Microbiologically Influenced Corrosion Testing

Kearns/Little, editors

ASTM

STP 1232

STP 1232

Microbiologically Influenced Corrosion Testing

Jeffery R. Kearns and Brenda J. Little, Editors

ASTM Publication Code Number (PCN)
04-012320-27

ASTM
1916 Race Street
Philadelphia, PA 19103
Printed in the U.S.A.

Library of Congress Cataloging-in-Publication Data

Microbiologically influenced corrosion testing / Jeffery R. Kearns and
Brenda J. Little, editors.
cm.—(ASTM special technical publication ; 1232)
Includes bibliographical references and index.
ISBN 0-8031-1892-9
1. Microbiologically influenced corrosion. 2. Materials—
—Microbiology. I. Kearns, Jeffery R., 1956– . II. Little,
Brenda J., 1945– . III. Series.
TA418.74.M543 1994
620.1'1223—dc20 94-5900
CIP

Photocopy Rights

Peer Review Policy

Each paper published in this volume was evaluated by three peer reviewers. The authors addressed all of the reviewers' comments to the satisfaction of both the technical editor(s) and the ASTM Committee on Publications.

The quality of the papers in this publication reflects not only the obvious efforts of the authors and the technical editor(s), but also the work of these peer reviewers. The ASTM Committee on Publications acknowledges with appreciation their dedication and contribution to time and effort on behalf of ASTM.

Printed in Fredericksburg, VA
April 1994

Foreword

The symposium on Microbiologically Influenced Corrosion Testing was presented at Miami, Florida on 16–17 Nov. 1992. ASTM Committee G-1 on Corrosion of Metals sponsored the symposium. Jeffery R. Kearns, Allegheny Ludlum Corporation, and Brenda J. Little, Naval Research Laboratory, served as co-chairs for the symposium and were co-editors of the resulting publication.

Contents

SURFACE ANALYSIS

SRB CHARACTERIZATION

NON-METALLICS

Overview

ASTM Committee G-1 on Corrosion of Metals began the development of standards on Microbiologically Influenced Corrosion (MIC) Testing in 1991. There were several challenges. The first was to organize an interdisciplinary task group with expertise in the use of electrochemical, metallurgical, surface analytical, microbiological, and biotechnological techniques. This was a particularly difficult problem because of limited communication between the different disciplines. Microbiologists had the skills necessary to manipulate and characterize microbial behavior and, consequently, their contributions tended to dominate the field. In addition, many practicing corrosion engineers were skeptical of claims made about the unique characteristics of MIC, since most of the observed corrosion could be accounted for by traditional concepts of localized and underdeposit corrosion.

The second challenge in developing standardized MIC tests was that much of the information on the performance and testing of materials in microbiologically active environments consisted of anecdotal evidence and descriptive case histories. There was virtually no consensus on how to conduct corrosion tests in microbiologically active environments or how to interpret test results. Exaggerated claims about the possible corrosive effects of microbial activity alarmed many people, but the lack of reliable, quantitative test data prevented the inclusion of microbiological factors in engineering designs. Although significant progress was made in solving industrial problems related to MIC and in developing analytical tools for studying biofilms, important issues related to materials testing, such as reproducibility and bias, were all but ignored. Field test results were considered to be site specific and the population dynamics of microbial consortia in natural waters were considered to be too complex to reproduce in the laboratory. Few considered the essential question of "What factor actually accelerates corrosion in a microbiologically active system?"

Faced with this situation, people with important materials selection decisions to make devised testing strategies based on the assumption that the factors that caused MIC are essentially the same chemical and physical factors that are well known to cause severe pitting and crevice corrosion in tests that do not intentionally involve microbes (abiotic tests). The controversy over a representative test and how to conduct it has persisted for over a decade.

MIC demands attention primarily because of the growing number of rather spectacular failures associated with the presence and activity of microbes in environments that would otherwise have been considered to be rather benign. All over the world, process and natural waters are becoming more corrosive for several reasons. Traditional methods of mitigation through cleaning and water treatment are becoming less effective because of high maintenance costs and more restrictive legislation on the chemical contents of process water effluents. Industrial waters are recycled more often, which tends to concentrate corrosive elements. MIC has resulted in premature failures of system components, increased downtime of equipment for repairs and maintenance, and increased operating costs associated with mitigation measures. MIC has forced premature replacement of tanks, heat exchangers, and piping systems with a severe detrimental effect on plant production. Cases of MIC have been reported in nuclear and fossil-fueled power plants, oil production, chemical processing industries, pulp and paper, transportation, and water distribution networks. If materials change-out and up-grade options are to be used for new and existing plants and vessels, reliable accelerated test methods have to be developed. MIC testing should be regarded as an essential part of the mitigation and control of corrosion in natural waters.

As a first step toward developing consensus on technical issues and toward creating a multidisciplinary task group that would develop standards on MIC within the ASTM G-1 Committee, a symposium on MIC Testing was organized. The participants in the symposium were from Argentina, Canada, England, France, Germany, Italy, Japan, New Zealand, and the United States and represented the multiple disciplines and industries engaged in MIC testing.

This ASTM Special Technical Publication (STP) resulted from the First International Symposium on Microbiologically Influenced Corrosion (MIC) Testing held in Miami during November of 1992. The STP consists of a Keynote Address and twenty-one papers arranged in six topical sessions: Electrochemical Methods, On-Line Monitoring Methods, Surface Analysis Techniques, SRB Characterization, Non-Metallic Materials, and Service Water Systems. The reader is advised that several papers deserve to be under two or more of these headings. Two papers are reviews of the state-of-the-art on electrochemical and surface analytical techniques for the study of MIC, and a third review addresses the effects of marine biofilms on corrosion of stainless steels.

The Keynote Address describes the evolution of the study of MIC from phenomenological case histories toward a mature multidisciplinary science. The most advanced technologies for determining cellular constituents within biofilms and for identifying and measuring MIC are described. Emphasis is given to recent developments in image analysis systems, electron, atomic and laser microscopy that have made it possible to image biological materials in hydrated states. New insights into complex interactions between biofilms and metal surfaces have lead to important findings, such as the absence of a correlation between the numbers and types of microbial cells and the occurrence of localized corrosion.

Electrochemical Methods

The development of an accelerated test for assessing the susceptibility of materials to MIC is very difficult because the usual methods of accelerating corrosion, such as increasing the temperature and concentration of aggressive chemical species, can alter the microbiological activity in the system, and hence bias test results. New methods of acceleration and detection are proposed.

Three types of electrochemical techniques are recommended since they do not perturb the microbiologically active system during the measurement: electrochemical noise measurement (ENM), electrochemical impedance spectroscopy (EIS), and zero resistance ammetery (ZRA). Measurements made in the field were combined with laboratory studies. For example, ENM was used to detect and monitor the ingress of oxygen into a biofouled test vessel at an Ontario Hydro nuclear power plant. Laboratory studies were conducted when it was necessary to explore specific issues or when more control of key test variables, such as temperature and oxygen content, were required. Successes in producing MIC in the laboratory and in identifying the crucial factors that accelerate corrosion are described. Inorganic analogs for simulating these factors in laboratory tests are also proposed.

The advantage of field tests over laboratory tests in microbiologically active systems is that the data generated are more directly applicable to the system of interest. However, field testing has three main limitations: (1) corrosion can take a long time to occur since no critical factor is accelerated, (2) natural fluctuations in the environment can mask significant changes in localized corrosion behavior, and (3) individual parameters are difficult to discriminate. A combination of failure analyses, laboratory studies, and field simulations is recommended to determine the mechanism of corrosion.

A biofilm limits oxygen diffusion to the surface of a metal or alloy and affects the pH at the biofilm/alloy interface. In addition, the biofilm may also contain electrically conductive

(or semiconductive) phases, such as pyrroles. Factors such as these can catalyze oxidation-reduction reactions and thereby accelerate localized corrosion. The pH at the biofilm/alloy interface was measured by two different techniques. In one case, a sophisticated micro-electrode apparatus was used to achieve outstanding spatial resolution, and in the other case various alloys in the form of wire mesh electrodes are monitored while cathodically polarized in natural and artificial seawater.

On-Line Monitoring Methods

Four different experiences with on-line monitoring methods for MIC and biofouling in industrial cooling water systems, service water systems, and secondary oil recovery water injection systems are documented in this section. Conventional monitoring methods tend to be too slow or are of insufficient sensitivity to permit reliable process control and water treatment in microbiologically active systems. This limitation means that mitigation activities are often costly, both environmentally and in terms of the direct costs of the anti-microbial chemicals. The papers in this section present proven alternatives to conventional methods of monitoring. The papers describe monitoring systems for heat exchangers and water distribution pipelines where the objective is to maintain heat transfer efficiency or flow. This is done by controlling the formation of biological deposits, while not compromising the effectiveness of corrosion inhibitors or promoting scale formation. The capabilities and test parameters for the on-line monitoring systems were developed in the laboratory and the effectiveness of the system was demonstrated at sites such as the Amoco Chemical Company Chocolate Bayou petrochemical plant and the Tennessee Valley Authority Browns Ferry nuclear plant. Electrochemical monitoring methods were the primary tool used in three of the four papers. However, as described in the second paper of this section, it was necessary to monitor water microbiology and chemistry at Husky Oil Operations Limited's Wainwright waterflood operation in order to improve the water treatment practice.

Surface Analysis Techniques

Surface analytical techniques provide powerful tools for understanding MIC. X-ray Photoelectron Spectroscopy (XPS) was shown to provide detailed information about the oxidation and reduction of metals as transformed by microbial metabolism. More specifically, XPS was used to determine quantitative chemical information on the interaction of *Desulfovibrio sp.* with the corrosion products from stainless steels (Fe, Cr, Ni and Mo ions) under anoxic conditions. Microbial sulfate reduction produced multiple reduced sulfur species (SO_3^{2-}, elemental S and S^{2-}), as well as reduced molybdate and ferric ions.

The utilization of conventional surface analytical techniques in failure analysis and laboratory studies is reviewed in the second paper of the section. Surface analysis techniques were utilized for elucidating the processes involved with MIC and for establishing causal relationships between microbial activity and corrosion.

SRB Characterization

The traditional microbiological methods as well as the latest genetic techniques for the characterization of SRB (Sulfate-Reducing Bacteria) are described in two of the three papers in this section. A thermodynamic analysis of SRB behavior is presented in the first paper. Efforts to characterize SRB contribute to the identification of "fingerprints" for the presence and activity of SRB that can be unequivocally linked to corrosion.

For many years all SRB were cultured on standard media using lactate as the electron donor and carbon source. Two modern alternatives are presented: Sulfur Isotope Fractionation is presented as a definitive tool for identifying MIC by SRB, and, the molecular biological technique of reverse sample genome probing (RSGP) is demonstrated to be of practical industrial value in solving a biofouling/MIC problem in the heavy oil operations of the Wainwright and Wildmere fields in Alberta, Canada.

Non-Metallic Materials

Although the majority of work on MIC is concerned with metals and alloys, in this section, three novel papers on the MIC of polymers, concrete, and natural sandstone are presented. A unique test system developed in Germany is to simulate the combined effects of atmospheric gaseous pollutants (SO_2 and NO_x) and nitrifying bacteria (biogenic nitric acid) on natural sandstone and calcium alginate mortars. This system revealed that gaseous pollutants (SO_2) remove microbiologically produced nitrite and nitrate which effectively reduces the rate of corrosion. It is rather ironic that the reduction of sulfur dioxide in the atmosphere increases the risk of damage to historical buildings by biogenic nitric acid corrosion.

From historical buildings to ships: a US Navy field test program evaluated the seawater corrosion resistance of several conductive caulks and sealants that are used to protect ship antenna arrays. Environmental scanning electron microscopy was used as a non-destructive means of observing the activity of biofilms on the caulks. A nickel-based conductive caulk with a corrosion inhibitor resisted degradation well in all of the field and accelerated laboratory tests over a period of 15 months. Consequently, this material was recommended for this application.

Results from chemical tests can be misleading when it comes to predicting the behavior of materials in natural environments because the influence of bacteria on the corrosion process is not well represented. For example, calcium aluminate cement has performed well in sewage systems for many years, although the results of conventional chemical tests indicate that it was inadequate for this application. To obtain more reliable test results, a simulation chamber for biogenic sulfuric acid corrosion was created at the University of Hamburg. By optimizing the growth conditions for microbes in the simulation chamber, the aggressive conditions in the Hamburg sewer system were created within a year. The city of Hamburg now requires this test to qualify new materials for the sewage system.

Service Water Systems

Nearly 60 years ago, Wolzogen and Van der Vlugt considered the influence of SRB on corrosion of cast iron pipe in soil. The second paper of this section reconsidered this topic with one of the newest electrochemical monitoring techniques—Electrochemical Impedance Spectroscopy (EIS). The strong correlation between EIS data and weight loss data recommend this method for accelerated testing and monitoring.

Effective measures for mitigating MIC often have to be developed, substantiated and introduced into practice to protect existing installations even though the mechanism for MIC is not known. Two examples of such cases are presented in regard to the potable water distribution systems in several European hospitals. First, the corrosion was confirmed to be MIC by the presence of solid corrosion products mixed with a gelatinous film consisting of polysaccharides, polysilicates, lactate and pyruvate. Then the factors related to operating conditions were discriminated from those related to piping system design. This was done by means of test rigs installed at various locations within a hospital. A combination of ultra-

violet radiation and bicarbonate additions mitigated the corrosion of the copper piping in cold water supply, while maintaining the water above 55°C solved the corrosion problem in hot water supply. The likelihood of MIC increased drastically after an induction period. Consequently, accelerated, short term tests were devised to simulate the induction period. In order to further accelerate the processes that lead to corrosion and overcome seasonal changes in microbial activity, the test rigs were inoculated with bacteria from corroding sites.

Laboratory tests for service water systems are often criticized for not being representative of actual field situations because pure strains of bacteria are grown on enriched media then exposed to alloys under stagnant flow conditions. These limitations are addressed in an accelerated test system built at the Center for Environmental Biotechnology which simulates the ecological, physiological and nutritional requirements for the various species of bacteria found in the sediments, slime, tubercles, and corrosion products at an operating plant. Test solutions were prepared to simulate field conditions with nutritional supplements to stimulate the growth of microbes. Electrochemical techniques were used to monitor corrosion of mild steel without perturbing the biofilm. The system provided a means to simulate and accelerate MIC of mild steel.

Summary

The combined offerings of the contributors to this STP will provide the reader with a review of the state-of-the-art of MIC testing in the early 1990s. Many industrial needs in the area of MIC testing are identified in these papers along with latest laboratory and field testing techniques. Strategies to monitor and control corrosion and biofouling in water distribution systems, underground pipelines, buildings, and marine vessels are discussed. From this a consensus emerges on how to evaluate and reliably simulate microbiological factors in real systems and laboratory tests. It is hoped that some of the proposed test methods and guidelines presented in this STP will gain wider acceptance and eventually lead to the development of new ASTM standards.

Jeffery R. Kearns

Allegheny Ludlum Corporation, Backenridge, PA; symposium co-chair and co-editor.

Brenda J. Little

Naval Research Laboratory, Stennis Space Center, MS; symposium co-chair and co-editor.

Keynote Address

Brenda J. Little[1] *and Patricia A. Wagner*[1]

Advances in MIC Testing

REFERENCE: Little, B. and Wagner, P., **"Advances in MIC Testing,"** *Microbiological Influenced Corrosion Testing, ASTM STP 1232,* Jeffery R. Kearns and Brenda J. Little, Eds., American Society for Testing and Materials, Philadelphia, 1994, pp. 1–11.

ABSTRACT: The study of microbiologically influenced corrosion (MIC) has progressed from phenomenological case histories to a mature interdisciplinary science including electrochemical, metallurgical, surface analytical, microbiological, biotechnological, and biophysical techniques. With microelectrodes and gene probes it is now possible to measure interfacial dissolved oxygen, dissolved sulfide and pH, and to determine microbial species responsible for localized chemistry. Biofilms can be tailored to contain consortia of specific microorganisms and naturally-occurring biofilms can be dissected into cellular and extracellular constituents. Scanning vibrating electrodes can be used to map the distribution of anodic electrochemical activity. Electrochemical impedance spectroscopy and electrochemical noise analysis techniques have been developed to non-destructively evaluate localized corrosion due to MIC. The development of environmental scanning electron, atomic force, and laser confocal microscopy makes it possible to image cells on surfaces and to accurately determine the spatial relationship between microorganisms and localized phenomena. Transport of nutrients through biofilms can be modeled using techniques including optical density measurements to precisely locate the water/biofilm interface and nuclear magnetic resonance imaging to visualize flow characteristics near surfaces colonized with microorganisms. The ways in which new techniques can be used to understand fundamental mechanisms and to discriminate MIC will be discussed in this paper.

KEYWORDS: microbiologically influenced corrosion (MIC), culture techniques, electrochemistry, surface analyses

Introduction

Corrosion associated with microorganisms has been recognized for over 50 years, yet the study of MIC is a relatively new, multidisciplinary field. In 1985 an International Conference on Biologically Influenced Corrosion was sponsored by the National Association of Corrosion Engineers (NACE). Of the thirty-six papers in the proceedings volume, roughly half the papers are descriptive case studies and ten titles contain the words sulfate-reducing bacteria (SRB) [*1*]. In 1985 many of the techniques for evaluating MIC depended on characterizing shape, color, and smell of surface deposits in addition to the presence of specific types of bacteria, usually SRB. In contrast, today there is general recognition that SRB contribute and control many cases of MIC, but that it is the total community of bacteria within the biofilm that is responsible for MIC and there is no correlation between numbers and types of cells and localized corrosion [*2*]. Electrochemical, surface analytical, and microbiological techniques are now routinely combined to elucidate the complexities of microbial interactions with metal substrata.

[1] Research chemist and oceanographer, respectively, Naval Research Laboratory, Stennis Space Center, MS 39529-5004.

Techniques for Determining Cellular Constituents Within Biofilms

Culture Techniques

For many years, the standard for evaluating MIC has been the enumeration of SRB either in bulk liquids or in surface deposits using a liquid or solid [*3*] medium with sodium lactate as the carbon source [*4,5*]. When SRB are present in the sample, sulfate is reduced to sulfide which reacts with iron in solution to produce black ferrous sulfide. Blackening of the medium over a 28-day period signals the presence of SRB. Usually, 1 mL samples are injected by syringe into media bottles for 10-fold dilutions. It is assumed that only a single living bacterium is required to blacken a bottle. The simplest interpretation of test results is to consider that if one bottle is blackened, the sample contained at least 1 organism, if two bottles are blackened, the sample contained 10 organisms; three bottles, 100 organisms and so on. Agar slants can be inoculated by dipping a pipe cleaner into a liquid sample and inserting it into a single vial of solid or semi-solid agar. Mineral oil and a CO_2-generating tablet are usually added to exclude oxygen, and the vial is capped, incubated for 5 days, and checked daily for blackening.

The distinct advantage of culturing techniques is that they are extremely sensitive. Low numbers of SRB grow to easily detectable higher numbers in the proper culture medium. However, growth media tend to be strain-specific. For example, lactate-based media sustain the growth of lactate oxidizers but not acetate-oxidizing bacteria. Incubating at one temperature is further selective. Culturing methods using agar media cannot distinguish between a single SRB cell and a clump of SRB cells [*3*]. The present trend in culture techniques is to attempt to culture several physiological groups including aerobic, heterotrophic bacteria; facultative anaerobic bacteria; and acid-producing bacteria in addition to sulfate-reducing bacteria [*6*]. A complex SRB medium containing multiple carbon sources that can be degraded to both acetate and lactate has been developed and compared to five other commercially available media using natural and produced waters and surface deposits [*7*].

Biochemical Assays

Biochemical assays have been developed for the detection of specific microorganisms associated with MIC. Unlike culturing techniques, biochemical assays for detecting and quantifying bacteria do not require growth of the bacteria. Instead, biochemical assays measure constitutive properties including adenosine triphosphate (ATP) [*8*], phospholipid fatty acids (PLFA) [*2*], cell-bound antibodies [*9,10*], and DNA [*11*]. Adenosine-5'-phosphosulfate (APS) reductase [*3*], hydrogenase [*12*], and radiorespirometric measurements have been used to estimate SRB populations and activity [*13,14*].

ATP assays estimate the total number of viable organisms by measuring the amount of adenosine triphosphate in a sample. ATP is a compound found in all living matter. The procedure requires that a water sample be filtered to remove solids and salts which may interfere with the test. The filtered sample is added to a reagent that releases cell ATP. An enzyme then reacts with the ATP to produce a photochemical reaction. Emitted light is measured with a photometer and the number of bacterial cells is estimated from the total light emitted.

Biofilm community structure can be analyzed using cluster analysis of the PLFA profiles [*2*]. PLFA profiles for natural biofilms have been shown to be more complex than profiles for laboratory biofilms. None of the laboratory profiles clustered closely with profiles from natural biofilms. In addition, the PLFA profiles for attached bacteria clustered separately

from profiles of the same bacteria in the bulk phase, suggesting that either the community or the physiology of attached bacteria differ from that of bulk phase bacteria.

Immunofluorescence techniques have been developed for the identification of specific bacteria in biofilms [*15,16*]. Epifluorescence cell surface antibody (ECSA) methods for detecting SRB are based on the use and subsequent detection of specific antibodies, produced in rabbits, that react with SRB cells [*9,10*]. A secondary antibody, produced in goats, is then reacted with the primary rabbit antibodies bound to SRB cells. In some cases, goat antibodies are linked to a fluorochrome which enables bacterial cells marked with the secondary antibody to be viewed with an epifluorescence microscope. In other cases, goat antibodies are conjugated with an enzyme (alkaline phosphatase) that can then be reacted with a colorless substrate to produce a visible color proportional to the quantity of SRB present. The detection limits for the field test are 10 000 SRB/mm^2 filter area. The color reagent used for the field tests is unstable at room temperature and tends to bind nonspecifically with antibodies adsorbed directly at active sites on the filter, creating a false positive that may interfere with the detection of SRB at levels below 10 000 cells/mm^2. Antigenic structures of marine and terrestrial strains are distinctly different and therefore antibodies to either strain did not react with the other. Furthermore, SRB antibodies did not react with non-SRB bacteria. The developers report a poor response of rabbit antibodies developed from pure SRB cultures to mixed populations [*10*]. Rabbit SRB antibodies generated from fresh SRB strains from Prudhoe Bay, Alaska, as well as terrestrial and marine locations, were found to react better with SRB from natural sources. It is possible to differentiate individual species within a biofilm by reacting them with monoclonal antibodies specific to outer cell membrane antigens. Hogan [*11*] described a non-isotopic semi-quantitative procedure for the detection of *Desulfobacterium* and *Desulfotomaculum* using DNA probes labeled with an acridinium ester that is sensitive to 10^4 organisms per mL.

Direct molecular characterization of natural microbial populations can be accomplished with sequence analysis of 5S rRNAs [*17,18*]. More recently, fluorescent dye-labeled oligonucleotide probes have been used for microscopic identification of single cells and characterization of mixed populations. Polymerase chain reaction amplification, comparative sequencing and whole cell hybridization have been combined to selectively identify and visualize SRB both in established and developing multispecies biofilms [*19*].

APS reductase is an intercellular enzyme found in all SRB. Briefly, cells are washed to remove interfacing chemicals, including hydrogen sulfide, and lysed to release APS reductase. The lysed sample is washed, added to an antibody reagent and exposed to a color-developing solution. In the presence of APS reductase a blue color appears within 10 min. The degree of color is proportional to the amount of enzyme and roughly to the number of cells from which the enzyme was extracted. Similarly, a procedure has been developed to quantify hydrogenase from hydrogenase-positive SRB requiring cells to be concentrated by filtration from water samples [*12*]. Solids, including corrosion product and sludge, can be used without pretreatment. The sample is exposed to an enzyme extracting solution for 15 min and placed in an anaerobic chamber from which oxygen is removed by hydrogen. The enzyme reacts with excess hydrogen and simultaneously reduces an indicator dye in solution. The activity of the hydrogenase is established by the development of a blue color in less than 4 h. The intensity of the blue color is proportional to the rate of hydrogen uptake by the enzyme. The technique does not attempt to estimate specific numbers of SRB.

Roszak and Colwell [*20*] reviewed techniques commonly used to detect microbial activities in natural environments, including transformations of radiolabelled metabolic precursors. Phelps et al. [*21*] and Mittelman et al. [*22*] used uptake or transformation of ^{14}C-labelled metabolic precursors to examine activities of sessile bacteria in natural environments and

in laboratory models. Phelps et al. [*21*] used a variety of ^{14}C-labelled compounds to quantify catabolic and anabolic bacterial activities associated with corrosion tubercles in steel natural gas transmission pipelines. They demonstrated that organic acid was produced from H_2 and CO_2 in natural gas by acetogenic bacteria, and that acidification could lead to enhanced corrosion of the steel. Mittelman et al. [*22*] used measurement of lipid biosynthesis from ^{14}C-acetate, in conjunction with measurements of microbioal biomass and extracellular polymer, to study effects of differential fluid shear on physiology and metabolism of *Alteromonas* (formerly *Pseudomonas*) *atlantica*. Increasing shear force increased the rate of total lipid biosynthesis, but decreased per cell biosynthesis. Increasing fluid shear also increased cellular biomass and greatly increased the ratio of extracellular polymer to cellular protein.

Techniques for analyzing microbial metabolic activity at localized sites are also being developed. Franklin et al. [*23*] incubated microbial biofilms with ^{14}C-metabolic precursors and autoradiographed the biofilms to locate biosynthetic activity on corroding metal surfaces. The uptake of the labelled compounds was related to localized electrochemical activities associated with corrosion reactions.

A major breakthrough in determining bacterial activity within biofilms has been the use of "reporter" genes that can signal the induction of specific metabolic pathways. King et al. [*24*] engineered the incorporation of a promotorless cassette of *lux* genes into specific operons of *Pseudomonas* so that these operons induce bioluminescence during the degradation of naphthalene. Mittelman et al.[2] used the bioluminescent reporter gene to provide a quantitative measure of attachment of microorganisms onto metal and glass surfaces in a laminar flow system. They found that biofilm light production was directly correlated with biofilm cell numbers in a range of 10^5–10^7 cells/cm^2. Using reporter genes, Marshall et al. [*25*] demonstrated that bacteria immobilized at surfaces exhibit physiological properties not found in the same organisms in the aqueous phase. Some genes are turned on at a solid surface despite not being expressed in liquid or on solid media. It is also likely that other genes are turned off at surfaces. They identified acid- and alkali-inducible genes in *E. coli*. Marshall et al. [*25*] further demonstrated gene transfers within biofilms even in the absence of imposed selection pressure.

Rosser and Hamilton [*13*], with subsequent modifications [*14*], developed a test tube technique for a ^{35}S sulfate radiorespirometric assay to measure SRB metabolic activity on the surface of metal coupons after exposure to corrosive environments. The coupon is placed into anaerobic filtered sterile seawater containing ^{35}S-sulfate. Oxygen-free zinc acetate is immediately injected onto an enclosed filter paper wick and the entire system is incubated. Oxygen-free hydrochloric acid is then injected past the wick into the solution. Volatile acid sulfides, including any $H_2{}^{35}S$ formed, are trapped during an equilibration period. The wick is removed from the tube and the radioactivity measured using a liquid scintillation counter, after which the sulfate reduction rate is calculated. This technique has been used for both bulk and coupon samples.

Techniques for Identification and Measurement of MIC

Electrochemical Techniques

Mansfeld and Little [*26*] recently reviewed electrochemical techniques applied to MIC studies and no attempt will be made to discuss all the innovations in electrochemical techniques. Three nondestructive electrochemical techniques, the scanning vibrating electrode technique (SVET), electrochemical impedance spectroscopy (EIS), and electrochemical

[2] M. W. Mittelman, J. M. H. King, G. S. Sayler, and D. C. White, unpublished data, University of Tennessee, Knoxville, TN, 1992.

noise analysis (ENA) are currently being used to provide unique insights into mechanisms for MIC.

SVET is used to determine the magnitude and sign of current densities over freely corroding metals in solution [*27*]. Franklin et al. [*28*] used SVET to show a spatial relationship between localized corrosion and bacterial cells on carbon steel surfaces. Pit propagation depended on the presence of bacteria. The authors proposed that biofilms inhibited migration of aggressive ions from pits or migration of inhibiting ions from the bulk solution into pits.

EIS techniques record impedance data as a function of the frequency of an applied signal at a fixed potential [*29*]. A large frequency range (65 kHz to 1 mHz) must be investigated to obtain a complete impedance spectrum. Dowling et al. [*30*] and Franklin et al. [*31*] demonstrated that the small signals required for EIS do not adversely affect the number, viability, and activity of microorganisms within a biofilm.

EIS data may be used to determine polarization resistance, the inverse of corrosion rate. Sophisticated models have been developed for localized corrosion [*32,33*] that provide additional information from EIS data. Several reports have been published in which EIS has been used to study the role of SRB in corrosion of buried pipes [*34–36*] and reinforced concrete [*37–39*]. The formation of biofilms and calcareous deposits on three stainless steels and titanium during exposure to natural seawater was followed using EIS and surface analysis [*40,41*]. Ferrante and Feron [*42*] used EIS data to conclude that the material composition of steels was more important for MIC resistance than bacterial population, incubation time, sulfide content, and other products of bacterial growth. Jones et al. [*43*] used EIS to determine the effects of several mixed microbiological communities on the protective properties of epoxy coatings on steel. A damage function was defined which allowed qualitative assessment of coating deterioration due to MIC.

ENA follows fluctuations of potential or current as a function of time or experimental conditions. Analysis of the structure of the electrochemical noise using the frequency dependence of the power spectral density can provide information concerning the nature of corrosion processes and magnitude of corrosion rate. King et al. [*36*] interpreted noise measurements for steel pipes in environments containing SRB as being indicative of film formation and breakdown. Iverson [*44,45*] used ENA to monitor corrosion of mild steel in a trypticase seawater culture of a marine SRB and concluded that breakdown of the iron sulfide film was accompanied by the generation of potential electrochemical noise.

Surface Analytical Techniques

Nivens et al. [*46*] demonstrated that attenuated total reflectance infrared spectroscopy (ATR-FT/IR) can be used to detect changes in sessile microbial biomass. The ATR-FT/IR studies showed that changes in the physiological properties of attached bacteria were induced by changes in the bulk phase. They demonstrated that the number of attached *Caulobacter sp.* was directly correlated with the intensity of the infrared amide II asymmetrical stretch band at 1543 cm^{-1}, corresponding to bacterial protein. The technique was sensitive to 10^6 bacteria/cm^2, and changes in the physiological status of the attached bacteria could be measured. For example, production of the intracellular storage lipid, poly-B hydroxyalkanoate, and production of extracellular polymer, were monitored by absorbance at 1730 cm^{-1} (C=O stretch) and 1084 cm^{-1} (C—O stretch), respectively.

Geesey and Bremer [*47*] used ATR-FT/IR to evaluate non-destructively, in real time, interactions of bacteria with thin films of copper deposited on germanium. Changes in the thickness of the copper films were measured as increased intensity of the infrared water absorption band at 1640 cm^{-1}. The authors compared copper loss in the presence of bacteria

isolated from corroded copper samples and were able to observe differences between two cultures. Using this technique, Jolley et al. [*48*] observed copper oxidation by three polymers, including bacterial exopolymer.

Nivens et al. [*46*] investigated the use of the quartz crystal microbalance (QCM), a very sensitive mass-sensing device, for detecting attached microbial films. The QCM was more sensitive to changes in biomass than ATR-FT/IR, with a detection limit of 10^4 bacteria/cm^2 and a linear range of at least two orders of magnitude. An interesting aspect of both ATR-FT/IR and the QCM is that substrata of both techniques can be used for electrochemical analyses so that corrosion information can be obtained while changes in microbial biofilms are monitored.

It is now generally recognized that biofilms alter biofilm/metal interfacial chemistries. Direct chemical measurements are restricted by biofilm thickness and the heterogeneous anisotropic nature of biofilms [*49*]. Ion-selective and gas sensing microprobes with tip diameters less than 10 μm have been developed for direct biofilm measurements. Lewandowski [*49*] measured dissolved oxygen profiles in a continuous flow, open channel reactor with a mixed biofilm on a metal surface. Van Houdt et al. [*50*] developed a rugged iridium oxide pH microelectrode with a 3 to 5 μm tip diameter to measure a pH profile across a mixed population biofilm on a polycarbonate disc.

An in-situ microtechnique has been developed for evaluating parameters of diffusion-controlled reactions in biofilms [*51*]. A microprobe 15 μm in diameter was used to simultaneously measure dissolved oxygen and optical density at different depths in a submerged biofilm. The diffusion coefficient for dissolved oxygen, the dissolved oxygen flux, and the half velocity coefficient were then calculated.

Nuclear magnetic resonance imaging (NMRI), a non-invasive method, uses radiofrequency magnetic fields in the presence of a strong magnetic field to provide information about the concentration and physical state of specific atomic nuclei. Lewandowski et al. [*52*] demonstrated the use of NMRI to show distribution of water, flow velocities, and biomass in a biofilm/polycarbonate reactor system.

Recent developments in image analysis systems and electron, atomic and laser microscopies make it possible to image biological materials in the hydrated state. Muellar et al. [*53*] were able to determine rate coefficients for early bacterial colonization on copper, silicon, stainless steel and glass using a chemostat, a flow cell, and a microscope equipped with an image analysis system. Substrata were monitored using reflective light from a microscope equipped with a Nomarski lens and video camera recorder. Transmitted light was used for transparent surfaces. They demonstrated that surface roughness and surface free energy correlated positively with biological and abiological sorption processes.

Little et al. [*54*] used environmental scanning electron microscopy/energy-dispersive X-ray analysis (ESEM/EDS) to study biofilms on stainless steel surfaces, observing a gelatinous layer in which microalgae were embedded. Extracellular polymeric acidic polysaccharides bind and precipitate heavy metals. ESEM/EDS spectra indicated local concentrations of Al, Ni, and Ti. Images of the same specimens made using traditional scanning electron microscopy (SEM) demonstrated a loss of cellular and extracellular material. Dehydration of the biofilm with solvents, required for SEM, either extracted bound metals from the biofilm by ion exchange/solvent extraction or removed the metals with the extracellular polymeric material.

Laser confocal microscopy permits one to create three-dimensional images, see surface contour in minute detail, and accurately measure critical dimensions by mechanically scanning the object with laser light [*55*]. A sharply focused image of a single horizontal plane within a specimen is formed while light from out of focus areas is repressed from view. The process is repeated again and again at precise intervals on horizontal planes and the visual data from all images compiled to create a single, multidimensional view of the subject.

Geesey[3] used laser confocal microscopy to produce three-dimensional images of bacteria within scratches, milling lines and grain boundaries.

The atomic force microscope (AFM) is related to the scanning tunneling microscope (STM). The STM uses an atomically sharp conductive tip held angstroms from the surface to profile surface features with angstrom resolution. When the tip is electrically biased with respect to the sample, a current will flow between the surface atom closest to the tip and the nearest tip atom by the quantum mechanical process of electron tunneling. While the STM requires the sample to be electrically conductive or coated with a conductive material, the AFM can be used to image non-conducting surfaces and does not rely on tunneling current. AFM provides exceptional detail and allows viewing of specimens in the hydrated state. AFM uses an extremely sharp scanning probe mounted on a flexible cantilever to record x,y,z coordinates of a sample in fractions of a nanometer. Photodiode electrical outputs mimic sample topography and serve as the basis for the resulting image. AFM images of copper exposed to a bacterial culture medium for 7 days showed biofilms distributed heterogeneously across the surface with regard to both cell numbers and depth [*56*]. Bacterial cells were associated with pits on the surface of the copper coupons.

Conversion of metals to sulfides by SRB has been studied since the late 1800s [*57*]. Baas-Becking and Moore identified mackinawite, gregrite and smythite as indicators for SRB corrosion of ferrous metals in anaerobic environments [*58*]. McNeil et al. analyzed sulfide mineral deposits on copper alloys colonized by SRB in an attempt to identify specific mineralogies that were indicative of SRB activity [*59*]. They concluded that the formation of non-adherent layers of chalcocite (Cu_2S) and the presence of hexagonal chalcocite were indicators of SRB-induced corrosion of copper. The compounds were not observed abiotically and their presence in near-surface environments could not be explained thermodynamically.

Sulfur isotope fractionation was demonstrated by Little et al. in sulfide corrosion deposits resulting from the activities of SRB within biofilms on copper surfaces [*60*]. ^{32}S accumulated in sulfide-rich corrosion products, and ^{34}S was concentrated in the residual sulfate in the culture medium. Accumulation of the lighter isotope was related to surface derivatization or corrosion as measured by weight loss. Use of this and the preceeding mineralogical technique to identify SRB-related corrosion requires sophisticated laboratory procedures.

Conclusions

The combined testing approaches of microbiology, electrochemistry, and surface chemistry have been reviewed to provide insight into complex interactions between biofilms and metal surfaces. Multimedia microbiological cultures, biochemical assays and genetic probes are being used to demonstrate the presence of specific types of bacteria. ESEM, AFM and laser confocal microscopy have demonstrated the spatial relationship between bacteria and localized corrosion on hydrated surfaces. Dissolved oxygen, dissolved sulfides, pH and optical density profiles through biofilms have been made with microprobes. Electrochemical testing, including EIS, SVET and ENA, has been used to demonstrate MIC for many alloys in a large number of environments.

Acknowledgments

This work was supported by the Office of Naval Research, Program Element 0601153N through the Defense Research Sciences Program, NRL Contribution Number PR 92:077:333.

[3] G. G. Geesey, unpublished data, Montana State University, Bozeman, MT, 1992.

References

[1] *Biologically Induced Corrosion*, S. C. Dexter, Ed., National Association of Corrosion Engineers, Houston, Texas, 1986.

[2] Franklin, M. J. and White, D. C., "Biocorrosion," *Biotechnology*, Vol. 2, 1991, pp. 450–456.

[3] Tatnall, R. E., Stanton, K. M., and Ebersole, R. C., "Methods of Testing for the Presence of Sulfate-Reducing Bacteria," *Corrosion/88*, Paper No. 88, National Association of Corrosion Engineers, Houston, Texas, 1988.

[4] Postgate, J. R., *The Sulphate-Reducing Bacteria*, Cambridge University Press, Great Britain, 1979.

[5] American Petroleum Institute, API Recommended Practice for Biological Analysis of Subsurface Injection Waters, API, New York, 1965.

[6] Soracco, R. J., Pope, D. H., Eggars, J. M., and Effinger, T. N., "Microbiologically Influenced Corrosion Investigations in Electric Power Generating Stations," *Corrosion/88*, Paper No. 83, National Association of Corrosion Engineers, Houston, Texas, 1988.

[7] Scott, P. J. B. and Davies, M., "Survey of Field Kits for Sulfate-Reducing Bacteria (SRB)," *Materials Performance*, Vol. 31, No. 5, 1992, pp. 64–68.

[8] Littman, E. S., "Oilfield Bactericide Parameters as Measured by ATP Analysis," Paper No. 5312, International Symposium of Oil Field Chemistry of the Society of Petroleum Engineers of AIME, Dallas, Texas, 1975.

[9] Pope, D. H., "Discussion of Methods for the Detection of Microorganisms Involved in Microbiologically Influenced Corrosion," *Biologically Induced Corrosion*, National Association of Corrosion Engineers, Houston, Texas, 1986, pp. 275–283.

[10] Pope, D. H., "Development of Methods to Detect Sulfate-Reducing Bacteria—Agents of Microbiologically Influenced Corrosion," MTI No. 37, Materials Technology Institute of the Chemical Process Industries, Inc., National Association of Corrosion Engineers, Houston, Texas, 1990.

[11] Hogan, J. J., "A Rapid, Non-Radioactive DNA Probe for the Detection of SRBs," presented at *Institute of Gas Technology Symposium on Gas, Oil, Coal, and Environmental Biotechnology*, New Orleans, LA, 1990.

[12] Boivin, J., Laishley, E. J., Bryant, R. D., and Costerton, J. W., "The Influence of Enzyme Systems on MIC," *Corrosion/90*, Paper No. 128, National Association of Corrosion Engineers, Houston, TX, 1990.

[13] Rosser, H. R. and Hamilton, W. A., "Simple Assay for Accurate Determination of [^{35}S] Sulfate Reduction Activity," *Applied and Environmental Microbiology*, Vol. 45, 1983, pp. 1956–1959.

[14] Maxwell, S. and Hamilton, W. A., "The Activity of Sulphate-Reducing Bacteria on Metal Surfaces in an Oilfield Situation," *Biologically Induced Corrosion*, National Association of Corrosion Engineers, Houston, TX, 1986, pp. 284–290.

[15] Zambon, J. J., Huber, P. S., Meyer, A. E., Slots, J., Fornalik, M. S., and Baier, R. E., "In Situ Identification of Bacterial Species in Marine Microfouling Films by Using an Immunofluorescence Technique," *Applied and Environmental Microbiology*, Vol. 48, No. 6, 1984, pp. 1214–1220.

[16] Howgrave-Graham, A. R. and Steyn, P. L., "Application of the Fluorescent-Antibody Technique for the Detection of *Sphaerotilus natans* in Activated Sludge," *Applied and Environmental Microbiology*, Vol. 54, No. 3, pp. 799–802.

[17] Stahl, D. A., Flesher, B., Mansfield, H. R., and Montgomery, L., "Use of Phylogenetically Based Hybridization Probes for Studies of Ruminal Microbial Ecology," *Applied and Environmental Microbiology*, Vol. 54, pp. 1079–1084.

[18] Stahl, D. A., Lane, D. J., Olsen, G. J., and Pace N. R., "Analysis of Hydrothermal Vent-Associated Symbiosis by Ribosomal RNA Sequences," *Science*, Vol. 224, 1984, pp. 409–411.

[19] Ammann, R. I., Stormley, J., Devereux, R., Key, R., and Stahl, D. A., "Molecular and Microscopic Identification of Sulfate-Reducing Bacterial in Multispecies Biofilms," *Applied and Environmental Microbiology*, Vol. 58, No. 2, 1992, pp. 614–623.

[20] Roszak, D. B. and Colwell, R. R., "Survival Strategies of Bacteria in the Natural Environment," *Microbiological Reviews*, Vol. 51, 1987, pp. 365–379.

[21] Phelps, T. J., Schram, R. M., Ringelberg, D., Dowling, N. J., and White, D. C., "Anaerobic Microbial Activities Including Hydrogen Mediated Acetogenesis Within Natural Gas Transmission Lines," *Biofouling*, Vol. 3, 1991, pp. 265–276.

[22] Mittelman, M. W., Nivens, D. E., Low, C., and White, D. C., "Differential Adhesion, Activity, and Carbohydrate: Protein Ratios of *Pseudomonas atlantica* Attaching to Stainless Steel in a Linear Shear Gradient," *Microbial Ecology*, Vol. 19, 1990, pp. 269–278.

[23] Franklin, M. J., Guckert, J. B., White, D. C., and Isaacs, H. S., "Spatial and Temporal Relationships Between Localized Microbial Metabolic Activity and Electrochemical Activity of Steel," *Corrosion/91*, Paper No. 115, National Association of Corrosion Engineers, Houston, TX, 1991.

[24] King, J. M. H., DiGrazia, P. M., Appelgate, B., Buriage, R., Sanseverino, J., Dunbar, P., Larimer, F., and Sayler, G. S., "Rapid, Sensitive Bioluminescent Reporter Technology for Naphthalene Exposure and Biodegradation," *Science*, Vol. 249, 1990, pp. 778–781.

[25] Marshall, K. C., Power, K. N., Angles, M. L., Schneider, R. P., and Goodman, A. E., "Analysis of Bacterial Behavior During Biofouling of Surfaces," in *Biofouling/Biocorrosion in Industrial Water Systems*, G. G. Geesey, Z. Lewandowski, and H.-C. Flemming, Eds., Lewis Publishers, Inc., Chelsea, MI, in press.

[26] Mansfeld, F. and Little, B., "A Technical Review of Electrochemical Techniques Applied to Microbiologically Influenced Corrosion," *Corrosion Science*, Vol. 32, No. 3, 1991, pp. 247–272.

[27] Isaacs, H. S. and Ishikawa, Y., "Application of the Vibration Probe to Localized Current Measurements," *Corrosion/85*, Paper No. 55, National Association of Corrosion Engineers, Houston, TX, 1985.

[28] Franklin, M. J., White, D. C., and Isaacs, H. S., "Pitting Corrosion by Bacteria on Carbon Steel, Determined by the Scanning Vibrating Electrode Technique," *Corrosion Science*, Vol. 32, No. 9, 1991, pp. 945–952.

[29] Mansfeld, F. and Lorenz, W. J., *Techniques of the Characterization of Electrodes and Electrochemical Processes*, R. Varma and J. R. Selman, Eds., J. Wiley and Son, 1991, p. 581.

[30] Dowling, N. J. E., Franklin, M., White, D. C., Lee, C. H., and Lundin, C., The Effect of Microbiologically Influenced Corrosion on Stainless Steel Weldments in Artificial Seawater," *Corrosion/89*, Paper No. 187, National Association of Corrosion Engineers, Houston, TX, 1989.

[31] Franklin, M. J., Nivens, D. E., Guckert, J. B., and White, D. C., "Effect of Electrochemical Impedance Spectroscopy on Microbial Biofilm Cell Numbers, Viability, and Activity," *Corrosion*, Vol. 47, 1991, pp. 519–522.

[32] Kendig, M., Mansfeld, F., and Tsai, S., "Determination of the Long Term Corrosion Behavior of Coated Steel with AC Impedance Measurements," *Corrosion Science*, Vol. 23, 1983, p. 317.

[33] Mansfeld, F., Kendig, M., and Tsai, S., "Evaluation of Corrosion Behavior of Coated Metals with AC Impedance Measurements," *Corrosion*, Vol. 38, 1982, pp. 478–485.

[34] Kasahara, K. and Kajiyama, F., "Role of Sulfate Reducing Bacteria in the Localized Corrosion of Buried Pipes," *Biologically Induced Corrosion*, National Association of Corrosion Engineers, Houston, TX, 1986, pp. 171–183.

[35] Kasahara, K. and Kajiyama, F., "Electrochemical Aspects of Microbiologically Influenced Corrosion on Buried Pipes," *Microbially Influenced Corrosion and Biodeterioration*, University of Tennessee, Knoxville, TN, 1991, pp. 2-33–2-37.

[36] King, R. A., Skerry, B. S., Moore, D. C. A., Stott, J. F. D., and Dawson, J. L., "Corrosion Behavior of Ductile and Grey Iron Pipes in Environments Containing Sulphate-Reducing Bacteria," *Biologically Induced Corrosion*, National Association of Corrosion Engineers, Houston, TX, 1986, pp. 83–91.

[37] Moosavi, A. N., Dawson, J. L., and King, R. A., "The Effect of Sulfphate-Reducing Bacteria on the Corrosion of Concrete," *Biologically Induced Corrosion*, National Association of Corrosion Engineers, Houston, TX, 1986, pp. 291–308.

[38] Mansfeld, F., Shih, H., Postyn, A., Devinny, J., Islander, R., and Chen, C. L., "Corrosion Monitoring and Control in Concrete Sewer Pipes," *Corrosion/90*, Paper No. 113, National Association of Corrosion Engineers, Houston, TX, 1990.

[39] Mansfeld, F., Shih, H., Postyn, A., Devinny, J., Islander, R., and Chen, C. L., "Corrosion Monitoring and Control in Concrete Sewer Pipes," *Corrosion*, Vol. 47, 1991, pp. 369–375.

[40] Mansfeld, F., Tsai, C. H., Shih, H., Little, B., Ray, R., and Wagner, P., "Results of Exposure of Stainless Steels and Titanium to Natural Seawater," *Corrosion/90*, Paper No. 109, National Association of Corrosion Engineers, Houston, TX, 1990.

[41] Mansfeld, F., Liu, G., Tsai, C. H., Shih, H., and Little, B., "Evaluation of Polarization Curves for Copper Alloys Exposed to Natural and Artifical Seawater," *Corrosion/92*, Paper No. 213, National Association of Corrosion Engineers, Houston, TX, 1992.

[42] Ferrante, V. and Feron, D., "Microbially Influenced Corrosion of Steels Containing Molybdenum and Chromium: A Biological and Electrochemical Study," *Microbially Influenced Corrosion and Biodeterioration*, University of Tennessee, Knoxville, TN, 1991, pp. 3-55–3-63.

[43] Jones, J., Walch, M., and Mansfeld, F., "Microbial and Electrochemical Studies of Coated Steel Exposed to Mixed Microbial Communities," *Corrosion/91*, Paper No. 108, National Association of Corrosion Engineer, Houston, TX, 1991.

[44] Iverson, W. P., "Transient Voltage Changes Produced in Corroding Metals and Alloys," *Journal of the Electrochemical Society*, Vol. 115, 1968, pp. 617–618.

[45] Iverson, W. P., Olson, G. J., and Heverly, L. F., "The Role of Phosphorous and Hydrogen Sulfide in the Anaerobic Corrosion of Iron and the Possible Detection of This Corrosion by an Electro-

chemical Noise Technique," *Biologically Induced Corrosion,* National Association of Corrosion Engineers, Houston, TX, 1986, pp. 154–161.

[46] Nivens, D. E., Chambers, J. Q., and White, D. C., "Non-Destructive Monitoring of Microbial Biofilms at Solid-Liquid Interface Using On-Line Devices," *Microbially Influenced Corrosion and Biodeterioration,* University of Tennessee, Knoxville, TN, 1991, pp. 5-47–5-56.

[47] Geesey, G. G. and Bremer, P. J., "Application of Fourier Transform Infrared Spectrometry to Studies of Copper Corrosion Under Bacterial Biofilms," *Marine Technology Society Journal,* Vol. 24, 1990, pp. 36–43.

[48] Jolley, J. G., Geesey, G. G., Hankins, M. R., Wright, R. B., and Wichlacz, P. L., "In Situ, Real-Time FR-IR/CIR/ATR Study of the Biocorrosion of Copper by Gum Arabic, Alginic Acid, Bacterial Culture Supernatant and *Pseudomonas atlantica* Exopolymer," *Journal of Applied Spectroscopy,* Vol. 43, 1989, pp. 1062–1067.

[49] Lewandowski, Z., "Chemistry Near Microbially Colonized Surfaces," in *Biofouling/Biocorrosion in Industrial Water Systems,* G. G. Geesey, Z. Lewandowski and H.-C. Flemming, Eds., Lewis Publishers, Inc., Chelsea, MI, in press.

[50] Van Houdt, P., Lewandowski, Z., and Little, B., "Iridium Oxide pH Microelectrode," *Biotechnology and Bioengineering,* Vol. 40, 1992, pp. 601–608.

[51] Lewandowski, Z., Walser, G., and Characklis, W. G., "Reaction Kinetics in Biofilms," *Biotechnology and Bioengineering,* Vol. 38, No. 8, 1991, pp. 877–882.

[52] Lewandowski, Z., Altobelli, S. A., Majors, P. D., and Fukushima, E., "NMR Imaging of Hydrodynamics Near Microbially Colonized Surface," *Water Science and Technology,* Vol. 26, No. 3–4, 1992, pp. 577–584.

[53] Muellar, R. F., Characklis, W. G., Jones, W. L., and Sears, J. T., "Characterization of Initial Events in Bacterial Surface Colonization by Two Pseudomonas Species Using Image Analysis," *Biotechnology and Bioengineering,* Vol. 39, 1992, pp. 1161–1170.

[54] Little, B., Wagner, P., Ray, R., Pope, R., and Scheetz, R., "Biofilms: An ESEM Evaluation of Artifacts Introduced during SEM Preparation," *Journal of Industrial Microbiology,* Vol. 8, 1991, pp. 213–222.

[55] Baak, F. B., Thunnissen, J. M., Oudejans, C. B. M., and Schipper, N. W., "Potential Clinical Uses of Laser Scan Microscopy," *Applied Optics,* Vol. 26, 1987, pp. 3413–3416.

[56] Bremer, P. J., Geesey, G. G., and Drake, B., "Atomic Force Microscopy Examination of the Topography of a Hydrated Bacterial Biofilm on a Copper Surface," *Current Microbiology,* Vol. 24, 1992, pp. 223–230.

[57] deGouvernain, M., "Sulfiding of Copper and Iron by a Prolonged Stay in the Thermal Spring at Bourbon l'Archambault," *Comptes Rendus Hebdomadaires des Seances de l'Academie des Sciences,* Vol. 80, 1875, p. 1297.

[58] Baas-Becking, G. M. and Moore, D., "Biogenic Sulfides," *Economic Geology,* Vol. 56, 1961, p. 259.

[59] McNeil, M. B., Jones, J. M., and Little, B. J., "Production of Sulfide Minerals by Sulfate Reducing Bacteria During Microbiologically Influenced Corrosion of Copper," *Corrosion,* Vol. 47, No. 9, 1991, pp. 674–677.

[60] Little, B., Wagner, P., and Jones-Meehan, J., "Sulfur Isotope Fractionation by Sulfate-Reducing Bacteria in Corrosion Products," *Biofouling,* Vol. 6, 1993, pp. 279–288.

DISCUSSION

Tom Jack[1] *(written discussion)*—I was interested by one subject that you did not mention but which is probably going to be very important: kinetics of transport phenomena in biofilms. Could you comment on the state of the art?

B. Little and P. Wagner (authors' closure)—Techniques for determining biofilm reaction kinetics and the related diffusion coefficients depend on two types of testing: (1) chemical analyses of bulk water and (2) measurements inside the biofilm using microsensors. Le-

[1] NRTC, Calgary, Ab, Canada.

wandowski et al. developed a microtechnique that allows evaluation of diffusion-controlled reactions within biofilms. They presented an algorithm and instrumentation for measuring respiration reaction kinetics in biofilms and simultaneously measured dissolved oxygen and optical density through a biofilm. The biofilm diffusion coefficient for dissolved oxygen, the dissolved oxygen flux through the biofilm surface and the half velocity coefficient were calculated. The procedure is general and can be used for organic compounds or dissolved gases for which a concentration profile across a biofilm can be measured. See "Reaction Kinetics in Biofilms" by Z. Lewandowski, G. Walser and W. Characklis in *Biotechnology and Bioengineering*, Vol. 38, 1991, pp. 877–882.

Electrochemical Methods

Alex M. Brennenstuhl[1] *and Tracey S. Gendron*[2]

The Use of Field Tests and Electrochemical Noise to Define Conditions for Accelerated Microbiologically Influenced Corrosion (MIC) Testing

REFERENCE: Brennenstuhl, A. M. and Gendron, T. S., **"The Use of Field Tests and Electrochemical Noise to Define Conditions for Accelerated Microbiologically Influenced Corrosion (MIC) Testing,"** *Microbiologically Influenced Corrosion Testing, ASTM STP 1232,* Jeffery R. Kearns and Brenda J. Little, Eds., American Society for Testing and Materials, Philadelphia, 1994, pp. 15–27.

ABSTRACT: The problem associated with the development of an accelerated test for assessing the susceptibility of materials to microbiologically influenced corrosion (MIC) is an uncommonly difficult one. The usual methods of accelerating corrosion such as increasing the temperature and concentration of aggressive species cannot be used. Both these factors have to be maintained within relatively tight limits, otherwise unacceptable changes in the biology of the system will result. Conventional, anodic polarization techniques can produce misleading information because the very high fields produced at the metal surface during polarization are incompatible with the maintenance of viable microorganisms. Other methods of acceleration and detection must therefore be sought.

A combination of failure analyses, laboratory studies, and field simulations has been useful to determine the mechanism of corrosion of Ontario Hydro's freshwater cooled heat exchangers (HXs) and to identify the most detrimental operating conditions. During field simulations of the worst conditions, electrochemical noise monitoring has identified a reproducible response that could be an MIC signature. This signature may be used to verify the relevance of proposed accelerated MIC tests to field operation.

This paper describes the methods and results of field experiments using electrochemical noise monitoring and their implications for accelerated MIC testing.

KEYWORDS: electrochemical noise, sulphate-reducing bacteria, hypochlorination, stagnation, hydrogen sulphide oxidation

The advantage of using field "test rigs" over experimentation in the laboratory is a better simulation of the system under study. Therefore, the data generated are more directly applicable to that system. This is particularly true when complex biological factors are part of the operating environment. However, field testing in isolation has three main limitations:

(1) The degradation processes occur at the same rate as they do in the system under study, that is, there is no acceleration of the processes of the degradation. Therefore, obtaining predictive information is impossible unless testing is commenced prior to commissioning of the system.

[1] Research scientist, Ontario Hydro, Metallurgical Research Department, 800 Kipling Avenue, Toronto, Ontario, Canada, M8Z 5S4.

[2] Research scientist, Chalk River Laboratories, System Chemistry and Corrosion, Chalk River, Ontario, Canada, K0J 1J0.

(2) Unavoidable natural fluctuations in the environment can lead to confounded results. This is often the case when testing is influenced by seasonal changes.
(3) Complex environments and operating conditions can make it difficult to obtain mechanistic information by isolating the effects of individual parameters.

In order to overcome these deficiencies, Ontario Hydro and Atomic Energy of Canada (AEC) employed a combination of failure analyses, field testing, and laboratory tests to determine the degradation mechanism of the stainless-steel and nickel-alloy tubing and piping employed in some of Ontario Hydro's CANDU reactors. Moderator heat exchangers (HXs) shutdown coolers and fuel bay HXs are the systems most prone to localized corrosion. Electrochemical noise monitoring was used in field testing to help verify a proposed degradation mechanism. In the process, the most detrimental operating condition was identified. In addition, an electrochemical response was recorded that may be useful as an MIC signature and as the basis of an accelerated laboratory test.

Systems Under Study

Ontario Hydro's CANDU reactors employ untreated lake water for cooling its stainless steel and nickel alloy HXs. This lake water is conveyed to some of these HX systems through stainless-steel piping. The HXs and piping are prone to underdeposit corrosion. Failure analysis, field simulations, and laboratory studies have indicated that microorganisms play a role in the degradation processes [*1*]. Aerobic slime-forming bacteria (for example, pseudomonas) are first to colonize the surface of the tubes. They secrete an extra-cellular polymeric substance that leads to the stabilization of sediments on the tube surface. By excluding oxygen beneath the fouled layer, aerobic bacteria provide anoxic habitats for anaerobic bacteria such as methanogenic and sulphate-reducing bacteria (SRB). Methanogenic bacteria produce CO_2 as a metabolic product that drives calcite deposition. SRB generate a local aggressive environment by metabolizing sulphate to sulphide [*2*]. The resulting fouled layer concentrates potentially aggressive species such as chloride and sulphide that lead to occluded regions where local acidification can take place.

In regions where the fouling has become detached or where high-flow rates have prevented biofilm attachment, oxygen in the lake water has access to the tubing. The role of oxygen is thought to be threefold. First, oxygen acts to increase the corrosion potential of the tubing provided activating species such as chloride and thiosulphate, or both, are present. Second, reduction of oxygen is the cathodic reaction that drives metal dissolution within the pits. Finally, it is believed that oxygen reacts with sulphide to produce thiosulphate, which can be a very aggressive pit activator for these materials.

Field Monitoring Technique

Technique Description

The electrochemical-noise technique was employed to monitor electrochemical-corrosion transients during this study. Electrochemical noise is the generic term used to describe the low-amplitude, low-frequency random fluctuations of current and potential observed in many electrochemical corrosion processes; the current and potential are related to anodic metal dissolution and cathodic processes, or both. Mechanistic information can be obtained by analyses of the individual transients making up the noise signal [*3*]. The detailed nature of the transient is the result of specific events associated with corrosion.

The electrochemical noise technique employed during this study uses a three-electrode configuration comprised of nominally-identical electrodes, one of which is a pseudo-refer-

ence. With this arrangement, the potential and coupling current fluctuate to the positive and negative of a mean value due to net polarity of the electrodes switching from being anodic to cathodic.

Sample Description

The electrode configuration was comprised of three 25-mm diameter AISI Type 304L stainless steel discs embedded in epoxy resin. Electrical leads were connected to each disc so that pairs of electrodes could be coupled. One of the electrodes was a common electrode; the potential and current between it and the other two electrodes were measured with the CAPCIS-MARCH digital electrochemical noise interrogation system. The surface finish of the samples was No. 20 grit, this is similar to that which might be present on an as-received pipe or HX tube.

Equipment Settings and Outputs

The electrochemical equipment was programmed to interrogate the test electrodes at 4s intervals during the monitoring period. Each data file was comprised of 1024 points and took 4096 s to acquire. This was found to be the minimum time necessary to characterize the electrochemical noise signatures produced by the environmental changes imposed on the system during the study. The equipment was initially allowed to settle for 30 min before monitoring.

The following information was obtained from each data set:

(1) corrosion potential (pseudo-reference),
(2) electrochemical potential noise (EPN),
(3) RMS coupling current, and
(4) electrochemical current noise (ECN).

Specific features of interest in the time domain plot can be extracted for local statistical analyses.

Testing consisted of exposing samples to: (a) untreated lake Erie water and (b) water that had been continuously treated with 0.5 ppm residual chlorine. The water used for these experiments was drawn directly from the lake. Poly-vinyl chloride spool pieces (test vessels) (see Fig. 1), were used to contain the test samples. The test coupons were inserted in the spool pieces in July 1991 and exposed to water flowing at a rate of 0.7 m/s^{-1}. Both samples were exposed initially to untreated water for a period of two weeks. Slight crevice attack and pitting was evident on the surface of both samples at the end of this initial flowing untreated water phase of the experiment. Sodium hypochlorite was then added to one of the spool pieces. A thick layer of fouling comprised of lake sediment and organic material, including microorganisms, quickly became established on the surface of the sample exposed to untreated water. The sample subjected to hypochlorination treatment remained free of fouling throughout the exposure. After a stagnation period of 30 days, electrochemical data was obtained from both the untreated and sterile samples. This was started prior to allowing naturally-oxygenated lake water to enter the spool piece to obtain baseline data for the stagnant conditions. During this pre-exposure period, aliquotes of water were removed from each spool piece for SRB examination.

The stagnant water contained in the spool piece was at a temperature of 16°C. After the stagnant baseline signal acquisition period, oxygenated lake water at 2°C was then allowed to make contact with the samples by opening the inlet valve; the outlet remained closed. The inlet valve was opened approximately 10 min into the monitoring period.

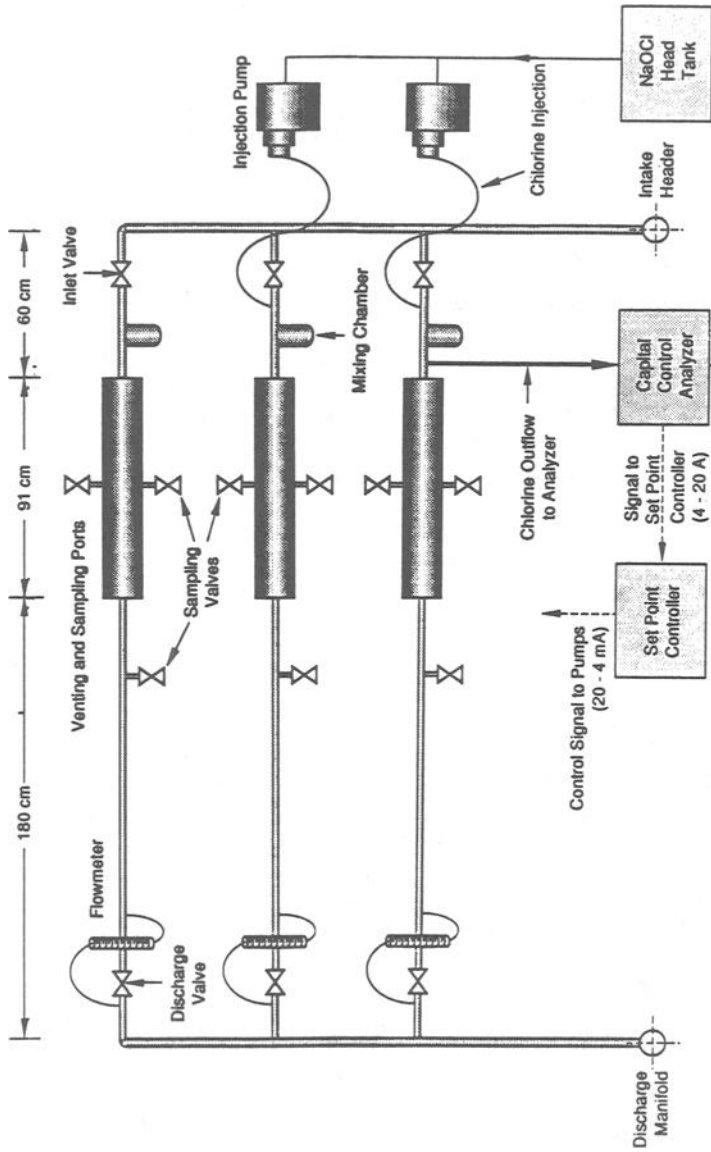

FIG. 1—*Experimental setup.*

Opening the inlet valve represents the worst case condition; oxygen enters the cell by diffusion. Flow is undesirable because it leads to the rapid removal of metabolites that are thought to have a major role in accelerated corrosion.

Analysis of Water Samples

Water samples were cultured in Postgate C medium. Serial dilution was used to establish the number of bacteria present.

Results

Untreated Sample

Figure 2 displays the results of the monitoring period for stagnant conditions followed by exposure to oxygenated lake water. The initial part of the plot, Region [I], represents the stagnant condition.

Figure 3 is a subset of Fig. 2 and is the first 10 min of the time domain plot (that is, Region [I]). The mean values for this part of the plot are given in Table 1. All electrochemical outputs are low.

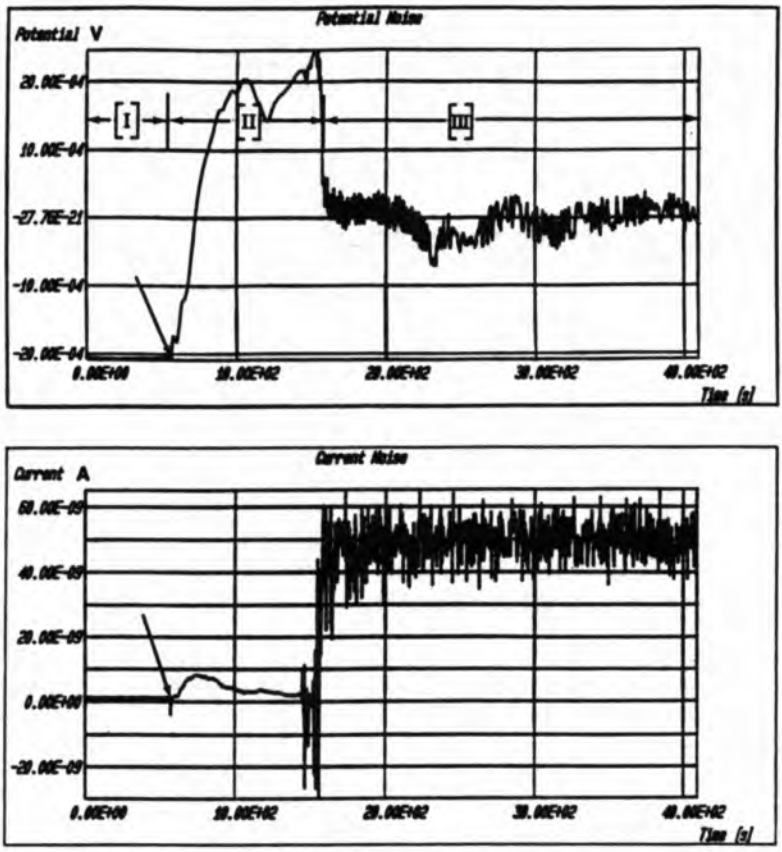

FIG. 2—*Electrochemical results data for the untreated sample. The arrow indicates when the inlet valve was opened.*

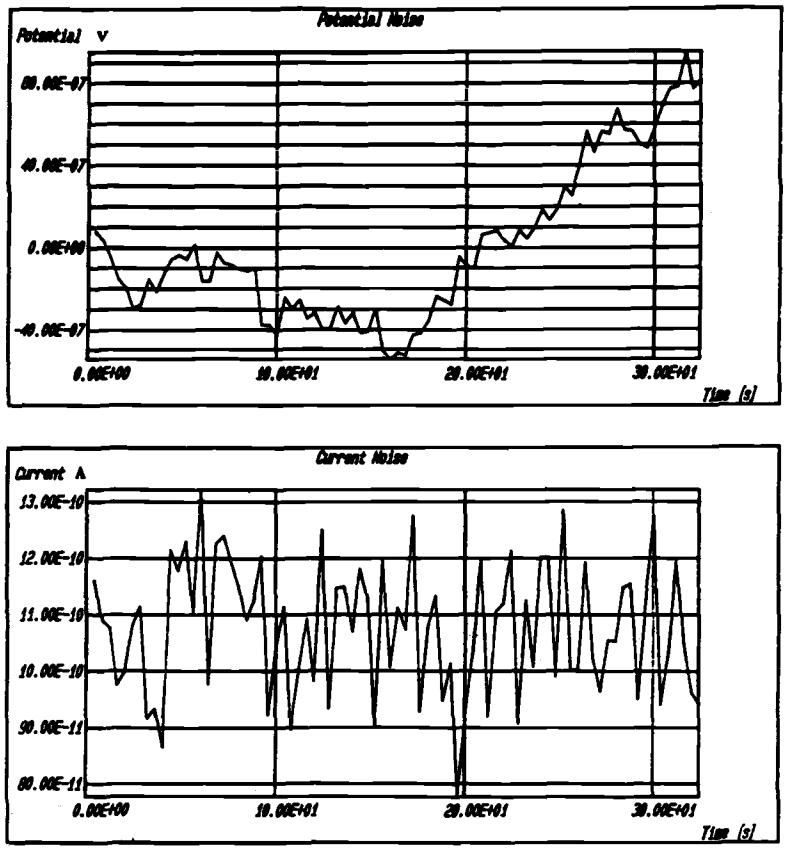

FIG. 3—*Detail of the electrochemical noise prior to opening the inlet valve (Region [I] and Fig. 2).*

When the inlet valve was opened, an increase in potential immediately occurred. The potential reached a maximum, decayed slightly then increased again, reached another maximum and then decayed sharply. This reduction in potential was followed by a period of relative stability. However, during this period of "stability" the potential displayed high-frequency fluctuations that appear to decrease in frequency with time. The current noise plot contrasts with the potential noise output. Initially, a decrease in current was observed; this was followed by a rapid recovery. A slight increase then occurred followed by a decay to a value similar to that observed before the valve was opened. Approximately 12 min

TABLE 1—*Summary of electrochemical outputs for untreated (Regions [I-III]) and the samples.*

	Untreated			
	Region [I]	Region [II]	Region [III]	Sterile
Potential/mV	−14.3	−12.21	−12.21	0.02
EPN/mV	0.0038	1.45	0.23	0.005
Coupling Current/nA	1.1	55.3	50.0	20.07
ECN/nA	0.12	2.6	59.4	0.7

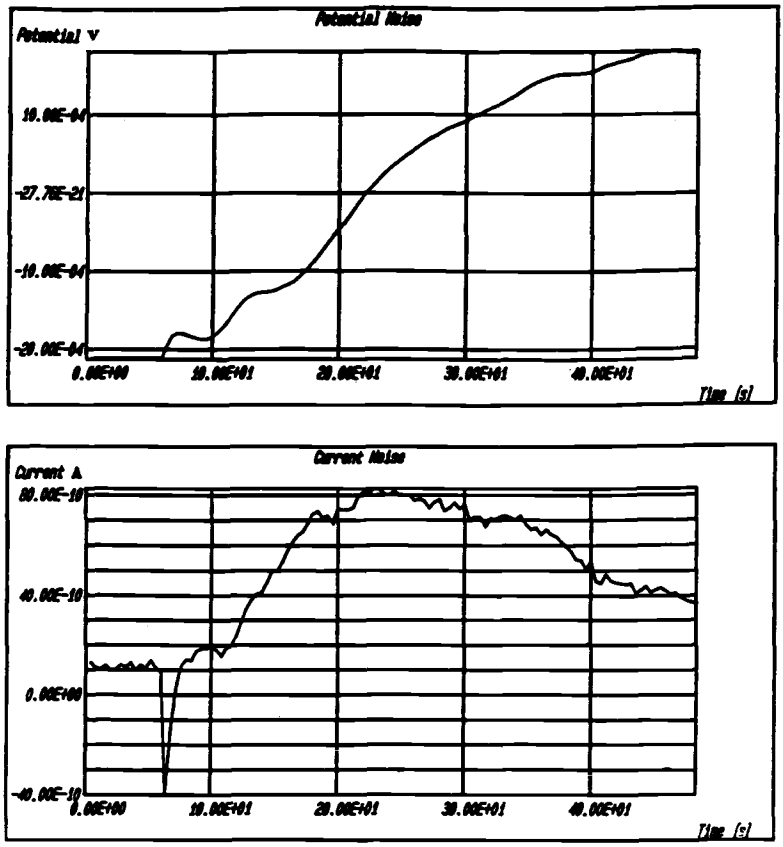

FIG. 4—*Region [II], showing detail of the transition in Fig. 2.*

after the inlet valve was opened, a sharp increase in the current occurred. This increase coincided with the second drop in potential. The current then reached a relatively high value, and, like the potential signal, exhibited large fluctuations in the current noise. Figure 4 shows detail of the transition region (Region [II] on Fig. 2). Table 1 gives the summary statistics for Region [II].

Figure 5 illustrates the electrochemical noise outputs for Region [III] in Fig. 2. The arrow on the potential plot shows an area where propagation appears to have occurred before repassivation. Summary statistics for this part of the plot are given in Table 1.

Both potential and current gradually decay with time. It took approximately 2 h to reach a level slightly above that observed before the inlet valve was opened.

The results of the SRB analysis of water removed from the spool piece indicated 10^6 cell/mL. A strong smell of hydrogen sulphide was also noted during the removal of a sample from the spool piece.

Sterile Sample

A time domain plot for the sterile sample can be seen in Fig. 6. As was the case with the untreated lake water sample, the inlet valve was opened 10 min into the monitoring cycle.

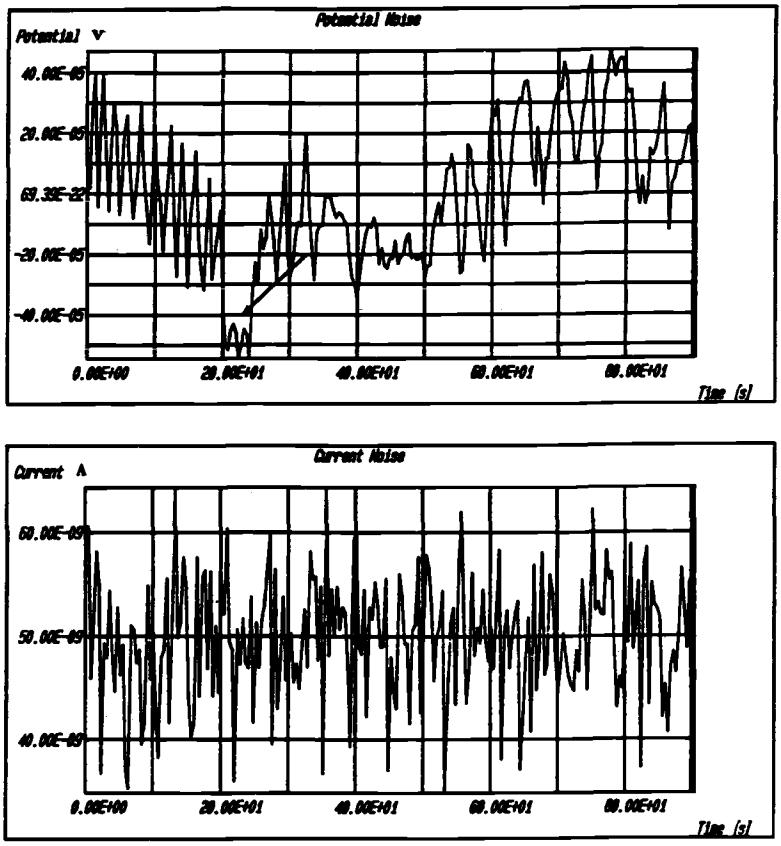

FIG. 5—*Region [III], showing detail of the metastable events in Fig. 2.*

No readily discernible perturbation of the potential or current signal was evident when this was done. However, on close inspection it might be argued that the potential decreased when the valve was opened. The signal drift prior to valve opening makes it difficult to make a definitive statement regarding this. After approximately 30 min, one high amplitude noise transient occurred on both the potential noise and current noise plots. Table 1 gives the summary statistics for this plot.

SRB analysis of water removed from the sterile spool piece revealed 10^1 cells/mL.

Both of these experiments have been repeated several times and each time a similar response has been observed. Further, the transients observed for the sample exposed to untreated lake water also occur after shorter times of stagnation, but the magnitude of change was not as great.

Discussion

Important Factors

The largest increase in electrochemical activity was observed when oxygen was allowed to enter the system after a period of stagnation. Attack, which was inferred by an increase in coupling current, was greatest when the flow rate was zero, that is, when oxygen was

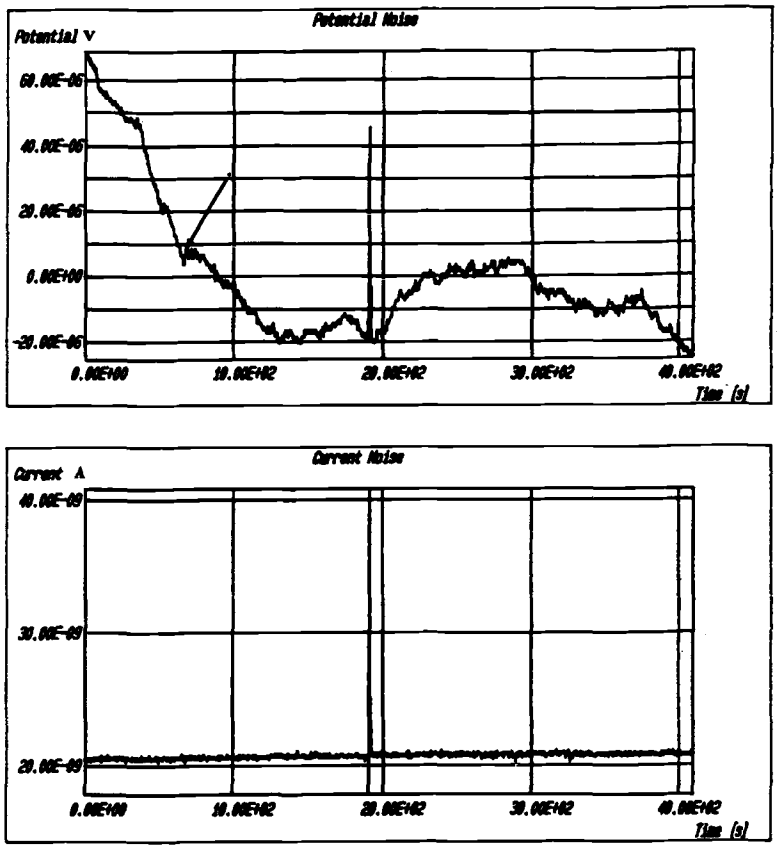

FIG. 6—*Electrochemical noise data for the "sterile" sample. The arrow indicates when the inlet valve was opened.*

allowed to diffuse into the stagnant water. This condition might occur in an operating plant when equipment valves are opened but before water-pump activation is initiated.

Untreated Water Exposure

Initially, potential appears to be very sensitive to oxygen ingress, and potential increases almost immediately. This was taken to infer that oxygen was leading to passive film thickening and repair, or both.

The coupling current and ECN observations contrasted with the potential and EPN results. Apart from a very short initial transient, very little activity was observed until approximately 12 min into the oxygenated-water exposure. Clearly, the changes in the environment, which lead to an increase in ECN, are relatively sluggish.

Based on the water chemistry, which has a low Cl^- ion concentration relative to other anions, it is likely that microorganisms have an indirect role in corrosion. The $S_2O_3^{2-}$ mechanism proposed by Newman et al. and Roberge [*4–6*], is likely to be applicable in this specific case. This mechanism involves the oxidation of biogenic H_2S to $S_2O_3^{2-}$. Thiosulphate is a source of sulphur. Sulphur inhibits repassivation by absorbing on the metal surface. The

relatively slow rate of oxidation of H_2S to $S_2O_3^{2-}$ is a possible explanation for the delay in activity when fresh water is allowed to enter the system.

The activity reported here is associated with testing during the winter months and was relatively short lived; both coupling current and electrochemical noise eventually decayed to a lower value. This phenomenon might be explained by the following:

(1) The ions responsible for oxide breakdown (that is, $S_2O_3^{2-}$) become depleted with time. If this metastable pitting process is catalyzed by sulphur, a change in the optimum $SO_4^{2-}/S_2O_3^{2-}$ ratio of 10 to 30 for pitting would lead to a decrease in corrosion.
(2) The reduction in temperature of the stagnant water contained in the vessel (at 16°C), due to contact with the oxygenated lake water at 2°C. This would result in a decrease in the rates of most processes involved in the localized corrosion process.
(3) A combination of the above.

It should be noted that exposure to 12°C lake water led to a large increase in electrochemical noise. This was followed by an increase in coupling current of over two order of magnitude, suggesting pit growth. Temperature appears to be an important factor.

We would like to point out that in our experience with electrochemical noise monitoring we have not found signal patterns like those seen during this investigation in any of the other systems that we have examined. This leads us to believe that it is possibly unique to the indirect MIC mechanism described.

Sterile Water Exposure

The virtual absence of activity, as shown by the electrochemical outputs of the sample exposed to sterile water, highlights the importance of bacteria and deposits.

Laboratory Test Design

The data generated during this investigation suggested that the worst operating condition in terms of accelerating corrosion is one that involves shutdown and stagnation followed by exposure to nonflowing oxygenated water. Based on comparison between the sterile and untreated water results it would appear that bacteria and deposits are essential for accelerated attack. When designing a laboratory test, these factors must therefore be taken into account. The stagnation period also appears to be important. A stagnation period of 2 to 4 weeks results in the greatest extent of activity. Increasing the temperature to a level that leads to maximum SRB growth should decrease the stagnation period required for accelerated attack. The effect of temperature, however, is better assessed in the laboratory where control is easier.

An accelerated MIC test must include a method for allowing oxygen to enter the system. The rate at which oxygen is allowed to enter the system to maximize corrosion has yet to be determined. The results of our experiments indicate that the greatest acceleration occurs when the supply of oxygen is diffusion-controlled. Flowing oxygenated water most likely leads to a more rapid departure from the optimum $SO_4^{2-}/S_2O_3^{2-}$ ratio of 10 to 30. Also, high flow rates leads to H_2S being purged from the system.

An accelerated laboratory test may therefore be comprised of a scaled-down field system in which parameters such as temperature and the oxygen ingress rate are carefully controlled to obtain maximum acceleration. Natural water and deposits should be employed to simulate

the physical, chemical, and biological conditions at the metal surface in the field. The test would involve cycling between stagnant and oxygenated conditions.

An alternative approach might employ culture medium instead of lake water. Culture-medium tests have advantages of a defined chemistry control and higher SRB growth rates. Lake water and natural deposits are often quite variable in terms of microorganisms and chemistry due to seasonal variations in the natural environment; this may lead to high scatter in the test data. However, the disadvantages of culture medium tests are (1) a further departure from the natural environment and (2) the introduction of species (constituents of the culture medium) that inhibit corrosion.

Another possibility is a test that does not employ bacteria. If thiosulphate is the real cause of the accelerated attack, and this would have to be verified by chemical analysis during testing, a test comprised of exposing the sample to anaerobic containing water with hydrogen sulphide added may approximate the crucial accelerating factors present under field conditions. Start-up would be simulated by allowing oxygen to enter the system. The advantage with this type of test is that it would not be necessary to wait for hydrogen sulphide to build-up as a result of microbial activity, and the variable concentration of H_2S caused by medium depletion would be eliminated.

Ultimately, the selection of conditions will depend on how near the electrochemical-noise signature is to those obtained in the natural environment.

Conclusions

(1) Field testing using ECN monitoring has been very useful for studying MIC of HX tubing in freshwater. Specifically, the preliminary results are:

   (a) the clearly demonstrated importance of bacterial activity on the corrosion of this system,
   (b) identification of specific operating conditions most likely to promote corrosion, and
   (c) produced reproducible electrochemical response that may be an MIC signature.

(2) Three accelerated MIC tests have been tentatively proposed, which reproduce the worst operating conditions artificially, immediately, and in the absence of other confounding factors. The electrochemical signature from field testing can be used to verify the relevance of the accelerated test to the field.

References

[1] Brennenstuhl, A. M., Gendron, T. S., and Doherty, P. E., "Fouling and Corrosion of Freshwater Heat Exchangers," 5th International Symposium on Environmental Degradation of Materials in Nuclear Power Systems—Water Reactors, Monterey, CA, 1991.

[2] Brennenstuhl, A. M., Gendron, T. S., and Cleland, B., "Mechanisms of Underdeposit Corrosion in Freshwater Cooled Austenitic Alloy Heat Exchangers," International Conference on Advances in Corrosion and Protection, University of Manchester Institute of Science and Technology (UMIST), Manchester, United Kingdom, June 1992.

[3] Eden, D. A., Eden, D. A., Hladky, K., John, D. G., and Dawson, J. L., CORROSION/86, Paper 274, National Association of Corrosion Engineers, Houston, TX, 1986.

[4] Newman, R. C., Wong, W. P., and Garner, A., "A Mechanism of Microbial Pitting in Stainless Steel," *Corrosion,* Vol. 42, No. 8, 1986, p. 489.

[5] Garner, A. and Newman, R. C., CORROSION/91 Paper 186, National Association of Corrosion Engineers, Cincinnati, 1991.

[6] Roberge, R., "Effects of the Nickel Content in the Pitting of Stainless Steel in Low Chloride and Thiosulphate Solutions," *Corrosion,* Vol. 44, No. 5, 1988, p. 274.

DISCUSSION

R. Walter[1] (*written discussion*)—Several presenters made comments about the presence and absence of bacteria in their studies. Alex Brennenstuhl mentioned that the experiments with 0.5 ppm Cl were sterile and that they could not culture sulphate-reducing bacteria (SRB). What culture medium was used and what was the detection level? I think we all need to be very careful in making these types of comments. I've found bacteria that can tolerate levels of chlorine as high as 1 ppm. Also, we all know that under these adverse conditions (biocide presence and/or lack of nutrients), the microorganisms will selectively congregate on surfaces, and sampling the bulk water will lead us to conclude that none are present.

A. M. Brennenstuhl and T. S. Gendron (*authors' closure*)—In our study, we reported that low (10^{-1} cells/liter) were detected when the lake water was treated with hypochlorite to a residual level of 0.5 ppm. The culture medium employed was Postage's B. During this study, we were not concerned with the effect of sodium chloride on SRB.

G. Licina[2] (*written discussion*)—In your test system, a stagnant leg is truly stagnant. In service, most applications that are called stagnant actually have some refreshment, transport of nutrients, and so forth, similar to your test conditions, while the inlet valve is open and the outlet valve is closed. How do your test results relate to dead legs, tanks, and so forth, in a plant?

A. M. Brennenstuhl and T. S. Gendron (*authors' closure*)—Our test system is truly stagnant, the inlet and outlet valves were checked before the experimental runs were started. We are aware that eventually the nutrients contained in the test vessel would be consumed and SRB activity would diminish. This would limit the quantity of hydrogen sulphide produced and available for oxidation on start-up. If the hydrogen sulphide can escape from the system, attack will not occur when oxygen is reintroduced into the water. We agree that the worst case would be one in which nutrients are continuously available to support SRB growth together with sufficient oxygen to promote the processes that lead to corrosion. Regarding, dead legs, tanks, and so forth, at present our results only relate to them if they are subjected to the sequence of events similar to those employed in our tests. Further work aimed at assessing the effects of oxygen concentration, sediment composition, and so forth, may yield information that can be used to predict the rate of corrosion in these parts of the system.

A. Stein[3] (*written discussion*)—(1) The author concludes that $S_2O_3^{2-}$ is responsible for corrosion. Was the oxyanion of sulfur detected or any other intermediate oxidation states of sulfur detected?

(2) The paper as presented, does not appear to conclusively demonstrate that the fluctuations in electrochemical noise are due to bacteria. Does the author have data to prove the noise is due to bacteria?

A. M. Brennenstuhl and T. S. Gendron (*authors' closure*)—(1) Corrosion activated by $S_2O_3^{2-}$ is based on the work of Newman (Refs *4* and *5*) and the composition of deposits and corrosion products found on our HXs and pipes. $S_2O_3^{2-}$ has not been detected because we

[1] Dow Chemical, Lawkin Laboratories, Midland, MI 48674.
[2] Structural Integrity Associates, 3150 Almaden Expressway, Suite 145, San Jose, CA 95118.
[3] Stone & Webster Engineering, 245 Summit Street, Boston, MA 02210.

have not yet looked for it. Ideally, we would like to have done this; however, it was not felt that this was absolutely necessary as there is a vast amount of data in the literature on the formation sulphur species in sediments containing SRB. These data suggest that it is highly likely that $S_2O_3^{2-}$ will be present in our deposits.

(2) Every series of tests that we have run clearly indicates that when bacteria are present there is an increase in noise on start-up. Potential increases almost immediately, and there is always a delay before a rise in current is seen. Further, the shape of the time domain outputs are almost identical; we have only seen electrochemical outputs like these when SRB have been present. In the case of the "sterile" samples, sometimes an increase in potential was observed when the inlet valve was opened but the current noise always remains virtually unaffected.

Barbara J. Webster[1] *and Roger C. Newman*[2]

Producing Rapid Sulfate-Reducing Bacteria (SRB)-Influenced Corrosion in the Laboratory

REFERENCE: Webster, B. J. and Newman, R. C., **"Producing Rapid Sulfate-Reducing Bacteria (SRB)-Influenced Corrosion in the Laboratory,"** *Microbiologically Influenced Corrosion Testing, ASTM STP 1232,* Jeffery R. Kearns and Brenda J. Little, Eds., American Society for Testing and Materials, Philadelphia, 1994, pp. 28–41.

ABSTRACT: Rapid corrosion influenced by sulfate-reducing bacteria (SRB) of a creviced stainless steel (Fe-15Cr-10Ni) has been produced potentiostatically at −250 mV (SCE) using specially designed media. SRB-influenced corrosion was also produced using a two-compartment cell where a small anode was connected through a zero resistance ammeter (ZRA) to a large-aerated cathode. By conducting potentiostatic and ZRA-coupling tests in a number of media, it was found that the corrosion process was influenced by anionic ratios, that is, the ratio of chloride-ion concentration to total-other-anion concentration.

In addition, studies of a convection-free stainless-steel electrode in a 'Microcell' assembly were conducted to investigate the stability of SRB-influenced corrosion in a bulk-aerated environment. These results suggest corrosion of stainless steel could occur in an anaerobic, convection-free microenvironment with SRB activity, by using oxygen reduction as the cathodic reaction elsewhere on the material.

KEYWORDS: sulfate-reducing bacteria (SRB), corrosion, stainless steel, mechanisms, test methods

Microbiologically influenced corrosion (MIC) failures of stainless steel have been reported in the literature and sulfate-reducing bacteria (SRB) have been implicated as either the cause or a contributing factor [*1–5*]. The most surprising failures occur in the lower grades of stainless steel in potable waters [*1–5*]. Laboratory attempts to simulate the rapid SRB-influenced corrosion that occurs in the field have either required polarization to unrealistic potentials (for example, >1 V versus SCE) [*6*] or have produced insignificant rates of corrosion [*7*]. These findings suggest that the laboratory tests were less aggressive than conditions under which the failures occur in the field. Without having a reliable laboratory method for producing SRB-influenced corrosion, the means for optimizing methods of detecting and monitoring it do not exist.

When investigating SRB-influenced corrosion, a number of documented findings regarding inorganic corrosion of stainless steel should be considered. Sulfur species, such as H_2S, produced by SRB, are known to activate corrosion of stainless steel. However, in order to activate significant rates of corrosion in an anaerobic environment, the corrosion has to be initiated at a relatively oxidizing potential and there has to be a cathodic reaction capable

[1] Research scientist, New Zealand Institute for Industrial Research and Development, P.O. Box 31-310, Lower Hutt, New Zealand.

[2] Reader, Corrosion and Protection Centre. UMIST, P.O. Box 88, Manchester, M60 1QD, United Kingdom.

of sustaining rapid corrosion. Consideration also needs to be given to the growth-medium composition. The medium contains anions regarded as inhibitors of stainless steel corrosion, for example, SO_4^{2-}, PO_4^{3-}. Literature suggests the concentration of these inhibiting anions relative to aggressive anions such as Cl^- will be important. These matters are discussed in more detail under subheadings below.

Corrosion of Stainless Steels in Inorganic Sulfurous Environments

Under inorganic near-neutral conditions, sulfide and other sulfur species are known to decrease both the pitting potential and repassivation potential of stainless steels [*8*]. These effects are believed to be due to the stabilizing effect that sulfur compounds have on the initiation and propagation of corrosion. Once a sulfur species is included in an actively-corroding site, it is believed to be adsorbed in the form of $S^{\delta-}_{ads}$ [*9,10*]. This species catalyses metal dissolution and hinders repassivation [*8,11*].

In sulfide-free, neutral environments, corrosion of stainless steel could only initiate by pitting at quite anodic potentials as no anodic current peak is evident on polarization curves. In neutral, anaerobic, sulfide-containing environments (such as SRB environments), however, a small anodic peak is evident [*12*] therefore, corrosion is possible at reducing potentials. Corrosion proceeding at reducing potentials in an anaerobic environment would have to be sustained using water reduction as the cathodic reaction, as no other reducible species are present. Water reduction could not sustain high rates of corrosion at neutral pH, therefore, corrosion rates would be expected to be insignificant. Furthermore, corrosion at reducing potentials in a neutral, anaerobic, sulfide-containing environment would not be localized.

Further evidence that supports the contention that rapid corrosion could not proceed in an anaerobic environment, is that all reported instances of inorganic stainless steel corrosion due to sulfur species occur at potentials more anodic than those that would prevail in an anaerobic SRB culture [*8,13–20*]. For example, Newman, et al. [*8*] conducted potentiodynamic scans of 304 stainless steel in 0.25 M NaCl solutions containing H_2S, KSCN, and $Na_2S_2O_3$ solutions (10^{-3}–10^{-1} M) and found that the pitting potentials were all above -250 mV versus SCE.

Obtaining SRB-influenced corrosion under oxidizing conditions poses some practical difficulties as SRB require anaerobic conditions for growth. It would require a locally anaerobic environment and a remote cathodic reaction. Alternatively, oxidizing conditions outside the site of microbial growth could permit formation of species such as polysulfides (or $S^0_{(aq)}$) and thiosulfate through oxidation of the H_2S. Like H_2S, these oxidized sulfur compounds are also indicated in the literature as causing corrosion of stainless steel [*8,13–20*].

Thiosulfate is one of the most corrosive sulfur species. It has a remarkable ability to catalyze pitting of Type 304 stainless steel in dilute solutions such as white water in newsprint paper machines [*13–17*]. Pitting occurs even in the absence of chloride, provided the ratio $[SO_4^{2-}]/[S_2O_3^{2-}]$ is in a certain range (about 10 to 30). Pitting has been obtained at thiosulfate concentrations as low as 1 ppm (10^{-5} M). As shown by Newman, et al., air-oxidized H_2S solutions could be an indirect mechanism of SRB pitting of stainless steels [*17*]. The aggressiveness of thiosulfate compared to sulfide arises, because like Cl^- and SO_4^{2-}, thiosulfate is attracted into the pit nuclei by electromigration. Sulfide, on the other hand, is uncharged at the acidic pH values near pits.

Polysulfides (H_2S_x) may be formed through air-oxidation of sulfide or through reaction of H_2S with elemental sulfur [*19,21*]. These or similar compounds at μM-concentration levels are believed to provide the cathodic reaction of stainless steel corrosion in sour gas environments, where pitting typically occurs at -300 to -350 mV versus SCE [*19,20*]. In this

environment, NaCl concentrations and temperatures are high (up to 20% and 200°C, respectively), CO_2 is present at many atmospheres pressure, and the pH may be as low as 3. As no free oxygen is present and hydrogen evolution is not thermodynamically possible at the pitting potential experienced in the sour-gas environment, it would appear that polysulfide (or $S^0_{(aq)}$) reduction is a feasible cathodic reaction.

Anionic Effects

Inorganic experiments have shown that some anions inhibit corrosion of stainless steels while others activate it. Chloride ions are aggressive to stainless steels. The pitting potential is reduced as the concentration of chloride increases [*22*]. Notably, a minimum chloride-ion concentration exists below which chloride does not cause pitting. Chloride is not the only aggressive anion. As discussed earlier, under certain conditions, sulfate can act as the 'aggressive' anion if thiosulfate is also present [*16*].

The effects of the aggressive anions are reduced by the presence of inhibiting anions, and microbial growth media contain several such anions. It has been shown that anions such as sulfate [*22*], hydroxide [*22,23*], phosphate [*24*], acetate [*24*], carbonate [*23,24*], and nitrate [*23*] inhibit pitting corrosion of stainless steel to varying extents. Many of these compounds inhibit corrosion by acting as buffers that restrict the pit solution from going acidic. At high concentrations, thiosulfate also inhibits corrosion through this buffering action, acting by disproportionating to the buffering bisulfite ion.

In this work, rapid SRB-influenced corrosion of a susceptible stainless steel has been produced. This required specialized test media and test methods. Guidance provided by the literature on inorganic corrosion of stainless steels allowed selection of experimental conditions. Some of the factors were selected based on the hypothesis that SRB-influenced corrosion of stainless steel is an H_2S-catalyzed dissolution process driven by remote reduction of oxygen or another suitable species. In addition, studies of the stability of the corrosion have been investigated using a convection-free Microcell electrode assembly.

Experimental

The cell assembly used for the experiments is shown in Fig. 1. Two 1 cm^2 Fe-15Cr-10Ni electrodes were exposed in the 2L 'anode' compartment. The Fe-15Cr-10Ni alloy simulates the composition of a chromium-depleted region around a δ-ferrite particle in Type 304 stainless steel weld metal. The electrodes were abraded to 600 grit and crevices of either masking lacquer or multicreviced washers were applied to the exposed surface. One electrode was potentiostatically polarized to −250 mV (versus SCE) and another was connected through a zero resistance ammeter (ZRA) to a large (40 cm^2) Type 304 stainless-steel cathode. The cathode was located in a separate 250 mL compartment, connected to the main body of the cell through an agar salt bridge. The 'cathode' compartment contained aerated 0.1 M NaCl and a saturated calomel reference electrode (SCE). Two platinum foil electrodes (1 cm^2) were also exposed in the 'anode' compartment. The tests usually lasted for a week following polarization of the electrodes, but in the event of significant corrosion, the test was terminated in less than a week.

The composition of the bacterial growth media used in the 'anode' compartment, along with descriptive names for each of the media tested, are listed in Table 1. The media differed in the sum of concentrations of nutrients and the concentration ratio of the nutrients to sodium chloride. Concentration ratios were estimated using conductivity measurements. The pH values of the media were adjusted to 7.2 with NaOH. The media contained no ferrous ions or reducing agents. Oxygen was removed from the media by purging with nitrogen

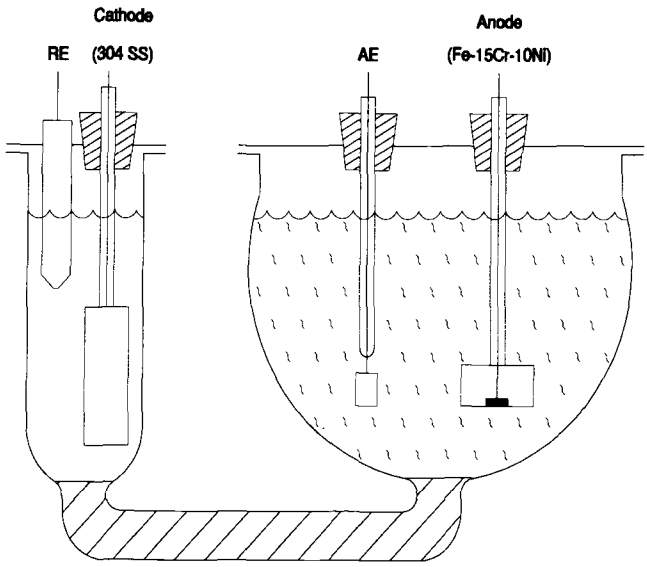

FIG. 1—*Outline of the two-compartment experimental cell.*

(>99.95% N_2) for 2 h before inoculating 3 mL of a 3-day-old subculture of *Desulfovibrio vulgaris*. SRB growth was monitored indirectly by measuring the sulfide concentration in solution using a potentiometric method [*25*]. Tests were conducted at 30°C, and generally, two tests were conducted in each medium. The exceptions were the chloride-rich medium and low-chloride medium in which four and one tests were conducted, respectively (see Table 2). To ensure that the starting conditions, with respect to sulfide concentration, were similar in the corrosion tests conducted, the electrodes were not polarized until the measured total H_2S concentration was at least 70% of the initial sulfate concentration of the medium.

Stability studies of propagating SRB-influenced corrosion of Fe-15Cr-10Ni were conducted using a specially-designed convection-free electrode assembly and the coupled-electrode ZRA technique. The 'Microcell' assembly used is shown in Fig. 2. As for the other ZRA tests, polarization of the electrode occurred when the total H_2S concentration in the bulk

TABLE 1—*Composition of the SRB-growth media.*

Composition, mmol · dm^{-3}	Medium Name				
	Chloride Rich	Chloride	Low Chloride	Undiluted	Dilute
$(NH_4)_2HPO_4$	1.1	1.1	1.1	3.8	0.2
$(NH_4)_2SO_4$	1.2	1.2	1.2	4.2	0.2
$CaSO_4$	2.1	2.1	2.1	7.4	0.4
$MgSO_4 \cdot 7H_2O$	2.3	2.3	2.3	8.1	0.5
Sodium lactate[a]	1.4	1.4	1.4	65.0	2.8[b]
Yeast extract[c]	290	290	290	1000	57.1
NaCl	100	20	4	100	20
Cl^-:Σ(all other anions)	**5:1**	**1:1**	**1:5**	**1.7:1**	**5:1**

[a] 70% solution (ml).
[b] 7% solution (ml).
[c] mg · dm^{-3}.

TABLE 2—*Results from ZRA tests.*

Medium	Cl^-:Σ(All Other Anions)	Crevice	Corrosion	I, μA	E, mV
Chloride-rich	5:1	castellated washer	+	40 → 80	−400
	5:1	castellated washer	+	30	−370
	5:1	½ lacquer	+	50 → 15	−410
	5:1	lacquer	+	27	−380
	5:1	lacquer	+	30	−350
Dilute	5:1	4-sided lacquer	+	30	−360
	5:1	4-sided lacquer	−	0.3	−114
Undiluted	1.7:1	4-sided lacquer	+	30 → 60	−380
	1.7:1	4-sided lacquer	+	6 → 4	−360, −320
Chloride	1:1	4-sided lacquer	+/−	0.2	+12
	1:1	½ lacquer	−	0.08	−40
Low chloride	1:5	½ lacquer	−	0.6	−127

was at least 70% of initial sulfate concentration. In addition to SRB being inoculated into the bulk medium, less than 0.1 mL of bacterial subculture was also inoculated into the Microcell. The bacteria were inoculated by syringe through the membrane covering the Microcell. The membrane was uncharged nylon with a pore size of 0.45 μm. The test was conducted in chloride-rich media.

In the Microcell experiments, corrosion of the Fe-15Cr-10Ni was initiated and allowed to stabilize before the bulk media was exchanged for fresh-aerated medium to increase the redox potential of the bulk solution. The nutrient medium was exchanged six times over a six-day period. On day nine, the nutrient media was replaced with 0.1 M NaCl solution.

No effort was made in any of these experiments to sterilize the medium, electrodes, or equipment, as the medium was selective to growth of SRB under deaerated conditions.

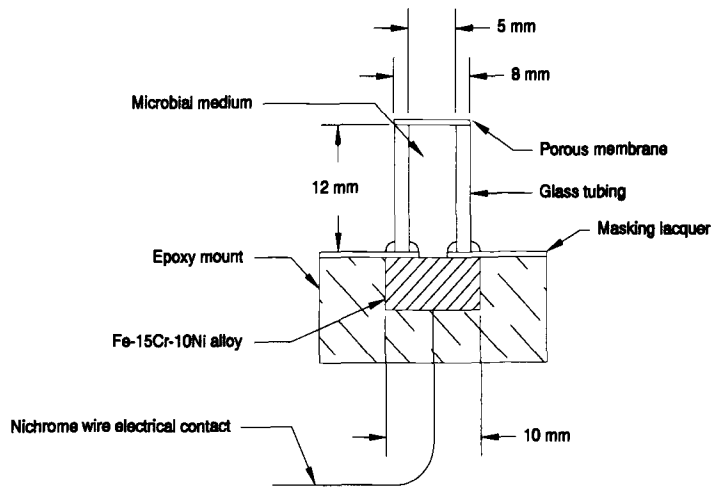

FIG. 2—*The 'Microcell' electrode assembly used for studies of stability of stainless steel corrosion in a bulk-aerated environment.*

Results and Discussion

As test conditions were found to be influential in producing rapid SRB-influenced corrosion, critical areas of experimental methodology have been discussed. Such a discussion should assist other workers in conducting more realistic corrosion tests in the laboratory.

Test Method Selection

Tests that involved prolonged exposure of stainless steels to quite oxidizing potentials were used in this work because of the stochastic nature of pitting (and crevice) corrosion. Of the 10^{13} atomic sites per square centimeter, initiation may only be possible at a few susceptible sites. Initiation of corrosion was also assisted by applying crevices to the electrode surfaces. Crevice and pitting corrosion both require local acidification at the site of initiation of corrosion through metal cation production and differ only in the distance that metal ions must diffuse to mix with the bulk solution. With crevice corrosion, the greater diffusion length permits acidification at lower anodic current densities, hence, corrosion can initiate at lower potentials [*26*]. Biofouling reduces convection at surfaces and may represent a condition close to that of crevice corrosion [*27*].

Medium Composition

In order to conduct laboratory studies of SRB-influenced corrosion of stainless steel, several requirements including anion concentration ratios were addressed in selecting the growth medium. The changes to the traditional media were as follows.

Inclusion of NaCl—This is necessary to obtain localized corrosion of stainless steel, except under extraordinary conditions.

Removal of Ferrous Ions—Preliminary investigations showed that precipitation of iron sulfide on the electrode gave spurious currents when the stainless-steel electrode was anodically polarized. These currents were presumably due to iron-sulfide oxidation. Furthermore, the removal of ferrous ions permitted build-up of H_2S.

Removal of Reducing Agents—Although not proven, indications were that ascorbic acid and sodium thioglycollate interfered with redox potentials, measurements that have proven valuable in monitoring SRB growth indirectly. Without the redox poising agents, deaeration for 2 h with a reasonable inoculum of growing SRB provided a sufficiently-reducing environment to permit growth. To ensure that yeast extract was not having a similar effect on redox potentials, this too was omitted from more recent tests. In the absence of yeast extract, SRB growth rates are reduced but nearly all interferences of medium composition on electrochemical measurements are removed.

H_2S Concentrations in Corrosion Tests

The amount of total sulfide (that is, H_2S plus HS^-, but presented as [H_2S]) produced in each test depends on the nutrient concentration of the individual medium. The maximum concentration of sulfide measured was usually between 70 to 90% of the total initial sulfate concentration of the medium (see Fig. 3). However, as is evident in Fig. 3, there was some variation in the time taken for the bacteria to produce this maximum concentration. The presence of H_2S/HS^- makes stainless steel susceptible to localized corrosion at lower potentials and stabilizes corrosion once initiated [*8,11*]. This is unlike corrosion of iron where high H_2S/HS^- concentrations passivate the material [*28,29*].

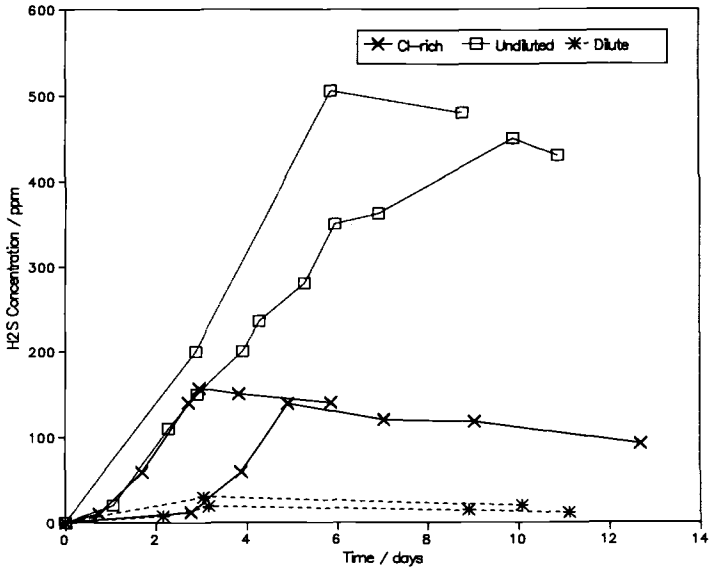

FIG. 3—*Total sulfide concentration (as H_2S) measurements versus time.*

Test Methods—Tests Conducted in Chloride-Rich Medium

In the chloride-rich media, rapid corrosion of the stainless steel was obtained for electrodes that were either potentiostatically polarized to −250 mV or were connected to the large cathode through the ZRA. Results from three potentiostatic tests are shown in Fig. 4 and an example of the potential/current data for a ZRA test is shown in Fig. 5. The chloride-rich medium had a concentration ratio (that is, $[Cl^-]$:Σ[all other anions]) of approximately 5:1 and the bacteria produced a maximum total sulfide concentration of around 150 ppm.

As is evident in Fig. 4, it took a period of time (varying between minutes and hours) before the corrosion initiated at −250 mV. Once initiated, however, the corrosion proceeded rapidly as it was driven by the potentiostat. The fact that corrosion was produced at −250 mV indicates that the environment was quite corrosive. Corrosion was achieved at potentials nearly 1 V less anodic than similar tests of stainless steels by other workers [7]. Initiation of corrosion at −250 mV suggests that the conditions may have been comparable to the inorganic sulfurous environments studied by Newman, et al. [8]. Corrosion occurred in three of the four tests conducted.

In the ZRA tests, immediate initiation of corrosion occurred when the Fe-15Cr-10Ni electrode was coupled to the large aerated Type 304 stainless-steel cathode. The highest potential attainable on connecting the electrodes was the open-circuit cathode potential. Generally, this was around 0 mV (SCE) following exposure to the NaCl solution for the period while the bacteria were growing. Following initiation of localized corrosion (which usually occurred at the edge of the crevice), the corrosion potential fell to just above the repassivation potential (see later discussion) and the current slowly increased, usually reaching a steady maximum value around 30 μA. Some variation in current was evident between tests; however, the currents were all sufficient to cause significant corrosion.

The potentiostatic tests were somewhat artificial in that once corrosion has initiated, the potentiostat was driving the corrosion. On the other hand, the ZRA tests were quite realistic. The large-aerated cathode and the deaerated anode could be envisaged as simulating a weld

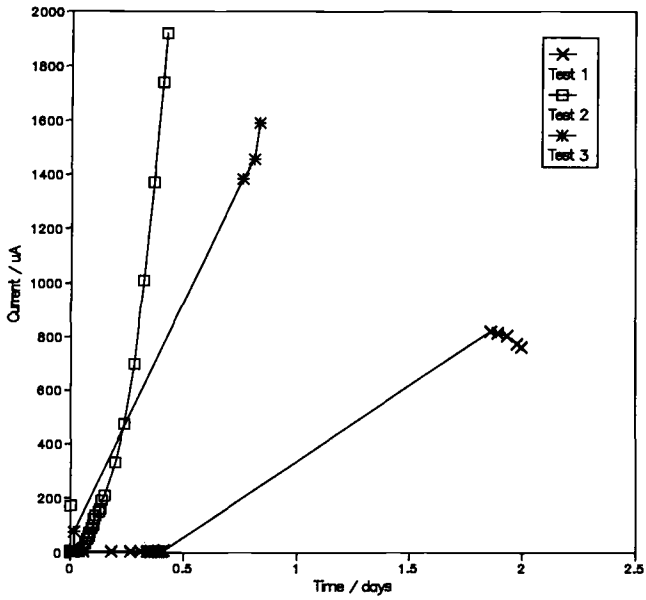

FIG. 4—*Results from potentiostatic tests conducted at −250 mV (SCE) in chloride-rich medium. Corrosion was initiated when in excess of 100 ppm H_2S had been produced.*

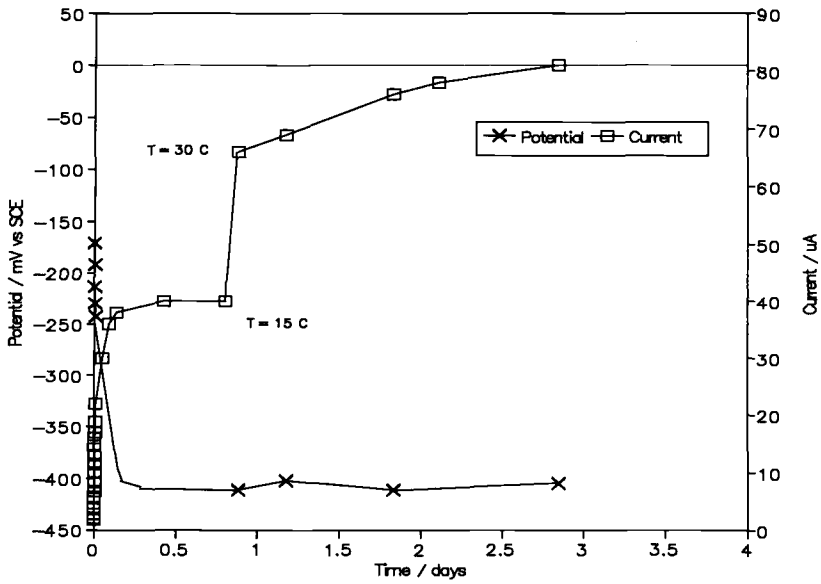

FIG. 5—*ZRA current and potential data for a test conducted in chloride-rich medium. Corrosion was initiated when in excess of 100 ppm H_2S had been produced. The step increase in current evident at approximately day 1 was probably the result of an increase in temperature.*

on a Type 304 stainless-steel pipe, where the weld surface was occluded by a biodeposit containing SRB, and the rest of the pipe was exposed to aerated solution.

The corrosion that occurred in the chloride-rich medium was shown to be due to the bacterial activity. Control-tests for both the potentiostatic and ZRA methods in 0.1 M NaCl (the same chloride concentration as the test medium but without inhibiting anions and H_2S) showed that no corrosion occurred. In the control tests, the current of the electrode at −250 mV was 0.01 μA and the ZRA coupling current was 0.1 μA at the end of the week-long polarizations.

Effect of Anionic Ratios

Inorganic studies have shown that the concentrations of inhibiting and aggressive anions affect the corrosion of stainless steels [*22–24*]. Presumably, the same would apply to MIC. For this reason, a selection of media of different $[Cl^-]$:Σ[all other anions] ratios was tested.

The effect of media composition was evident in the ZRA tests (see Table 2). In Table 2, it is shown that corrosion could not be sustained in *media of the same nutrient concentrations* if the $[Cl^-]$:Σ[all other anions] ratio was reduced below 5:1 (that is, a five-fold excess of chloride). When the ratio was reduced to 1:1 and 1:5 in the chloride[3] and low-chloride media, respectively, corrosion did not occur. This was despite the presence of over 100 ppm of H_2S. These results confirm the inhibiting effect of the anions other than chloride in the media.

In the chloride-rich medium, corrosion was repeatedly produced in the ZRA tests. It would be expected that corrosion would also proceed in a medium where the nutrients were diluted but the $[Cl^-]$:Σ[all other anions] ratio was 5:1 (as for the chloride-rich medium), provided the H_2S concentration was sufficient to initiate corrosion. Such tests were conducted in what has been called the 'dilute medium,' and corrosion occurred in one of the two tests conducted. The lack of corrosion in one of the tests may have resulted from insufficient H_2S to produce corrosion consistently. The H_2S concentration only reached a maximum of approximately 20 ppm (see Fig. 3).

Further support for the suggestion that H_2S concentration is influential in SRB-influenced corrosion of stainless steel (as mentioned at the beginning of the paper) may come from ZRA results of tests conducted in undiluted medium. In this medium, the $[Cl^-]$:Σ[all other anions] ratio was 1.7:1 and around 450 ppm of H_2S was produced. Corrosion occurred in two of the three tests conducted. Comparison of these data with that from the chloride medium, where the H_2S concentration was around 150 ppm but no corrosion occurred despite a similar anion ratio (1:1), suggests an H_2S effect. On the other hand, it may simply have been an anion ratio effect.

The concentrations of the inhibiting anions would be changing during the period of bacterial growth: for example, SO_4^{2-} would be converted to H_2S and HS^-. To reduce this problem, corrosion studies were started after the bacteria had consumed at least 70% of the initial sulfate concentration. At this time, the individual anion concentrations would not be the same as when the test started; however, the total conductivity did not change markedly over the test duration. An improvement to the test methodology may be to conduct similar tests in continuous rather than batch bacterial cultures where the anion ratios could be maintained at a stable level. Under these circumstances, however, the bulk H_2S concentration would tend to be lower than in batch cultures.

[3] At the start of one of the tests conducted in chloride-medium, a series of current events <1μA suggested initiation of corrosion. However, corrosion could not be sustained and the electrode immediately repassivated.

TABLE 3—*Results from the potentiostatic tests at −250 mV.*

Medium	Cl^-:Σ(All Other Anions)	Crevice	Corrosion	I_{end}, μA
Chloride-rich	5:1	castellated washer	+	···
	5:1	½ lacquer	+	···
	5:1	½ lacquer	+	···
	5:1	4-sided lacquer	−	<1
Dilute	5:1	4-sided lacquer	−	0.07
	5:1	4-sided lacquer	−	0.08
Undiluted	1.7:1	½ lacquer	+	···
	1.7:1	4-sided lacquer	−	1.3
Chloride	1:1	½ lacquer	−	0.07
	1:1	4-sided lacquer	−	0.01
Low chloride	1:5	castellated washer	−	0.3

The effect of media composition was quite evident in the ZRA tests conducted (see Table 2). However, in the potentiostatic tests conducted at −250 mV, the effect of media composition was not as clear cut and test results were not as reproducible (see Table 3). The lack of reproducibility in the potentiostatic tests may reflect the stochastic nature of the initiation process. That is, the likelihood of initiating corrosion at −250 mV (versus SCE) in the potentiostatic tests is lower than initiating corrosion in the ZRA tests at around 0 mV (versus SCE).

Potential-Time Data

Typical potential-time data for the Fe-15Cr-10Ni and a platinum electrode in chloride-rich medium are shown in Fig. 6. This figure shows that the potential of the stainless steel was quite reducing (around −600 mV) and was generally below that of the platinum electrode. Evidently, the passive-current density of the stainless steel was sufficient to make the mixed potential depart from the redox potential. This may be assisted by H_2S increasing the passive-current density. Examination of an Fe-15Cr-10Ni creviced electrode after exposure to the culture for 10 days, showed no visible corrosion; an estimated corrosion current would be $<<1\ \mu A \cdot cm^{-2}$. The brief excursion where the stainless-steel potential exceeds that of platinum from day 0 to day 0.5 is probably a kinetic effect. Platinum has a more catalytic surface than stainless steel, and therefore, would respond faster to changes in redox conditions.

The potential-time data given in Fig. 6 are useful when combined with repassivation potentials and redox potentials, to assess the feasibility of cathodic reactions other than oxygen evolution, which could sustain rapid SRB-influenced corrosion of stainless steel. The repassivation potential determinations are published elsewhere [*28–30*], but are discussed here in support of the comment made at the beginning of the paper that hydrogen evolution could not sustain such corrosion.

Repassivation potentials of corroding electrodes were determined by cathodically scanning electrodes corroding at −250 mV and electrodes used for polarization curves. These values were compared with ZRA current/potential data. The values were found to be between −420 and −500 mV (SCE) [*28–30*]. Therefore, from the definition of a repassivation potential, corrosion could not proceed at potentials below −500 mV. Hydrogen evolution would not proceed until potentials below −660 mV (SCE) at pH 7 were reached. Therefore, hydrogen evolution is not a feasible cathodic reaction.

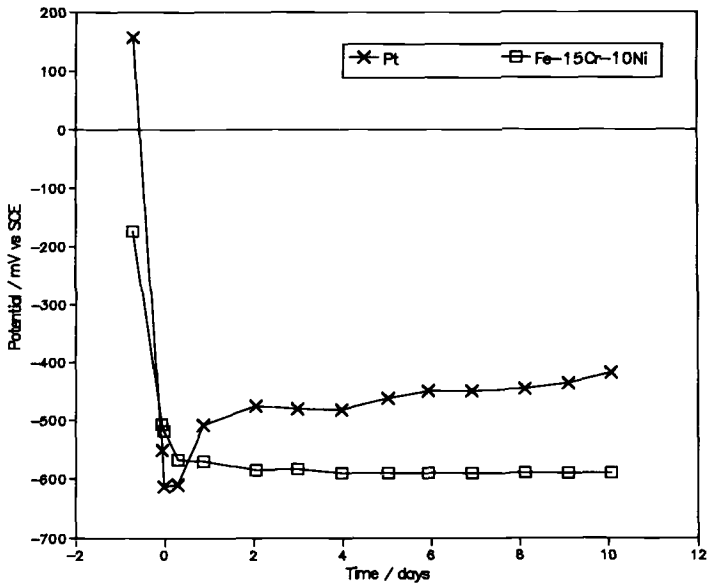

FIG. 6—*Typical potential versus time data for an Fe-15Cr-10Ni electrode and a platinum electrode.*

The maximum potential attainable by the Fe-15Cr-10Ni stainless steel is the redox potential of the medium, in this case around −400 mV. This potential is believed to be induced by the presence of polysulfides or $S^0_{(aq)}$ (formed through reaction of sulfide with residual or ingressing oxygen). It is above the repassivation potential; hence, theoretically, polysulfide or $S^0_{(aq)}$ reduction could sustain corrosion. Tests reported elsewhere have shown that once corrosion is initiated, polysulfide or $S^0_{(aq)}$ reduction can sustain corrosion, at least on this material [*29*]. No analytical tests were conducted to measure the concentration of polysulfides or $S^0_{(aq)}$.

Novel Test Electrode

As hydrogen evolution could not provide conditions sufficient to corrode stainless steel, a problem arises; SRB require anaerobic conditions, while the corrosion process requires more oxidizing conditions. Under many circumstances, the two situations could not coexist; however, because SRB produce sulfide, such a scenario is possible. Sulfide is an oxygen scavenger, hence, sulfide generated by the SRB could maintain an anaerobic microenvironment, provided growth was sufficient. This is the *minimum* requirement for stability of an anaerobic microenvironment; other organisms or reducing substances can also scavenge oxygen.

Convection-free electrode assemblies, referred to as Microcells, permitted the stability of SRB-influenced corrosion to be studied in an oxidizing environment. The Microcell test is an extension of the ZRA tests discussed above in that it is a step closer to artificially simulating field conditions in the laboratory.

Initial studies indicate that corrosion in a convection-free environment is stable provided nutrients are supplied to the bacteria (see Fig. 7). In this test, corrosion was sustained for approximately one week while exposed to aerated nutrients (days 1.8 to 9), but corrosion ceased soon after the medium was replaced with NaCl solution (day 10).

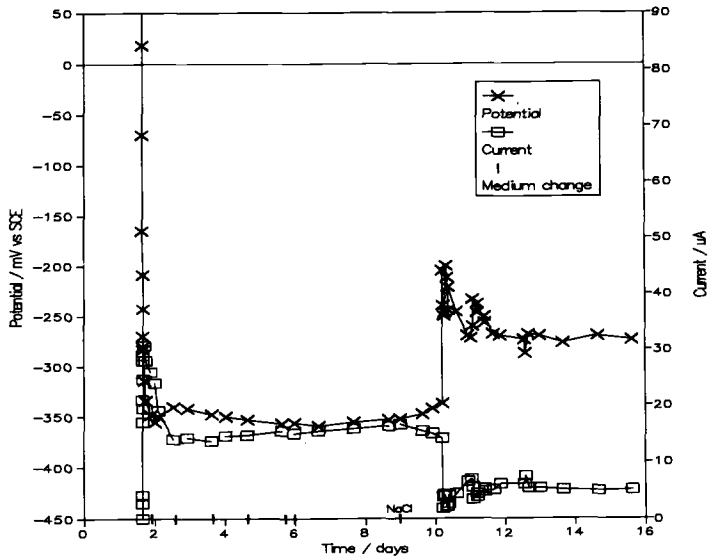

FIG. 7—*ZRA current and potential data from a corroding Fe-15Cr-10Ni 'Microcell' electrode. The x-axis markers indicate medium exchanges. Corrosion was initiated when the bacterial culture had produced 100 ppm H_2S. Notably, corrosion ceased soon after changing to NaCl solution.*

Attempts at replacing the two-compartment test cell with a single-compartment test cell to conduct the Microcell experiments were unsuccessful. A single compartment test cell required that the cathode was placed in aerated bacterial medium; in doing so, the cathode adopted a very reducing potential, around −580 mV (SCE). It seemed that a film of aerobes on the Type 304 stainless-steel surface altered its potential to a very reducing value. In this state, the cathode could not be used as such nor could it be used for initiation purposes. This result demonstrates how efficiently aerobes can provide local anaerobic niches within a bulk-aerated environment. This test highlighted the benefit of a two-compartment cell where the anode could be separated from the cathode. Keeping the cathode in a separate compartment and in an inorganic solution, not only restricted biological interferences but also permitted experimentation with different cathodic reactions, for example, polysulfide reduction.

These studies show that the 'Microcell' technique has promise for fundamental investigations of corrosion influenced by anaerobic bacteria in aerated media. It is also a promising tool for water treatment studies in which the effect of various biocidal substances, including oxygen, are examined under controlled mass transport conditions.

Conclusions

(1) The composition of SRB growth medium used in laboratory studies of stainless-steel corrosion is important. Critical factors are:

(a) the presence of chloride and
(b) the relative concentration of inhibiting anions to aggressive anions.

(2) A two-compartment test cell is required for testing SRB-influenced corrosion of stainless steel under artificial growth conditions in the laboratory. One compartment is

used for the bacterial culture while the other contains an inorganic solution to eliminate biofilms that interfere with the cathodic reaction.

(3) Rapid SRB-influenced corrosion of a susceptible stainless steel has been achieved using specially-designed media, creviced electrodes, and an oxygen-reduction cathode.

(4) The ZRA technique provided more consistent results than the potentiostatic technique. Using the ZRA technique, an effect of medium composition was apparent. An anion ratio of $[Cl^-]:\Sigma$[all other anions] of 5:1 consistently produced corrosion in these studies.

(5) Rapid SRB-influenced corrosion of stainless steel could not be sustained by hydrogen evolution as the cathodic reaction but may be sustainable by $S^0_{(aq)}$ reduction.

(6) Initial studies suggest that SRB-influenced corrosion of stainless steel may involve two distinct sites on the material: an anodic site located at the anaerobic, convection-free microenvironment of SRB activity and a cathodic site where oxygen reduction proceeds.

References

[1] Tiller, A. K. "Is Stainless Steel Susceptible to Microbial Corrosion?," *Microbial Corrosion,* The Metals Society, London, 1983, p. 104.

[2] Puckorius, P. R., *Materials Performance,* Vol. 22, No. 12, 1983, p. 19.

[3] Tatnall, R. E., *Materials Performance,* Vol. 22, No. 8, 1983, p. 41.

[4] Stott, J. F. D., *Metals and Materials,* Vol. 4, 1988, p. 224.

[5] Tapping, R. L., Doherty, P. E., Donaldson, J., and Lavoie, P. A., "Pitting of Fe-Ni-Cr Alloys in Freshwater," Environmental Degradation of Materials in Nuclear Power Systems - Water Reactors (4th International Symposium, Jekyll Island, GA), American Nuclear Society and the National Association of Corrosion Engineers (NACE), 1989.

[6] Ringas, C. and Robinson, F. P. A., *Corrosion,* Vol. 44, 1987, p. 386.

[7] Ringas, C. and Robinson, F. P. A., *Corrosion,* Vol. 44, 1988, p. 671.

[8] Newman, R. C., Isaacs, H. S., and Alman, B., *Corrosion,* Vol. 38, 1982, p. 261.

[9] Oudar, J. and Marcus, P., *Applications of Surface Science,* Vol. 3, 1979, pp. 48–67.

[10] Marcus, P. and Protopopoff, E., *Journal of the Electrochemical Society,* Vol. 137, 1990, p. 2709.

[11] Holt, D. and Cottis, R. A., in "The Effect of Trace Sulfur Compounds on the Pitting of Austenitic Stainless Steel in Potable Water," *Proceeding of the International Congress on Metallic Corrosion,* Vol. 3, N.R.C., Ottawa, Ontario, 1984, pp. 614–617.

[12] Moreno, D. A., Ibars, J. R., Ranninger, C., and Videla, H. A., *Corrosion,* Vol. 48, 1992, p. 226.

[13] Garner, A. and Newman, R. C., CORROSION/91, Paper 186, National Association of Corrosion Engineers (NACE), Houston, 1991.

[14] Newman, R. C., Wong, W. P., Ezuber, H., and Garner, A., CORROSION/87, Paper 202, National Association of Corrosion Engineers (NACE), Houston, 1987.

[15] Newman, R. C., *Corrosion,* Vol. 41, 1985, p. 450.

[16] Garner, A., *Corrosion,* Vol. 41, 1985, p. 587.

[17] Newman, R. C., Wong, W. P., and Garner, A., *Corrosion,* Vol. 42, 1986, p. 489.

[18] Roberge, R., *Corrosion,* Vol. 44, 1988, p. 274.

[19] Miyasaka, A., Denpo, K., and Ogawa, H., CORROSION/88, Paper 70, National Association of Corrosion Engineers (NACE), Houston, 1988.

[20] Kudo, T., Miyuki, H., Okamoto, H., Murayama, T., and Moroishi, T., CORROSION/82, Paper 127, National Association of Corrosion Engineers (NACE), Houston, 1982.

[21] Chen, K. Y. and Morris, J. C., *Environmental Science and Technology,* Vol. 6, 1972, p. 529.

[22] Leckie, H. P. and Uhlig, H. H., *Journal of the Electrochemical Society,* Vol. 113, No. 12, 1966, p. 1262.

[23] Ezuber, H., "Metallurgical and Environmental Factors Influencing Pitting Corrosion of Stainless Steel," PhD Thesis, University of Manchester Institute of Science and Technology, Manchester, United Kingdom, 1991.

[24] Szklarska-Smialowska, Z., *Pitting Corrosion of Metals,* National Association of Corrosion Engineers (NACE), Houston, 1986, p. 285.

[25] American Petroleum Institute, *RP45,* 2nd edition, Published by Division of Production, Dallas, 1981.

[26] Galvele, J. R., "Pitting Corrosion," *Treatise on Materials Science and Technology*, Academic Press, Vol. 23, 1983, p. 1.
[27] Characklis, W. G. and Marshall, K. C., *Biofilms*, John Wiley and Sons, Inc., 1990, p. 93.
[28] Newman, R. C., Rumash, K., and Webster, B. J., *Corrosion Science*, Vol. 33, No. 12, 1992, p. 1877.
[29] Webster, B. J., "Electrochemistry of Corrosion Influenced by Sulphate Reducing Bacteria," PhD Thesis, University of Manchester Institute of Science and Technology, Manchester, United Kingdom, 1991.
[30] Newman, R. C., Webster, B. J., and Kelly, R. G., *ISIJ International*, Vol. 31, No. 2, 1991, p. 201.

DISCUSSION

A. Stein[1] (*written discussion*)—Could you explain the need or significance of the S to the existence of corrosion with varying Cl^-:Σ (all other anion) ratio. Is H_2S required, and if so, was H_2S present with low Cl^-:Σ (all other anion) ratios when no corrosion was observed? If H_2S was present, was the effect of H_2S the same as at higher Cl^-:Σ (all other anion) ratios?

B. J. Webster and R. C. Newman (*authors' closure*)—The presence of sulfide is not necessary to see an effect of anion ratio on corrosion. Leckie and Uhlig found that the ratio of aggressive anions to inhibiting anions affected the pitting potential of stainless steel in the absence of H_2S [*22*]. Based on the findings of other workers, the presence of H_2S would probably stabilize metastable pitting, thereby permitting corrosion to occur at lower potentials [*13*].

In this work, H_2S was present in all experiments where the effect of anion ratio was investigated. In the ZRA tests, it was found that the anion ratio affected the corrosion of stainless steel. In low Cl^-:Σ (all other anion) ratios, no corrosion was obtained, whereas at high Cl^-:Σ (all other anion) ratios corrosion was obtained. For example, in a test conducted in low-chloride medium where the Cl^-:Σ (all other anion) ratio was 1:5 and the H_2S concentration was around 150 ppm, no corrosion was obtained. Similarly, no corrosion was obtained in tests conducted in chloride media where the Cl^-:Σ (all other anion) ratio was 1:1 and around 150 ppm of H_2S was present. In contrast, when the Cl^-:Σ (all other anion) ratio was 5:1 and around 150 ppm of H_2S was present, corrosion was consistently obtained.

[1] Stone & Webster Engineering, 245 Summit Street, Boston, MA 02210.

Florian Mansfeld[1] *and Hong Xiao*[1]

Electrochemical Techniques for Detection of Localized Corrosion Phenomena

REFERENCE: Mansfeld, F. and Xiao, H., **"Electrochemical Techniques for Detection of Localized Corrosion Phenomena,"** *Microbiologically Influenced Corrosion Testing, ASTM STP 1232*, Jeffery R. Kearns and Brenda J. Little, Eds., American Society for Testing and Materials, Philadelphia, 1994, pp. 42–60.

ABSTRACT: Most corrosion reactions in microbiologically influenced corrosion (MIC) are of localized nature. It is therefore necessary to develop methods that can provide information concerning the corrosion reactions occurring under biofilms. Electrochemical techniques such as electrochemical impedance spectroscopy (EIS), electrochemical noise analysis (ENA), and measurements of pit propagation rates for thin metal foils have been evaluated as tools for the study of localized corrosion in MIC. Initial studies have been carried out in abiotic NaCl solutions. Software has been prepared for collection and analysis of electrochemical noise data. It has been found that use of potential noise alone can lead to erroneous conclusions concerning the occurrence of pitting for Al alloys and the inhibition of corrosion of iron. However, current noise seems to be directly related to the extent of pitting. EIS has been used to detect the initiation and propagation of localized corrosion and to confirm the conclusions reached for the ENA-data. For iron in NaCl, the noise resistance had similar values as the polarization resistance determined by EIS. In thin foil tests, penetration of Al and nickel foils has been measured during exposure to 0.5 N NaCl.

KEYWORDS: impedance spectroscopy, electrochemical noise, pit propagation, iron, aluminum, polarization resistance, localized corrosion

In evaluating the use of electrochemical monitoring techniques for the detection and quantification of microbiologically influenced corrosion (MIC), a few limitations of such techniques have to be considered. A weakness of most electrochemical techniques is the failure to give quantitative results in cases of localized corrosion. These techniques give average readings for the surface of a test electrode and it is not clear whether a measured corrosion current corresponds to uniform corrosion of the entire surface or to localized corrosion of just a few sites on this surface. In the latter case, corrosion rates will be severely underestimated if the measured corrosion loss is not normalized to the area at which localized corrosion occurs, a quantity which is usually unknown. This general disadvantage of electrochemical techniques is especially bothersome in the case of MIC, where most corrosion processes are of a localized nature. Recently, techniques such as electrochemical impedance spectroscopy (EIS) have been shown to contain information that is specifically related to localized corrosion processes [*1–3*]. However, so far EIS has been used mainly as a laboratory technique for mechanistic studies. Another new technique is electrochemical noise analysis (ENA), which is considered by some as the ideal tool for the study of localized corrosion.

[1] Professor and Ph.D. candidate, respectively, University of Southern California, Department of Materials Science and Engineering, Los Angeles, CA 90089-0241.

ENA does not require an external signal and is relatively easy to apply. Unfortunately, very few studies have demonstrated that localized corrosion can be detected and analyzed quantitatively by ENA for a system, for which no previous information concerning its corrosion mechanism is available.

In a joint project with the Center for Interfacial Microbial Process Engineering at Montana State University, a number of electrochemical techniques are being evaluated for the study of localized corrosion phenomena in MIC. These techniques include EIS, ENA, and the thin foil technique for monitoring of pit growth rates. EIS has been used successfully in a number of areas of corrosion research such as the evaluation of polymer coatings, inhibitors, anodic films, and general studies of the kinetics of corrosion reactions [*4*]. ENA has been used in investigations of various types of corrosion for a variety of materials. Most frequently, this technique is applied in studies of localized corrosion phenomena. Different research groups have been working in different directions of data analysis; spectral analysis, statistical analysis, and theoretical approach. Several models of electrochemical noise generation during corrosion processes have been established [*5–9*], but most theories lack support from experimental investigations.

For the purpose of applying the electrochemical noise technique to MIC, the present investigation is focusing on the spectral analysis of pitting corrosion of an Al-based metal matrix composite. A statistical analysis is applied in the study of corrosion inhibition for iron with the goal of using this simple approach for corrosion monitoring. Electrochemical noise measurements follow either fluctuations of potential, often E_{corr}, or current as a function of time or experimental conditions. In this paper, most measurements are conducted with electrode couples of the same material thereby eliminating the noise from reference or counter electrodes. Many published papers concentrate on potential noise alone [*10–24*], while only a few investigators studied current noise [*25–29*]. In the present study, current noise as well as potential noise have been evaluated, and the current noise appears to be more related to localized corrosion than potential noise. The experimental noise data sets have been analyzed by an analysis program based on the maximum entropy method (MEM) through which the frequency domain information of noise data can be presented as power spectral density (PSD).

Another concern of this investigation is to detect pit penetration by the thin foil technique introduced by Hunkeler and Boehni [*30*]. A description of the results obtained for Al and nickel with a modification of the technique will be given.

Experimental Approach

Potential Noise Measurements

The experimental procedure for potential noise measurements is shown in Fig. 1. Two identical samples immersed in the test solution are connected to an HP3457A digital multimeter that is controlled by an IBM compatible computer. The potential fluctuations between the two samples are determined at a constant rate of 2 points per second and stored in the computer for further analysis. Pt wires were tested first in 0.5 N NaCl solution as background material that does not corrode in this environment. Al 2009/SiC, T8 metal matrix composite (MMC) samples containing 20% SiC particles were tested in 0.5 N NaCl for up to two weeks. Data obtained in 0.1 M Na_2SO_4 and deionized water have been reported elsewhere [*31*]. Pure iron foils (99.999%, 0.1-mm thickness) were exposed to 0.5 N NaCl open to air or deaerated with N_2. Some tests were performed with the addition of 0.01 M

[2] F. Mansfeld and H. Xiao, in preparation.

$NaNO_2$.[2] These tests were carried out for 24 h. At the end of each test series an impedance spectrum was recorded.

Current Noise Measurements

The experimental arrangement for the recording of current noise is shown in Fig. 2. In addition to the equipment used in potential noise measurements (Fig. 1), a Schlumberger model 1186 potentiostat is employed as a zero resistance ammeter (ZRA). The current fluctuations are sampled at the current output of the potentiostat by the computer-controlled multimeter. The sampling rate was 2 points per second and the collected data were stored in the computer for further processing. Pt, Al 2009/SiC, and iron were tested as in the potential noise measurements.

Thin Foil Tests

The experimental arrangement for measuring pit propagation rates is shown in Fig. 3. In a newly designed cell, a piece of metal foil with known thickness has one side exposed to the solution in the cell, while the other side is covered by a thin filter paper sheet. Next to the filter paper two closely spaced detector electrodes are pressed tightly to the filter paper by the outer cell wall. A small voltage is applied between the two parallel detector electrodes. When the paper is dry, no current flows across the two detector electrodes. However, if a pit has penetrated the test sample, the paper will be wetted and a current will be detected. Using this technique, the time for the fastest growing pit to penetrate the foil can be recorded for foils of different thicknesses and a pit propagation rate law can be determined. In order to test the experimental arrangement shown in Fig. 3, Al and Ni foils with varying thickness were exposed to 0.5 N NaCl. In order to reduce the time for foil penetration, the foils were polarized by a constant anodic current that exceeded the passivation current. The design used in the present study is slightly different from that of Hunkeler and Boehni [*30*], in which a voltage was applied between the test sample and the detector electrode, which may polarize the test electrode in an unpredictable and undesirable way.

In the thin foil tests reported here, only one half of the special test cell was used. For other types of investigations, the filter paper and the detector electrodes could be replaced

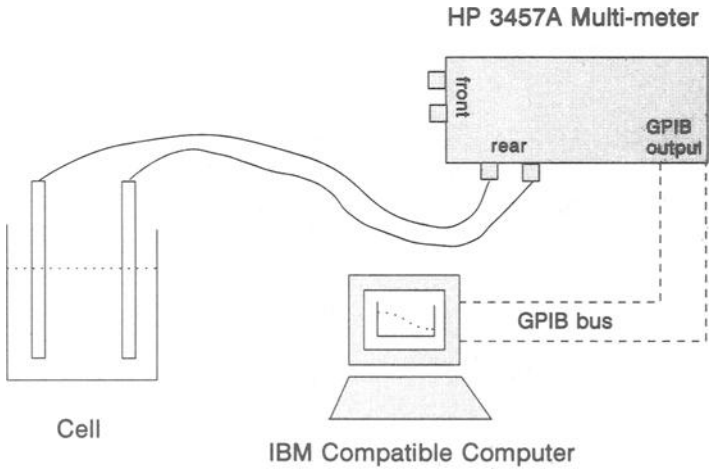

FIG. 1—*Experimental arrangement for potential noise measurements.*

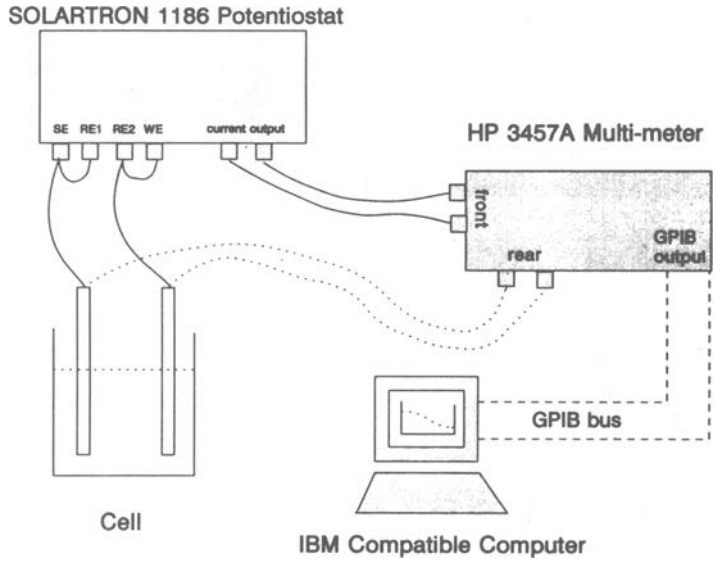

FIG. 2—*Experimental arrangement for current noise measurements.*

by another half cell, so that both sides of the thin foil would be exposed to different test solutions. For example, one solution could contain microorganisms, while the other would be an abiotic solution of the same composition similar to the dual-cell approach pioneered by Little et al. [*32*] for MIC applications. In further stages of this project, this PITCELL will be explored for its application in studies of MIC phenomena. For these tests, a modification of the detection system will be necessary.

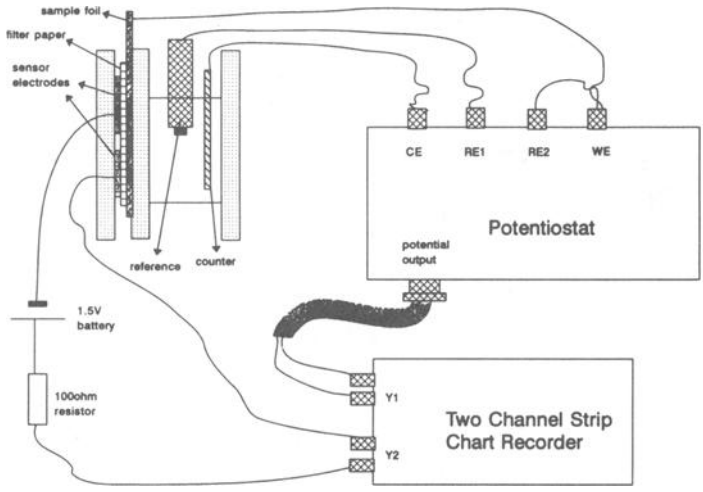

FIG. 3—*Experimental arrangement for pit foil measurements.*

Electrochemical Impedance Spectroscopy (EIS)

For a comparison and as conformation of the results obtained with the techniques described above, electrochemical impedance spectroscopy (EIS) measurements have been conducted. A significant amount of information has been collected previously with EIS in this laboratory for localized corrosion of Al alloys and models for the analysis of EIS-data have been prepared [*33*]. For the experiments with iron, the polarization resistance R_p has been determined [*4*]. EIS data have been collected for the two electrode systems as a function of exposure time immediately after each measurement of electrochemical noise data.

Data Analysis and Experimental Results

Spectral Analysis of Electrochemical Noise Data

For the analysis of electrochemical noise data, the fluctuations of potential or current are often difficult to interpret and are probably less meaningful than the frequency response behavior. The power spectral density (PSD) is defined as the average power of a signal in a certain frequency range [*34*]. A typical PSD plot of electrochemical noise data is given in Fig. 4, where the three most important parameters are the low-frequency limit P_o, the roll-off frequency f_r and the slope S_p. The correlation of these parameters with the mechanism of the corrosion process is still uncertain. However, it can be expected that higher values of P_o correspond to larger fluctuations of the measured signal and therefore to higher intensity of localized attack and that f_r and S_p are related to the type of corrosion of a given material (for example, uniform versus localized). Searson and Dawson [*10*], who determined potential noise, observed a slope of -20 dB/decade for pitting attack and -40 dB/decade for uniform corrosion.

In order to obtain the frequency domain information, the time series of noise data has to be transformed by certain functions. A computer program using the maximum entropy method (MEM) has been developed by the authors to obtain the PSD of the noise data collected in the present study. The MEM estimation of PSD is described by Eqs 1 and 2 [*35,36*]. In Eq 1, Φ_j is the autocorrelation function of the times series, a_k is the MEM coefficient array, M is called the order or the number of poles of the estimation approxi-

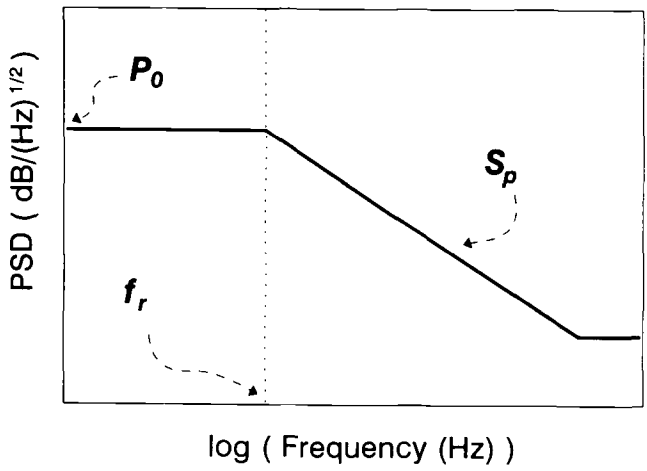

FIG. 4—*Schematic PSD plot.*

mation, and z refers to the Z-plane. Once the MEM coefficient, a_k, is obtained by Eq 2, the PSD can be calculated through Eq 1

$$\mathrm{PSD}(f) = \frac{a_0}{\left|1 + \sum_{k=1}^{M} a_k z^k\right|^2} = \sum_{j=-M}^{M} \Phi_j z^j \tag{1}$$

$$\begin{pmatrix} \Phi_0 & \Phi_1 & \Phi_2 & \dots & \Phi_M \\ \Phi_1 & \Phi_0 & \Phi_1 & \dots & \Phi_{M-1} \\ \Phi_2 & \Phi_1 & \Phi_0 & \dots & \Phi_{M-2} \\ \dots & \dots & & & \\ \Phi_M & \Phi_{M-1} & \Phi_{M-2} & \dots & \Phi_0 \end{pmatrix} \cdot \begin{pmatrix} 1 \\ a_1 \\ a_2 \\ \dots \\ a_M \end{pmatrix} = \begin{pmatrix} a_0 \\ 0 \\ 0 \\ \dots \\ 0 \end{pmatrix} \tag{2}$$

Compared to the FFT method, the MEM estimation has the advantage of sharper spectral features. Reducing M within certain accuracy limits can increase the calculation speed and smooth the spectra.

Statistical Analysis

For all tests carried out with iron in NaCl, the mean value and the standard deviation (rms) of the potential and current noise were calculated. From these data the noise resistance $R_n = dV/dI$, where dV is the rms of the corrosion potential fluctuation and dI is the rms of the current fluctuations [*37*], was calculated as a function of exposure time. Experimental values of R_n for carbon steel in NaCl have recently been reported by Lumsden et al. [*38*], who tried to correlate R_n with R_p, as determined from EIS. The exact relationship between R_n and R_p has not been established so far. Finally, the pit index PI, which has been defined as the ratio of the rms current noise and the mean coupling current [*39*], has been calculated.

Potential and Current PSD Data for Pt and Al 2009/SiC

Both potential noise and current noise data have been analyzed by the MEM program. Figure 5 shows the potential fluctuation-time records for Pt and Al 2009/SiC in 0.5 N NaCl measured during the first day of exposure and Fig. 6 shows the corresponding PSD plots. It is interesting that the potential noise for Pt, which does not corrode in this solution, is at the same level as that for Al 2009/SiC, which pitted severely in the first day of immersion. In Fig. 6, very similar P_o-values are observed for both systems. This very reproducible result gave the motivation for studying the current noise of these materials. Figure 7 shows the current fluctuation-time records for Pt and Al 2009/SiC in 0.5 N NaCl solution during the first day of immersion, while Fig. 8 shows the corresponding PSD plots. On the scale used in Fig. 7, the current fluctuations for Pt cannot be detected. The current noise PSD for Pt (Fig. 8) is at the same level as the background noise from the potentiostat. However, the current noise PSD for Al 2009/SiC is much higher at all frequencies and shows the typical shape observed in our studies for pitting of Al-based materials. This phenomenon indicates that localized corrosion is not the only cause of the observed potential fluctuations. The large potential fluctuations for Pt are likely due to fluctuations of the O_2 mass transport process in the stagnant solution that lead to large changes of the open-circuit potential of the passive Pt surface. This process does not involve corrosion reactions and the corresponding current fluctuations are very small. On the other hand, the Al 2009/SiC MMC experiences passive film breakdown processes as pits initiate during the first day of immersion and the current fluctuations are very large. Apparently, the current fluctuations are more

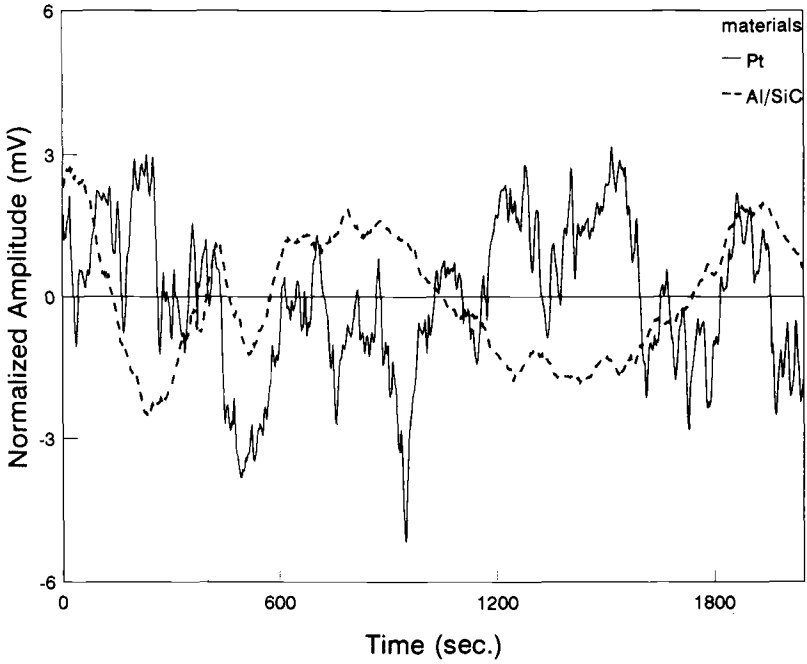

FIG. 5—*Normalized potential fluctuations for Pt and Al 2009/SiC measured during the first day of exposure in 0.5 N NaCl.*

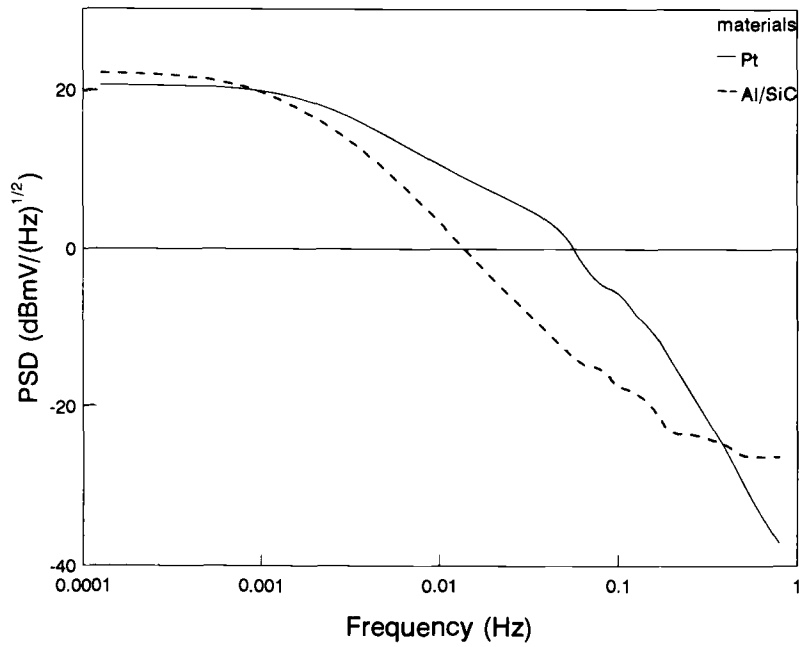

FIG. 6—*Potential PSD plots for Pt and Al 2009/SiC during the first day of exposure in 0.5 N NaCl; data of Fig. 5.*

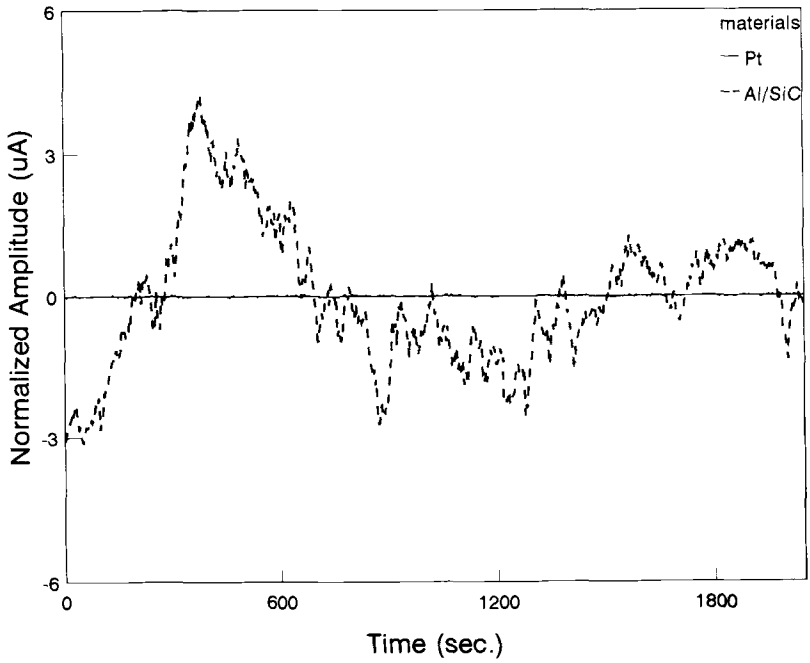

FIG. 7—*Normalized current fluctuations for Pt and Al 2009/SiC measured during the first day of exposure in 0.5 N NaCl.*

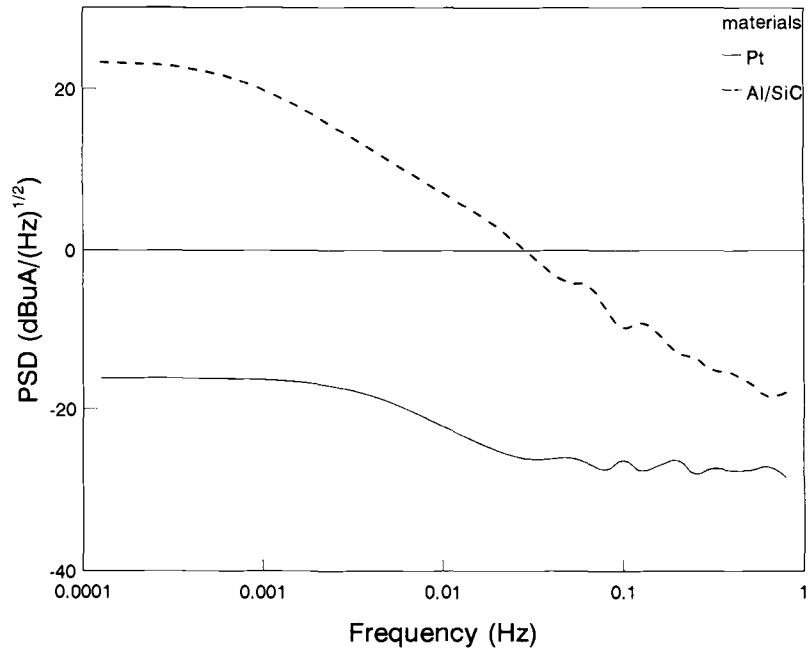

FIG. 8—*Current PSD plots for Pt and Al 2009/SiC during the first day of exposure in 0.5 N NaCl; data of Fig. 7.*

indicative of pit initiation and propagation than the potential fluctuations, and therefore more applicable to the study of MIC phenomena. Recording of potential noise alone could lead to erroneous conclusions concerning the type and extent of corrosion.

To illustrate the noise behavior of Al 2009/SiC in 0.5 N NaCl as a function of immersion time, Fig. 9 gives the potential fluctuation PSD curves for two weeks of immersion. No distinguishable features as a function of immersion time can be determined from these curves. However, in Fig. 10, which presents the current fluctuation PSD curves for the same experimental conditions, the curve obtained during the first day of immersion is much higher than those for the remainder of the exposure period that are almost identical (except for the 7th day for which an obvious artifact was found). All curves have a similar roll-off frequency f_r and similar linear slope S_p (except for the 7th day). The three parameters considered characteristic for both the potential and current PSD curves are tabulated in Table 1 as a function of exposure time. A comparison of the P_o-values in Table 1 shows that P_o does not change with exposure time for the potential noise data, but decreases significantly after the first day for the current noise data. The average value of f_r is about 0.5 mHz for the current noise and 0.9 mHz for the potential noise without significant changes with exposure time. The slope S_p does not seem to depend on exposure time either, but is significantly larger for the potential noise than for the current noise. The slopes observed for the potential noise data in Table 1 are close to that suggested to be indicative of pitting corrosion by Searson and Dawson [*10*].

EIS Data for Al 2009/SiC

For Al alloys, previous results obtained with EIS in this laboratory have shown that pits initiate within the first day of exposure to 0.5 N NaCl and propagate according to a time

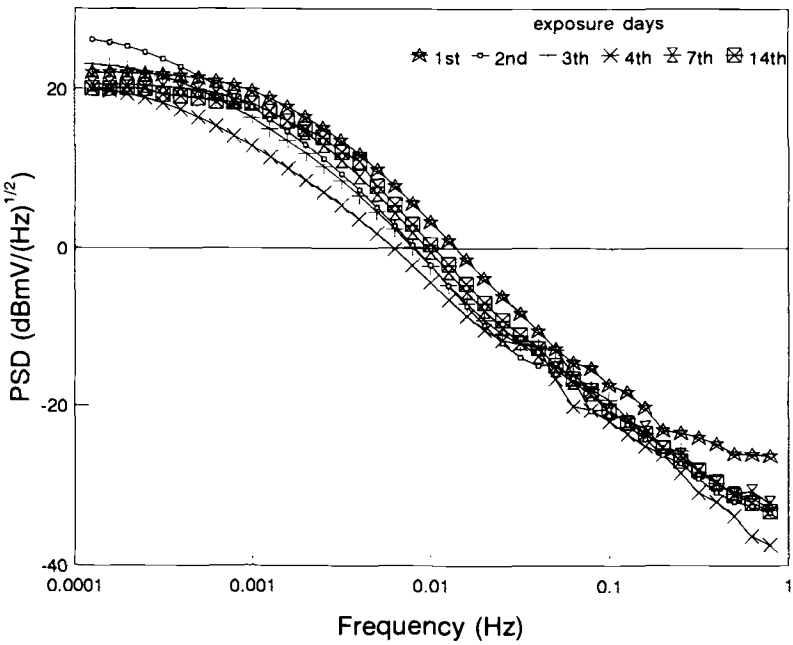

FIG. 9—*PSD plots for potential fluctuations for Al 2009/SiC as a function of exposure time to 0.5 N NaCl.*

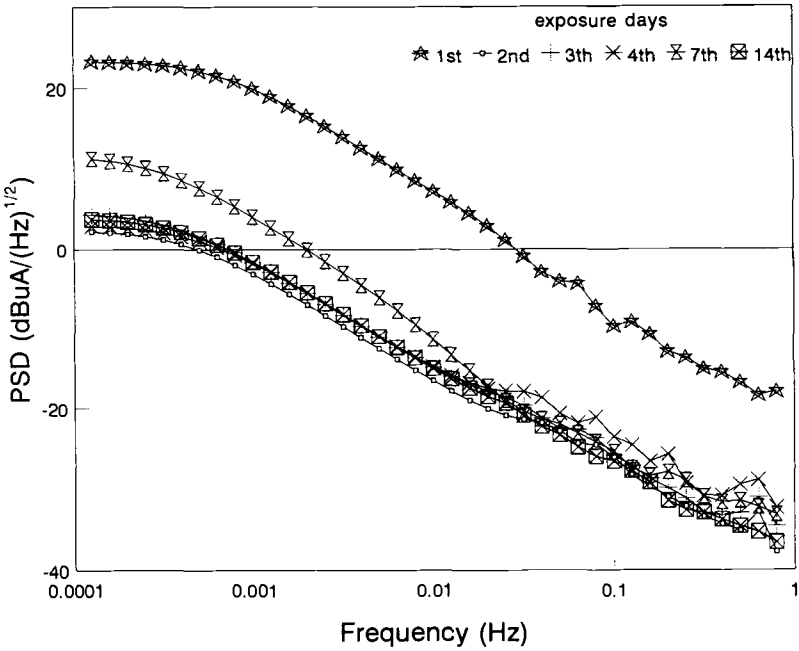

FIG. 10—*PSD plots for current fluctuations for Al 2009/SiC as a function of exposure time to 0.5 N NaCl.*

law that can be expressed as [*40*]

$$r = at^b \tag{3}$$

where r is the pit propagation rate, a is an experimental parameter, which depends on the metal/solution system, and b is an experimental parameter indicative of the mechanism of pit propagation. Figure 11 shows the impedance spectra for Al 2009/SiC in 0.5*N* NaCl solution as a function of immersion time. All curves show the typical pitting behavior described by the model discussed elsewhere [*1–3,40*]. The total capacitance observed in the frequency region between 5 and 500 Hz (Fig. 11) shows an increase from the first to the second day, indicating a large increase of the pitted area during this time. The polarization resistance of the pits that can be extracted from the spectra shown in Fig. 11 follows the time-dependence given in Eq 3.

TABLE 1—*PSD parameters for Al 2009/SiC in 0.5N NaCl.*

		Days					
		1st	2nd	3rd	4th	7th[a]	14th
Current	P_o (dB/$\sqrt{\text{Hz}}$)	22.5	2.4	4.3	3.3	11.4	4.0
	f_r (mHz)	0.7	0.5	0.5	0.6	0.3	0.5
	S_p (dB/dec)	−13.1	−12.1	−12.4	−12.2	−14.1	−12.3
Potential	P_o (dB/$\sqrt{\text{Hz}}$)	22.0	26.1	22.7	20.0	21.0	20.0
	f_r (mHz)	1.2	0.7	0.7	0.7	1.0	1.2
	S_p (dB/dec)	−21.8	−22.7	−20.4	−19.1	−21.6	−22.6

[a] Some artifacts were observed in the 7th day current fluctuation data.

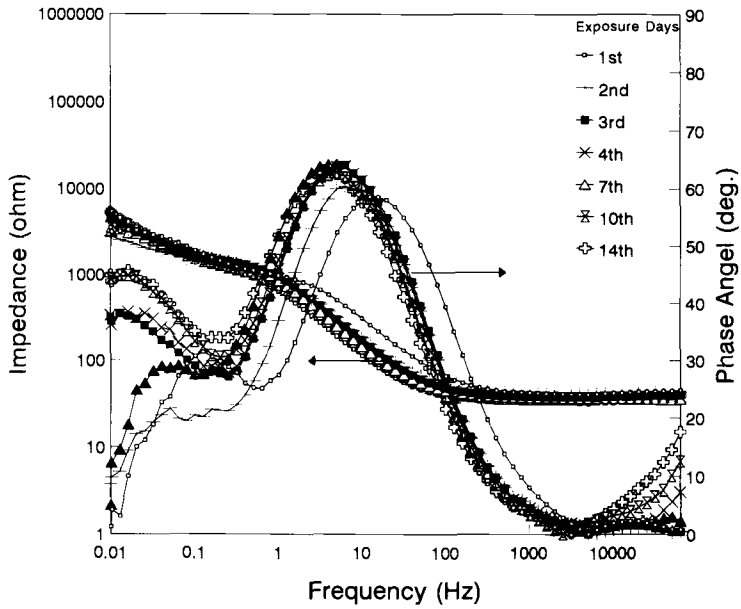

FIG. 11—*Impedance spectra for Al 2009/SiC as a function of exposure time to 0.5 N NaCl.*

ENA for Iron in NaCl

The mean values of E_{corr} for iron exposed to NaCl, which was open to air, deaerated or open to air with an addition of 0.01 M $NaNO_2$, are shown in Fig. 12, while Fig. 13 presents the mean values of the coupling current. These data were determined over a 24 h period. Potential values were measured versus a SCE reference electrode. At the beginning of each hour, potential noise was recorded first followed by current noise. Both potential and current were recorded at a sampling rate of 2 points/s and sampled for 500 s. The mean coupling current was very small for the deaerated and the inhibited solution, while both positive and negative peaks occurred in the aerated solution. The data shown in Fig. 13 are very different from those reported by Lumsden et al. [*38*] in which a very large dc current of 700 to 750 μA occurred, indicating large differences in the corrosion kinetics of the two steel samples.

Figures 14 and 15 show the rms values of potential and current, respectively. The largest rms potential values are observed for the inhibited solution where iron is in the passive state (Fig. 12) and the fluctuations of E_{corr} are larger similar to the results described above for Pt (Fig. 5). The rms current values are the lowest and show the least variations with time for the deaerated solution (Fig. 15). The noise resistance R_n, which is derived from the data in Figs. 14 and 15, is shown in Fig. 16 for the three solutions. The highest values (10 to 100 kohm) are observed for the inhibited solution. For the deaerated solution, a very stable time behavior is observed with R_n slowly increasing from about 1 to about 10 kohm after 24 h. The sample exposed to NaCl/air has the lowest R_n values with the largest fluctuations. Table 2 gives a comparison of the R_n and R_p values determined at the end of the test. Fairly good agreement between these two parameters is observed. Lumsden et al. reported much larger values of R_n than R_p for carbon steel in NaCl [*38*].

The pit index PI, which has been proposed as a tool for determining the type of corrosion [*39*], does not give meaningful information for the system iron/NaCl studied here. Very

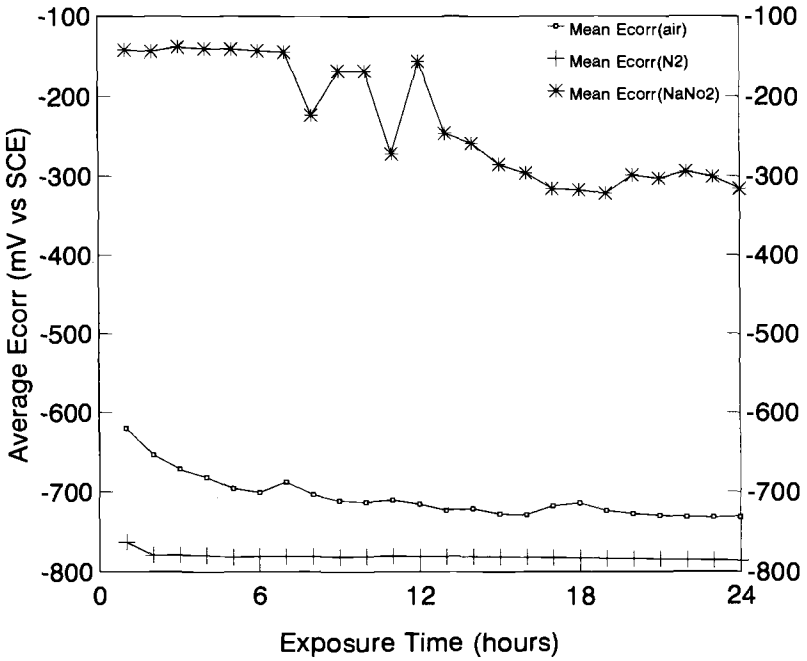

FIG. 12—*Time dependence of the mean E_{corr} for iron in three solutions.*

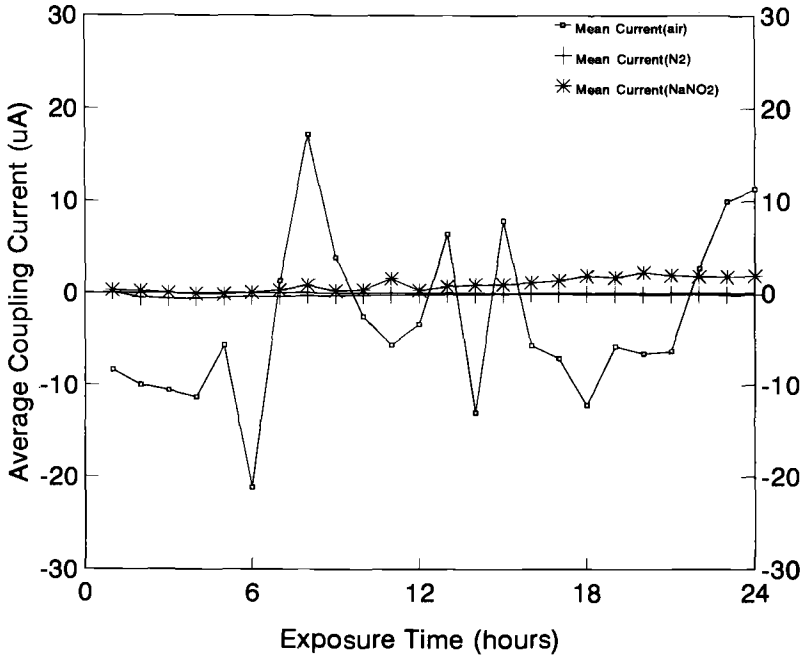

FIG. 13—*Time dependence of the mean coupling current for iron in three solutions.*

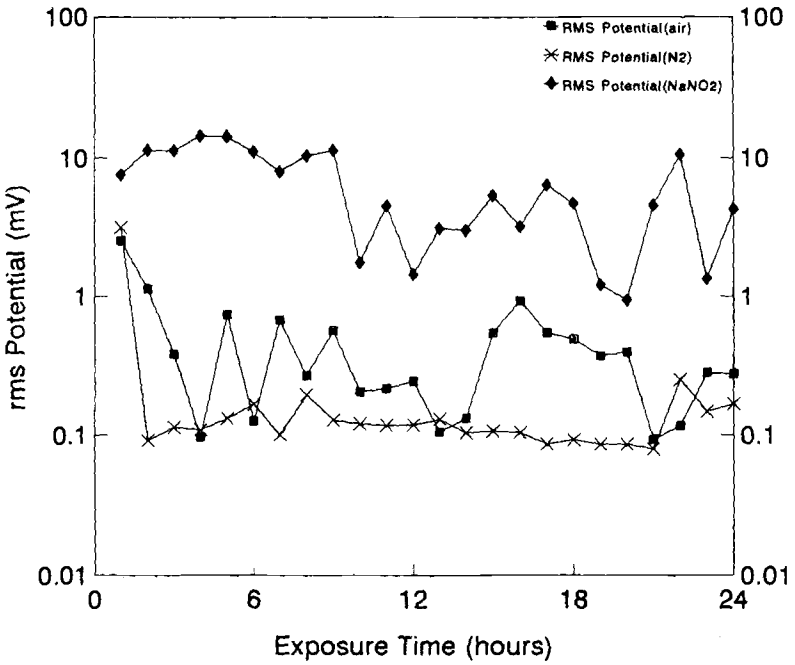

FIG. 14—*Rms potential values for iron in three solutions.*

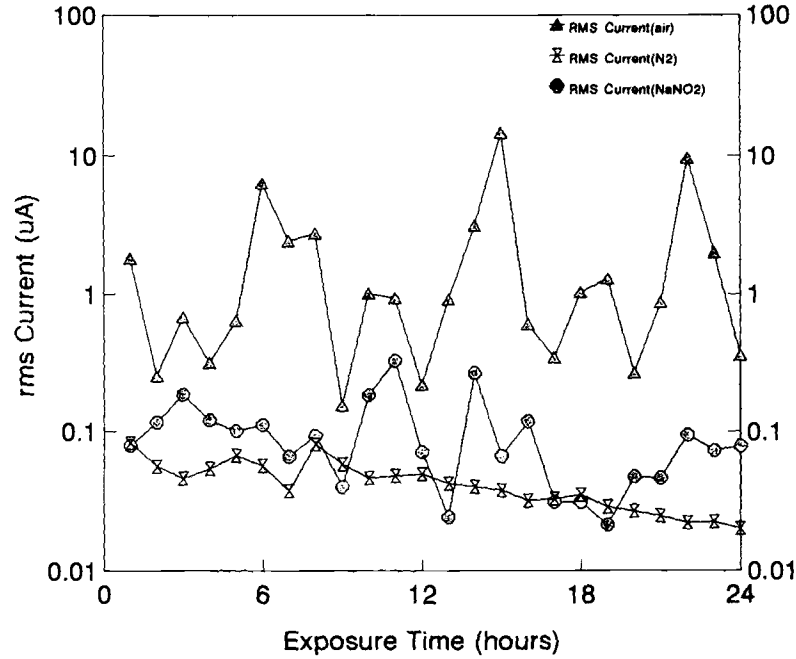

FIG. 15—*Rms current values for iron in three solutions.*

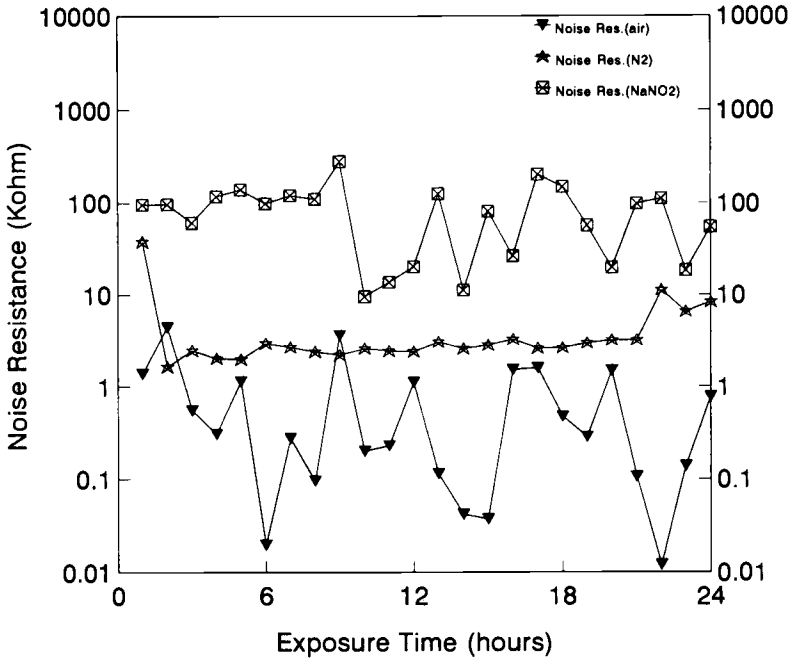

FIG. 16—*Noise resistance R_n for iron in three solutions.*

similar values of PI are observed in Fig. 17 for the three solutions of different corrosivity. For the inhibited solution, PI exceeds 1.0 several times in the first 6 h, which in the proposed approach [*39*], indicates initiation of pits. During the same time, the PI for NaCl/air is quite low. For NaCl/N_2 the PI is between 0.1 and 1 (Fig. 17), which supposedly indicates the occurrence of localized corrosion. However, localized corrosion was not observed in the deaerated and the inhibited solution.

Thin Foil Test Results

Figure 18 shows the detector current pattern for a pure Al foil (0.0254 mm) in 0.5 N NaCl for 20 $\mu A/cm^2$ applied anodic current density. Penetration of the foil was detected after exposure for 25 min which leads to a very high penetration rate of about 1 $\mu m/min$. By visual examination, two pits were found to have penetrated the foil. Figure 19 shows the detector current pattern for a Ni foil (0.124 mm) in 0.5 N NaCl for an anodic polarization

TABLE 2—*Comparison of R_n and R_p for three different test environments.*[a]

Environment	Open to Air	Deaerated(N_2)	Inhibitor($NaNO_2$)
R_n(KΩ)	~1	~10	~50
R_p(KΩ)	1.6	15.9	22.1

[a] The exposed area of each sample is about 5 cm^2.

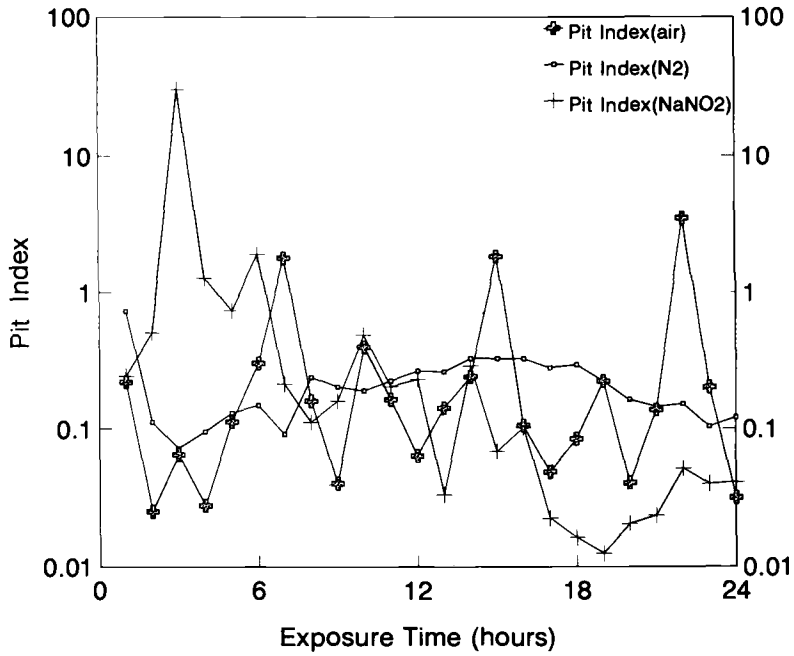

FIG. 17—*Pit index PI for iron in three solutions.*

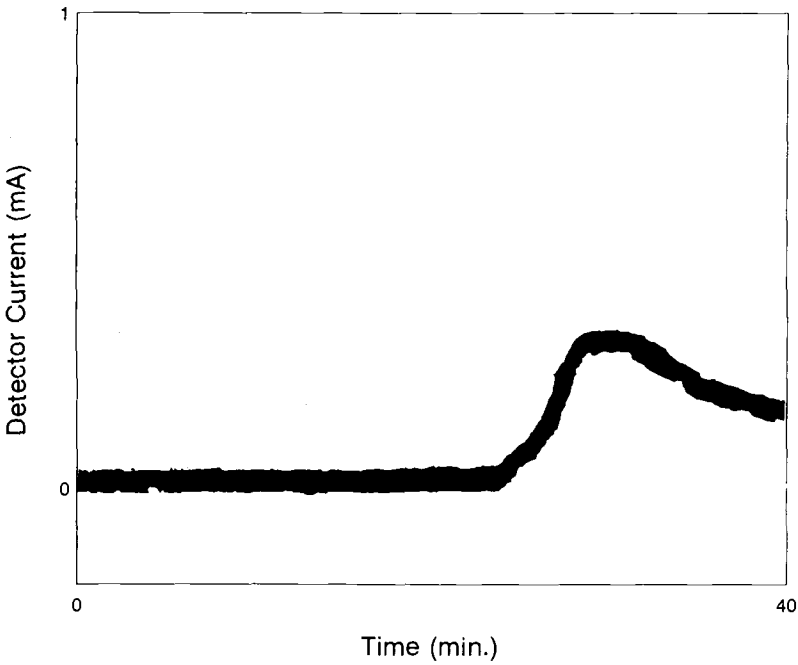

FIG. 18—*Detector current, time trace for Al foil exposed to 0.5 N NaCl at applied anodic current.*

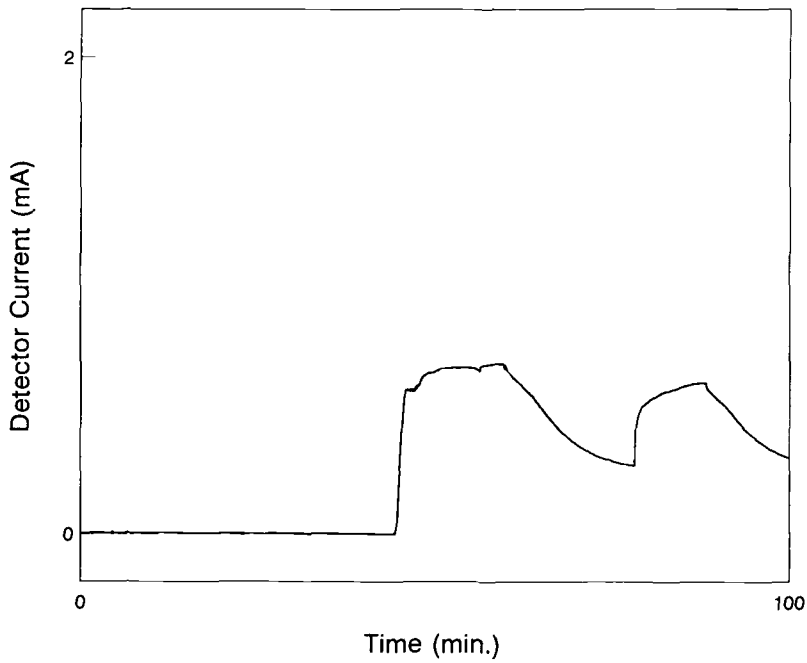

FIG. 19—*Detector current, time trace for Ni foil exposed to 0.5 N NaCl at applied anodic current.*

current density of 200 $\mu A/cm^2$. It is interesting that after the first penetration a second current burst can be seen. By microscopic observation, one pit was found on the surface. The pit shape from both sides of the foil is shown schematically in Fig. 20. Apparently, the growing pit produced undercutting of the exposed surface and the knife-like feature on the backside may be the cause of the second current burst triggered by an additional flux of electrolyte.

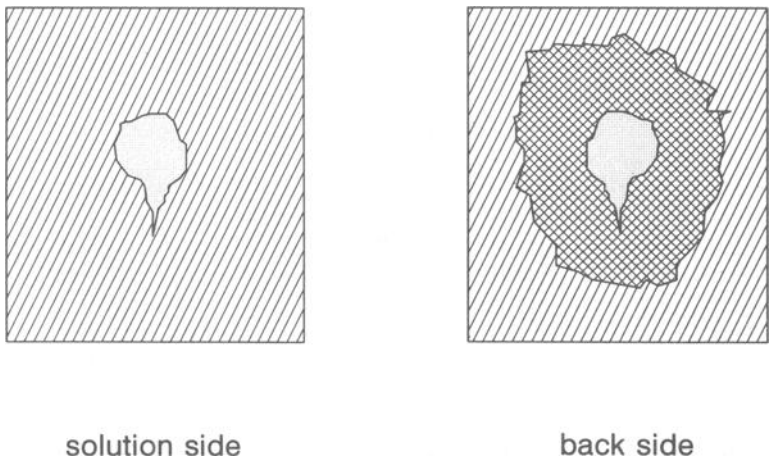

FIG. 20—*Appearance of Ni foil after pitting test (schematic).*

Conclusions

Electrochemical impedance spectroscopy (EIS) and electrochemical noise analysis (ENA) have been evaluated for their usefulness in studies of localized corrosion phenomena. An Al-based metal matrix composite has been used as a model system because of its known susceptibility to localized corrosion. Iron in NaCl solutions of different corrosivity has been used to evaluate concepts that have been proposed for corrosion monitoring purposes. A thin foil technique has also been evaluated because of its promise as a tool for detection of pit penetration during the early stages of the corrosion process.

Emphasis has been placed on the evaluation of ENA, which is a relatively new technique with the advantage that no external signal has to be applied in order to determine the corrosion characteristics of a system. For this reason, ENA is very promising as a tool not only for laboratory studies, but perhaps even more for field studies and corrosion monitoring. The effort in the initial phases of this project has concentrated on the development of software for the recording and analysis of electrochemical noise data. The maximum entropy method (MEM) has been chosen for data analysis and the results of this analysis have been displayed as power spectral density plots. An important result of the initial studies is the realization that potential noise can be misleading for systems in which mass transport plays an important role such as Pt in aerated, neutral NaCl. Since the open circuit potential of Pt in this environment is poorly biased, small fluctuations of the transport of O_2 to the surface can lead to large fluctuations of E_{corr} that could be mistakenly identified as being due to localized corrosion. On the other hand, current fluctuations seem to be mainly due to localized corrosion effects. While the PSD plots give a convenient overview of the frequency dependence of the electrochemical noise, the correlation of the characteristic parameters P_o, f_r, and S_p with the extent of corrosion and the type of corrosion is not clear at present. Therefore, these parameters have been used in this study for a qualitative description of the noise characteristics of different materials and exposure to different solutions.

For iron in 0.5 N NaCl, the mean and the rms values of E_{corr} and the coupling current between two electrodes of the same materials have been determined on an hourly basis for 24 h. From these data, the noise resistance R_n has been determined as a function of exposure time. This approach is promising for corrosion monitoring in studies of MIC since the experiment is easy to carry out and the equipment is inexpensive. Fairly good agreement between the polarization resistance R_p and R_n has been observed. However, the Pit Index (PI), which has been proposed as a tool for determining the type of corrosion, gave misleading results.

EIS, which is a more mature technique, has been used mainly to determine the extent of pitting of the Al-based MMC at certain time intervals, for establishment of a pit growth law according to Eq 3 and for comparison with the noise data. For iron in NaCl, R_p has been obtained for comparison with R_n.

A new experimental design has been completed for the thin foil technique that eliminates potential problems with previous detection systems for the penetration of the metal foil. This technique will be used at a later stage to determine pit growth rates with a nonelectrochemical technique by measuring the time for foil penetration as a function of foil thickness. The application of this technique lies in monitoring of MIC similar to the "pitting fuse" described by Kendig et al. [*41*]. A metal foil can be exposed as part of the system to be monitored and an alarm can be triggered when this foil has been penetrated by the fastest growing pit. The foil thickness can be adjusted, considering Eq 3 to cause such an alarm in a reasonable exposure time.

An important part of this project is the transfer of the software and hardware to the Center for Interfacial Microbial Process Engineering at Montana State University, where

the use of the candidate electrochemical techniques for the study of localized corrosion phenomena in MIC will be further evaluated. In initial studies, electrochemical noise data have been collected during aeration and deaeration for steel in the presence of sulfate reducing bacteria.[3]

Acknowledgment

This project has been funded by Montana State University under Subcontract 291435-01.

References

[1] Mansfeld, F., Lin, S., Kim, S., and Shih, H., *Journal of the Electrochemical Society*, Vol. 137, 1990, p. 78.
[2] Mansfeld, F., Lin, S., Kim, S., and Shih, H., *Electrochimica Acta*, Vol. 34, 1989, p. 1123.
[3] Mansfeld, F. and Little, B., *Corrosion Science*, Vol. 32, 1991, p. 247.
[4] Mansfeld, F. and Lorenz, W. J., in *Techniques for Characterization of Electrodes and Electrode Processes*, John Wiley & Sons, New York, 1991, p. 581.
[5] Blanc, G., Epelboin, I., Gabrielli, C., and Keddam, M., *Journal of the Electroanalytical Chemistry*, Vol. 75, 1977, pp. 94–124.
[6] Okata, T., *Journal of the Electroanalytical Chemistry*, Vol. 297, 1991, pp. 361–375.
[7] Okata, T., *Journal of the Electrochemical Society*, Vol. 92, 1991, p. 9.
[8] Hashimoto, M., Miyajima, S., and Murata, T., *Corrosion Science*, Vol. 33, No. 6, 1992, pp. 885–904.
[9] Kendig, M. and Hagen, G., Corrosion/88, Paper 383, National Association of Corrosion Engineers, (NACE), 1988.
[10] Searson, P. and Dawson, J., *Journal of the Electrochemical Society*, Vol. 135, 1988, p. 1908.
[11] Uruchurtu, J. and Dawson, J., *Materials Science Forum*, Vol. 8, 1986, pp. 113–124.
[12] Uruchurtu, J., *Corrosion*, Vol. 47, 1991, p. 472.
[13] Hladky, K. and Dawson, J., *Corrosion Science*, Vol. 21, 1981, p. 317.
[14] Hladky, K. and Dawson, J., *Corrosion Science*, Vol. 22, 1982, p. 231.
[15] Loto, C. and Cottis, R., *Corrosion*, Vol. 45, 1989, p. 136.
[16] Loto, C. and Cottis, R., *Corrosion*, Vol. 43, 1987, p. 499.
[17] Cottis, R. and Loto, C., *Corrosion*, Vol. 46, 1990, p. 12.
[18] Metikos-Hukovic, M., Loncar, M., and Zevnik, C., *Werkstoffe und Korrosion*, Vol. 40, 1989, pp. 494–499.
[19] Nachstedt, K. and Heusler, K., *Electrochimica Acta*, Vol. 33, 1988, p. 311.
[20] Bertocci, U. and Kruger, J., *Surface Science*, Vol. 101, 1980, pp. 608–618.
[21] Simoes, A. and Ferreira, M., *British Corrosion Journal*, Vol. 22, 1987, p. 21.
[22] Monticelli, C., Brunoro, G., Frignani, A., and Trabanelli, G., *Journal of the Electrochemical Society*, Vol. 139, 1992, p. 706.
[23] Hashimoto, M., Miyajima, S., and Murata, T., *Corrosion Science*, Vol. 33, 1992, p. 905.
[24] Hashimoto, M., Miyajima, S., and Murata, T., *Corrosion Science*, Vol. 33, 1992, p. 917.
[25] Tachibana, K., Miya, K., Furuya, K., and Okamoto, G., *Corrosion Science*, Vol. 31, 1990, p. 27.
[26] Smith, S. and Francis, R., *British Corrosion Journal*, Vol. 25, 1990, p. 285.
[27] Bertocci, U. and Yang-Xiang, Y., *Journal of the Electrochemical Society*, Vol. 131, 1984, p. 1011.
[28] Miyata, Y., Handa, T., and Takazawa, H., *Corrosion Science*, Vol. 31, 1990, pp. 465–470.
[29] Tsuru, T. and Sakairi, M., *Corrosion Engineering*, Vol. 39, 1990, p. 447.
[30] Hunkeler, F. and Boehni, H., *Corrosion*, Vol. 37, 1981, p. 645.
[31] Mansfeld, F. and Xiao, H., in *Biofouling/Biocorrosion in Industrial Water Systems*, G. G. Geesey, Z. Lewandowski and H. C. Flemming, Eds., Lewis Publishers, Inc., Chelsea, MI, in press.
[32] Little, B. J., Wagner, P., Gerchakov, S. M., Walch, M., and Mitchell, R., *Corrosion*, Vol. 42, 1986, p. 533.
[33] Mansfeld, F., Shih, H., and Tsai, C. H., "Software for Simulation and Analysis of Electrochemical Impedance Spectroscopy (EIS) Data," *Computer Modeling in Corrosion, ASTM STP 1154*, Raymond S. Munn, Ed., American Society for Testing and Materials, Philadelphia, 1992, pp. 186–195.

[3] F. Mansfeld, H. Xiao, and W. C. Lee, unpublished results.

[34] Oppenheim, A. and Schafer, R., *Discrete-Time Signal Processing,* Prentice Hall, Englewood Cliffs, NJ, 1989.
[35] Fougere, P., *Maximum Entropy and Bayesian Methods,* Kluwer Academic, Norwell, MA, 1990.
[36] Press, W., Flannery, B., Teukolsky, A., and Vetterling, W., *Numerical Recipes,* Cambridge University Press, Cambridge, MA, 1986.
[37] Rothwell, A. N. and Eden, D. A., Corrosion/92, Paper 223, National Association of Corrosion Engineers, Nashville, TN, 1992.
[38] Lumsden, J. B., Kendig, M. W., and Jeanjaquet, S., Corrosion/92, Paper 224, National Association of Corrosion Engineers, Nashville, TN, 1992.
[39] International Patent Application No. PCT/GB87/00310.
[40] Mansfeld, F., Wang, Y., Xiao, H., and Shih, H., Proc. Symp. "Critical Factors in Localized Corrosion," *The Electrochemical Society,* Proceedings Vol. 92-9, 1992, p. 469.
[41] Kendig, M. W., Mansfeld, F., and Jeanjaquet, S., *The Electrochemical Society,* Proceedings Vol. 83-1, 1983, p. 319.

Zbigniew Lewandowski,[1] *Thomas Funk,*[1] *Frank Roe,*[1] *and Brenda J. Little*[2]

Spatial Distribution of pH at Mild Steel Surfaces Using an Iridium Oxide Microelectrode

REFERENCE: Lewandowski, Z., Funk, T., Roe, F., and Little, B., **"Spatial Distribution of pH at Mild Steel Surfaces Using an Iridium Oxide Microelectrode,"** *Microbiologically Influenced Corrosion Testing, ASTM STP 1232,* Jeffery R. Kearns and Brenda J. Little, Eds., American Society for Testing and Materials, Philadelphia, 1994, pp. 61–69.

ABSTRACT: The distribution of pH near a metal surface indicates the positions of anodic (low pH) and cathodic sites (high pH). A microsensor, small enough that the pH sensing tip is confined to the diffusion layer, can be used to monitor pH near metal surfaces. This paper describes the mapping of pH near water-immersed mild steel surfaces using miniaturized iridium/iridium oxide pH microelectrodes in conjunction with a computer controlled micropositioner and data acquisition system. Two systems were analyzed: (1) a bare mild steel coupon exposed to artificial sea water, and (2) a mild steel coupon, first partially covered with the biopolymer, calcium alginate, and then exposed to artificial seawater. After 8 h exposure to seawater both coupons exhibited localized corrosion. On the coupon partially covered with calcium alginate gel, corrosion was limited to the area covered by biopolymer. On the bare coupon, corrosion was widespread. pH mapping of the coupons showed that low pH regions were identified with the corroded areas, and high pH regions with the uncorroded areas. These observations demonstrate that, in the abiotic environment, anodic sites on a mild steel surface can be fixed by partially covering the metal with biopolymer.

KEYWORDS: microelectrode, pH, iridium oxide, mapping, corrosion, mild steel, alginate, biopolymer, microbiologically influenced corrosion (MIC)

Microorganisms growing on water immersed metal surfaces form biofilms that are held together by extracellular polymeric substances (EPS). This type of microbial colonization is frequently associated with microbially influenced corrosion (MIC). The mechanisms relating microbial colonization and corrosion are not well understood. MIC costs the U.S. economy billions of dollars each year.

MIC is a function of a variety of environmental factors such as: metal alloy composition (for example, mild steel versus stainless steel), biofilm properties (for example, aerobic versus anaerobic organisms), and fluid characteristics (temperature, hydrodynamics, chemical composition) [*1,2*]. Corrosion mechanisms can be analyzed in terms of the anodic and cathodic processes that are occurring [*3*].

The rate limiting step of corrosion can be either oxidation of the metal or reduction of oxygen. Bare mild steel corrodes in dilute saline solutions showing no pronounced polari-

[1] Associate professor of civil engineering, and research associates, respectively, Montana State University, Bozeman, MT.

[2] Research chemist, Naval Oceanographic and Atmospheric Research Station, Stennis Space Center, MS.

zation; passivation rarely takes place and corrosion rates normally increase as corrosion potentials increase [*4*]. In this case, reduction of oxygen is normally the rate-limiting step due to diffusional or mixed diffusion/reaction control [*5*].

Biofilms have been implicated in both inhibition and promotion of corrosion of mild steel. Hernandez-Duque et al. [*6*] reported a drop in the corrosion rate of mild steel in the presence of a uniform layer of biofilm. This drop was attributed to respiration of the biofilm that resulted in a decline in oxygen concentration at the metal surface and associated decrease in rate of cathodic reduction oxygen. Smith et al. [*7*] reported the agar coated steel (artificial biofilm) also produced a very high polarization resistance and low corrosion rate. The last result suggests that biofilm metabolic activity may not be necessary for inhibition of corrosion by biopolymers.

Many researchers, on the other hand, have reported that biofilms promote MIC on mild steel surfaces [*8*]. Iverson [*9*] proposed that the natural patchiness of biofilms results in differential aeration cells at the metal surface; areas with more biofilm exhibit low oxygen concentrations and become anodic, while those with less biofilm are exposed to higher oxygen concentrations and become cathodic. This patchiness can also cause concentration gradients of other electrochemically active species within the biofilm [*10*]. Heterogeneities in biofilm structure and composition may be the key factor in determining whether biofilms enhance or inhibit corrosion rates. Consequently, MIC may not depend entirely on metabolically active biofilms.

This paper describes localized corrosion of mild steel in aerobic seawater. The role of biofilms in this process is under investigation. From the cited literature it is not clear if patchiness of biofilms alone promotes MIC to the extent observed, or whether some metabolic activity is necessary. Our study addresses the hypothesis that metabolic activity of biofilms is not always necessary in promoting MIC. This hypothesis was verified by forming an artificial patchy biofilm by partially coating a bare mild steel surface with the biopolymer, calcium alginate, and observing the location and extent of corrosion. If a differential aeration cell formed, localized corrosion would occur under the alginate and oxygen reduction would occur on the adjacent bare surface. A map of pH in the vicinity of the alginate spot should show a decrease in pH above the anodic site (the alginate spot) and an increase in pH above the cathodic site (bare surface).

Experimental Approach

Overview

A polished mild steel coupon was partially covered with calcium alginate biopolymer gel and immersed in artificial seawater. An iridium/iridium oxide pH microelectrode was used to map pH above the immersed coupon; results were compared to similar measurements over a bare polished control coupon.

Electrode Construction and Calibration

Briefly, an iridium wire is tapered electrochemically and covered with glass (Fig. 1). Excess glass is ground off to expose the tip of the iridium wire. The wire is then recessed a few micrometers into the glass to provide a protected area for the active iridium oxide. The iridium oxide layer is formed by potential cycling. This technique alternatively applies oxidation and reduction potentials to the exposed metal tip, oxidation being the slightly dominant process. The electrode tip is finally cleaned, aged in water, and calibrated. Details for electrode construction are given in the paper by VanHoudt et al. [*11*].

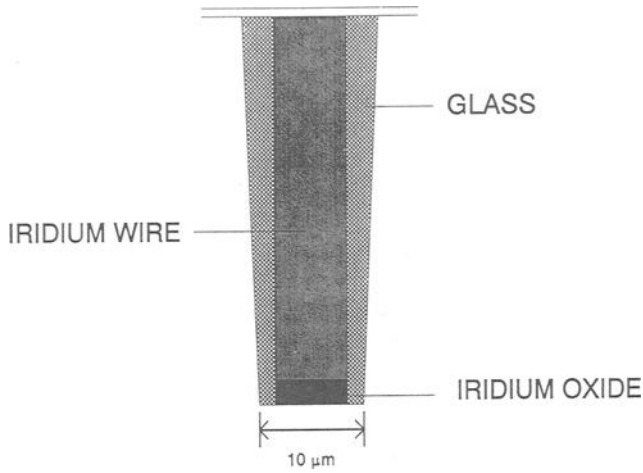

FIG. 1—*Tip of an iridium oxide pH microelectrode.*

Aging the Electrode—The pH-sensitive oxide is composed of hydrous and anhydrous iridium oxides. The degree of hydration changes with time causing a drift in calibration [*12*]. Furthermore, there is little consistency in the measured slope (mV/pH) for electrodes prepared using a single process. For electrochemically prepared electrodes, Kinoshita et al. [*13*] report 69.7 mV/pH-unit and Hitchman and Ramanathan [*14*] report 81.9 mV/pH-unit at 25°C. Our measurements indicated an initial slope of 77.3 mV/pH-unit that decreased after one week to 65.8 mV/pH-unit. Because the greatest change in oxide hydration occurs during the first 12 hours of equilibration [*12*], electrodes were aged in distilled water for 12 hours followed by aging in air for 2 hours. Data collected four times during the course of one week are shown in Fig. 2. Electrodes were stored in air.

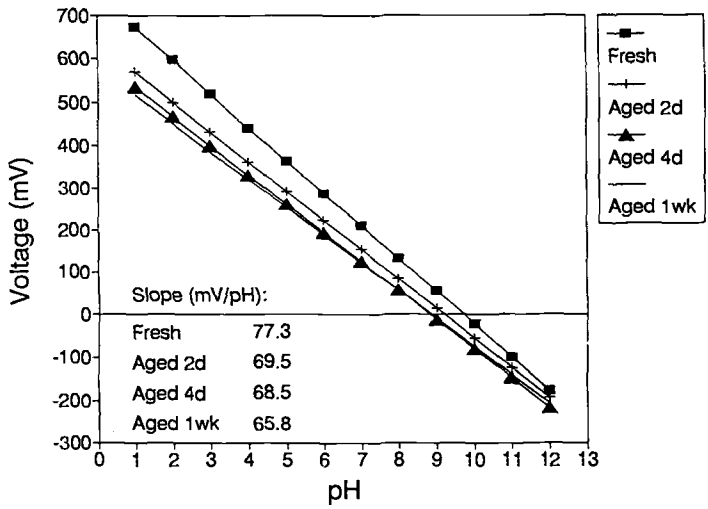

FIG. 2—*The effect of aging on pH response of an iridium/iridium oxide microelectrode.*

Calibration—Experimentation has shown that the internal impedance of iridium/iridium oxide microelectrodes can be as much as 10^{10} Ω. An electrometer with a minimum input impedance of 10^{12} Ω is used to measure the microelectrode potential relative to a reference electrode. This high impedance ensures that the meter does not load the electrode. A meter with an input impedance comparable to, or less than, 10^{10} Ω would produce inaccurate results by acting as a voltage divider. A low impedance volt meter can also damage the sensor by allowing current to flow through it. As a final caveat, the sensor should never be short-circuited to the reference electrode while both are in solution, since the voltage difference would cause current to flow and damage the electrode.

A World Precision Instruments model FD 223 electrometer (impedance = 10^{15} Ω) was used to measure pH from 1 to 12. The reference was Ag/AgCl with an internal fill solution of Ag^+ saturated 3M KCl. The Nernstian slope was 77.3 mV/pH-unit and E° was 751 mV. Slopes of 70 to 80 mV/pH unit were typical of freshly prepared electrodes. As noted above, slopes usually settled to ≈65 mV/pH-unit after several calibrations and uses, or both, as reported above. Response was immediate for most pH buffers.

Although Midgley [*15*] reported that the iridium/iridium oxide pH electrode was not sensitive to Fe^{2+} and Fe^{3+} ions, we found that the presence of Fe^{2+} did influence the response of the electrode. Increasing the ferrous ion concentration led to underestimating the acidic nature of the media by, at most, one pH unit. Valid qualitative conclusions can be drawn in spite of this interference.

Surface Mapping pH Near the Metal Surface

An iridium/iridium oxide pH microelectrode was used to map pH over metal coupon surfaces. The coupons were mounted in the bottom of a rectangular polycarbonate vessel located on an XY-axis positioning table. The pH microelectrode was mounted on the shaft of a stationary Z-axis positioner above the coupon. The polycarbonate vessel was filled with artificial sea water (Instant Ocean™ Aquarium Systems, Mentor, OH), and guided under computer control in a plane perpendicular to the stationary pH probe. Measurements taken at 100 μm intervals in two dimensions were used to construct an evenly spaced grid of pH data. The experimental apparatus is shown schematically in Fig. 3. All corrosion and surface mapping took place at room temperature.

XYZ micropositioner—The micropositioning system was manufactured by Micro Kinetics (Laguna Hills, CA). The XY table consisted of an X-Y stage with 4 in. travel driven by two encoder motors with gear heads. The Z-positioner consisted of a Drivemaster™ (Microkinetics) positioner with a gear ratio of 1670:1 and a maximum travel of 1 in. The XYZ-positioning system had a resolution of 0.1 μm. A three axis motor controller, connected to a personal computer through an RS232 serial interface, provided control of the positioning motors. Custom software integrated the motion of the positioner with collection of data. The large matrix of pH versus X and Y coordinates was plotted in three dimensions using Graph Tools™ (3D Vision Corp. Torrance, CA) software.

Polycarbonate reaction vessel—Mild steel coupons (diameter = 1.6 cm) were embedded in threaded PVC plugs using epoxy cement. A reaction vessel was made of 1.27-cm-thick polycarbonate. The vessel was 5-cm square and 2-cm deep with a raised bottom into which the coupons were mounted (Fig. 3).

Coupon preparation—The coupons, which had been previously mounted in PVC plugs, were cleaned and brought to near-mirror smoothness by polishing with graded silicon carbide sand papers down to a 1200 grit coarseness. They were then rinsed with distilled water and air dried.

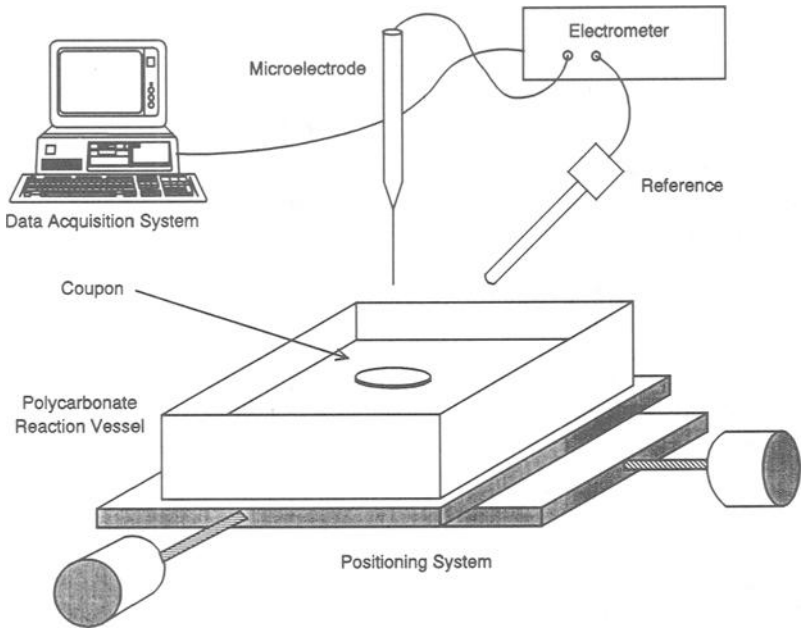

FIG. 3—*Experimental apparatus.*

Control coupon—Localized corrosion was induced on a clean bare mild steel coupon surface by masking all but a portion of it (0.04 cm^2) with water proof tape and immersing it in artificial seawater (Instant Ocean) for approximately 8 h at room temperature. This procedure created intense localized corrosion in the exposed region. The tape was removed just before scanning.

Corrosion of a coupon coated with a spot of calcium alginate gel—Another clean, bare, mild, steel coupon was also masked with waterproof vinyl tape except for a 0.04 cm^2 area in the middle of the coupon. The exposed area was sprayed with 0.4% sodium alginate using an artists air brush. The coupon was then submerged in 1M $CaCl_2$ for 45 to 60 min to complete cross-linking of the biopolymer gel. The estimated thickness of the coating was 40 μm. Finally, the tape was removed and the coupon placed in artificial sea water for 8 h.

Scanning procedure—The procedure for scanning was the same for both the control coupon and for the alginate coated coupon. The vessel holding the corroded coupon and the pH microelectrode (tip diameter = 50 μm) was positioned on the 3-D table for the scan. The electrode, as viewed through a binocular microscope, was moved to within approximately 50 μm of the metal surface using the 3-D positioner and held at that height (stationary z-axis) for the entire scan. There was no visible agitation of the solution in the reactor during scanning. The pH microelectrode was referenced to a silver/silver chloride electrode. The potential proportional to pH was measured with a Keithley Model 617 programmable electrometer that has an analog output proportional to the input from the electrode. This output was connected to a Keithley/Metrabyte model DAS-8 data acquisition board mounted in a Zenith 486DX PC. A map consisted of a matrix of data points, 40 rows by 40 columns, scanned one row at a time. Each row was scanned from the same direction to eliminate hysteresis in mechanical positioning. The mapped region covered the entire exposed portions of the coupons.

Results and Discussion

Each coupon exhibited visually distinct regions after 8 h exposure to seawater. The control coupon displayed a reddish-orange deposit over its entire 0.04 cm^2 exposed surface, indicating significant corrosion. The coated region of the alginate-coated coupon also displayed a reddish-orange deposit indicative of corrosion, while the region outside of the coating appeared uncorroded.

Figure 4 shows a map of experimental pH data for the control coupon. The data is displayed in two formats; first, as a 3-D plot, and second, as a contour plot projected below the 3-D representation. The dip in pH matches the visible corrosion spot on the coupon. Figure 5 shows the map of experimental pH data for the calcium alginate coated coupon and is displayed in the same formats.

The entire exposed region of the control coupon displayed low pH values as well as visible corrosion. High pH was observed only at the edge of the exposed region.

Similar results were obtained for the calcium alginate coated surface. The reddish-orange cast, indicative of corrosion, rapidly developed in association with the alginate-coated zone; pH was lower above the same region. These observations were consistent with a rapidly corroding surface underneath the alginate, and a simultaneous transport of hydrogen ions through the alginate gel to the bulk water. Outside of the alginate coated zone, corrosion was less and the associated drop in pH was significantly lower.

The corrosion regions and associated pH differences were not unexpected on metal surfaces with both anodic and cathodic sites. The local interfacial equilibrium chemistry can be represented by Eqs 1 through 4.

$$Fe^0 \rightarrow Fe^{2+} + 2e^- \qquad \text{anodic region} \qquad (1)$$

$$Fe^{++} + 2H_2O \rightarrow Fe(OH)_2 + 2H^+ \qquad \text{hydrolysis} \qquad (2)$$

$$2Fe(OH)_2 + 1/2\ O_2 \rightarrow Fe_2O_3 + 2H_2O \qquad \text{further oxidation} \qquad (3)$$

$$2e^- + H_2O + 1/2\ O_2 \rightarrow 2OH^- \qquad \text{cathodic region} \qquad (4)$$

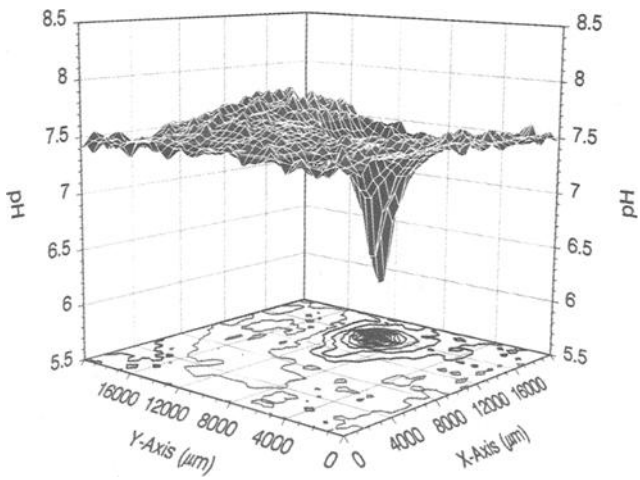

FIG. 4—*3D-map of pH at a fixed height (50 μm) above the surface of a freely-corroding mild steel coupon.*

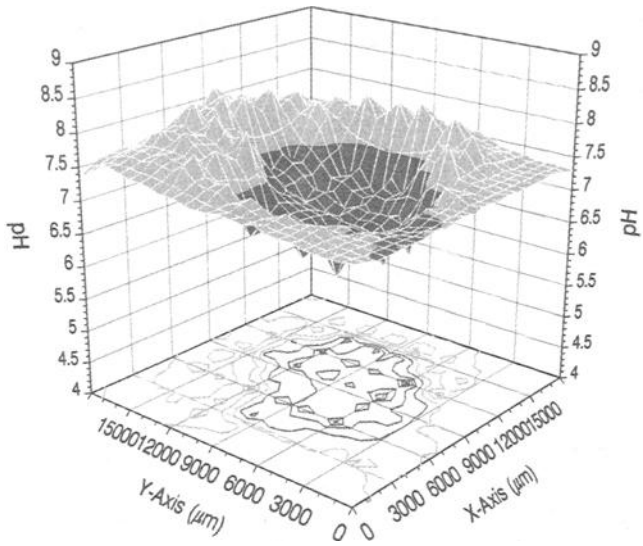

FIG. 5—*3D-map of pH at a fixed height (50 μM) above a calcium-alginate spot on a mild steel coupon.*

Comparing the two coupons revealed that corrosion in the uncoated region of the alginate-coated coupon was not as intense, nor did it develop as rapidly, as did corrosion on the control coupon. Both coupons were exposed to seawater for approximately the same length of time. In addition, pH above the control coupon was considerably lower than pH above the uncoated region of the alginate-coated coupon. It appears that the alginate coating stimulates formation of an anodic region beneath the coating that inhibits corrosion in the surrounding area. This preliminary observation is consistent with the concept that a patchy biofilm creates an electrochemical environment conducive to corrosion.

It is possible that the alginate coating on the coupon limits oxygen transport to the metal surface and, hence, creates a differential aeration cell [*16*]. In the bare area, this would encourage hydroxide ion generation and cathodic behavior, while in the alginate-coated region, anodic behavior and corrosion would result. This appears to be the case even though oxygen transport to metal below the alginate coating was expected to be nearly the same as that in the uncoated region, that is: (1) the system was stagnant and there was little or no convective mixing, (2) the alginate coating was thin, on the order of 100 μm; and (3) for small molecules, diffusion coefficients in calcium-alginate gels are nearly the same as in water [*17*]. LaQue [*18*] demonstrated that very small differences in oxygen mass transport, such as those created on rotating disks in aerated water, can produce differential aeration cells resulting in pronounced corrosion. Consequently, the very small oxygen gradients expected in our system could produce differential aeration cells similar to those seen by LaQue.

Another observation may suggest a second contributing factor. When the coupon is dried, the alginate coating can be peeled off the metal surface. And, when this is done, the red-orange ferric oxide remains with the alginate, exposing a bare, but somewhat dull, metal surface. It appears that the ferric oxide forms in the calcium-alginate gel rather than at the metal surface.

Alginic acid is a naturally occurring linear polymer consisting of manuronic and guluronic acid subunits. Each acid contains a carboxylic acid functional group. The affinity of calcium

alginate for divalent metal ions is well documented [*19–21*]. It is possible that in the presence of alginate gel, Eqs 2 and 3 can be expanded

$$\text{Alg-Ca} + \text{Fe}^{2+} \rightarrow \text{Alg-Fe} + \text{Ca}^{2+} \quad (5)$$

$$\text{Alg-Fe} + 1/4\ \text{O}_2 + \text{H}_2\text{O} \rightarrow 1/2\ \text{F}_2\text{O}_3 + 2\text{H}^+ + \text{Alg}^{2-} \quad (6)$$

$$\text{Alg}^{2-} + \text{Ca}^{2+} \rightarrow \text{Alg-Ca} \quad (7)$$

In Eqs 5 through 7, Alg is a binding site for a divalent metal ion in the alginate-gel polymer. It is possible that the Alg-complexed ferrous ion could oxidize more rapidly than the soluble hydrated ion, which is a catalytic effect. From mass action considerations, the decreased ferrous ion concentration could promote corrosion underneath the alginate coating.

These results may have significant implications for the mechanism of microbially influenced corrosion (MIC). If biopolymer alone can stimulate corrosion, then merely killing the microorganisms that form a biofilm will not stop MIC. In addition, if this is the principal mechanism for MIC, then there is little need to search for a mechanism involving viable organisms; instead, one should study the role of structural heterogeneity (patchiness) of biofilms in MIC.

Conclusions

(1) The pH distribution above a corroding mild steel coupon was measured using an iridium oxide microelectrode in conjunction with a computer-controlled micropositioning system.

(2) Variations in pH were correlated with visible corrosion sites on the coupon. As expected, corrosion was associated with anodic regions of low pH adjacent to cathodic regions of high pH.

(3) Preliminary observations indicated that the presence of a calcium-alginate gel spot on the surface of mild steel influenced the corrosion process: (a) the mild steel surface under the gel spot corroded faster than the surrounding bare area and (b) the area surrounding the gel spot corroded more slowly than the surface of a bare-control coupon.

(4) Accelerated corrosion under the biopolymer gel could be due to either a differential aeration cell (crevice corrosion), or complexation of ferrous ion by the alginate gel, or some combination of the two processes.

References

[*1*] Little, B. J., Wagner, P. A., Characklis, W. G., and Lee, W., *Biofilms,* W. G. Characklis and K. C. Marshall, Eds., John Wiley & Sons, New York, NY, 1990, pp. 635–670.

[*2*] Ford, T. and Mitchell, R., "The Ecology of Microbial Corrosion," *Advanced Microbial Ecology,* Vol. 17, 1990, pp. 231–262.

[*3*] Buchannan, R. A. and Stansburg, E. E., "Fundamentals of Coupled Electrochemical Reactions as Related to Microbially Influenced Corrosion," Proceedings, *Microbially Influenced Corrosion and Biodeterioration,* Knoxville, TN, Oct. 1990, N. J. Dowling, M. W. Mittleman, and J. C. Danko, Eds., University of Tennessee, Knoxville, 1990, pp. 1.11–1.17.

[*4*] Uhlig, H., *Corrosion and Corrosion Control,* John Wiley and Sons, New York, NY, 1971, p. 92.

[*5*] Bonnel, A., Dabosi, F., Deslouis, C., Duprat, M., Keddams, M., and Tribollet, B., "Corrosion Study of Carbon Steel in Neutral Chloride Solutions by Impedance Techniques," *Journal of the Electrochemical Social Society,* Vol. 130, 1983, p. 753.

[6] Hernandez-Deque, G., Pedersen, A., Thierry, D., Hermansson, M., and Kucera, V., "Bacterial Effects of Corrosion of Steel in Seawater," Proceedings, *Microbially Influenced Corrosion and Biodeterioration*, Knoxville, TN, Oct. 1990, N.J. Dowling, M. W. Mittleman, and J. C. Danko, Eds., University of Tennessee, Knoxville, 1990, pp. 2.41–2.51

[7] Smith, C. A., Compton, K. G., and Coley, F. H., "Aerobic Marine Bacteria and the Corrosion of Carbon Steel in Sea Water," *Corrosion Science*, Vol. 13, 1973, p. 677.

[8] Pope, D., Duquette, D., Wayner, P. C., Jr., and Arland, H. J., *Microbiologically Influenced Corrosion: A State-of-the-Art Review*, MTI Publication 13, Materials Technology Institute of the Chemical Process Industries, Inc., St. Louis, MO, June 1984.

[9] Iverson, W. P., "Microbial Corrosion of Iron," *Microbial Iron Metabolism*, J. B. Nieland, Ed., Academic Press, New York, NY, 1974, pp. 475–512.

[10] Costerton, J. W. and Boivin, J., "The Role of Biofilms in Microbial Corrosion," Proceedings, *Microbially Influenced Corrosion and Biodeterioration*, Knoxville, TN, Oct. 1990, N. J. Dowling, M. W. Mittleman, and J. C. Danko, Eds., University of Tennessee, Knoxville, 1990, pp. 5.85–5.89.

[11] VanHoudt, P., Lewandowski, Z., and Little, B., "Iridium Oxide pH Microelectrode," *Biotechnology and Bioengineering*, Vol. 40, 1992, pp. 601–608.

[12] Burke, L. D., Mulcahy, J. K., and Whelan, D. P., "Preparation of an Oxidized Iridium Electrode and the Variation of its Potential with pH," *Journal of Electroanalytical Chemistry*, Vol. 163, 1984, p. 117.

[13] Kinoshita, E., Ingman, F., Edwall, G., Thulin, S., and Glab, S., "Polycrystalline and Monocrystalline Antimony, Iridium and Palladium as Electrode Material for pH-Sensing Electrodes," *Talanta*, Vol. 33, 1986, pp. 125–134.

[14] Hitchman, M. L. and Ramanathan, S., "Evaluation of Iridium Oxide Electrodes Formed by Potential Cycling as pH Probes," *Analyst*, Vol. 113, 1988, pp. 35–39.

[15] Midgley, D., "A Review of pH Measurements at High Temperature," *Talanta*, Vol. 37, No. 8, 1990, pp. 767–781.

[16] Jones D., *Principles and Prevention of Corrosion*, MacMillan Publishing Company, New York, 1992, pp. 189–196.

[17] Tanaka, H., Matsumura, M., and Veliky, I. A., "Diffusion Characteristics of Substrates in Ca-Alginate Gel Beads," *Biotechnology and Bioengineering*, Vol. 26, 1984, pp. 53–58.

[18] Laque, F. L., "Theoretical Studies and Laboratory Techniques in Sea-Water Corrosion Testing Evaluation," *Corrosion*, Vol. 13, 1957, p. 303.

[19] Jang, L. K., Brand, W., Resong, M., Mainieri, W., and Geesey, G. G., "Feasibility of Using Alginate to Absorb Dissolved Copper from Aqueous Media," *Environmental Progress*, Vol. 9, 1990, pp. 269–274.

[20] Smidsrød, O. and Haug, A., "Dependence Upon Uronic Acid Composition of Some Ion-Exchange Properties of Alginates," *Acta Chemica Scandinavica*, Vol. 22, 1968, pp. 1989–1997.

[21] Smidsrød, O., "Molecular Basis for Some Physical Properties of Alginates in the Gel State," Faraday Discussions of the Chemical Society, Vol. 57, 1974, pp. 263–274.

Gabriele Salvago,[1] *Giorgio Taccani,*[1] *and Gabriele Fumagalli*[2]

Review of Effects of Biofilms on the Probability of Localized Corrosion of Stainless Steels in Seawater

REFERENCE: Salvago, G., Taccani, G., and Fumagalli, G., **"Review of Effects of Biofilms on the Probability of Localized Corrosion of Stainless Steels in Seawater,"** *Microbiologically Influenced Corrosion Testing, ASTM STP 1232,* Jeffery R. Kearns and Brenda J. Little, Eds., American Society for Testing and Materials, Philadelphia, 1994, pp. 70–95.

ABSTRACT: Measurements have been made of pH values in the layer adjacent to fine-meshed screens immersed in artificial and natural seawater. The results obtained on platinum, bronze, nickel-based alloys, stainless-steel and carbon-steel screens indicate that acidic environments can be formed beneath the biofilm on even cathodically polarized metallic materials. From an examination of data regarding the exposure of different materials in galvanic couples to natural and artificial environments, it seems clear that stainless steels exposed to the acidification of the artificial environment:

(1) leads to depolarization phenomena of the cathodic processes, with effects qualitatively but not quantitatively similar to those observed in natural seawater; and
(2) enhances the localized corrosion onset probability, though the attack penetration depth is lower than values observed in natural seawater.

The different procedures for obtaining polarization curves in seawater, as well as the significance of the numeric values achieved, are discussed herein. The electrochemical complexity of biofilms is emphasized. Some aspects of the biofilms formed on stainless steel exposed to seawater are similar to those observed for conductive polymer films, such as polypyrroles.

KEYWORDS: marine corrosion, biofilm, pH, polypyrrole, stainless steel, electrochemical techniques, localized corrosion, microbiologically influenced corrosion (MIC)

It is well known that one of the greatest limitations in the use of stainless steels in marine environments is their susceptibility to localized corrosion. Though studies on passivation phenomena date back to the Industrial Revolution [*1*], the scientific problem of the passive film breakdown and subsequent onset of localized corrosion, even in solutions merely containing sodium chloride, is still widely discussed [*2*]. In seawater, and, more generally, in biologically active environments, the problem is complicated further, compared to sodium-chloride solutions, by the presence of biofilms.

Engineering, chemistry-physics, and biology are interconnected, and among themselves, interactive. Different authors, with different cultural backgrounds, give their contribution in the solution of these problems, each of them emphasizing one aspect over the other.

At present, several microbiologically influenced corrosion (MIC) researchers have considered the pH variations that could take place through the biofilms formed at sea on the

[1] Professor and corrosion research engineer, respectively, CNR-ITM Via Bassini 15, 20133 Milano, Italy.
[2] Doctor, CNR-CESPEL Politecnico di Milano, P.za L. da Vinci 32, 30133 Milano, Italy.

different materials [*3–7*]. Such pH variations have been related to hypothetical modifications of the oxygen-reduction cathodic process [*3*] and the different susceptibility to localized corrosion exhibited by stainless steels in seawater compared to abiotic sodium-chloride solutions.

Therefore, it seemed to be quite interesting to consider the following aspects:

- methodology of pH measurement near metallic surfaces,
- correlation between cathodic polarization curves and kinetic aspects of cathodic processes, and
- electrochemical characterization of biofilms.

Moreover, it seemed to be useful to consider localized corrosion susceptibility of stainless steels as if it were divided into two distinct phases or periods, one relating to the onset probability of localized corrosion and the other pertaining to the penetration rate of the corrosive attack.

pH Values at a Metal/Environment Interface

Effect of pH on Cathodic Process

pH changes, as well as any changes in the oxygen content near the metal/environment interface, are connected to the system's heterogeneity. However, pH changes cannot affect any values regarding homogeneous equilibrium conditions such as the equilibrium voltage of the oxygen-reduction cathodic process. This value depends only on the initial and the final state of the system under steady-state conditions. In this specific case, the voltage for cathodic reduction depends on the oxygen content and on pH value in the bulk solution. However, the characteristics of the metal/environment interface can play an essential role concerning the kinetic aspects of the various processes and the relation to corrosion.

No general agreement has been reached yet on the effects of the biofilm on pH variations. Certain authors hypothesize the activity of acidification phenomena at the metal/biofilm [*3–5,7*] interface, whereas others [*6*] hypothesize the predominance of alkalinization phenomena. Surface acidification phenomena have been called up to justify the ennoblement of corrosion potential for stainless steels exposed to seawater in absence of localized corrosion [*3,5*].

Depolarization effects of the cathodic-oxygen reduction process observed on stainless steels exposed to seawater have been thought to be either favored by surface alkalinization by some authors [*6*] or connected to surface acidification phenomena by other authors [*7*]. As far as the kinetics of the cathodic oxygen-reduction process on stainless steel is concerned, some similarities have been observed in the behavior between natural seawater at pH values near 8.2 and abiotic artificial seawater at pH near 4. These similarities in cathodic properties have been connected to possible variations of electronic properties of the passive film [*7–9*].

Certain authors observe acidification phenomena in biotic solutions as a result of biological processes [*10–11*] and even in solutions taken beneath the fouling layer on cathodically protected metallic materials exposed to marine environments [*12*].

Other authors tried to measure pH variations, using microelectrodes, near electrically polarized metallic surfaces in artificial environments [*13–15*] or natural seawater [*16*].

If pH measurements are to be made at metal/biofilm interface, the only practical techniques are those of the potentiometric types. This is because the pH measurements obtained by optical, colorimetric techniques, as well as various sampling techniques would not be at the metal/biofilm interface [*17*].

In potentiometric techniques, pH measurement consists of measuring the potential difference between an electrode (the potential of which is dependent on the activity of H^+ ions) and a reference electrode (the potential of which is not dependent on the activity of H^+ ions). Any potential changes, even not related to variations in the activity of H^+ ions would be misinterpreted by the measurement system as connected to variations in the activity of H^+ ions.

Therefore, pH measuring techniques that utilize an H^+ sensitive electrode macroscopically separated from the reference electrode, cannot provide reliable pH measurements in proximity of surfaces subject to current flows. Such current flows can even be caused by superficial inhomogeneities and could give rise to a net balance between cathodic and anodic currents. This is the case for many metallic materials exposed to seawater under free corrosion conditions, due to the patchy nature of the biofilm [*18–19*].

pH Measurement

Therefore, in order to experimentally measure the pH value at the metal/biofilm interface, we have used a technique that has been used by other authors [*20*] to measure pH values at cathodes during metallic electrodeposition.

Several alloys have been used in the form of fine-mesh screens (Fig. 1). These screens have the greatest mesh values among those commercially available:

bronze:	185 mesh, wire diameter 0.05 mm,
UNS S30400:	185 mesh, wire diameter 0.05 mm,
carbon steel:	55 mesh, wire diameter 0.11 mm,
UNS N06600:	350 mesh, wire diameter 0.032 mm, and
platinum:	85 mesh, wire diameter 0.06 mm,

For pH measurement, a flat-bottomed glass electrode and a calomel reference electrode have been pressed against the same side of a metallic screen (26 mm in diameter) (Fig. 2(*a*)). On the other side, a reference electrode has been positioned to measure the potential of the metallic screen. A counter-electrode has been positioned in order to perform cathodic or anodic polarizations at the desired value. The system described above is able to measure an average pH value within a layer adjacent to the screen comparable in size to that of the wire diameter even if the metallic screen is to be electrically polarized [*20*].

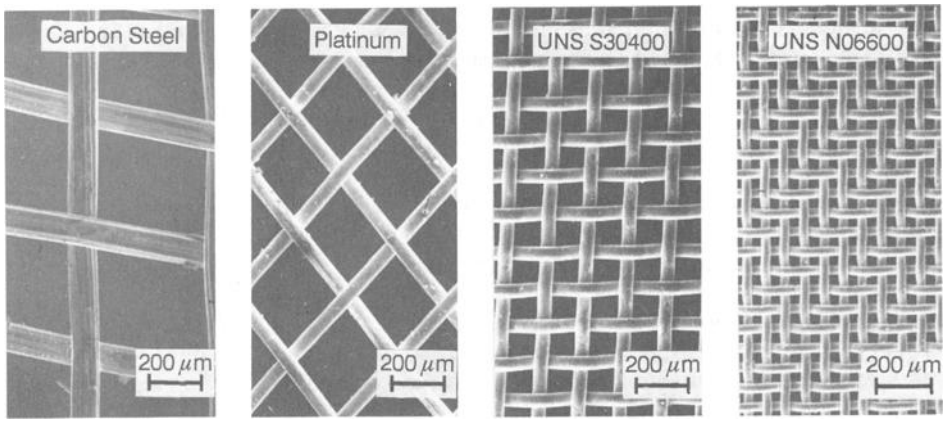

FIG. 1—*Metallic wire screens used as specimen.*

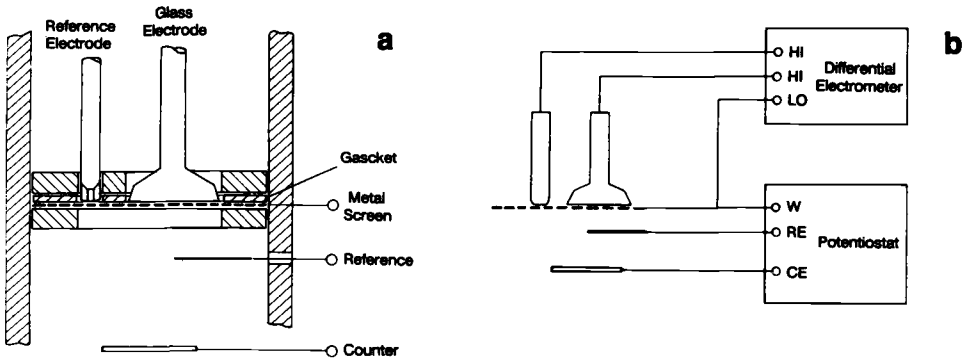

FIG. 2—*Schematic arrangement of apparatus for pH measurement near a screen electrode.*

When measuring the potential difference between the glass electrode and the calomel reference electrode, a normal floating pH-meter is used. The metallic screen is connected as the working electrode to a floating ground. Significant deviations of pH value can be observed. Any instrument noises or errors have been eliminated using high-impedance differential electrometer following the scheme of Fig. 2(*b*).

The cell shown in Fig. 2 was positioned vertically inside a 5 L container. The container was continuously fed to renew the solution ten times per h. On the feed line, a combined glass electrode was positioned for pH control in the solution. The electric continuity of the waste-line was interrupted by an adequate dripping system of the solution.

Results of pH Measurement in Artificial Seawater

In the tests performed in artificial seawater (ASTM D 1141 Specification for Substitute Ocean Water, pH = 8.2) and under free-corrosion conditions, corrosion-resistant materials exhibited no significant pH variations in the layer near the metallic screen.

Again, in artificial seawater, but under cathodic polarization conditions, cathodic polarization currents tended to decrease in time and to oscillate. The oscillation was more significant at lower polarization potentials. pH-values on the layer adjacent to the electrode tended to increase with time by increasing the average value of the cathodic current. The typical trends of stainless steel are shown in Fig. 3. The behavior of the other corrosion-resistant alloys only slightly differed from that described for stainless steel; see the case of platinum reported in Fig. 4. The differences observed could be easily explained by taking into account the different cathodic behaviors of the various materials and the different mesh sizes that led to different thicknesses for the layer in which the pH was measured [*20*].

Under anodic polarization conditions, the pH value in the layer adjacent to the screen tends to decrease in time; the more it decreases, the higher the anodic current density is. Particularly notable pH reductions have been observed in artificial seawater on stainless steel at the initiation of crevice corrosion (Fig. 5).

A far different behavior is presented by carbon steel. Under free corrosion condition in artificial seawater, the pH value near the screen exhibits an oscillating trend (Fig. 6). Some alkalinization phenomena within the layer adjacent to the metallic surface are initially present, even under anodic dissolution conditions. Acidification phenomena appear to become particularly important at the same time of passivation phenomena (Fig. 7).

For all the materials considered in artificial seawater and in absence of localized corrosion, the pH value measured in the layer near metallic screen depended on the metallic material, the mesh size, and the log of the current (Fig. 8).

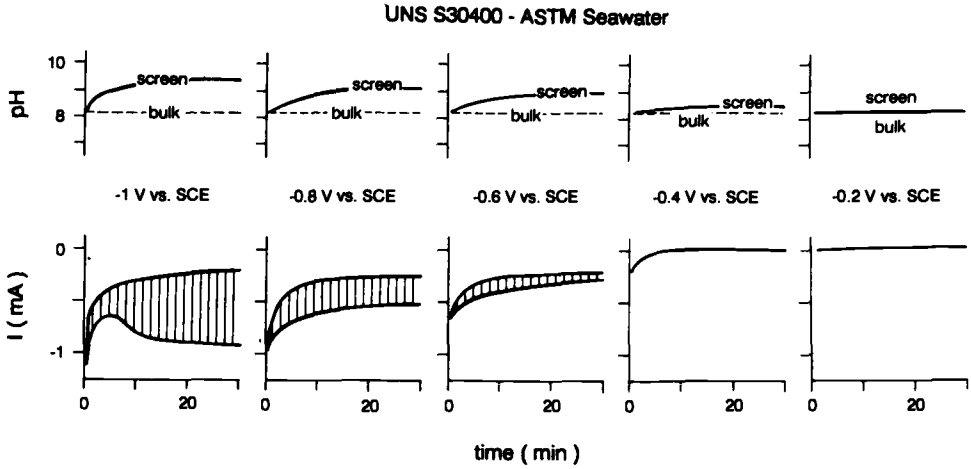

FIG. 3—*Polarization currents and near-screen-pH versus time curves for UNS S30400 stainless steel screens in ASTM D 1141 seawater at different polarization potentials.*

Results of pH Measurement in Natural Seawater

In our tests performed in natural seawater, the involved phenomenology was completely different from that described for artificial seawater. Parallel and repeated measurements were, at best, only qualitatively reproducible.

Under free-corrosion conditions, there is a general tendency leading to acidification phenomena within the layer near the metallic screen. This is the case regardless of the nature

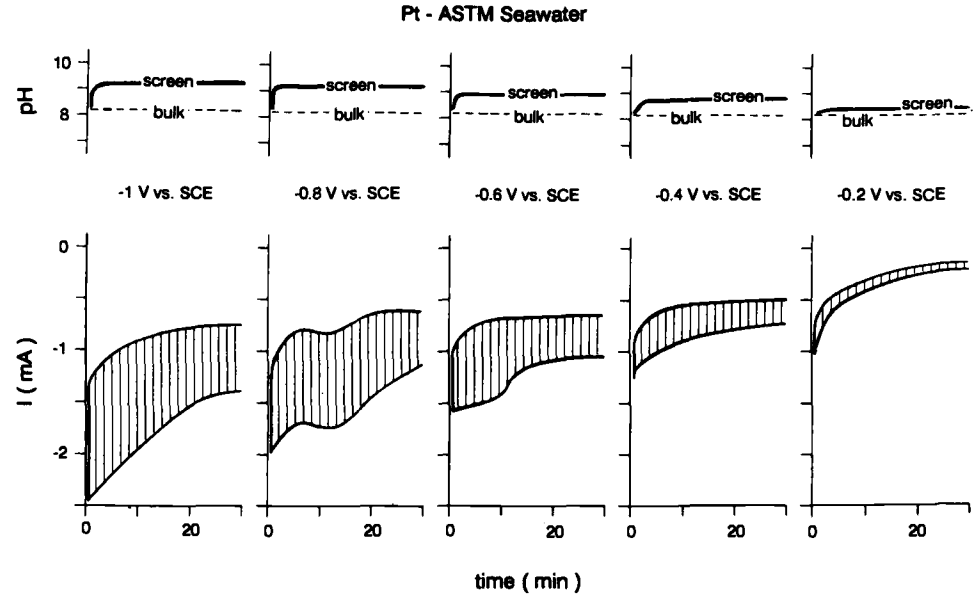

FIG. 4—*Polarization currents and near-screen pH versus time curves for platinum screen in ASTM seawater at different polarization potentials.*

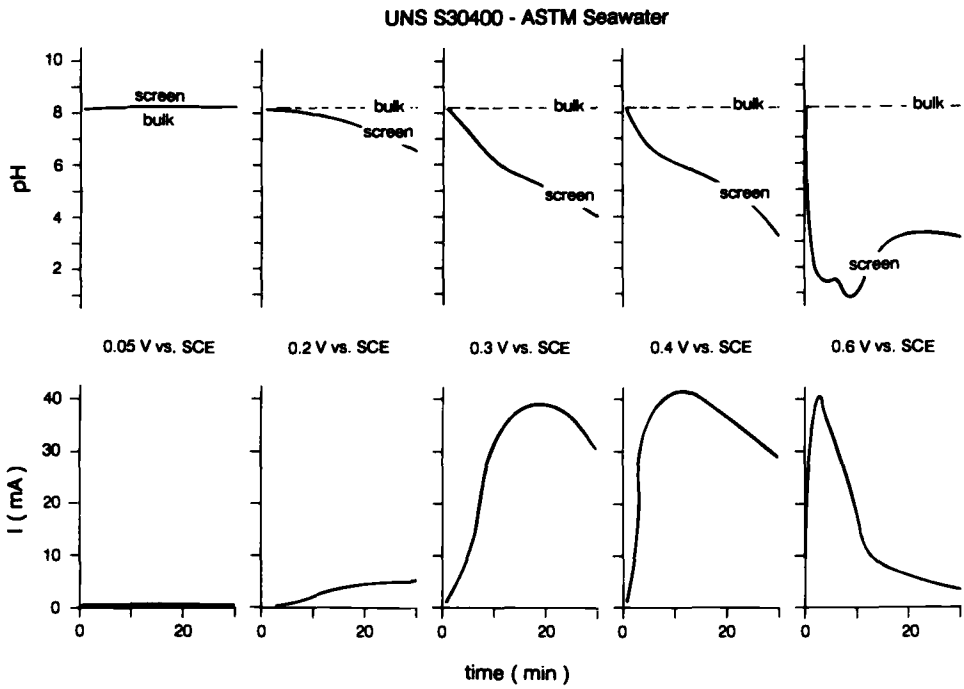

FIG. 5—*Aodic polarization currents and near-screen-pH versus time curves for UNS S30400 stainless steel screens in ASTM seawater.*

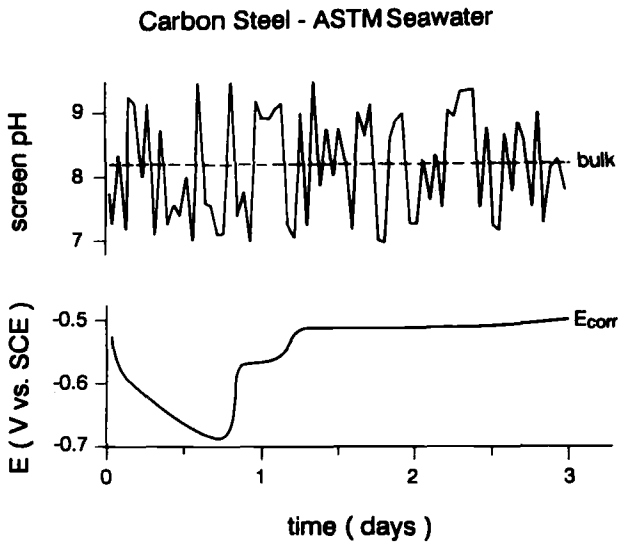

FIG. 6—*Near-screen-pH and free corrosion potentials versus time curves for carbon-steel screens in ASTM seawater.*

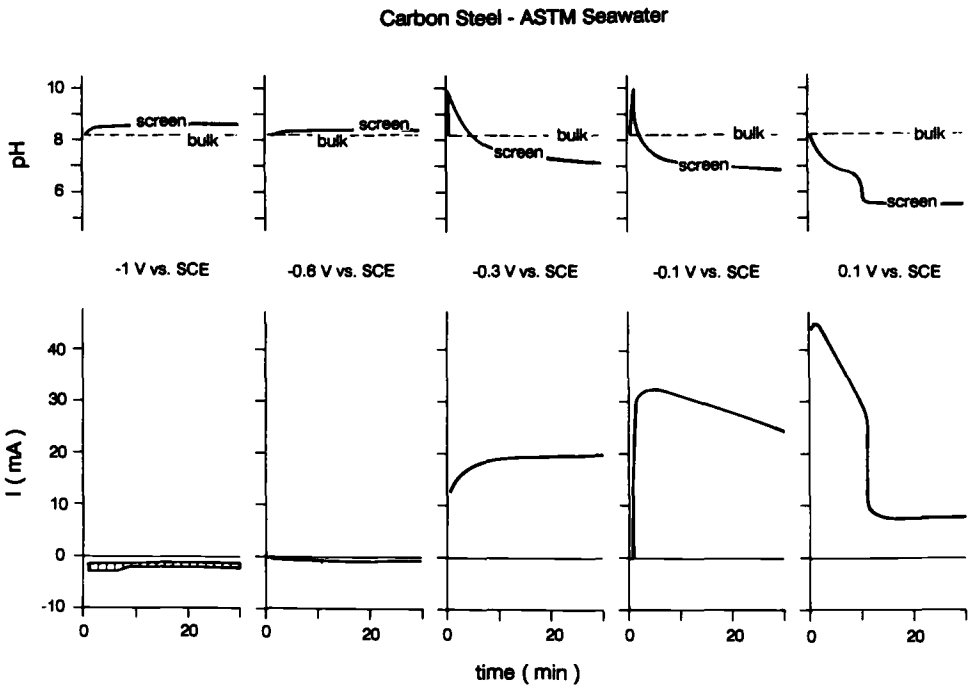

FIG. 7—*Near-screen-pH and polarization currents versus time curves for carbon-steel screens in ASTM seawater.*

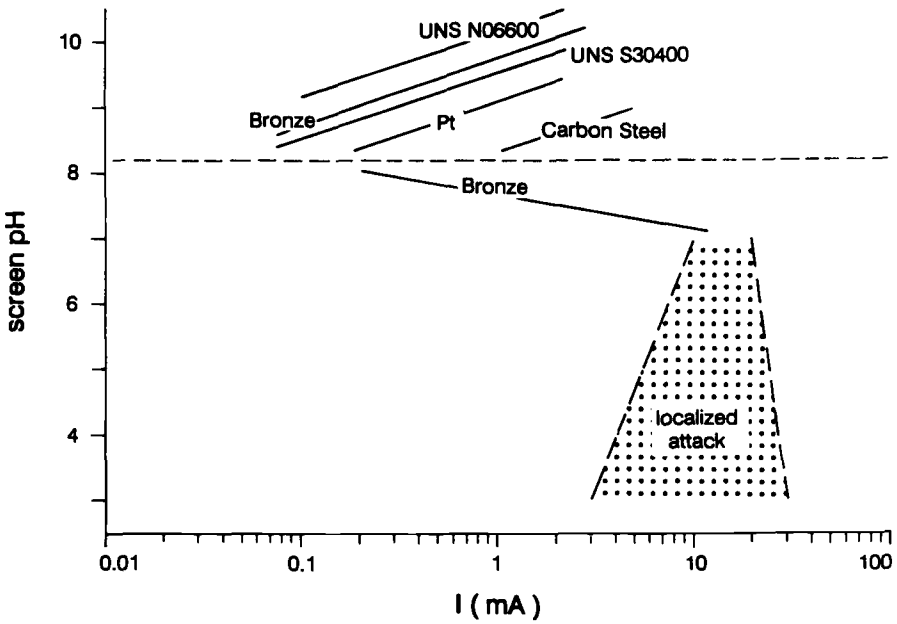

FIG. 8—*Near-screen-pH versus polarization currents for different screens.*

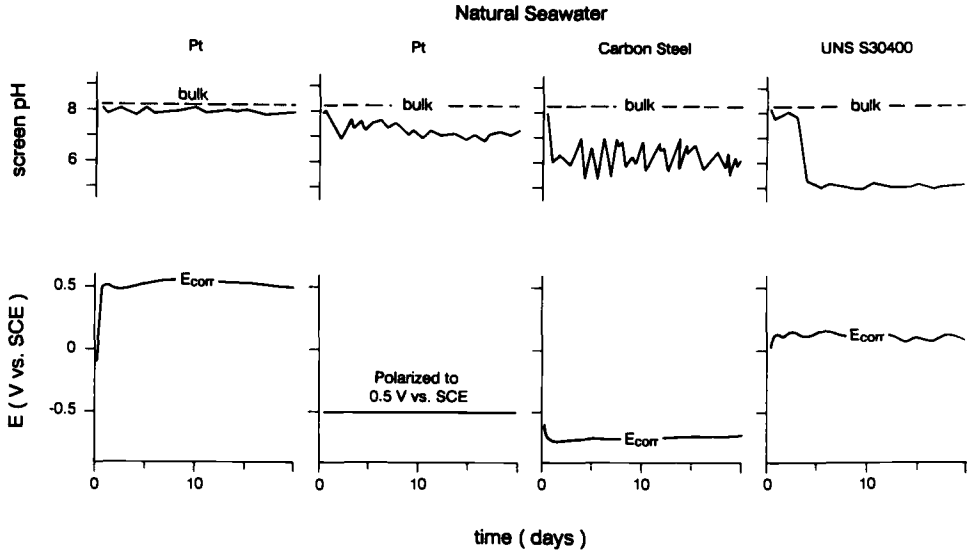

FIG. 9—*Near-screen-pH versus time and free corrosion potentials curves for different screens in flowing natural seawater.*

of the material (Fig. 9) and even under cathodic polarization conditions, according to Ref *12*. Any disturbances in the hydrodynamic regime or in the polarization potential, regardless of their sign, seem to give rise to layer-transient acidification with scarcely reproducible values.

Anyway, our results confirm the presence of acidification phenomena not directly connected to current-flowing phenomena at metal surface in natural seawater. Moreover, such results suggest that the pH calculation models for the pH at polarized metal surfaces already developed [*16*], could not be applied to natural seawater.

Cathodic Polarization Curves and Oxygen-Reduction Kinetics on Stainless Steels in Seawater

Techniques for Recording Polarization Curves

The recording of polarization curves represents one of the traditional techniques used in the electrochemical study of corrosion phenomena. In this technique, the external current (J_e) flowing between a working electrode (W) and a counterelectrode is equal to the sum of the currents pertaining to all anodic and cathodic processes simultaneously operating on the working electrode.

The currents (J) are generally assumed to be proportional to the surface of the electrode and the results are expressed in terms of current density (i). Such an assumption is justified only in case of homogeneous surfaces and in absence of localized corrosion.

The current J_e depends on the potential of the working electrode (E^W) as well as on time, $J_e = J_e(E^W,t)$.

The potential of the working electrode can be artfully forced to vary in time, following any law $E^W = E^W(t)$, giving rise to potentiodynamic or potentiokinetic techniques. In these cases, the current J_e is a function of time $J_e = J_e(E^W,t) = J_e(E(t),t)$ although results are usually expressed in the form $i_e = i_e(E^W)$ or $E^W = E^W(i_e)$.

The potential of the working electrode can be artfully maintained constant and corresponding to a value $E^W = \bar{E}$ for a time $t = \bar{t}$, giving rise to potentiostatic techniques. The curve $i_e = i_e(E^W)$ can be constructed point by point, in relation to a given time $t = \bar{t}$. Assuming that the current value measured at a given potential tends to take constant values in time, that is $\lim_{t\to\infty} = (\delta J_e/\delta t)E^W = \bar{E} = 0$ then the curve $i_e = i_e(E^W)$ potentiostatically determined can be hypothesized regardless of time, at least for times exceeding a given value.

Under free-corrosion conditions, the sum of the currents relating to anodic processes equals that relating to cathodic processes and no external current (J_e) appears. Under conditions near free-corrosion conditions, external current cannot be considered as representative of the kinetics of cathodic or anodic processes, but only of their algebraic sum.

Effect of the Passivity Current

As far as stainless steels exposed to seawater and under passivity conditions are concerned, the passivity current values observed in a wide range of potential values are normally comprised between 0.01 and 1 $\mu A/cm^2$. In this case, cathodic polarization curves can be representative of the kinetics of cathodic processes, except for an error up to 1 $\mu A/cm^2$ due to the uncertainty on passive current density values.

The evolution of cathodic polarization curves observed by several authors on stainless steels exposed to seawater for increasing times, is not necessarily indicative of depolarization phenomena with time of cathodic processes. For external current density values lower than 1 $\mu A/cm^2$, it could only reveal some diminution with time of the passive current density.

Effect of the Passive Film Thickness Modifications

The thickness of passive films on stainless steels is in the order of 10 Å [*1–2*]. One Å per cm^2 corresponds to a volume of 10^{-8} cm^3. Assuming that the passive film has a density > 1 g/cm^3 and an equivalent weight < 100, it follows that to 1 Å thickness corresponds a superficial concentration $> 10^{-10}$ geq./cm^2 corresponding to a superficial charge of about 10^{-5} C/cm^2. Any variation < 1 Å in the passive film thickness can determine the flow of a charge amount exceeding 10 $\mu A \cdot s/cm^2$.

Accepting a 1 $\mu A/cm^2$ error in the current density measurement, what results is an error greater than 10 s in the time measurement. This can cause some difficulties in the interpretation of results obtained on stainless steels or other passivated materials, when using quick potential scanning techniques or the measurement of low current densities.

Figure 10 shows the effect of the presence of different passive films on the stainless steel surface on cyclic cathodic polarization curves and Fig. 11 shows the effect of sharp transition of cathodic polarization potential value on current.

Effect of Environmental Pollution

In natural environments, some dissolved substances in concentrations lower than 0.1 ppm can usually be considered as impurities and can be neglected by standard analytical tests.

Hypothesizing for the impurity an equivalent weight < 100, at a concentration of 0.1 ppm, corresponds to a concentration in equivalent $> 10^{-6}$ eq./L. If in seawater, the diffusion coefficient values for ions are approximately 10^{-5} cm^2 s^{-1} then the impurity maintains a diffusion limited current density approximately equal to $i_l = zFDc = 10^5 \cdot 10^{-5} \cdot 10^{-6}$ $A/cm^2 = 1$ $\mu A/cm^2$.

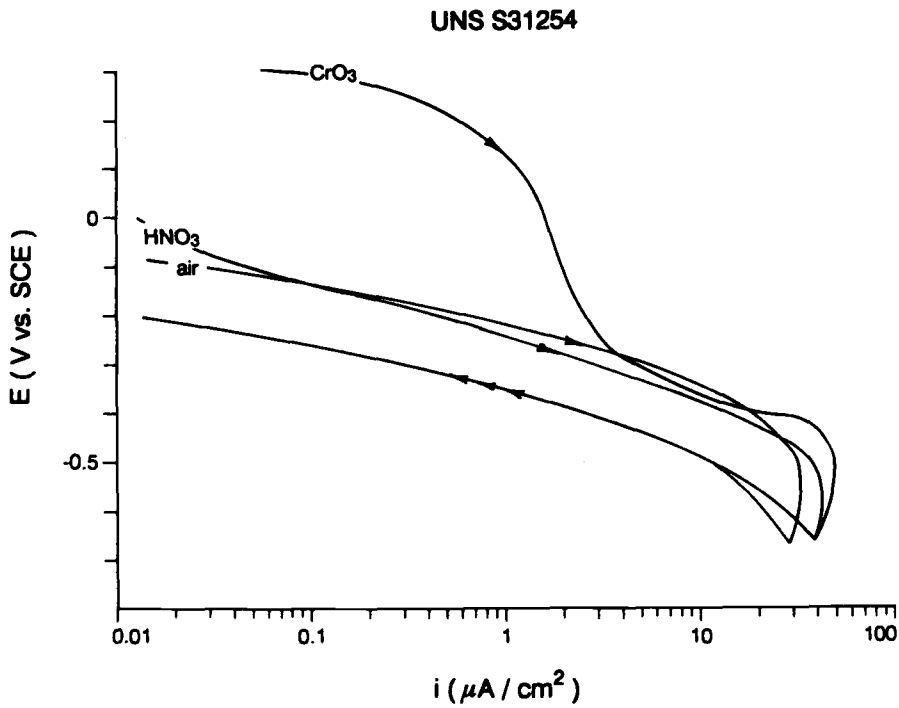

FIG. 10—*Cyclic cathodic polarization curves for UNS S31254 in 3.5% NaCl solution at 60°C after passivation treatment in different environments: air: 25°C, wet, relative humidity 100%, 100 h; HNO_3: 80°C, 2M HNO_3, 1 h; CrO_3: 45°C, 2.5 M CrO_3, 15 h.*

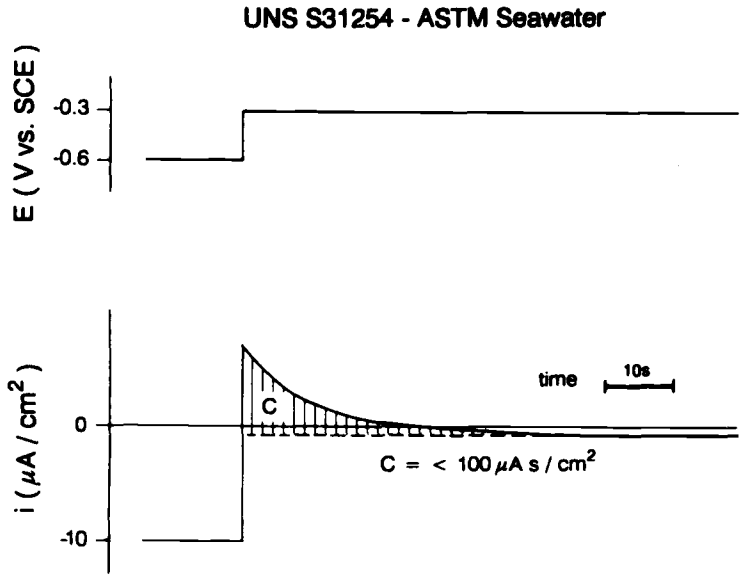

FIG. 11—*Polarization current on UNS S31254 in ASTM seawater after a sharp transition of polarization potential from −0.6 to −0.3 V versus saturated calomel electrode (SCE).*

Such current density can also be pointed out by polarization curves, but it cannot be associated with a given electrodic process unless the impurity is known. The values of such currents are of the same order of magnitude as the passivity current density values of stainless steels exposed to seawater and can therefore greatly affect free-corrosion potential.

In the event that impurities might deposit on the metallic surface, altering its characteristics, electrodic polarization curves can also be influenced. Let us consider the case of copper alloys, for which even occasional sulfide contamination leads to the depolarization of the anodic dissolution process and, to a greater extent, to the depolarization of the oxygen-reduction cathodic process [*8,9,21*]. Sulfides affect the corrosion behavior of copper alloys, though present in concentrations as low as 0.01 ppm [*22*], which is lower than the sensitivity limits of the usual testing procedures. The behavior of sulfides in stainless steels greatly differs from that of sulfides with copper alloys. In our tests, the sensitivity to sulfide contamination for stainless steels was far less than that for copper alloys. The effects of sulfide absorption appeared to be equally persistent in time, after such contamination has been removed. Whereas, according to Ref *23*, the presence of passive films appears to hinder this absorption.

Contrary to the case of copper alloys, the presence of sulfides on stainless steels seems to hamper the oxygen-reduction cathodic process, or at least it seems to remove the depolarizing effect, observed after long exposure to seawater (Fig. 12).

These differences in behavior have been attributed to the different electronic properties of passive films [*8,9*]. The passive films on stainless steels are generally n-type semiconductors, whereas those present on copper alloys are generally p-type semiconductors.

Again, as to copper alloys, the effect of sulfide contamination on free-corrosion potentials, in even abiotic seawater, appeared more drastic in the case of stainless steels (Fig. 13) due to their low passive currents.

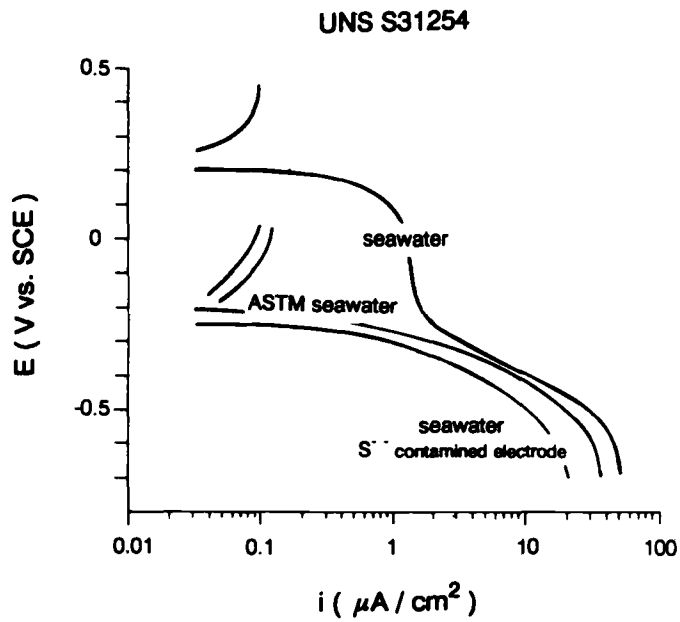

FIG. 12—*Polarization curves in ASTM seawater on UNS S31254 and in natural seawater on fouled samples after and before stainless steel surface sulphide contamination.*

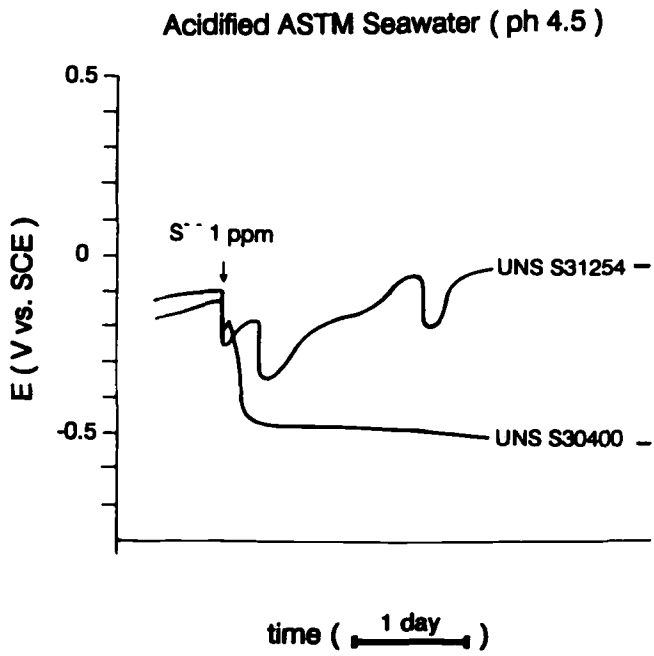

FIG. 13—*Transient of free corrosion potentials on stainless steels in acidified ASTM seawater, pH 4.5, after sulphide contamination.*

In seawater, hydrogen-sulfide can be created *in situ* by bacterial sulfate reduction [*24*], but anaerobic activity does not necessarily mean sulfide formation. The hydrogen-sulfide formed can be reoxidized or partly adsorbed by the metallic surface. Sulfide adsorption on the metallic surface may depend on the stability of the passive state reached by the surface upon contact with sulfides. In these cases, corrosion potentials, even in absence of localized corrosion, depend on a very complicated galvanic couple situation between different areas.

Some areas can present aerobic biological activity, others anaerobic biological activity. The relative extension of the surfaces and the amount of sulfides adsorbed may vary greatly, depending on hydrodynamic conditions, on the type and level of the biological activity, and on the passive state reached by the surface.

It is no wonder that differences in corrosion potential versus time for stainless steels and other easily passivated materials exposed to seawater, have been reported by several authors [*3–9*].

Polarization Curves in Seawater

It is well-known that the polarization curves obtained using potentiodynamic techniques may differ greatly from those obtained using potentiostatic techniques. This applies to stainless steels in seawater. In potentiodynamic tests, the continuous changes in the potential value might prevent these tests from reaching equilibrium conditions within passive films and steady conditions within biofilms. This causes some hysteresis phenomena to occur, if polarization scanning would be cyclically carried out or would be repeated. In potentiostatic tests, the polarization curve is traced by different points; to set n points, it is necessary to perform n tests that can be either successive or simultaneous. Successive tests are time-

consuming and are not suited well for environments such as seawater, the characteristics of which vary greatly with time. Simultaneous tests require the use of several potentiostats and several measuring cells.

The use of several potentiostats involves high costs and problems related to grounding, whereas the use of several measuring cells imposes problems regarding secondary current distributions that may cause interferences between cells. In certain cases, special attention [*25*] has been given to these problems. However, several measuring cells are sometimes used or several measurements are made simultaneously in the same cell, without considering these problems. When using continuous loops or lines taking and discharging directly into the sea, significant errors could be made.

During potentiostatic tests, any accidental events, such as a power black-out or any failure, can disconnect the potentiostats, thus nullifying or interrupting tests performed for long times.

At sea, on stainless steels cathodically protected at fixed potential and in our tests, the hypothetical $\lim_{t\to\infty} = (\delta J_e/\delta t)E^W = \overline{E} = 0$ did not take place at least for $t < 6$ months and $E > -1000$ mV versus saturated calomel electrode (SCE), in accordance with Ref *12*.

Free-corrosion potentials at sea are usually subject to marked fluctuations in time, both in presence and in absence of localized corrosion. The condition $E = \overline{E}$, typical of potentiostatic tests, is an unreal situation from a corrosion point of view. It corresponds to the situation of an electrode able to supply or to absorb a current density up to an even infinite value, provided that its potential would not be changed. In such a situation, the development of the biofilm and the possibility of localized attack could be modified.

Cathodic Polarization Curves from Galvanic Couple Data

In the event that the metallic material examined, W, is galvanically coupled with a metal, M, through an external electric resistance, R, the potential assumed by W in the couple depends on: M, on the relative extension of metallic surfaces, on resistance R, on time, and has all typical characteristics of a corrosion potential. The sum of cathodic currents on the two metals of the couple must be equal to the sum of anodic currents:

$$-(J_c^W + J_c^M) = (J_a^W + J_a^M) \text{ from which } -(J_a^M + J_c^M) = (J_a^W + J_c^W) = J_e^W = -J_e^M = J^{WM}$$

Therefore, the galvanic couple current equals the external current related to W, in correspondence of the potential assumed by W in the galvanic couple.

The exposure to the environment of the metallic material examined galvanically coupled with a metal can be used in the construction of polarization curves under conditions that seem to be closer to real corrosion conditions than those normally realized in traditional potentiodynamic or potentiostatic methods. The external electric resistance permits the current to be easily measured. The potential values observed depend on the processes occurring on the surfaces of metal M and W, as well as on electric resistor value R applied. By changing metal M and resistor R value, or both, different potential values can be obtained for W within all the potential range of practical interest.

The measurement system is economical and reliable. It requires different metallic materials, calibrated electric resistors, reference electrodes, and one electrometer with a data logger. No potentiostats are needed. Possible failures or power black-outs do not necessarily suspend the test.

Table 1 reports a series of readings for W/M galvanic couples after 20-day exposures to seawater. Figure 14 shows the cathodic polarization curve for the stainless steel, as it can be deduced from the galvanic couple data shown in Table 1. Such curves are then compared

TABLE 1—*Data of W/M[a] galvanic coupling after 20 days exposure in seawater.*

	12.9.91	C001	C002	C003	C004	C005	C006	C007	C008	C009	C010	C011	C012	C013
M		Mo	Cu-Ni	Brass	Brass	Brass	Brass	Brass	Brass	Brass	Bronze	Sn	Fe	Fe
R	(Ω)	10	10	10	1000	2000	3000	4000	5000	10 000	10	10	10	100
ΔV	(mV)	0.5	0.5	0.7	60.4	109.6	168.4	204	264.1	402.1	0.8	0.9	6.2	54.7
i	(mA/cm²)	5	5	7	6	5.5	5.6	5.1	5.3	4	8	9	62	55
	12.9.91	C014	C015	C016	C017	C018	C019	C020	C021	C022	C023	C024	C025	C026
M		Fe	Fe	Fe	Fe	Fe	Cd	Zn	Zn	Zn	Zn	Zn	Zn	Zn
R	(Ω)	200	300	400	500	1000	10	10	100	200	300	400	500	1000
ΔV	(mV)	96.8	116.9	136.7	148.2	182.3	7.2	8.1	79.6	158.5	225.8	324.2	336.4	552.4
i	(mA/cm²)	48	39	34	30	18	72	81	80	79	75	81	67	55

[a] W = UNS S31254 stainless steel (10 cm² in surface) and M = coupled metal.

to the polarization curves obtained using potentiodynamic method (1 V/h scanning rate) or potentiostatic method on the same type of steel.

pH Effects on Cathodic Polarization Curves

Cathodic polarization curves, obtained from galvanic couple data, have already been used to point out the evolution of the cathodic process kinetics on stainless steels exposed for different periods of time to natural seawater (Fig. 15) and to artificial ASTM D 1141 seawater (Fig. 16) [7]. The results reported in Fig. 16 show that the acidification at a metal/environ-

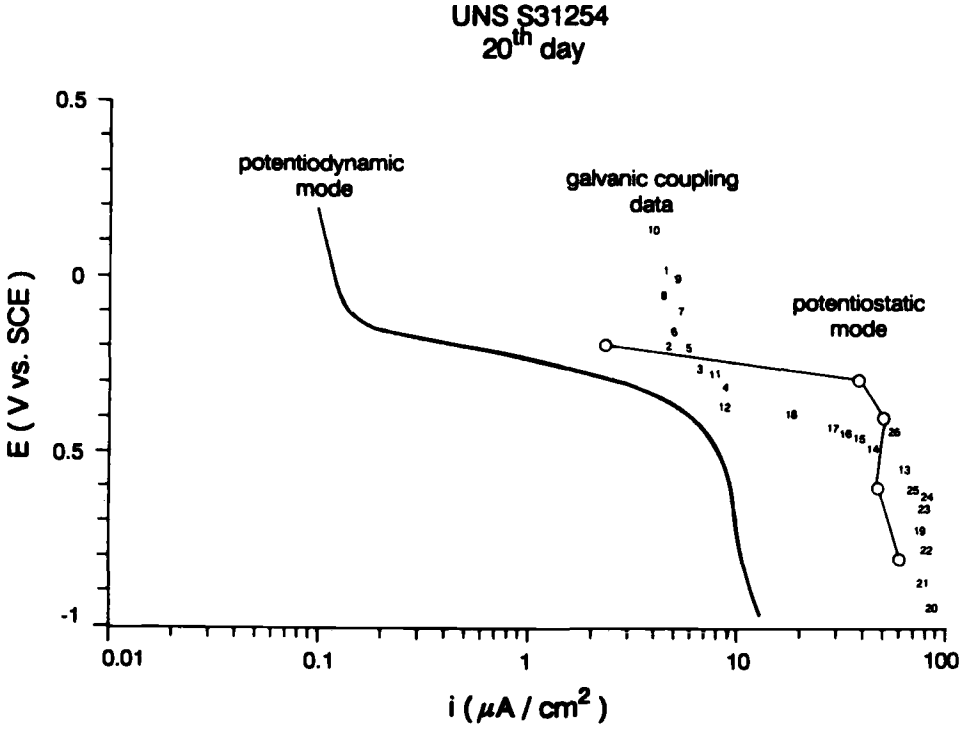

FIG. 14—*Cathodic polarization curves on UNS S31254 stainless steel, after 20 days of exposure in natural seawater, obtained by potentiodynamic or potentiostatic scans or calculated from the galvanic coupling data of Table 1.*

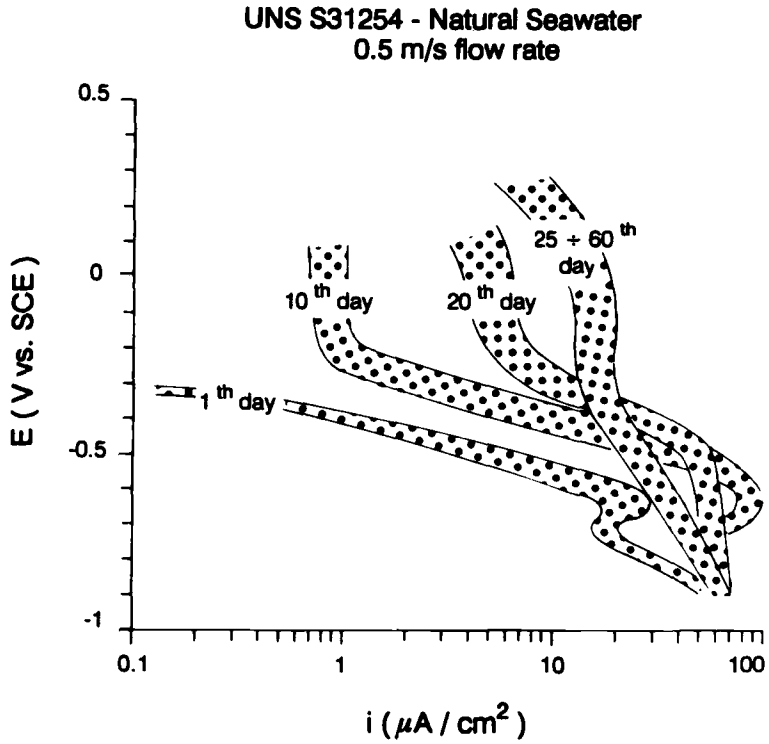

FIG. 15—*Cathodic polarization curves on UNS S31254 stainless steel obtained by galvanic coupling after different times of exposure in natural seawater.*

ment interface depolarizes cathodic process on stainless steels exposed to artificial ASTM D 1141 seawater.

Such contribution has been attributed to the alteration of the electronic properties of passive films on stainless steels, due to a permanence in an acid environment [*7*]. The comparison between Fig. 15 and Fig. 16 points out that acidification alone cannot be sufficient to fully explain the depolarization observed in natural seawater. The addition to artificial seawater of acids of the same type as those involved in biological cycles (for example, carbon dioxide, lactic acid, acetic acid or hydrogen sulfide) did not produce cathodic polarization curves quantitatively similar to those observed in natural seawater.

Electrochemical Characterization of Biofilms Formed on Stainless Steel Exposed to Seawater

Electrochemical Nature of Biofilms

The biofilms formed on the different materials in various environments can be considered as an electrolyte that can cause complicated electrochemical reactions. In the case of biofilms formed at sea on stainless steels, some authors suggest that, with regard to electrochemical impedance spectrum analyses, the behavior of the biofilm can be quite similar to that of a layer of seawater [*26*]. This does not seem to be true when trying to remove the biofilm of thick consistency from the surface.

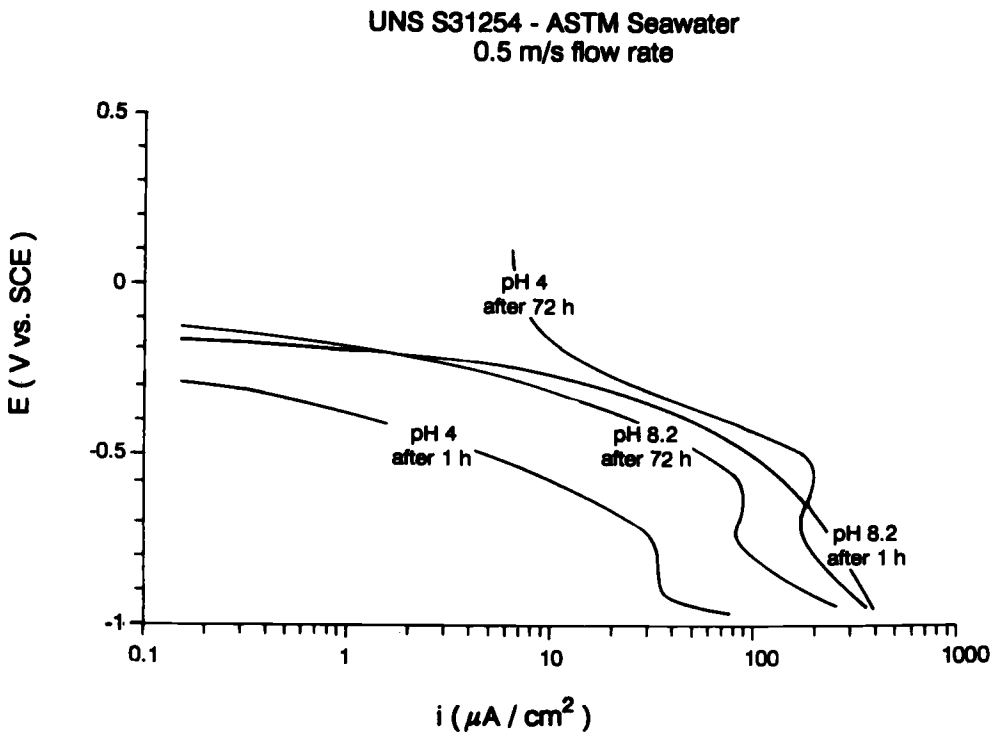

FIG. 16—*Cathodic polarization curves on UNS S31254 stainless steel obtained by galvanic coupling in aerated ASTM seawater at different pH values and after different exposure times.*

Oxygen-reduction processes through the biofilm can even follow other ways than the electrodic reduction on a metallic surface. The reduction of molecular oxygen can take place at biofilm/sea interface by an enzyme with oxidase activity, whereas the electron transfer from the metallic surface to the enzyme can be carried out by means of mediators [*27*]. Such a mechanism, which provides for the diffusion of the oxidase enzyme through the biofilm, does not seem to be able to withstand high current densities.

Electron transfer in organic matrices are demonstrated both as intramolecular phenomena, as in the case of polypeptides [*28*], and as intermolecular phenomena, as in the case of proteins [*29*]. Also, organic polymers with semiconductive properties and high electronic conductivity exist and have been widely studied [*30*]. Electron transfer phenomena could occur even within biofilms that would assume semiconductive behaviors.

Oxygen-reduction processes could be of an electrodic type and take place at the biofilm/seawater interface. Phenomena of mediatorless activation of electron reduction of molecular oxygen by enzymes are well-known and can withstand current densities on the order of mA/cm^2 [*27*].

Among the various studies on marine fouling of stainless steels, some authors [*31*] emphasize the presence in the biofilms of an organic material having high electronic density in the form of layers or capsules around bacterial colonies. Other authors [*32*] have suggested that the ennoblement of the corrosion potential would be caused not by the metabolism but by the metabolite of the sea diatoms included in the thin organic film. Some other authors [*33*] observed the presence, upon cathodic polarization, of an anodic electrodic capacity linked to the presence of biofilms.

Naturally Occurring Pyrrole Derivatives

Within marine biology, the importance of the role played by pyrrole derivatives is well-known [*34*]. The heme and most chlorophyll pigments are macrocyclic tetrapyrroles and the bile pigments are linear tetrapyrroles. Bile pigments have been isolated: from red and blue-green algae, from the pigment of the calcareous skeleton of *Helipora coerulea* blue coral, and from the secretions of gasteropod mollusks type *Aplysia limacina* and *Aplysia californica*. Tetrahydropyrrole derivatives have been isolated from red algae *Digenea simplex* and *Chondria armata*. A phenylsubstitute bromopyrrole has been isolated from a bacterium *Pseudomonas bromoutilis* and simple bromopyrroles has been isolated from sponges *Agelas oroides* [*34*].

Polypyrrole Films

Aqueous solutions containing pyrrole can easily give rise to the formation of ionic polymers called polypyrroles, which appear as a black powder or film. Such formations can take place by air oxidation, by reaction with hydrogen peroxide, ozone, metallic ions (among which Fe^{3+} and Cu^{2+}), or by anodic oxidation [*35*].

Polypyrroles are semiconductors that, dependent on preparation conditions, can present electrical conductivities close to that of metals [*30*]. Polypyrroles can be reduced and reoxidized several times, can be used as electrodes for secondary batteries [*36*], can incorporate metal complexes, and present high catalytic activities in the cathodic processes of oxygen reduction [*37*].

We do not have available any direct experimental evidence of the presence of polypyrroles in biofilms; nevertheless, we are able to obtain polypyrrole films on platinum by anodic oxidation, at potentials over 200 mV versus SCE of artificial seawater solutions containing pyrrole additions to 0.1 moles/L. The formation of polypyrrole films causes a severe acidification at anodes and, at current density $> 100\ \mu A/cm^2$, pH values less than 2 were measured. The nucleation of polypyrrole films on stainless steels points out some difficulties that have been overcome by performing the nucleation at 600 mV versus SCE. Figure 17 reports micrographs of polypyrrole films obtained on stainless steels by anodic oxidation in artificial seawater with pyrrole addition. Energy dispersion system (EDS) chemical analyses carried out on the sample reported in Fig. 17(*d*) reveals, along with the absence of sodium ions, the presence of both chlorine and sulfur. The sulfur is present in a relative molecular percentage that decreases from 23% in the layer near the metal to 11% in the layer towards the solution. Therefore, the presence of both chlorides and sulphates as anions in polypyrrole films so obtained can be hypothesized, with a greater sulphate/chloride ratio than that present in the formation solution.

The cathodic polarization curves obtained potentiostatically in artificial seawater on stainless-steel samples coated with polypyrrole film (Fig. 18(*a*)) are similar to those obtained in natural seawater on samples of the same steel coated with biofilms (see Fig. 14). The cathodic polarization curves obtained through cyclic potentiodynamic method (Fig. 18(*b*)) point out the capability of the polypyrrole film to be reduced and reoxidized.

A marked anodic capacity, after cathodic reduction, is also exhibited by stainless-steel samples, as well as by platinum samples upon exposure to natural seawater and formation of biofilm. This capacity, shown in Fig. 19, is greater than that related to passive-film modifications (Fig. 11), and cannot be attributed to hydrogen-retention phenomena [*33*]. Hydrogen evolution is not thermodynamically possible under the cathodic reduction conditions ($E = -600$ mV versus SCE, pH 8.3).

Therefore, the presence within the biofilms naturally formed on stainless steels at sea, of phases having electronic conductivity, and oxidation-reduction capability of the type shown

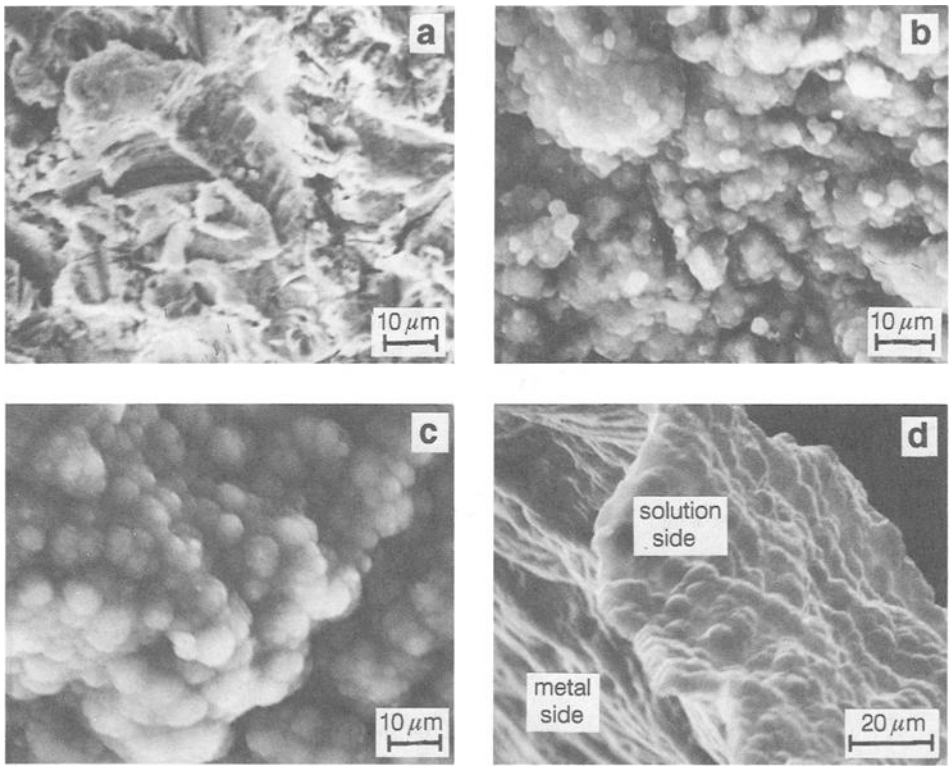

FIG. 17—*SEM images of polypyrrole film obtained on UNS S31254 stainless-steel surfaces by anodic polarization at room temperature from ASTM seawater with addition of pyrrole to 0.1 M solution.* (a) *stainless steel surface after 80 mesh Al_2O_3 blasting,* (b) *polypyrrole film nucleated at 600 mV versus SCE,* (c) *polypyrrole film growth at 300 mV versus SCE, and* (d) *polypyrrole film detached from the surface.*

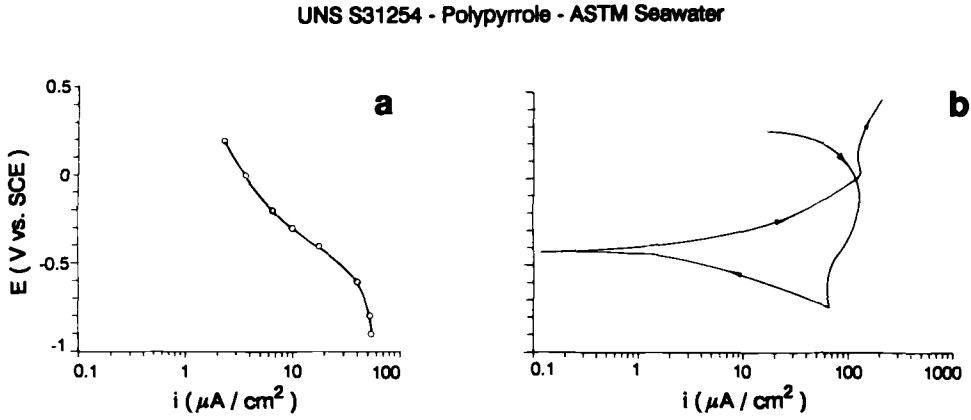

FIG. 18—*Cathodic polarization curves obtained in ASTM seawater on bare or on polypyrrole-coated UNS S31254 stainless steel. Tests were conducted in* (a) *potentiostatic mode and* (b) *cyclic potentiodynamic mode.*

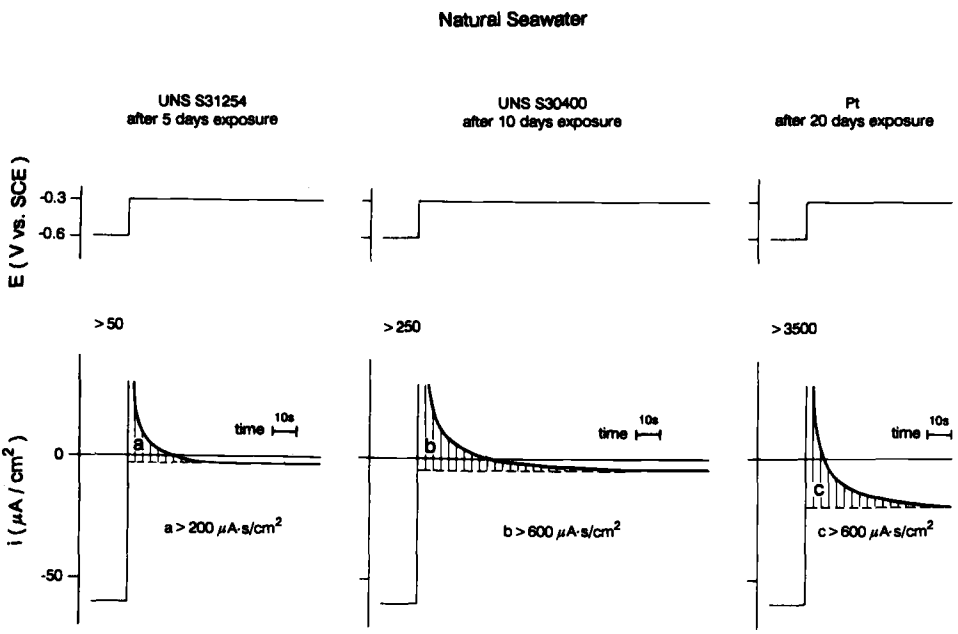

FIG. 19—*Polarization currents on different materials exposed to natural seawater for different times after a sharp transition of polarization potential from −0.6 to −0.3 V versus SCE.*

by polypyrroles cannot be excluded. Biofilms cannot be considered as "mere" electrolytes. from an electrochemical point of view.

Localized Corrosion

Stochastic Nature of Localized Corrosion

In the study of localized corrosion on passive materials, much attention has been made to the breakdown potential or to other potentials obtained from potentiodynamic tests. Such potentials have been used widely in order to predict the susceptibility to localized corrosion of a given material in a given environment.

Today, corrosion researchers believe that localized corrosion is determined by stochastic laws at various potentials, rather than deterministic laws [*38*]. The breakdown potentials or other similar electrochemical parameter cannot be univocally determined. Their values are statistically distributed in ranges even exceeding some hundred mV in amplitude [*39–43*]. Figure 20 reports the distribution of breakdown potential values for an AISI type 316 (UNS S31600) stainless steel in anaerobic marine mud and in flowing seawater [*8,9*].

Localized corrosion can even fail to occur for a length of time. Once initiated, it can proceed at high penetration rates or even stop. Instead of speaking about the general term of "corrosion rate," it is necessary therefore to distinguish different periods of the corrosion process. As far as the onset of localized attack is concerned, there can be the probability of corrosion initiation [*44*] or the sample-survival probability [*41,43*].

As to the localized attack propagation rate, the corrosion rate deduced from polarization resistance measurement results, as experimentally verified [*45*], are quite insignificant. Even the current density value assessed with respect to the whole electrodic surface, has no significance, since the metal dissolution is localized on a small portion of the total surface.

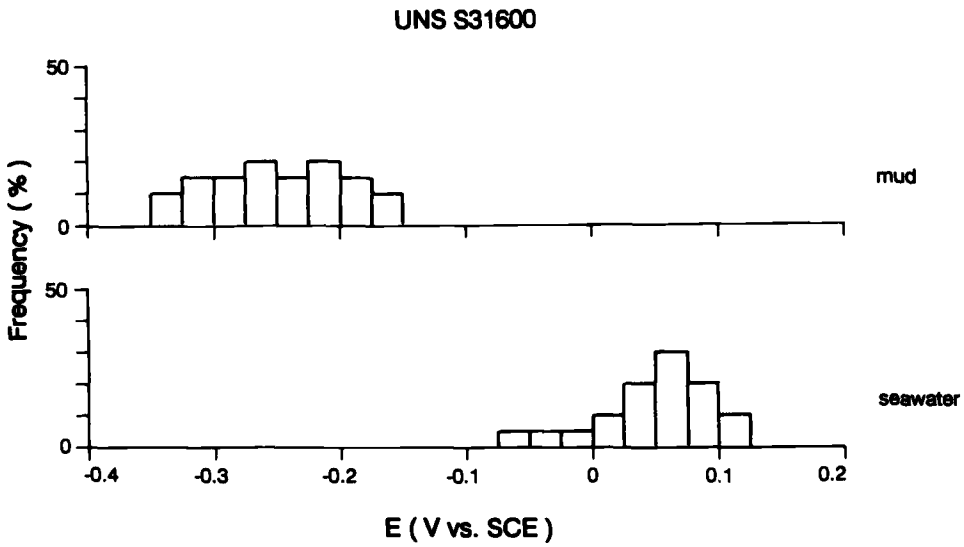

FIG. 20—*Breakdown potential distribution for UNS S31600 stainless steel in flowing seawater or in anaerobic marine mud with a several hundred ppm sulphide concentration.*

In case of only one attack site, as has occurred in many crevice corrosion experiments, it is preferable to speak about total corrosion current [*46–48*] or to refer to the maximum penetration depth and to its statistical distribution [*45,49*]. Also, the recording of real current density distributions on the electrodic surface can be carried out through the Scanning Vibrating Electrode Technique (SVET) [*18,50*].

Results of Tests on Galvanic Couples of Localized Corrosion Onset

In our experiments, several tests have been conducted by galvanically coupling UNS S31600 anodes with UNS S31254 (AVESTA 254 SMO^{R} alloy) cathodes [*8,9,51,52*]. The cathodic behavior of the two stainless steels, in the environments examined, is substantially similar, whereas the localized attack onset probability is markedly different for the two materials. The decision to adopt two different materials for anode and cathode has been made in order to eliminate the frequency of localized attack on the cathode. The tests have been performed in biologically active anaerobic marine mud, in unpolluted natural seawater, in artificial seawater, in artificial seawater brought to pH 4 using hydrochloric acid or acetic acid, in artificial seawater saturated with air and carbon dioxide (50:50) or with air, carbon dioxide, and hydrogen sulfide (50:45:5).

Figure 21 summarizes the results regarding survival probabilities, that is the complement to one of localized corrosion onset probabilities, in dependence of the time and the environment type. From Fig. 21(*a*), it can be noted that the localized corrosion onset probability seems to be negligible for materials completely submerged in anaerobic marine mud. In some experiments, marine animals such as cirripeds, patellae, and mussels settled on AISI Type 316 sheets exposed to seawater and have been sealed onto metal using epoxy resins. Eighteen months later, the surfaces exposed to the degradation products of marine animals showed no signs of corrosion, in accordance with Fig. 21(*a*).

The localized corrosion onset probability was highest for anodes immersed in mud and cathodes immersed in flowing seawater (Fig. 21(*b*)). Such results support the observation

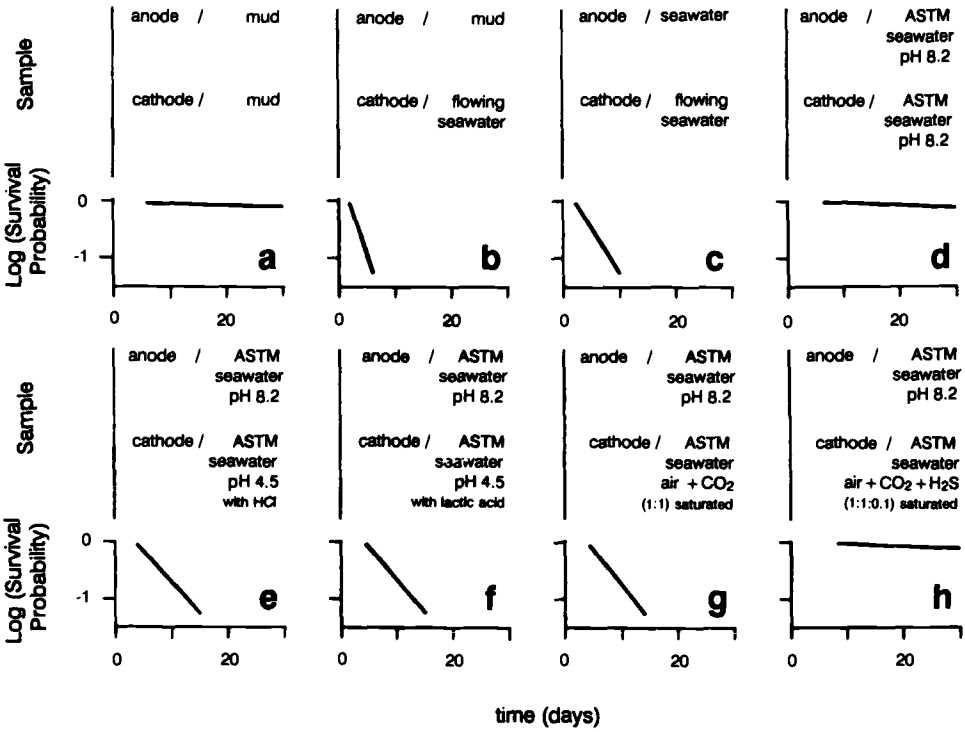

FIG. 21—*Survival probability of samples of UNS S31600 anodes coupled with UNS S31254 in the same or different artificial or natural environments.*

of one of the most frequent corrosion forms for stainless steels in seawater, which is crevice attack along the edge of dead animal shells on freely exposed surfaces [*53*]. The localized corrosion onset probability in the case shown in Fig. 21(*b*) is greater than that regarding materials freely immersed in seawater (Fig. 21(*c*)), thus confirming the tendency of sulfide to facilitate localized corrosion onset. The localized corrosion onset probability, in the case of material freely immersed in artificial seawater (Fig. 21(*d*)) was far lower than that of the material immersed in natural seawater.

In the case where artificial seawater is acidified, the cathodic process was depolarized (see Fig. 16) and the role of cathodic-current availability in favoring the localized corrosion onset is seen by comparing Fig. 21(*e*) or 21(*f*) to Fig. 21(*d*). These results support the fact that the greater the crevice corrosion onset probability, the greater the ratio between the unshielded (cathodic) surface and the shielded (anodic) surface [*44*].

While the presence of sulfides on the anodic area seems to facilitate the onset of localized corrosion (Fig. 21(*b*)), the presence of sulfides on the cathodic area may involve the polarization of the oxygen reduction cathodic process. The localized corrosion onset probability can be drastically reduced, as in Fig. 21(*a*) and 21(*h*). This confirms the importance of cathodic processes, besides anodic processes, in influencing localized corrosion onset [*52*].

Results of Tests on the Penetration Rate of Localized Corrosion

In crevice corrosion tests of stainless steels with separate anodes and cathodes, like remote crevice-assembly testing [*47*], the corrosion current tends to assume an average value constant

in time. This value can be referred to when speaking about the penetration rate of localized corrosion.

The corrosion current in seawater is not proportional to the extension of the cathodic surface area (*Sc*) at least for $Sc > Sa$, where *Sa* is the anodic surface area, but it tends to be independent of the cathodic surface area in our experiments, and according to Ref *48*.

In our tests, the crevice corrosion currents had an average value that in artificial environments was one order of magnitude lower than that observed in natural environments (Fig. 22). Such a difference can be observed even if the replacement of the natural environment by an artificial one is only limited to the anodic or the cathodic side. Similar differences persist also in cases where the cathodic surface area is increased ($Sc/Sa \leq 100$) or if artificial seawater is acidified (pH ≥ 4) so as to depolarize the cathodic process.

All of these events demonstrate that, in relation with stainless steels, any differences in the corrosion behavior assumed in natural or in artificial seawater are not limited merely to effects on the anodic and cathodic side, or both; such effects are present on both sides, where they interact and are enhanced often.

Polymer films can hinder the diffusion of anodic products and promote the development of occluded cells by hampering repassivation [*50,54*]. If these films have the properties described for polypyrroles, they can also supply the high cathodic current densities required to promote the localized attack onset [*55*].

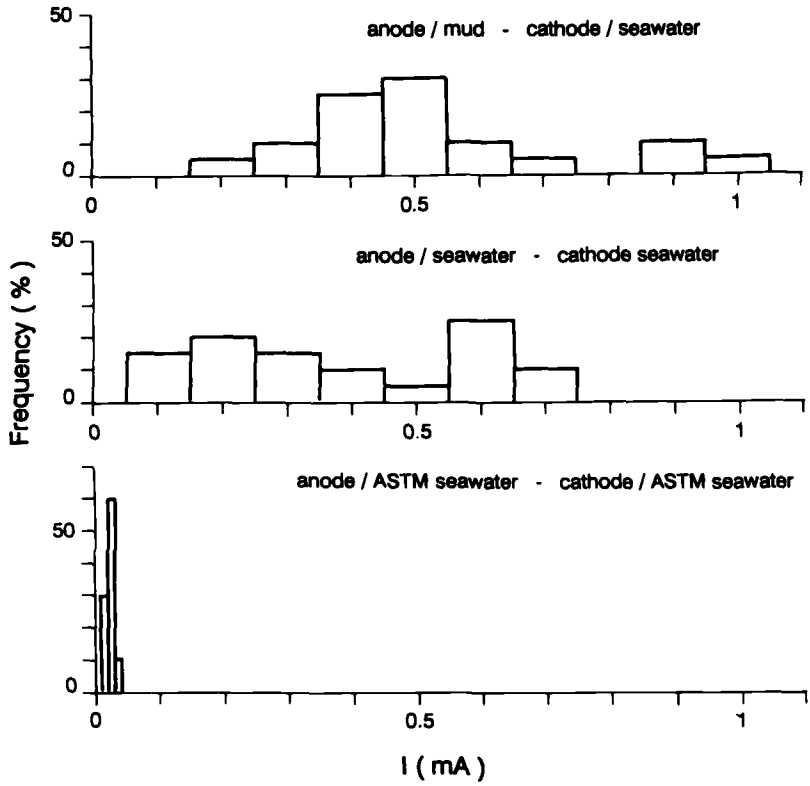

FIG. 22—*Galvanic current distribution of UNS S31254 and S30400 stainless steels coupled after 30 days of exposure to cited environments.*

Summary

Among the major effects of the biofilm on stainless steels' behavior, special consideration is given to:

(1) effects of pH at a metal/environment interface,
(2) effects of cathodic processes,
(3) effects of semiconductor presence in biofilms, and
(4) effects of the stochastic nature of localized corrosion process.

The methodology for pH measurement near metallic surfaces is shortly discussed.

In our tests in artificial seawater and in absence of localized corrosion forms, the pH value measured in the layer near metallic screen is proportional to the log of the current.

In natural seawater there is a general tendency leading to acidification within a layer near the metallic screen.

The construction of polarization curves is briefly discussed.

A methodology for deducing polarization curves from galvanic couple data is herein presented. The effect of biofilm on the kinetics of oxygen reduction on stainless steels in seawater seems to occur through an action of the biofilm on the passive film.

pH decrease at a metal/biofilm interface seems to contribute, though not explain fully the depolarization observed in natural seawater.

The electrochemical nature and complexity of biofilm are pointed out, and the presence, inside the biofilms, of phases having electrical conductivity and oxidation-reduction capability of the type shown by pyrroles is hypothesized.

The stainless steels localized corrosion susceptibility is presented through the results of tests relating to the onset probability of localized corrosion and through the results of tests relating to the penetration rate of corrosive attack.

References

[1] Uhlig, H. H., "Passivity in Metal and Alloys," *Corrosion Science*, Vol. 19, 1979, pp. 777–791.
[2] "Passivation of Metals and Semiconductors," *Corrosion Science*, Sapporo 1989, N. Sato and K. Hashimoto, Eds., Vol. 31, 1990.
[3] Dexter, S. C. and Lin, S. H., "Mechanism of Corrosion Potential Ennoblement by Marine Biofilm," in Proceedings, *7th International Congress on Marine Corrosion and Fouling*, Universidad Politecnica, Valencia, España, 1988.
[4] Little, B., Ray, R., Wagner, P., Lewandowski, Z., CheeLee, W., Characklis, W. G., and Mansfeld, F., "Electrochemical Behaviour of Stainless Steels in Natural Seawater," Corrosion/90, Paper 150, National Association of Corrosion Engineers (NACE), Houston, TX, 1990.
[5] Dexter, S. C. and Zhang, H. J., "Effect of Biofilms on Corrosion Potential of Stainless Alloys in Estuarine Waters," in Proceedings, *11th International Corrosion Congress*, Vol. 4, Associazione Italiana di Metallurgia, Milano, Italy, 1990, pp. 4.333–4.340.
[6] Mollica, A., Ventura, G., and Traverso, E., "On the Mechanism of Corrosion Induced by Biofilm Growth on the Active-Passive Alloys in Seawater," in Proceedings, *Microbially Influenced Corrosion and Biodeterioration*, N. J. Dowling, M. W. Mittleman, and J. C. Danko, Eds., University of Tennessee, Knoxville, TN, 1990, pp. 2.25–2.31.
[7] Salvago, G., Taccani, G., and Fumagalli, G., "Electrochemical Approach to Biofilms Monitoring," in Proceedings, *Microbially Influenced Corrosion and Biodeterioration*, N. J. Dowling, M. W. Mittleman, and J. C. Danko, Eds., University of Tennessee, Knoxville, TN, 1990, pp. 5.1–5.7.
[8] Salvago, G., Fumagalli, G., Taccani, G., Cristiani, P., and Rocchini, G., "Electrochemical and Corrosion Behaviour of Passive and Fouled Metallic Materials in Seawater," in Proceedings, *2nd European Federation of Corrosion Workshop on Microbial Corrosion*, C. A. C. Sequeira and A. K. Tiller, Eds., European Federation of Corrosion, Institute of Materials, Glasgow, 1992, pp. 33–49.

[9] Salvago, G., Taccani, G., and Olzi, E., "Role of Biofouling on Seawater Aggressiveness," in Proceedings, *2nd International Offshore and Polar Engineering Conference*, R. S. Puthli, J. F. Dos Santos, S. Berg, C. P. Elinas, and Y. Ueda, Eds., Vol. IV, International Society of Offshore and Polar Engineering, Golden, CO, 1992, pp. 156–164.

[10] Efird, K. D. and Lee, T. S., "Putrid Seawater as a Corrosive Medium," *Corrosion*, Vol. 35, No. 2, 1979, pp. 79–83.

[11] Edyvean, R., "Algal-Bacterial Interaction and Their Effects on Corrosion and Corrosion-Fatigue," in *Microbial Corrosion—1*, C. A. C. Sequeira and A. K. Tiller, Eds., Elsevier, London, 1988, pp. 40–52.

[12] Nekoksa, G. and Gutherman, B., "Determination of Cathodic Protection Criteria to Control Microbially Influenced Corrosion in Power Plant," in Proceedings, *Microbially Influenced Corrosion and Biodeterioration*, N. J. Dowling, M. W. Mittleman, and J. C. Danko, Eds., University of Tennessee, Knoxville, TN, 1990, pp. 6.1–6.8.

[13] Lewandowski, Z., Lee, W. C., Characklis, W. G., and Little, B., "Dissolved Oxygen and pH Microelectrode Measurements at Water-Immersed Metal Surfaces," *Corrosion*, Vol. 45, No. 2, 1989, pp. 92–98.

[14] Lewandowski, Z., Lee, W. C., Characklis, W. G., and Little, B., "pH at Polarized Metal Surfaces: Theory, Measurement and Implication for MIC," in Proceedings, *Microbially Influenced Corrosion and Biodeterioration*, N. J. Dowling, M. W. Mittleman, and J. C. Danko, Eds., University of Tennessee, Knoxville, TN, 1990, pp. 2.19–2.24.

[15] Little, B., Ray, R., Wagner, P., Lewandoski, Z., Lee, W. C., Characklis, W. G., and Mansfeld, F., "Impact of Biofouling on the Electrochemical Behaviour of 304 Stainless Steels in Natural Seawater," *Biofouling*, Vol. 3, 1991, pp. 45–59.

[16] Dexter, S. C. and Lin, S. H., "Calculation of Seawater pH at Polarized Metal Surfaces with Calcareous Deposits and Biofilms," *Corrosion/91*, Paper 499, National Association of Corrosion Engineers (NACE), Houston, TX, 1991.

[17] Kuhn, A. T. and Chlan, C. Y., "pH Changes at Near-Electrode Surfaces," *Journal of Applied Electrochemistry*, Vol. 13, 1983, pp. 189–207.

[18] Franklin, M. J., Guckert, J. B., White, D. C., and Isaacs, H. S., "Spatial and Temporal Relationships Between Localized Microbial Metabolic Activity and Electrochemical Activity of Steel," *Corrosion/91*, Paper 115, National Association of Corrosion Engineers (NACE), Houston, TX, 1991.

[19] Characklis, W. G., Little, B. J., Stoodley, P., and McCoughey, M. S., "Microbial Fouling and Corrosion in Nuclear Power Plant Service Water Systems," *Corrosion/91*, Paper 281, National Association of Corrosion Engineers (NACE), Houston, TX, 1991.

[20] Romankiv, L. T., "pH Changes at the Cathode During Electrolysis of Ni, Fe, Cu and Their Alloys and a Simple Technique for Measuring pH Changes at Electrodes," in Proceedings, *International Symposium on Electrodeposition Technology, Theory and Practice*, L. T. Romankiv and D. R. Turner, Eds., The Electrochemical Society, Inc., Pennington, NJ, 1987, pp. 301–325.

[21] Schiffrin, D. J. and De Sanchez, S. R., "The Effect of Pollutants and Bacterial Microfouling on the Corrosion of Copper Base Alloys in Seawater," *Corrosion*, Vol. 41, No. 1, 1985, pp. 31–38.

[22] Gudas, J. P. and Hack, H. P., "Sulfide Induced Corrosion of Copper Nickel Alloys," *Corrosion*, Vol. 35, No. 2, 1979, pp. 67–73.

[23] Tsinman, A. I., Kolesnichenko, V. N., and Makeeva, T. V., "Influence of Hydrogen Sulfide on Pitting Corrosion," *Zashchita Metallov*, Vol. 19, No. 4, 1983, pp. 592–595.

[24] Edyvean, R. G. J., "Hydrogen Sulfide—A Corrosive Metabolite," *International Biodeterioration*, Vol. 27, 1991, pp. 109–120.

[25] Scully, J. R., Hack, H. P., and Tipton, D. G., "Effect of Exposure Time on the Polarization Behaviour of Marine Alloys under Flowing and Quiescent Conditions," *Corrosion/83*, Paper 214, National Association of Corrosion Engineers (NACE), Houston, TX, 1983.

[26] Mansfeld, F., Tsai, R., Shih, H., Little, B., Ray, R., and Wagner, P., "Results of Exposure of Stainless Steels and Titanium to Natural Seawater," *Corrosion/90*, Paper 109, National Association of Corrosion Engineers (NACE), Houston, TX, 1990.

[27] Torasevich, M. R., "Bioelectrocatalysis," *Comprehensive Treatise of Electrochemistry*, Vol. 10, Chpt. 4, S. Srinivasan, Y. A. Chizmadzhev, J. O'M. Bockris, B. E. Conway, and E. Yeager, Eds., Plenum Press, New York, 1985, p. 231.

[28] Isied, S. S., Ogawa, M. Y., and Wishart, J. F., "Peptide-Mediated Intramolecular Electron Transfer: Long-Range Distance Dependence *Chemical Rev.*, Vol. 92, 1992, pp. 381–394.

[29] McLendon, G. and Hake, R., "Interprotein Electron Transfer," *Chemical Review*, Vol. 92, 1992, pp. 481–490.

[30] Simon, J. and Andrè, J. J., *Molecular Semiconductors*, J. M. Lehn and Ch. W. Rees, Eds., Springer-Verlag, Berlin, 1985.

[31] Varjonen, O., Hakkarainen, T., Nurmiaho-Lassila, E. L., and Salkinoja-Salonen, M., "Brackish Water Biofilm on Stainless Steels: An Electrochemical and Morphological Study," in *Microbial Corrosion—1*, C. A. C. Sequeira and H. K. Tiller, Eds., Elsevier Applied Science, New York, 1988, pp. 164–178.

[32] Motoda, S., Suzuki, Y., Shinohara, T., and Tsujikawa, S., "The Effect of Marine Fouling on the Ennoblement of Electrode Potential for Stainless Steels," *Corrosion Science*, Vol. 31, 1990, pp. 515–520.

[33] Videla, A., de Mele, M. F. L., and Brankevich, G., "Biofouling and Corrosion of Stainless Steels and 70/30 Copper-Nickel Samples after Several Weeks of Immersion in Seawater," *Corrosion/89*, Paper 291, National Association of Corrosion Engineers (NACE), Houston, TX, 1989.

[34] Schever, P. J., *Chemistry of Marine Natural Products*, Chpt. 4, Academic Press, New York, 1973, pp. 135–141.

[35] Goosauer, A. and Nesvadba, P., "Oxidation and Reduction of the Pyrrole Ring," in *Pyrroles—Part 1*, Chpt. 3.5, R. Alan Jones, Ed., John Wiley & Sons, New York, 1990, pp. 499–536.

[36] Mermilliod, N., Tanguy, J., and Petiot, F., "A Study of Chemically Synthesized Polypyrrole as Electrode Material for Battery Applications," *Journal of the Electrochemical Society*, Vol. 133, No. 6, 1986, pp. 1073–1079.

[37] Seeliger, W. and Hamnett, A., "Novel Electrocatalysts for Oxygen Reduction," *Electrochimica Acta*, Vol. 34, No. 4, 1992, pp. 763–765.

[38] Sharland, S. M., "A Review of the Theoretical Modelling of Crevice and Pitting Corrosion," *Corrosion Science*, Vol. 27, 1987, pp. 289–323.

[39] Shibata, T. and Takeyama, T., "Stochastic Theory of Pitting Corrosion," *Corrosion*, Vol. 33, 1977, pp. 243–251.

[40] Baroux, B., "The Kinetics of Pit Generation on Stainless Steels," *Corrosion Science*, Vol. 28, 1988, pp. 969–983.

[41] Shibata, T., "Stochastic Studies of Passivity Breakdown," *Corrosion Science*, Vol. 31, 1990, pp. 413–423.

[42] Videla, H. A., de Mele, M. F. L., Morena, D. A., Ibars, J. R., and Ranninger, C., "Influence of Microstructure on the Corrosion Behaviour of Different Stainless Steels," *Corrosion/91*, Paper 104, National Association of Corrosion Engineers (NACE), Houston, TX, 1991.

[43] Salvago, G. and Fumagalli, G., "The Distribution of Stainless Steel Breakdown Potentials: Experimental Method and the Effect of Metallurgical Conditions," *Corrosion Science*, Vol. 33, 1992, pp. 985–995.

[44] Anderson, D. B., "Statistical Aspects of Crevice Corrosion in Seawater," in *Galvanic and Pitting Corrosion—Field and Laboratory Studies, STP 576*, R. Baboian, W. D. France, L. C. Rowe, and J. F. Reynewicz, Eds., American Society for Testing and Materials, Philadelphia, 1976, pp. 231–242.

[45] Gehring, G. A., Jr., Pond, R., Cramblitt, V. L., Jr., and Shulder, J. J., Accelerate Failure of Copper-Nickel Condenser Tubing," in Proceedings, *Condenser Technology Conference*, Electric Power Research Institute, Palo Alto, CA, 1990, p. 16.

[46] Lee, T. S., Kain, R. M., and Oldfied, J. W., "The Effect of Environmental Variables on Crevice Corrosion of Stainless Steels in Seawater," *Materials Performance*, Vol. 23, No. 7, 1984, pp. 9–15.

[47] Kain, R. M. and Klein, P. A., "Crevice Corrosion Propagation Studies for Alloy N066225: Remote Crevice Assembly Testing in Flowing Natural and Chlorinated Seawater," *Corrosion/90*, Paper 158, National Association of Corrosion Engineers (NACE), Houston, TX, 1990.

[48] Shone, E. B. and Gallagher, P., "Galvanic Compatibility of Selected High Alloy Stainless Steels in Seawater," in *Corrosion in Seawater Systems*, Part I.4, A. D. Mercer, Ed., Ellis Horwood, London, 1990, pp. 40–49.

[49] Kain, R. M., Klein, P. A., and Ferrara, R. J., Crevice Corrosion of Nickel-Chromium-Molybdenum Alloys in Natural Seawater and Chlorinated Seawater," *Corrosion/89*, Paper 112, National Association of Corrosion Engineers (NACE), Houston, TX, 1989.

[50] Isaacs, H. S., "The Localized Breakdown and Repair of Passive Surfaces During Pitting," *Corrosion Science*, Vol. 29, 1989, pp. 313–323.

[51] Salvago, G., Fumagalli, G., Mollica, A., and Ventura, G., "A Statistical Evaluation of AISI 316 Stainless Steel Resistance to Crevice Corrosion in 3.5% NaCl Solution and in Natural Seawater after Pre-Treatment in HNO_3," *Corrosion Science*, Vol. 27, 1987, pp. 927–936.

[52] Salvago, G., Fumagalli, G., Mollica, A., and Ventura, G., "Surface Finishing Effects on Crevice Corrosion Resistance of AISI 316 Stainless Steel," in Proceedings, *International Conference on Corrosion and Corrosion Control for Offshore and Marine Construction*, J. Xiao, R. Zhu, and Y. Xu, Eds., International Academic Publishers, Pergamon Press, New York, 1988, pp. 651–663.
[53] La Que, F. L., *Marine Corrosion*, Chpt. 4, John Wiley & Sons, New York, 1975.
[54] Franklin, M. J., White, D. C., and Isaacs, H. S., "Pitting Corrosion by Bacteria on Carbon Steel, Determinated by Scanning Vibrating Electrode Technique," *Corrosion Science*, Vol. 32, 1991, pp. 945–952.
[55] Isaacs, H. S. and Ishikawa, Y., "Current and Potential Transients During Localized Corrosion of Stainless Steel," *Journal of the Electrochemical Society*, Vol. 132, No. 6, 1985, pp. 1288–1293.

DISCUSSION

T. Jack[1] *(written discussion)*—I was intrigued by your work with the biological pyrrole polymers acting as semiconductors. From our work, we believe "FeS" matrices act as a galvanically coupled pathway for removal and distribution of electrons from corrosion through the biofilm. Would you care to speculate on the impact of such a distributed semiconductor on the spatial distribution of organisms and processes in biofilm?

Salvago et al. (authors' closure)—The issue raised by Mr. Tom Jack regards several subjects, not only biological corrosion. In our work we have noticed that some aspects of the electrochemical behavior of passive and fouled metal surfaces would be easily explained assuming the presence inside the biofilm of substances with electrochemical features similar to those of the polypyrroles. This presence allows high values of redox potential to be reached, even where dissolved molecular oxygen is practically absent; for example, under biofilm of high thickness.

It appears logical, therefore, to think that the presence of polypyrrole can influence the distribution of processes and mechanisms inside the biofilms. But this influence could not also result solely by the influence of polypyrrole on the electrodic behavior of the surface.

The ability of polypyrrole to fix some enzymes is well known, as is the use of polypyrrole in the field of biological electrodes. In our personal view, we believe that considering the ability of polypyrrole to produce filiform structures of high electronic density and a certain degree of long range order, the polpyrrole could also interfere directly in the biological mechanisms of electrical conduction and information transmission. These aspects of the problem appear as fascinating as they are complex.

[1] NRTC, Calgary, Alberta, Canada.

On-Line Monitoring Methods

Patrick S. N. Stokes,[1] *Michael A. Winters,*[2] *Patricia O. Zuniga,*[3] *and David J. Schlottenmier*[4]

Developments in On-Line Fouling and Corrosion Surveillance

REFERENCE: Stokes, P. S. N., Winters, M. A., Zuniga, P. O., and Schlottenmier, D. J., **"Developments in On-Line Fouling and Corrosion Surveillance,"** *Microbiologically Influenced Corrosion Testing, ASTM STP 1232,* Jeffery R. Kearns and Brenda J. Little, Eds., American Society for Testing and Materials, Philadelphia, 1994, pp. 99–107.

ABSTRACT: Corrosion and fouling impact the operation of cooling water systems in terms of reduced heat-transfer capability, increased maintenance cost, loss of plant availability, and water contamination. Conventional test methods have focused separately on measurement of fouling build-up by electrically-heated or pressure-drop apparatus and corrosion detection by electrical resistance or electrochemical methods. A major drawback of conventional fouling monitors has been the inability to indicate real-time corrosion activity beneath surface deposits. Consequently, it has been necessary to destructively evaluate test heat exchanger tubes and/or rely upon use of corrosion coupons and probes, or both, under nonheat flux conditions. A recent test method, focusing on two simultaneous effects, monitors localized corrosion (pitting, etc.) promoted beneath a fouled heat exchanger tube. The corrosion tendency of a surface under heat flux differs from corresponding surfaces without heat transfer in two respects. First, higher temperature increases the rate of corrosion reaction kinetics. Secondly, scales or biofilms prevent uniform corrosion and promote localized attack, often in the form of pitting. Furthermore, the presence of deposits creates a microenvironment at the heat-transfer interface that can prevent the ingress of certain species (inhibitors, biocides) and increase the concentration of others (acidity, bacteria). Contrary to expectation, the presence of scales or biofilms will often exacerbate damage, not prevent it. An overview of the test method and recent field results carried out at Amoco Chemical Company's Chocolate Bayou Plant are presented and discussed.

KEYWORDS: fouling, under deposit corrosion, on-line surveillance, electrochemical noise

Background

The operation of cooling water systems can be adversely affected by fouling and corrosion by reducing heat transfer efficiency, increasing maintenance costs, reducing plant availability, and increasing contamination. A major drawback of field monitors has been the inability to indicate real-time corrosion activity beneath fouled deposits. In the past it has been necessary to destructively evaluate heat exchanger tubes and rely upon use of coupons and probes exposed under nonrepresentative conditions, or both. A recent initiative has been the development of a combined corrosion and fouling monitoring instrument. This unit is capable of providing an indication of corrosion activity under heat transfer conditions at the tube wall and has a high potential for use in microbiologically influenced corrosion (MIC)

[1] Project engineer, CAPCIS MARCH Ltd, Granby Row, Manchester M1 2PW, United Kingdom.
[2] Water treatment consultant, Amoco Corporation, PO Box 3011, Naperville, IL 60566.
[3] Associate chemical engineer, Amoco Chemical Company, PO Box 1488, Alvin, TX 77511.
[4] Senior mechanical engineer, Bridger Scientific, PO Box 1923, Sandwich, MA 02563.

applications. The following sections present an overview of the testing method with examples of recent field trial results.

Instrumentation

The combined instrument comprises a miniature heat exchanger (incorporating a novel corrosion sensor arrangement), an electronic flow and heat control unit, and a data collection device that is linked to an electronic storage device. The heat exchanger uses a segmented tube (typically carbon steel) that is coated with heat transfer paste and mechanically clamped in an electrically heated block. A side stream of cooling water is fed through the exchanger and a paddle-wheel flow meter enables the flow to be maintained between 0.30 and 4.6 ms^{-1}. Equating to Reynolds numbers between 10 000 and 100 000, the flow is kept within $\pm$ 0.02 ms^{-1} of the set value. The other variable that may be set is either heat transfer rate or wall temperature. Platinum resistance temperature detectors (RTDs) measure the temperature of the fluid and the temperature of the block outside the tube. The inside wall temperature is calculated from these measurements. If the heat transfer rate is set, then as the surface of the tube fouls, the wall temperature will rise to maintain the set heat rate. If the wall temperature is set, the heating rate would decrease to maintain the set wall temperature as the resistance to heat transfer increases. Making allowance for convective and conductive resistance, changes in heat transfer resistance from that of the clean-surface condition are found analytically. Measured values of variables, scanned every minute, are fed to a personal computer for storage. Heat transfer rate can be set between 50 and 1000 Watts. This equates to a typical skin temperature between 30 and 90°C. The heat transfer rate is set typically at 200 Watts.

Electrochemical Techniques

In conjunction with the fouling tendency, the corrosion information is obtained using four electrochemical techniques: zero resistance ammetry (ZRA), electrochemical current noise (ECN), electrochemical potential noise (EPN), and linear polarization resistance (LPRM).

Zero resistance ammetry has been used conventionally to determine the galvanic current between two dissimilar electrodes, but may be also used to determine the current between two nominally identical electrodes. It has been found that "identical" electrodes normally have different balances of anodic and cathodic areas and hence take up slightly different potentials. When the electrodes are coupled via with ZRA, a measurable current will flow. The dc value of the current during active corrosion is proportional to the corrosion activity in progress on the electrodes [*1*].

ZRA time records complement the information obtained by EPN and ECN measurements. Film breakdown, for example, is characterized by sporadic transients in the current flow. These currents are drawn from any available cathodic sites, including those of the second electrode, and the current transients are observed via the ZRA.

The EPN technique measures low-level random fluctuations of the corrosion potential. The fluctuations are usually of low amplitude, less than a millivolt, and of low frequency, in the range 1 Hz and below [*2*]. The EPN measurement provides data that can be correlated with the mode of corrosion attack, since the random fluctuations recorded are characteristic of the corrosion processes. The signatures of pitting corrosion and crevice attack are especially clear. For a fixed electrode area, it has been shown that data obtained at the free corrosion potential can be related to the degree of localized attack occurring at the time of measurement [*3*]. The electrochemical noise techniques are sensitive to the onset of uniform attack (general corrosion), and can characterize propagation of pitting or crevice corrosion.

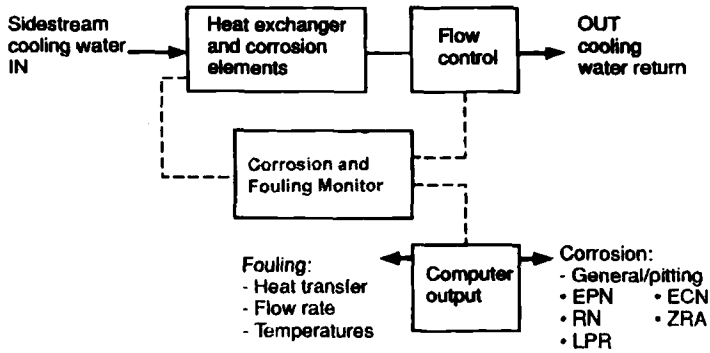

FIG. 1—*Schematic of combined corrosion and fouling system set-up.*

The ECN technique is similar to EPN, except that fluctuations in the coupling current between the two similar electrodes, typically less than 1 microamp, are recorded and analyzed. It is possible to relate current and potential noise to localized attack propensity [*4*]. ECN and EPN are also used to obtain the resistance noise (Rn) value. This value is used to estimate corrosion rates from the Stern-Geary approximation [*5,6*]. Unlike the LPR technique, the noise techniques are nonperturbative. No external voltage or current is applied. The potential and current measurements made are due to naturally occurring spontaneous fluctuations associated with the corrosion processes taking place on the surface of the material.

Linear polarization resistance is a dc method used for measurement of uniform corrosion. The technique assesses the electrode potential versus current potential relationship close to the corrosion potential. This is achieved by monitoring the external current flow between two nominally identical electrodes held at a known potential difference. The difference is kept small, typically 10 mV, and the change of potential relative to the change of current, gives the polarization resistance, Rp. The corrosion current is then given by the simple relationship (again from Stern-Geary)

$$i_{corr} = B/Rp$$

where B is a polarization constant dependent on the type of metal or alloy used for the electrode probe and on the environment. The LPR method is used extensively for prediction of general or uniform corrosion rates but has limited value in the presence of scales or deposits that can introduce an increased resistance, as can low conductivity electrolytes. The technique is also insensitive to localized corrosion. A schematic illustration of the set-up used in the field is given in Fig. 1.

Applications

Fouling Tendency

The combined unit gives an indication of the fouling tendency of the cooling water stream. Heat flux and flow parameters are usually set to encourage continuous fouling, that is, high-temperature flux and low flow. Operation of the monitor in this manner permits fine tuning of the water treatment program because the unit is sensitive to changes in chemical treatment that affect the fouling rate. System upsets also show up immediately as changes in the fouling curve slope. Conditions of operation can also be set to mimic a critical heat exchanger, thus

tracking fouling at a key location in the cooling system. Recent field trials have shown that the fouling mode of operation of the unit has a major influence on the corrosion activity. The rate of corrosion attack is very sensitive to the nature and degree of fouling sustained.

In the past there has been a tendency to consider that fouled/scaled heat transfer surfaces are protected by the presence of the scale itself. This assumption has shown to be misplaced by the recent experiences/results from the field studies. Fouling has an immediate and significant impact on the surface corrosion condition. Operation of the unit such that it mimics critical heat exchanger conditions is therefore imperative in order to obtain a representative indication of corrosion activity in that location.

Corrosion Information

The combined unit gives real-time corrosion information on fouled heat transfer surfaces. The unit gives a continuous on-line indication of the corrosion rate and the pitting tendency on a single graphical output. The data are also stored for more detailed retrospective evaluation.

The unit has demonstrated the capability to monitor changes to pit initiation and propagation from general corrosion under the influence of heat transfer or changes in the effectiveness of the chemical treatment package. A side-by-side comparison of test data with results from conventional LPRM probes used under nonheat flux conditions can also be obtained.

Results

Baseline Tests

Prior to the field trials, laboratory tests were carried out to ensure that the fouling tendency within the combined unit was similar to that of a stand-alone proven fouling monitor [*7*]. Technical descriptions and reported field experiences of the stand-alone fouling monitor have been reported elsewhere [*8,9*]. The results confirmed that the combined unit had fouling characteristics that were closely similar to the stand-alone fouling unit (Fig. 2). These results confirmed that the modifications to the heater block design (in order to incorporate corrosion sensors) did not adversely affect the fouling capability of the combined unit.

Field Trials

The unit was used for one year on a cooling water system of a petrochemical plant in Texas. This plant uses river water make-up to the cooling towers and has suffered severe under-deposit corrosion caused by particulate settlement and oxygen-induced attack. Steps have been taken over the years to minimize the corrosion and fouling tendency of the cooling water but problems are still evident due to low flow rate and high-temperature conditions in the system, or both. When first installed in the field, the unit recorded very little corrosion on the heated surface of the clean-exchanger tube, confirming the results obtained with conventional instrumentation. However, after only two weeks of monitoring, indications of increased corrosion activity were evident. This was attributed to under-deposit attack of the fouled exchanger tube. The trend was not detected by an unfouled LPRM sensor probe that was also exposed to the flowing stream.

There were prolonged periods in the early stages of the program when virtually no fouling took place. However, when the flow rate was reduced from 1 · 5 to 1 · 3 fps, the data recorded indicated some increased activity that coincided with the onset of a slight fouling curve, as indicated by the heat-transfer-resistance time record (Fig. 3).

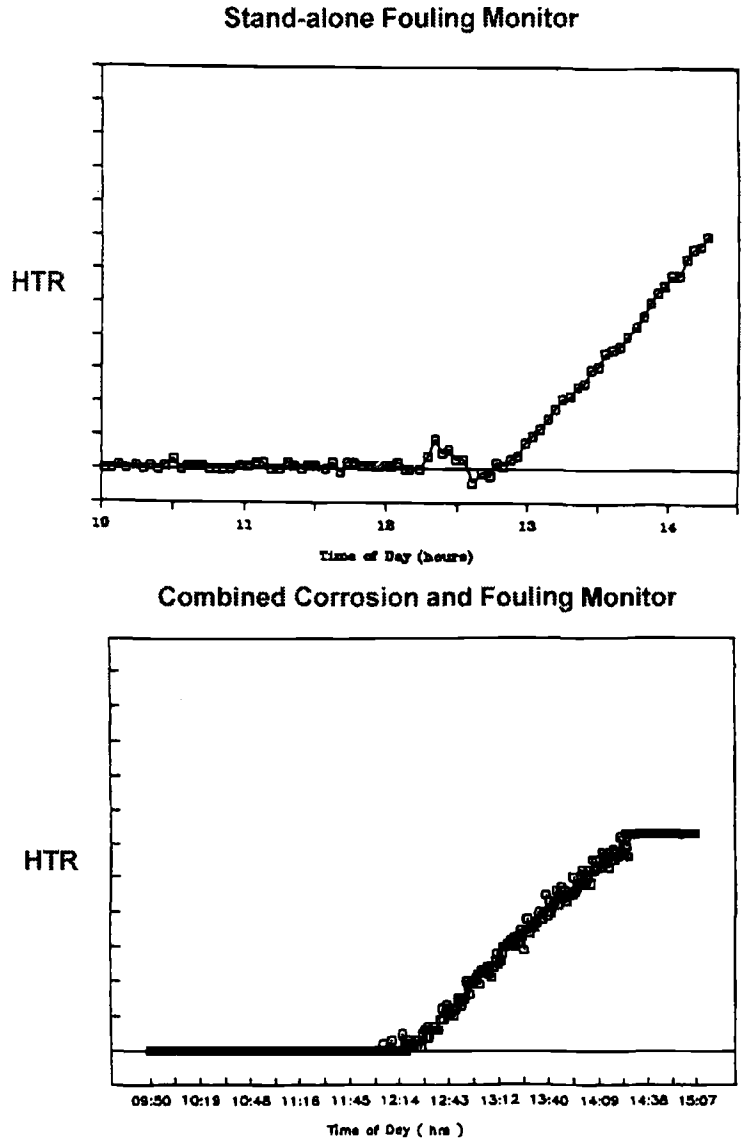

FIG. 2—*Comparison of fouling tendency of combined and stand-alone fouling monitor.*

Figure 4 is typical of the differences between corrosion activity on a heated surface in a fouled condition and after cleaning, done midway through the trials. Before cleaning, the value of ECN and ZRA were always near full-scale; the trace of EPN showed transients typical of pit initiation. After cleaning, EPN became flat and featureless and the ECN and ZRA values dropped by two and one orders of magnitude, respectively. By contrast, the LPR output indicated a larger active area of apparently increased corrosion activity. Information provided by the noise technique and ZRA, however, are more representative of

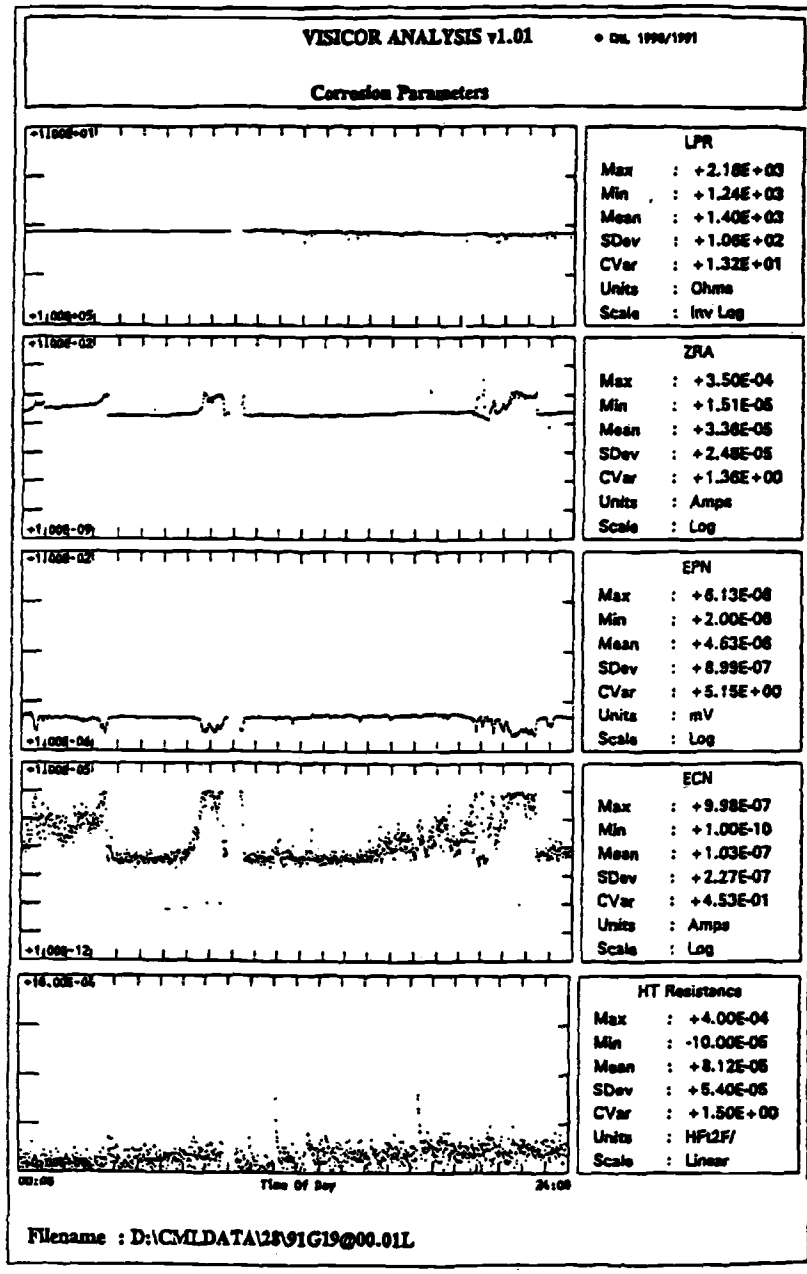

FIG. 3—*Increased corrosion activity on monitor coinciding with onset of a slight fouling curve.*

corrosion because they reflect increased attack occurring on a reduced area beneath fouling deposits.

The combined monitor is also sensitive to biocide feed. Figure 5 illustrates the effect of chlorine overfeed on the corrosion behavior of the fouled unit. Increased corrosion activity

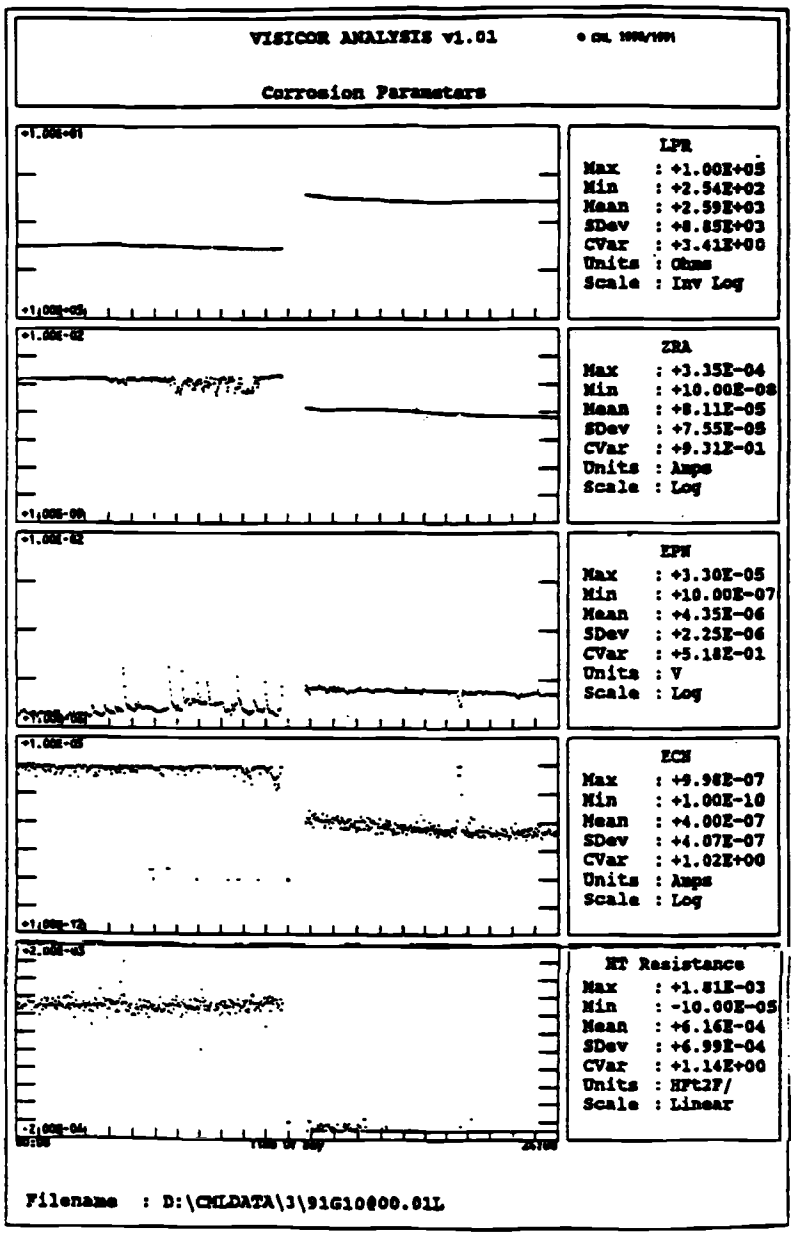

FIG. 4—*Difference between corrosion activity on a heated surface in a fouled condition and after cleaning, done midway through the trials.*

on this day was attributed to residual chlorine levels that were five times the normal recommended working level in this cooling water system. From plant data it was found that the overfeed began at approximately 7 a.m. From the time records for the corrosion data, this had an immediate and simultaneous effect on all the techniques being used. The resistance values from linear polarization and electrochemical noise were reduced, indicating

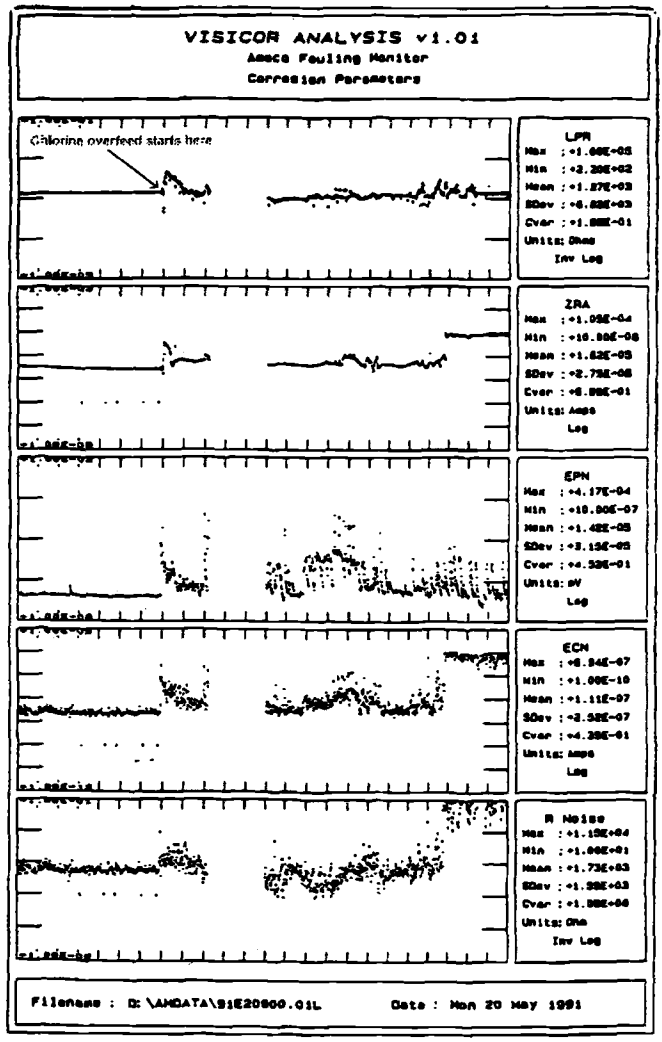

FIG. 5—*Effect of chlorine overfeed on corrosion behavior of fouled unit.*

increased activity. The increased noise on the potential and current noise signals as well as increased ZRA current were further indications of increased activity. The use of such biocides to stop the occurrence, growth, or metabolic activities of a variety of microorganisms is a well-established practice. The combined unit can evaluate the efficiency of such biocides in terms of fouling and corrosion activity. It can be used to indicate periods of biocide overfeed in cases where such overfeed has a marked effect on the corrosion behavior as typified by the chlorine example.

During the field trial, corrosion rates as high as 100 mpy due to under-deposit corrosion were indicated. Confidence in these rates were only obtained once confirmatory metallographic examination of the sensors was carried out. Metallography of the fouled sensor elements confirmed that the elements had sustained considerable attack similar to that experienced in plant heat exchangers where excessive fouling occurs due to slow flow rates

and high particulate loading in the cooling water. The depth of pits observed agreed well with estimates produced from electrochemical data.

Conclusions

1. Electrochemical methods of corrosion appraisal can be applied under heat transfer conditions to provide a continuous indication of corrosion status from beneath scale or fouling deposits.
2. A new system combining a proven fouling monitor and modern corrosion appraisal methods has been developed and used in the laboratory and in the field.
3. The system has potential for monitoring MIC. Initial results have shown that it may be able to assist in the selection, control, and optimization of chemical and biocide treatment packages, thereby reducing heat transfer losses, repair, and maintenance expenditure and lost availability.

References

[1] Hladky, K. and Dawson, J. L., *Corrosion Science,* Vol. 23, 1982, p. 231.
[2] Dawson, J. L., Eden, D. A., and Hladky, K., "Electrochemical Noise—Some New Developments in Corrosion Monitoring," Corrosion/83, Institute of Corrosion Science and Technology, Birmingham, United Kingdom, Nov. 1983.
[3] Dawson, J. L., Farrell, D. M., Aylott, P. J., and Hladky, K., Corrosion/89, Paper 31, National Association of Chemical Engineers (NACE), New Orleans, LA, 1989.
[4] Hladky, K., UK Patent Application 8,200,196, Jan. 1982, U.S. Patent 4,575,678, March 1986.
[5] Eden, D. A., Dawson, J. L., and John, D. G., UK Patent Application 8,611,518 May 1986.
[6] Stern, M. and Geary, A., *Journal of the Electrochem. Society,* Vol. 56, No. 104, 1957.
[7] Deposit Accumulation Testing System (DATS) Fouling Monitor System, Bridger Scientific, Inc., PO Box 1923, Sandwich, MA 02563.
[8] Zuniga, P. O., Klee, H., Miller, K., and Winters, M. A., Corrosion/90, Houston, TX, 1990.
[9] Zuniga, P. O., Miller, K., and Winters, M. A., "Cooling Water Fouling Monitor Senses Upsets, Evaluates Changes," *Chemical Processing,* 1990.

Thomas R. Jack,[1] *Ed Rogoz,*[2] *B. Bramhill,*[3] *and Pierre R. Roberge*[4]

The Characterization of Sulfate-Reducing Bacteria in Heavy Oil Waterflood Operations

REFERENCE: Jack, T. R., Rogoz, E., Bramhill, B., and Roberge, P. R., **"The Characterization of Sulfate-Reducing Bacteria in Heavy Oil Waterflood Operations,"** *Microbiologically Influenced Corrosion Testing, ASTM STP 1232,* Jeffery R. Kearns and Brenda J. Little, Eds., American Society for Testing and Materials, Philadelphia, 1994, pp. 108–117.

ABSTRACT: This study was carried out in an oilfield waterflood operation in which produced brine is reinjected to displace oil from the reservoir. Significant corrosion problems are associated with bacterial colonization of the water handling system. Previous work has focused on optimizing biocide treatments, but there are limits to what is economically achievable by this approach.

This report describes results of an audit of chemical, biological and corrosion parameters measured across the Wainwright waterflood operation over a 30-month period. The intent of the audit was to provide a basis for understanding and improving monitoring and control practices in such operations.

Corrosion-monitoring methods generally failed to correlate in a simple way with corrosion failures. Failure frequency correlated with several water chemistry parameters. Common treatment chemicals showed evidence of promoting bacterial growth. Sulfate-reducing bacterial numbers were found to be a function of position in the system, population composition and water chemistry.

Based on the insights obtained, a series of runs was carried out in a special test facility to assess the effects of trace nitrate, oxygen scavenger, and nutrient addition on the sessile bacterial populations present in an operating unit. Results are briefly described.

KEYWORDS: sulfate-reducing bacteria, corrosion, acid-producing bacteria, biocides, treatment chemicals, water chemistry, monitoring

Introduction

The control of biofilm development and related corrosion problems in oilfield water piping systems has been the aim of extensive and expensive effort in the oil industry for many years. Despite this effort, state-of-the-art technology provides only a qualified level of risk assessment and control. Even under selected biocide treatment using the best products available, fouling and microbial growth persist. Indeed, microbial levels below 100 viable cells per cm^2 seem unattainable within economic constraints. Furthermore, spontaneous shifts in microbial numbers due to variations in other factors rival biocide effects in magnitude.

Figure 1 illustrates typical field performance. Biocide A injected at Month 4 gradually reduced sessile sulfate-reducing bacterial counts at the waterplant over a nine-month period before control was lost. Introduction of another product, Biocide B, showed a rapid kill

[1] Research Supervisor, Novacor Research & Technology Corporation, 2928 16th St. NE, Calgary, Alberta, Canada, T2E 7K7.

[2] Staff Technologist, Husky Oil, Lloydminster, Saskatchewan, Canada, S9V, 0Z8.

[3] Scientist, Novacor Research & Technology, Calgary, Alberta, Canada, T2E 7K7.

[4] Professor, Royal Military College, Kingston, Ontario, Canada, K7K 5L0.

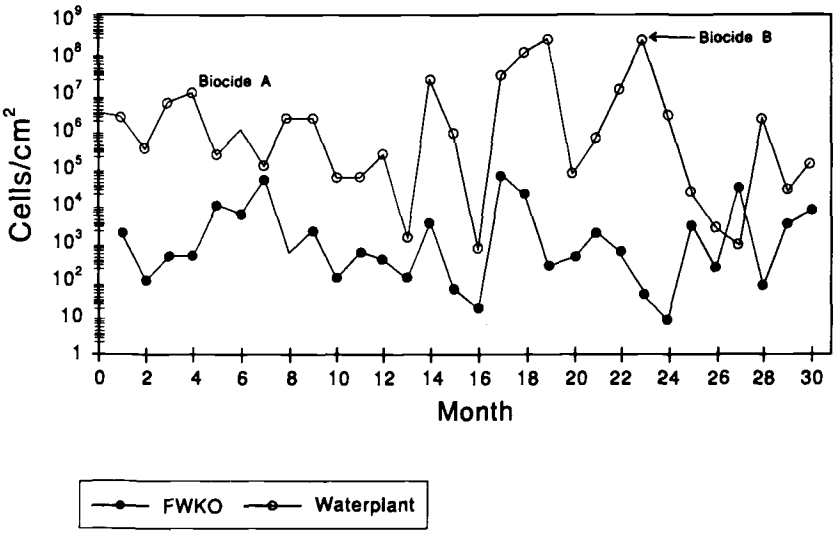

FIG. 1—*Field performance of Biocides A and then B showing level of control attainable and importance of other factors influencing sessile bacterial numbers.*

over a four-month response. Both biocides had the same active ingredient, cocodiamine, but differed in their formulation, illustrating the importance of other components. More importantly, Fig. 1 shows the significant variability of the population even under treatment.

The implication is that much better understanding of the microbial populations in the field and the factors which influence them will be required before a significant improvement in practice can be achieved.

A first attempt to understand the nature of the variability shown in Fig. 1 involved tracking changes in the sessile population in a given field unit with variations in water chemistry [*1*]. These results were sufficiently encouraging that a field-wide audit of chemical, corrosion and microbial parameters was undertaken over a 30-month period. An attempt was then made to discover parameters which were interrelated and to rationalize the correlations found. This report summarizes the findings of that effort.

Based on the hypotheses developed in this process as well as correlations seen in earlier work [*1*], a series of runs was carried out in a special field test facility to assess the effects of trace addition of nitrate, an oxygen scavenger, and selected nutrients on the sessile population in an operating unit. These results will be briefly presented as part of the conclusions here.

Field Audit

The Field

A database of chemical, corrosion, and microbiological parameters over a 30-month period was prepared for the Wainwright waterflood operation run by Husky Oil Operations Ltd. This field is on the edge of a major heavy oil area centered about Lloydminster on the Alberta, Saskatchewan border. The field is in unconsolidated sand with a connate sodium chloride rich brine at about 600-m depth and roughly room temperature. The field is divided

into a number of more or less self-contained units each of which produces a mixture of oil and water, separates the fluids, and reinjects the brine more or less independently of the other operating units in the field.

A schematic of a typical water-handling operation is shown in Fig. 2. A free water knock out (FWKO) receives produced fluids from the production wells and separates most of the water from them. Water is concentrated in the waterplant (WP) for reinjection. Most corrosion occurs internally in the water piping system towards the downstream end of the system beyond the WP. Consequently, biocide addition is usually done between the FWKO and WP. All subsequent data and discussion treat these separately unless otherwise noted.

Units of interest here are: 1, 5, 6, 12, 13 (location of field test facility), 14, 20, and 28. In addition, a truck pit operation collects trucked fluids from various sources in the surrounding area for processing. The quality of fluids received is variable and can be suspect. Most units have source wells to augment water injection but most are of limited capacity. Only Unit 14 shows a marked dilution of produced brine with fresh source well water. Conductivity falls from 76 to 31 mS/cm in going from the FWKO to the WP. Other units show less than a 5% drop in conductivity.

Parameters

Sessile bacterial populations were measured on pairs of bull plug coupons in each unit; one set in the FWKO and one in the WP. Sulfate-reducing bacteria (SRB) were counted by the most probable number (MPN) method using a lactate medium. So-called acid-producing bacteria (APB) were counted using a proprietary medium from Bioindustrial Technologies Incorporated, Georgetown, Texas. This medium is based on the fermentation of a sugar to give acid and constitutes a useful complementary assay for characterizing other organisms in a mixed population with SRB.

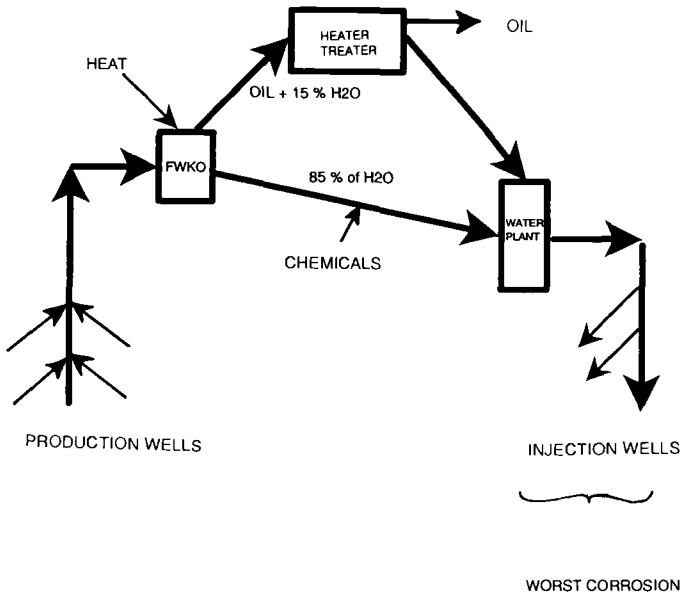

FIG. 2—*Schematic diagram of Water Handling Facility, Wainwright Oilfield.*

Other parameters measured included: pH, anions, cations, density, conductivity, oil and grease, hardness, dissolved solids, suspended solids, and residuals for scale inhibitor, oxygen scavenger, corrosion inhibitor, and oxygen. Corrosion rates were obtained using weight loss coupons (1018 carbon steel, United Corrosion, Edmonton) and instantaneous corrosion rates and pitting indices using a Petrolite Model M 4100 analyzer. Failure frequency and costs were documented by operating personnel, Husky Oil, for all corrosion failures.

Correlations were attempted between all parameters taken in pairs. Due to the difficulty in comparing individual sampling times and locations and in order to make the task practical, averaged data were used for each unit over the 30-month period. Plots of parameter pairs were developed to see if correlations existed. In most cases, visual inspection was sufficient to distinguish correlations from senseless scatter.

Results

Produced Water

Produced water handled in these facilities is a strong sodium chloride brine (47 to 76 mS/cm) of near neutral pH (6.5 to 7.0), rich in suspended solids (57 to 1600 mg/L) as well as oil and grease (182 to 10 000 mg/L). Immiscible materials are highest at the FWKO and drop markedly downstream of this unit.

In general, produced water chemistry correlations were straightforward. For example, low sulfate levels correlated with high soluble barium indicating barite precipitation was controlling available soluble sulfate. Total hardness, density, calcium concentration, and conductivity all correlated with each other and inversely with pH.

Corrosion Measurements

Seven parameters were used to track corrosion: soluble iron, soluble manganese, weight loss from coupons, instantaneous corrosion rate measurements (general corrosion rate and pitting index), and failures (cost and frequency). Attempts to correlate these parameters over the audit period revealed little consistency.

The aim of any corrosion control program is to abate failures; yet, the only correlation seen between failure data and corrosion-monitoring parameters was a correlation between pitting indices from electrochemical methods and failure frequency at FWKOs. All other corrosion measurements failed to correlate with either the cost or observed failure frequency.

A relationship was noted between averaged general corrosion rates measured by weight loss coupons and electrochemical methods; however, the electrochemical readings were several fold higher (Fig. 3). This correlation all but disappeared when individual data points for a given unit were used in place of 30-month averages for the whole field.

Soluble manganese and iron correlated, with manganese readings at about 3% of the iron readings, consistent with the primary source of both ions being the corrosion of steel. The concentration of iron fell off in going from FWKO to WP, presumably due to its precipitation in the system. Elevated manganese to iron ratios indicate selective precipitation of iron is occurring at the WP, probably as iron sulfide [*2*].

Corrosion and Water Chemistry

Failures correlated with water conductivity and water hardness, consistent with the importance of electrolyte and scaling in corrosion processes. Suspended solids and oil and grease also correlated with system failures presumably through the promotion of fouling,

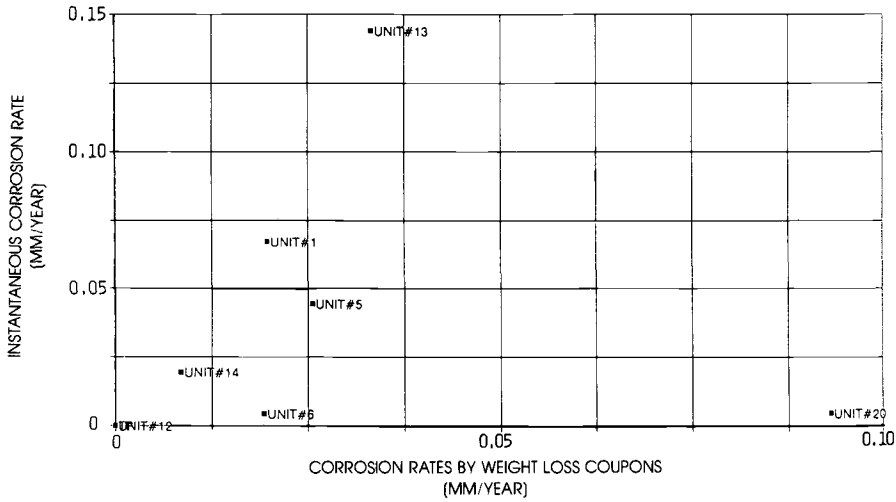

FIG. 3—*Correlation of instantaneous corrosion rate measurements and weight loss coupon corrosion rates. Each point represents the average of monthly readings over a 30-month period.*

deposits, provision of nutrients, and possible interference with treatment chemical performance. These correlations were pronounced at the FWKO but largely lost for the downstream WP data due to the loss of suspended materials along the water handling system. Sulfate levels also correlated with failure frequency in these systems consistent with the role of the sulfate-reducing bacteria in sustaining the corrosion process. Failure frequency exhibited this correlation with sulfate levels despite control by barite precipitation.

Corrosion and Treatment Chemicals

Residual sulfite levels from the addition of ammonium bisulfite oxygen scavenger and residuals from the addition of a filming amine corrosion inhibitor exhibited an inverse correlation with failure costs at the WPs. This is satisfactory from a treatment point of view, but the case for sulfite as an oxygen scavenger is compromised by the correlation of residual concentrations and corrosion rates for both weight loss coupon and electrochemical data (both general corrosion rates and pitting data).

Microbiology

Almost all units show an increase in the density of sulfate-reducing bacteria from FWKO to WP downstream (Fig. 4). Acid-producing bacteria (APB) show no such spatial distribution. A surprising and robust correlation, however, was found between the number of acid-producing bacteria in a system and the increase in sulfate reducers going from the FWKO to WP (Fig. 5). This correlation is sustained even when data for individual units are plotted over the 30-month period. While APB have been cited by Pope in studies funded by the Gas Research Institute [*3*], as agents of corrosion, independent of SRB, this is the first time a correlation or relationship between these groups of organisms has been seen in a field system. It is tempting to suggest that the APB represent organisms capable of breaking down complex substrates to feed the SRB and that in these water-handling systems, hydrocarbons present in the FWKO are being degraded to support the increase of SRB in the downstream elements (WP).

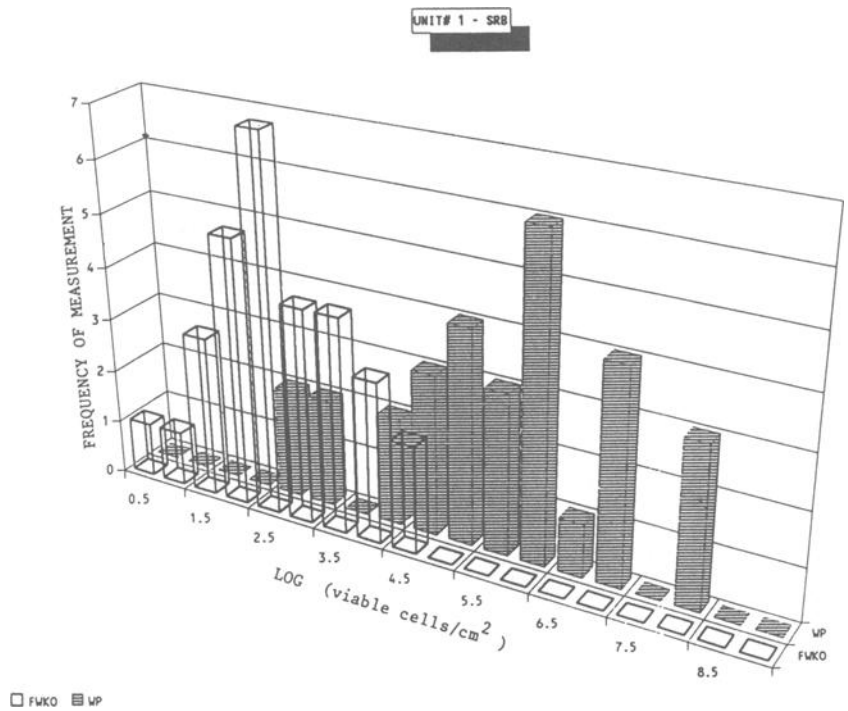

FIG. 4—*Distribution of viable cell counts for sulfate-reducing bacteria in Unit 1, free water knock out, and waterplant over a 30-month period.*

Microbiology and Water Chemistry

Observation of changes in sessile microbial numbers with spontaneous variations in water chemistry at Unit 13 [*1*] suggested that sulfate-reducing bacterial populations in the waterplant respond positively to chance increases in sulfate concentration but negatively to chance

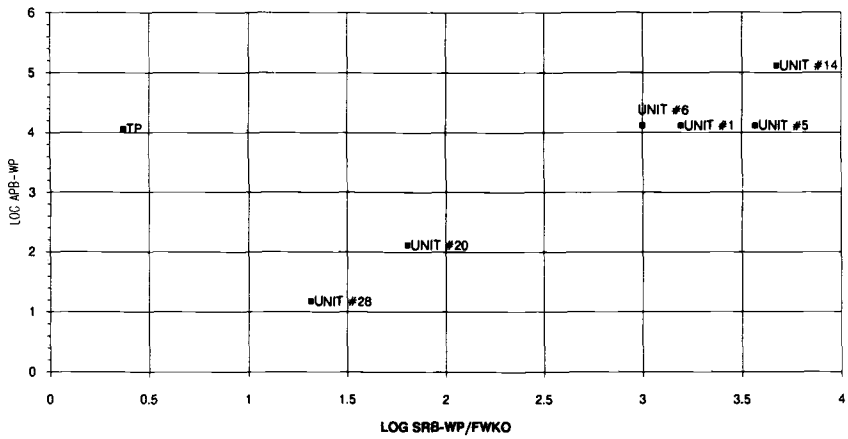

FIG. 5—*Correlation between acid-producing bacteria and increase in sulfate-reducing bacteria between free water knock out and waterplant.*

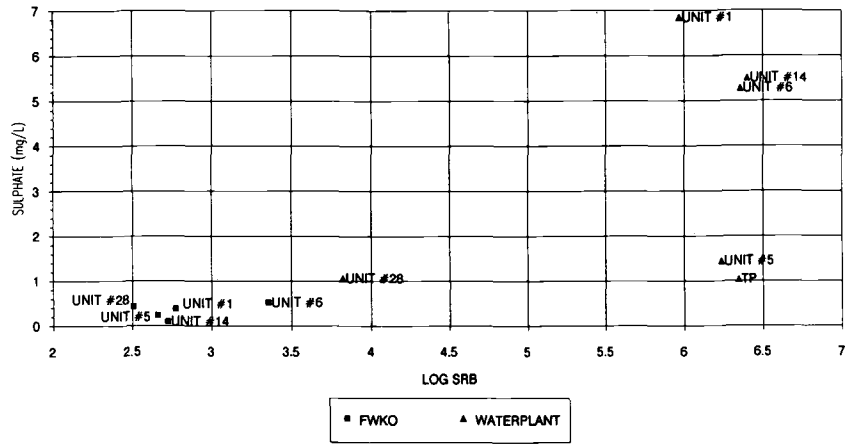

FIG. 6—*Correlation of soluble sulfate with density of sulfate-reducing bacteria in biofilms.*

increases in nitrate and magnesium concentrations. Unfortunately, nitrate was not monitored in the audit, and a separate investigation had to be carried out in the field test facility as briefly described in the next section.

Audit data did show inverse correlations between APB numbers generally and SRB numbers at the WP with magnesium and, more importantly, hardness. It may be that total brine strength is the key since there is no obvious reason why magnesium in itself should be inhibitory at these concentrations. The general increase in sessile bacterial counts between the FWKO and waterplant did show an inverse correlation with conductivity at the waterplant consistent with this view.

Correlation of soluble sulfate with SRB numbers (Fig. 6) indicates that significant sessile SRB populations are sustained at 2-mg/L soluble sulfate. Given the total water flow in these systems (hundreds of cubic meters/day), adequate sulfate is apparently available from a steady-state concentration in this range.

Higher pH favors both sulfate reducers and the so-called acid-producing bacteria (Fig. 7). Ability to ferment sugars in the APB assay medium may not indicate acid production in a mixed community in the field.

APB numbers correlated with suspended solids entering the FWKO and inversely with residual oxygen. The latter observation is consistent with the use of adventitious oxygen by these organisms.

Microbiology and Treatment Chemicals

Biocides were being injected into field units during the audit. No comment will be included here on their efficacy. Figure 1 illustrates that other parameters act on biofilm populations with at least comparable potency.

Residual sulfite from the ammonium bisulfite oxygen scavenger and residuals from the phosphate rich scaling inhibitor used in this field both correlated with the increase in numbers of APB and SRB at the WP.

Microbiology and Corrosion

Figure 8 shows the correlation of corrosion rate by weight loss coupon with the increase in SRB population in going from the FWKO to the WP. A correlation also exists between

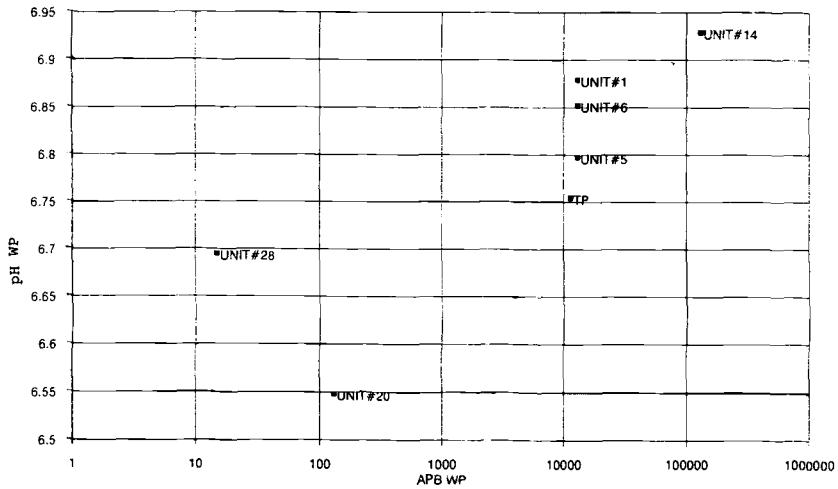

FIG. 7—*Correlation of pH and density of acid-producing bacteria (APB) in waterplant biofilms.*

the SRB in the FWKO and weight loss data. These observations support the use of SRB numbers as an index of biocide performance in these field systems. No other correlation between corrosion measurements and microbial numbers was found.

Field Test Facility

The field test facility is a set of five instrumented side streams located in the Unit 13 waterplant. Each 1-in. (2.54-cm) line is equipped for independent chemical injection, and flow can be controlled separately. Water is pumped through the unit once without recycle.

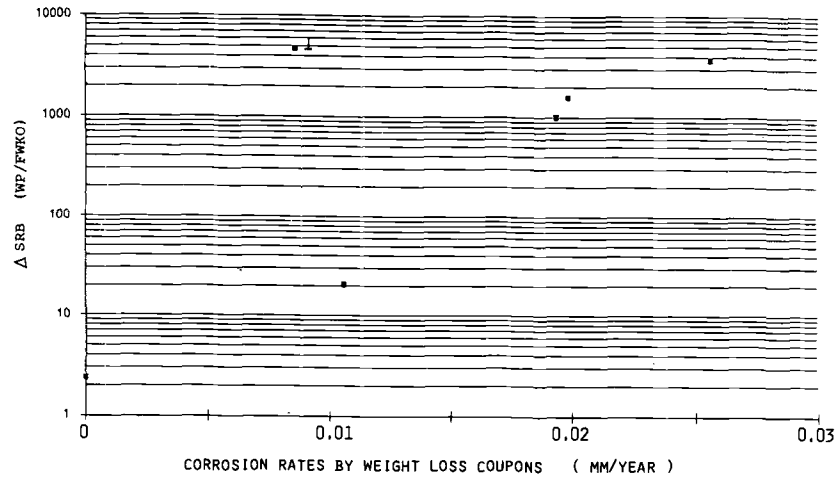

1. UNIT #14 IS ANOMOLOUS. CONDUCTIVITY DROPS FROM 76 TO 31 MS/CM FROM FWKO TO WATERPLANT DUE TO FRESHWATER MAKEUP. 'OTHER UNITS DROP LESS THAN 5%.

FIG. 8—*Correlation between increase in sulfate-reducing bacteria from free water knock out to waterplant and corrosion rates by weight loss coupon.*

To test several ideas emerging from this study, trace levels of nitrate, oxygen scavenger and acetate/lactate nutrient were injected into separate lines in this facility and the effect on lactate and acetate utilizing SRB as well as APB in the sessile population monitored over ten weeks. While details of these experiments will be reported separately, conclusions are included in the next section for the sake of completeness.

Conclusions

Useful correlations in audit data between corrosion-monitoring measurements are almost nonexistent. This means that field corrosion personnel must use a combination of indicators interpreted through experience to optimize control programs. Long-term plots of corrosion failure frequency and cost remain the final proof of efficacy.

Electrochemical measurement of corrosion rate gives a general correlation with corrosion weight loss data; however, absolute values differ and individual measurements taken locally seem unlikely to agree.

Corrosion failures in these systems do correlate with the conductivity of the water, hardness, suspended solids, oil and grease, and soluble sulfate. The last correlation is interesting since soluble sulfate is limited by barite precipitation to very low levels. The importance of sulfate and a correlation between corrosion rates by weight loss coupon and the increase in SRB going from the FWKO to the WP suggests that bacterial corrosion is important.

The addition of corrosion inhibitor correlates with reduced failures and has no relationship with measured corrosion rates or with bacterial numbers in the downstream part of the systems most prone to corrosion damage.

Residual sulfite from addition of ammonium bisulfite as an oxygen scavenger correlates not only with lower failure costs but also with increased corrosion rates and increased bacterial biofilm densities in waterplants. Experimental results from the field test facility confirmed an increase in lactate utilizing SRB results from trace sulfite addition. These observations make its use suspect.

Increased bacterial populations in waterplants correlated with excess use of scaling inhibitor, and it seems likely that both scaling inhibitor and oxygen scavenger may be promoting bacterial growth by providing necessary nitrogen, sulfite, and phosphorus in opposition to the effect of biocide addition.

In contrast to the positive influence of these treatment chemicals, water conductivity and hardness appear to limit bacterial numbers. The pH is a particularly key variable even over a range of 0.5 pH units. The correlation of high APB numbers with higher pH indicates that these organisms are not controlling the system pH in the field through acid production. They are also promoted by suspended solids and oil and grease entering the system. An inverse correlation with residual oxygen is consistent with their use of oxygen in breaking down complex hydrocarbons as a nutrient source for the community. Consequent production of lactate/acetate type organics by the mixed community would then explain the growth of SRB numbers through the system from FWKO to WP, being dependent on the APB numbers present. This is the first indication of a relationship existing between APB and SRB in a field system. Addition of trace levels of acetate and lactate to a slip stream in the field test facility in the Unit 13 waterplant confirmed that both lactate and acetate utilizing sulfate-reducing bacteria are limited by organic nutrients.

Sulfate concentration in these high flow water systems is limiting only below 2 mg/L. The common idea that systems low in sulfate will not have SRB problems is clearly at variance with the data here. It is the total availability of sulfate, not its concentration, that is the key to the importance of SRB in a given site.

Earlier observation that chance nitrate excursions reduced SRB numbers in the Unit 13 waterplant [*1*] was confirmed by the intentional injection of nitrate into the field test facility. The addition of low concentrations of nitrate has been observed to inhibit sulfide production previously and has even been suggested as a way to control the activity of sulfate-reducing bacteria in the reservoir [*4,5*]. Addition of 100 mg/L of sodium nitrate to a test stream in the field test facility did suppress sulfide production. Iron sulfide, a common constituent in biofilms from these systems, was not seen on this line after 70 days injection. Nevertheless, a very thick biofilm did develop and corrosion rates measured by electrochemical methods and weight loss coupons increased markedly. Thus, nitrate does not appear to be a desirable inhibitor for field use.

Extensive studies of this kind provide a context for discussion of measurement and enumeration of bacteria associated with field corrosion and fouling problems. It is clear from the insights of this audit that single or even limited data sets based on a few microbial samplings can be very misleading, and factors other than biocide treatment can have profound and competitive impact on microbial numbers. It seems probable that the state of the art biocide technology is close to its economic limits of performance and that any advance in practice will have to come through a better understanding and manipulation of the factors influencing sessile populations in the field.

Acknowledgments

The authors gratefully acknowledge CANMET, Energy, Mines and Resources, Ottawa for partial support of this work.

References

[*1*] Jack, T. R., Bramhill, B. J., and Ferris, F. G., "Field Studies of Biocorrosion and its Control in Water Piping Systems," in *Proceedings of the Eighth Annual General Meeting of BIOMINET, October 31, 1991*, W. D. Gould and S. Lord, Eds, CANMET, EMR, Ottawa, 1992, pp. 1–18.

[*2*] Ferris, F. G., Jack, T. R., and Bramhill, B. J. "Corrosion Products Associated with Attached Bacteria at an Oil Field Water Injection Plant," *Canadian Journal of Microbiology*, Vol. 38, 1992, pp. 1320–1324.

[*3*] Pope, D. H., *Annual Report: Microbiologically Influenced Corrosion in the Natural Gas Industry*, Gas Research Institute, Chicago, 1991.

[*4*] Jack, T. R., Lee, E. G., and Mueller, J. C., "Anaerobic Gas Production: Controlling Factors," in *Microbes and Oil Recovery, Proceedings of the International Conference on Microbial Enhancement of Oil Recovery, Fountainhead, Oklahoma, May 20–25, 1984*. J. E. Zajic and E. C. Donaldson, Eds., Petroleum Bioresources, El Paso, 1985, pp. 167–180.

[*5*] Jenneman, G. E., McInerney, M. J., and Knapp, R. M. "Effect of Nitrate on Biogenic Sulfide Production," *Applied and Environmental Microbiology*, Vol. 51, 1986, pp. 1205–1211.

George J. Licina,[1] *George Nekoksa,*[2] *and Robert L. Howard*[3]

An Electrochemical Method for On-Line Monitoring of Biofilm Activity in Cooling Water Using the BIOGEORGE™[4] Probe

REFERENCE: Licina, G. J., Nekoksa, G., and Howard, R. L., **"An Electrochemical Method for On-Line Monitoring of Biofilm Activity in Cooling Water Using the BIoGEORGE™ Probe,"** *Microbiologically Influenced Corrosion Testing, ASTM STP 1232,* Jeffery R. Kearns and Brenda J. Little, Eds., American Society for Testing and Materials, Philadelphia, 1994, pp. 118–127.

ABSTRACT: The presence of active microorganisms on piping and components in cooling water systems can have a profound effect on the corrosion performance of such systems. Microbiologically influenced corrosion (MIC) can result in premature failures of critical and support systems, increased downtime of equipment for repairs and maintenance, and increased operating costs associated with mitigation measures. In some cases, MIC has forced premature replacement of tanks, heat exchangers, and piping systems with a severe effect on plant availability.

Monitoring methods that alert plant operators that biofilm formation is occurring on pipe work and components permit the operators to initiate mitigation actions before biofouling becomes severe or MIC has occurred. The effectiveness of common water treatment chemicals is also increased substantially by prompt actions. Unfortunately, most monitoring activities rely upon process controls or batch methods that are too slow or of insufficient sensitivity to permit reliable control and implementation of mitigation techniques. Those methods are also too slow to be utilized for process controls of biocide additions, hence, mitigation activities are often excessively costly, both environmentally and in terms of direct costs of antimicrobial chemicals.

An electrochemical probe to permit on-line monitoring of biofilm activity under power plant or other industrial exposure conditions is under development. This device, the BIoGEORGE[4] electrochemical biofilm monitor, permits on-line evaluations of the effects of biofilm formation upon the surfaces of passive alloys such as stainless steels exposed to cooling water environments. Benchtop experiments have shown that biofilm formation on stainless steel surfaces can be detected by an electrochemical indication well in advance of any visual evidence of biofilm or corrosion on the electrodes. The probe may be used to provide an early warning to plant operators to take appropriate actions such that biofouling and MIC may be avoided. The simplicity of the design and operation sequence are such that probes may be installed and left to operate unattended for extended periods with only minimal operator interaction.

The design of the probe, results of benchtop experiments, and a description of its installation at the Browns Ferry Nuclear Plant are described.

KEYWORDS: monitoring, microbiologically influenced corrosion (MIC), electrochemical methods

[1] Associate, Structural Integrity Associates, 3150 Almaden Expressway, Suite 145, San Jose, CA 95118.

[2] President, Corrosion Failure Analysis and Control, 209 Gaucho Court, San Ramon, CA 94583.

[3] Engineer, Tennessee Valley Authority, Browns Ferry Nuclear Plant, P.O. Box 2000, Decatur, AL 35602.

[4] Trade name of Structural Integrity Associates, San Jose, CA.

Background

Microbiologically Influenced Corrosion (MIC) is a significant source of degradation in nuclear and fossil-fueled power plants, oil production, chemical processing industries, pulp and paper, transportation, and water distribution networks. Damage due to MIC results in increased downtime of equipment, increased operating costs, and can jeopardize the safe operation of plant equipment. Control methods include: mechanical and chemical cleaning, water treatment, and thermal treatments. In many cases, system replacement has been required. Chemical methods are the most common mitigation approach. Such treatments can be expensive in terms of increased operator activity, the costs of the water treatment chemicals and the chemical delivery systems, and environmental impact. Simple and reliable methods for monitoring biofilm activity that permit an accurate and early indication of biofilm formation provide a means to improve MIC control significantly. Monitors can also help to optimize water treatment by eliminating costly and environmentally unsound over-treatment of waters. On-line methods permit the system operator to take mitigation actions **before** a damaging biofilm becomes established while using the optimum treatment. Over-treatment of the water is avoided resulting in lower operating costs.

On-line biofilm monitors, like all in-plant equipment must be:

- **Simple to Use**—Installation and routine maintenance of the probe should not impact power plant operations.
- **Simple to Interpret**—Results should be readily interpreted by operations personnel. Corrosion specialists should not need to be consulted routinely. Outputs should be amendable to automation (alarms, and so forth).
- **Rugged**—The probes and equipment must be sufficiently rugged that frequent, unscheduled maintenance is avoided. Sensitivity to external noise (for example, welding, the plant's turbine-generators) is unacceptable.
- **Sensitive**—Detectable electrochemical effects should appear on the probe before thick biofilms are established on plant components.
- **Accurate**—A monitoring device must provide reliable detection of biofilm activity with a minimum of false calls.
- **Economical**—Cost for installation, maintenance, and operation must be cost effective, as reflected by potential savings realized as a result of the improved monitoring capabilities.

The following sections will discuss the design and performance of the BIoGEORGE probe relative to these requirements.

Approach

The BIoGEORGE probe monitors changes in electrochemical reactions produced by biofilms on stainless steel electrodes. This method was selected in preference to other candidate approaches as discussed in Ref *1*. The use of electrochemical methods to monitor the effects of biofilms on corrosion have been discussed elsewhere [*2–5*].

The BIoGEORGE probe (Fig. 1) consists of two identical electrodes (where each electrode is made up of a series of identical stainless steel discs), mounted on a threaded stainless steel body, and a simple control and data acquisition system. One set of discs is polarized relative to the other for a short time (~ one hour) each day. Polarity always remains the

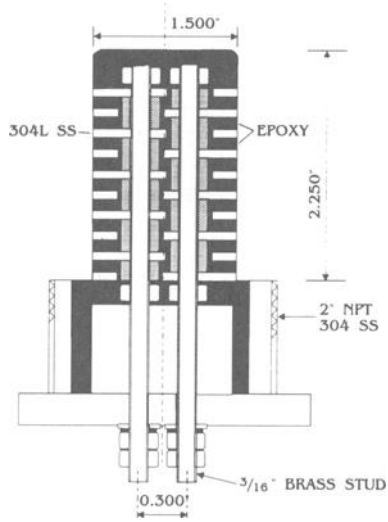

FIG. 1—*BIoGEORGE probe.* (© Copyright 1993 by NACE International. All rights reserved by NACE; reprinted by permission.)

same. At all other times, the electrodes are connected through a zero resistance ammeter. Currents and potentials are monitored continuously. Deposits that produce an increase in the current required to achieve the applied potential, such as biofilms, may be detected by monitoring the current that flows during the polarization cycle. For example, biofilms that catalyze oxygen reduction in aerated environments (Fig. 2) or produce alternative cathodic

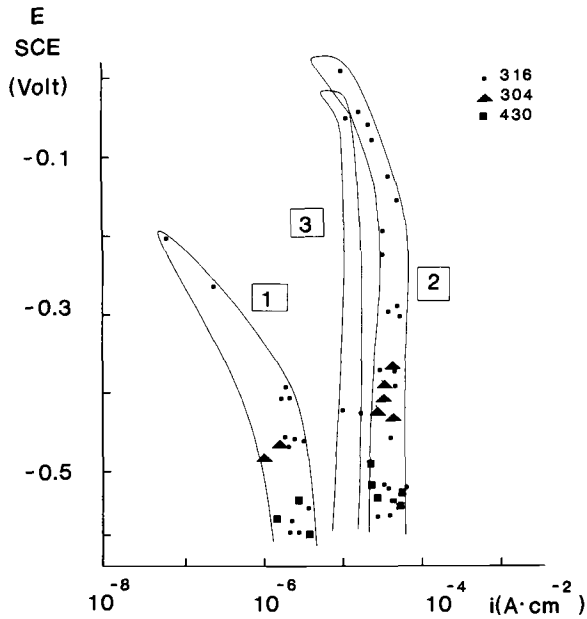

FIG. 2—*Oxygen reduction rates measured on stainless steels exposed to natural seawater. Curve 1 is measured within 1 to 2 days of immersion; Curve 2 is observed fourteen days later; Curve 3 is observed after a long term (from Ref* 15).

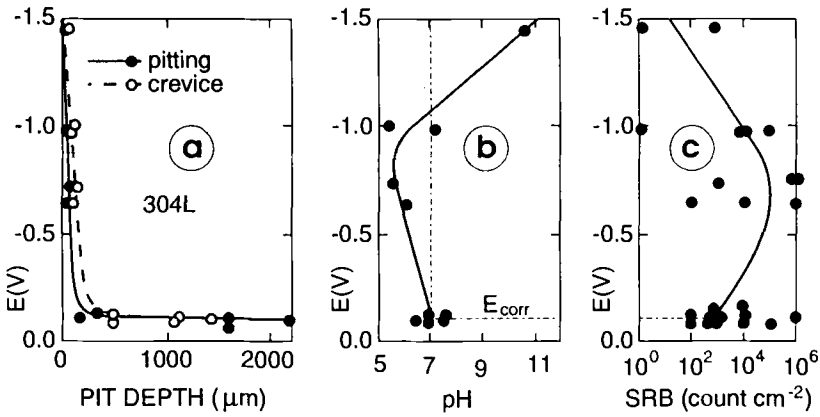

FIG. 3—*Correlation of cathodic protection potential on Type 304L stainless steel versus (a) corrosion, (b) pH on the sample, and (c) SRB count. E = potential (SCE); PD = pit depth (max); and CP = corrosion potential (from Ref* 13). (© Copyright 1993 by NACE International. All rights reserved by NACE; reprinted by permission.)

reactions (for example, the result of SRB or acid-producing bacteria) should be readily detectable, simply by monitoring changes in the current during the polarization cycle. The low level of polarization also simulates conditions conducive to microbial colonization such as those resulting from local anodic sites like inclusions or weldments. The "gentle" cathodic polarization can also encourage microbial colonization, similar to that observed on cathodically protected structures in biologically active environments [6,7] (Fig. 3).

The standard probe design uses a threaded pipe plug of nominal 2 in. (50 mm) size. Other sizes and configurations can be accommodated, including smaller dimensions, amenable to the use of fittings that permit insertion or removal at full temperature and pressure as used for the installation in the fire protection system at the Tennessee Valley Authority's Browns Ferry Nuclear Plant (Fig. 4).

Methods

Laboratory Experiments

In the initial laboratory studies, probes constructed using Type 304L stainless steel discs and PVC probe bodies (as compared to the stainless steel body as shown in Fig. 1) were exposed to soil extracts under stagnant, passively aerated conditions. Soils known to be rich in biological activity were mixed with deionized water (one volume of soil to ten volumes of water). Steels buried in the soil used for Soil Extract 1 had exhibited a history of rapid corrosion. The soil itself exhibited a high total organic carbon content and a definite sulfide odor. The soil used for the second soil extract experiment was removed from a garden that supported a variety of flora and fauna. In both soil extract experiments, half of the soil/water mixture was boiled for ten min to decrease its microbiological activity. This sample was used to provide a "sterile" control. Both probes were exposed in 600 mL beakers that were shielded from light to minimize the influences of algae. The test cells were covered but not hermetically sealed, thus permitting communication of the environment with ambient air.

A potential of 200 mV was applied between the two stainless steel electrodes for 30 min every day. The electrodes were shorted to each other the remaining 23½ h of the day.

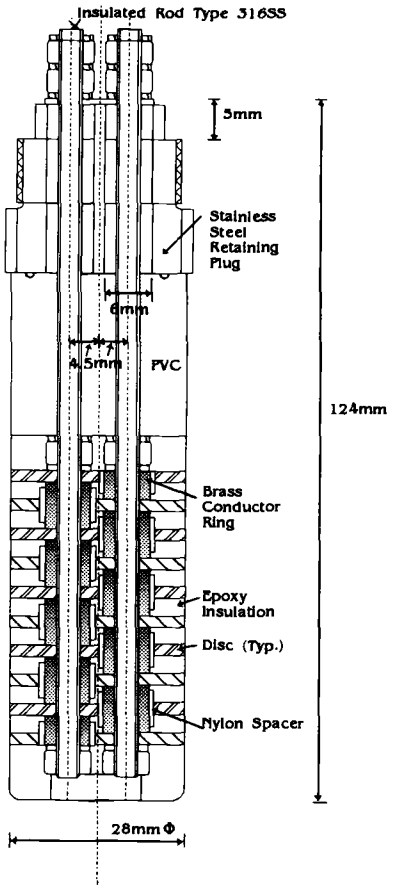

FIG. 4—*BIoGEORGE probe for installation at Browns Ferry.* (© Copyright 1993 by NACE International. All rights reserved by NACE; reprinted by permission.)

Currents were monitored continuously. These currents were plotted to illustrate trends and to discern when the local environments on the electrodes had changed significantly, as would result from the formation of a biofilm that would influence cathodic or anodic half-reactions.

Once trends in current had stabilized, the polarization was ceased but measurements of current were continued or potentials were measured against a saturated calomel electrode.

Post-test characterization of probe surfaces consisted of carefully scraping deposits from the "positive" and "negative" electrodes using sterile tools. These films and the bulk environment were then characterized by serial dilution using MICKITS[5], via Hach Biological Activity Reaction Test Kits,[6] and a portable pH sensor.

Plant Exposures

The initial plant exposures, done at the Tennessee Valley Authority's Browns Ferry Nuclear Plant, required a slightly different design for the probe (Fig. 4). The plant had

[5] Trade name of Bioindustrial Technologies, Inc., Grafton, NY.
[6] Trade name of Hach, Inc., Loveland, CO.

installed a number of high-pressure access fittings that permitted sensors, coupons, and so forth, to be installed or removed with the system at full pressure and temperature. These fittings were of a much smaller diameter than that of the standard probe. A smaller diameter probe was built, using the Caproco bore seal nut as the probe body. That approach permitted the probe to be installed through these fittings. One probe was installed into an 8-in. (200 mm) carbon steel pipe in the plant's high-pressure fire protection system. The probe was exposed to raw water at ambient temperatures that, historically, range from about 1 to about 32°C.

As for the laboratory tests, one probe was used as a "sterile" control. The control environment was prepared by extracting several liters of water from the fire protection system, then boiling it vigorously for ten min. The control probe was exposed to this environment in a beaker covered with metal foil.

Both probes were polarized to 200 mV for 30 min each day, then shorted the remainder of the time. Currents were monitored continuously using a Johnson-Yokogawa HR-2400 hybrid recorder. Plots of current during the polarization (a time approximately ten min into the polarization cycle was selected as a representative value) and with the external polarization off (immediately prior to the start of the polarization cycle) were made to indicate trends in these current values.

Results

Laboratory Experiments

Over the first week or two of the initial soil extract experiment, the current required to achieve this potential (the "applied current") remained steady at a value of approximately 0.5 μA. After about two weeks' exposure, the current began to increase steadily, an effect consistent with the formation of a biofilm (Fig. 5, top). No change in current was observed for the "sterile" control.

The biologically active sample produced an interesting and unexpected effect. Shortly after the apparent onset of biofilm formation (signaled by the increase in the current required to achieve the preset potential of 200 mV), it was found that current flow continued, **even after the impressed potential was removed** (Fig. 5, bottom). That is, the biologically-active cell continued to generate currents from 1 to 2 μA even after the impressed potential was removed. The biologically active sample continued to exhibit a potential difference of 40 to 300 mV and a current of several tenths of a micro-amp between the electrodes for another month, although no potential was applied during that time. Generated currents and potentials remained zero in the control cell.

Post-test examination revealed no corrosion or mineral deposits and only minor discoloration of one set of discs. The observed currents were of a magnitude that should have produced measurable corrosion. This suggested a second test to delve more deeply into the source of the observed currents.

A second test in the extract of a different soil showed similar behavior to that noted in the initial exposure (Fig. 6). Post-exposure characterization of the electrodes from the second soil extract experiment showed that material scraped from the "positive" and "negative" electrodes exhibited a difference in pH of approximately 1 pH unit. The "positive" electrode was the more acidic. Microbiological characterization was done using MICKITS and Biological Activity Reaction Tests. These procedures showed that viable acid producing bacteria (1000 to 10 000 cells/cm^2 of sample)[7] were present on the "positive" electrode. The soil extract itself contained sulfate reducing bacteria, iron oxidizers, and slime formers.

[7] Approximately 1 cm^2 was examined.

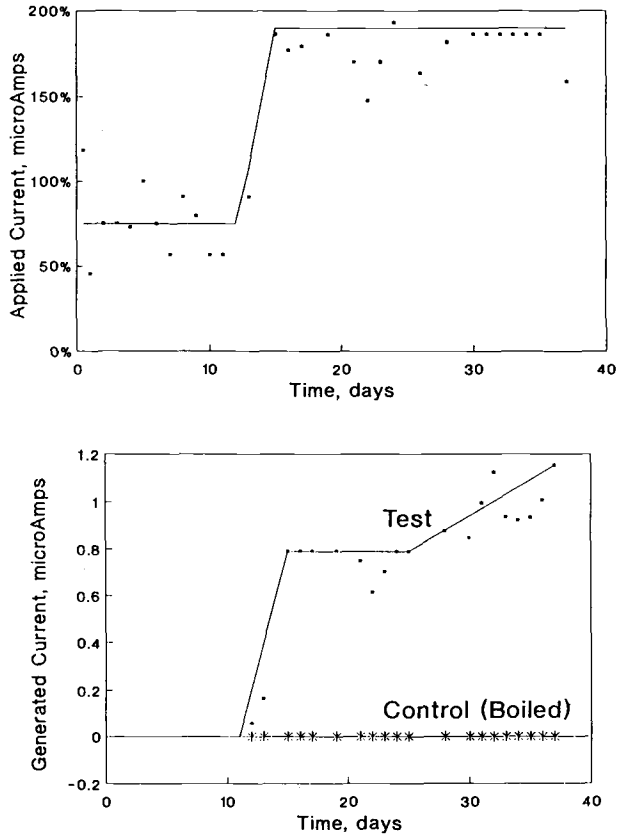

FIG. 5—*Current applied on and generated by MIC monitoring probe versus time. (Benchtop experiments in soil extract 1).* (© Copyright 1993 by NACE International. All rights reserved by NACE; reprinted by permission.)

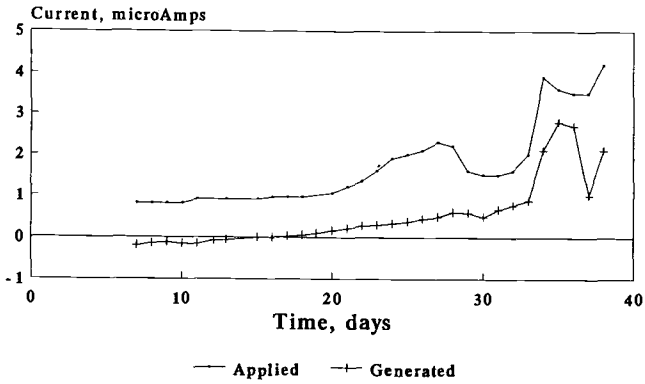

FIG. 6—*BIoGEORGE probe soil extract test 2.* (© Copyright 1993 by NACE International. All rights reserved by NACE; reprinted by permission.)

Plant Exposure

The probes installed at Browns Ferry were polarized to 200 mV for 30 min each day. Figure 7 presents the results of approximately 6½ months' exposure. The probe was installed in October, when the water temperature was fairly low. As would be expected, both the applied and generated currents remained low for the first 35 to 40 days' exposure. About December 15, after approximately 52 days' exposure, both the applied and generated currents for the probe in the fire protection system exhibited a very definite increase. The applied current steadily increased from approximately 1 to 17 μA. The generated current (the current that persists even after the electrodes have been shorted to one another) exhibited a similar trend beginning at about the same time; increasing from essentially zero to nearly 4 μA.

Seasonal conductivity and temperature variations that this line experienced had little effect on the probe. Increases in flow (for example, hydrant testing during January and February) did not corrupt the signal.

Late in January, the generated current began to decrease, although the applied current remained fairly constant at a value of approximately 17 μA. A definite generated current of approximately 0.5 μA persisted throughout February, March, and much of April, then suddenly decreased to zero.

Throughout the entire exposure, the applied current on the control sample (exposed to water from the fire protection system that had been boiled for ten min to kill microbes) remained at very low levels and no generated current was observed. The BIOGEORGE probe continues to be exposed to the Browns Ferry fire protection system environment.

Discussion

Outputs from a BIOGEORGE probe may signal the system operator to take mitigation or prevention actions. These actions may include: additions of biocide or increases in dosage of biocide additions, verification of the proper operation of biocide addition equipment, or initiation of flow on a stagnant loop. Traces from a BIOGEORGE probe may also be used to tune biocide treatments such that the minimum addition is made that prevents biofilm formation.

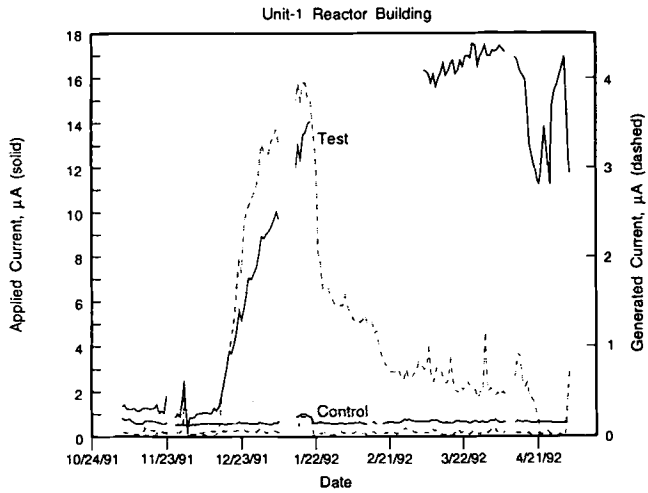

FIG. 7—*BIOGEORGE probes at Browns Ferry.* (© Copyright 1993 by NACE International. All rights reserved by NACE; reprinted by permission.)

Biological consortia on metallic surfaces often affect the electrochemical nature of the surface. Biological activity can influence the rates and nature of such reactions, particularly, the cathodic half-reaction. For example, stainless steels in aerated seawater undergo a noble shift in the open circuit potential (OCP) as a result of such effects [*8–11*]. Similar effects have been observed in fresh waters as well [*12,13*]. Experience with cathodically protected structures also suggests that microbiological growth can be stimulated by cathodic protection [*6,7*]. The two-electrode BIOGEORGE probe uses this experience to provide a simple and reliable method for encouraging microbiological colonization that should be accelerated relative to that of plant structures while providing a means for monitoring that settlement. Further, the use of a "gentle," intermittent polarization schedule also provides the opportunity to optimize microbial attachment on surfaces and their influences on electrochemical processes. These factors make the probe amenable to a variety of environments including both flowing and normally stagnant systems.

Increases in applied current signal the existence of a deposit or a change in the surface characteristics of the metal. A film that increases the rate of operative half-reactions (typically cathodic half-reactions) or permits more rapid, alternative half-reactions to occur will cause the applied current to increase. Most inorganic films would be expected to have only minimal effect on the applied current as they typically present an impediment to such reactions. Calcareous deposits dramatically reduce the current required to maintain a cathodic protection potential. Biofilms, on the other hand, would be expected to cause the reaction rates to increase [*2,8,10–13*]. The existence and nature of surface films may also be monitored by measuring their ohmic resistance. This method provides a third, independent method for detecting films, both biological and nonbiological.

The "generated" current (that is, the current that persists even after the applied potential is removed) appears to provide a measure of the activity of the biofilm on the metal. The laboratory tests and recent data from the plant exposure show that the generated current is much more sensitive to operating conditions (for example, temperature) and aging. In long exposures, the generated current often decreases to near zero signaling inactivity of the film. Future work will be devoted to evaluating this effect.

Conclusions

An electrochemical probe has been designed for industrial use. The multiple disc electrodes and intermittent cathodic polarization schedule provide an environment that is amenable to microbiological colonization. By tracking the current required to achieve the preselected potential, biofilm formation can be monitored on line.

The probe has been tested in the laboratory as well as in a power plant environment. The probe requires only minimal attention and interpretation of results and does not require the day-to-day involvement of a corrosion specialist. The probe produces consistent and stable outputs that do not appear to be affected by the normal dirt, noise, and electromagnetic interference inherent in a large power plant.

In laboratory tests in a passively aerated environment, the probe has provided a definitive indication of biological activity on the electrode surfaces. The probe appears to be readily amenable to the variable aeobisis of the plant environments.

Acknowledgments

Patent rights to the BIOGEORGE probe are owned by the Electric Power Research Institute. The cooperation of Mr. R. E. Taylor and Mr. A. Camp of the Tennessee Valley Authority are gratefully acknowledged.

References

[1] Licina, G. J., Nekoksa, G., and Howard, R. L., "An Electrochemical Method for On-Line Monitoring of Biofilm Activity in Cooling Water," CORROSION/92, Paper 177, National Association of Corrosion Engineers, Houston, TX, 1992.

[2] Mollica, A., Traverso, E., and Ventura, G., "Electrochemical Monitoring of the Biofilm Growth on Active-Passive Alloy Tubes of Heat Exchanger Using Seawater as Cooling Medium," *Proceedings, 11th International Corrosion Congress*, Florence, Italy, April, Associzione Italiana di Metallurgia, 1990.

[3] Dexter, S. C., Duquette, D. J., Siebert, O. W., and Videla, H. A., "Use and Limitations of Electrochemical Techniques for Investigating Microbiological Corrosion," *Corrosion*, Vol. 47, No. 4, 1991, pp. 308–318.

[4] Mansfeld, F. and Little, B. J., "The Application of Electrochemical Techniques for the Study of MIC - A Critical Review," CORROSION/90, Paper 108, National Association of Corrosion Engineers, Houston, TX, 1990.

[5] White, D. C., Sayler, G. S., Mittleman, M. W., Nivens, D. E., and King, J. H., "Nondestructive, On-Line Monitoring of Microbiologically Influenced Corrosion," CORROSION/91, Paper 114, National Association of Corrosion Engineers, Houston, TX, 1991.

[6] Nekoksa, G. and Gutherman, B., "Cathodic Protection Criteria for Controlling Microbially Influenced Corrosion in Power Plants," EPRI NP-7312, Electric Power Research Institute, Palo Alto, CA, May 1991.

[7] Guezennec, J., et al., "Cathodic Protection in Marine Sediments and the Aerated Seawater Column," *Microbially Influenced Corrosion and Biodeterioration*, N. J. Dowling, M. W. Mittleman, and J. C. Danko, Eds., University of Tennessee, 1991.

[8] Dexter, S. C. and Gao, G. Y., "Effect of Seawater Biofilms on Corrosion Potential and Oxygen Reduction of Stainless Steel," CORROSION/87, Paper 377, National Association of Corrosion Engineers, Houston, TX, 1987.

[9] Gundersen, G., Johansen, B., Gartland, P. O., Vintermyr, I., Tunold, R., and Hagen, G., "The Effect of Sodium Hypochlorite on the Electrochemical Properties of Stainless Steel and on Bacterial Activity in Seawater," CORROSION/89, Paper 108, National Association of Corrosion Engineers, Houston, TX, 1989.

[10] Scotto, V., "Electrochemical Studies of Biocorrosion of Stainless Steel in Seawater," *Proceedings*, 1988 EPRI Microbial Corrosion Workshop, EPRI ER-6345, G. J. Licina, Ed., Electric Power Research Institute, Palo Alto, CA, 1989.

[11] Holthe, R., Bardal, E., and Gartland, P. O., "The Time Dependence of Cathodic Properties of Stainless Steels, Titanium, Platinum and 90-10 CuNi in Seawater," CORROSION/89, Paper 393, National Association of Corrosion Engineers, Houston, TX, 1989.

[12] Dexter, S. C. and Zhang, H.-J., "Effect of Biofilms, Sunlight, and Salinity on Corrosion Potential and Corrosion Initiation of Stainless Alloys," EPRI Report NP-7275, Electric Power Research Institute, Palo Alto, CA, May 1991.

[13] Buchanan, R. A., Li, P., Zhang, X., Dowling, N. D. E., Stansbury, E. E., Danks, J. C., and White, D. C., "Electrochemical Studies of Microbiologically Influenced Corrosion," EPRI Report NP-7468, Electric Power Research Institute, Palo Alto, CA, Sept. 1991.

Hector A. Videla,[1] *F. Bianchi,*[2] *M. M. S. Freitas,*[2] *C. G. Canales,*[2] *and J. F. Wilkes*[3]

Monitoring Biocorrosion and Biofilms in Industrial Waters: A Practical Approach

REFERENCE: Videla, H. A., Bianchi, F., Freitas, M. M. S., Canales, C. G., and Wilkes, J. F., **"Monitoring Biocorrosion and Biofilms in Industrial Waters: A Practical Approach,"** *Microbiologically Influenced Corrosion Testing, ASTM STP 1232,* Jeffery R. Kearns and Brenda J. Little, Eds., American Society for Testing and Materials, Philadelphia, 1994, pp. 128–137.

ABSTRACT: This paper describes a practical approach to the assessment of biotic and abiotic processes at the metal/solution interface, introducing a nonconventional multipurpose sampling device that can be used in a conventional side-stream corrosion rack. The complete monitoring program for biofilms and corrosion in water-using systems includes parallel field and laboratory measurements, in addition to the sampler exposures. This device can simplify collection of samples for biofilm and corrosion product analyses, facilitate field and laboratory studies for biocide selection, and provide a useful source of samples for assessing corrosion and biofouling effects in the system. Two practical cases, involving an industrial cooling water system and a secondary oil recovery water injection line, are briefly described to illustrate the effectiveness of the monitoring program.

KEYWORDS: biocorrosion, biofouling, monitoring devices, sampling devices, cooling water, injection water

Introduction

Corrosion and scaling control monitoring have been the two primary objectives of cooling water treatment programs in past years. Since the beginning of the present decade, biofouling and biocorrosion are finally getting the attention they deserve. The major concern now is to improve methods for maintaining heat transfer efficiency, by control of biological deposits, while preserving corrosion inhibition and avoiding scale formation.

Biocorrosion is rarely linked to a single mechanism or to a single species of microorganisms. Biofilms mediate the interaction between metal surfaces and the aqueous environment leading to an important modification of the metal/solution interface. Thus, a complementation of microbiological, electrochemical and surface analysis techniques is mandatory [*1*].

Microbiological fouling of pipelines and heat exchangers is a multi-step process that involves a series of biological and inorganic changes, all of which alter the metal/solution interface. To understand this process, a realistic monitoring program is needed to clarify the relationships between biotic and abiotic variables, which permit differentiation between abiotic corrosion and biological reactions. Although corrosion data obtained from standard

[1] Senior research biochemist, Bioelectrochemistry Section, INIFTA, University of La Plata, Suc. 4, CC 16, La Plata 1900, Argentina.

[2] Senior chemical engineers and micro-biologist, respectively, GRACE-Aquatec Quimica, Sao Paulo, Brazil.

[3] Consulting chemical engineer, Titusville, FL.

test methods like weight loss, electrical resistance or fouling tendency under heat transfer conditions are useful, they do not provide complete information needed for the evaluation and measurement of biocorrosion.

This paper describes a practical approach for monitoring the effects of biofilms on the corrosion behavior of metal surfaces used in heat exchangers and pipelines. This approach uses a new multipurpose sampling device and a complete monitoring program based on field and laboratory measurements. Results from two industrial water systems (a cooling tower of a nitrochemical plant and an oilfield waterflood system) will be presented to illustrate the suggested approach for monitoring biofouling and biocorrosion in industrial waters.

Present Monitoring Programs for Biofouling and Biocorrosion

Monitoring programs for biofouling and biocorrosion have been mainly devoted to assessments of planktonic populations in water samples and of corrosion by using weight loss measurements (corrosion coupons), electrical resistance, or polarization resistance probes.

The main objections to these types of biological monitoring programs are: the planktonic population does not properly reflect the type and number of organisms living in the biofilm and causing biodeterioration problems; and, the susceptibility of planktonic microorganisms to antimicrobial agents differs markedly from that of sessile microorganisms within the biofilm, because of the protective action of the extracellular polymeric substances (EPS). Thus, sessile bacteria are rarely affected by levels of biocides that completely kill planktonic cells in the same systems [*2*]. The use of biocides to control corrosion-causing bacteria requires killing bacteria in the structured consortia at the bottom of biofilms. This information can only be obtained in well-established biofilms like those developed in the water system.

From the corrosion side, the electrical resistance method is excellent for indicating a change in the general corrosion rate. Results are difficult, however, to interpret in the presence of localized forms of corrosion such as pitting, the most common form of attack found in biocorrosion cases [*3*]. Corrosion coupons and linear polarization are also most useful for systems undergoing uniform corrosion. If biofilms or localized corrosion are present, the polarization resistance will reveal that something is happening, but may not give an accurate measure of the rate of corrosion.

Only a different approach with other electrochemical methods or parameters assessing localized corrosion damage can provide valuable data for monitoring deleterious effects of biocorrosion and biofouling.

The economic consequences of biofouling are the primary reasons for industrial and research interest in the fouling of cooling water systems and pipelines. The deleterious effects of biofouling include: (1) energy losses due to increased fluid frictional resistance and increased heat transfer resistance; (2) increased capital costs for excess surface area in heat exchange equipment to account for fouling heat transfer resistance; (3) increased capital costs for replacement of equipment suffering under-deposit corrosion; (4) downtime, resulting in loss of production, to clean metal surfaces which fouled at an unanticipated rate; (5) quality control problems derived from fouling of equipment or fouling of the product stream; (6) safety problems resulting from leaks caused by corrosion pits which penetrate the wall thickness of heat exchangers and pipelines.

In the last decade, several fouling monitoring devices that measure the effects of deposits on transport processes (that is, heat transfer and fluid frictional resistance) have been developed for industrial water systems. Two common fouling monitors are: (1) devices with an annular flow passage and heated surface, and (2) devices with flow inside externally heated tubes. In the first example, the test section is internally heated and microfouling

develops in its outer area. The device is placed inside a container tube, forming an annulus between both tubes through which flow circulates. The container tube is generally made of glass to facilitate observation of the fouling surface. Devices of the second type measure thermal transfer degradation coefficient and fluid-frictional resistance. This configuration directly reproduces the flow regime in a condenser tube, and a sample of a condenser tube can be used as the test section. Even if these monitoring devices supply useful information on overall fouling effects, they are not able to: discriminate between inorganic fouling and biofilms; provide information on the nature and diversity of microbial components of deposits; or easily sample deposits on the internal surface of the tube.

Owing to the differences in biofouling and biocorrosion, an effective monitoring program must necessarily supply information on water quality, corrosive attack, sessile and planktonic bacteria, biofilm characteristics, and chemical composition of inorganic and biological deposits. Sampling devices for monitoring biofilms can be used to assess corrosive attack both before and after the removal of biological and inorganic deposits, giving wider and more useful information. There are two main types of monitoring devices: (1) directly implanted, and (2) side-stream implanted. Metal coupons, generally made from the same structural material as the system, present a known surface area, and enable an accurate count of sessile bacteria/cm^2 after biofilm detachment. Coupons are mounted in holding assemblies and inserted in the pipework of the laboratory or industrial system.

The main characteristics to be fulfilled by a good sampling device are: (1) to ensure that metal coupons experience a flow regime similar to the rest of the pipe surface; (2) to be inexpensive and easily manufactured; (3) to be easily withdrawn from the system; (4) to hold several sampling coupons for allowing duplication of tests and a higher diversity of assays per sampling device; (5) to be easily fitted in any conventional access to the system pipework or laboratory flow loops; and (6) when used in pressurized lines, to have a suitable design for being compatible with existing high-pressure fittings, avoiding a partial shut-down and depressurization.

A Practical Approach for Monitoring Biocorrosion and Biofouling in Industrial Waters

A new multipurpose side-stream sampling device, that can be fitted in any conventional corrosion rack, has recently been developed [*4*]. The sampler, identified as RENAprobe™ (Reusable Non-conventional Appliance), consists of a Teflon™ holding rod, alternately drilled on opposite faces to hold eight round metal coupons (0.5 cm^2 surface area each) four on each face of the holder (Fig. 1). The sampler can be side-stream implanted in a conventional corrosion rack for corrosion coupons. In this way, eight different samples can be collected simultaneously or at different exposure periods. After exposure, the entire assembly is withdrawn and the coupons removed for biofouling and corrosion assessment according to a suitable schedule. A typical scheme would be: (1) sessile bacterial counts; (2) biofilm observation by scanning electron microscopy (SEM); (3) surface analysis of corrosion products and biofilms; (4) optical microscopy and SEM evaluation of metal attack after removal of biological and inorganic deposits; and (5) electrochemical corrosion measurements in the laboratory or the field to assess localized corrosion. These studies are generally complemented with field and laboratory measurements such as: (1) water quality control; (2) field corrosion monitoring; (3) field redox potential measurements; and (4) other analytical data according to particular characteristics of each system (dissolved oxygen, sulfides, etc.).

For microbiological assessment, after the desired exposure period, the RENAprobe™ is removed from the system, and transported to the laboratory in a closed, sterile carrier (Fig. 1), for removal of biological and inorganic deposits by scraping or ultrasonic cleaning.

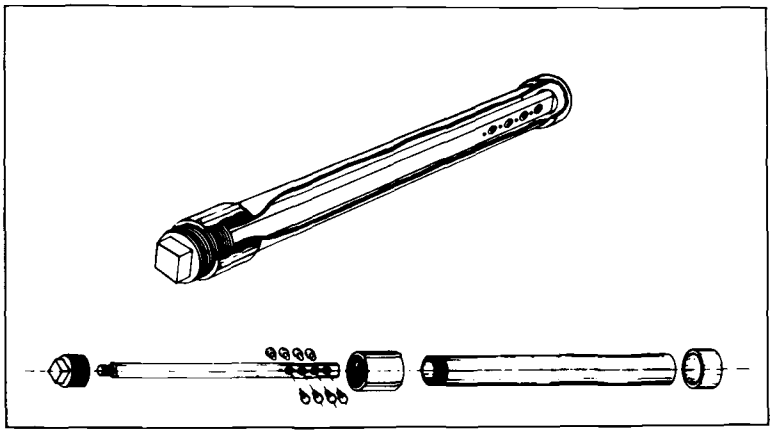

FIG. 1—*Scheme of the RENAprobe™ and carrier.*

Observations of biofilms and sessile bacteria with SEM require fixation of samples with a glutaraldehyde solution in phosphate buffer, followed by gradual dehydration through a series of acetone dilutions, and critical point or freeze drying. SEM observations of the corrosion attack do not require fixation, dehydration, and drying, only removal of the biofilm. In all cases, non-conductive samples must be coated prior to examination by sputtering a carbon or a palladium/gold coating layer. For energy dispersive X-ray analysis (EDXA) or any other surface analysis of biological or inorganic deposits, the use of metallization should be avoided to eliminate interferences with elementary analysis. In such cases, the application of a carbon coating is advisable.

RENAprobe™ coupons are generally constructed from the same structural material as the system (for example, carbon steel) (Fig. 2). However, a corrosion resistant substrate,

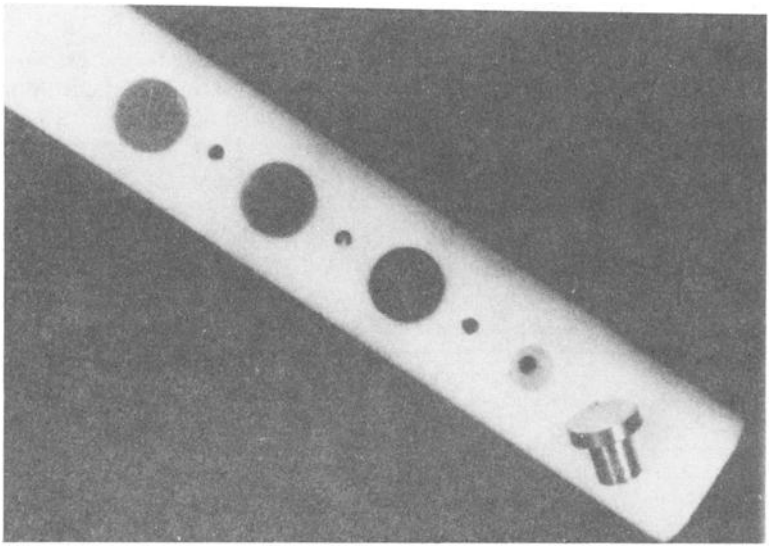

FIG. 2—*Close up of the RENAprobe™ sampling device (from Ref 5 with permission of NACE, Houston, TX).*

like stainless steel, is preferred for SEM observation of the biofilms and sessile bacteria, to avoid the presence of copious corrosion products that impede bacterial visualization.

Monitoring Biofouling and Biocorrosion in Industrial Waters: Two Case Histories

Chemical Industry Cooling Water Systems

Cooling waters of two open recirculating systems were studied [5]. The cooling water of both systems was treated using an organic phosphonate (PBTC) and zinc salt blend for corrosion control. Selective dispersant agents were also added to avoid scaling. To assess biofouling effects, chlorine was used in only one of the cooling systems (System 1), whereas no biocide was added to the water of the other circuit (System 2) during a testing period of 15 days.

Conventional weight loss method and linear polarization measurements were used to assess corrosion inhibition efficiency. Water chemical analyses and standard plate counts for planktonic bacteria were also performed as routine measurements in the plant. Electrochemical techniques conducted in the laboratory complemented field evaluations. For biofouling and biocorrosion monitoring, RENAprobe™ samplers were placed in one of the sampling sites of the side-stream corrosion rack of the cooling water system. After an exposure period of 5 days, the holder was removed and the biocoupons withdrawn immediately for culturing or for SEM observations.

Results of bacterial enumeration for System 2 showed hazardous levels of contamination with aerobic and anaerobic bacteria. Conversely, sessile bacteria counts for cooling water of System 1 were considerably lower (Table 1). These results were in close agreement with SEM observations of the biofilm. A comparison between carbon steel coupons from both systems revealed that, whereas metal attack was inhibited in the cooling water of System 1, steel coupons of System 2 presented copious corrosion products, even for the shortest exposure periods assayed. Pitting attack under these deposits was markedly different in size and shape from that observed in the biologically controlled cooling water.

Considering that the composition of the cooling water of both systems was similar and the operational conditions (corrosion and scale inhibition treatments) were equal, the biological source of the metal attack was evident.

Experimental evidence drawn from this case history shows that the adverse effects generated by biofouling can defeat the protective action of a conventional corrosion control water treatment, facilitating the initiation of localized attack.

Oilfield Water Injection Systems

Several factors affect biocorrosion and biofouling in secondary oil recovery operations: (1) velocity, temperature, oxygen level and redox potential of the injection water; (2)

TABLE 1—*Chemical industry cooling water system: sessile and planktonic bacteria enumeration and identification after 5 days exposure.*

	System 1 Microbiological Control		System 2 No Microbiological Control		
Tests No.	1	2	3	4	Units
Total aerobic bacteria	1.0×10^0	3.9×10^3	2.0×10^5	1.0×10^7	
Total anaerobic bacteria	$<10^0$	1.0×10^1	1.0×10^3	2.0×10^4	CFU/cm^2
Iron related bacteria	$<10^0$	8.6×10^3	3.3×10^4	3.3×10^6	

[a] CFU = Colony forming units—Measurement basis = CFU/cm^2.

chemical composition, pH, amount of organic matter and depth of pumping of the injection water; and (3) effectiveness of the biocide to gain access to the sessile bacteria within the biofilms. On this basis, a complete monitoring program for biofouling and biocorrosion using two types of sampling devices and several field and laboratory measurements, was scheduled [*6*]. The goals of the program were to perform a quick evaluation of the bacteriological status of the system, and to implement an effective biocide treatment for sessile bacteria. The limited information available before implementing the program was restricted to sporadic planktonic counts for aerobic bacteria and sulfate reducing bacteria (SRB), analytical data on water quality, and corrosion assessment based on weight loss measurements of metal coupons.

The simplified scheme for microbiological assessment was limited to the evaluation of SRB sessile population at three different locations (Fig. 3): (1) at Station I, between the coalescer tank and the depurator-separator system; (2) at Station II, between the filtered water storage tank and the injection pumps; and (3) at a point, under pressure, of the injection line, after the injection pumps. In Stations I and II, side-stream implanted RENAprobes™ were used, whereas a directly implanted Bioprobe™ sampler was installed in the pressurized injection water line. Samples from Station I were used to observe biofilms and corrosion attack on metal samples exposed to injection water without biocide treatment. Station II and the sampling point in the pressurized line were used to assess the effects of the biocide to mitigate biodeterioration.

After each exposure period (1 and 5 days), the coupon holder was withdrawn and the coupons removed for examination. Coupon distribution for analysis (per RENAprobe™) was as follows: one stainless steel coupon for biofilm observations by SEM; two carbon steel coupons for sessile SRB counts (in duplicate); two carbon steel coupons for biofilms/passive layers observations by SEM; one carbon steel coupon for EDXA of biological and inorganic deposits; and one carbon steel coupon for corrosion potential versus time measurements at the laboratory. In each case, two identical samplers were installed per station to allow for duplication.

For sessile SRB counts, the entire sampler holder was taken to the laboratory within a period of 12 h, in a closed receptacle filled with system water (Fig. 1). Biofilms were detached

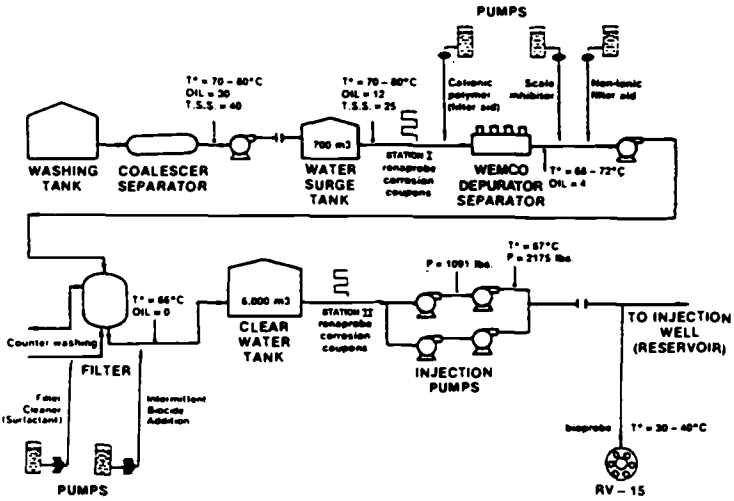

FIG. 3—*Plant scheme of the water injection systems. Location of sampling stations I and II can be seen in the figure.*

TABLE 2—*Chemical analysis of injection water.*

		Units
pH	6.7	
Total Alkalinity	117.0	ppm $CaCO_3$
Total Hardness	3190.0	ppm $CaCO_3$
Calcium Hardness	2900.0	ppm $CaCO_3$
Magnesium Hardness	300.0	ppm $CaCO_3$
Chlorides	15300.0	ppm Cl^-
Silica	100.0	ppm SiO_2
Sulphates	451.0	ppm $SO_4^=$
Total Iron	0.9	ppm Fe
Total Diss. Solids	30300.0	ppm
Dissolved Oxygen[a]	50.0	ppb
H_2S[a]	0.4	ppm $S^=$

[a] Average values at Station I.

by scraping with a sterile scalpel blade and poured into 10 mL of sterile injection water. Enumeration of viable SRB bacteria was made by serial dilution in liquid Postgate C medium with a saline content similar to the injection water (Table 2), according to the standard extinction dilution method. Dilutions were incubated for 2 weeks within the temperature range of the injection water (65 to 75°C). Readings of viable counts were made after 12 h of inoculation, and continued on a daily basis for 290 h (Table 3).

Corrosion was measured in the field by means of corrosion coupons located at both stations, by linear polarization measurements made in the field, and potentiodynamic polarization and corrosion potential versus time runs made in the laboratory. In addition to SEM observations of biofilms and EDXA analysis of corrosion products and biological deposits, water analysis included total iron, sulfates, total dissolved solids (TDS), dissolved oxygen, hydrogen sulfide and other physical and chemical determinations.

Macroscopic observations of samples made immediately after the removal of the samplers from Station I revealed black adherent deposits. Metal coupons from Station II (after biocide addition) had few surface deposits after 1 day of exposure. After 5 days of exposure, the deposits could not be detected. SEM observations confirmed the macroscopic differences observed in samples from both stations. Carbon steel samples were layered with copious corrosion products that hindered observation of sessile bacteria. Conversely, in samples exposed to injection water in the station without biocide treatment, stainless steel coupons exhibited copious biofilms of sessile rod-shaped and filamentous bacteria embedded in their mucilage. Biocide effects were observed in samples of Station II and after the battery of injection pumps. The stainless steel coupons exposed for 1 and 5 days to injection water had no sessile bacteria and the amount of deposits was negligible.

Metal attack observed after removal of deposits from the metal surfaces confirmed the marked differences found in samples of both stations. Carbon steel coupons, exposed for

TABLE 3—*Oilfield water injection system: results of sessile SRB monitoring from the waterflood injection line (Standard Extinction Dilution Method in Postgate C saline liquid medium).*[a]

Exposure of coupons, days	Reading time, h	Station I, CFU/cm^2	Station II, CFU/cm^2
1	290	10^8	10^7
5	290	10^8	10^6

[a] Results are the average values of triplicate runs.

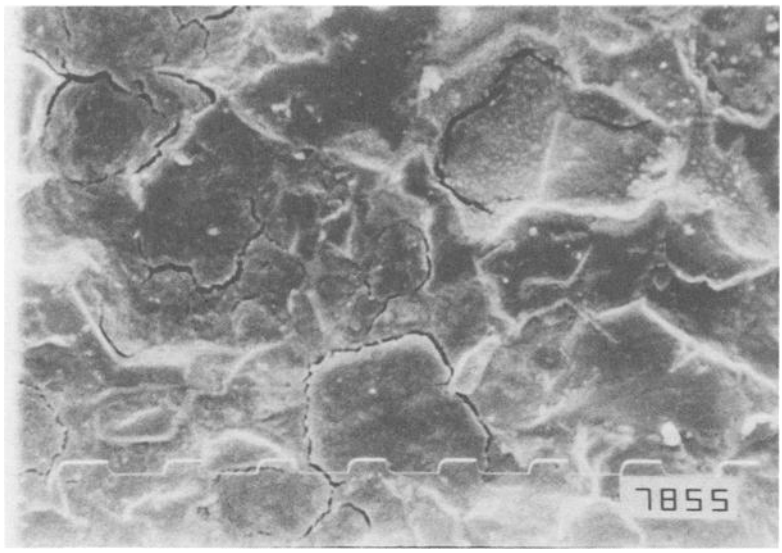

FIG. 4—*SEM micrograph of the corrosive attack on a carbon steel surface after a 5 day exposure to injection water at the Station I. Deposits were previously removed by mechanical cleaning (Magnification × 1500).*

only 1 day to injection water without biocide, presented localized attack and selective dissolution at the grain boundaries (Fig. 4). Conversely, after biocide injection, carbon steel samples presented scarce areas of micropitting and intergranular attack was absent (Fig. 5).

Corrosion experiments performed in the laboratory confirmed SEM observations and field measurements. Potentiodynamic polarization experiments revealed the absence of passive

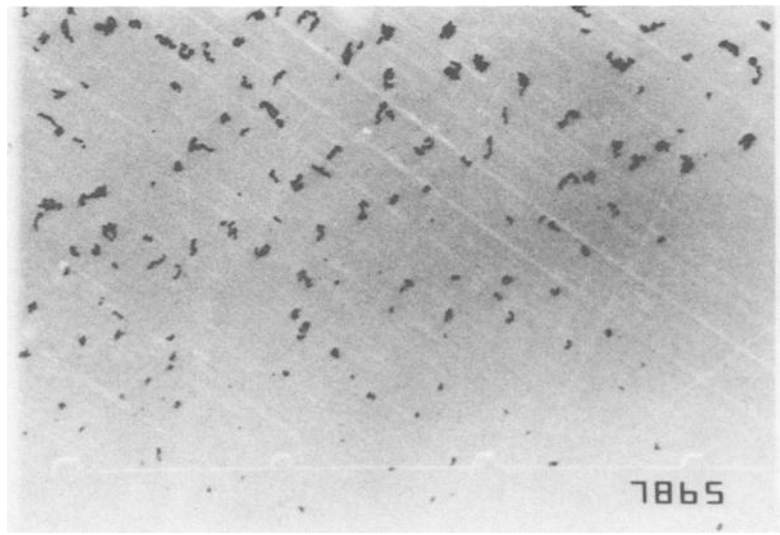

FIG. 5—*SEM micrograph of the corrosive attack on a carbon steel surface after a 5 day exposure to injection water at the Station II. Deposits were previously removed by mechanical cleaning (Magnification × 350).*

TABLE 4—*Percentage elementary analysis (EDAX) of deposits.*[a]

Element	Station I	Station II
Iron	80.606	69.735
Cromium	0.242	0.631
Manganese	0.750	1.276
Sulphur	4.794	0.697
Chlorine	7.693	5.908
Calcium	1.156	1.144
Sodium	2.991	0.551
Silicon	0.929	18.900
Aluminum	0.526	0.800

[a] Carbon steel coupons exposed to injection water for 1 day.

behavior for carbon steel in injection water as well as an active dissolution of metal surfaces. After 48 h of immersion, coorosion potential remained stable at active potentials, ranging from −0.600 to −0.700 V (versus standard calomel electrode (SCE)), confirming polarization results.

The results of this monitoring program suggest that the severe degree of attack of carbon steel coupons, with its localized morphology can not be attributed only to the corrosivity of injection water, characterized by the uniform dissolution observed in all samples. Laboratory experiments and EDXA analysis of biological and inorganic deposits (Table 4) support this conclusion.

The partial reduction of SRB viable counts, and the decrease in the intensity of the corrosive attack after biocide addition, suggest that preliminary biocide treatment assayed in the system was insufficient to achieve microbiological control (Table 3). However, an appropriate optimization of the biocide treatment, in conjunction with an improvement in some operational procedures, will achieve an adequate and effective control of the bacteriological status of the system.

Conclusions

Biofouling and biocorrosion can overcome the inhibitory effects achieved by a conventional corrosion and scale control program, leading to an enhanced localized attack in short periods of exposure of metal samples. Good performance alloys like some high quality stainless steels can be affected by deleterious effects derived from biofilms/corrosion products interactions that condition the corrosion behavior of structural metals and alloys. Thus, an appropriate monitoring program for biofouling and biocorrosion will be mandatory to implement an effective water treatment strategy. An updated program of this kind will necessarily cover microbiological, electrochemical and surface analysis measurements to guarantee a proper assessment of all the biodeterioration causes.

The sampling device presented in this paper, together with different field and laboratory evaluations included in the monitoring programs previously described, represent a significant improvement in industrial water treatments.

Acknowledgments

The authors wish to thank the contributions of M. F. L. de Mele, P. S. Guiamet and O. R. Pardini (Bioelectrochemistry Section, INIFTA) as co-authors of the case histories presented in this paper.

References

[1] Videla, H. A., "Microbially Induced Corrosion: An Updated Overview," *Biodeterioration and Biodegradation 8*, H. W. Rossmoore, Ed., Elsevier Applied Science, London, 1991, pp. 63–88.

[2] Costerton, J. W. and Geesey, G. G., "The Microbial Ecology of Surface Colonization and of Consequent Corrosion," *Biologically Induced Corrosion*, S. C. Dexter, Ed., National Association of Corrosion Engineers (NACE), Houston, TX, 1986, pp. 223–232.

[3] Dexter, S. C., Duquette, D. J., Siebert, O. W., and Videla, H. A., "Use and Limitations of Electrochemical Techniques for Investigating Microbiological Corrosion," *Corrosion*, Vol. 47, No. 4, April 1991, pp. 308–318.

[4] Amaral, M. C., Silva, R. A., Canales, C. G., and Videla, H. A., "Field and Laboratory Evaluation of a New Multipurpose Sampling Device for Monitoring Microbially Influenced Corrosion and Biofilms in Recirculating Cooling Water Systems," *Biodeterioration and Biodegradation 8*, H. W. Rossmoore, Ed. Elsevier Applied Science, London, 1991, pp. 592–594.

[5] Videla, H. A., de Mele, M. F. L., Silva, R. A., Bianchi, F., and Gonzales Canales, C., "A Practical Approach to the Study of the Interaction Between Biofouling and Passive Layers on Mild Steel and Stainless Steel in Cooling Water," *Corrosion/90*, Paper No. 124, NACE, Houston, TX, 1990.

[6] Videla, H. A., Guiamet, P. S., Pardini, O. R., Echarte, E., Trujillo, D., and Freitas, M. M. S., "Monitoring Biofilms and MIC in an Oilfield Water Injection System," *Corrosion/91*, Paper No. 103, NACE, Houston, TX, 1991.

Surface Analysis

Clive R. Clayton,[1] *Gary P. Halada,*[2] *Jeffery R. Kearns,*[3] *Jeffrey B. Gillow,*[4] *and A. J. Francis*[5]

Spectroscopic Study of Sulfate Reducing Bacteria-Metal Ion Interactions Related to Microbiologically Influenced Corrosion (MIC)

REFERENCE: Clayton, C. R., Halada, G. P., Kearns, J. R., Gillow, J. B., and Francis, A. J., **"Spectroscopic Study of Sulfate Reducing Bacteria-Metal Ion Interactions Related to Microbiologically Influenced Corrosion (MIC),"** *Microbiologically Influenced Corrosion Testing, ASTM STP 1232,* Jeffery R. Kearns and Brenda J. Little, Eds., American Society for Testing and Materials, Philadelphia, 1994, pp. 141–152.

ABSTRACT: It has long been recognized that sulfate reducing bacteria (SRB) found in natural and industrial waste waters promote microbiologically influenced corrosion (MIC) of certain metals and alloys. Corrosion may be enhanced biologically, through direct enzymatic action of the bacteria, or abiotically, as a result of reaction with metabolic byproducts or changes in local conditions (for example, pH) brought about by bacterial activity. In this study, X-ray photoelectron spectroscopy (XPS) is utilized in conjunction with conventional microbiological and quantitative chemical analytical techniques to analyze the effects of localized environmental conditions similar to those found near the surface of a passive stainless steel on the behavior of SRB, and to determine the ability of these bacteria to alter local environmental conditions in such a way as to create conditions that accelerate corrosion. Specifically, the interactions of Fe, Cr, Ni and Mo ions with *Desulfovibrio sp.* under anoxic conditions were studied in order to determine the influence of passive dissociation products on the extent of sulfate reduction and to determine the resulting speciation of the metal ions and sulfur. In all cases, XPS revealed the presence of multiple reduced sulfur species (SO_3^{2-}, elemental S and S^{2-}), as well as reduction of both the molybdate and ferric ions. Localized reduction in pH due to SRB metabolic activity was presumed to play a role in the formation of stable molybdenum disulfide and ferrous species.

KEYWORDS: sulfate reducing bacteria (SRB), X-ray photoelectron spectroscopy (XPS), microbiologically influenced corrosion (MIC)

Introduction

Sulfate reducing bacteria (SRB) are ubiquitous to both natural and industrial waters. Nearly sixty years ago Wolzogen and Van der Vlught [*1*] considered the influence of SRB

[1] Professor and Chair, Department of Materials Science and Engineering, SUNY, Stony Brook, NY 11794-2275.

[2] Graduate student, Department of Materials Science and Engineering, SUNY, Stony Brook, NY 11794-2275.

[3] Senior corrosion engineer, Allegheny Ludlum Corporation, Technical Center, Brackenridge, PA 15014.

[4] Biology associate, Brookhaven National Laboratory, Upton, NY 11973.

[5] Microbiologist and group leader, Brookhaven National Laboratory, Upton, NY 11973.

on microbiologically influenced corrosion (MIC). More recent studies have established strong evidence that SRB are involved in the corrosion process of some metals [*2*]. However, to establish the causal relation between SRB activities and corrosion of metals, one must be certain to find a link between corrosion sites and the presence of a definable corrosion cell involving a biogenic agency. The components of such a cell may include a biofilm and liquid and solid metabolic products. Since corrosion is not always associated with such biofilms it is necessary to determine the critical conditions which are required to initially accelerate localized corrosion. To initiate a study to determine the nature of such conditions, it is necessary to analyze and catalogue the constituents of a biofilm in close proximity to a corroded site and to formulate a rationale for the production of such constituents. Consideration must be given to the possibility of both biotic and abiotic formation of sulfur compounds. Traditional models of SRB-driven corrosion have generally failed to consider these differences. Furthermore, because of the possible action of enzymes, thermodynamic data alone cannot predict the nature of the sulfur products [*3*]. Of special interest would be any evidence of sulfur products, for instance, which can reliably be predicted not to form abiotically but otherwise can be formed by SRB. Such a case has recently been made for the formation of mackinawite by SRB [*4*], although in this case abiotic synthesis is not entirely excluded [*5*].

The work of Mohagheghi [*6*] seems to illustrate that metal ions bound to cell walls of SRB are more reactive with bacteriogenic sulfur than the same ions involved in an equivalent abiotic process occurring on a metal surface exposed to a solution containing sulfur. The formation of sulfides in biomasses must be considered a potential source of cathodic activation of the corrosion cell [*7–10*]. Additionally, Newman, et al. [*11*], have reported that $Na_2S_2O_3$, $Na_2S_4O_6$, KSCN, Na_2S, Na_2SO_3 and H_2S in neutral chloride solutions are all capable of promoting the pitting of 304 stainless steel.

Characterization of corrosion products associated with MIC presents considerable constraints on the nature of the analytical system which can be used. For example, the importance of low atomic number species limits the usefulness of such techniques as energy dispersive X-ray analysis. Similarly, few techniques can provide determination of speciation. By contrast, X-ray photoelectron spectroscopy (XPS) provides a method for determination of the chemical state of high and low atomic number species on the surface of both inert biological material [*12–15*] as well as the surfaces of living cells [*16–19*]. In this paper we demonstrate the use of XPS in determining the extent to which SRB may alter local environmental chemistry. We have considered the effects of Fe, Cr, Ni and Mo ions on the activity of *Desulfovibrio sp.* in a modified Postgate's medium C.

The nature of metal ion-bacteria interactions is important to understand since metal ions released from stainless steels, even under passive conditions, may bring about nutrient or toxic conditions. The concentration and types of metal ions released from a stainless steel under passive conditions (10^{-5} A/cm^2) were considered in this study [*20*].

Experimental Procedure

Culture

Desulfovibrio sp. 1CA3 was isolated from waste disposal leachate in Postgate's medium B. Upon isolation, the bacterium was maintained in Postgate's medium C. The bacterium is a gram negative vibrioid rod, desulfoviridin positive, which produces acetic acid as a major end product when grown in the presence of lactic acid and vigorously reduces sulfate with hydrogen sulfide gas production.

Medium

Modified Postgate's medium C consisting of (g/L deionized water): 1 NH_4Cl, 2.25 lactate; 0.06 $MgSO_4 \cdot 7H_2O$; 4.5 Na_2SO_4; 1 yeast extract; 0.5 KH_2PO_4; 0.06 $CaCl_2 \cdot 2H_2O$; 0.004 $FeSO_4 \cdot 7\ H_2O$, pH adjusted to 7.8 with KOH. The modification consisted of the addition of lactate as lactic acid instead of sodium lactate. The medium was prereduced by boiling and purging with ultra-high purity nitrogen, and 40 mL was dispensed into each 60 mL serum bottle in a nitrogen filled glove box as described previously [*21*]. The bottles were capped with butyl-rubber stoppers, sealed and autoclaved at 121°C, 20 psi for 20 min. The final pH of the medium after sterilization was 7.4. The bottles each contained 900 μmoles lactate and 1800 μmoles sulfate.

Metals

Ultra high purity (UHP) nitrogen purged solutions of iron (III) chloride ($FeCl_3 \cdot 6\ H_2O$), sodium molybdate (Mo(VI)) ($Na_2MoO_4 \cdot 2\ H_2O$), chromium (III) chloride ($CrCl_3 \cdot 6\ H_2O$) and nickel (II) chloride ($NiCl_2 \cdot 6\ H_2O$) were separately added to the sterile medium in the glove box for a final concentration of 0.2 mM. The solutions containing the metal ions were added to the sterile medium after filtration through a 0.22 μm filter. The pH was adjusted to 7.4 after addition with sterile acid or base. Sodium molybdate was also added to a series of bottles for a final concentration of 0.2, 1, 10 and 20 mM molybdate. Specific sample bottles were reserved without metal additions as controls. Metal concentrations were measured by atomic absorption spectrophotometry.

Inoculation

One milliliter of a 24 h culture of *Desulfovibrio sp.* 1CA3 was added to each bottle and incubated in the dark at 26 ± 1°C. Uninoculated samples and inoculated samples without metals were prepared and used as controls.

Microbiological and Chemical Analyses

After incubation for five days the following analyses were performed: (1) total gas production by using an analog pressure gauge (Marcsh Co.) attached to a 22 gauge needle, (2) lactic acid consumption and acetic and propionic acid production by high performance liquid chromatography (HPLC) with a UV/VIS (Spectra-Physics) and refractive index (Shimadzu) detector after filtration through a 0.22 μm filter [*22*], (3) the pH, (4) sulfate reduction spectrophotometrically by precipitation with barium chloride [*23*], and (5) metal remaining in solution by atomic absorption spectrophotometry on a filtered, acidified aliquot. Turbidity was not used as a measure of growth because of the formation of metal sulfide precipitates. The biomass along with any precipitate was recovered by centrifugation at 10 000 rpm for 15 min in 40 mL acid-washed, anaerobically sealed centrifuge tubes. The cell pellets (bacterial cells and sulfide precipitate) were placed in a desiccator and allowed to dry under anoxic conditions for two days.

Sample Preparation for XPS Analysis

The dried cell pellets were stored under nitrogen and transferred to an argon-purged glove box. The cell pellets were then crushed onto indium foil, mounted onto the XPS

sample holder and transferred to the spectrometer, all in a glove box under an argon atmosphere to prevent surface chemical oxidation and contamination.

XPS Analysis

All XPS measurements were performed with a modified V.G. Scientific ESCA 3 Mark II spectrometer controlled by a VGX 900 computer-based data acquisition system, located in the Department of Materials Science and Engineering at the State University of New York at Stony Brook. Special features of the XPS unit include an environmental cell, multiple injection ports and a probe with heating and liquid nitrogen cooling capabilities. A cold stage was specifically added to prevent the degradation of biological samples during analysis and to avoid contaminating the chamber. Ultra-high vacuum conditions (base pressure was 1 to 2 $\times$ 10^{-9} torr) were maintained in order to optimize the quality of the signal coming from the specimen surface to the detector and to prevent accumulation of contaminants on the surface from the gas phase. Further details on XPS instrumentation, particularly for biological applications, can be found elsewhere [*24–29*]. A summary of the advantages and limitations of the use of XPS for the study of MIC is given in Table 1.

In all cases, the incident radiation was $AlK\alpha_{1,2}$ X-radiation from a non-monochromatized source operated at 400 W. All XPS measurements were carried out at a high take-off angle (50°) measured with respect to the plane of the sample. The entrance and exit slit widths for the hemispherical analyzer were 4 mm, which resulted in a half angle for photoelectron emission of 0.095 radians. In each case, 1000 eV survey scans were run to locate the most intense peaks. These peaks were repeatedly scanned to improve the sensitivity and signal-to-noise ratio. The metal and sulfur peaks were first identified and then separate narrow scan peaks were obtained. A 20 eV pass energy was used for all narrow scan analysis providing a full width at half maximum (FWHM) for the $Au4f_{7/2}$ singlet of 1.35 eV. For reference, the binding energy of the $Au4f_{7/2}$ singlet was found to be 83.8 eV and that of the $Cu2p_{3/2}$ singlet was found to be 932.4 eV. All binding energies were corrected for charge shifting by referencing to the C1s line from the adventitious carbon at 284.6 eV. Details of the curve fitting procedures and data analysis routines may be found elsewhere [*30*]. Standards data for all peak parameters and sensitivity factors were developed from work done on compounds in this laboratory. Powdered standards were crushed into the surface of indium foil under argon and transferred under argon to the spectrometer to ensure a clean surface for analysis. Sulfur 2p and sulfur 2s level photoelectron binding energies determined in this way are presented in Table 2.

TABLE 1—*Advantages and limitations of the application of XPS to the study of MIC.*

ADVANTAGES
• Sensitivity to a wide range of elements (all except H and He)
• Provides data on speciation of all elements present
• Non-destructive technique
• Relatively straightforward method of data analysis
LIMITATIONS
• All analysis must take place in a UHV environment, hence sample must be dry and biological samples must be liquid nitrogen cooled to prevent outgassing or decomposition
• Severe sample charging may occur; in some cases use of a low energy electron flood gun may be necessary
• Complex C1s photoelectron signal may not be useful for charge referencing
• Fairly complex apparatus for analysis

TABLE 2—*Sulfur 2s and 2p X-ray photoelectron binding energies.*

Compound	Species	S2s B.E., eV[a]	S2p B.E., eV
FeS	S^{2-}	225.8	161.9
Pure S	S	228.8	164.2
Na_2SO_3	S^{4+}	231.3	166.1
$FeSO_4$	S^{6+}	232.8	169.2

[a] Note: All binding energy values are ±0.1 eV.

The ion bombardment operation that is typically done (with 2.5 kV argon ions) to remove surface contaminants was found to reduce sulfur species (Fig. 1) and therefore has limited value in a study of this kind. Contaminants found in the vacuum system were attributed to the egress of certain sulfur compounds (especially elemental sulfur and ferrous sulfide, FeS) within the biomass when under vacuum. Sample cooling with liquid nitrogen greatly reduced the severity of outgassing.

Results and Discussion

Microbiological Analysis

Gas production and sulfate reduction by *Desulfovibrio sp.* 1CA3 in the presence of Fe, Cr, Ni and Mo ions are presented in Table 3. The pH dropped slightly in inoculated samples

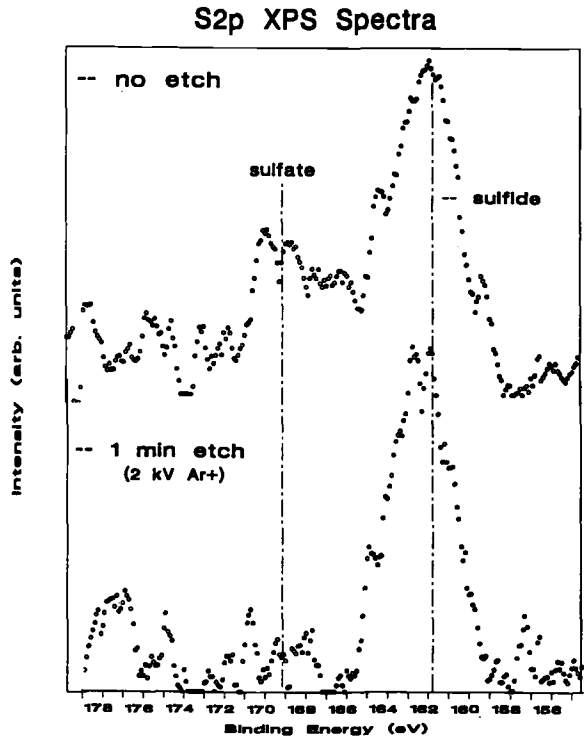

FIG. 1—*S2p XPS spectra from a non-inoculated sample showing the reduction in photoelectron intensity from sulfate following a one minute etch with 2kV Ar^+ ions.*

TABLE 3—*Effect of metal ions on the activity of sulfate reducing bacteria.*

Treatment	pH	Gas Produced, ml	Sulfate Reduced, %	Metal Remaining in Solution, %	Organic Acids (μmoles)		
					Lactic	Acetic	Propionic
No metal added							
Uninoculated	7.46 ± 0.06	ND[a]	ND	ND	855 ± 49	ND	ND
Inoculated	6.96 ± 0.05	6.8	15	ND	ND	941 ± 25	283 ± 7
Chromium							
Inoculated	6.95 ± 0.05	6.8	30	90	ND	773 ± 22	274 ± 5
Iron							
Inoculated	7.00 ± 0.01	9.5	23	3	ND	816 ± 111	174 ± 72
Molybdenum							
Inoculated	6.86 ± 0.01	6.8	39	<1	ND	704 ± 51	265 ± 11
Nickel							
Inoculated	7.10 ± 0.01	6.8	24	4	ND	1050 ± 26	88.6 ± 4

[a] ND = none detected.

due to acid production. Gas production (CO_2 and H_2S) was greatest in the presence of Fe, presumably due to increased metabolic activity by *Desulfovibrio* in response to the abundance of available Fe. *Desulfovibrio* has an exceptionally high requirement for inorganic iron [3]. However, sulfate reduction was greatest in the presence of molybdate, with almost 40% of the added sulfate reduced. All the metals, except chromium (III), were removed from solution. Addition of 0.2 mM Fe, Cr, Ni and Mo ions to *Desulfovibrio sp.* 1CA3 did not inhibit microbial activity (Fig. 2) as indicated by acid production, sulfate reduction and gas production (Table 3).

XPS Analysis

The XPS technique involved the irradiation of the cell pellet sample by a soft X-ray beam which induced the emission of photoelectrons from the core atomic levels in the outermost layer of the sample surface. The kinetic energies of the emitted electrons were analyzed to determine their binding energies in the species of interest according to the following relationship:

$$h\nu = E_{kin} + E_{be} + \phi \quad (1)$$

where $h\nu$ is the energy of the incident X-rays, E_{kin} is the kinetic energy of the emitted photoelectrons, E_{be} is the electron binding energy, and ϕ is the work function of the spectrometer. Peaks in the deconvoluted spectra were associated with specific elements and particular valence states or compounds of those elements by comparison to standards.

The XPS S2p spectra from the inovulated SRB are referred to in an earlier study [31]. In all cases, sulfur exists in the original sulfate form and as three reduced states: sulfide, elemental sulfur and sulfite. The amount of sulfate reduced as determined by analysis of sulfate remaining in solution after incubation in the presence of various metals is presented in Table 3. The sample inoculated with molybdate showed the maximum amount of sulfate reduction. The XPS sulfur spectral data from the biomass (Fig. 2) confirmed this finding. The presence of low levels of iron sulfide in the biomass is due to its high vapor pressure and hence volatility in the vacuum system of the XPS unit.

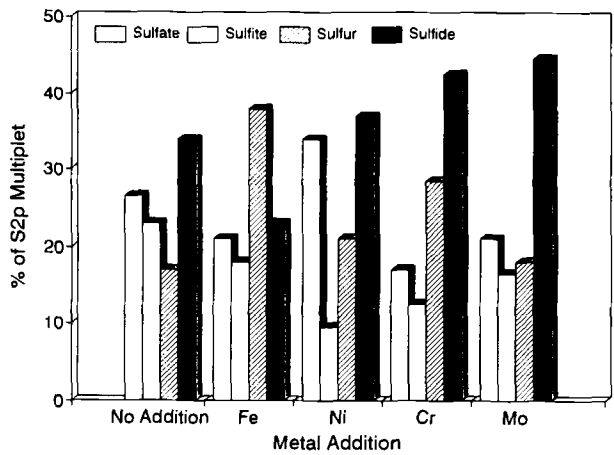

FIG. 2—*XPS analysis of sulfur species in biomass of* Desulfovibrio sp. *incubated in the presence of Fe, Ni, Cr and Mo.*

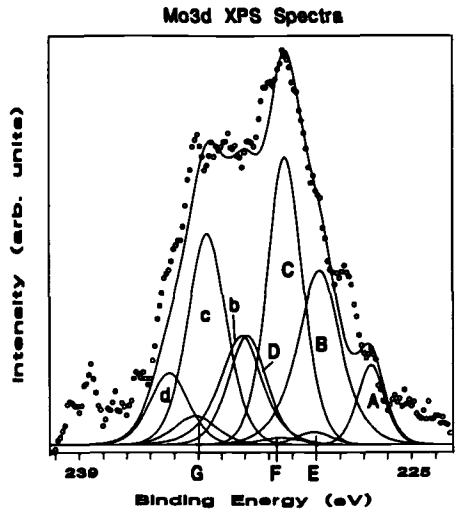

FIG. 3—*Mo3d (and overlapping S2s) XPS spectra from* Desulfovibrio sp. *biomass exposed to 0.2 mM sodium molybdate. Peak identification:* (A) S^{2-} *(from* MoS_2*),* (B) Mo^{4+} $3d_{5/2}$ *(from* MoS_2*),* (b) Mo^{4+} $3d_{7/2}$ *(from* MoS_2*),* (C) Mo^{5+} $3d_{5/2}$, (c) Mo^{5+} $3d_{7/2}$, (D) Mo^{6+} $3d_{5/2}$, *(from molybdate),* (d) Mo^{6+} $3d_{7/2}$, *(from molybdate),* (E) *S* (F) SO_3^{2-} (G) SO_4^{2-}.

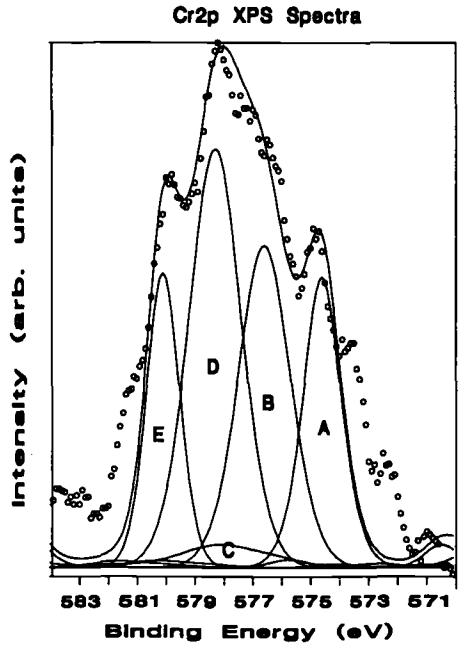

FIG. 4—*Cr2p*$_{3/2}$ *XPS spectra from* Desulfovibrio sp. *biomass exposed to 0.2 mM chromic chloride. Peak identification:* (A) Cr^{3+} *(from* Cr_2S_3*),* (B) Cr^{3+} *(from* $CrOOH$ *or* $Cr(OH)_3$*),* (C) *satellite from* $Cr2p_{1/2}$ *photoelectron peak,* (D) Cr^{3+} *(from* $CrCl_3$*), and* (E) Cr^{3+} *(from* $Cr_2(SO_4)_3$*).*

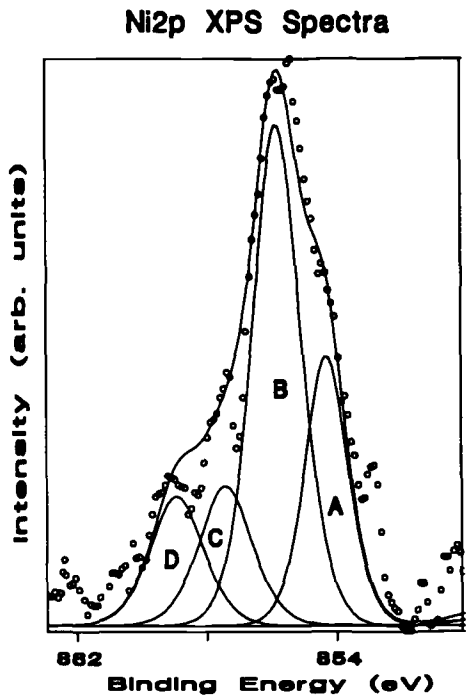

FIG. 5—*$Ni2p_{3/2}$ XPS spectra from* Desulfovibrio sp. *biomass exposed to 0.2 mM nickelous chloride. Peak identification:* (A) *Ni^{2+} (from NiS)*, (B) *Ni^{2+} (from $Ni(OH)_2$)*, (C) *Ni^{2+} (from $NiCl_2$)*, *and* (D) *Ni^{2+} (from $NiSO_4$). (Note—No satellite from $2p_{1/2}$ component included in multiplet due to larger value of spin-orbit splitting.)*

The XPS metal spectra appear in Figs. 3 through 6. Photoelectron spectra were analyzed for the Fe2p, Ni2p, Cr2p and Mo3d core levels for the samples inoculated with the respective metal ions. The Mo3d spectra (Fig. 3) is complicated by its overlap with the S2s core photoelectron spectra. The formation of metal sulfides from cationic (Fe, Cr and Ni) metal complexes in a neutral pH medium was not surprising, but evidence of molybdenum disulfide was. One possible explanation is that molybdenum disulfide may form by direct reaction of molybdate with hydrogen sulfide, but this requires acidic conditions [*32*]. In the bulk medium with neutral pH, the formation and stability of a sulfide would require microbial production of hydrogen sulfide gas in a region of low pH, which could possibly be created by the acetic acid and propionic acids that were observed to be produced by the bacteria. It is of interest to note that molybdate has been found to play an important role as an electron acceptor in the outermost layer of passive films formed on Mo-bearing stainless steels and hence any reduction of molybdate to lower valent species would adversely affect the ability of the passive film to inhibit ingress of anionic species such as Cl^- [*33*]. In addition, we noted that the Mo3d photoelectron spectra show a strong signal from a pentavalent reduction product, possibly a precurser to disulfide formation or part of a molybdenum oxy-hydroxide complex, or both.[6] Further clarification is currently being sought.

All other metal spectra indicated the presence of the respective chloride in the cell pellet as well as the metal sulfides and sulfate compounds. The Cr2p, Ni2p and Fe2p spectra also

[6] D. G. Kim, Ph.D Thesis, SUNY Stony Brook, NY, 1993.

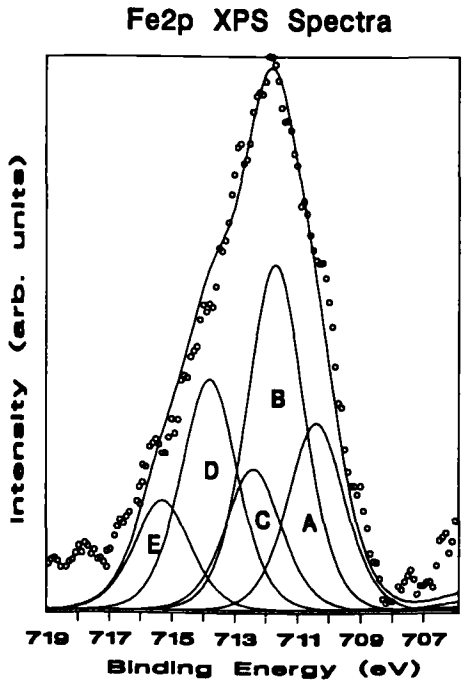

FIG. 6—*Fe2p$_{3/2}$ XPS spectra from* Desulfovibrio sp. *biomass exposed to 0.2 mM ferric chloride. Peak identification:* (A) *Fe^{3+} (from Fe_2O_3 or FeOOH or $Fe(OH)_3$),* (B) *Fe^{3+} (from $FeCl_3$),* (C) *Fe^{2+} (from FeS),* (D) *Fe^{2+} (from $FeSO_4$), and* (E) *Fe^{3+} (from $Fe_2(SO_4)_3$). (Note—No satellite from $2p_{1/2}$ component included in multiplet due to larger value of spin-orbit splitting.)*

indicated the formation of oxy-hydroxides or hydroxides of the respective metal ions, most likely a result of the interaction of the aliquot with the metal species during the process of sulfate reduction. By analogy this would further suggest the presence of stable pentavalent molybdenum as part of an oxy-hydroxide complex. Both the Cr and Ni spectra exhibited only a single valent state; however, there is evidence of both ferric and ferrous compounds in the Fe2p photoelectron spectra (Fig. 6). According to the Pourbaix diagram for the iron-water system [*34*], a shift to lower pH due to SRB metabolic activity creates a condition favorable for the reduction of the ferric (III) ion to the ferrous (II) ion. The Fe2p XPS spectra, in fact, show evidence of not only ferric (III) chloride but also ferrous (II) sulfide and sulfate. The Cr(III) and Ni(II) ions are predicted to be stable in acidic environments, and hence no reduction to lower valent states (unlikely in any case) is expected.

Conclusions

1. Exposure of *Desulfovibrio sp.* to solutions containing 0.2 mM concentrations of Fe, Cr, Ni and Mo metal ions was not found to inhibit the activity of the microorganism as indicated by lactic acid consumption, acetic acid production, sulfate reduction and gas production.
2. Of the four metal ions tested (Fe(III), Cr(III), Ni(II) and Mo(VI)), the highest rate of sulfate reduction by *Desulfovibrio sp.* occurred in the presence of molybdate.
3. XPS revealed the presence of metal sulfides in the biomass that had been inoculated by both cationic (Fe, Cr and Ni) and anionic (Mo) metal ions. The formation of cationic

metal sulfides in neutral pH medium was not surprising. However, the abiotic formation of molybdenum sulfide by reaction of hydrogen sulfide requires acidic conditions. The formation and stability of the sulfide may be facilitated by the microbial production of hydrogen sulfide gas, acetic and propionic acids which may sufficiently lower the pH at localized sites. In addition, enzymatic reduction of Mo(VI) by *Desulfovibrio sp.* may also occur. In any case, both the production of sulfides and the reduction of molybdate may limit the protective capabilities of passive films formed on stainless steels.

4. Fe2p XPS spectra revealed evidence of iron(II) which may result from the localized reduction in pH due to SRB activity.
5. XPS appears to be an invaluable tool in elucidating the possible mechanisms and processes involved in corrosion in the presence of sulfate reducing bacteria, such as *Desulfovibrio sp.* Though limitations exist, primarily due to the ultra-high vacuum environment and the possibility of high sample charging, corrections can be made and techniques utilized which enable XPS to determine quantitative chemical information for a variety of biological samples.

Acknowledgments

This work was funded in part by the Office of Naval Research (Dr. A. J. Sedriks, contract officer) under contract number N0001485K0437. The authors would like to thank Mr. C. J. Dodge (Brookhaven National Laboratory) for the analysis of metals.

References

[1] Von Wolzogen, C. A. H. and Van der Vlught, L. S., *Water (The Hague)*, Vol. 18, 1934, p.147.
[2] Little, B. J., Wagner, P. A., Characklis, W. G., and Lee, W., "Microbial Corrosion" in *Biofilms*, W. G. Characklis and K. C. Marshall, Eds., Wiley Interscience, New York, 1990, pp. 635–670.
[3] Postgate, J. R., *The Sulfate Reducing Bacteria*, 2nd ed., Cambridge University Press, Cambridge, U.K., 1984, p. 132.
[4] McNeil, M. B. and Little, B. J., *Corrosion*, Vol. 46, No. 7, 1990, p. 599.
[5] MacDonald, D. D., Roberts, B., and Hyne, J. B., *Corrosion Science*, Vol. 18, 1978, p. 411.
[6] Mohagheghi, A., Updegraff, D. M., and Oldhaber, M. B., *Geomicrobiology*, Vol. 5, 1984, p. 153.
[7] Smith, J. S. and Miller, J. D. A., *British Corrosion Journal*, Vol. 10, 1975, p. 136.
[8] Marcus, P. and Talah, H., *Corrosion Science*, Vol. 29, 1989, p. 455.
[9] Newman, R. C., Webster, B. J., and Kelly, R. G., *ISIJ International*, Vol. 31, 1991, p. 201.
[10] Schmidt, G., *Corrosion*, Vol. 47, 1991, p. 285.
[11] Newman, R. C., Isaacs, H. S., and Alman, B., *Corrosion*, Vol. 3, No. 8, 1980, p. 261.
[12] Andrade, J. D., in "Surface and Interfacial Aspects of Biomedical Polymers," Vol. 1, Chapter 5, J. D. Andrade, Ed., Plenum Press, New York, 1985, pp. 105–195.
[13] Defosse, C. in *Characterization of Heterogeneous Catalysts*, Chapt. 6, F. Delannay, Ed., Marcel Dekker, New York, 1984, pp. 225–298.
[14] Ratner, B. D. and McElroy, B. J., in *Spectroscopy in the Biomedical Sciences*, Chapt. 5, R. M. Gendreau, Ed., CRC Press, Boca Raton, 1986, pp. 107–140.
[15] Siegbahn, K., *Philosophical Transactions of the Royal Society of London, Series A*, Vol. 318, 1986, p. 3.
[16] Magnusson, K. E. and Johansson, L., *Studia. Biophysica*, Vol. 66, 1977, p. 145.
[17] Millard, M. M. and Bartholomew, J. C., *Analytical Chemistry*, Vol. 49, 1977, p. 1290.
[18] Pickart, L., Millard, M. M., Beiderman, B., and Thaler, M. M., *Biochimica Biophysica Acta*, Vol. 544, 1978, p. 138.
[19] Van Haecht, J. L., Defosse, C., Vandenbogaert, R., and Rouxhet, P., *Colloids and Surfaces*, Vol. 4, V.H.C Inc., New York, 1982, p. 343.
[20] Nash, B. K. and Kelly, R. G., "The Use of Ion Chromatography for the Study of Localized Corrosion," *Journal of Chromatography*, in press.
[21] Francis, A. J. and Dodge, C. J., *Applied and Environmental Microbiology*, Vol. 54, 1988, p. 1009.

[22] Francis, A. J., Dodge, C. J., Gillow, J. B., and Cline, J. E., *Radiochimica Acta*, Vols. 52–53, 1991, p. 311.
[23] *Standard Methods for the Examination of Water and Wastewater*, 14th ed., American Public Health Association–American Water Association, 1976, p. 496.
[24] *Handbook of X-ray and Ultraviolet Photoelectron Spectroscopy*, D. Briggs, Ed., Heydon and Son, London, 1977.
[25] *Practical Surface Analysis by Auger and X-ray Photoelectron Spectroscopy*, D. Briggs and M. P. Seah, Eds., 2nd ed., John Wiley, New York, 1990.
[26] *Electron Spectroscopy: Theory, Techniques and Applications*, Vol. 1, C. R. Brundle and A. D. Baker, Eds., Academic Press, New York, 1977.
[27] Carlson, T. A., *Photoelectron and Auger Spectroscopy*, Plenum Press, New York, 1975.
[28] Nefedov, V. I., *X-ray Photoelectron Spectroscopy of Solid Surfaces*, VSP/BV, Ultrecht, 1988.
[29] Siegbahn, K., Nordling, C., Fahlman, A., Nordberg, R., Hamrin, K., Hedman, J., Johansson, G., Bergmark, T., Karlsson, S. E., Lindgren, I., and Lindberg, B., *ESCA: Atomic, Molecular and Solid State Structure Studies by Means of Electron Spectroscopy*, Series IV, Vol. 20, Nova Acta Regiae Soc. Sci., Uppsaliensis Almqvist and Wiksells Boktryckeri AB, Uppsala, 1967.
[30] Halada, G. P. and Clayton, C. R., *Journal of the Electrochemical Society*, Vol. 138, 1991, p. 2921.
[31] Kearns, J. R., Clayton, C. R., Halada, G. P., Gillow, J. B., and Francis, A. J., *Materials Performance*, Vol. 31, No. 10, 1992, p. 48.
[32] Cotton, F. A. and Wilkenson, G., *Advanced Inorganic Chemistry*, 5th ed., John Wiley and Sons, Inc., New York, 1980, p. 810.
[33] Lu, Y. C. and Clayton, C. R., *Journal of the Electrochemical Society*, Vol. 133, 1986, p. 2465.
[34] Pourbaix, M., in *Atlas of Electrochemical Equilibria in Aqueous Solutions*, Pergamon Press, New York, 1966, p. 312.

Patricia A. Wagner[1] *and Richard I. Ray*[1]

Surface Analytical Techniques for Microbiologically Influenced Corrosion—A Review

REFERENCE: Wagner, P. A. and Ray, R. I., **"Surface Analytical Techniques for Microbiologically Influenced Corrosion—A Review,"** *Microbiologically Influenced Corrosion Testing, ASTM STP 1232,* Jeffery R. Kearns and Brenda J. Little, Eds., American Society for Testing and Materials, Philadelphia, 1994, pp. 153–169.

ABSTRACT: Microbiologically influenced corrosion (MIC) has received increasing attention from engineers, materials scientists, and corrosion specialists. In field and laboratory studies, basic surface analytical examinations must be correlated to knowledge of the overall corroding system in order to conclude the presence of MIC. Preliminary observations and microbiological, chemical, microscopic, and metallurgical techniques are discussed.

KEYWORDS: microbiologically influenced corrosion (MIC), biofilms, surface analysis

Microorganisms attach to all engineering materials in contact with natural waters and colonize surfaces to produce biofilms. The biofilms are varied in composition but usually include bacteria, algae, and fungi, in addition to exopolymeric material that provides attachment and structural integrity. A large fraction of the biofilm is adsorbed and entrapped materials such as solutes, heavy metals, and inorganic particulates, in addition to cellular constituents [*1*]. Cells within biofilms grow, reproduce, and form colonies that are physical anomalies on a metal surface; local anodes and cathodes and differential aeration cells result (Fig. 1). Under aerobic conditions, areas under respiring colonies can become anodic and surrounding areas cathodic. A thick biofilm can prevent diffusion of oxygen to cathodic sites and diffusion of aggressive anions, such as chloride, to anodic sites. Outward diffusion of metabolites and corrosion products is also impeded. If areas within the biofilm become anaerobic, the cathodic mechanism can change to reduction of water or microbiologically produced H_2S.

Biofilms can be either beneficial or detrimental in industrial processes. They remove dissolved and particulate contaminants in fixed film biological systems, such as trickling filters, rotating biological contactors, and fluidized bed wastewater treatment plants. Biofilms can determine water quality by influencing dissolved oxygen content and by serving as a sink for toxic and/or hazardous materials. Microorganisms within biofilms can be used to recover minerals and to degrade hydrocarbons [*2*]. However, biofilms form undesirable deposits on engineering surfaces causing reduced heat transfer [*3*], increased fluid frictional resistance [*3*], plugging [*4*], and corrosion [*4*].

The term microbiologically influenced corrosion (MIC) is used to designate corrosion resulting from the presence and activities of microorganisms within biofilms on a material

[1] Oceanographer and Physical Science technician, respectively, Naval Research Laboratory, Stennis Space Center, MS 39529-5004.

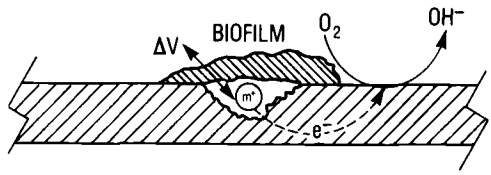

FIG. 1—*Differential aeration cell resulting from microbial colony on metal surface.*

surface. Microorganisms can accelerate and control corrosion reactions by several mechanisms: formation of differential or concentration cells, formation of aggressive metabolites, such as sulfides and organic and inorganic acids; metal oxidation and reduction, and deactivation of corrosion inhibitors. Iron-oxidizing, sulfur-oxidizing, iron-reducing, sulfate-reducing, acid-producing, slime-producing, ammonia-producing, and hydrogen-producing bacteria have been implicated in the corrosion of metals and alloys. Sulfate-reducing bacteria (SRB) are commonly found to be responsible for MIC in anaerobic environments through the production of H_2S. Metal-depositing bacteria, especially iron-oxidizing genera, form dense deposits of cells and metal ions, creating oxygen concentration cells and under-deposit corrosion. Acidic bacterial exopolymers can bind metal ions from the aqueous phase, increasing corrosion rates by providing an additional cathodic reaction.

MIC has received increased attention by corrosion scientists and engineers in recent years with the development of surface analytical and electrochemical techniques that can quantify the impact of microbes on electrochemical phenomena and provide details of corrosion mechanisms. MIC has been documented for metals exposed to seawater, fresh water, demineralized water, process chemicals, food stuffs, soils, aircraft fuels, human plasma, and sewage. The chemical process, oil and gas, and power generation industries and the U.S. military have acknowledged the occurrence and prevalence of MIC in their operating systems. In the past ten years there have been at least 20 international conferences that included sessions on the subject.

Investigations for MIC can usually determine only if conditions are appropriate for MIC. Experience has shown that MIC is considered only when other forms of nonbiological corrosion have been eliminated. This paper will review field and laboratory surface analytical procedures for investigating a corroding system to determine if MIC may be a causative agent. Some are applicable to field and laboratory use, while others are only useful for research. Related electrochemical techniques used to identify mechanisms and monitor and quantify electrochemical parameters and corrosion rates have been discussed elsewhere [*5*].

Preliminary Examination of a Corrosion System

The Corroding Sample

1. Metal Composition—Metals listed as commercially pure actually contain a variety of impurities and imperfections that influence corrosion. In general, as purity increases, the tendency for a metal to corrode is reduced. However, high purity metals frequently have low mechanical strength, leading to the use of alloying elements to improve mechanical, physical, fabrication, and corrosion characteristics [*6*]. Alloy composition, manufacturing specifications such as surface finish and heat treatments, and presence of protective coating influence susceptibility to MIC [*7*].

2. Macroscopic Examination—Color photographs of the corroded material while still wet and before extensive handling can be invaluable for reference and documentation.

a. *Visible fouling*

Extensive biological fouling with filamentous material, slime, and debris suggests the presence of algae, in addition to fungi and bacteria. In the presence of light, algae produce oxygen (photosynthesis) that can accumulate in the biofilm. In the absence of light, algae consume oxygen (respiration) and reverse the process. Dowling et al. [*8*] showed that a photosynthetic biofilm may influence ennoblement of the open circuit potential of type 316L stainless steel so that it approaches the potential above which pits can initiate and grow (Fig. 2). Algae and fungi may also produce aggressive metabolites. Additionally, Little et al. have shown that there is no correlation between the thickness of the biofilm and the chemistry at the biofilm/metal interface [*9*]. Localized cells of pH values 5.2-9.2 were measured randomly at depths within an estuarine biofilm on type 304 stainless steel.

b. *Localized corrosion*

(1) Forms—MIC is localized corrosion and can appear as pitting, crevice corrosion, under-deposit corrosion, dealloying, or stress corrosion cracking. The form, shape, and depth of the corroded areas should be noted. Pits associated with MIC often have a small surface opening with a larger subsurface cavity. SRB produce open pitting or gouging on stainless steel. When SRB are active along edges of gasketed joints, shallow crevice corrosion is often found under adjacent gaskets. Subsurface tunneling has been observed along ferrite stringers in weld areas of stainless steel [*10*]. SRB attack on cast iron typically produces graphitization where the corroded areas are filled with a soft skeleton of graphite [*11*]. On nickel and cupronickel alloys, SRB are reported to produce conical pits containing concentric rings [*12*].

(2) Location—Distribution of corrosion within the sample is important. Frequently, pitting of stainless steels is located in the heat-affected zone, fusion line, and adjacent base metal of welds [*10*]. Kobrin described pitting attack in weld seams of a type 316L stainless steel storage tank after hydrotesting due to metal-depositing bacteria (Fig. 3) [*12*]. Regions of low flow such as in bends, elbows, or crevices due to engineering design and fabrication are common sites for MIC, especially where low oxygen concentrations encourage anaerobic bacterial growth. Any recurring directional pattern of localized attack may be related to turbulence or impinging flow.

(3) Material within Pits—Tatnall reviewed a case history where fine dark particles were found in open pits in galvanized steel, identified to include aerobic sulfur-oxidizing bacteria and anaerobic SRB [*13*].

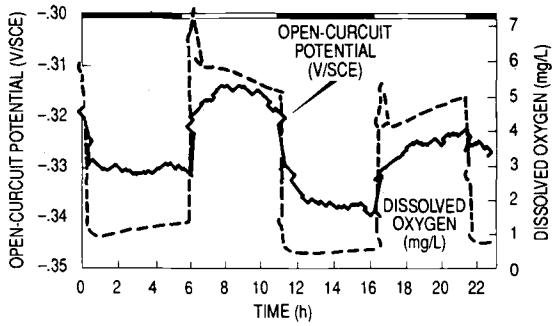

FIG. 2—*Open-circuit potential and dissolved oxygen oscillations associated with an* Anabena *sp. biofilm under a 6h light/dark regime. Light period denoted by white slot, dark period denoted by black slot* [*8*].

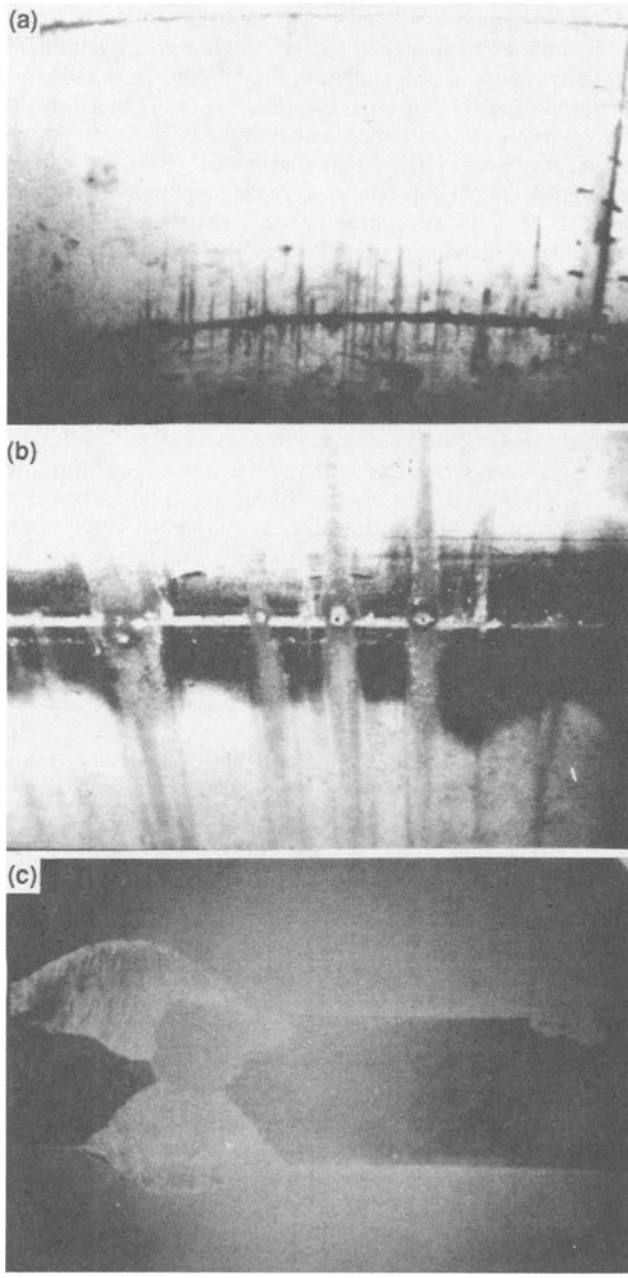

FIG. 3—*Tubercle formation on stainless steel [12]: (a) = rust colored streaks normal to weld seams in sidewall of 316L tank formed after 1 month exposure to stagnant hydrotest water, (b) = wet deposit of metal-depositing bacteria, and (c) = cross-section through pitted weld seam.*

c. *Corrosion products*

Discrete mounds or columns (tubercles) can develop on metal surfaces as a result of microbial activities. Morphology and location are often indicative of the causative microbial species. Deposit shape, color, and texture should be noted. SRB produce characteristic black deposits of FeS on steel and stainless steels. Distinctive reddish-brown, hemispherical, or conical tubercles with a small "chimney shape" near the center on the surface of steel and subsurface pitting are characteristics of iron bacteria activity [*14*].

Bacterial deposits usually have a soft slimy texture when fresh and wet. In the presence of slime-formers, deposits are more irregular and may appear layered. In anaerobic conditions where SRB involvement is suspected, the deposit may be screened for the presence of H_2S by odor and testing with HCl [*11*].

Environment of the Corroding System

In an ideal investigation of MIC, the corrosion environment would be available for inspection. Factors of interest include the following:

(1) Presence, Absence, Cycles of Light—This would influence biofilm composition, respiration, and metabolic activities [*8*].

(2) Aqueous Medium—Microorganisms within the biofilm are capable of maintaining an environment that is radically different from that of the bulk medium in terms of pH, dissolved oxygen, and organic and inorganic species [*9*]. Interfacial chemistry cannot be predicted from measurement of any set of parameters in the bulk medium. Similarly, the numbers and types of bacteria within biofilms cannot be predicted or determined by measuring planktonic microorganisms [*15*]. The following parameters for the aqueous medium offer supportive data for investigation of MIC and causative organisms.

a. *Temperature*—Microorganisms have been found at water temperatures from 1°C in Antarctic waters [*16*] to 320°C in deep-sea hydrothermal vents [*17*].

b. *Salinity*—Bacteria are commonly found in fresh and open ocean waters.

c. *Dissolved oxygen*—Bacteria are found in 0 to 100% O_2 concentrations.

d. *Water chemistries*—Including organic carbon nutrients, NO_3, CO_2, O_2, SO_4, and other compounds that may serve as terminal electron acceptors in respiratory metabolism. The presence and concentration of nitrites, phosphates, and sulfides; ionic materials such as chlorine, sulfur and phosphorous; metals, and acids is important. For example, breakdown of the protective passive oxide film on stainless steel occurs in the presence of the chlorides.

e. *Water microbiology*—See microbiology discussion.

f. *Direction and velocity of flow*—Hydrodynamic shear stress, related to flow, influences transport, transfer, and reaction rates within the biofilm, as well as biofilm detachment.

(3) System Relationship to Nearby Upstream Industry—Environmental ground or air pollution and terrestrial influence, as compared to open ocean.

(4) Operating History of Corroding System—As an example, there have been several documented cases of MIC in the nuclear industry where shutdown after hydrotesting with natural waters has resulted in extensive pitting failures [*18*]. Inadequate drainage left stagnant areas conducive to bacterial attack. Antifouling and cathodic protection measures in use should be known.

Collection and Transport of Corroding Sample and Medium

Pope [*11*], Tatnall [*14*], and Stoecker [*19*] have described sample collection for the study of MIC. Swabs should be obtained from the base metal and within pits beneath tubercles. Samples of tubercular material and aqueous medium, in addition to any other items in the environment of interest should be collected. General recommendations are to collect and analyze intact specimens, maintained in natural liquid medium, as soon as possible after disturbing the normal operating system. Samples should be taken in clean sterile containers and chilled until examination within 12-24 h. Specimens to be studied microscopically should be fixed in preservatives such as 2-4% formaldehyde or glutaraldehyde to maintain structural integrity.

Microbiology

It must be remembered that biofilms are a total community with synergistic relationships between organisms, producing activities different than those from isolated species. Cultures only provide identification of species present.

Standard microbiological practices for general and selective cultures are commonly described. General plate counts may be misleading because results do not necessarily correlate with bacteria directly related to MIC. Using knowledge of the corroding system, including oxygen content, metal alloy involved, and other parameters, a microbiologist could determine investigative directions such as using Postgate medium [*20*] where SRB are suspected.

Commercially prepared media and test kits are available for on-site and laboratory screening. Little et al. have described several for the detection of SRB [*21*].

Culture Techniques

The American Petroleum Institute (API, New York, NY) Recommended Practice (RP 38) [*22*] for the enumeration of SRB in subsurface injection waters specifies sodium lactate as the carbon source. When bacteria are present in the sample, they reduce sulfate in the medium to sulfide that reacts with iron in solution to produce black ferrous sulfide. Blackening of the medium over a 28-day period signals the presence of SRB. A solid medium technique termed "agar deeps" uses a modification of API with sodium sulfite as the reducing agent/oxygen scavenger [*23*]. An agar slant is inoculated, oxygen is excluded, tube is sealed, incubated for 5 days, and observed for blackening.

Direct Methods

Unlike culturing techniques, direct methods for detecting and quantifying SRB do not require SRB growth. Instead, direct methods measure constitutive properties including: adenosine-5′-phosphosulfate (APS) reductase [*23*], hydrogenase [*24*], cell-bound antibodies [*25*], and DNA [*26*]. Attempts have also been made to use adenosine triphosphate (ATP) [*27*] and radiorespirometric measurements for estimates of SRB activity [*28*].

The APS reductase antibody method was developed by Tatnall [*23*]. APS reductase is an intercellular enzyme found in all SRB. Briefly, cells are washed to remove interfering chemicals including hydrogen sulfide and lysed to release APS reductase. The lysed sample is washed and exposed to a color-developing solution. In the presence of APS reductase a blue color appears within 10 min. The degree of color is proportional to the amount of enzyme and roughly to the number of cells from which the enzyme was extracted. Similarly, a procedure has been developed to quantify hydrogenase from SRB that requires that cells

be concentrated by filtration from water samples [*24*]. Solids, including corrosion products and sludge, can be used without pretreatment. The sample is exposed to an enzyme extracting solution for 15 min and placed in an anaerobic chamber from which oxygen is removed by hydrogen. The enzyme reacts with excess hydrogen and simultaneously reduces an indicator dye in solution. The activity of the hydrogenase is established by the development of a blue color within 4 h. Color intensity is proportional to rate of hydrogen uptake.

Field and laboratory epifluorescence cell surface antibody methods for detecting SRB have been developed by D. H. Pope [*25*]. Both methods are based on the use and subsequent detection of specific antibodies, produced in rabbits, that react with SRB cells. A secondary antibody, produced in goats, is then reacted with the primary rabbit antibodies bound to the SRB cells. In the laboratory method, the goat antibodies are linked to a fluorochrome that enables bacterial cells marked with the secondary antibody to be viewed with an epifluorescence microscope. In the field method, the goat antibodies are conjugated with an enzyme (alkaline phosphatase) that can then be reacted with a colorless substrate to produce a visible color proportional to the quantity of SRB present.

Hogan has described a nonisotopic, semiquantitative procedure for the detection of *Desulfobacterium* and *Desulfotomaculum* using DNA probes that are labeled with an acridinium ester and is sensitive to 10^4 organisms/mL [*26*]. DNA probes are directed towards ribosomal RNA and may be viewed as consisting of three to four steps: (1) sample handling, (2) binding the probe to the target, (3) removal or destruction of the unbound probe, and (4) detection and quantification of the reporter group on the bound probe.

ATP assays estimate the total number of viable organisms by measuring the amount of ATP in a sample. ATP is a compound found in all living matter. Littman proposed that ATP assay techniques may be used with oilfield water samples to estimate relative numbers of SRB [*27*]. The procedure requires that a water sample be filtered to remove solids and salts that may interfere with the test. The filtered sample is added to a reagent that releases cell ATP. An enzyme then reacts with the ATP to produce a photochemical reaction. Emitted light can be measured with a photometer and the number of bacterial cells is estimated from the total light emitted.

Microscopy

Because MIC cannot be verified by morphology of localized corrosion or composition of corrosion products, it is essential in the diagnosis of MIC that a spatial relationship be established between microorganisms, substratum metal, and corrosion. Several microscopic techniques have been used to document numbers and types of microorganisms on surfaces. Epifluorescence microscopy has been used to evaluate the distribution of cells on corroded surfaces [*25*]. This technique requires sample fixation and staining. It is often difficult to distinguish individual cells within a densely populated biofilm using epifluorescence microscopy and it is sometimes impossible to penetrate corrosion products with stains. Transmission electron microscopy (TEM) has been used to demonstrate microbial cells distributed throughout corrosion layers [*29*]. TEM requires sample fixation, dehydration, embedding and thin sectioning. Traditional scanning electron microscopy (SEM), coupled with energy dispersive spectroscopy (EDS), has been used extensively to demonstrate bacteria in corroded areas and to determine surface chemistries resulting from MIC. Elemental chemistry of the base metal, pit area, corrosion products, and general biofilm should be identified. Presence, morphology, and distribution of microorganisms within the biofilm, and the presence of polymeric material must be determined. Figure 4 shows localized corrosion and distribution of bacteria in corrosion products from a copper/nickel piping system after 1 year of service [*30*].

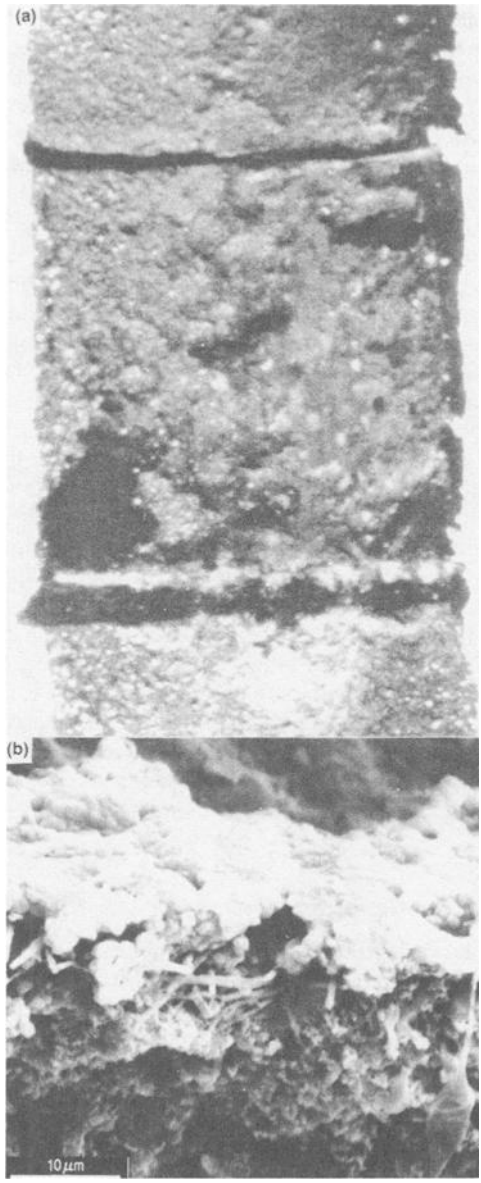

FIG. 4—*Pitting in copper/nickel piping system after 1 year in service [30]: (a) = pitted area and (b) = bacteria in cross-section of pitted area.*

Preparation of biological material for SEM requires extensive manipulation, including fixation, dehydration, and either air or critical-point drying because the SEM operates at high vacuum. Nonconducting samples, including biofilms, must be coated with a conductive film of metal before the specimen can be imaged. Uncoated nonconductors build up local concentrations of electrons, referred to as "charging," that prevent the formation of usuable images. EDS can be used to determine the elemental composition of surface films in the

SEM, but EDS analyses must be completed prior to deposition of a thin metal coating. EDS data are typically collected from an area, the specimen removed from the specimen chamber and coated with a conductive layer, and returned to the SEM. The operator attempts to relocate and photograph the precise area from which the EDS data were collected. Little et al. [*31*] demonstrated that sample preparation for SEM, including the solvent removal of water and air or critical point drying, decreases areal coverage of the surface by the biofilm, removes cells from the biofilm, removes extracellular polymeric material that may contribute to corrosion, and decreases the concentration of metals bound within the matrix of the exopolymer (Fig. 5).

Environmental scanning electron microscopy (ESEM) was used to demonstrate that the number and types of microorganisms on copper surfaces have been underestimated by SEM. ESEM provides fast, accurate images of a biofilm (Fig. 6), its spatial relationship to a corrosion site, as well as surface chemistry, without extensive manipulation of the sample. This instrument uses a unique secondary electron detector capable of forming high resolution images at pressures in the range of 0.1 to 20 torr. At these relatively high pressures, specimen

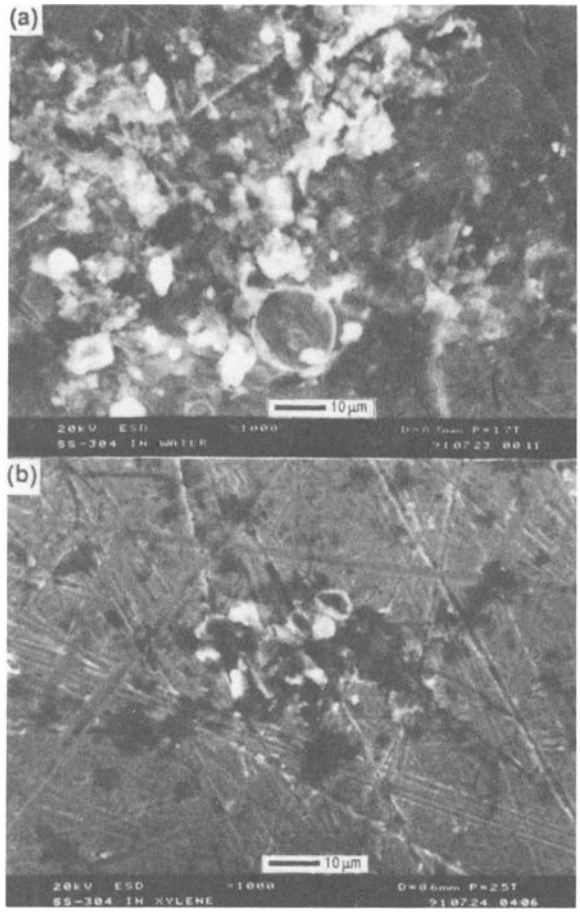

FIG. 5—*ESEM images comparing biofilm coverage when wet and after removal of water* [*31*]: (*a*) = *as taken directly from water and* (*b*) = *after acetone-xylene removal of water.*

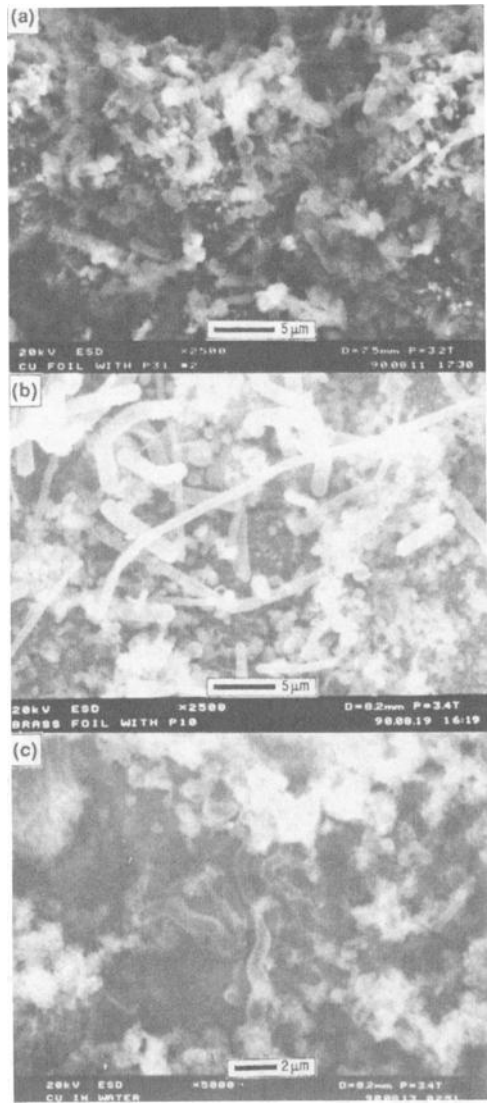

FIG. 6—*ESEM micrographs of bacterial cells within biofilms.*

charging is dissipated into the gaseous environment of the specimen chamber, enabling direct observation of uncoated, nonconductive specimens. If water vapor is used as the specimen environment, wet samples can be observed directly, and EDS data can be collected at the same time as sample morphology and topography are photographed. Figure 7 shows a flow diagram for sample preparation for SEM compared to that for ESEM.

Corrosion and sulfide film formation on copper-containing metals can be followed using ESEM/EDS. In the presence of S^{2-}, a porous layer of cuprous sulfide with the general stoichiometry Cu_2-xS, $O < x < 1$ forms [*32*]. Copper ions migrate through the layer, react with more sulfide to produce a thick black scale. It has been argued that if the copper sulfide

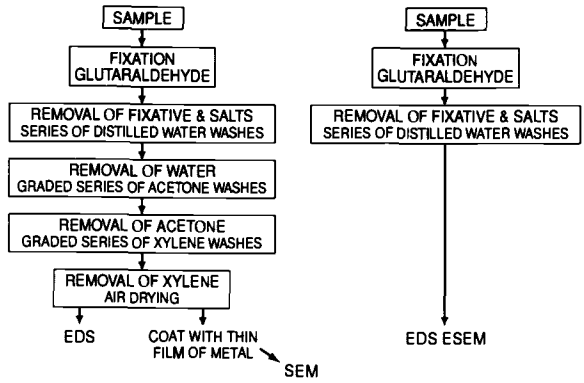

FIG. 7—*Flow chart comparing sample preparation for SEM and ESEM.*

layer were djurleite ($Cu_{1.96}S$) the sulfide layer would be protective. However, even if such a sulfide film were technically passivating, the film's mechanical stability is so poor that sulfide films are useless for corrosion protection. In the presence of turbulence, the loosely adherent sulfide film is removed, exposing a fresh copper surface to react with the sulfide ions. Preparation of microbiologically-produced sulfide corrosion products on copper foils for the SEM physically or chemically, or both, removes material from the surface.

An important feature of wet biofilms on copper-containing metals was that the microorganisms were distributed throughout the copper/nickel/iron-rich surface layers and not on top of these layers as some traditional scanning electron micrographs have indicated. Fixation, dehydration, and critical-point drying resulted in a loss of material from the surface so that many bacteria were removed with the surface deposits. It has been previously reported that bacterial cells attached to the base metal were tenaciously attached to the surface and were not removed or distorted during the SEM preparation [*31*]. TEM has been used to demonstrate that bacteria were intimately associated with the corrosion products and that on copper surfaces, the bacteria were found between layers of corrosion products and attached to base metal [*29*]. Similarly, ESEM images demonstrate that SRB were distributed throughout the sulfur-rich corrosion layers.

Dealloying of nickel from copper/nickel alloys and intergranular corrosion as a result of MIC has been reported by several investigators. Little et al. used EDS to demonstrate selective dealloying of Monel 400 in the presence of SRB from an estuarine environment (Fig. 8) [*30*]. The first evidence of a spatial relationship between the constituents of the biofilm and dealloying within pits covered with bacteria and diatoms has been presented. Little et al. demonstrated that diatoms are easily removed from marine biofilms during preparation for SEM and advanced the opinion that the role of diatoms in MIC has been neglected (Fig. 5) [*31*].

Several new forms of microscopy have been recently developed. Brief descriptions of those with potential application to the research study of biofilms follow.

Confocal laser scanning microscopy uses mechanical scanning of the object and a laser light source. A pinhole diaphragm just before the photomultiplier allows detection of light from very small specimen areas. High spatial resolution is achieved where horizontal optical sections can be collected and compiled for 3-dimensional image analysis [*33*]. Geesey has used this technique to study multidimensional images within a biofilm[2].

[2] G. G. Geesey, personal communication, 1992.

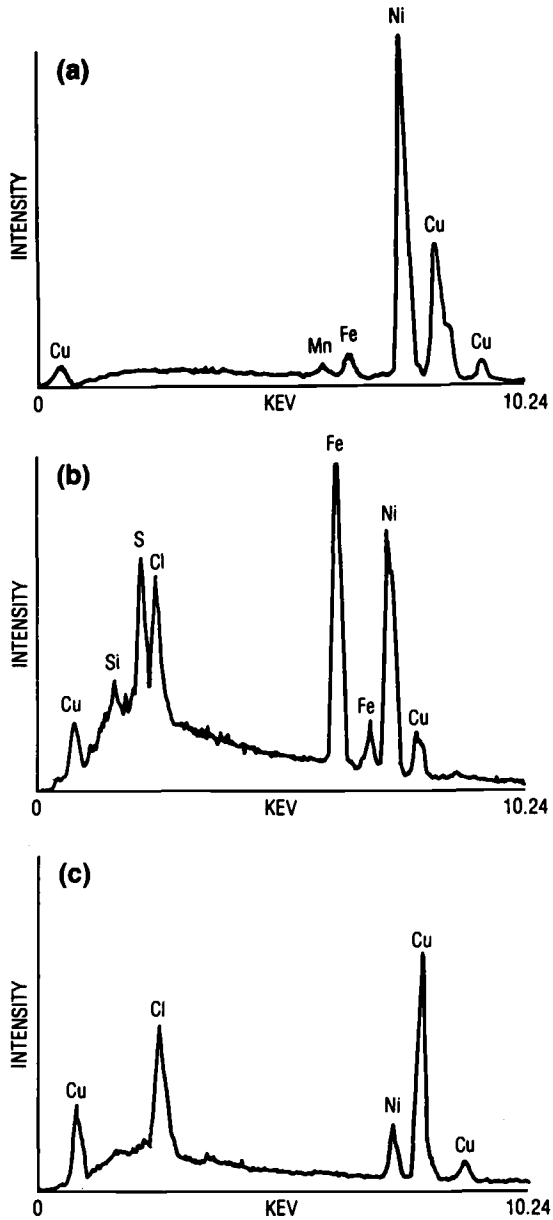

FIG. 8—*EDS spectra for nickel alloy Monel 400 before and after exposure to estuarine water [30]: (a) = unexposed, (b) = exposed for 6 months, showing accumulations of Si, S, and Cl with increased Fe and Ni, and (c) = residual metal in base of pit showing Ni depletion and Cu enrichment.*

Scanning tunneling microscopy uses the principle of quantum mechanical tunneling. The microscope tip and the sample form two electrodes between which tunneling can occur through a nonconductor, usually a vacuum, but can be other media such as water or an electrolyte. The tip moves in x,y,z dimensions to yield a surface map of local density states.

This technique has been applied to imaging unstained, uncoated viruses [*34*]. Atomic force microscopy provides contour images, as used by Bremer et al., to show spatial relationship between a bacterium and a pit on a copper surface [*35*]. Probes use x,y,z piezotranslation to position a sample in contact with a microfabricated cantilever where it is scanned in a raster pattern.

Chemistry

(1) Aqueous Medium

Chemical analyses of the liquid medium from the corrosion system has been described previously and should be performed according to standard methodology.

(2) Base Metal and Corrosion Products

Elemental analysis of base metal and corrosion deposits using SEM/EDS or ESEM/EDS has been described. EDS spectra are obtained while the electron beam scans the area of interest to obtain true average compositions and avoid bias associated with selecting a specific point on an inhomogenous surface. Associated dot mapping shows distribution of an element of interest within a field. Figure 9 illustrates use of dot mapping in investigation of delamination of a zinc coating on galvanized steel[3].

Scanning Auger microprobe analyses were used by Lee et al. to show metallic segregation in butt-welded 90/10 Cu/Ni piping [*36*]. The composition of the heat-affected zone was profiled by a series of overlapping images to allow calculation of percentage compositions from peak amplitudes. As an example, Fig. 10 shows a profile of percent concentration calculated from Auger data for carbon across the heat affected zone of a copper/nickel butt weld.

McNeil et al. analyzed sulfide mineral deposits on copper alloys colonized by SRB in an attempt to identify specific mineralogies that could be used to fingerprint SRB activity [*32*]. They concluded that the formation of nonadherent layers of chalcocite (Cu_2S) and the presence of hexagonal chalcocite were indicators of SRB-induced corrosion of copper. The compounds were not observed abiotically and their presence in near-surface environments could not be explained thermodynamically. Others have identified mackinawite, gregrite, and symthite as indicators for SRB corrosion of ferrous metals in anaerobic environments [*37*].

Sulfur isotope fractionation was demonstrated by Little et al. in sulfide corrosion deposits resulting from the activities of SRB within biofilms on copper surfaces [*38*]. ^{32}S was accumulated in sulfide-rich corrosion products and ^{34}S was concentrated in the residual sulfate in the culture medium. Conventionally, the amplitude of each isotope is not reported individually, but a ratio is established and compared to the isotope ratio of a standard to yield a value $\delta^{34}S$ expressed as parts per thousand. Negative δ values indicate a concentration of ^{32}S, and positive values indicate an accumulation of ^{34}S. Accumulation of the lighter isotope was related to surface derivatization or corrosion as measured by weight loss. Use of this and the preceding mineralogical technique to identify SRB-related corrosion requires sophisticated laboratory procedures.

[3] B. Little, unpublished work, 1987.

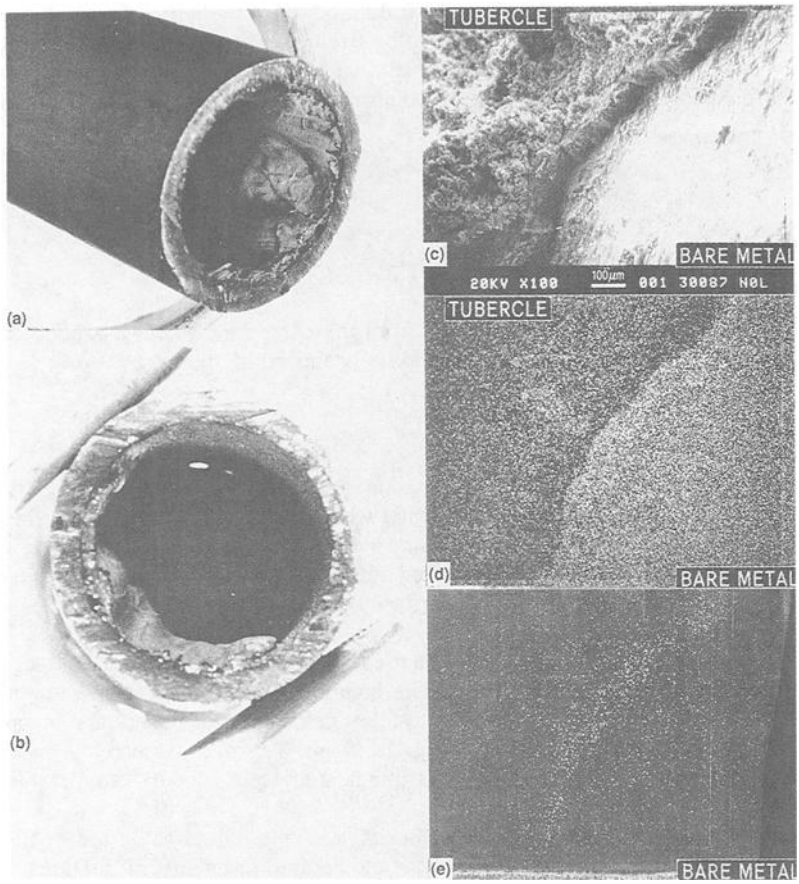

FIG. 9—*Delamination of zinc coating on galvanized steel: (a & b) = galvanized steel pipe containing tubercles of iron-oxidizing bacteria, (c) = SEM micrograph of tubercle, (d) = EDS dot map for Fe for area shown in (c), and (e) = EDS dot map for Zn for area shown in (c).*

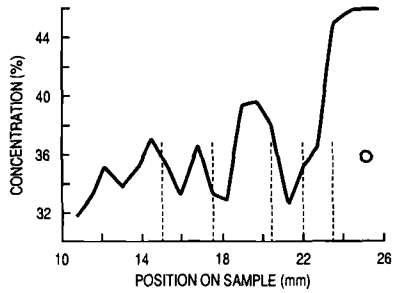

FIG. 10—*Profile of percent concentration of carbon across heat affected zone of a copper/nickel butt weld [36]. Weld bead starts at 22 mm and proceeds to the right, melt zone at approximately 16 mm.*

(3) Interfacial Chemistries

Including pH, dissolved oxygen, and sulfides have been measured by Lewandowski et al. [*9*], and VanHoudt et al. [*39*]. Microelectrodes were developed to profile these parameters systematically through the biofilm from external surface to the metal/biofilm interface.

Kearns et al. used X-ray photoelectron spectroscopy to characterize the interaction of metal ions and SRB for interfacial studies [*40*]. The biomass was irradiated to induce photoelectron ejection. By measuring kinetic energies of the photoelectrons, the binding energy of the electrons can be calculated. The binding energy value contributes to elemental identifications. Shifts in binding energy identifies oxidation state of the element.

Metallurgy

Alloy composition, mechanical properties, and microtopography provide indicators of corrosion susceptibility. Examples of localized attack for specific alloys have been discussed earlier. Deformation of grain structure, presence of inclusions, and any other manufacturing defects provide sites of decreased corrosion resistance [*6*]. In certain environments, heat-affected zones of welds in stainless steels are very susceptible to MIC [*10*]. In metallographic examination after exposure, identification of localized attack, carbides from graphitization, and hydrides from hydrogen-producing bacteria may suggest MIC.

Conclusions

In ideal circumstances, basic examination of a corrosion system includes preliminary knowledge of the corroding material and its operating environment. Initial visual observations of the undisturbed sample and subsequent microbiological, microscopic, chemical, and metallurgical examinations should provide reliable evidence for MIC.

Acknowledgment

This work was supported by the Office of Naval Research, Program Element 0601153N, through the NRL Defense Research Sciences Program. Approved for public release, unlimited distribution. NRL Contribution Number PR 92:060:333.

References

[*1*] Characklis, W. G. and Marshall, K. C., "Biofilms: A Basis for an Interdisciplinary Approach," *Biofilms*, Wiley Interscience, New York, NY, 1990, p. 4.

[*2*] Ehrlich, H. L. and Brierly, C. L., *Microbial Mineral Recovery*, McGraw-Hill, New York, NY, 1990.

[*3*] Characklis, W., Turakhia, M., and Zelver, N., "Transport and Interfacial Transfer Phenomena," *Biofilms*, Wiley Interscience, New York, NY, 1990, p. 265.

[*4*] Moreton, B. B. and Glover, T. G., "New Marine Industry Applications for Corrosion and Biofouling Resistant, Copper-Nickel Alloys," *Biologia Marina*, Graficas Orbe, Madrid, Spain, 1980, p. 267.

[*5*] Mansfeld, F. and Little, B., "A Technical Review of Electrochemical Techniques Applied to Microbiologically Influenced Corrosion," *Corrosion Science*, Vol. 3, 1991, p. 247.

[*6*] *Corrosion Basics*, National Association of Corrosion Engineers, Houston, TX, 1984, p. 49.

[*7*] Borenstein, S. W., "Microbiologically Influenced Corrosion of Austenitic Stainless Steel Weldments," *Materials Performance*, Vol. 30, No. 1, 1991, p. 52.

[*8*] Dowling, N. J. E., Guezennec, J., Bullen, J., Little, B., and White, D. C., "Effect of Photosynthetic Biofilms on the Open-Circuit Potential of Stainless Steel," *Biofouling*, 1992, p. 6.

[9] Little, B., Ray, R., Wagner, P., Lewandowski, Z., Lee, W. C., Characklis, W. G., and Mansfeld, F., "Impact of Biofouling on the Electrochemical Behaviour of 304 Stainless Steel in Natural Seawater," *Biofouling*, Vol. 3, 1991, p. 45.

[10] Borenstein, S. W., "Why Does Microbially Influenced Corrosion Occur Preferentially at Welds?" Proceedings, Corrosion/91, Paper 286, National Association of Corrosion Engineers, Houston, TX, 1991.

[11] Pope, D. H., Duquette, D., Wayner, P., Johannes, A., and Freeman, A., *Microbiologically Influenced Corrosion: A State-of-the-Art Review*, Materials Technology Institute, *MTI 13*, National Association of Corrosion Engineers, Houston, TX, 1989.

[12] Kobrin, G., "Corrosion by Microbiological Organisms in Natural Waters," *Materials Performance*, Vol. 15, No. 7, 1976, p. 38.

[13] Tatnall, R. E., "Case Histories: Bacteria-Induced Corrosion," Proceedings, Corrosion/81, Paper 130, National Association of Corrosion Engineers, Houston, TX, 1981.

[14] Tatnall, R. E., "Fundamentals of Bacteria-Induced Corrosion," *Materials Performance*, Vol. 20, No. 9, 1981, p. 32.

[15] Costerton, J. W., Geesey, G. G., and Jones, P. A., "Bacterial Biofilms in Relation to Internal Corrosion Monitoring and Biocide Strategies," *Materials Performance*, Vol. 27, No. 4, 1988, p. 49.

[16] Maki, J. S., Little, B. J., Wagner, P., and Mitchell, R., "Biofilm Formation on Metal Surfaces in Antarctic Waters," *Biofouling*, Vol. 2, 1992, p. 27.

[17] Tunnicliffe, V., "Hydrothermal-Vent Communities of the Deep Sea," *American Scientist*, Vol. 80, July–Aug., 1992, p. 336.

[18] Soracco, R. J., Pope D. H., Eggars, J. M., and Effinger, T. N., "Microbiologically Influenced Corrosion Investigations in Electric Power Generating Stations," Proceedings, Corrosion/88, Paper 83, National Association of Corrosion Engineers, Houston, TX, 1988.

[19] Stoecker, J. G., "Guide for the Investigation of Microbiologically Induced Corrosion," *Materials Performance*, Vol. 23, No. 8, 1984, p. 48.

[20] Postgate, J. R., *The Sulphate Reducing Bacteria*, Cambridge University Press, Cambridge, United Kingdom, 1979, p. 26.

[21] Little, B. and Wagner, P., "Standard Practices in the United States for Quantifying and Qualifying Sulphate Reducing Bacteria in Microbiologically Influenced Corrosion," Proceedings Symposium Redefining International Standards and Practices for the Oil and Gas Industry, London, United Kingdom, sponsor, National Association of Corrosion Engineers, Houston, TX, 1992.

[22] American Petroleum Institute, *API Recommended Practice for Biological Analysis of Subsurface Injection Waters*, American Petroleum Institute (API), New York, NY, 1965.

[23] Tatnall, R. E., Stanton, K. M., and Ebersole, R. C., "Methods of Testing for the Presence of Sulfate-Reducing Bacteria," Proceedings, Corrosion/88, Paper 88, National Association of Corrosion Engineers, Houston, TX, 1988.

[24] Boivin, J., Laishley, E. J., Bryant, R. D., and Costerton, J. W., "The Influence of Enzyme Systems on MIC," Proceedings, Corrosion/90, Paper 128, National Association of Corrosion Engineers, Houston, TX, 1990.

[25] Pope, D. H., "Development of Methods to Detect Sulfate-Reducing Bacteria Agents of Microbiologically Influenced Corrosion," MTI 37, Materials Technology Institute of the Chemical Process Industries, Inc., sponsor, National Association of Corrosion Engineers, Houston, TX, 1990.

[26] Hogan, J. J., "A Rapid, Non-Radioactive DNA Probe for the Detection of SRBs," presented at the Institute of Gas Technology Symposium on Gas, Oil, Coal and Environmental Biotechnology, New Orleans, LA, 1990.

[27] Littman, E. S., "Oilfield Bactericide Parameters as Measured by ATP Analysis," Paper 5312, *International Symposium of Oilfield Chemistry, Preprints*, Society of Petroleum Engineers of the American Institute of Mining, Metallurgical, and Petroleum Engineers (AIME), New York, NY, 1975, pp. 171–181.

[28] Rosser, H. R. and Hamilton, W. A., "Simple Assay for Accurate Determination of [^{35}S] Sulfate Reduction Activity," *Applied and Environmental Microbiology*, Vol. 45, 1983, p. 1956.

[29] Blunn, G., "Biological Fouling of Copper and Copper Alloys," *Biodeterioration VI*, CAB International, Slough, United Kingdom, 1986, p. 567.

[30] Little, B., Wagner, P., Ray, R., and McNeil, M., "Microbiologically Influenced Corrosion in Copper and Nickel Seawater Piping Systems," *Marine Technology Society Journal*, Vol. 24, No. 3, 1990, p. 10.

[31] Little, B., Wagner, P., Ray, R., Pope, R., and Scheetz, R., "Biofilms: An ESEM Evaluation of Artifacts Introduced During SEM Preparation," *Journal of Industrial Microbiology*, 1991, p. 213.

[32] McNeil, M. B., Jones-Meehan, J., and Little, B. J., "Production of Sulfide Minerals by Sulfate Reducing Bacteria during Microbiologically Influenced Corrosion of Copper," *Corrosion*, Vol. 47, No. 9, 1991, p. 674.
[33] Baak, J., Thunnissen, F., Oudejans, C., and Schipper, N., "Potential Clinical Uses of Laser Scan Microscopy," *Applied Optics*, Vol. 26, No. 16, 1987, p. 3413.
[34] McCormick, D. and McCormick, L., "Applications of Scanning Tunneling Microscopy to Biological Materials," *Biotechnology Laboratory*, 1990, p. 55.
[35] Bremer, P., Geesey, G., and Drake, B., "Atomic Force Microscopy Examination of the Topography of a Hydrated Bacterial Biofilm on a Copper Surface," *Current Microbiology*, Vol. 24, 1992, p. 223.
[36] Lee, R. N., Norr, M. K., Jacobus, O. J., Little, B. J., and Wagner, P. A., "Composition Variations in Copper-Nickel Butt Welds," *Corrosion*, Vol. 47, No. 8, 1991, p. 645.
[37] Baas-Becking, G. M. and Moore, D., "Biogenic Sulfides," *Economic Geology*, Vol. 56, 1961, p. 259.
[38] Little, B. Wagner, P., and Jones-Meehan, J., "Sulfur Isotope Fractionation by Sulfate-Reducing Bacteria in Corrosion Products," *Biofouling*, Vol. 6, 1993, p. 279.
[39] VanHoudt, P., Lewandowski, Z., and Little, B., "Iridium Oxide pH Microelectrode," *Biotechnology and Bioengineering*, Vol. 40, 1992, p. 601.
[40] Kearns, J. R., Clayton, C. R., Halada, G. P., Gillow, J. B., and Francis, A. J., "The Application of XPS to the Study of MIC," Proceedings, Corrosion/92, Paper 178, National Association of Corrosion Engineers, Houston, TX, 1992.

SRB Characterization

Michael B. McNeil[1] *and A. L. Odom*[2]

Thermodynamic Prediction of Microbiologically Influenced Corrosion (MIC) by Sulfate-Reducing Bacteria (SRB)

REFERENCE: McNeil, M. B. and Odom, A. L., **"Thermodynamic Prediction of Microbiologically Influenced Corrosion (MIC) by Sulfate-Reducing Bacteria (SRB),"** *Microbiologically Influenced Corrosion Testing, ASTM STP 1232,* Jeffery R. Kearns and Brenda J. Little, Eds., American Society for Testing and Materials, Philadelphia, 1994, pp. 173–179.

ABSTRACT: Sulfiding corrosion induced by the action of consortia containing sulfate-reducing bacteria (SRB) in biofilms is a problem with most common engineering materials. It is now possible to use a model based on basic thermodynamic reasoning and information on complexation and alteration kinetics to make some predictions about the mineralogy and form of the corrosion products. This analysis, applied to a variety of materials, gives predictions in agreement with experimentation.

KEYWORDS: microbiologically influenced corrosion (MIC), sulfate-reducing bacteria (SRB), stability diagrams

Microbiologically influenced corrosion (MIC) resulting from the sulfiding action of consortia, including SRB, was reported before sulfate-reducing bacteria (SRB) had been characterized microbiologically [*1–3*]; the basic chemistry of SRB MIC of iron was identified in 1934 [*4*], and a general review of SRB MIC of metals was published in 1961 [*5*]. Notwithstanding these activities, and significant engineering research on SRB-influenced MIC [*6–9*], little or no effort was made to understand why SRB MIC was common in certain alloy systems and rare or unknown (or very slow) in others, or to explain the nature of the corrosion products. This is still true despite advances in knowledge of microbiological aspects of biomineralization [*10,11*].

The availability of modern experimental techniques, especially the environmental scanning electron microscope (ESEM) [*12*], and various other probes that have permitted much more accurate measurements of conditions in biofilms [*13*] and the nature of corrosion products [*14,15*], have made it possible to construct and test models for microbiological-corrosion processes. This paper presents a model that can be used to interpret sulfiding corrosion resulting from the direct action of consortia of microorganisms within a biofilm attached to the surface of a metal or alloy, assuming that the *net* primary reaction is that between sulfide ions produced by the SRB and metal atoms from the solid, though this net reaction is the sum of several reactions, at least one of which involves metal ion solubilization. The term "corrosion" will be used to characterize the reactions associated with this phenomenon, though it is recognized that some of the reactions involving species such as malachite ($Cu_2CO_3(OH)_2$) are of the sort more commonly described as alteration. The focus on the

[1] Nuclear Regulatory Commission, Office of Nuclear Regulatory Research, Washington, DC 20555.
[2] Professor, Florida State University, Department of Geology, Tallahassee, FL 23206.

sulfiding reactions does not imply that nonsulfiding reactions are unimportant in corrosion. For example, to understand the overall reactions involved in SRB MIC of iron in natural environments (which are almost never wholly oxygen-free), one must consider anodic reactions leading to products such as green rust [*16*] and other oxidized species; otherwise, one cannot account for the fact that in some cases of iron corrosion, metal consumption is greater than can be accounted for on the basis of iron-sulfide stoichiometry. The purpose of this paper is to address the question of whether basic thermochemical data can be used to predict vulnerability to sulfiding MIC rather than to pursue detailed kinetic issues, even those that are very important practically.

Status of Database

The following are mineralogical observations that have been made on the products of SRB-influenced corrosion/mineralization reactions. Patterns refer to X-ray powder patterns when not otherwise described.

- Al—No data.
- Ag—MIC leads to production of acanthite, Ag_2S [*17*].
- Ag-Cu Alloys—MIC leads to production of acanthite, sometimes argentite, the high-temperature polymorph of Ag_2S or jalpaite, Ag_3CuS_2 [*17*].
- Be—No data.
- Cd—No direct data, but evidence of cadmium sulfide (CdS) formation [*18*].
- Ce, Other Rare Earths—No data.
- Cr—No data.
- Cu—SRB MIC produces complex suites of sulfide minerals; the most common product is chalcocite, Cu_2S, though final product in many cases is blue-remaining covellite, CuS_{1+x} [*19*].
- Cu-As, Cu-Sb Alloys—No data.
- Cu-Ni Alloys—Corrosion products are similar to those of Cu, but with significant djurleite, $Cu_{31}S_{16}$. No Ni minerals are observed [*19*].
- Cu-Sn Alloys—Corrosion products similar to those in Cu.
- Cu-Zn Alloys—Complex patterns with no familiar mineral lines.
- Fe (Carbon Steel)—Final product is pyrite, FeS_2; intermediate reactions involve a number of compounds. Crystals tend to be small [*6,7,20*].
- Fe (Stainless Alloys)—Rate are slower than pure Fe or carbon steel. No Ni minerals have been detected. Stainless steels with 6% or more Mo appear to be very resistant.
- Ir—SRB MIC of oxidized Ir surfaces produces complex patterns.
- Mg—No data.
- Ni—SRB produce millerite, NiS, from Ni ions [*15*]; Ni and high-Ni alloys are vulnerable to SRB MIC but Ni minerals are rarely detected.
- Pb—SRB MIC produces galena, PbS [*21,22*].
- Sn—No data.
- Ti—Apparently not affected by SRB [*23*].
- Zn—SRB MIC produces a sulfide conjectured to be sphalerite, ZnS [*5*].
- Zr—Apparently not affected by SRB.

There are three basic sources for thermodynamic data. Two are published books: *The National Bureau of Standards Handbook of Thermodynamic Data* [*24*] and *Woods' and Garrels' Compilation of Data on Minerals* [*25*]. The third is the Data Program for Alloy Phase Diagrams, which maintains files of thermodynamic data at the University of Toronto (Dr. V. Itkin) and at the University of Notre Dame (Professor C. B. Alcock).

Model for Pure Metals

The observations summarized above are consistent with the following general model. SRB MIC is initiated by sulfide-rich, reducing conditions in the biofilm. Under these conditions the oxide layer on the metal (or, in the case of Ag, perhaps the metal itself) is destabilized and acts as a source of metal-containing ions [*26*]. These ions are generally complexes of some sort (possibly sulfide complexes; see Refs *15*, *27*, and *28*). At the surfaces of the microbes, these ions react to produce sulfide compounds in micron size particles that are, at least for Ni, crystalline [*15*], though they may at first be amorphous, in the case of iron [*29*]. The consumption of metal ions at microbe surfaces is balanced by release from the surface, so the net reaction is as follows:

$$MO \longrightarrow MS \tag{1}$$

until the oxide is totally consumed, and thereafter (or throughout) the reaction, in the case of Ag)

$$M \longrightarrow MS \tag{2}$$

where *M* is the metal, *MO* the oxide, and *MS* the sulfide. If the reaction to produce *MS* from *MO* has a positive Gibbs free energy under surface conditions, the sulfides will not strip the protective oxide; if the reaction from *M* to *MS* has a positive Gibbs free energy, the metal, even when exposed, is immune.

The sulfide microcrystals then redissolve and reprecipitate as larger, generally more sulfide-rich crystals, ultimately altering the sulfide minerals stable under biofilm conditions. The sulfide-sulfide alteration reactions generally follow Ostwald's principle [*30*] stating that less stable, and generally sulfide-poor minerals are precursors to more stable end products, and the simplexity principle [*31*], which states that solutions rich in impurity ions tend to precipitate high-temperature, high-entropy polytypes that can accommodate alien cations. Ultimately, in the presence of dissolved oxygen, the sulfides may react to other compounds; this is particularly true in piping situations where oxygenated water may be brought into contact with the biofilm.

Microbiological and inorganic chemical processes interact in MIC, and it is clear that at least in some cases this interaction is extremely complex [*32*]. The model put forth here treats the microbiological processes purely as a machinery for adjusting local water chemistry and reduces the whole process of MIC and biomineralization to a special case of inorganic alteration. Clearly this is not always adequate if one wishes to predict the composition [*29*] or morphology [*32*] of minerals forming, for example, in magnetotactic bacteria. The evidence in this paper indicates that it is adequate to make predictions of whether materials are subject to MIC, and to make some general predictions about corrosion-product mineralogy.

This model can be tested in several ways. First, it should explain why SRB MIC is not found on certain metals. While considerations of acidity, dissolved oxygen, sulfide levels, and so forth change the details, it is clear that this model says that if reaction [*1*] has a sizeable negative standard-free energy of reaction, SRB MIC is possible, while if the reaction has a sizeable positive standard-free energy of reaction, SRB MIC will not happen.

Using the data in the most recent National Institute of Standards and Technology (NIST) table [*24*], one can examine possible sulfidation reactions for a number of metals at 298.16 K. First, two familiar cases

$$Cu_2O + HS^- \longrightarrow Cu_2S + OH^-$$

The standard-free energy of reaction is −110.2 kJ.

$$CuO + HS^- \longrightarrow CuS + OH$$

The standard-free energy of reaction is −103.2 kJ.
Fe:

$$Fe_3O_4 + 4HS^- \longrightarrow 2Fe_{1-x}S(\text{pyrrhotite}) + FeS_2 + 4OH^-$$

The standard-free energy of the reaction is −29.6 kJ using the thermodynamic values for iron-rich pyrrhotite near the composition FeS; however, assuming that the products were pyrite and sulfur-rich pyrrhotite would give a standard-free energy of reaction below −100 kJ.

Consider two metals that are not normally considered subject to SRB MIC, but which have been observed to undergo such reactions
Pb:

$$PbO + HS^- \longrightarrow PbS + OH^-$$

The standard-free energy of reaction is −80.79 kJ.
Ir:

$$IrO_2 + 2HS^- \longrightarrow IrS_2 + 2OH^-$$

The standard-free energy of reaction is −191 kJ.

As a further check, one can examine metals that appear not to exhibit SRB MIC, Ti and Zr. In these cases we have no free-energy data. Standard enthalpies of reaction will be calculated; reference to the NIST tables indicates that entropy difference terms are generally fairly minor contributions to the free energies of solid sulfides. The hypothetical sulfide product on Ti is assumed to be TiS, not TiS_2, because no data are available even on the enthalpy of formation of TiS_2.
Ti:

$$TiO_2 + HS^- \longrightarrow TiS + OH^- + \tfrac{1}{2}O_2$$

The standard enthalpy of reaction is +587 kJ.
Zr:

$$ZrO_2 + 2HS^- \longrightarrow ZrS_2 + 2OH^-$$

The standard enthalpy of reaction is +206 kJ.

Standard-free energies of reaction are not identical to standard enthalpies of reaction, but it is still hard to imagine conditions on the surface of the earth that would produce negative free energies for the hypothetical Ti and Zr SRB MIC reactions; certainly it would require conditions antithetical to the growth of organisms. Using the familiar formula for equilibrium constants, $\ln K = -\Delta G_0/kT$, one can see that to produce TiS_2 from TiO_2 by increasing the concentration of HS^- at atmospheric oxygen pressure would require an HS^- activity of the order of e^{268}. Analyses of the implications of obtaining this conversion by other chemical means also lead to unphysical requirements. Calculations on other metals for which data are available also support three general conclusions concerning SRB MIC.

The first conclusion, based on thermodynamic equilibrium reasoning, is: *If, under all plausible biofilm conditions, the sulfides of a metal have higher free energy than the metal or oxide, the metal is immune to SRB MIC.*

This reasoning suggests the possibility of finding a way of making alloys passive to SRB MIC, by introducing surface films that are composed of minerals, other than oxides, that are more stable than the metal sulfides; for example, copper might be protected by a layer of dioptase, $CuSiO_3 \cdot H_2O$. However, if the coating on the metal (oxide or not) resists SRB MIC, but the underlying metal is not immune, one has a version of passivity and the metal would be vulnerable to localized attack at flaws in the coating.

Two further conclusions can be drawn concerning SRB MIC. Consideration of metal mass transport from the oxide (or other) surface to the SRB leads to a second conclusion: *Metals that do not dissolve easily in the biofilm will exhibit slower SRB MIC than those that do; and if the coating on the metal is of such a nature as to suppress dissolution or complexing, it will reduce the rate of SRB MIC.* These assertions are again supported by the observation that Cu, particularly pure Cu, shows quite rapid SRB MIC, while Ni and its alloys, although almost equally vulnerable from the thermodynamic standpoint, are much more resistant because the Ni^{++} ion has a kinetic resistance to solubilization [*26*]. Furthermore, Ni^{++} ions do not have easily-formed sulfide complexes like Cu^{+}, so nickel minerals once formed in the biofilm are not as reactive.

Since the reason stainless steel is stainless is that the Cr and Ni stabilize the oxide and the model predicts that one-phase stainless steels undergo sulfiding MIC more slowly than carbon steels, which is observed.

The third conclusion concerning SRB MIC arises from the fact that almost all of the reactions at the surface involve charge transport: *A metal with a surface coating having low electrical conductivity will show lower SRB MIC than the same metal with a coating having a higher electrical conductivity.*

Application of the Model to Alloys

The most straightforward way to apply the reasoning previously stated to metals in aqueous solutions, whether or not cathodically protected, is by use of Pourbaix diagrams [*33*] that display regions of stability for phases and ionic species as functions of Eh and pH, and are widely used in abiotic corrosion research. However, there are three problems in the use of conventional Pourbaix diagrams in studying SRB MIC in commercial alloys. First, Pourbaix diagrams tell one nothing about kinetics; a minor alloying element may fundamentally change the nature of a surface oxide, changing all reaction rates radically. Second, conventional Pourbaix diagrams address only pure metals, and cannot deal with either the thermodynamic affects of alloying or with dealloying. Third, conventional Pourbaix diagrams treat all corrosion-product minerals as having unique stoichiometries, and many do not (notably mackinawite, pyrrhotite, and covellite).

The model may be applicable to answering questions that appear to be questions about oxide reaction rates (for example, why does the addition of 6% Mo to a stainless steel suppress SRB MIC?), but such an application will require a careful study of the thermodynamics and kinetics of oxide alteration. In general, one may say that an alloying element that makes the surface oxide more stable thermodynamically will retard MIC.

The use of conventional Pourbaix diagrams is unlikely to predict immunity where there is vulnerability to SRB MIC. Such diagrams do not take into account either the thermodynamic effects associated with alloying or those associated with the formation of minerals having variable stoichiometry, but the errors in reaction energies associated with substitutional alloy formation are generally small. A large error could be introduced by the formation

of a nonsubstitutional mixed-cation mineral, but this would be unusual. However, the inability of conventional Pourbaix diagrams to accommodate thermodynamic effects of alloying and mixed-cation mineral formation does mean that they cannot readily be used to interpret dealloying, and many types of corrosion products also cannot be understood with conventional diagrams.

Conclusions

The use of thermodynamic arguments to predict immunity or vulnerability to MIC by SRB gives correct predictions for all pure metals for which experimental data are available. Extension of thermodynamic reasoning to alloys appears to require thermodynamic analyses of not only alloys and mixed-cation corrosion products, but also analyses of surface oxides.

References

[1] Daubree, G. A., *Bulletin de la Societe Geologique de France,* Vol. 19, 1862, p. 529.
[2] de Gouvernain, M., *Comptes Rendus,* Vol. 80, 1875, pp. 1297–1300.
[3] Daubree, G. A., *Comptes Rendus,* Vols. 92 and 93, 1881, and p. 57 and 572, respectively.
[4] von Wolzogen Kuhr, C. A. H. and van der Vlught, L. S., *Water,* Vol. 8, 1934, pp. 147–165.
[5] Baas Becking, G. M. and Moore, D., *Economic Geology,* Vol. 56, 1961, pp. 259–272.
[6] King, R. A., Dittmer, C. K., and Miller, J. D. A., *British Corrosion Journal,* Vol. 11, 1976, pp. 105–107.
[7] King, R. A. and Miller, J. D. A., *Anti-Corrosion,* Aug. 1977, p. 9.
[8] Smith, J. S. and Miller, J. D. A., *British Corrosion Journal,* Vol. 10, 1975, pp. 136–143.
[9] Pope, D. H., Duquette, D., Wayner, P. C., and Johannes, A. H., in *Microbially Influenced Corrosion,* Materials Technology Institute of the Chemical Process Industries, St. Louis, MO, 1984.
[10] Hamilton, W. A., *Annual Review of Microbiology,* Vol. 39, 1985, pp. 195–217.
[11] Gorby, Y. A., Beveridge, T. J., and Blakemore, R. P., *Journal of Bacteriology,* Vol. 170, 1988, pp. 834–841.
[12] Little, B. J., *Journal of Industrial Microbiology,* Vol. 8, 1991, pp. 213–222.
[13] Jolley, J. G., Geesey, G. G., Hankins, M. R., Wright, R. B., and Wichlacz, P. A., *Applied Surface Science,* Vol. 37, 1989, pp. 469–480.
[14] MacLean, R. J. C. and Beveridge, T. J., "Metal Binding Capacity of Bacterial Surfaces and their Ability to Form Mineralized Aggregates," *Microbial Mineral Recovery,* H. L. Ehrlich and C. L. Brierley, Eds., McGraw-Hill, New York, 1990.
[15] Ferris, F. G., Fyfe, W. S., and Beveridge, T. J., *Geology,* Vol. 10, 1988, pp. 149–152.
[16] Olowe, A. A., Bauer, Ph., Genin, J. M. R., and Guezennec, J., *Comptes Rendus,* Vol. 314, Series II, 1992, pp. 1157–1163.
[17] McNeil, M. B., "Microbiologically Influenced Corrosion of Silver in Marine Environments," *Microbiologically Influenced Corrosion and Biodegradation,* N. J. Dowling, M. W. Mittelman, and J. C. Danko, Eds., University of Tennessee Press, Knoxville, TN, 1991, pp. 8.17–8.22.
[18] Davies-Colley, R. J., Nelson, P. O., and Williamson, K. J., *Marine Chemistry,* Vol. 16, 1985, pp. 173–186.
[19] McNeil, M. B., Jones, J. M., and Little, B. J., *Corrosion,* Vol. 47, 1991, pp. 674–679.
[20] McNeil, M. B. and Little, B. J., *Corrosion,* Vol. 46, 1990, pp. 599–600.
[21] Duncan, S. J. and Ganiaris, H., "Some Sulphide Corrosion Products on Copper Alloys and Lead Alloys from London Waterfront Sites," *Recent Advances in the Conservation and Analysis of Artifacts,* J. Black, Ed., London Summer Schools Press, London, 1987.
[22] Stoffyn, P. and Buckley, D. E., "The *Titanic* 80 Years Later: Initial Observations on the Microstructure and Biogeochemistry of Corrosion Products," *Proceedings of the 50th Annual Meeting of the Electron Microscope Society of America,* San Francisco Press, San Francisco, CA, 1992.
[23] Little, B. J., "An Experimental Evaluation of Titanium's Resistance to Microbiologically Influenced Corrosion," *Corrosion 92,* Paper 173, National Association of Corrosion Engineers (NACE), Houston, TX, 1992.
[24] Wagman, D. D., Evans, W. H., Parker, V. B., Schumm, R. W., Harlow, I., Bailey, S. M., Churney, K. L., and Nuttall, R. L., *Journal of Physical and Chemical Reference Data,* Vol. 11, 1982, Supplement 2.

[25] Woods, T. L. and Garrels, R. M., *Thermodynamic Values at Low Temperature for Natural Inorganic Materials*, Oxford University Press, Oxford, 1987.
[26] Casey, W. H., *Journal of Colloid and Interface Science*, Vol. 146, 1991, pp. 586–589.
[27] Crerar, D. A. and Barnes, H. L., *Economic Geology*, Vol. 71, 1976, pp. 772–794.
[28] Shea, D. and Helz, G. R., *Geochimica et Cosmochimica Acta*, Vol. 53, 1989, pp. 229–236.
[29] Parise, J. B. and Schoonen, M., "An Extended X-Ray Fine Structure (EXAFS) Spectrographic Study of Amorphous FeS," Paper 22224, Geological Society of America, Annual Meeting, 1990.
[30] Ostwald, W., *Lehrbuch der Allgemeinen Chemie*, Engleman, Leipzig, 1897.
[31] Goldsmith, J., *Geological Magazine*, Vol. 61, 1953, pp. 539–551.
[32] Bazylinski, D. A., Garratt-Reed, A. J., Abedi, A., and Frankel, R. B., "Copper Association with Iron Sulfide Magnetosomes in a Magnetotactic Bacterium," *Archives of Microbiology*, 1992.
[33] Pourbaix, M. J. N., *Atlas of Electrochemical Equilibria in Aqueous Solutions*, 2nd Edition. Cebelcor, Brussels, Belgium, 1974. Translated from French by J. A. Franklin, National Association of Corrosion Engineers (NACE), Houston, TX, 1979.

Brenda J. Little,[1] *Patricia Wagner,*[1] *and Joanne Jones-Meehan*[2]

Sulfur Isotope Fractionation in Sulfide Corrosion Products as an Indicator for Microbiologically Influenced Corrosion (MIC)

REFERENCE: Little, B., Wagner, P., and Jones-Meehan, J., **"Sulfur Isotope Fractionation in Sulfide Corrosion Products as an Indicator for Microbiologically Influenced Corrosion (MIC),"** *Microbiologically Influenced Corrosion Testing, ASTM STP 1232,* Jeffery R. Kearns, and Brenda J. Little, Eds., American Society for Testing and Materials, Philadelphia, 1994, pp. 180–187.

ABSTRACT: Sulfur isotope fractionation was demonstrated in corrosion products resulting from the activities of sulfate-reducing bacteria within biofilms on copper surfaces. ^{32}S accumulated in corrosion products, while ^{34}S was concentrated in the culture medium due to fractionation. The accumulation of the lighter isotope was related to surface derivatization or corrosion as measured by weight loss.

KEYWORDS: sulfur isotopes, sulfate-reducing bacteria (SRB), corrosion, mass spectrometry, copper alloys, seawater, environmental scanning electron microscopy (ESEM)

Introduction

Sulfate-reducing bacteria (SRB) are responsible for microbiologically influenced corrosion (MIC) of numerous metals and alloys [*1–5*]. Obligate anaerobic SRB within biofilms can reduce sulfate at metal/biofilm interfaces in both oxygenated and anaerobic bulk media [*6,7*]. When sulfate is reduced by SRB, there is a net release of free energy used for growth and the concomitant production of large amounts of sulfide [*8*]. Sulfides react aggressively with many metals to form corrosion products.

MIC resulting from the activities of SRB does not produce any unique form of localized corrosion. Instead, pitting, crevice corrosion, dealloying, and underdeposit corrosion have been attributed to SRB. Recently, McNeil, Jones, and Little [*9*] attempted to identify mineralogical fingerprints for SRB-influenced corrosion on copper surfaces by identifying unique copper sulfide minerals formed by SRB in biofilms that do not form abiologically at standard conditions of temperature and pressure. The formation of non-adherent layers of chalcocite (Cu_2S) and the presence of hexagonal chalcocite were indicators of SRB-influenced corrosion. During sulfate reduction by SRB, the stable isotopes of sulfur (^{32}S and ^{34}S) are selectively metabolized and the sulfide is enriched in ^{32}S [*10*]. The ^{34}S isotope accumulates in the starting sulfate as the ^{32}S isotope is removed and becomes concentrated in the sulfide. Isotope fractionation by SRB has been used to interpret the origin of sulfides in modern and ancient environments, including sediments and groundwaters [*11–16*]. The

[1] Research chemist and oceanographer, respectively, Naval Resarch Laboratory, Stennis Space Center, MS 39529-5004.

[2] Microbiologist, Naval Surface Warfare Center, Silver Spring, MD 20903-5000.

authors of this paper evaluated isotope fractionation from a sulfate-rich medium by examining sulfide corrosion products produced by SRB on copper surfaces and correlating the degree of fractionation with corrosion as measured by weight loss.

Materials and Methods

Replicate strips of 90Cu:10Ni were preweighed and exposed for 3 months to two mixed cultures. These cultures contained facultative and obligate anaerobic bacteria isolated from corrosion failures and were known to contain SRB. Isolation, maintenance and identification techniques have been described elsewhere [*9*]. Three replicates were used for environmental scanning electron microscopy (ESEM) [*17*] and corrosion weight loss (ASTM Practice for Preparing, Cleaning, and Evaluating Test Specimens, G 1).

Sulfur isotope fractionation analyses were performed by Global Geochemistry (Canoga Park, CA). Three replicates were used to evaluate sulfur isotope fractionation in the corrosion products and in the growth medium. Controls were prepared with foil strips and sterile media to which no SRB were added. The foil strips were not sterilized, and control samples did develop microbial growth.

Each metal strip exposed to SRB was removed from the culture medium, rinsed with distilled water to remove residual sulfates, air dried and clipped into small pieces. The culture medium was centrifuged and the liquid medium decanted. Solid material was rinsed with distilled water, air-dried and combined with the dried foil pieces in a ceramic crucible that contained iron chips. Samples were combusted at high temperature (about 1400°C) under oxygen to convert sulfur to sulfate [*18–20*]. Sulfur concentration was analyzed as sulfate precipitated as $BaSO_4$. Quartz powder and the $BaSO_4$ precipitate were combusted at 900°C in a quartz tube to remove organic material, cooled and reheated to convert SO_4 to SO_2. SO_2 was analyzed with a dual collecting, stable isotope ratio mass spectrometer. The culture medium was treated and analyzed as above. The amount of sulfur was calculated by relating the weight of precipitated $BaSO_4$ to the starting liquid volume. Conventionally, the amplitude of each isotope is not reported individually, but a ratio is established and compared to the isotope ratios of a standard to yield a value termed $\delta\ ^{34}S$ expressed as parts per thousand (‰), as follows:

$$\delta\ ^{34}S\ ‰ = \frac{^{34}S/^{32}S \text{ sample} - {}^{34}S/^{32}S \text{ standard}}{^{34}S/^{32}S \text{ standard}} \times 1000$$

Negative δ values indicate a concentration of ^{32}S, and positive numbers indicate an accumulation of the heavier ^{34}S. The standard for the sulfur isotope is meteorite troilite (FeS).

Results

After exposure to mixed cultures containing SRB, all foils were covered with a continuous black corrosion layer (Fig. 1). Control foils exposed to identical conditions, but not inoculated with SRB, were covered with a light brown slime layer. Bacteria were distributed throughout the black corrosion layers associated with the sulfide corrosion products (Fig. 2*a*, *b*). Some cells were encrusted with sulfur-rich deposits (Fig. 3). Localized corrosion was observed under discrete deposits (Fig. 4).

Tables 1 and 2 show sulfur concentrations in the solid corrosion products and growth medium for controls and cultures of SRB. Copper foils exposed to SRB developed sulfur-rich corrosion products (4321 to 36 695 ppm sulfur), whereas the controls accumulated

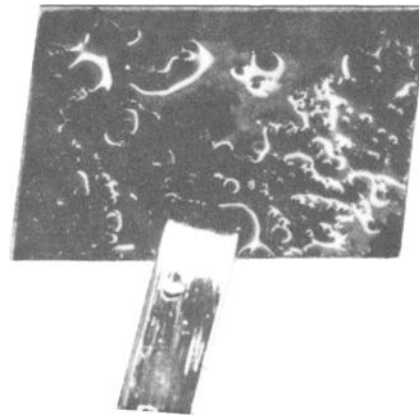

FIG. 1—*90Cu:10Ni surface colonized by SRB* ($\times 3$).

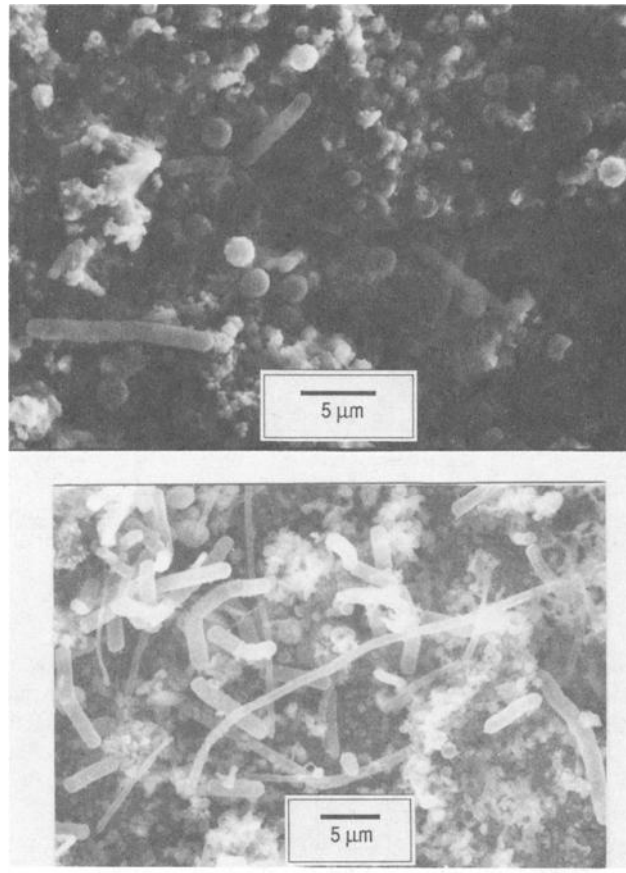

FIG. 2—*ESEM micrographs of biofilms on copper alloy foils.*

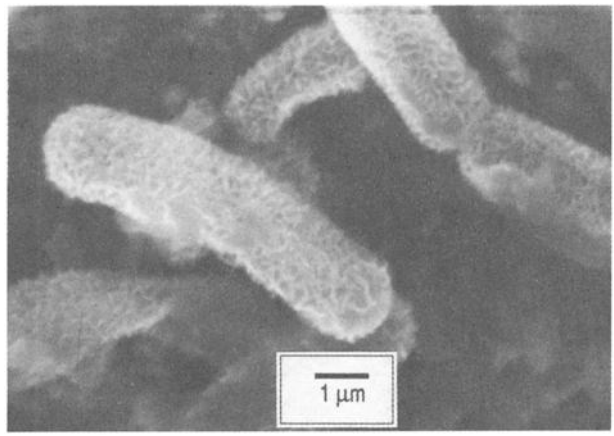

FIG. 3—*ESEM image of sulfide deposits on cell from 90Cu:10Ni in SRB culture.*

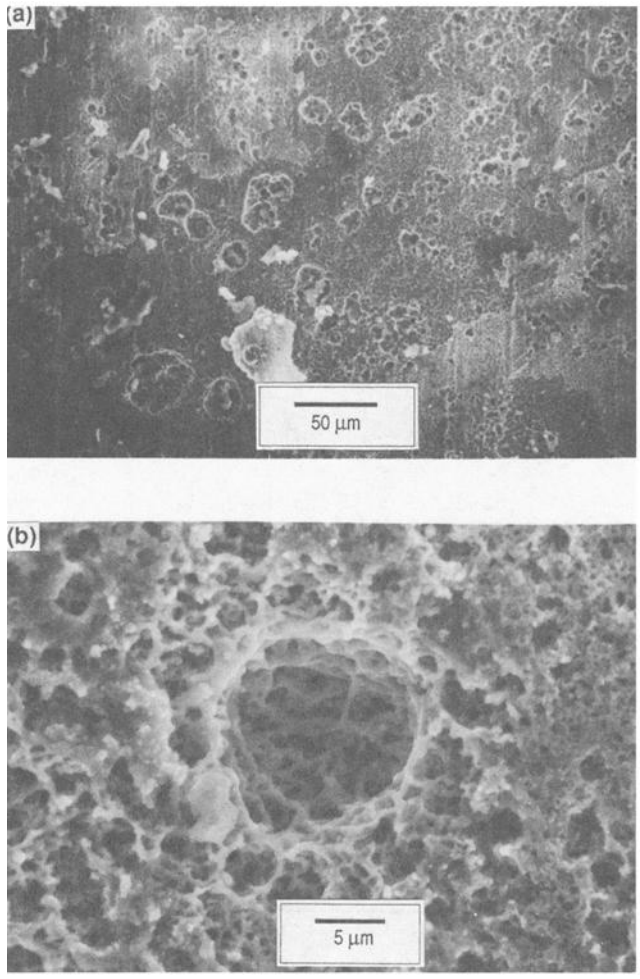

FIG. 4—*ESEM image of pits on copper foil after exposure to SRB.*

TABLE 1—*Sulfur isotope and corrosion data after three months exposure.*

Sample	Sulfur Concentration in Solid, ppm	$\delta\ ^{34}S$ in Solid, ‰	Sulfur Concentration in Medium, ppm	$\delta\ ^{34}S$ in Medium, ‰	Weight Loss $mg/mm^2 \times 10^{-3}$ for Similarly Treated Foils
Control	747	10.2	372	0.3	15.9
	900	12.3	514	0.4	30.2
	613	16.5	580	0.2	29.9
SRB Culture I	26627	−0.4	7	[a]	226.3
	36618	−1.3	20	3.7	131.7
	36695	−0.8	16	8.7	178.6
SRB Culture II	4321	0.6	20	23.8	99.4
	3371	1.5	18	25.8	227.2
	19490	−0.7	11	[a]	169.5

[a] Insufficient sulfur.

surface layers with low concentrations of sulfur (613 to 900 ppm). Similarly, sulfur was depleted in the culture media inoculated with SRB relative to the controls without SRB.

Weight loss and sulfur isotope fractionation data are also included in Tables 1 and 2. The starting sulfates in the culture medium had a $\delta\ ^{34}S = -0.88$, indicating a slight enrichment of the lighter isotope. The ^{32}S isotope accumulated in all corrosion products resulting from the activities of SRB, and the residual sulfur in the growth medium was enriched in ^{34}S. Using an F test for analysis of variance, there was a significant difference between means of $\delta\ ^{34}S$ for foils exposed to SRB and controls at the 95% confidence level. There was also a significant difference between means of weight loss for foils with SRB + NaCl compared to the controls at the 95% confidence level. There was no significant difference in weight loss for foils with SRB − NaCl compared to controls. Sample weight loss cannot be directly correlated with accumulation of ^{32}S.

TABLE 2—*Sulfur isotope and corrosion data after six months exposure.*

Sample	$\delta\ ^{34}S$ in Solid, ‰	$\delta\ ^{34}S$ in Medium, ‰	Weight Loss $mg/mm^2 \times 10^{-3}$ for Similarly Treated Foils
Control	9.8	−0.3	76.4
	13.8	0.1	95.1
	16.2	−0.3	59.7
SRB Culture I	−0.4	10.7	138.5
	−0.2	20.4	261.5
	−1.5	[a]	158.8
	−0.2	[a]	364.1
	−1.6	[a]	282.6
	−0.6	[a]	
SRB Culture II	−1.1	0.6	351.8
	−0.4	5.9	247.6
	−0.3	30.3	329.1
	−1.9	29.3	313.0
	−0.5	[a]	229.4
	−0.2	[a]	

[a] Insufficient sulfur.

Discussion

SRB are a diverse group of anaerobic bacteria that can be isolated from a variety of environments [*8,21*] including seawater [*22*], where the concentration of sulfate is typically 2 g/L. Even though the oxygen content of seawater ranges from 6 to 10 ppm, anaerobic microorganisms survive in anaerobic microniches until conditions are suitable for their growth [*23,24*]. If the aerobic respiration rate within a biofilm is greater than the oxygen diffusion rate, the metal/biofilm interface can become anaerobic and provide a niche for sulfide production by SRB [*25*].

The impact of sulfides on the corrosion of copper alloys has received a considerable amount of attention. Little et al. [*26,27*] published several reports documenting localized corrosion of copper alloys by SRB in estuarine environments. Others reported the failure of copper alloys in polluted seawater containing waterborne sulfides that stimulate pitting and stress corrosion cracking [*28*]. Copper alloys suffer accelerated corrosion attack in seawater containing 0.01 ppm sulfide after 1-day exposure [*29*]. A porous layer of cuprous sulfide with the general stoichiometry Cu_2-xS, $O < x < 1$ forms in the presence of sulfide ions [*30*]. Copper ions migrate through the layer, react with more sulfide, and produce a thick, black scale.

It has been argued that if the copper sulfide layer were djurelite ($Cu_{1.96}S$), the sulfide layer would be protective [*31*]. Even if such a sulfide film were technically passivating, the film's mechanical stability is so poor as to be useless for corrosion protection. In the presence of turbulence, the loosely adherent sulfide film is removed, exposing a fresh copper surface to react with sulfide ions. In the presence of oxygen, the possible corrosion reactions in a copper sulfide system are extremely complex because of the large number of stable copper sulfides [*32*], their differing electrical conductivities, and catalytic effects. Transformations between sulfides or of sulfides to oxides result in changes in volume that weaken the attachment scale and oxide subscale, leading to spalling. Bared areas repassivate forming cuprous oxide. The lack of tenacity of the copper sulfide corrosion products was evident during sample manipulation.

Most scanning electron microscopy (SEM) images of SRB on copper surfaces have indicated a monolayer of cells overlaying a sulfur-rich layer. Transmission electron microscopy has been used to demonstrate that bacteria were intimately associated with corrosion products and that on copper-containing surfaces, the bacteria were found between alternate layers of corrosion products and attached to base metal [*33*]. ESEM image presented in Fig. 2 demonstrates that SRB were distributed through the sulfur-rich corrosion layers. The ESEM is capable of accommodating wet biological material without dehydration and metal coating. Artifacts introduced into SRB biofilms as a result of fixation for SEM have been reviewed by Little et al. [*17*].

During abiotic chemical reduction of sulfate, a kinetic isotope effect results in a predominance of ^{32}S in the sulfide [*34*]. Bacterial sulfate reduction results in $\delta\ ^{34}S$ values greater than that predicted by the chemical kinetic isotope effect [*20*]. Enhanced isotope fractionation has been explained in terms of additive effects associated with two or more enzymes in the microbial sulfate reduction pathway [*35*]. Isotopic fractionation during sulfate reduction is inversely proportional to the rate of reduction when lactate and ethanol are used as electron donors and is directly proportional when molecular hydrogen is the electron donor [*18*]. Both temperature and sulfate concentration influence the rate of reduction and therefore the extent of fractionation, but the impact of sulfate concentration is reportedly minor [*20*]. The most negative values for $\delta\ ^{34}S$ have been reported for microbial reductions with slow reaction rates when the sulfide can be trapped and analyzed immediately after formation.[3]

[3] Isaac R. Kaplan, Global Geochemistry, Canoga Park, CA, personal communication, 1991.

The δ ^{34}S values reported in this study are small by comparison to many of the literature values for microbiological fractionation and may reflect fast conversion rates and the inability to trap the sulfide as it forms. Sulfide corrosion products were allowed to form over 3- and 6-month periods. During that time the isotope ratio of the starting medium became enhanced in the heavier isotope so that further sulfate reductions would not have the original pool of isotopes from which to select. With aging and further sulfate reductions, one would expect the δ ^{34}S values of the sulfide corrosion products and the medium to reach equilibrium. For example, the consequence of biological sulfate reduction through geological time has been to transfer ^{32}S to marine sediments and to leave the seawater sulfate enriched in ^{34}S by 20‰ relative to meteoritic sulfur [*18*].

Conclusions

Sulfur isotope fractionation was demonstrated in corrosion products resulting from the activities of SRB on copper surfaces. Accumulation of ^{32}S in sulfide corrosion products may be a useful indicator of MIC.

Acknowledgments

This work was supported by the Office of Naval Research, Program Element 61153N, through the NOARL Defense Research Sciences Program. Work performed at NAVSWC was supported by Capt. Steve Synder, ONR Code 1141 MB. NOARL Contribution number PR92:022:333.

References

[*1*] Alanis, I., Berardo, L., De Cristofaro, N., Moina, C., and Valentini, C., "A Case of Localized Corrosion in Underground Brass Pipes," in *Biologically Induced Corrosion*, S. C. Dexter, Ed., National Association of Corrosion Engineers, Houston, Texas, 1986, pp. 102–108.

[*2*] Gouda, V. K., Banat, M. I., Riad, T. W., and Mansour, S. I., "Microbial-Induced Corrosion of Monel 400 in Seawater," in *Proceedings Corrosion '90*, Paper No. 90107, National Association of Corrosion Engineers, Houston, Texas, 1990.

[*3*] Hamilton, W. A., "Sulphate-Reducing Bacteria and Their Role in Biocorrosion, in *Biofouling and Biocorrosion in Industrial Water Systems*, H.-C. Flemming, G. G. Geesey, Eds., Springer-Verlag, Berlin, 1990, pp. 187–193.

[*4*] Little, B., Wagner, P., Ray, R., and McNeil, M., "Microbiologically Influenced Corrosion in Copper and Nickel Seawater Piping Systems," *Marine Technology Society Journal*, 1990, Vol. 24, No. 3, pp. 10–17.

[*5*] Pope, D. H., "A Study of Microbiologically Influenced Corrosion in Nuclear Power Plants and a Practical Guide for Countermeasures," Electric Power Research Institute, Palo Alto, CA, 1986.

[*6*] Hamilton, W. A. and Maxwell, S., "Biological and Corrosion Activities of Sulphate-Reducing Bacteria within Natural Biofilms," in *Biological Induced Corrosion*, S. C. Dexter, Ed., National Association of Corrosion Engineers, Houston, Texas, 1986, pp. 131–136.

[*7*] Rosser, H. R. and Hamilton, W. A., "Simple Assay for Accurate Determination of [^{35}S] Sulfate Reduction Activity," *Applied and Environmental Microbiology*, 1983, Vol. 45, pp. 1956–1959.

[*8*] Postgate, J. R., "The Sulphate-Reducing Bacteria," Cambridge University Press, Great Britain, 1979.

[*9*] McNeil, M. B., Jones, J. M., and Little, B. J., "Production of Sulfide Minerals by Sulfate-Reducing Bacteria During Microbiologically Influenced Corrosion of Copper," *Corrosion*, 1991, Vol. 47, pp. 674–677.

[*10*] Chambers, L. A. and Trudinger, P. A., "Microbiological Fractionation of Stable Sulfur Isotopes: A Review and Critique," *Geomicrobiology Journal*, 1979, Vol. 1, pp. 249–293.

[*11*] Dickman, M., Thode, H. G., Rao, S., and Anderson, R., "Downcore Sulphur Isotope Ratios and Diatom Inferred pH in Artificially Acidified Canadian Shield Lake," in *Environmental Pollution*, J. P. Dempster and W. J. Manning, Eds., Elsevier Applied Science, England, 1988, pp. 265–288.

[12] Dockins, W. S., Olson, G. J., McFeters, G. A., Turbak, S. C., and Lee, R. W., *Sulfate Reduction in Ground Water of Southeastern Montana,* USGS/WRD/WRI-80/040, 1980, pp. 1–18.
[13] Kaplan, I. R., Sweeney, R. E., and Nissenbaum, A., "Sulfur Isotope Studies on Red Sea Geothermal Brines and Sediments," in *Hot Brines and Recent Heavy Metal Deposits in the Red Sea,* E. T. Degens and D. A. Ross, Eds., Springer-Verlag, New York, 1969, pp. 474–498.
[14] Lyalikova, N. N., "Role of Bacteria in Oxidation of Sulfide Ores in Copper-Nickel Deposits of Kola Peninsula," *Mikrobiologiya,* 1961, Vol. 30, No. 1, pp. 135–139.
[15] Sweeney, R. E. and Kaplan, I. R., "Stable Isotope Composition of Dissolved Sulfate and Hydrogen Sulfide in the Black Sea," *Marine Chemistry,* 1980, Vol. 9, pp. 145–152.
[16] Vaynshteyn, M. B., Tokarev, V. G., Shakola, V. A., Yu Lein, A., and Ivanov, M. V., "The Geochemical Activity of Sulfate-Reducing Bacteria in Sediments in the Western Part of the Black Sea," *Geokhimiya,* 1985, Vol. 7, pp. 1032–1044.
[17] Little, B., Wagner, P., and Ray, R., "Biofilms: An ESEM Evaluation of Artifacts Introduced During SEM Preparation," *Journal of Industrial Microbiology,* 1991, Vol. 8, pp. 213–222.
[18] Kaplan, I. R., "Stable Isotopes as a Guide to Biogeochemical Processes," *Proceedings Royal Society of London B.,* 1975, Vol. 189, pp. 183–211.
[19] Kaplan, I. R. and Rafter, T. R., "Fractionation of Stable Isotopes of Sulfur by Thiobacilli," *Science,* 1958, Vol. 127, pp. 517–518.
[20] Kaplan, I. R. and Rittenberg, S. C., "Microbiological Fractionation of Sulphur Isotopes," *Journal of General Microbiology,* 1964, Vol. 34, pp. 195–212.
[21] Pfennig, N., Widdel, F., and Truper, H. G., "The Dissimulatory Sulfate-Reducing Bacteria," in *The Prokaryotes: A Handbook on Habitats,* M. P. Starr, et al., Eds., Springer-Verlag, New York, 1981, pp. 926–940.
[22] Battersby, B. L., "Sulphate-Reducing Bacteria," in *Methods in Aquatic Bacteriology,* B. Austin, Ed., John Wiley and Sons, New York, 1988, pp. 269–299.
[23] Costerton, J. W. and Geesey, G. G., "The Microbial Ecology of Surface Colonization and of Consequent Corrosion," in *Biologically Induced Corrosion,* S. C. Dexter, Ed., National Association of Corrosion Engineers (NACE), Houston, Texas, 1986, pp. 223–232.
[24] Staffeldt, E. E. and Kohler, D. A., "Assessment of Corrosion Products Removed from 'La Fortuna'," *Petrolia e Ambiente,* Punta del Mar, Venezia, 1973, pp. 163–170.
[25] Little, B., Ray, R., Wagner, P., Lewandowski, Z., Lee, W. C., Characklis, W. G., and Mansfeld, F., "Electrochemical Behavior of Stainless Steels in Natural Seawater," *Corrosion/90,* Paper No. 150, National Association of Corrosion Engineers, Houston, Texas, 1990.
[26] Little, B., Wagner, P., and Jacobus, J., "The Impact of Sulfate-Reducing Bacteria on Welded Copper-Nickel Seawater Piping Systems." *Materials Performance,* 1988, Vol. 27, No. 8, pp. 57–61.
[27] Little, B., Wagner, P., Jacobus, J., and Janus, L., "Evaluation of Microbiologically Induced Corrosion in an Estuary," *Estuaries,* 1989, Vol. 12, No. 3, pp. 138–141.
[28] Rowlands, J. C., "Corrosion of Tube and Pipe Alloys Due to Polluted Seawater," *Journal of Applied Chemistry,* 1965, Vol. 15, pp. 57–63.
[29] Gudas, J. P. and Hack, H. P., "Sulfide-Induced Corrosion of Copper-Nickel Alloys," *Corrosion,* 1979, Vol. 35, pp. 67–73.
[30] Syrett, B. C., "The Mechanism of Accelerated Corrosion of Copper-Nickel Alloys in Sulfide Polluted Seawater," *Corrosion/80,* Paper No. 33, National Association of Corrosion Engineers, Houston, Texas, 1980.
[31] North, N. A. and MacLeod, I. D., "Corrosion of Metals," in *Conservation of Archeological Object,* C. Pearson, Ed., Butterworths, London, 1987, pp. 68–98.
[32] Ribbe, P. H., Ed., "Sulfide Mineralogy," *Mineralogical Society of America,* Washington, D.C., 1976.
[33] Blunn, G., "Biological Fouling of Copper and Copper Alloys," in *Biodeterioration VI,* CAB Int., Slough, UK, 1986, pp. 567–575.
[34] Harrison, A. G. and Thode, H. G., "The Kinetic Isotope Effect in the Chemical Reduction of Sulphate," *Transactions of the Faraday Society,* 1957, Vol. 53, pp. 1648–1651.
[35] Rees, C. E., "A Steady State Model for Sulphur Isotope Fractionation in Bacterial Reduction Processes," *Geochimica et Cosmochimica Acta,* 1973, Vol. 37, pp. 1141–1162.

Gerrit Voordouw,[1] *Thomas R. Jack,*[2] *Julia M. Foght,*[3] *Phillip M. Fedorak,*[3] *and Donald W. S. Westlake*[3]

Application of Reverse Sample Genome Probing to the Identification of Sulfate-Reducing Bacteria

REFERENCE: Voordouw, G., Jack, T. R., Foght, J. M., Fedorak, P. M., and Westlake, D. W. S., **"Application of Reverse Sample Genome Probing to the Identification of Sulfate-Reducing Bacteria,"** *Microbiologically Influenced Corrosion (MIC) Testing, ASTM STP 1232,* Jeffery R. Kearns and Brenda J. Little, Eds., American Society for Testing and Materials, Philadelphia, 1994, pp. 188–199.

ABSTRACT: Reverse sample genome probing (RSGP) has been used for the analysis of sulfate-reducing bacteria (SRB) in samples obtained from heavy oil operations in the Wainwright/Wildmere fields in Western Canada. These reservoirs are shallow (600 m), roughly 25°C, and host a 6% brine. Master filters containing up to 35 independently hybridizing SRB standards were used for analysis of DNA prepared from the samples. The standards represented the diversity of SRB that is now recognized, for example, SRB using lactate, ethanol, benzoate, propionate, decanoate, or acetate as their carbon and energy source. These had previously been isolated from Alberta oil and gas field environments either by single colony purification or by liquid culture enrichment. Twenty four sites were analyzed by RSGP following liquid culture enrichment of SRB on media with one of these six carbon sources. Combination of the results of this method for all enrichments indicated on average the presence of six different SRB at each site. No significant differences were observed in the types of SRB cultured from the two fields. Also, the same SRB standards were recovered by growth of either sessile or planktonic samples. Some oil field production waters were analyzed by direct extraction of DNA from the bacterial population and RSGP analysis. This indicated that the natural population is dominated by lactate- and benzoate-utilizers. Oil fields therefore harbor a variety of SRB. Biocide treatment schemes should ideally take into account this variety and be based on identification of the SRB involved, their known effects on field operations, and their documented biocide sensitivity. In this scheme, RSGP can help in the rapid identification of SRB and others, for example, acid-producing bacteria associated with corrosion.

KEYWORDS: sulfate-reducing bacteria, corrosion, DNA probe, hydrogenase, oil and gas industry, microbial identification techniques

Introduction

Sulfate-reducing bacteria (SRB) are held responsible for a number of problems in the oil and gas industry, particularly corrosion of steel works and souring of fields. Their metabolic activity may thus result in the physical deterioration of equipment and reduction of the economic value of the fields [*1*].

[1] Professor of biochemistry, The University of Calgary, Department of Biological Sciences, Calgary, Alberta, T2N 1N4.

[2] Research supervisor, Nova Husky Research Corporation, 2928 16th Street, N. E., Calgary, Alberta, T2E 7K7.

[3] Research associate, professor, and professor emeritus, respectively, University of Alberta, Department of Microbiology, Edmonton, Alberta, T6G 2E9.

The classical assay for the presence of SRB is a growth-based metabolic activity test in which samples are injected into anaerobic medium, containing lactate as the carbon and energy source and sulfate as the respiratory substrate (lactate-sulfate medium). This test indicates the presence of lactate-utilizing SRB by the formation of black particles of iron sulfide. Use of a dilution series allows the number of these bacteria present in the sample to be estimated by the most probable number method. SRB detected with this method could belong to six different genera [2], the best known being *Desulfovibrio*.

However, some SRB (most members of the genus *Desulfobacter* and some of the genera *Desulfobacterium, Desulfonema,* and *Desulfotomaculum*) are not capable of metabolizing lactate. Cord-Ruwisch et al. [3] showed that these bacteria were present in higher numbers than the lactate-utilizing SRB in an oil treater. They would therefore be overlooked with the lactate-sulfate test. The potential metabolic variety among SRB is even greater, as demonstrated by Aeckersberg et al. [4], who have recently isolated a sulfate-reducing bacterium capable of growing anaerobically on saturated hydrocarbons. This strain did not grow on lactate, ethanol, H_2, or alkanes with chains shorter than C_{12}. The evaluation of the presence of these bacteria would seem to be particularly relevant to the estimation of the potential for oil and gas field souring.

Another problem with growth-based metabolic activity or plate tests is that their evaluation may take a long incubation time, for example, several weeks. Attempts have therefore been made to design rapid assays for the presence of SRB. Ideally, the assay should be sufficiently simple to be carried out in the field and yield results in a short time, for example, in less than one h. When these criteria are met, and if the results truly indicate the potential for microbiologically influenced corrosion, then the assay results can serve as a factor in instant decision making on remedial procedures, like the application of biocides. Two systems have been developed. The first relies on the detection of the enzyme hydrogenase, considered a key enzyme in anaerobic microbial corrosion [1]. In this assay, color formation by hydrogenase-catalyzed reduction of a redox dye serves as a measure for the presence of SRB [5]. The second determines the presence of a key enzyme in sulfide formation, adenosine-5'-phosphosulfate (APS) reductase, with an immunological procedure [6].

Although both tests may be very useful they are not without disadvantages. For example, not all SRB have hydrogenase activity and the structure of the enzyme APS reductase of a single species may not be sufficiently conserved to allow its detection with antibodies generated against this APS reductase in all other SRB [7]. We have been working since 1988 on the development of DNA probes for the detection of SRB in oil and gas fields and other environments. Although field-based DNA probe techniques are currently not available, these assays do offer the advantage of being both rapid (assays can be completed within 4 days) and of allowing monitoring at different levels (single species, single genus, whole community). As an example of a single genus assay, we discovered that of three different hydrogenase genes found in SRB of the genus *Desulfovibrio,* the genes for the [NiFe] hydrogenase were found in all of 22 members of the genus tested [8]. The DNA containing these genes was used as a genus-specific probe, and the presence of at least five different *Desulfovibrio* species was demonstrated in oil field samples, following growth on lactate-sulfate medium [8].

The determination of the nucleotide sequence of 16S rRNA (the ribosomal RNA of the small subunit of the ribosome, present in all bacteria and other life forms) also offers a powerful system for bacterial classification. Sequences can be linked in phylogenetic trees, which provide a measure for the genetic and evolutionary relationships between species in the tree. Determination of 16S rRNA sequences for SRB has not only led to the generation of a phylogenetic tree defining eight distinct genera [2,9], but has also provided the information necessary to design genus-specific oligonucleotide probes. As a result, fluorescent

oligonucleotide probes targeted against (1) all eubacteria, (2) *Desulfovibrio desulfuricans* and SRB of the genus *Desulfotomaculum,* (3) SRB of the genus *Desulfobacter,* or (4) *Desulfovibrio desulfuricans* and SRB of the genus *Desulfobacter,* are now available [*10*].

Fluorescent oligonucleotide probes have been used successfully to elucidate the position of selected SRB in biofilms by microscopy [*11*]. A potential disadvantage of both the hydrogenase- and the 16S rRNA-directed probes is that they target only one species or genus in the entire community.

In searching for a method in which the presence of multiple species can be assayed simultaneously, we discovered (1) that the total genomic DNA of a bacterial species (referred to here on as a "standard," different standards being defined as bacterial species with genomes that do not cross-hybridize) can be used as a sensitive specific probe for its presence in a sample and (2) that a large number of standards can be assayed if the hybridization process is reversed [*12*], as outlined in Fig. 1. Thus, in this technique, known as reverse sample genome probing (RSGP), DNA isolated from a sample is not spotted on a filter for analysis by hybridization with labeled DNA from a standard, as in conventional gene probe assays. Instead, a filter containing denatured DNAs from a number of standards in a known configuration (the "master filter"), is hybridized with labeled sample DNA and the standards prevailing in the sample are determined in a single step. It is advisable to spot the denatured, but unlabeled, sample DNA on the master filter just prior to the hybridization process. This sample DNA serves as a positive control for two reasons: (1) lack of hybridization of any of the standards on the master filter with the labeled reverse sample genome probe with strong self-hybridization to the sample DNA indicates that the standards spotted on the filter are not representative for those present in the sample, whereas (2) absence of self-hybridization can indicate failed labeling of sample DNA, although another reason for failed self-hybridization can be that the sample DNA is of exceeding complexity (contains se-

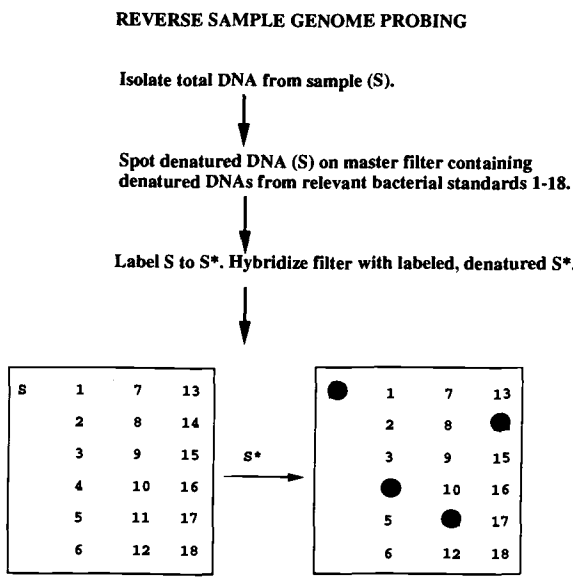

FIG. 1—*Principle of RSGP. The master filter containing denatured DNAs from 18 standards (1 to 18), as well as the sample (S) is hybridized with the labeled, denatured reverse sample genome probe (S*). Following development to detect the hybridization, it appears that standards 4, 11, and 14 are present in the sample.*

quences from many different standards). This situation can arise especially if DNA isolated directly from the environment, without prior liquid enrichment, is analyzed.

RSGP was shown to be a useful method for the identification of SRB from oil fields in the Province of Alberta, Canada [*12*], which appear to harbor two distinct communities depending on the field salinity [*13*].

In this paper, the microbial composition in the Wainwright and Wildmere oil fields in Alberta, as determined by RSGP with growth on enrichment media, is analyzed in more detail. In addition, the possibility of analyzing microbial communities by RSGP without enrichment is discussed.

Materials and Methods

Biochemical Reagents

Enzymes used for primer extension labeling were obtained from Pharmacia LKB Biotechnology, Inc. (Baie d'Urfe, Quebec, Canada). The Hybond-N hybridization transfer membrane was from Amersham Canada Ltd., (Oakville, Ontario, Canada). Radiolabeled [α-^{32}P]dCTP (3000 Ci/mmol, 10 mCi/mL) was from ICN Biomedicals Canada Ltd. (St-Laurent, Quebec, Canada). Random hexadeoxyoligonucleotides were obtained from the DNA Synthesis Laboratory of The University of Calgary. Reagent grade chemicals were purchased from either Fisher Scientific Canada Ltd. (Edmonton, Alberta, Canada) or Sigma Chemical Co. (St. Louis, MO).

Collection of Samples

Sites in the Wainwright and Wildmere fields in Alberta from which samples were collected are indicated in Table 1. These reservoirs are shallow (600 m), roughly 25°C, and host a 6% brine. Oil is recovered by water flooding. Several production units, consisting of a free water knockout and a water plant, were functioning in the separation of the oil-water mixture. The produced water was reinjected into the field. The truckpit received oil-water mixtures from different field locations. Sessile samples were taken from a plug surface and planktonic samples were taken directly from the fluid present at the site (Table 1). Sampling methods have been described elsewhere [*12,13*]. It should be noted that some of the sites were revisited (Table 1, for example, WW1 and WW15). The actual number of sites from which samples were taken is thus smaller than 24. Nevertheless, the terms site and sample will be used interchangeably in the sections below.

Liquid Enrichment of SRB

Liquid SRB enrichment cultures grown on media described by Pfennig et al. [*14*], using lactate, ethanol, benzoate, decanoate, propionate, or acetate as the carbon source at 22, 30 or 35°C. Usually, 7.5 mL of the sample was used to inoculate a serum bottle with 75 mL of Pfennig's medium. The temperature chosen for incubation reflected that of the sample at the time of collection (Table 1). The salinity of the medium was likewise adjusted to reflect that of the sample (Table 1). One of two salinities were chosen: saline (s), 20 g of NaCl and 3 g of $MgCl_2$ per liter or, brackish (b), 7 g of NaCl and 1.2 g of $MgCl_2$ per liter. These liquid enrichment cultures were used either for isolation of DNA or stored, as described elsewhere [*13*]. SRB standards were named according to the carbon source used for their first isolation and an identifying number, for example, *Lac*6 is standard 6 isolated on lactate. The names used in Tables 2 and 3 represent the same standards as in earlier works [*12,13*].

TABLE 1—*Survey of sites in either the Wainwright or Wildmere fields from which samples were taken for SRB enrichment and subsequent RSGP analysis. A total of 24 sites were sampled.*

Field	Site[a]	Description	Year[b]	Type[c]	Salinity[d]	Temperature, °C[e]
Wainwright	WW1	waterplant 13	1989	p	s	30
Wainwright	WW2	waterplant 13	1989	s	s	30
Wainwright	WW3	waterplant truckpit	1989	p	s	30
Wainwright	WW4	waterplant	1989	s	s	30
Wainwright	WW5	truckpit	1989	p	s	30
Wainwright	WW6	waterplant 1	1989	s	s	30
Wainwright	WW7	waterplant 20	1989	p	s	30
Wainwright	WW8	waterplant 28	1989	s	s	30
Wildmere	WM10	lower waterplant	1989	s	s	30
Wainwright	WW11	waterplant 20	1990	p	s	30
Wainwright	WW12	waterplant 20	1990	s	s	30
Wainwright	WW13	truckpit	1990	p	s	30
Wainwright	WW14	waterplant truckpit	1990	p	s	30
Wainwright	WW15	waterplant 13	1990	p	s	30
Wainwright	WW16	waterplant 13	1990	s	s	30
Wainwright	WW17	waterplant 1	1990	p	s	30
Wainwright	WW18	waterplant 28	1990	p	s	30
Wainwright	WW19	waterplant 6	1990	p	s	30
Wildmere	WM20	lower waterplant	1990	s	b	22
Wildmere	WM21	washtank	1990	s	b	22
Wainwright	WW22	waterplant truckpit	1990	s	b	22
Wainwright	WW23	washtank truckpit	1990	s	b	22
Wainwright	WW24	waterplant 20	1990	s	b	22

[a] The same site codes are used in Table 3.
[b] Year in which the sample was collected.
[c] Sample type, either planktonic (p) or sessile (s).
[d] Salinity used for sample cultivation, either saline (s) or brackish (b).
[e] Temperature used for cultivation of the sample.

Colony Purification of SRB

The liquid enrichment cultures were used as source for the colony purification of SRB standards. Colony purification of 10 of the 35 standards has so far been achieved [*12,13*]. Of the remaining 25 standards, 2 were type cultures, 14 were stable liquid cultures, while the remaining 9 were unstable liquid cultures [*13*]. The status of each standard is indicated in Table 2. Most of these standards have been further characterized with molecular biological techniques; Southern blot hybridization has indicated specific hybridization patterns with 16S rRNA and in some cases with the [NiFe] hydrogenase gene probe [*13*].

DNA Isolation and Preparation of Master Filters

DNA was extracted and purified from cells collected from liquid enrichment cultures or from liquid cultures of the colony purified standards, as described elsewhere [*8,12,13*]. The DNA preparations were dissolved to a concentration of 1 to 1000 ng/μL, as determined fluorimetrically [*12*], in 10 mM Tris/HCl, 0.1 mM EDTA pH 8 (TE). Master filters were prepared by spotting 2 μL volumes of heat denatured DNAs at 10 ng/μL in a known pattern on Hybond-N filter membrane. DNAs were covalently linked to the filters by irradiation with ultraviolet light [*13*].

TABLE 2—*Number of observations of 35 SRB standards in liquid culture enrichments from both the Wainwright and Wildmere fields with different carbon sources.*

Carbon Source:		Lactate	Ethanol	Benzoate	Decanoate	Propionate	Acetate	Total
Standard[a]	Status[b]							
*Lac*1,2[c]	CP	2	2	...	...	1	...	5
*Lac*3	TC	4	1	...	...	...	1	6
*Lac*4	CP	9	12	...	...	2	...	23
*Lac*5	CP	16	11	...	...	2	1	30
*Lac*6	CP	7	14	1	...	8	4	34
*Lac*7	CP	...	1	...	...	...	...	1
*Lac*8	--	...	...	...	...	...	...	...
*Lac*10	CP	4	6	...	1	2	2	15
*Lac*12	LC	3	1	...	...	1	...	5
*Lac*15	CP	...	...	1	...	...	...	1
*Lac*17	CP	...	...	...	...	...	...	...
*Lac*21	CP	...	1	...	...	1	...	2
*Eth*2	--	...	...	...	...	3	...	3
*Eth*3	LC	5	6	...	...	...	...	11
*Ben*1	LC	...	9	20	4	7	13	53
*Ben*3	--	...	...	...	...	4	...	4
*Ben*4	--	...	3	1	...	10	3	17
*Ben*6	--	...	...	...	...	2	1	3
*Dec*1	LC	...	1	3	8	2	1	15
*Dec*3	LC	...	...	...	6	...	...	6
*Dec*4	LC	...	...	...	...	...	...	...
*Dec*6	LC	...	...	...	...	...	...	...
*Dec*7	--	...	...	...	...	1	...	1
*Dec*8	--	...	...	...	...	2	...	2
*Pro*1	LC	...	1	1	1	8	3	14
*Pro*4	CP	...	...	1	...	8	...	9
*Pro*5	LC	...	...	...	...	1	...	1
*Pro*7	--	...	...	...	...	1	...	1
*Pro*10	LC	...	...	...	...	...	...	...
*Pro*11	LC	...	...	...	...	1	...	1
*Pro*12	LC	...	1	2	...	3	...	6
*Ace*1	LC	2	3	4	4	1	11	25
*Ace*3	TC	1	1	...	4	...	5	11
*Ace*4	--	1	...	...	...	...	3	4
*Ace*5	LC	...	...	...	...	1	1	2
Total		54	74	34	28	72	49	311

[a] Standards are named by the first three letters of the carbon source used for their first isolation and an identifying number.

[b] The status is either colony purified (CP), type culture (TC), stable liquid culture (LC), or unstable liquid culture (--).

[c] *Lac*1 and *Lac*2 are variants of the same genotype *D. vulgaris* subspecies *oxamicus* Monticello. They are referred to as a single standard *Lac*1,2, because their genomes strongly crosshybridize.

DNA Labeling for RSGP Analysis

As a first step in the analysis, 2 μL of 10 ng/μL of the denatured sample DNA preparation to be analyzed (Fig. 1, S) was spotted on the master filter to provide a positive hybridization control. Reverse sample genome probes were made by primer extension for which 6 μL of denatured sample DNA solution, 6 μL of primer extension mix, 2 μL of Klenow polymerase

TABLE 3—*Number of observations of 35 SRB standards in samples obtained from the sites listed in*

Field:		Wainwright											
	Number:[a]	4	3	13	5	10	3	7	4	5	6	7	7
	Site:	WW1	WW2	WW3	WW4	WW5	WW6	WW7	WW8	WW11	WW12	WW13	WW14
Standard													
*Lac*1,2		1	...	...	...	...	...	1	1	...	...	...	...
*Lac*3		...	...	...	...	...	...	...	1	1	...	...	...
*Lac*4		2	...	2	2	1	1	2	1	2	...	1	...
*Lac*5		3	2	8	2	4	...	3	...	...	...	1	...
*Lac*6		...	...	...	1	...	1	...	2	3	3	3	2
*Lac*7		...	...	...	...	...	1	...	...	...	...	...	...
*Lac*8		...	...	...	...	...	...	...	...	...	...	...	...
*Lac*10		1	...	1	2	1	...	1	3	...	...	...	...
*Lac*12		...	...	...	...	...	...	...	...	...	...	...	...
*Lac*15		...	...	...	...	...	...	...	...	...	...	...	...
*Lac*17		...	...	...	...	...	...	...	...	...	...	...	...
*Lac*21		...	...	...	...	...	...	...	...	...	...	...	...
*Eth*2		...	...	...	...	...	...	...	...	...	...	...	...
*Eth*3		...	...	...	...	...	2	...	...	1	2	...	...
*Ben*1		1	1	3	3	3	2	4	1	4	2	1	2
*Ben*3		...	...	...	...	1	...	...	...	...	...	...	...
*Ben*4		...	...	1	1	3	...	...	...	...	...	...	...
*Ben*6		...	...	...	...	...	...	...	...	...	...	...	...
*Dec*1		...	...	...	...	...	...	...	...	3	1	...	...
*Dec*3		...	...	1	...	1	...	...	...	...	...	...	1
*Dec*4		...	...	...	...	...	...	...	...	...	...	...	...
*Dec*6		...	...	...	...	...	...	...	...	...	...	...	...
*Dec*7		...	...	...	...	...	...	...	...	...	...	...	...
*Dec*8		...	...	...	...	...	...	...	...	...	...	...	...
*Pro*1		...	...	...	...	3	...	1	...	3	...	...	...
*Pro*4		...	...	...	...	...	...	...	...	...	1	1	1
*Pro*5		...	...	...	...	...	...	...	...	...	...	...	...
*Pro*7		...	...	...	...	...	...	...	...	...	...	...	...
*Pro*10		...	...	...	...	...	...	...	...	...	...	...	...
*Pro*11		...	...	...	...	...	...	...	...	...	...	...	...
*Pro*12		...	...	2	1	2	...	...	...	...	...	...	...
*Ace*1		...	...	...	...	...	...	3	...	...	3	5	4
*Ace*3		...	...	...	...	...	...	...	...	...	2	3	...
*Ace*4		...	...	...	...	...	...	...	...	...	...	1	1
*Ace*5		...	...	...	...	...	...	...	...	...	...	...	...
Total[a]		8	3	18	12	19	7	15	9	17	14	16	11
Variety[b]		5	2	7	7	9	5	7	6	7	7	8	6

[a] The number of RSGP assays performed on a sample is indicated.
[b] The total number of identifications made is given.
[c] The variety indicates the number of different SRB standards in the sample.

(2 units/μL), 2 μL of [α-^{32}P]dCTP (3000 Ci/mmol, 10 mCi/mL) and 14 μL of H_2O were mixed in a 1.5 mL microcentrifuge tube [*13*]. The primer extension reaction was allowed to proceed for 3 to 5 h at 22°C after which the probes were boiled and added to the prehybridized master filters. Prehybridization, hybridization, and washing of the filters were done with the high stringency procedure described before [*12,13*]. The filters were then dried and subjected to autoradiography.

RSGP Analysis Without Growth

The feasibility of analyzing DNA preparations directly isolated from injection water samples was evaluated. Samples of ~1L were collected and subjected to centrifugation for 10

Table 1. SRB were identified by RSGP following liquid culture enrichment or isolation of single colonies.

Wainwright										Wildmere				
11 WW15	7 WW16	8 WW17	10 WW18	6 WW19	6 WW22	6 WW23	3 WW24	131 Total	Total (%)	12 WM10	4 WM20	5 WM21	21 Total	Total (%)
...	1	...	...	1	...	...	...	5	1.9	...	...	...	...	...
...	...	...	...	...	1	1	1	5	1.9	...	...	1	1	2.4
...	1	1	1	1	1	1	...	20	7.4	1	...	2	3	7.1
...	...	...	...	...	...	...	...	23	8.6	5	...	2	7	16.7
3	2	3	5	2	1	1	1	33	12.3	...	1	...	1	2.4
...	...	...	...	...	...	...	...	1	0.4	...	...	...	...	...
...	...	...	...	...	...	...	...	...	...	...	...	...	...	...
...	...	...	...	...	1	...	...	10	3.7	4	1	...	5	11.9
...	...	1	1	...	1	1	...	4	1.5	...	...	1	1	2.4
...	...	...	...	...	...	...	...	...	...	...	...	1	1	2.4
...	...	...	...	...	...	...	...	...	...	...	...	...	...	...
...	...	1	1	...	...	...	...	2	0.7	...	...	...	...	...
...	...	1	...	...	...	...	...	1	0.4	1	1	...	2	4.8
1	1	3	...	1	...	...	...	11	4.1	...	...	...	...	...
3	2	3	3	1	4	4	1	48	17.8	3	1	1	5	11.9
...	...	1	...	...	...	...	1	3	1.1	...	...	1	1	2.4
1	...	...	...	...	1	2	3	12	4.5	1	2	2	5	11.9
...	...	...	1	...	1	...	...	2	0.7	...	1	...	1	2.4
1	2	...	1	2	1	2	...	13	4.8	...	...	2	2	4.8
1	1	...	1	...	...	...	...	6	2.2	...	...	...	...	...
...	...	...	...	...	...	...	...	...	...	...	...	...	...	...
...	...	...	...	...	...	...	...	...	...	...	...	...	...	...
...	...	...	...	...	...	...	...	...	...	1	...	...	1	2.4
...	...	...	1	...	...	...	...	1	0.4	1	...	...	1	2.4
...	...	...	1	...	2	...	...	10	3.7	3	...	1	4	9.5
3	2	...	...	1	...	...	...	9	3.3	...	...	...	...	...
...	...	...	1	...	...	...	...	1	0.4	...	...	...	...	...
...	...	...	1	...	...	...	...	1	0.4	...	...	...	...	...
...	...	...	...	...	...	...	...	...	...	...	...	...	...	...
...	...	...	1	...	...	...	...	1	0.4	...	...	...	...	...
...	...	...	1	...	...	...	...	6	2.2	...	...	...	...	...
3	...	3	1	3	...	...	...	25	9.3	...	...	...	...	...
3	...	1	...	2	...	...	...	11	4.1	...	...	...	...	...
...	1	...	...	1	...	...	...	4	1.5	...	...	...	...	...
...	...	...	...	...	1	...	...	1	0.4	...	1	...	1	2.4
19	13	18	21	15	15	12	7	269	100.0	20	8	14	42	100.0
9	9	10	15	10	11	7	5			9	7	10		

min at 27 500 × g (where g is the gravitational acceleration). The pellet containing bacterial cells and other solids was suspended in 1 mL of 0.15 M NaCl, 0.1 M EDTA, pH 8, and stored at −20°C. DNA was purified from aliquots (50 to 200 μL) of this frozen stock with the modified Marmur procedure [*8,12,13*]. Following fluorimetric concentration determination, dilution to 10 ng/μL, and heat denaturation, these sample DNA preparations were spotted on a master filter and labeled exactly as described above.

Results and Discussion

RSGP Analysis with Growth

In this method, samples collected from the 24 sites listed in Table 1 were grown on Pfennig's medium with one of the six carbon sources. Many of the primary enrichments were trans-

ferred again into medium with the same carbon source. These primary or subsequent enrichments were also used to generate colony purified standards. These procedures resulted in the generation of 152 liquid cultures for the 24 site samples that were used for DNA extraction and RSGP analysis. The number of RSGP assays done for each sample is given in Table 3. For the 21 samples analyzed for the Wainwright field (Table 3, WW1-WW24), a total of 131 RSGP assays was performed, whereas for the 3 samples analyzed in the Wildmere field (Table β, WM10-WM21), 21 RSGP assays were done. The data analyzed in Tables 2 and 3 are a subset of those obtained earlier for six different oil fields and one oil storage facility [*13*]. The main conclusion of that study was that there are two distinct SRB communities, a saline and a freshwater community. Of 34 SRB standards, 18 were typical for the saline and 10 were associated with the fresh water community, while 6 organisms were detected in both populations. Five of the fields studied, including Wainwright and Wildmere, harbored the saline community, whereas one field (Pembina) had the different fresh water community [*13*]. The data set for the saline Wainwright and Wildmere fields will be analyzed in more detail in this paper.

It should be noted first of all that all sites in these two fields have a variety of SRB. A minimum of 2 and a maximum of 17 different standards was detected (Table 3). Several standards (*Lac*7, *Lac*17, *Dec*4, *Dec*6, *Dec*7, *Pro*5, and *Pro*10) were found very infrequently (0 or 1 observations). These are now known to belong to the freshwater oil field community [*13*] and are therefore not expected to be cultured from the saline Wainwright and Wildmere fields. The most prevalent standard cultured was *Ben*1, an SRB first isolated on Pfennig's medium containing benzoate. This standard was found following enrichment on benzoate at all 24 sites. *Lac*6 and *Lac*5 were also frequently observed. Both have been identified as *Desulfovibrio* species in view of their hybridization with the [NiFe] hydrogenase gene probe [*13*]. The two organisms seem to be mutually exclusive; sites from which *Lac*5 was cultured did not yield *Lac*6 and vice versa. It remains to be determined whether this is representative of the true population or whether this exclusion occurs during cultivation. This can be resolved by doing RSGP assays without growth, as discussed below.

Frequently observed SRB were also *Lac*4 and *Ace*1, although the latter has only been found in the Wainwright field. Surveying the entire population for both fields, it appears that in 311 identifications, lactate utilizers were found most frequently (120), followed by benzoate-(77), acetate-(42), decanoate-(24), propionate-(28) and ethanol-utilizers (14). Again, proof that the SRB population in the field consists mainly of lactate- and benzoate-utilizers can be obtained if the RSGP technique is applied to samples not subjected to culturing in the laboratory (see RSGP without growth below). Lactate utilizers *Lac*1,2, *Lac*3, *Lac*4, *Lac*5, *Lac*6, *Lac*10, and *Lac*12 generally also grow well on ethanol-containing enrichment medium (Table 2). Standard *Eth*3, first isolated on Pfennig's medium with ethanol as the carbon source, is likewise frequently found in lactate-based enrichment media. These standards are all [NiFe] hydrogenase positive [*13*], which identifies them as belonging to the genus *Desulfovibrio*. This result is in agreement with the known capacity of most members of this genus to use both lactate and ethanol as carbon and energy source.

The data in Table 2 should be interpreted with caution, since they indicate the frequency of occurrence of the SRB standards on Pfennig's medium with different carbon sources both for enrichment and pure cultures. The growth of acetate utilizers on lactate and ethanol likely resulted from coculture with an acetate-producing lactate-utilizer. With this reservation in mind, it appears that the lactate- and ethanol-utilizers present in the Wainwright and Wildmere fields are unable to grow on decanoate and benzoate. Conversely, the benzoate- and decanoate-utilizers do not readily grow on lactate. The SRB population from the Wildmere field is similar to that from Wainwright. It is also interesting that most SRB cultured from sessile samples are also recovered from planktonic samples (Table 4). The acetate-

TABLE 4—*Frequency of detection of SRB standards*[a] *following culturing of planktonic or sessile samples. The data are derived from those in Table 3.*

Standard	Planktonic[b]	Sessile[b]	Total
*Lac*1,2	3	2	5
*Lac*3	1	5	6
*Lac*4	13	10	23
*Lac*5	19	11	30
*Lac*6	21	13	34
*Lac*10	4	11	15
*Lac*12	2	3	5
*Lac*21	2	...	2
*Eth*2	1	1	2
*Eth*3	6	5	11
*Ben*1	28	25	53
*Ben*3	2	2	4
*Ben*4	5	7	12
*Ben*6	1	2	3
*Dec*1	7	8	15
*Dec*3	5	1	6
*Dec*8	1	1	2
*Pro*1	8	6	14
*Pro*4	6	3	9
*Pro*12	5	1	6
*Ace*1	22	3	25

[a] Standards observed in total only once or not at all are not included in the table.
[b] A total of 11 planktonic and 13 sessile samples were surveyed (Table 1). Culturing of these 24 samples gave rise to 152 DNA preparations, which were analyzed by RSGP as explained in the text.

utilizers form a possible exception and are primarily recovered from planktonic samples. Therefore, it appears that the SRB standards found in the bulk fluid are also present on the surfaces of many of the sampling sites.

RSGP Analysis Without Growth

The above data clearly indicates that a diverse, albeit similar SRB population is present both in the Wainwright and Wildmere oil fields. The growth-based sulfide production and enzyme-based biochemical tests described in the Introduction would have provided enumeration of only a fraction of this population. On the other hand, although RSGP with growth provides information on diversity, it does not give any quantitative information because growth will selectively favor some members of the community. The need to develop RSGP assays without prior growth is therefore evident. This is more difficult primarily because: (1) DNA isolated directly from the environment must be sufficiently clean to allow *in vitro* enzymatic labeling and (2) the number of different standards present in the environment, for example, SRB and other bacteria, may be very large relative to the number that has been isolated and is present on the filter. Thus, upon labeling, only a small fraction of the ^{32}P-label may be incorporated in genomic DNAs present as standards on the master filter. Following hybridization, weak signals (as detected by autoradiography) may be expected.

Preliminary results of RSGP without prior growth are shown in Fig. 2 and these confirm the latter expectation. In Fig. 2 (*a*) and 2(*b*), RSGP is used to confirm the identity of two colony purified samples. As expected, the hybridization reactions with *Lac*5 (Fig. 2(*a*) and *Pro*12 (Fig. 2(*b*) are strong, that is, of the same order as the sample self-hybridization. Lack

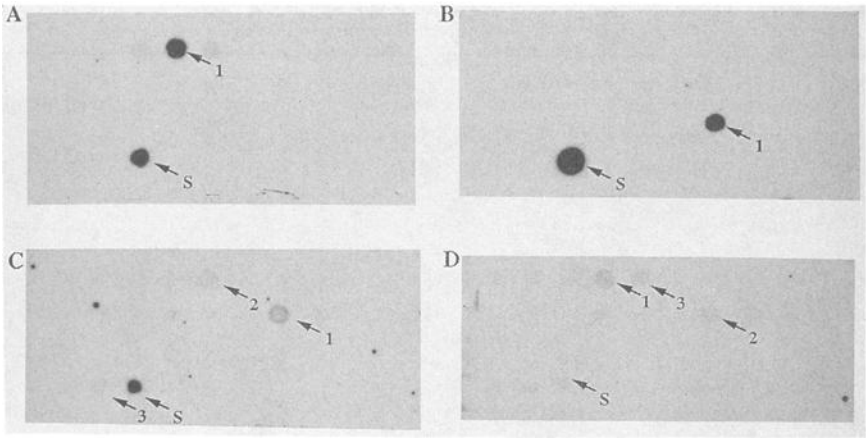

FIG. 2—*Identification of SRB by RSGP. Denatured chromosomal DNAs of 35 different SRB standards (Table 2) were spotted on each of the master filters. The sample DNA preparations to be analyzed were spotted at the indicated positions (S) and were from either a colony purified isolate (A, B) or an uncultured water sample (C, D). The observed hybridizations have been labeled in order of decreasing hybridization intensity (1→3). (A) 1* = Lac5, *(B) 1* = Pro12, *(C) 1* = Ben6, *2* = Lac6, *3* = Ace5; *and (D) 1* = Lac5, *2* = Ben6, *3* = Lac6.

of hybridization with other standards confirms that the samples represent pure cultures. In Fig. 2(*c*) and 2(*d*), RSGP of total community DNA isolated from two Wainwright production waters, as indicated in the Materials and Methods section, is presented. The signals observed are weaker, relative to the sample self-hybridization in Fig. 2(*c*). In Fig. 2(*d*), sample self-hybridization is not observed, possibly due to the high complexity of the sample DNA, as discussed at the beginning of the paper. The three most intense spots have been marked in order of decreasing hybridization intensity (1→3). For Fig. 2(*c*), these are: (1) *Ben*6, (2) *Lac*6, and (3) *Ace*5, whereas for Fig. 2(*d*), these are (1) *Lac*5, (2) *Ben*6, and (3) *Lac*6. The observation of *Lac*6 in both samples is in accord with the fact that this standard is frequently cultured from Wainwright sites (Table 2). The preliminary results in Fig. 2(*c*) and 2(*d*) should be confirmed by conventional genome probing in which defined amounts of denatured total community DNA are spotted on a filter and probed with a labeled standard (for example, *Lac*6). Inclusion of known amounts of denatured *Lac*6 DNA on the filter (for example, in the range 0.1 to 10 ng) will provide a positive control and will allow quantitation of *Lac*6 in samples of total communities. Once the absolute number of bacteria in a sample is known for one of the standards, the others can be derived by densitometry, assuming that relative numbers are proportional to the hybridization intensities in Fig. 2(*c*) and 2(*d*). These studies are currently in progress.

Application of RSGP without growth is described in detail in Ref *15*.

Acknowledgments

This work was supported by a Strategic Grant of the Natural Science and Engineering Research Council of Canada (NSERC) and by an NSERC Collaborative Research and Development Grant with NOVA HUSKY Research Corp. The authors are indebted to Husky Oil Ltd. for access to their field facilities and assistance in sampling. The contributions of Sara Ebert, Neili Sifeldeen, Johanna K. Voordouw, and Brenda Bramhill are gratefully acknowledged.

References

[1] Hamilton, W. A., "Sulphate-Reducing Bacteria and Anaerobic Corrosion," *Annual Reviews of Microbiology*, Vol. 39, 1985, pp. 195–217.

[2] Devereux, R., Delaney, M., Widdel, F., and Stahl, D. A., "Natural Relationships Among Sulfate-Reducing Eubacteria," *Journal of Bacteriology*, Vol. 171, 1989, pp. 6689–6695.

[3] Cord-Ruwisch, R., Kleinitz, W., and Widdel, F., "Sulfate-Reducing Bacteria and Their Activities in Oil Production," *Journal of Petroleum Technology*, Vol. 39, 1987, pp. 97–106.

[4] Aeckersberg, F., Bak, F., and Widdel, F., "Anaerobic Oxidation of Saturated Hydrocarbons to CO_2 by a New Type of Sulfate-Reducing Bacterium," *Archives of Microbiology*, Vol. 156, 1991, pp. 5–14.

[5] Bryant, R. D., Jansen, W., Boivin, J., Laishley, E. J., and Costerton, J. W., "Effect of Hydrogenase and Mixed Sulfate-Reducing Bacterial Populations on the Corrosion of Steel," *Applied and Environmental Microbiology*, Vol. 57, 1991, pp. 2804–2809.

[6] Odom, J. M., Gawell, L. J., and Ng, T. K., "Sulfate-Reducing Bacteria Detection," Patent Application ICR 7780-USSN946, 547, Du Pont Co., Wilmington, DE.

[7] Odom, J. M., Jessie, K., Knodel, E., and Emptage, M., "Immunological Cross-Reactivities of Adenosine-5′-Phosphosulfate Reductases from Sulfate-Reducing and Sulfide-Oxidizing Bacteria," *Applied and Environmental Microbiology*, Vol. 57, pp. 727–733.

[8] Voordouw, G., Niviere, V., Ferris, F. G., Fedorak, P. M., and Westlake, D. W. S., "The Distribution of Hydrogenase Genes in Desulfovibrio and Their Use in Identification of Species from the Oil Field Environment." *Applied and Environmental Microbiology*, Vol. 56, 1990, pp. 3748–3754.

[9] Devereux, R., He, S.-H., Doyle, C. L., Orkland, S., Stahl, D. A., LeGall, J., and Whitman, W. B., "Diversity and Origin of *Desulfovibrio* Species: Phylogenetic Definition of a Family," *Journal of Bacteriology*, Vol. 172, 1990, pp. 3609–3619.

[10] AccuSearch, "Chemiluminescent DNA Probe and Detection System. Sulfate-Reducing Bacteria," Gen-Probe®, 1990.

[11] Amann, R. I., Stromley, J., Devereux, R., Key, R., and Stahl, D. A., "Molecular and Microscopic Identification of Sulfate-Reducing Bacteria in Multispecies Biofilms," *Applied and Environmental Microbiology*, Vol. 58, 1992, pp. 614–623.

[12] Voordouw, G., Voordouw, J. K., Karkhoff-Schweizer, R. R., Fedorak, P. M., and Westlake, D. W. S., "Reverse Sample Genome Probing, a New Technique for Identification of Bacteria in Environmental Samples by DNA Hybridization, and its Application to the Identification of Sulfate-Reducing Bacteria in Oil Field Samples," *Applied and Environmental Microbiology*, Vol. 57, 1991, pp. 3070–3078.

[13] Voordouw, G., Voordouw, J. K., Jack T. R., Foght, J. M., Fedorak, P. M., and Westlake, D. W. S., "Identification of Distinct Communities of Sulfate-Reducing Bacteria in Oil Fields by Reverse Sample Genome Probing," *Applied and Environmental Microbiology*, Vol. 58, pp. 3542–3552.

[14] Pfennig, N., Widdel, F., and Truper, H. G., "Dissimilatory Sulphate-Reducing Bacteria," *The Prokaryotes*, Vol. 1, M. P. Starr, Ed., Springer Verlag, Inc., New York, 1991, pp. 926–940.

[15] Voordouw, G., Shen, Y., Harrington, C. S., Telang, A. J., Jack, T. R., and Westlake, D. W. S., "Quantitative Reverse Sample Genome Probing of Microbial Communities and Its Application to Oil Field Production Waters," *Applied and Environmental Microbiology*, Vol. 59, pp. 4101–4114.

Non-Metallics

Reiner Mansch[1] *and Eberhard Bock*[1]

Simulation of Microbiologically and Chemically Influenced Corrosion of Natural Sandstone

REFERENCE: Mansch, R. and Bock, E., **"Simulation of Microbiologically and Chemically Influenced Corrosion of Natural Sandstone,"** *Microbiologically Influenced Corrosion Testing, ASTM STP 1232,* Jeffery R. Kearns and Brenda J. Little, Eds., American Society for Testing and Materials, Philadelphia, 1994, pp. 203–216.

ABSTRACT: A test system for the simulation of a combined chemically (gaseous pollutants) and microbiologically (nitrifying bacteria) influenced corrosion on natural sandstone is presented. A high stone moisture was essential for the growth of nitrifying bacteria on test stones. Under optimum conditions, a nitrifying biofilm developed on the calcareous Ihrlersteiner green sandstone, reducing the evaporation from the stone surface. Biofilm cells adapted well to high concentrations of gaseous pollutants.

The mean metabolic activities of ammonia oxidizers were 11 and those of nitrite oxidizers 30 times higher than mean values of samples from historical buildings.

The microbiologically influenced nitric acid corrosion alone was stronger than the chemically influenced corrosion by a smog atmosphere (1065-$\mu g/m^3$ sulphur dioxide, 850-$\mu g/m^3$ nitric oxide, and about 450-$\mu g/m^3$ nitrogen dioxide). While 72 μmol of calcium were solubilized per week of exposure to the smog atmosphere, 161 μmol of calcium per week were solubilized by the nitric acid produced by nitrifying bacteria.

If gaseous pollutants were added, the microbiologically produced nitrite and nitrate were removed by the action of sulphur dioxide. Thus, the combined attack of nitrifying bacteria and gaseous pollutants did not result in increased corrosion.

KEYWORDS: building, air pollution, stone deterioration, corrosion, simulation, acceleration, biodeterioration, endolithic microorganisms, nitrifying bacteria, nitrification, nitric acid

In the last decades, accelerated stone deterioration has been observed. This phenomenon has mostly been explained by an increased rate of man-made pollution of the atmosphere [*1,2*]. The gaseous pollutants sulphur dioxide (SO_2), nitrogen dioxide (NO_2) and nitric oxide (NO) interact with stone surfaces by forming sulphate (SO_4^{2-}), nitrite (NO_2^-) and nitrate (NO_3^-) [*3,4*]. The deteriorating effect of SO_2 alone, and together with other gaseous pollutants as nitrogen dioxide, hydrogen fluoride and ozone has been demonstrated in several simulation experiments [*3,5–8*]. The gases react mainly according to their solubility in water which is $SO_2 > NO_2 > NO$ [*7*]. Therefore, the deteriorating effect of NO_2 and NO seems to be of less importance. However, in urban environments with high photochemical pollution, the deposition of NO_3^- can overcome the deposition rate of SO_4^{2-} [*9*].

Building stone is a natural habitat for epi- and endolithic microorganisms [*10,11*]. The question arises as to what extent these microorganisms contribute to stone deterioration. This subject is part of a research project on preservation of historical buildings and mon-

[1] Biologist and professor of microbiology, respectively, Institut für Allgemeine Botanik, Abteilung Mikrobiologie, Ohnhorststrasse 18, 22609 Hamburg, Germany.

uments in Germany which started in 1985 [*12*]. Microbiological investigations include integral inventory evaluation of field data, test fields and simulation experiments.

Nitrifying bacteria have been found in natural stones of 25 historical buildings in Germany [*13*]. They consist of two groups of specialized organisms ubiquitously present in soil. The ammonia oxidizers convert ammonia to nitrous acid and the nitrite oxidizers transform nitrite into nitrate according to the following equations:

$$NH_4^+ + 1.5\ O_2 \rightarrow NO_2^- + H_2O + 2\ H^+ \quad (1)$$

$$NO_2^- + 0.5\ O_2 \rightarrow NO_3^- \quad (2)$$

The substrate ammonia, deposited on stone surfaces, mainly originates from livestock-breeding, fertilization and industry [*14*]. The nitric acid produced by nitrifying bacteria dissolves calcareous binding materials and contributes to high nitrate concentrations in building stone [*15*].

Microbiologically influenced nitric acid corrosion was first simulated by Bock et al. [*16*] in a salt spray cabinet. This paper describes improved simulation experiments. Biogenic nitric acid corrosion and chemically influenced corrosion by gaseous pollutants were simulated in a specially constructed double-chamber cabinet.

The aim was: (1) to differentiate between the impact of gaseous pollutants and biogenic nitric acid corrosion, (2) to quantify the individual effects each process has in stone deterioration, and (3) to characterize synergistic effects between microbiology and chemistry.

Experimental Procedures

Experimental Concept

Each experiment consisted of three different tests performed simultaneously.

Test 1—simulating biogenic nitric acid corrosion together with chemically influenced corrosion by SO_2, NO_2, and NO.

Test 2—simulating chemically influenced corrosion by SO_2, NO_2, and NO in the absence of biogenic nitric acid corrosion.

Test 3—simulating biogenic nitric acid corrosion in the absence of gaseous pollutants.

Tests 1 and 2 were done in a double-chamber cabinet (see Fig. 1). Test 3 was done in a separate climatic chamber. This report summarizes the results of two long-term experiments performed in 1991 and 1992.

Double-Chamber Cabinet

The double-chamber cabinet (DCC) consisted of two identical climatic chambers (Weiss-Technik, Reiskirchen, Germany) combined with a gas supplying system (Messer-Griesheim, Duisburg, Germany) and housed in a thermostated laboratory container (see Fig. 1).

Each unit had a volume of 1.5 m^3. The temperature of both units (A, B) was regulated between 20 to 40°C by Heater I and the relative humidity was adjusted between 60 and 100% relative humidity. Temperature and relative humidity (Dew Point Instrument Model DP 3-D, MBW Electronics, Wettingen, Switzerland) were recorded. The air flow was regulated between 0 and 1.2 m^3/h. Unit B could be operated separately between 20 and 60°C by Heater II and relative humidity between 60 and 100% by Humidifier II.

Polluted air was produced by feeding NO and SO_2 into the humidified air stream. Gas flow regulation was achieved with flow controllers (Tylan, Eching, Germany). The sulphur

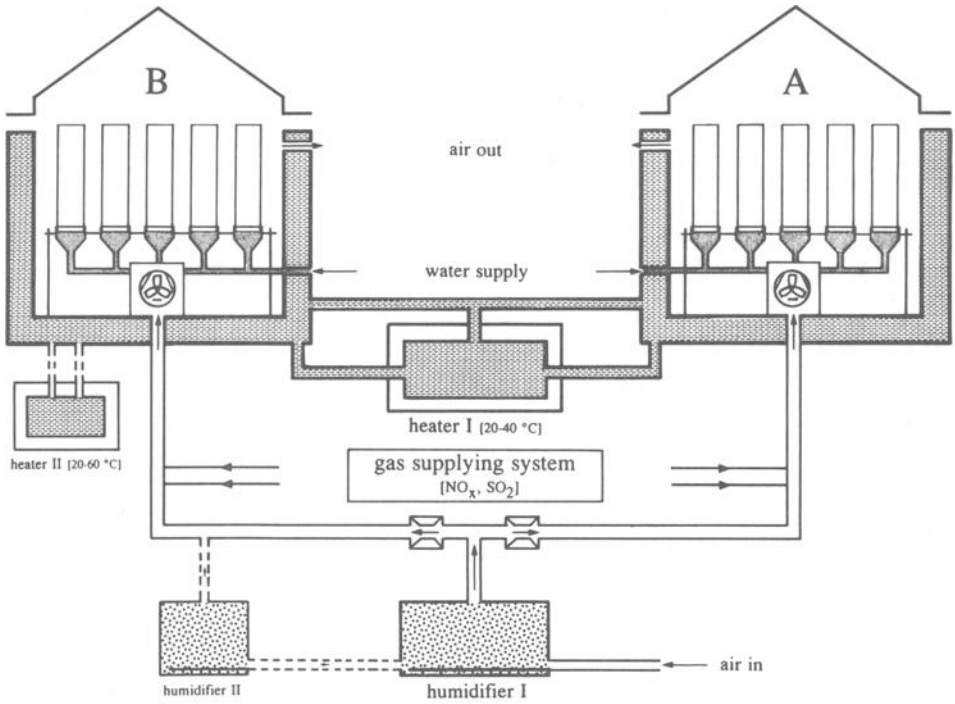

FIG. 1—*Schematic diagram of the double chamber cabinet (DCC) for the simulation of chemically and microbiologically influenced corrosion of natural sandstone. In Chamber A, the combined weathering of gaseous pollutants plus nitrifying bacteria is simulated, while in Chamber B chemical weathering without nitrifying bacteria is simulated. In each chamber, test blocks with the closed watering system are depicted.*

dioxide concentration was automatically adjusted to a nominal value, while the nitric oxide concentration was manually adjusted. To get an even distribution of the gases, the atmospheres were vigorously ventilated by a tangential blower, which mixed the atmospheres about 1000 times per hour. Gas concentrations were measured at two control-points in each chamber. The sample air was diluted tenfold with dry, clean air using a heated gas mixing probe. Nitrogen oxides were measured with a chemoluminescence detector (Oxides of Nitrogen Analyser, Columbia Scientific Industries, CSI 1600), and sulphur dioxide was measured with a sulphur detector (Sulfur Analyser CSI, SA 285).

Climatic Chamber

A control experiment without gaseous pollutants was conducted in a closed climatic chamber. The bottom of the chamber was filled with water to give an atmosphere of nearly maximum relative humidity.

Experimental Conditions

All experiments were done at 28°C and 95 ± 2% relative humidity. Test blocks in Tests 1 and 2 were exposed to an atmosphere of 1065-$\mu g/m^3$ SO_2, 820-$\mu g/m^3$ NO, and about 450-$\mu g/m^3$ NO_2. These values resemble concentrations measured at smog situations in urban

environments. Under these conditions, NO_2 resulted from the oxidation of NO. Ventilation and the exchange of air (0.9 m^3/h) caused a net evaporation from the stone surfaces. In contrast to Tests 1 and 2, the blocks of Test 3 were not exposed to a polluted atmosphere but they were kept in a steady and moist atmosphere. Under these conditions, the evaporation was negligible.

Test Blocks

Test blocks were made of "Ihrlersteiner green sandstone," a variety of the calcitic ($CaCO_3$) and dolomitic [$CaMg(CO_3)$] "Regensburger green sandstone." This stone was green in color as a result of an iron bearing clay mineral, glauconite.

Test blocks had a size of 5 by 5 by 30 cm with sealed flanks. They were sealed for the following reasons: (1) to reduce the evaporation and (2) to simulate the situation in a stone wall where only one face is exposed to the atmosphere. To grow bacteria on the stone surface, the test blocks in the DCC had an additional water reservoir on the upper surface (see Fig. 2). The test blocks were fitted into a water reservoir, tightened with silicone and connected to a reservoir outside the chambers (see Fig. 1). Additional experiments used 1.5 by 1.5-cm cubes of unsealed stone material.

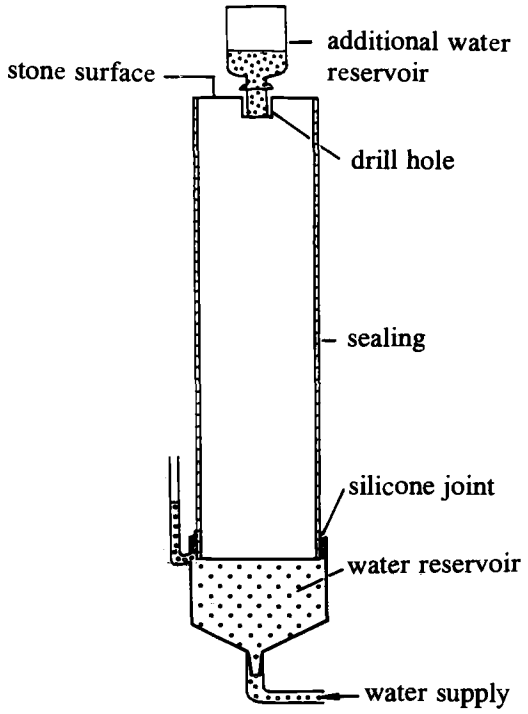

FIG. 2—*Cross section of a test block from the double chamber cabinet with a closed water reservoir at the bottom and an additional water reservoir on the upper stone surface.*

Modeling a Nitrifying Microflora

At the beginning of each experiment, the watered test stones for Tests 1 and 3 were inoculated with pure cultures of nitrifying bacteria on the upper stone surface. Blocks for Test 2 were inoculated with a suspension of killed cells. All strains had been originally isolated from building stones. The ammonia oxidizers belonged to the genus *Nitrosovibrio* strain K 7.1 [*17*] and *Nitrosomonas* strain R 1.24. The nitrite oxidizers belonged to the species *Nitrobacter vulgaris* strain K 48 [*18*].

All stones were supplied weekly with 3 mL of 500m*M* ammonium-chloride solution and kept at nearly 100% of their maximum water-holding capacity (about 5.6% weight). The test blocks in Test 2 were heated monthly at 60°C to kill any nitrifying bacteria that might have infected the stones during the testing.

Sampling

Every six weeks a set of test blocks was removed and analyzed. The test blocks were sawed to give distinct stone samples with depths of 0 to 5, 5 to 15, 15 to 25, 25 to 35, 35 to 50, 50 to 100, 100 to 150, 150 to 200, 200 to 250, and 250 to 300 mm. The layers were cut off using a hammer and chisel, and then the layers were ground using a pestle and mortar.

Microflora Characterization

The nitrifying microflora was characterized by the amount of nitrite (NO_2^-) and nitrate (NO_3^-) in the test stones, by nitrification potential measurements, and by cell numbers as determined by a most probable number test.

To measure the nitrification potential of ammonia- and nitrite oxidizers, 3 g of stone material were washed with 0.2% (wt/vol) sterile sodium chloride (NaCl) and centrifuged at ×20 000 *g* for 15 min. The sediment was resuspended in 15-mL basal salts solution (pH 7.5) containing 5m*M* ammonium-chloride (NH_4Cl) or sodium nitrite ($NaNO_2$), respectively. The resuspended sediments were incubated at 28°C on a shaker (150 rpm). The formation of NO_2^- and NO_3^- was followed in each sample. Nitrite and nitrate were determined by high pressure liquid chromatography (HPLC; see description that follows). Activities were calculated from the amount of metabolic endproducts formed during the first 60 h.

Cell numbers of ammonia- and nitrite oxidizers were determined using a three-tube most probable number (MPN) test from serial dilutions of stone suspensions. The suspensions were made from 2 g of stone material suspended in 10 mL of 0.9% (wt/vol) sterile NaCl solution and homogenized at 150 rpm for 1 h. The MPN test tubes contained 5 mL of basal salts solution with 10m*M* of NH_4Cl or 5m*M* $NaNO_2$, respectively. Heterotrophic bacteria were counted on DEV gelatin agar (Merck) and fungi on SABOURAUD-4% maltose agar (Merck) diluted 1:10. Agar plates were counted after one week, and MPN-tubes were examined qualitatively for nitrite and nitrate production after six weeks of incubation at 28°C.

Monitoring the Corrosion

As an indicator for corrosion and the formation of gypsum from SO_2, the amount of water-soluble calcium (Ca^{2+}) and sulphate (SO_4^{2-}) in the test stones was determined. Three sets of 0.5-g stone material from each layer were washed with 20 mL of distilled water for 1 h at 150 rpm and the stone material was sedimented at ×20 000 *g* for 15 min. If necessary,

this procedure was repeated. The Ca^{2+} concentrations were measured by Atomic Absorption Spectrometry (AAS) using an AAS Perkin Elmer 1100 B. All data termed "solubilized" Ca^{2+} were corrected for the amount of soluble Ca^{2+} in fresh stone material.

Sulphate was determined indirectly by a modified barium chloride precipitation assay [*19*] with barium being measured by AAS.

To measure nitrite and nitrate in the stones, 1 g of material was sterilized, extracted with 10 mL of distilled water for 12 h on a shaker (150 rpm), and sedimented. Nitrite and nitrate concentrations were measured by HPLC with 5m*M* tetrabutyl-ammoniumhydrogensulphate/10% methanol buffer (6.5) as the solvent. The separations used a Hypersil-ODS-5μ column with detection at 225 nm.

Scanning Electron Microscopy (SEM)

Surface samples were immediately frozen in liquid nitrogen. Samples were transferred into a cryopreparation chamber SCU 020 (Baltec Company), sputtered with platinum and scanned with a field emission electron microscope (Hitachi S 400).

Results and Discussion

Colonization of Natural Sandstone in the Laboratory and Under Environmental Conditions

The Importance of Stone Moisture and Stone Characteristics—In simulation experiments, a stone moisture of nearly 100% of the maximum water-holding capacity was essential for the survival of nitrifying bacteria. Because of a high evaporation from the stone surface in Test 1, an additional water reservoir was necessary (see Fig. 2). In Test 3, the stone moisture caused by capillary attraction was sufficient for bacterial growth.

The second major growth factor for nitrifying bacteria was the stone itself. Nitrifiers preferred the calcareous Ihrlersteiner green sandstone (pH 8.5), which was heavily colonized. In contrast, the siliceous Rüthener green sandstone (pH 6.5) was not colonized. These findings were in accordance with the results of a statistical evaluation of data from 18 historical buildings in Germany [*20,21*]. Nitrifying bacteria preferred stones with a calcareous binding material, a pH of 8.0 to 8.5 and a medium pore size between 1 and 10 μm.

Colonization of Test Blocks—High nitrification potentials and cell numbers of nitrifying bacteria were measured in the upper layer of test blocks from Ihrlersteiner green sandstone. The mean metabolic activities calculated for the two experiments were 44 nmol/h $\times$ g^{-1} for ammonia oxidizers and 172 nmol/h $\times$ g^{-1} for nitrite oxidizers. Cell numbers ranged between 1×10^6 and 1×10^7 cells/g stone. Uninoculated test stones (Test 2) were easily infected if they were not regularly pasteurized (60°C). All stones were strongly colonized with heterotrophic microorganisms. In the upper layer, the cell numbers of fungi ranged between 1×10^6 and 1×10^7 cells/g and the heterotrophic bacterial numbers were approximately 1×10^8 cells/g.

The cell numbers of nitrifying bacteria and fungi decreased in the deeper layers of sealed test blocks, while unsealed stones were colonized evenly. Oxygen deficiency in the deeper layers of sealed stones seemed to be the main reason for this. Ammonia oxidizers were restricted to the upper 4 cm, whereas nitrite oxidizers were found up to 10 cm deep. Heterotrophic bacteria were not affected by the sealing.

Influence of Gaseous Pollutants on the Nitrifying Microflora—After preincubation without gaseous pollutants, a smog situation was simulated. After five weeks of exposure to the

polluted atmosphere, the activities of ammonia and nitrite oxidizers in the first experiment were markedly reduced, while they remained at the same level in the second experiment. However, in both cases the activities of ammonia- and nitrite oxidizers increased during the time of exposure reaching values 1.5 to 11 times higher than before exposure to the polluted atmosphere. For nitrite oxidizers this was surprising because there was nearly no nitrite available (see following discussion). *Nitrobacter* cells may have grown with nitric oxide instead of nitrite [*22*] or with organic matter [*18*].

If biological questions are considered in smog simulation experiments, it is essential to assure that the organisms tolerate the applied pollutant concentrations. Naturally occurring values should not be greatly exceeded.

The Nitrifying Biofilm—Nitrifying bacteria and chemoorganotrophic microorganisms formed a "nitrifying biofilm" (Tests 1 and 3). The stone surface was almost entirely covered by the biofilm (see Fig. 3, left panel). On stones inoculated with dead nitrifiers, the stone surface was only partly covered with cell debris (see Fig. 3, right panel). The biofilm contained different types of microcolonies formed by heterotrophic bacteria and nitrifying bacteria (data not shown). Microcolonies of endolithic nitrifying bacteria have already been described for building stone [*15*] and, thus, seem to be their natural growth form. As biofilm cells can develop new characteristics, for example, resistance against pollutants or desiccation [*23–25*], their impact on corrosion may increase.

The evaporation from the stone surface was markedly reduced by the biofilm. After 30 weeks, 15 mL evaporated per day from test blocks colonized with nitrifiers compared with 45 mL for test stones without nitrifiers.

Correlation with Field Data—The mean values of metabolic activities for ammonia-oxidizers in the simulation experiments (see previous discussion) were 11 times and those of nitrite oxidizers 30 times higher than the mean activities determined for samples from historical buildings [*20*]. This stands for a mean acceleration factor of 11 for simulated biogenic nitric acid corrosion. This is comparable with a factor of 8 ascertained for the simulation of biogenic sulphuric acid corrosion [*26*].

If the age of historical buildings is taken into consideration, it is obvious that the acceleration by simulation experiments may be even higher. This can be derived from the fact

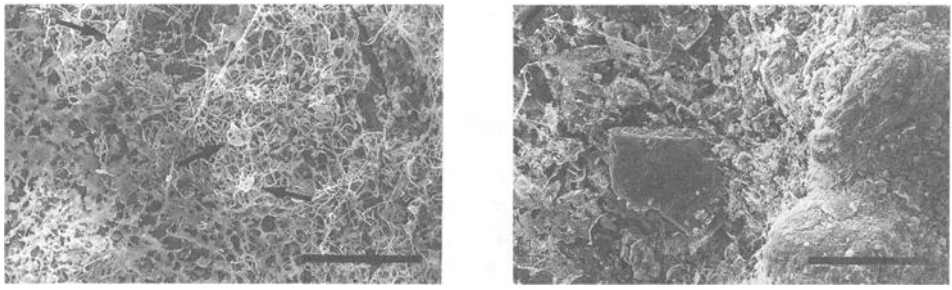

FIG. 3—*SEMs of Ihrlersteiner green sandstone surfaces colonized* (left) *and not colonized with nitrifying bacteria after 36 weeks of experimental time and after 26 weeks of exposure to gaseous pollutants* (right). *The left stone surface is nearly entirely covered with a biofilm consisting of nitrifying bacteria, chemoorganotrophic microorganisms, and extracellular polymeric substances. Some microcolonies of heterotrophic bacteria are visible and indicated* (→). *The stone surface on the right is partially covered with cell debris from the inoculation with dead nitrifiers, but microorganisms are not visible. Bars = 60 μm.*

that under natural conditions the colonization of Ihrlersteiner green sandstone by nitrifying bacteria was very slow. After five years of exposure on a test field in the urban area of Duisburg (Germany), test blocks were scarcely colonized with nitrifiers. In contrast, fungi and heterotrophic bacteria exhibited maximum cell numbers within one year. This finding indicates that aging of the stone material, for example, chemical weathering, deposition of ammonia and colonization with chemoorganotrophic and phototrophic microorganisms, may play an important role for colonization by nitrifying bacteria.

Chemical Attack by Sulphur Dioxide (Tests 1 and 2)

After 17 weeks of exposure to the simulated atmosphere, the concentrations of sulphate and solubilized calcium in the upper layer of the test blocks amounted to 3260 μg/g of sulphate and 1069 μg/g of calcium in Test 1 and 4760 μg/g of sulphate and 1751 μg/g of calcium for Test 2. In the second layer (0.5 to 1 cm depth), sulphate and solubilized calcium were not detectable.

These values give a total amount of 958 μmol of sulphate deposited and 833 μmol of calcium solubilized in stones colonized with nitrifiers (Test 1) and 1400 μmol of sulphate deposited and 1218 μmol of calcium solubilized for stones without nitrifiers (Test 2). In Test 2, about 72 μmol of calcium per week were solubilized by the smog atmosphere.

The amounts of sulphate formed and calcium solubilized correspond well. Thus the corrosion in both tests can mainly be explained by the reaction of SO_2 with the calcitic binding material and the formation of gypsum. During this reaction, sulfite (SO_3^{2-}) is formed as an intermediate according to the following equations [*4*]:

$$CaCO_3 + SO_2 + 2\,H_2O \rightarrow CaSO_3 \times 2\,H_2O + CO_2 \quad (3)$$

$$CaSO_3 \times 2\,H_2O + 1/2\,O_2 \rightarrow CaSO_4 \times 2\,H_2O \quad (4)$$

Some of the SO_2 reacted with $MgCO_3$ (data not shown), which made about 10% of the binding material. Surprisingly, the corroding effect of SO_2 did not increase on stones colonized with nitrifying bacteria (Test 1), as we suspected from the fact that nitrite enhances the oxidation of sulfite [*15*]. In contrast, the deposition of SO_2 was lowered, which may be caused by the biofilm covering the stone surface.

Chemical Attack by Nitrogen Dioxide (Test 2)

Compared with SO_2, the chemical attack of NO_2 was negligible. After 17 weeks of exposure to the simulated atmosphere, 8 μmol of nitrite plus nitrate were found on test blocks (Test 2). This was equivalent to 4 μmol calcium solubilized (data not shown), which was about 0.4% compared to the amount of calcium solubilized by SO_2 (Test 2). On the other hand, NO_2 might have promoted the formation of gypsum from SO_2 as described in the literature [*3,6,7*].

Biogenic Nitric Acid Corrosion (Test 3)

In this experiment, the total amount of nitrate produced by the nitrifying biofilm in the absence of gaseous pollutants increased with time (see Fig. 4, left panel). Although nitri-

fication occurred only in the upper few centimeters, within 27 weeks nitrate was distributed by diffusion in the whole test block. In layers deeper than 2 cm, nitrite was found which confirmed the oxygen deficiency inside the blocks (see previous discussion). Because the total amount of nitrite was negligible, only nitrate will be discussed in the following paragraphs.

The nitrate content represented the amount of nitric acid which reacted with calcium carbonate ($CaCO_3$). After 27 weeks of incubation, 5.0 mmol of nitrate were formed per block with 4.4 mmol of Ca^{2+} being solubilized (see Fig. 5). This represents 162 μmol of Ca^{2+} solubilized per week. Because the acid generating first step of nitrification produces two protons (see introduction), one mol of Ca^{2+} was solubilized per mol nitrate. The oxidation of NH_4Cl on the test blocks and the solubilization of calcium carbonate can be described by the following equations:

$$NH_4Cl + 2O_2 \rightarrow NO_3^- + Cl^- + 2H^+ + H_2O \quad (5)$$

$$CaCO_3 + 2H^+ + NO_3^- + Cl^- \rightarrow Ca^{2+} + NO_3^- + Cl^- + CO_2 \quad (6)$$

The fact that 162 μmol of Ca^{2+} per week were solubilized by biogenic nitric acid corrosion compared with only 72 μmol of Ca^{2+} per week by the smog atmosphere shows the highly corrosive potential of microbiologically influenced corrosion (see Fig. 5).

Biogenic Nitric Acid Corrosion in Polluted Atmospheres (Test 1)

In this experiment, soluble substances (for example, NO_3^- and Ca^{2+}), were transported to the stone surface by the evaporating water. Nitrite was not detected in these test blocks. At first, the nitrate content increased during the pre-incubation without gaseous pollutants. After the exposure to the complex atmosphere, the nitrate content decreased, although the activities of nitrifiers were high. If sulphur dioxide was omitted from the gas mixture, the nitrate content increased again (see Fig. 4, right panel). During the experiment, a significant increase in the concentration of nitric oxide was observed.

On sterilized stone material supplied with $NaNO_2$ and $NaNO_3$, nitrate (NO_3^-) was stable while nitrite (NO_2^-) was not. From these findings it seems obvious that NO_2^- was removed by the action of sulphur dioxide and may have been reduced to nitric oxide. This process dominated the oxidation of NO_2^- by the nitrite oxidizers and, consequently, nitrate was not formed. Because NO_3^- was stable on sterilized stone material, the disappearing NO_3^- must have been reduced enzymatically to NO_2^-. Many microorganisms possess a nitrate-reductase, and even the nitrite-oxidoreductase, the key enzyme of *Nitrobacter,* has nitrate-reductase activity producing NO_2^- [*22*].

Neither biologically produced NO_2^- (Test 1) nor the addition of $NaNO_2$ increased the amount of SO_4^{2-} formed on the test stones. These data are in contrast to a reported increase in SO_4^{2-} formation catalyzed by nitrogen dioxide [*3,6,7*] and to the enhanced oxidation of sulfite in the presence of NO_2^- [*15*]. Consequently, a reaction of sulphur dioxide with NO_2^- can be excluded. We conclude that NO_2^- is removed as a result of the acidification of the surface water film by sulphur dioxide. This acid-catalyzed NO_2^- reduction, which becomes significant at pH-values below 5.0 is known as chemodenitrification [*27*] and generates nitric oxide as the predominant gaseous product.

Although NO_3^- was not formed during ammonia oxidation in the presence of sulphur dioxide, there can be no doubt that nitric acid was produced in amounts comparable to

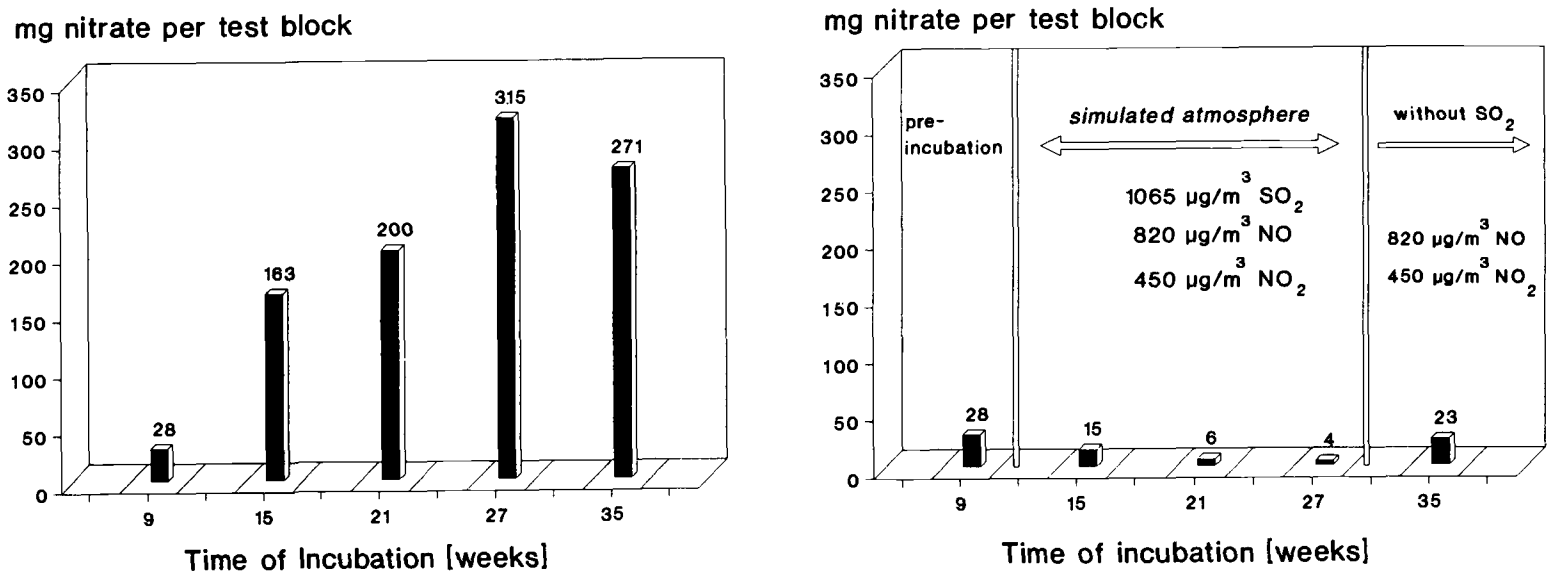

FIG. 4—*Total amounts of nitrate determined for test blocks of Ihrlersteiner green sandstone with high metabolic activities of nitrifying bacteria.* Left: *Test blocks incubated in an atmosphere of ambient, clean air.* Right: *After 9 weeks of pre-incubation, test blocks were exposed to a complex atmosphere of 1065-µg/m³ SO_2, 850-µg/m³ NO, and about 450-µg/m³ NO_2. After 27 weeks, SO_2 was omitted from the gas mixture.*

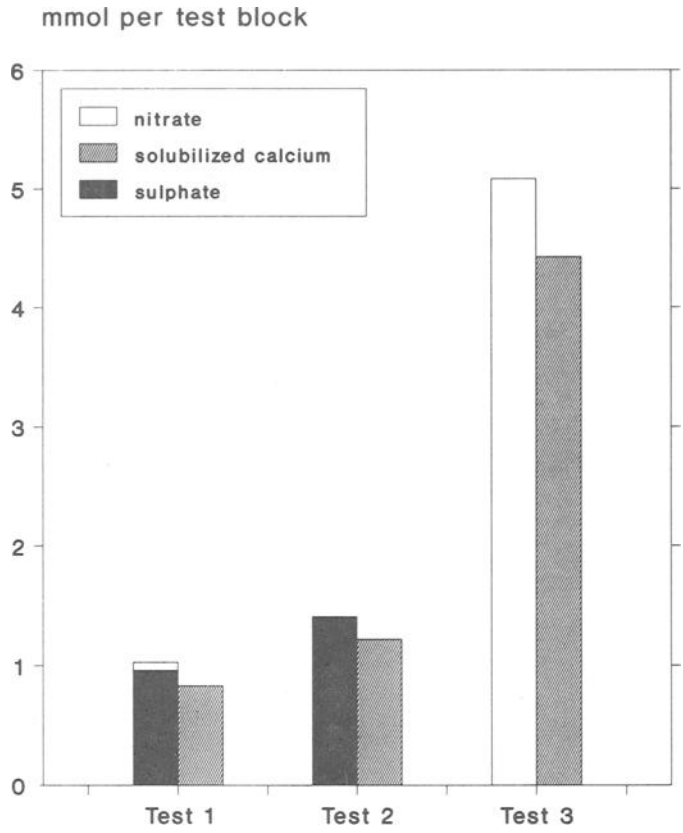

FIG. 5—*Solubilized calcium as an indicator for corrosion of weathered test blocks of Ihrlersteiner green sandstone after 27 weeks. The influence of biogenic nitric acid corrosion is indicated by the amount of nitrate, and the influence of chemical sulfuric acid corrosion is indicated by the amount of sulphate.* Test 1: *Combined weathering of nitrifying bacteria and a complex gas atmosphere of 1065-μg/m³ SO_2, 850-μg/m³ NO, and about 450-μg/m³ NO_2.* Test 2: *Weathering of the complex gas atmosphere without nitrifying bacteria.* Test 3: *Weathering of nitrifying bacteria in an atmosphere of ambient, clean air.*

those of Test 3. The question arises as to whether the intermediately produced nitric acid had a corrosive effect. A comparison of the amounts of solubilized Ca^{2+} for Test 1 and Test 2 shows that in the presence of gaseous pollutants there was no accelerated weathering by the nitrifying microflora. Chemically influenced weathering by sulphur dioxide was the dominating process.

However, the colonization with nitrifying bacteria was clearly visible (see Fig. 6). The surfaces of the chemically plus microbiologically weathered stones appeared to be clogged with many efflorescences. Zones of brown and white coloring were distinguishable, while the chemically weathered stone surfaces were only slightly colored. The latter exhibited an open surface, with small cavities and only a few efflorescences on it. The brown coloring might be caused by a formation of melanin [*28*] or by the mobilization and precipitation of iron. The white coloring could be attributed to fungal growth. In addition, certain changes

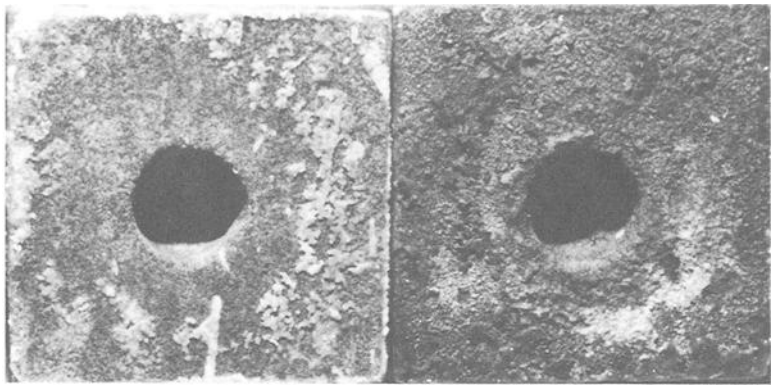

FIG. 6—*Stone surfaces (5 by 5 cm) of Irhlersteiner green sandstone test blocks after 17 weeks of combined weathering by nitrifying bacteria and a complex atmosphere of 1065-μg/m³ SO_2, 850-μg/m³ NO, and about 450-μg/m³ NO_2* (right test block) *compared to a stone surface weathered by the same complex atmosphere without nitrifying bacteria* (left test block). *The chemically plus microbiologically weathered stone* (right) *showed brown coloring with many efflorescences. Light areas could be attributed to fungal growth. In comparison, the chemically weathered stone was only slightly colored with few efflorescences. The light areas represent calcit inclusions.*

in the mineralogical composition of the stone may have occurred, but were not detectable with the methods used in this study. Mineralogical investigations are in progress.

Concluding Remarks

A high acceleration of the biogenic nitric acid corrosion was achieved with the described test system. Therefore, the system could be used for regular testing of natural sandstones concerning their resistence to microbiologically influenced corrosion (MIC).

In the absence of gaseous pollutants, the microbiologically influenced corrosion was greater than the chemically influenced corrosion from a smog atmosphere. This confirms the highly corrosive potential of nitrifying bacteria.

For the first time, a combined microbiologically and chemically influenced weathering of natural sandstone was simulated. Surprisingly, this did not cause increased corrosion, but revealed yet unknown interactions between sulphur dioxide and microbiologically produced nitrite and nitrate. These results suggest that in polluted environments nitrate in contrast to sulphate is not stable. Consequently, the nitrate content of building stone will not reflect the weathering processes that took place during a building's history. Conclusions drawn from the sulphate to nitrate ratio [*2*] will overestimate the importance of sulphuric acid influenced corrosion. Taking into consideration that emissions of sulphur dioxide are decreasing [*2*], the danger to historical buildings by biogenic nitric acid corrosion may increase in the future.

Acknowledgments

This work was funded by a grant from The Federal Minister for Research and Technology in Germany. We gratefully appreciate the support of Dr. H. Schulze.

We thank M. Langenfeld and Professor R. Blaschke from the Amtliche Materialprüfanstalt (MPA) Bremen, Germany for the contribution of scanning light electron microscopy. Dr.

W. Sand provided valuable help with the manuscript and S. Schröder provided excellent technical assistance. This article is based on a doctoral study by R. Mansch in the Faculty of Biology, University of Hamburg.

References

[1] Graedel, T. E. and McGill, R., "Degradation of Materials in the Atmosphere," *Environmental Science and Technology*, Vol. 20, 1986, pp. 1093–1100.

[2] Leysen, L., Roekens, E., and Van Grieken, R., "Air-Pollution-Induced Chemical Decay of a Sandy-Limestone Cathedral in Belgium," *The Science of the Total Environment*, Vol. 78, 1989, pp. 263–287.

[3] Johansson, L.-G., Lindqvist, O., and Mangio R. E., "Corrosion of Calcareous Stones in Humid Air Containing SO_2 and NO_2," *Durability of Building Materials*, Vol. 5, 1988, pp. 439–449.

[4] Gauri, K. L. and Holden G. C., Jr., "Pollutant Effects on Stone Monuments," *Environmental Science & Technology*, Vol. 15, No. 4, 1981, pp. 386–390.

[5] Vale, J. and Martin, A., "Deterioration of a Sandstone in Simulated Atmospheres," *Durability of Building Materials*, Vol. 3, 1986, pp. 183–196.

[6] Vale, J. and Martin, A., "Deterioration of a Calcareous Stone in Simulated Atmospheres," *Durability of Building Materials*, Vol. 3, 1986, pp. 197–212.

[7] Haneef, S. J., Dickinson, C., Johnson, J. B., Thompson, G. E., and Wood, G. C., "Report on a Research Project Supported by the Commission of the European Communities," *European Cultural Heritage News Letter on Research*, Vol. 4, No. 3, 1990, pp. 9–16.

[8] Johnson, J. B., Haneef, S. J., Hepburn, B. J., Hutchinson, A. J. Thompson, G. E., et al., "Laboratory Exposure Systems to Simulate Atmospheric Degradation of Building Stone Under Dry and Wet Deposition Conditions," *Atmospheric Environment*, Vol. 24A, No. 10, 1990, pp. 2585–2592.

[9] Deloupoulou, P. and Sikiotis, D., "The Corrosion of Penthelic Marble by the Dry Deposition of Nitrates and Sulphates," *The Science of the Total Environment*, Vol. 120, 1992, pp. 213–224.

[10] Bock, E. and Sand, W., "The Microbiology of Masonry Biodeterioration," *Journal of Applied Bacteriology*, Vol. 74, 1993, pp. 503–514.

[11] Torre de la, M. A., Gomez-Alarcon, G., Melgarejo, P., and Saiz-Jimenez, C., "Fungi in Weathered Sandstone from Salamanca Cathedral, Spain," *The Science of the Total Environment*, Vol. 107, 1991, pp. 159–168.

[12] The Federal Minister for Science and Technology, "Outline of Research in the Federal Republic of Germany on the Preservation of Historic Natural Stone Buildings and Monuments," *European Cultural Heritage News Letter on Research*, Vol. 2, No. 1, 1988, pp. 16–20.

[13] Bock, E. and Sand, W., "Microbially Influenced Corrosion of Concrete and Natural Sandstone," in *Microbially Influenced Corrosion and Biodeterioration*, N. J. Dowling, M. W. Mittelman, and J. C. Danko, Eds., The University of Tennessee, Knoxville, 1990, pp. 29–33.

[14] Buijsman, E., Maas, H. F. M., and Asman, W. A. H., "Anthropogenic NH_3 Emissions in Europe," *Atmospheric Environment*, Vol. 21, 1987, pp. 1009–1022.

[15] Bock, E., "Biologisch Induzierte Korrosion von Naturstein-Starker Befall mit Nitrifikanten," *Bautenschutz und Bausanierung*, Vol. 10, No. 5, 1986, pp. 24–26.

[16] Bock, E., Ahlers, B., and Meyer, C., "Biogene Korrosion von Beton und Natursteinen Durch Salpetersäure Bildende Bakterien," *Bauphysik*, Vol. 4, 1989, pp. 141–145.

[17] Meincke, M., Krieg, E., and Bock, E., "*Nitrosovibrio* spp., the Dominant Ammonia-Oxidizing Bacteria in Building Sandstone," *Applied and Environmental Microbiology*, Vol. 55, No. 8, 1989, pp. 2108–2110.

[18] Bock, E., Koops, H. P., Möller, U. C., and Rudert, M., "A New Falcultatively Nitrite Oxidizing *Bacterium Nitrobacter Vulgaris* sp. nov.," *Archives of Microbiology*, Vol. 153, 1990, pp. 105–110.

[19] Dunk, R., Mostyn, R. A., and Hoare, H. C., "The Determination of Sulfate by Indirect Atomic Absorption Spectroscopy," *Atomic Absorption Newsletter*, Vol. 8, 1969, pp. 79–81.

[20] Fahrig, N., "Mikroorganismen in Steinen Historischer Bauten-eine Datenanalyse," Diploma thesis, University of Hamburg, 1991.

[21] Wilimzig, M., Fahrig, N., and Bock, E., "Biologically Influenced Corrosion of Stones by Nitrifying Bacteria," in *Proceedings of the 7th International Congress on Deterioration and Conservation of Stone*, J. D. Rodrigues, F. Henriques, and F. T. Jeremias, Eds., Laboratório Nacional de Engenharia Civil, Lisbon, Portugal, 1992, pp. 459–469.

[22] Freitag, A. and Bock, E., "Energy Conservation in *Nitrobacter*," *FEMS Microbiology Letters*, Vol. 66, 1990, pp. 157–162.

[23] Costerton, J. W. and Boivin, J., "The Role of Biofilms in Microbial Corrosion," in *Microbially Influenced Corrosion and Biodeterioration,* N. J. Dowling, M. W. Mittelman, and J. C. Danko, Eds., The University of Tennessee, Knoxville, 1990, pp. 85–86.

[24] Flemming, H. C., "Biofilms as a Particular Form of Microbial Life," in *Biofouling and Biocorrosion in Industrial Water Systems, Proceedings of the International Workshop on Industrial Biofouling and Biocorrosion,* H. C. Flemming and G. G. Geesey, Eds., Springer, Berlin, Heidelberg, New York, 1991, pp. 1–6.

[25] Allison, S. M. and Prosser, J. I., "Survival of Ammonia Oxidising Bacteria in Air Dried Soil," *FEMS Microbiology Letters,* Vol. 79, 1991, pp. 65–68.

[26] Sand, W., Ahlers, B., Krause-Kupsch, T., Meincke, M., Krieg, E., et al., "Mikroorganismen und Ihre Bedeutung für die Zerstörung von Mineralischen Baustoffen," *Zeitschrift für Umweltchemie und Ökotoxikologie,* Vol. 3, 1989, pp. 36–40.

[27] Tiedje, J. M., "Ecology of Denitrification and Dissimilatory Nitrate Reduction to Ammonia," in *Biology of Anaerobic Microorganisms,* A. J. B. Zehnder, Ed., Wiley, New York, 1989, pp. 179–244.

[28] Wilimzig, M., Fahrig, N., Meyer, C., and Bock, E., "Biogene Schwarze Krusten auf Gesteinen," *Bautenschutz und Bausanierung,* Vol. 16, No. 2, 1993, pp. 22–25.

Joanne Jones-Meehan,[1] *Kunigahalli L. Vasanth,*[1] *Regis K. Conrad,*[1] *Maria Fernandez,*[2] *Brenda J. Little,*[3] *and Richard I. Ray*[3]

Corrosion Resistance of Several Conductive Caulks and Sealants from Marine Field Tests and Laboratory Studies with Marine, Mixed Communities Containing Sulfate-Reducing Bacteria (SRB)

REFERENCE: Jones-Meehan, J., Vasanth, K. L., Conrad, R. K., Fernandez, M., Little, B. J., and Ray, R. I., **"Corrosion Resistance of Several Conductive Caulks and Sealants from Marine Field Tests and Laboratory Studies with Marine, Mixed Communities Containing Sulfate-Reducing Bacteria (SRB),"** *Microbiologically Influenced Corrosion Testing, ASTM STP 1232*, Jeffery R. Kearns and Brenda J. Little, Eds., American Society for Testing and Materials, Philadelphia, 1994, pp. 217–233.

ABSTRACT: Due to seawater intrusion and moisture accumulation, corrosion of antenna foundations/ship's super-structure has been observed and was attributed to galvanic corrosion of the aluminum with the silver-based conductive caulk used for electromagnetic interference/electromagnetic pulse (EMI/EMP) conductivity between the antennas and the ship's super-structure. Several conductive caulks and sealants were field tested and evaluated to determine if the environment would degrade their performance, for the prevention of seawater intrusion, and to prevent potential failures due to corrosion. A nickel-based conductive caulk with a corrosion inhibitor (PRC 1764) performed well in all of the field tests over a period of 15 months. Because of the excellent corrosion resistance, adequate EMI/EMP and shielding characteristics, the nickel-loaded caulk with a corrosion inhibitor has been recommended for antenna applications. Among the sealants, GE RTV 157, GE RTV 167 and Product Research Corporation ProSeal 870 polysulfide performed well. GE RTV 157 is already in use for topside applications and its use is being continued.

Three conductive caulks (PRC 1764, PI 8500, PI 8505) were applied to 4140 steel coupons. Caulked coupons were exposed to five mixed, microbial cultures in the laboratory for 15 months. At the end of the exposure period, environmental scanning electron microscopy (ESEM) analyses were used to demonstrate that bacteria including sulfate-reducing bacteria (SRB) were found under the conductive caulks. In laboratory testing, there was water and bacterial intrusion which resulted in corrosion of the steel under the conductive caulk. The laboratory caulked samples were not covered with a sealant such as RTV as described previously for the field test samples.

KEYWORDS: conductive caulks, corrosion-resistant sealants, electromagnetic interference/electromagnetic pulse (EMI/EMP) sealants, antenna arrays, environmental scanning electron microscopy (ESEM), energy dispersive X-ray spectrometry (EDS), microbiologically influenced corrosion (MIC), biodegradation, sulfate-reducing bacteria (SRB)

[1] Microbiologist, research chemist, and materials research engineer, respectively, Naval Surface Warfare Center, 10901 New Hampshire Ave., Silver Spring, MD 20903-5000.

[2] Materials engineer, Naval Surface Warfare Center, 1650 Southwest 39th St., Ft. Lauderdale, FL 33315-3528.

[3] Research chemist and physical science technician, respectively, Naval Research Laboratory-Detachment, Stennis Space Center, MS 39529-5004.

AN/SPY-1 antenna arrays are highly critical systems on ships. Both the ship's superstructure and the antennas are made from aluminum alloy Al 6061-T6. A conductive caulk is needed to fill gaps between the antenna and super structure in order to preserve electrical continuity. A silver-plated copper filled conductive caulk was used in the gap along the perimeter of the arrays. A nonconductive sealant (room temperature vulcanized rubber [RTV]) was applied as an overcoat to prevent seawater intrusion.

Kohlman [*1*] reported that the primary failure mode of electromagnetic and radio frequency interference (EMI/RFI) sealants was due to galvanic corrosion. In an earlier investigation of a damaged antenna, seawater intrusion and moisture accumulation resulted in corrosion of the antenna foundation. This crevice corrosion was attributed to galvanic corrosion of aluminum with the silver-based conductive caulk (PI 8500) or silver copper loaded caulk (Chobond 4669, PI 8505) used for mounting the antennas on the ship's superstructure (see Fig. 1).

In this report, the authors describe an evaluation of several conductive caulks and sealants for the prevention of seawater intrusion and to prevent potential failures due to corrosion. The conductive caulks were tested in flume tanks (constant immersion and alternate immersion) and on atmospheric racks at NAVSWC, Ft. Lauderdale, FL. Coating deterioration in the presence of an adherent biofilm (that is, mixed communities containing SRB; microbial metabolites, polymers, and enzyme activities; inorganic ion deposits) is of interest to our laboratories. Coating deterioration was assessed by visual observations, environmental scanning electron microscopy (ESEM) and energy dispersive X-ray spectrometry (EDS).

Materials and Methods

Conductive Caulks and Sealants Tested

In field testing experiments, we evaluated several conductive caulks (Chomerics Chobond 4669, AI Technology PI 8500 and PI 8505, Products Research Corp. PRC 1764, Emerson

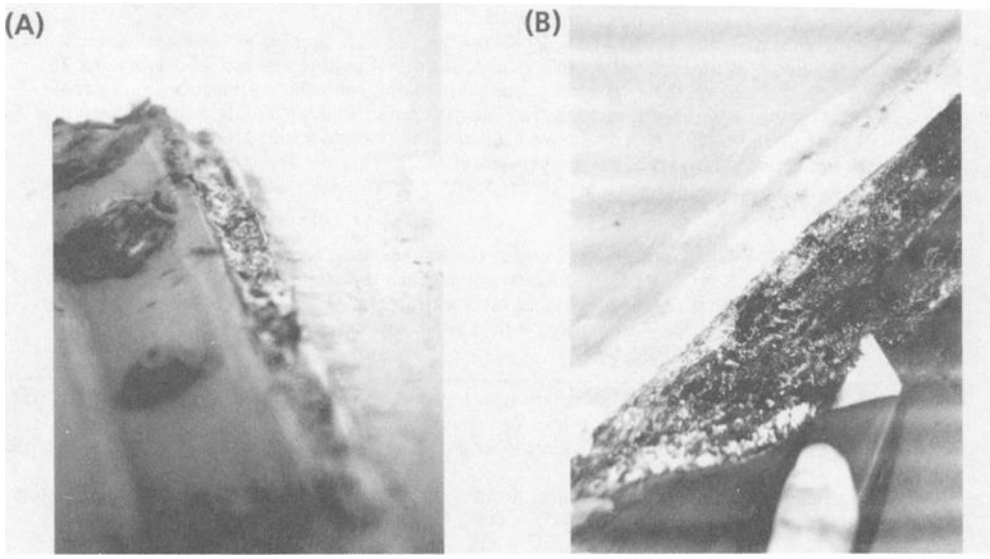

FIG. 1—*In-service corrosion problems (including flaking off of the Chobond 4669) between the antenna and the ship's superstructure.*

Cummings Inc. Ecoshield VY-NC) and sealants (Product Research Corp. 870-B2 Polysulfide, RayChem GelTeK, GE RTV 157, GE RTV 167) for the prevention of seawater intrusion and to prevent potential failures due to corrosion. These conductive caulks were tested in natural seawater flume tanks (that is, constant immersion with seawater circulated at about 3 gal/min; alternate immersion with repeating cycles of sample immersion for 24 h followed by a 6 day exposure to the atmospheric marine environment) and on atmospheric exposure racks at the NAVSWC Marine Corrosion Field Test Facility at Ft. Lauderdale, FL. Environmental parameters (range) measured in the constant immersion flume tank were: pH, 8.0 to 8.25; air SO_2, 0 to 0.38 ppm; tank temperature, 25 to 28°C; conductivity, 53 to 55.3 × 10^3 μΩ; salinity, 3.5% (wt/vol) NaCl and dissolved oxygen, 3 to 5.8 mg/L.

Sample Configurations for Field Tests

The following two sample configurations were tested: (1) scratch test coupons, and (2) assemblies to simulate the interface between the aluminum antenna array and the ship's aluminum foundation. For scratch test coupons, the surface was scribed to simulate damage which was covered with conductive caulk or a sealant. This test was used to determine the adhesion of a conductive caulk or sealant, as well as to determine whether these caulks/sealants protected the scribed areas from corrosion. The assembly perimeters were sealed using a layer of conductive caulk or conductive caulk with an RTV 157 sealant overcoat. Some assemblies were constructed with a bottom plate of Al 6061 and a Plexiglas® top plate for visual assessment of the bottom plate; these assemblies were tested in the flume tanks described previously.

Microbial Communities and Caulks Tested in the Laboratory

Five marine, mixed communities were isolated from corroding, in-service materials (see Table 1). The isolation, maintenance and characterization of the mixed communities containing SRB has been described previously [2]. All cultures were grown anaerobically at room temperature in sealed bottles. These mixed cultures contained strict anaerobes (SRB)

TABLE 1—*Hydrogenase activity in the mixed, microbial populations containing sulfate-reducing bacteria (SRB).*

Culture[a]	Isolated Originally On: Material + Topcoat(s)	Hydrogenase Activity[b] 2½ h	4 h	24 h
P10	4140 Steel + 5 Step Iron Phosphate	0	+1	+2
P14	4140 Steel + 5 Step Iron Phosphate + Epoxy	+1	+1	+2
49Z	4140 Steel + Zinc Plate	+2	+2	+2
I14	4140 Steel + IVD-Aluminum + Nylon	+2	+2	+2
CPNC	Aluminum Alloy + Epoxy + Polyurethane	0	0	+2

[a] Cultures P10–I14 were isolated from a constant immersion flume tank at NSWC/Ft. Lauderdale, FL. SRB in cultures P10–I14 require NaCl for growth (halophilic). Culture CPNC was isolated from moisture trapped under the cargo ramp of a C-130 transport plane at the NADEP in Cherry Point, NC. SRB in culture CPNC are facultative halophiles (do not need NaCl for growth but can grow in seawater concentrations of NaCl).

[b] Activity of the hydrogenase enzyme is measured with a Caproco Hydrogenase Test Kit. The rating system is from 0 to 3. A negative reaction is rated as 0, weak reaction is +1 (0 to 0.5 nmol of hydrogen uptake/min), moderate reaction is +2 (0.05 to 5 nmol of hydrogen uptake/min) and a strong reaction is +3 (5 to 5000 nmol of hydrogen uptake/min).

TABLE 2—*Conductive caulks applied to 4140 steel for use in ESEM/EDS analyses.*

Characteristic[a]	PRC 1764	PI 8500/8505[b]
Color	Black	Silver Gray
Filler	Ni	Ag
Inhibitor	Chromate	None
Corrosion Behavior After 1000 h Salt Fog	No Corrosion	Resistant to Salt Fog

[a] Information provided by the vendors (PRC 1764, Product Research and Chemical Corporation, 5430 San Fernando Road, Glendale, CA 91203; PI 8500/8505, AI Technology, Inc., Chemical Division, P.O. Box 3081, Princeton, NJ 08543).

[b] PI 8505 is listed by the vendor as a silver loaded conductive caulk, but our EDS analyses show PI 8505 to be a silver copper loaded conductive caulk.

and facultative anaerobes (non-sulfate reducers). The SRB mixed communities were tested for hydrogenase activity using Caproco Hydrogenase Test Kits (Caproco Limited, Edmonton, Alberta, Canada). Color development is rated after 4 h, but to detect weak enzyme activities, color development is allowed to occur for 24 h (see Table 1).

Three conductive caulks (PRC 1764, PI 8500, PI 8505) were applied to coupon surfaces (¾ by ¾ in. 4140 steel and 4140 steel with an IVD-aluminum primer coat). Some characteristics of these three conductive caulks are shown in Table 2. The laboratory caulked samples were not covered with a sealant such as RTV as already described for the field test samples. Caulked steel coupons were exposed to the mixed cultures in an anaerobic environment in the laboratory at room temperature for 15 months. At the end of the exposure period, ESEM analyses were used to demonstrate that bacteria including SRB were found under the conductive caulks.

ESEM/EDS Studies

At the end of the laboratory exposure period of 15 months, surface topography and chemistry were documented using an Electroscan Model E-30 environmental scanning electron microscope and a Tracor Northern Model 5502 energy dispersive X-ray spectrometer (ESEM/EDS). Coupons were removed from the culture medium, carried through a series of salt water/distilled water washes and examined directly from distilled water.

Results

Constant Immersion Testing

After 2 months of constant immersion, scribed coupons with PI 8500 (silver particle loaded conductive caulk) or PI 8505 (silver copper loaded conductive caulk) showed severe deterioration of the caulk, which resulted in corrosion of the scribed aluminum region under the caulk. Chobond 4669 (silver loaded conductive caulk by Chomerics) showed a mild degradation of the caulk. In contrast, no degradation of PRC 1764 (nickel loaded conductive caulk and chromate as a corrosion inhibitor) was observed. Figure 2 shows no degradation/corrosion on the PRC 1764 coated coupon after 2 months constant immersion in natural seawater, but severe corrosion was observed with PI 8505 on chromated Al 6061 and on

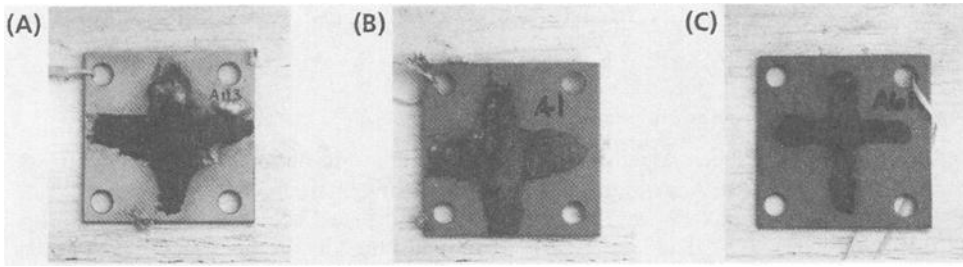

FIG. 2—*Visual observations after 2 months constant immersion:* A, *PI 8505 on chromated Al 6061 showed severe corrosion;* B, *PI 8505 on topcoated Al 6061 showed severe corrosion; and* C, *PRC 1764 showed no corrosion.*

topcoated Al 6061. Figure 3 shows no corrosion of the scribed coupon coated with PRC 1764 after 6 months of constant immersion. After 12 months of constant immersion, the silver loaded conductive caulks showed significant degradation and loss of adhesion resulting in corrosion of the aluminum substrate, while the nickel loaded conductive caulk showed no degradation or loss of adhesion to the substrate.

The assemblies exposed to constant immersion showed results similar to the scribed coupons. The PI 8500 and PI 8505 silver loaded conductive caulks performed poorly (that is, the caulk came off the steel bolt heads which allowed for severe corrosion of the steel substrate). Ecoshield VY-NC is a nickel loaded, black-colored caulk (does not contain an inhibitor) that shrank and cracked along the perimeter during curing, therefore this conductive caulk does not meet the necessary requirements for prevention of water intrusion.

Among the sealants, GE RTV 157 and PRC 870-B2 showed good adhesion and no signs of degradation after a 12 month constant seawater immersion test. GE RTV 157 is already in use for topside applications and its use is being continued.

Alternate Immersion Testing

Similar results for the conductive caulks and sealants on scribed coupons and on assemblies were obtained after 12 months of alternate seawater immersion testing as was seen in the constant seawater immersion testing. Figure 4 shows PRC 1764 coated test assemblies ex-

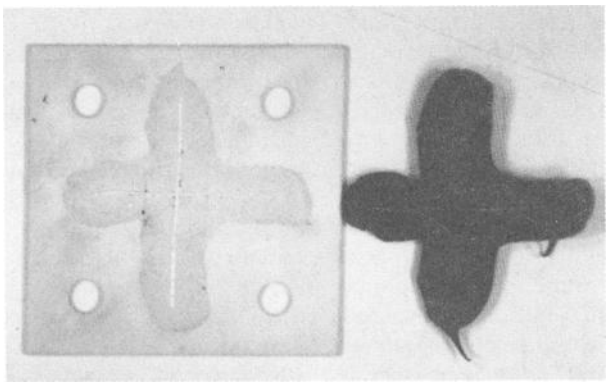

FIG. 3—*Scribed coupon coated with PRC 1764 showed no corrosion under the caulk after 6 months constant immersion.*

posed to alternate immersion testing for 2½ months and for 8 months. Some surface fouling was seen but no corrosion was observed.

Atmospheric Exposure Testing

Similar results for the conductive caulks and sealants were obtained after 12 months of atmospheric exposure as was observed in the constant and alternate immersion testing. The PI 8500 and PI 8505 caulks showed severe corrosion of the steel bolts due to loss of adhesion of the caulk (see Fig. 5). The scratch test failed due to the loss of adhesion of these caulks to the substrates. PRC 1764 performed very well with no loss of adhesion to the substrate.

ESEM Studies and Visual Observations

EDS data were collected at the same time as the sample morphology and topography were photographed. A variety of cell morphologies (including short rods, long rods, vibrio, spirillum and cocci) were seen in the mixed communities attached to the coupon surfaces. Bacteria were attached to the steel surface and were distributed throughout the biofilm layers of corrosion products, bacterial exopolymers and inorganic ion deposits. Figures 6 and 7 show the microbial biofilm on the 4140 steel surface under PRC 1764. The chemical composition (EDS spectra) of the steel surface under the PRC 1764 is shown for a mixed culture grown without NaCl and a mixed culture grown with NaCl (note Cl concentrated in this biofilm under the caulk at the steel surface; see Fig. 8).

Figures 9 and 10 show microbial intrusion for PRC 1764 on IVD-aluminum coated 4140 coupons. Figures 11 and 12 show microbial intrusion for PI 8500 on 4140 steel and on IVD-aluminum coated 4140 steel, respectively. Table 3 is a summary of EDS analyses of the steel surface underneath the conductive caulks. Water intrusion (Cl peak or Cl and Na peaks) and bacterial intrusion including SRB (S peak) resulted in corrosion of the steel surface under the conductive caulks.

Discussion

A nickel-based conductive caulk with a corrosion inhibitor (PRC 1764) has performed well in all of the field tests over a period of 15 months [*3,4*]. Because of the excellent corrosion resistance, adequate EMI and shielding characteristics, PRC 1764 has been recommended for antenna applications. Kohlman [*1*] evaluated eight corrosion resistant EMI/RFI sealants and selected a nickel-filled polythioether sealant (PRC 1764) based on its relatively low cost, excellent corrosion resistance and superior shielding effectiveness.

Among the sealants, GE RTV 157 and some of the other sealants performed well. GE RTV 157 is already in use for topside applications and its use is being continued. It is important that the surface be properly treated and good quality control be followed in the application of RTV to prevent seawater intrusion through pinholes or areas that received inadequate sealant coverage.

Corrosion is often extremely rapid at small discontinuities in coatings, and breaks or blisters in coatings may allow access of corrosion-inducing microbes, such as sulfate-reducing bacteria (SRB), to the metal beneath [*5*]. SRB are a diverse group of anaerobic bacteria that can be isolated from many anaerobic environments but their principal habitat is the marine environment where the concentration of sulfate in seawater is high and fairly constant [*6*]. Jones et al. [*2*], using SEM/EDS and EIS, described the microbial attack of epoxy, polyurethane and nylon coated 4140 steel by mixed communities of strict anaerobes (SRB) and facultative anaerobes isolated from corroding, in-service naval materials. For protective coatings to be effective, they must be resistant to microbial degradation.

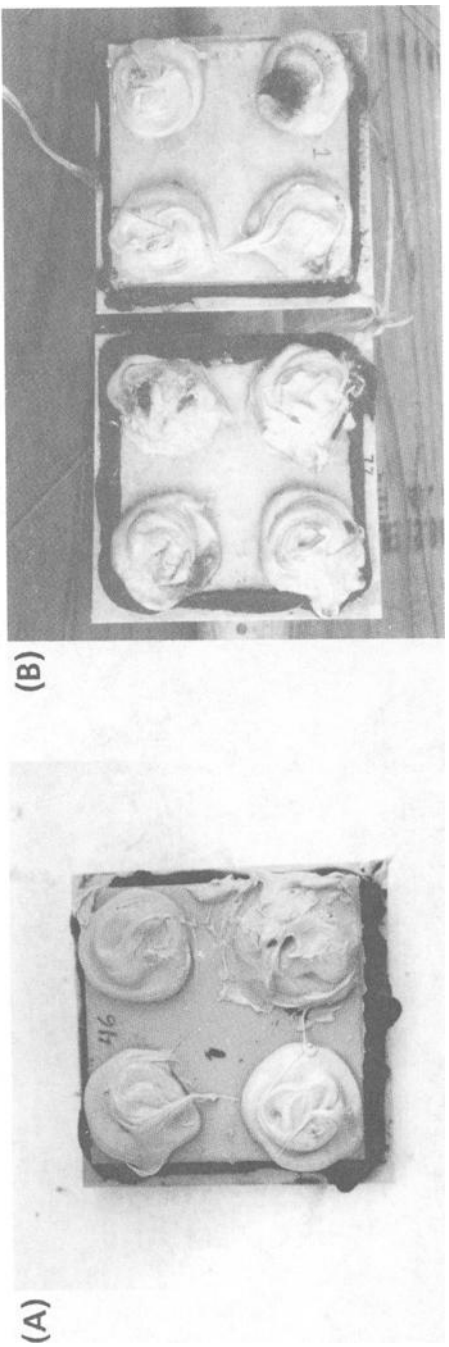

FIG. 4—*PRC 1764 coated assemblies showed no corrosion problems after a 2½ month (panel* A*) and a 9 month (panel* B*) exposure to alternate immersion.*

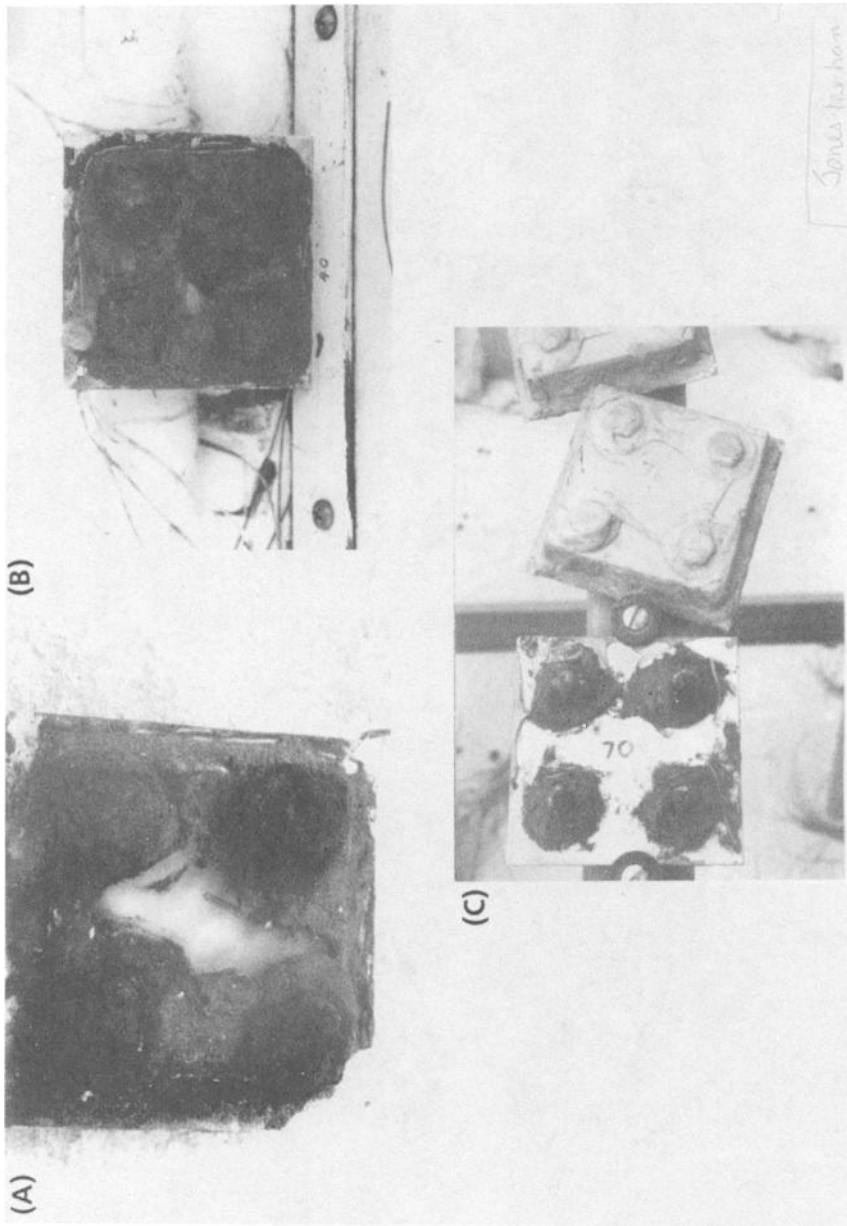

FIG. 5—*Severe corrosion of the steel bolts due to loss of adhesion of PI 8500 was observed with 4 months alternate immersion of PI 8500 on a clear plastic assembly* (A), *with 4 months constant immersion of PI 8500 on a clear plastic assembly* (B) *and with an 8 month exposure on an atmospheric rack (coupon marked 70 on left side of panel* C).

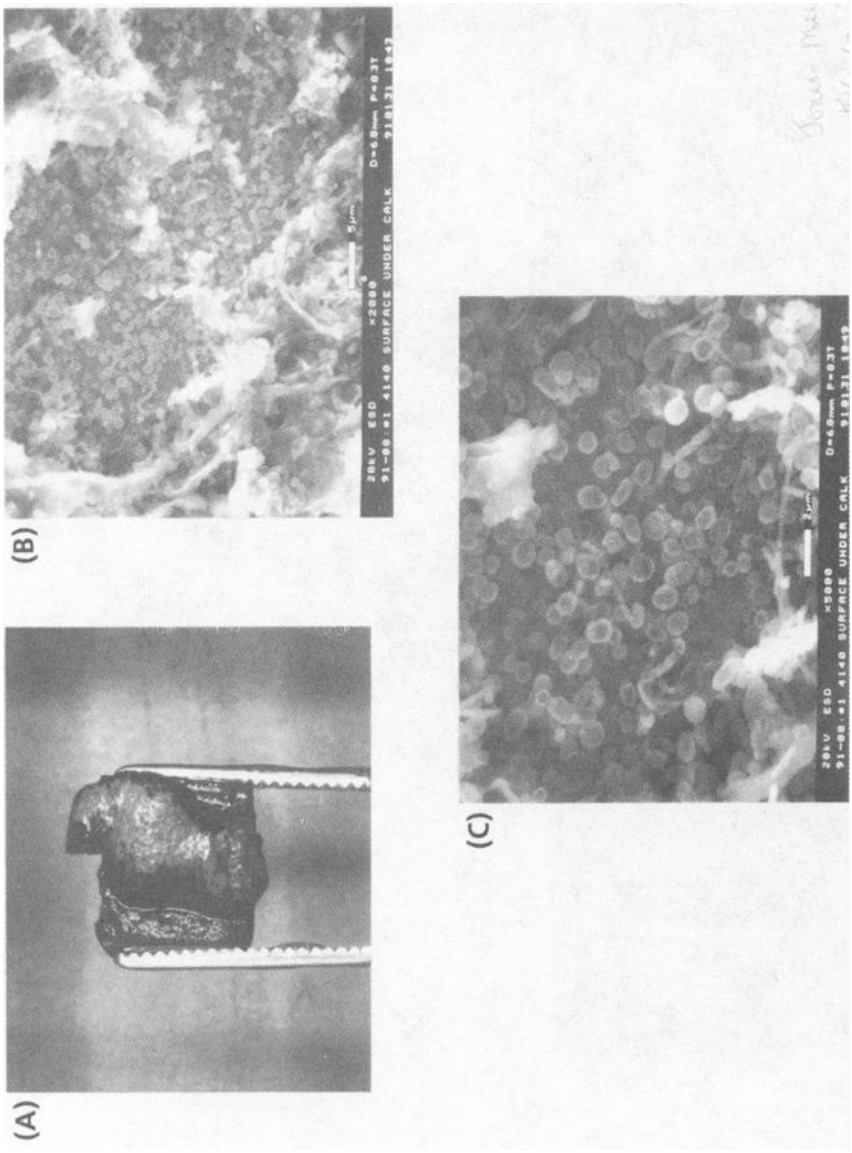

FIG. 6—A, *photograph of the corrosion seen for PRC 1764 on 4140 steel after exposure for 15 months to CPNC mixed culture (growth medium did not contain NaCl);* B *and* C, *ESEM of the microbial biofilm on the steel surface under the PRC 1764.*

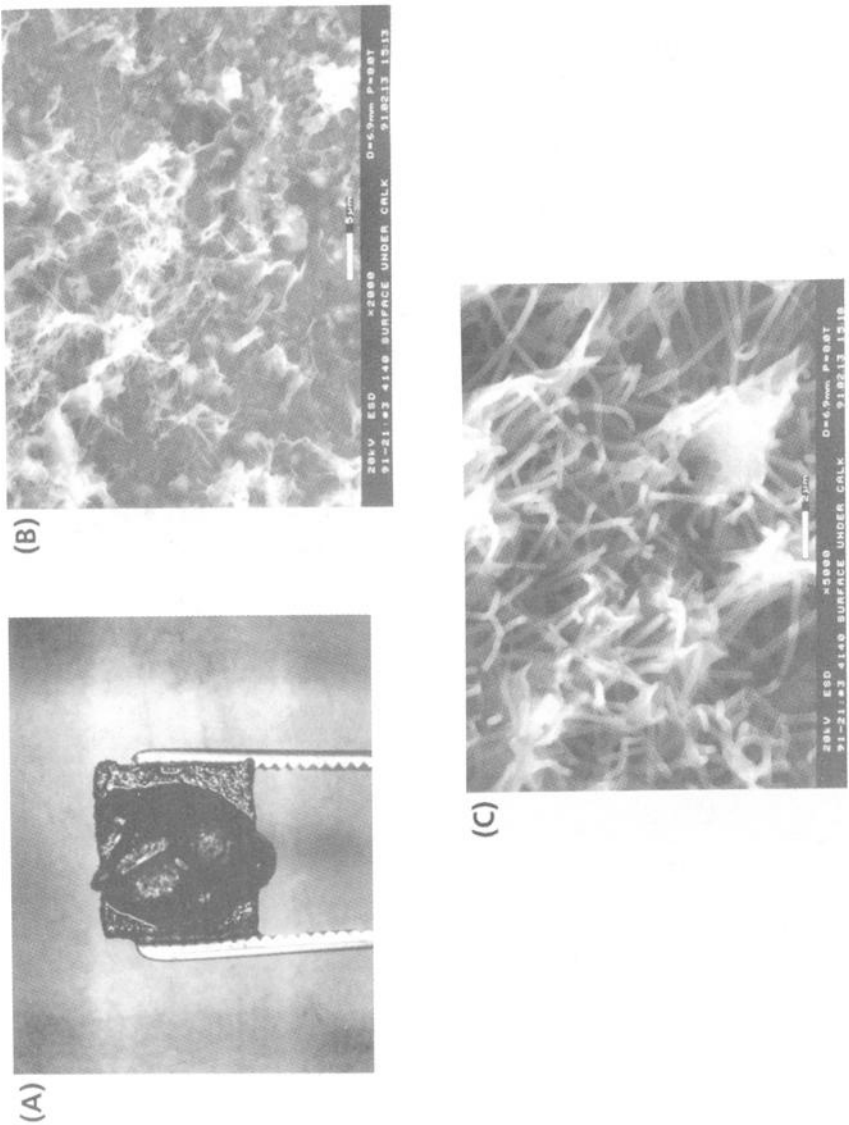

FIG. 7—A, *photograph of the corrosion seen for PRC 1764 on 4140 steel after exposure for 15 months to 114 mixed culture (growth medium contained NaCl);* B *and* C, *ESEM of the microbial biofilm on the steel surface under the PRC 1764.*

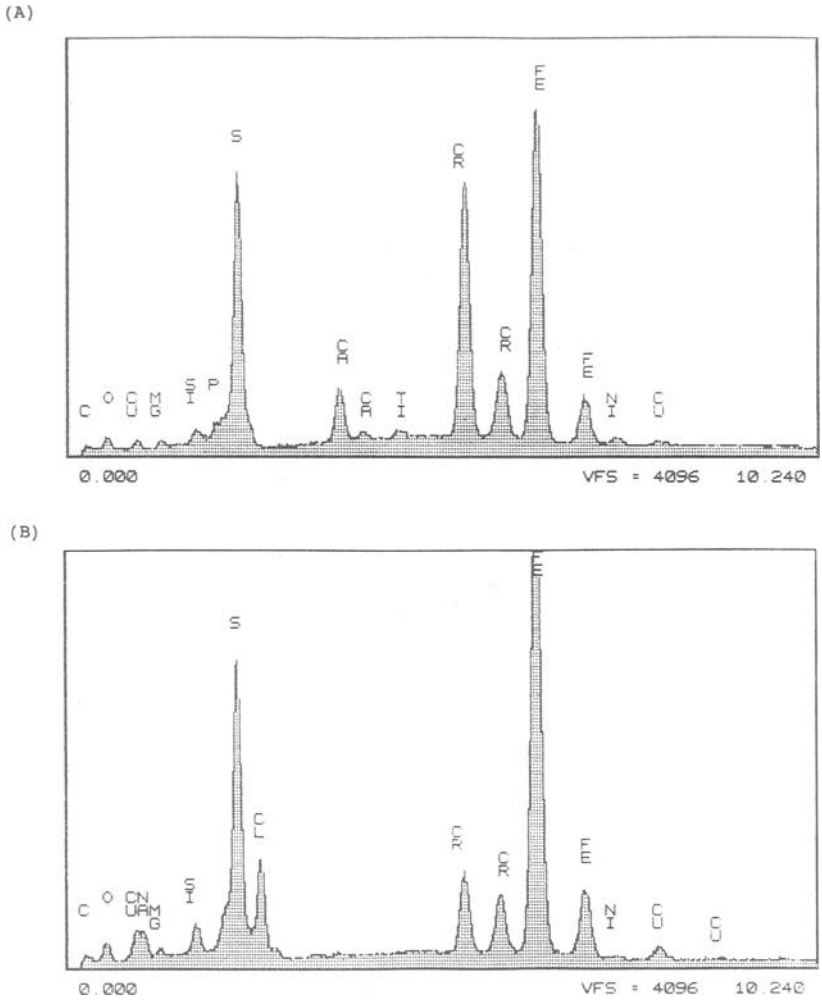

FIG. 8—*EDS spectra of the 4140 steel surface under PRC 1764 after exposure to CPNC mixed culture in growth medium without NaCl* (A) *and after exposure to 114 mixed culture in growth medium with NaCl* (B; *note the concentration of Cl in the biofilm at the steel surface*).

Breaches in protective coatings can lead to rapid localized corrosion and may allow access of other bacteria to the underlying metal, perhaps further exacerbating the corrosion problem [*5*]. Stranger-Johannessen [*7*] has described blistering and debonding of corrosion protective coatings by marine and soil microbes, as well as, fungal deterioration of coatings. Stranger-Johannessen and Norgaard [*8*] reported on observations that indicate microbial attack at the coating surface thereby changing its chemical and physical properties. Many other protective coatings may also be subject to biodeterioration, given that bacteria are capable of degrading an incredible variety of organic polymers and materials.

Environmental scanning electron microscopy (ESEM) offers a nondestructive method for observing the activity of microbial biofilms. The applicability and advantages of ESEM/EDS in studies of microbiologically influenced corrosion (MIC) have been discussed by

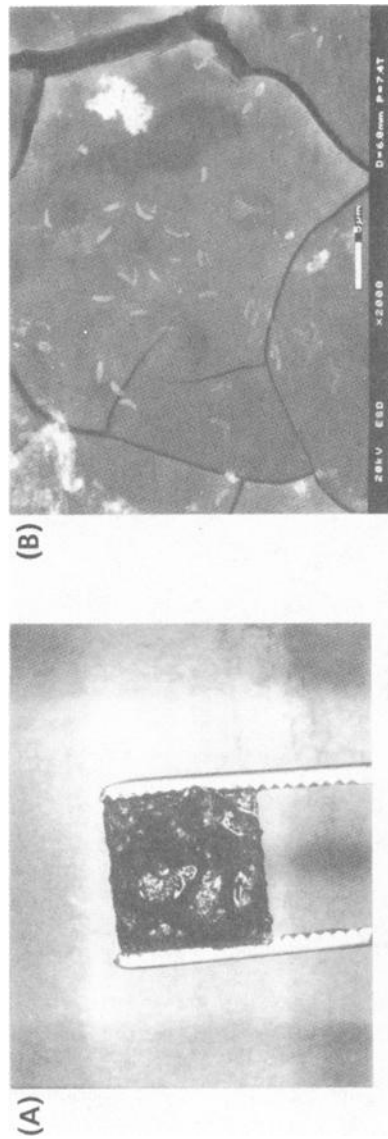

FIG. 9—A, *photograph of the corrosion seen for PRC 1764 on IVD-Al coated 4140 steel after 15 month exposure to 114 mixed culture (growth medium contained NaCl);* B, *ESEM of the microbial biofilm on the IVD-Al steel surface under the PRC 1764.*

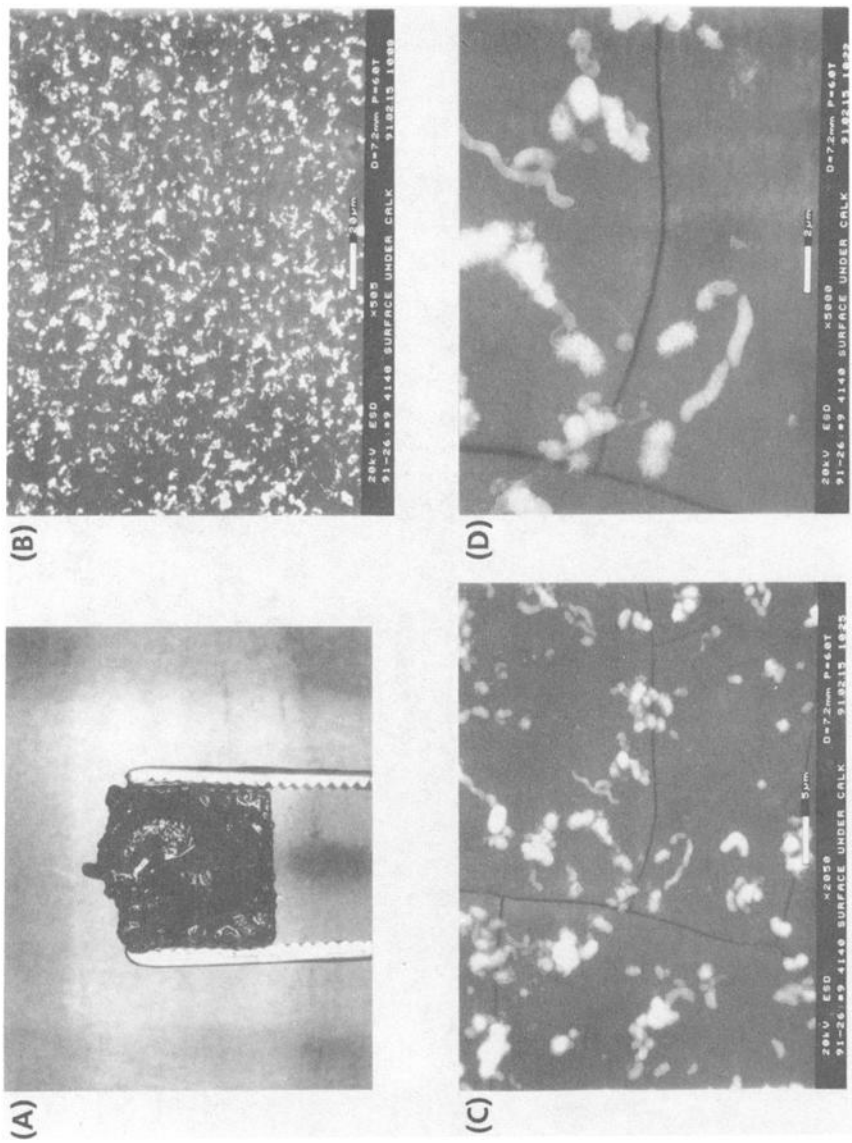

FIG. 10—A, *photograph of the corrosion seen for PRC 1764 on IVD-Al coated 4140 steel after 15 month exposure to 49Z mixed culture (growth medium contained NaCl);* B–D, *ESEM of the microbial biofilm on the IVD-Al steel surface under the PRC 1764.*

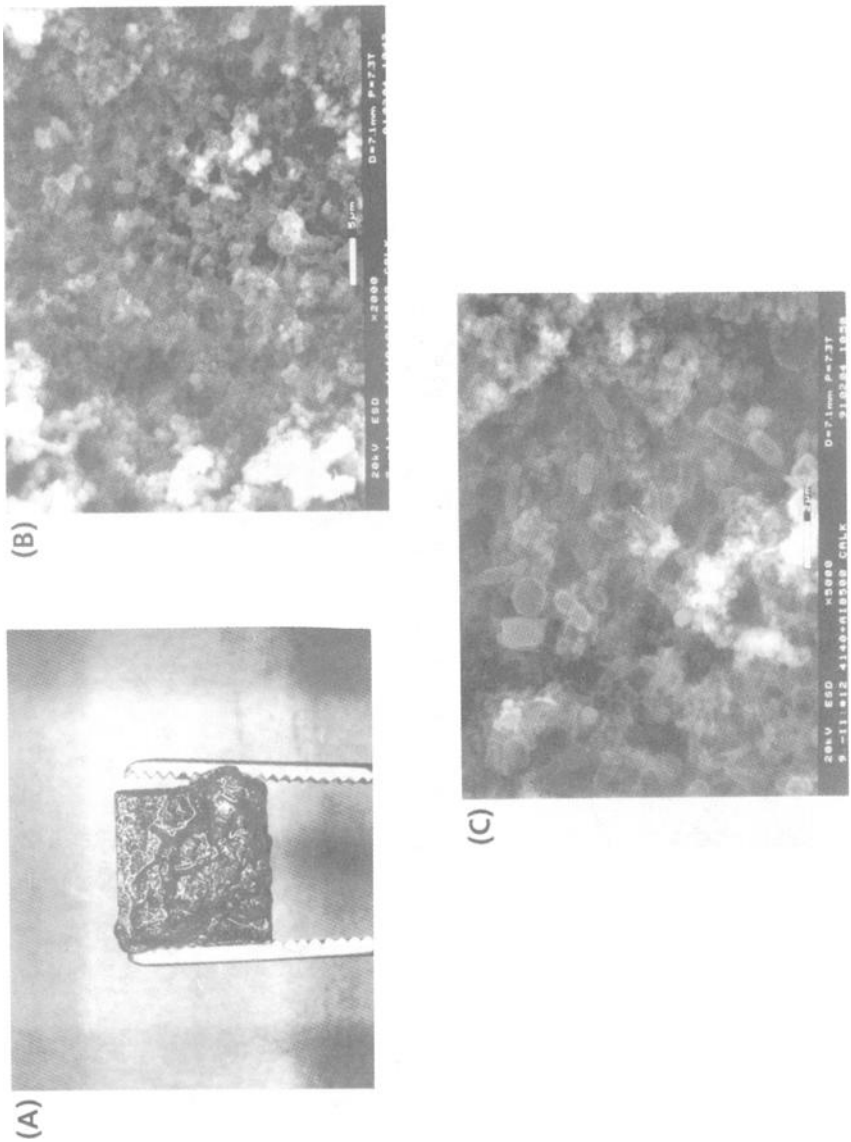

FIG. 11—A, *photograph of the corrosion seen for PI 8500 on 4140 steel after 15 month exposure to CPNC mixed culture (growth medium did not contain NaCl);* B–C, *ESEM of the microbial biofilm on the steel surface under the PI 8500.*

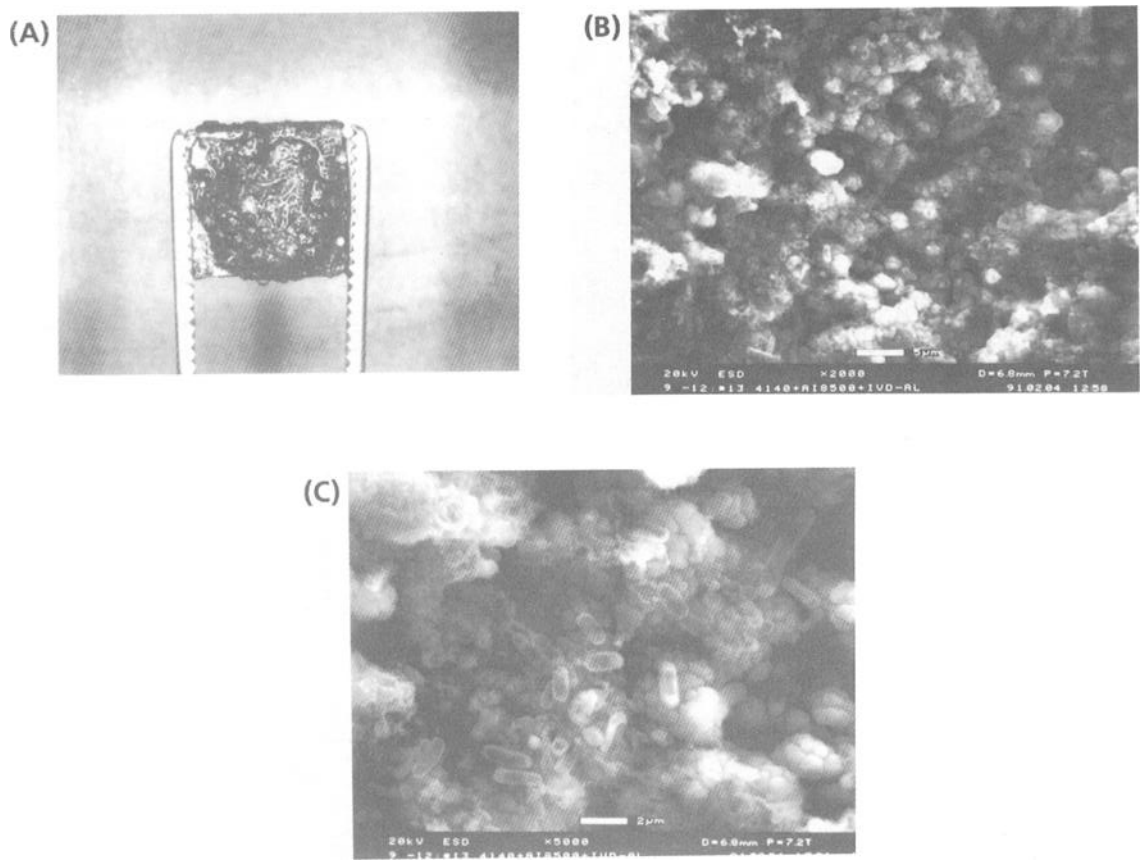

FIG. 12—A, *photograph of the corrosion seen for PI 8500 on IVD-Al coated 4140 steel after 15 month exposure to CPNC mixed culture (growth medium did not contain NaCl);* B–C, *ESEM of the microbial biofilm on the IVD-Al steel surface under the PI 8500.*

TABLE 3—*Detection of water intrusion and SRB on the steel surface under the conductive caulks by EDS analyses.*

Culture	Medium	Detected on Steel Surface Under Caulk Using EDS[a]		
		Cl	Na	S
PRC 1764 ON 4140 STEEL				
P10	+ NaCl	Yes	No	Yes
I14	+ NaCl	Yes	No	Yes
49Z	+ NaCl	Yes	No	Yes
P14	+ NaCl	Yes	No	Yes
CPNC	− NaCl	No	No	Yes
PRC 1764 ON IVD-AL COATED 4140 STEEL				
P10	+ NaCl	Yes	No	Yes
I14	+ NaCl	Yes	Yes	Yes
49Z	+ NaCl	No	No	Yes
P14	+ NaCl	Yes	Yes	Yes
CPNC	− NaCl	No	No	Yes
PI 8500 ON 4140 AND ON IVD-AL COATED 4140 STEEL				
CPNC	− NaCl	No	No	Yes
PI 8505 ON 4140 AND ON IVD-AL COATED 4140 STEEL				
CPNC	− NaCl	No	No	Yes

[a] PRC 1764 contains sulfur, therefore the EDS data for the S peak would be from the activity of sulfate reducing bacteria (SRB) and any residual caulk that may have remained on the steel surface. EDS data from the controls (uninoculated PI 8500 and PI 8505; PI 8500 and PI 8505 exposed to growth medium without SRB) did not show a sulfur peak. Therefore, the large S peak seen when these caulks were exposed to the CPNC culture was due to SRB activity in the biofilm attached to the steel surface under the caulks.

Little et al. [*9*] and Wagner et al. [*10*]. ESEM/EDS have been used in this study to show water intrusion (that is, EDS spectra showed chlorides concentrated in some of the SRB biofilms on steel surfaces) and bacterial intrusion (as shown in ESEM photographs) which resulted in corrosion of the steel under the conductive caulk.

SRB hydrogenase activity may influence the biocorrosion process and may be repressed or induced depending on the substrate and the bacterial consortia present in the biofilm [*9*]. The microbial composition of the mixed population which included SRB and the presence or absence of hydrogenase enzyme were two variables that influenced the biocorrosion process on SAE 1020 steel [*11*]. All the mixed SRB populations used in this study were hydrogenase-positive. To our knowledge, no one has looked at hydrogenase-negative and hydrogenase-positive mixed SRB populations to determine whether the hydrogenase enzyme plays a role in the microbial degradation of coatings, caulks and sealants.

Further MIC and coating degradation studies using pure and mixed SRB cultures (including hydrogenase-negative and hydrogenase-positive SRB) will provide more information about whether SRB hydrogenase plays a role in coating degradation. Laboratory MIC studies need to be performed with the conductive caulks covered by a sealant (that is, RTV) to determine if seawater and microbial intrusion would occur. If this intrusion occurred with the RTV topcoat over the conductive caulk, there would be corrosion problems at the metal/caulk interface.

Acknowledgments

Work at NSWCDDWODET was supported by the AEGIS Combat Systems Program Office NO5 (NAVSWC/Dahlgren, VA). Work at NRL-Detachment was supported by a contract from NSWCDDWODET (Code R301) and by the Office of Naval Research, Program Element 0601153N, through the Defense Research Sciences Program.

References

[1] Kohlman, S. D., "Corrosion Resistant EMI/RFI Sealant Evaluation," *Corrosion 89*, Paper No. 44, National Association of Corrosion Engineers (NACE), Houston, TX, 1989.

[2] Jones, J. M., Walch, M., and Mansfeld, F. B., "Microbial and Electrochemical Studies of Coated Steel Exposed to Mixed Microbial Communities," *Corrosion/91*, Paper No. 108, NACE, Houston, TX, 1991.

[3] Vasanth, K. L. and Conrad, R. K., "New Conductive Caulk for AN SPY-1 Antenna Array," *NAVSWC Corrosion Technology Newsletter*, June 1991.

[4] Vasanth, K. L. and Conrad, R. K., "Characterization of SPY-1A Antenna Foundation Corrosion in Marine Environment," *Navy Research & Development Exchange Conference Proceedings*, April 1991.

[5] Miller, J. D. A., *Microbial Aspects of Metallurgy*, American Elsevier Publishing Co., Inc., New York, 1970, pp. 31 and 97.

[6] Battersby, N. S., "Sulphate-Reducing Bacteria," *Methods in Aquatic Bacteriology*, B. Austin, Ed., John Wiley & Sons Ltd., New York, 1988, pp. 269–299.

[7] Stranger-Johannessen, M., "The Role of Microorganisms in the Blistering and Debonding of Corrosion Protective Organic Coatings," *Proceedings of the XVIII FATIPEC- Congress*, Venezia, 1986, Vol. 3, pp. 1–13.

[8] Stranger-Johannssen, M., Norgaard, E., "Deterioration of Anticorrosive Paints by Extracellular Microbial Products," *International Biodeterioration*, Vol. 27, 1991, pp. 157–162.

[9] Little, B., Wagner, P., Ray, R., Pope, R., and Sheetz, R., "Biofilms: An ESEM Evaluation of Artifacts Introduced During SEM Preparation," *Journal of Industrial Microbiology*, Vol. 8, 1991, pp. 213–222.

[10] Wagner, P. A., Little, B. J., Ray, R. I., Jones-Meehan, J., "Investigations of Microbiologically Influenced Corrosion Using Environmental Scanning Electron Microscopy," *Corrosion/92*, Paper No. 185, NACE, Houston, TX, 1992.

[11] Bryant, R. D., Jansen, W., Boivin, J., Laishley, E. J., "Effect of Hydrogenase and Mixed Sulfate-Reducing Bacterial Populations in the Corrosion of Steel," *Applied and Environmental Microbiology*, Vol. 57, 1991, pp. 2804–2809.

Wolfgang Sand,[1] *Thierry Dumas,*[2] *and Serge Marcdargent*[3]

Accelerated Biogenic Sulfuric-Acid Corrosion Test for Evaluating the Performance of Calcium-Aluminate Based Concrete in Sewage Applications

REFERENCE: Sand, W., Dumas, T., and Marcdargent, S., **"Accelerated Biogenic Sulfuric-Acid Corrosion Test for Evaluating the Performance of Calcium-Aluminate-Based Concrete in Sewage Applications,"** *Microbiologically Influenced Corrosion Testing, ASTM STP 1232,* Jeffery R. Kearns and Brenda J. Little, Eds., American Society for Testing and Materials, Philadelphia, 1994, pp. 234–249.

ABSTRACT: The corrosion of concrete structures in sewage environments is a major problem in some areas. The phenomena leading to formation and stripping of H_2S are now reasonably well understood. By a biologically-influenced process, the metabolism of thiobacilli, hydrogen sulfide is converted into sulfuric acid. This acid reacts with concrete and causes deterioration.

For the purpose of testing materials, this environment is often simulated by laboratory tests with concentrated acid solutions. Such tests, however, do not consider the bacterial aspect of the reality, and therefore, can lead to irrelevant conclusions.

For a reliable result, the interactions between living organisms and their substratum are essential and need to be taken into account. This task is achieved by the use of our simulation chamber for biogenic sulfuric-acid corrosion. The biologically-influenced corrosion is remodeled under conditions favoring the relevant microorganisms. Thus, an acceleration of the natural process is achieved.

Recent investigations conducted on calcium-aluminate-based mortars in the bacterial-corrosion chamber of Hamburg University demonstrated for these materials a good resistance against biogenic sulfuric-acid attack. These results are confirmed by on-site observations of sewer pipelines made of calcium-aluminate-based concrete inspected after up to 35 years of service in harsh environments.

KEYWORDS: biogenic sulfuric acid, corrosion, thiobacilli, Thiobacillus thiooxidans (T. thiooxidans), simulation, materials testing, biotest, calcium aluminate cement

Biogenic Sulfuric-Acid Corrosion (H_2S Corrosion)

The term biogenic sulfuric-acid corrosion is used for an attack of biologically-produced sulfuric acid on cement-bound materials. The acid is excreted by lithotrophic sulfur and sulfur compounds oxidizing bacteria as endproduct of their metabolism, or both. Therefore, this type of corrosion should be precisely called biogenic sulfuric-acid corrosion of cement-bound materials.

The biogenic sulfuric-acid corrosion occurs mainly in sewage pipelines/installations made of cement-bound concrete. In addition, cement-bound mortar (between bricks) is also de-

[1] University of Hamburg, Mikrobiologie, Ohnhorststraße 18, D-2000 Hamburg 52, Germany.
[2] Lafarge Fondu International, 157 avenue Charles de Gaulle, 92521 Neuilly, France.
[3] Lafarge Fondu International, ZI du Parc de Chesues, 95 rue du Montmurier, Saint Quentin Fallavier, 38291 La Verpillière, France.

stroyed. In general, all materials are destroyed that may react (chemically) with sulfuric acid.

Beyond the scope of this report are working materials that themselves may be used as substrate by microorganisms like some resins, sulfur-bound concrete, natural materials, and so forth. Even though these materials are of great public interest, the underlying corrosion mechanism is different from the one for biogenic sulfuric-acid corrosion and, thus, clearly differentiates them from the materials concerned here.

The fact that concrete sewers carrying sulfide-bearing sewage were subject to a rapid and extensive destruction was observed as early as 1900 [*1*]. It was observed that the destroyed concrete was highly acidic due to the presence of sulfuric acid.

Although various authors, including Morris in 1940 [*2*] and Pomeroy and Bowlus in 1946 [*3*] recognized the possibility that this sulfuric acid could have been produced by bacteria, it was generally thought that the corrosion process was due essentially to chemical transformations by which H_2S in the sewer air was converted to sulfate. The following extract from Lea and Desch's authoritative book on cement chemistry (1936) is indicative of the viewpoint: "It seems probable that the calcium sulfide or hydrosulfide first produced by the action of the hydrogen sulfide on the concrete, becomes converted in the presence of oxygen to calcium sulfide and sulfate. It is possible, however, that direct oxidation of hydrogen sulfide to sulfur dioxide may occur or that the calcium hydrosulfide may be oxidised to calcium thiosulfate, which subsequently decomposed by carbon dioxide, liberating thiosulfuric acid, as Rodt has suggested. Thiosulfuric acid readily decomposes to form sulfurous acid [*4*]."

In 1945, Parker published the discovery of strongly acid-forming bacteria from samples of corroded concrete sewage pipelines [*5*]. He called them Thiobacillus (T.) concretivorus, a synonym to T. thiooxidans (correct name). Since this discovery, the understanding began to develop that this type of corrosion is caused by the action of sulfur-oxidizing bacteria belonging mainly to the genus Thiobacillus.

Since, several reports have been published elucidating the mechanism of the biogenic sulfuric-acid corrosion in sewage pipelines [*6–12*]. Summarizing the literature, it becomes clear that the corrosion is a result of bacterial activity. It is to be assigned to the sulfur cycle, which in contrast to the carbon cycle (global warming), attracts considerably less public attention, although the phenomenon biogenic sulfuric-acid corrosion results to a considerable extent from the habits of the population. As it has been mentioned, the main source for biogenic sulfuric acid is the sulfur compound hydrogen sulfide, H_2S. It is produced by microorganisms that live in the sewage, in the mud at the bottom of the pipelines, and in the slime layer coating the surfaces of sewage pipelines above and below the water level. The layer may be called a biofilm. Under anaerobic conditions, sulfate-reducing bacteria (SRB) are active in these habitats, reducing oxidized sulfur compounds to H_2S. As H_2S is a weak acid, it becomes dissolved in the sewage under neutral or alkaline conditions. If the pH value decreases, for example, due to acidification, H_2S is emitted into the sewage atmosphere. Turbulences in the sewage flow are another reason for H_2S emission. Even at comparably low concentrations H_2S escapes into the gas phase (stripping). Once H_2S has reached the atmosphere it may react with oxygen to elemental sulfur that is deposited on the walls. In fact, this reaction may be accelerated catalytically by an alkaline surface. Sulfur is a good substrate for thiobacilli. By their metabolism, sulfur is oxidized to sulfuric acid. The energy obtained is used for CO_2-fixation for cell mass production. Figure 1 gives an overview of the sulfur cycle.

The endproduct sulfate may be used again by SRBs as a source of chemically-bound oxygen. Thus, the sulfur cycle is closed. As a side reaction, thiosulfate may also occur in sewage pipelines. Sulfur reacts chemically with sulfur dioxide, SO_2, to form thiosulfate. The

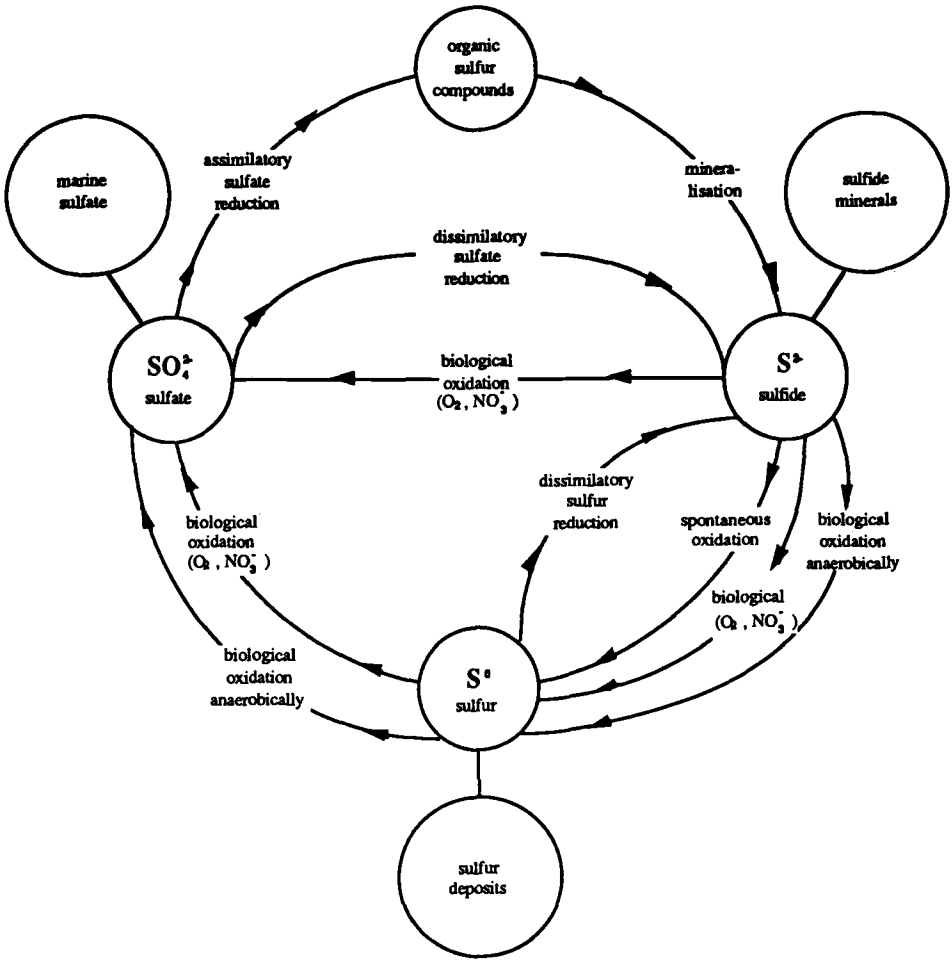

FIG. 1—*The sulfur cycle.*

thiobacilli themselves are one source for sulfur dioxide. During sulfur oxidation, T. thiooxidans produced measurable quantities of SO_2, probably indicating an overflow of the primary sulfuroxidation as compared with the sulfite oxidation. All these compounds have been detected by König and coworkers in sewage pipelines [*1–5,7,13,14*]. This type of sulfur cycle occurs in sewage pipelines, as illustrated in Fig. 2.

The H_2S production often seems to be the limiting factor, as H_2S is the substrate for conversion into sulfuric acid. However, man influences H_2S production in several ways. Most important is the temperature of the sewage itself. Because of an increasing use of hot water (for dishwashers, washing machines, showers, baths, and so forth), during the last decades the temperature of the sewage increased by several degrees celsius. Estimations range up to 10°C. It is well known that microorganisms convert their substrate at high temperatures more rapidly than at low temperatures, although the rate does not double, as in chemistry (10°C to → doubled reaction rate). Thus, increased acidification is caused. The second reason for increased H_2S production is the increased use of detergents containing

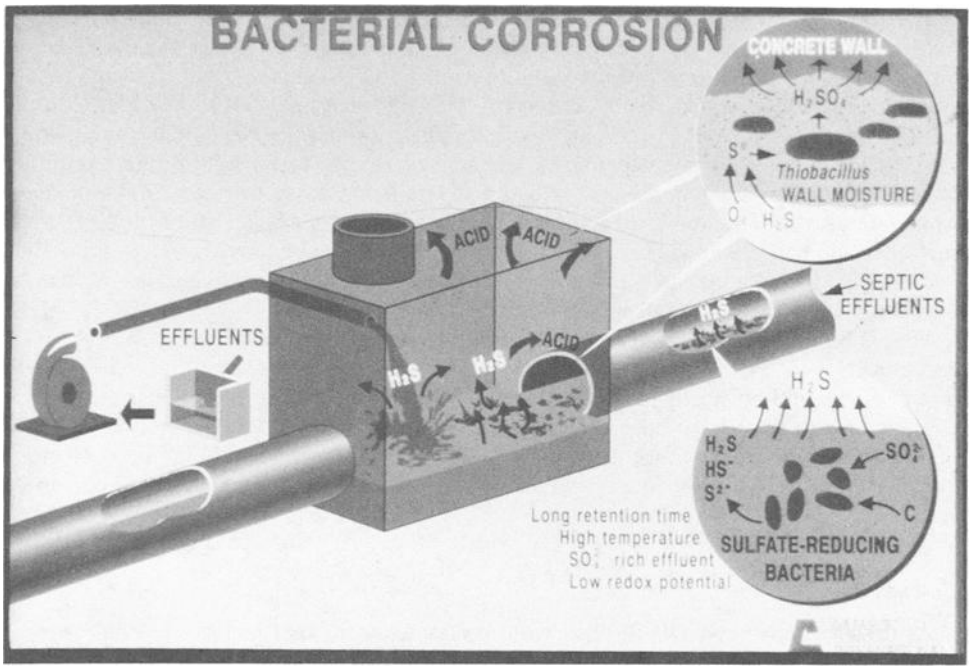

FIG. 2—*The sulfur cycle as it occurs in the sewage systems.*

sulfates and the increase in protein consumption. Whereas sulfates may be used by SRBs in the way described above, protein is reaching the sewage after digestion of food. It is degraded into amino acids. Two amino acids, methionine and cystein/cystin, contain sulfur atoms. The degradation of methionine usually yields methylmercaptan, CH_3SH (methanethiol), whereas cystein gives rise to H_2S under aerobic and anaerobic conditions. Thus, H_2S may be produced aerobically as well. The third reason for an increase in H_2S production are the spreading cities. Because people tend to live in green suburbs, far outside town, long sewage networks have to be installed for treating household sewage. Due to the long distances, especially in flat areas, the sewage has long residence times until it reaches the treatment plant. As a consequence, a lot of degradation takes place during the flowtime, producing volatile sulfur compounds like H_2S. Often pressure pipes are used to reduce residence time. However, if these pipes are not ventilated and aerated, for example, by pressurized air, they tend to develop anaerobic conditions, giving rise to H_2S again. Summarizing, it becomes obvious that man's way of life influences the sulfur cycle and its reactions finally causing an increased possibillity of attack on working materials by biogenic sulfuric acid.

Concrete Systems

Ordinary concrete systems are very sensitive to the production of sulfuric acid. Concrete consists of a hydraulic mixture of cement fines with coarse aggregates, sand, and water. The cement first dissolves into water, then precipitates, leading to formation of hydrates. The interpenetration of these hydrates leads to setting and final hardening, giving the structure its mechanical strength.

The most common cement material is Portand cement. It is mainly composed of the following mineral anhydres: tricalcium silicate ($3CaO \cdot SiO_2$), dicalcium silicate ($2CaO \cdot SiO_2$), tricalcium aluminate ($3CaO \cdot Al_2O_3$), and tetracalcium ferro aluminate ($4CaO \cdot Fe_2O_3Al_2O_3$). These anhydrates react with water to form a number of hydrated oxides, including high amounts of calcium hydroxide $Ca(OH)_2$, which is water soluble. In addition to silica, alumina, and iron compounds, cement also contains small amounts of adventitious compounds such as sodium, potassium, and magnesium oxides, phosphates, and sulphates, which are also water soluble. In a normal clean atmosphere, any moisture on a concrete surface would have dissolved in it small quantities of these compounds, as well as some CO_2 and oxygen. In polluted city atmospheres, the air contains SO_2, ammonia, and oxides of nitrogen. These also will be dissolved in the moisture.

The alkaline hydrates react to acid attack-forming calcium sulfates such as gypsum ($CaSO_4$) and ettringite ($6CaO \cdot Al_2O_3 \cdot 3SO_4 \cdot 32H_2O$). This is all the more true since $Ca(OH)_2$ is water soluble and especially reactive even deep inside the concrete structure.

Many observations have been conducted on-site that illustrate this general behavior of ordinary concretes under concentrated acid attack. The photography in Fig. 3 was taken in a manhole of the Arcachon system, France, where severe biogenic sulfuric-acid corrosion is encountered.

Corrosion Tests

As described above, H_2S will react with oxygen to sulfur that is deposited on the wall surface. If thiobacilli are present, sulfur will be oxidized to sulfuric acid causing corrosion of susceptible mineral materials.

In order to help in predicting the behavior of pipe materials to this phenomenon, tests are often conducted by materials scientists immersing cement-bound test materials in sulfuric

FIG. 3—*Corroded manhole of ordinary Portland concrete, Arcachon sewer, France.*

acid. With this type of test it is conceived that the cement-bound material is destroyed by a purely chemical reaction with the acid. The nature of the acid and its concentration may vary from assay to assay. The acidic solution is renewed from time to time, and the loss of weight due to chemical reaction is measured. The corrosion rate is then calculated from these values.

However, the experience of many years indicates that corrosion does not occur uniformly in sewage pipelines. From one joint to another, a pipe may be severely corroded, whereas the adjacent pipe (of the same material) exhibits only negligible corrosion. The reason for these differences are not known and, thus, predictions about the possible rate of corrosion of materials in sewage environments remain difficult.

Moreover, Wierig [*15*] showed in his experiments that in concentrated sulfuric acid (pH 1 to 2), concretes exhibit corrosion rates of similar order though being very different materials; all samples but one lost 50% of their initial weight between the 8th and the 16th week. Taking into account the expected service life of pipes of 50 to 80 years, the differences observed have little significance. The results are shown in Fig. 4.

These results come in contradiction to the field experience, where at severely endangered parts of the sewage system, pH values between 1 and 2, sometimes even below 1, occur although the grade of corrosion shows considerable variation. As a consequence, besides the action of sulfuric acid, there must be another factor determining the resistance of a cement-bound material against biogenic sulfuric-acid attack.

Similarly, immersion tests conducted with calcium-aluminate-based cements in the laboratories of the Lafarge Coppée Group led to the conclusion that such mineral systems, though generally exhibiting better corrosion resistance than traditional cements, would not withstand severe sulfuric-acid attacks such as in sewage networks facing harsh H_2S stripping

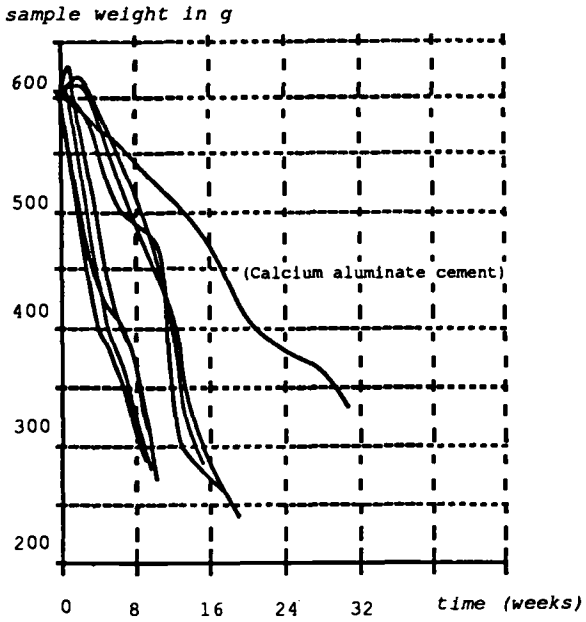

FIG. 4—*Loss of weight of samples of various Portland and blast furnace-type cements after immersion in sulfuric acid at pH 1. Additionally, the behavior of a calcium-aluminate cement is shown* [15].

problems. This is consistent with the results shown in Fig. 4 [*15*] and with other information found in the literature [*16*].

These conclusions, however, were clearly contradicted by observations conducted on site [*17*]. The site of El Berka, Greater Cairo, Egypt, is demonstrative in this aspect. The city transports its domestic wastes through a circa 5 km long and through flat open-air sewer. The long retention time and the hot climate promote septic reactions and favor the formation of H_2S in the effluent. Then the effluent enters four parallel sewer lines installed in 1981 with sudden increase in flow rate, leading to H_2S stripping. The sewer line is moreover bent at this particular place, inducing turbulences, further enhancing the stripping. The manholes are badly corroded and only two out of four could be opened. The concrete walls of the inspection chamber are covered with sulfur, giving evidence of H_2S stripping. The pH was measured on the surface of the concrete with pH paper and indicated values ranging between 1 and 2. The ordinary concrete was badly corroded, with reinforcement appearing, as can be seen in Fig. 5*a*.

The upstream pipe was 1500 mm in diameter. It was internally lined with a centrifuged concrete mortar made with calcium-aluminate cement. This mortar is in perfect shape and hard to hammer though the pH at the crown was ranging between 1 and 2, the same as on the walls of the inspection chamber. This is shown in Fig. 5*b*.

These observations clearly lead to the conclusion that corrosion testing based upon immersion in "simple" sulfuric acid is misleading and not appropriate when it comes to simulating the specific case of biogenic sulfuric-acid corrosion. The reason is obvious: bacteria produce the sulfuric acid. Because they are living organisms, they may thrive in suitable habitats, whereas in others, their growth is restricted. This means that the interactions between microorganisms and substratum must play an important role in the corrosion of cement-bound materials. This is to be taken into account in the testing procedure.

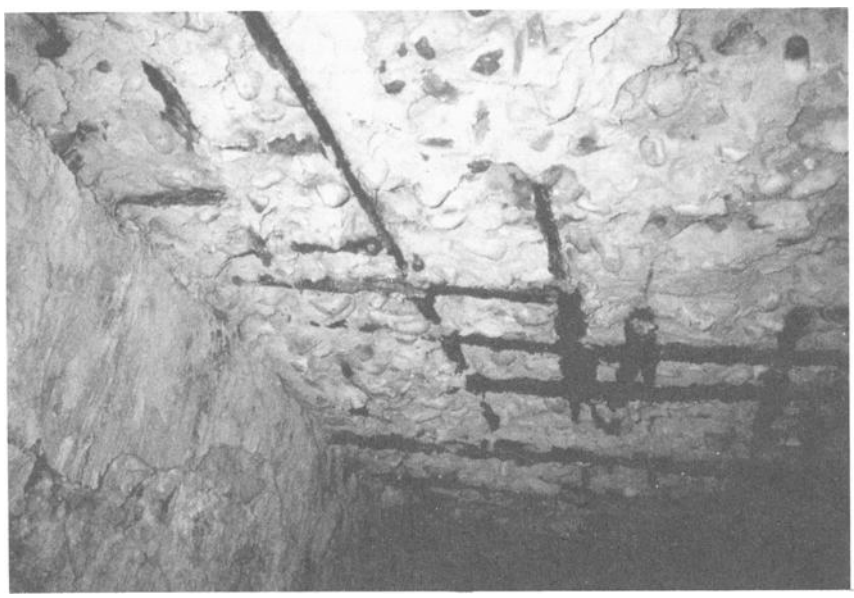

FIG. 5(*a*)—*The ordinary concrete of the manhole chamber is deeply degraded, giving evidence of harsh biogenic sulfuric-acid corrosion, Egypt, El Berka.*

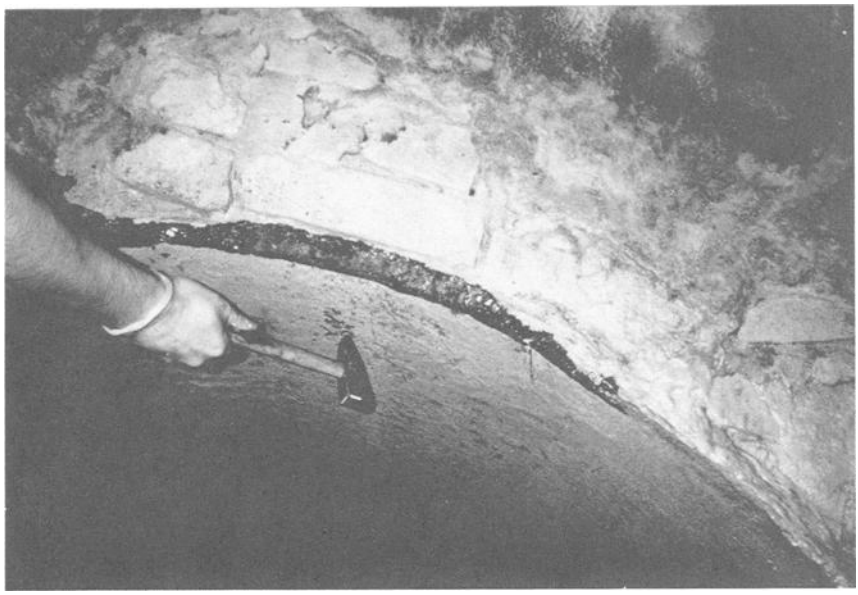

FIG. 5(*b*)—*Resistant-centrifuged calcium-aluminate-based mortar lining, El Berka, Egypt.*

Tests in a Simulation Chamber

Because of the apparent lack of an appropriate testing method, which would include microorganisms as the main corrosion-causing agents, a simulation chamber was constructed that allowed to remodel the conditions of a sewage pipeline. In this chamber the conditions for the main corrosion-causing agent, the sulfuric-acid-producing bacteria were optimized [*10*]. Thus, a possibility for the testing of materials was created that included the interactions between bacteria and substratum [*9*].

The first testings conducted with the experimental chamber confirmed the importance of the bacteria, and gave results that were consistent with on-site observations: two different materials may exhibit similar resistance to acid attack according to immersion tests, though having entirely different resistance to bacterially influenced corrosion. This is illustrated by results shown in Fig. 6. Two test blocks, one made of a blast-furnace cement, the other made of a portland cement, are shown. After having passed two simulation experiments, some difference is obvious. In this particular case, the Portland-cement-based formulation gave evidence of better resistance, though the purely chemical testing with sulfuric acid had caused insignificant differences [*15*].

Field experiments were conducted with Portland-cement-based concrete blocks in order to determine how much the simulation experiments were accelerated compared to natural conditions in Hamburg's most severely endangered sewers. Because the testing conditions are optimal to the bacteria in the experimental chamber, the test run produced corrosion on cement-bound concrete test blocks that needed more than eight times as long as under natural conditions in the aggressive atmosphere of a sewage pipeline [*8*].

Figure 7(*a*) gives an impression of the simulation chamber for reproduction of partially filled sewage pipelines. Figure 7(*b*) shows the diagram of the apparatus. The chamber has a volume of about 1 m^3. The walls and the bottom are thermostated separately, and the bottom is usually 2 to 3°C warmer than the walls. The chamber contains about 10 cm of

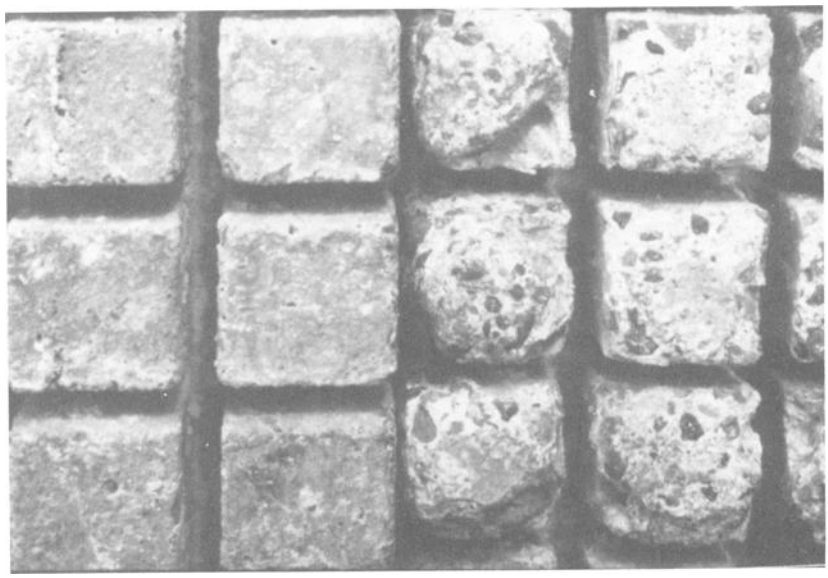

FIG. 6—(*a*) *Comparative testing of two test blocks of a German Portland cement and* (*b*) *a German blast-furnace cement.*

water. Due to the elevated temperature, water evaporates and condenses at the top lid and the walls, producing a high humidity in the gas space (usually above 98% relative humidity). The temperature is kept at 30°C. As a nutrient for the sulfur-oxidizing bacteria, H_2S gas is used. The concentration in the gas phase amounted to 10 ± 5 ppm H_2S. At both sides of

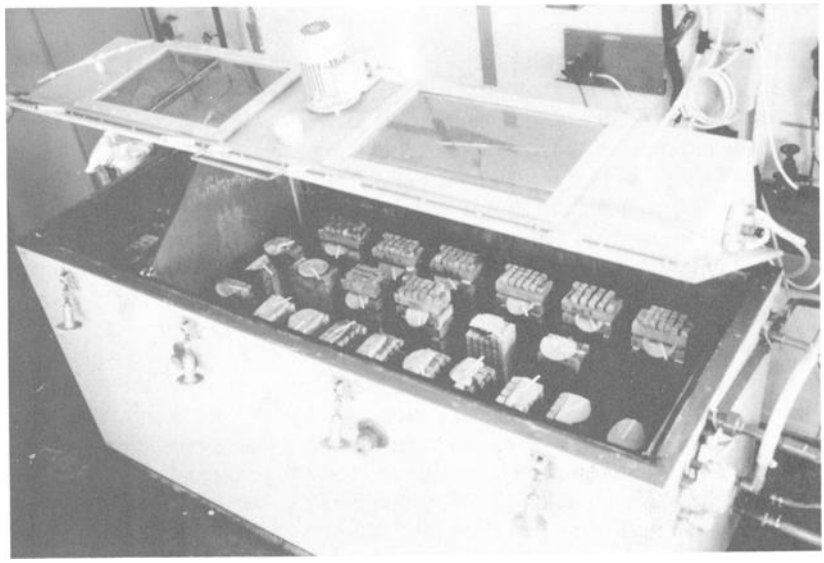

FIG. 7(*a*)—*Overview of the simulation chamber.*

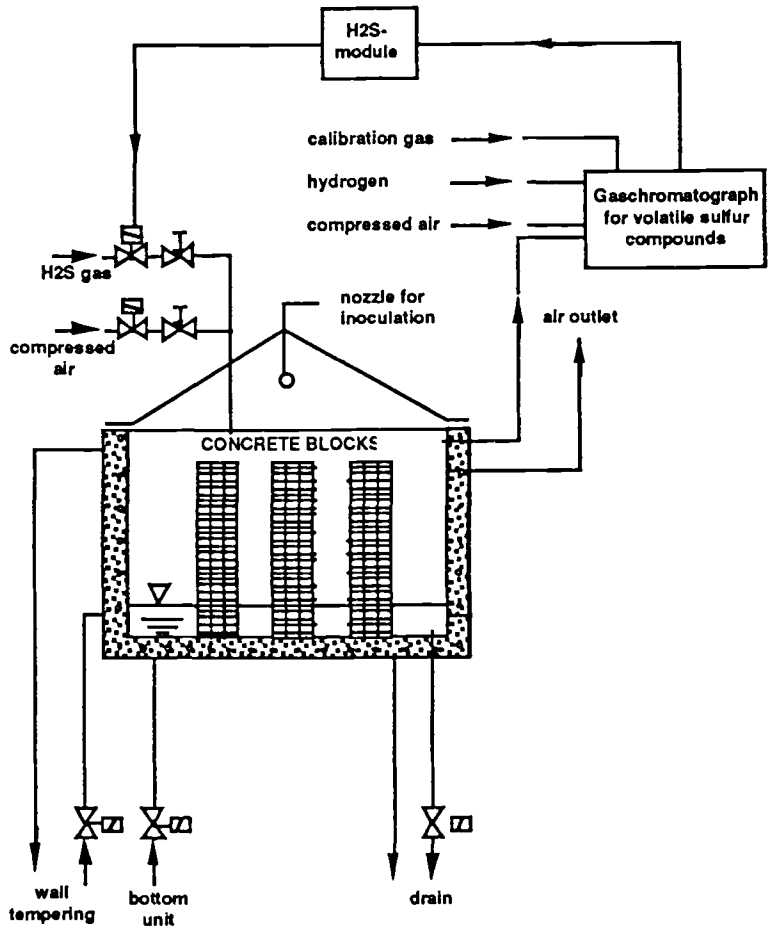

FIG. 7(*b*)—*Schematics of the simulation chamber.*

the lid a nozzle is installed. The nozzles are used for spraying a salt solution into the chamber that contains a supply of nitrogen and phosphorus for the bacteria (to avoid any shortage).

Secondly, the nozzles are used for inoculation of the test blocks with bacteria. Several strains of the species T. thiooxidans, T. neapolitanus, T. intermedius, and T. novellus (originating from samples of corroded sewers in Hamburg) are grown as mass cultures in the laboratory, harvested, and sprayed as an aerosol (fog) into the chamber. A total of 10^{13} cells are needed for the inoculation of one simulation experiment. A part of the aerosol settles on the surface of the test blocks. The results of 10 experiments show that by this inoculation method, cell densities of more than 10^6 cells/cm^2 are usually achieved. Compared with natural conditions this equals a cell count that occurs only at highly endangered parts of the sewage system [7]. Thus, a start of the experiment without lag-phase is achieved. The inoculation is done in intervals during a time period of about 90 days. A "resting" period of about 30 days follows, after which sampling for evaluation of resistance against biogenic sulfuric-acid attack starts.

Samples may be taken from the test materials two different ways. Either test blocks are presawn, giving cubes of 18 × 18 × 18-mm length that can be broken off easily, or single

cubes with similar measures have been used from the start of the experiment. The latter has the advantage that weight-loss measurements can be done precisely (weighing before and after incubation). For sampling and analysis, up to three cubes are removed, put into flasks with mineral salt solution (50 ml in 100 ml flasks) and incubated on a rotary shaker for 90 min for detachment of loose material (due to corrosion) and of adhering microorganisms. The resulting suspension is used consecutively for estimations of the cell counts of thiobacilli. For this purpose, dilution series are produced in steps of 1:10. Selective nutrient solutions are inoculated out of the dilution steps for strongly acidophilic T. thiooxidans, moderately acidophilic T. neapolitanus, and mixotrophic moderately acidophilic T. intermedius/T. novellus (the latter are detected together because of their growth requirements). At least three tubes of each nutrient solution are inoculated. Details have been published [*7,8,10*].

Evaluation of the test tubes takes place after 3 weeks. The cell counts are determined by the statistical method, most-probable-number (MPN). In parallel, weight-loss determinations are done. The cubes are dried and the loss of weight is determined by weighing. During the simulation test, the pH value of the surface water on the test blocks is measured additionally.

Test Results and Discussion

Typical results on a Portland cement-based concrete sample are shown in Fig. 8. The cement used is PZ 35 Alemannia, water/cement ratio is 0.5. The evolution of the bacterial cell count, loss of weight, and pH value of surface water during the experiment are reported in the same graph.

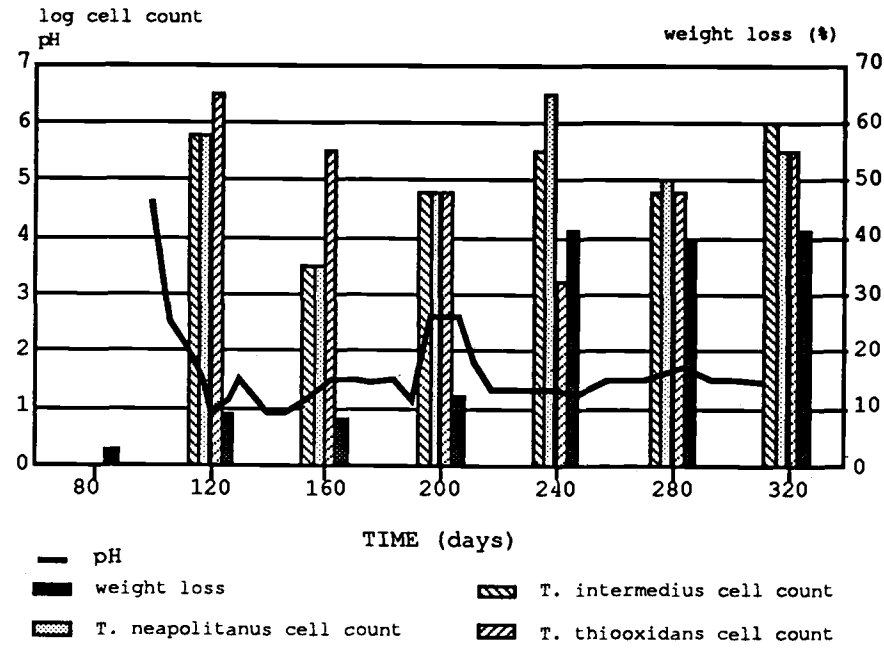

FIG. 8—*Evolution of the bacterial cell count, loss of weight, and pH value of surface water of a Portland-based concrete as a function of time in the simulation chamber.*

Because of the biogenic sulfuric acid the pH value of the surface water dropped from above 10 (fresh concrete) to less than pH 5 during the inoculation period (100 days). During the following incubation, the pH value decreased further to a range of about 1 and 1.5 and remained with minor deviations in this range. The cell counts of thiobacilli started between 10^6 and 10^7 cells/cm^2 test block surface. Although some deviations occurred, they remained at this level throughout the experiment. The weight loss measurements indicate a low loss after inoculation and 40% weight loss after 240 days until the end. It is evident from these data that such a test material is not suitable for construction of sewage pipelines.

Owing to the accelerated-simulation test, this result was achieved within 1 year, whereas at least 8 years would have been necessary to obtain the same information on site.

Similar tests were done with different cements, including calcium aluminate. The mortars were made with low-water-cement ratio and high-cement dosage, in order to simulate the behavior of centrifuged mortar lining inside metallic or concrete pipes. The mix composition is 600 g cement, 1380 g aggregates (0 to 5 mm), and 120 g sand (0 to 0.1 mm). The water/cement ratio is 0.38. The porosimetry of the sample by injection of mercury shows that most pores are around 0.3 μm, and almost all of them less than 1 μm. The results of the test are shown in Fig. 9.

The weight-loss measurements show with values of less than 10% that the biogenic attack is reduced considerably compared with the attack on the portland test material shown in Fig. 8, although only in conditions of pH less than 1.5. The conclusion is that:

1. The material exhibits good resistance against biogenic sulfuric acid corrosion. This is in good agreement with on-site observations.
2. The material exhibits a higher resistance than could be predicted by immersion tests and theories based solely upon traditional chemistry.
3. pH measurement alone is not appropriate for predicting the resistance of a material *in vitro* and, more important, *in situ* [*11*].

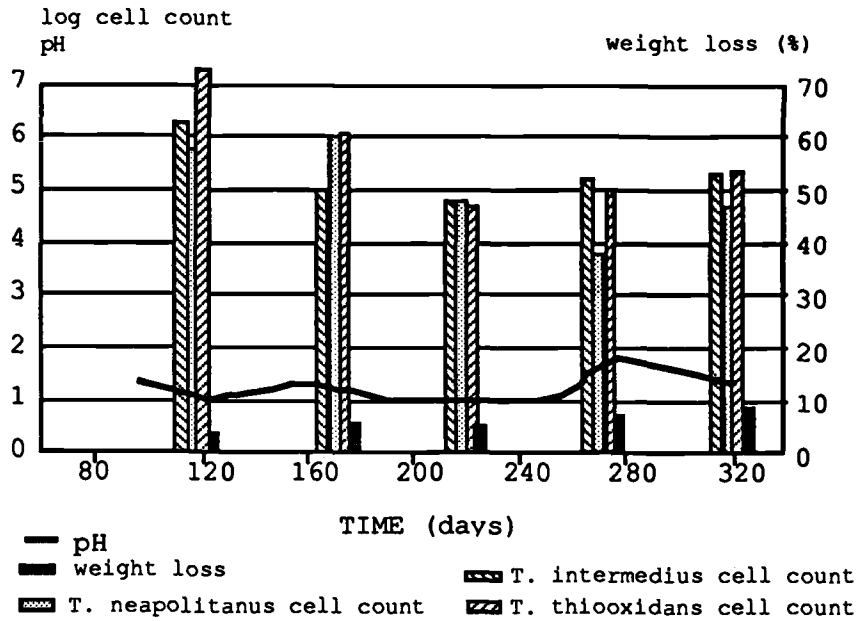

FIG. 9—*Corrosion test conducted on a calcium-aluminate-based mortar in the simulation chamber.*

Another important point is that the bacterial population shows a slight decrease in terms of cell counts. They started like the previous experiment of Fig. 8 at a level of 10^6 to 10^7/ cm^2 surface. In spite of some deviations, the cell counts declined to values of 10^5 cells/cm^2.

These results credit the statement that bacteria do not behave the same, that is, have different activity depending upon the substratum. For some reason, the calcium-aluminate system does have an effect in this aspect.

One test was conducted in order to investigate the role of the porosimetry on bacterial behavior. The mortar was composed of 480 g calcium aluminate, 120 g silica fumes, 1380 g aggregates, and 120 g sand. The water/binder ratio was 0.30. The porosimetry measurement indicated that most pores are in the range of 0.01 μm, all of them being less than 0.2 μm in diameter. The results of the corrosion tests are shown in Fig. 10.

The result demonstrates that the role of pores, within the range of porosity used, has little meaning in this aspect. Reversely, this confirms the importance of the interactions substratum-bacteria.

On the basis of this result, tests were conducted with an improved calcium-aluminate-based solution with synthetic aggregates produced by Lafarge (Alag®), whose composition is similar to that of the cement. The formulation is 600 g calcium-aluminate cement, 600 g Alag, 0 to 2 mm, and 1600 g Alag 0 to 5mm. The water cement ratio is 0.37. The results of the corrosion test are shown in Fig. 11.

The results show a great improvement in terms of corrosion resistance compared to the previous mortars (Figs. 8 to 10).

Examination of the surface of the samples shows that the corrosion progresses evenly from the surface. This is shown in Fig. 12.

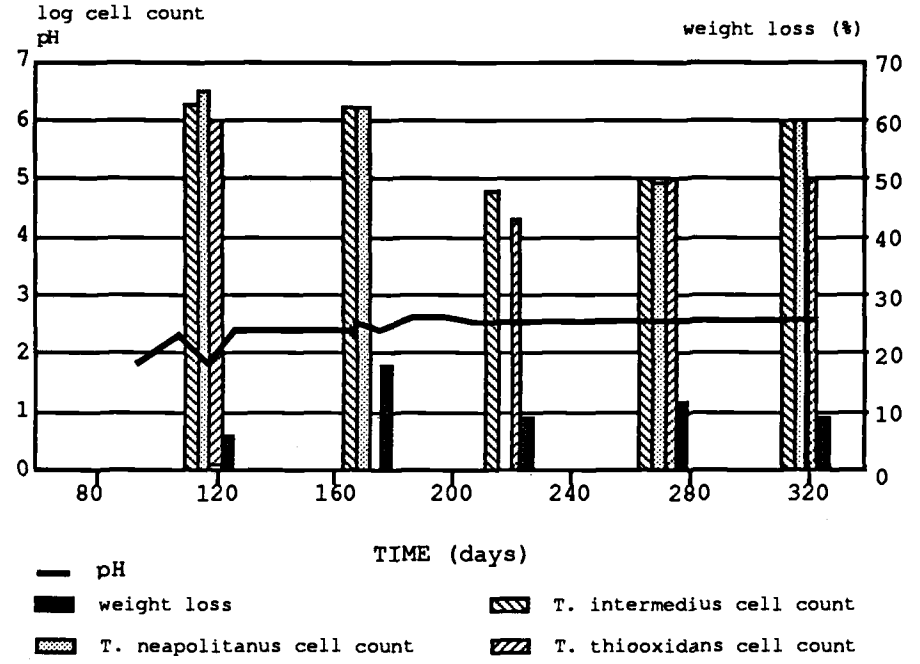

FIG. 10—*Corrosion test conducted on a calcium-aluminate-based mortar in the simulation chamber with "no" porosity.*

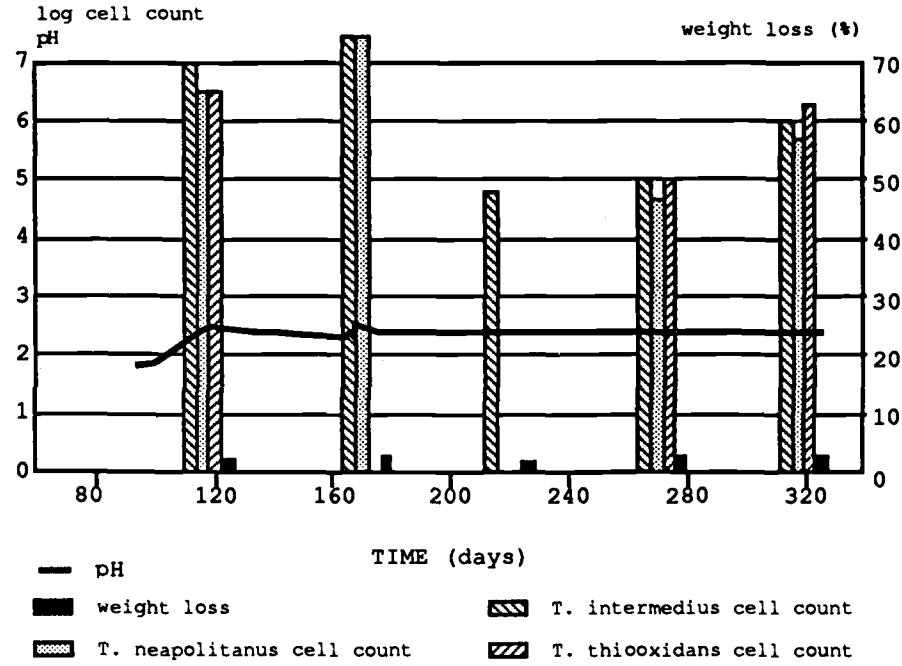

FIG. 11—*Influence of Alag aggregates on resistance of calcium-aluminate-based mortars.*

This is to be granted to the very homogeneous chemical and mineral composition of the material. Once hydrated, opposite to traditional cements, calcium aluminate is mainly composed by two minerals that are C3AH6 and AH3. In particular, it does not release free lime, opposite to Portland cements, nor does it contain high amounts of water soluble phases.

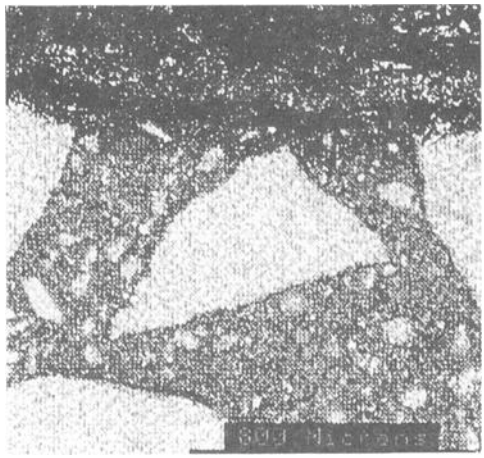

FIG. 12—*Even progress of biogenic sulfuric-acid corrosion on a calcium-aluminate based mortar (scanning electron microscopy).*

Summarizing, the result of this simulation test is the finding that:

1. Calcium-aluminate based materials are very resistant against biogenic sulfuric-acid attack and, thus, appropriate for use in sewage systems, within the range of placing conditions used for the tests.
2. Pores in the range below 1 μm do not play an important role.
3. The addition of Alag aggregates to this material considerably improve its resistance to biogenic sulfuric-acid attack.

Conclusions

Corrosion tests have been generally conducted in the past with little attention paid to the role of the bacteria in the process. This indeed helped classify the materials according to their chemical resistance to different acids with varying conditions. However, it was proven to be misleading when it came to predict the behavior of materials in natural conditions. A typical case is that of calcium-aluminate cement performing well, even after many years usage in harsh sewage environments; although calcium-aluminate cement is often classified as an inadequate material on the sole basis of purely chemical tests. The University of Hamburg developed a special corrosion test in a controlled-simulation chamber. The results observed came in good agreement with on-site observations, and confirmed the important role of the bacterial aspect in the particular context of biogenic sulfuric-acid corrosion. This was also confirmed in the case of calcium-aluminate cement.

Due to optimal breeding conditions, the chamber proved to work as an accelerated test, and to simulate within a year the corrosion results observed after 8 years in the most aggressive part of the Hamburg sewer system. Thus, this simulation apparatus is an excellent tool to sort out rapidly-appropriate cementitious working materials for use in sewage systems. The city of Hamburg's sanitation authority requires this test for any new material to be used in the city's sewage network.

It is now an understood fact that natural phenomena require expertise from different people. Biogenic sulfuric-acid corrosion is an excellent example where progress could be done through combined work of complementary expertises, such as mineral chemistry, materials science, and microbiology. Investigations are currently conducted in Hamburg of this nature, either for testing or for improving existing materials. In particular, the work permitted to understand the good field performances observed in sewers with calcium-aluminate cements. This in turn allowed to improve the existing material with regard to the substratum-bacterial interactions. The calcium-aluminate cement, combined with use of Alag aggregates, was found to give excellent results in this aspect with limited corrosion and minimized bacterial attack.

References

[1] Olmstead, W. M. and Hamlin, H., "Converting Portions of the Los Angeles Outfall Sewer into a Septic Tank," *Engineering News*, Vol. 44, 1900, pp. 317–318.

[2] Morris, S. S., "The Deterioration of Concrete in Contact with Sewage," *Journal of the Institute of Civil Engineering*, Vol. 13, 1940, p. 337.

[3] Pomeroy, R. and Bowlus, F. D., "Progress Report on Sulphide Control Research," *Sewage Works Journal*, Vol. 18, No. 4, 1946.

[4] Lea, F. M. and Desch, C. H., *The Chemistry of Cement and Concrete*, 3rd Ed., Edward Arnold, London, 1970.

[5] Parker, C. D., "The Corrosion of Concrete. I. The Isolation of a Species of Bacterium Associated with the Corrosion of Concrete Exposed to Atmospheres Containing Hydrogen Sulphide," *Australian Journal of Experimental Biology and Medical Science*, Vol. 23, 1945, pp. 81–90.

[6] Gilchrist, F. M. C., "Microbiological Studies of the Corrosion of Concrete Sewers by Sulphuric Acid Producing Bacteria," *The South African Industrial Chemist,* 1953, pp. 214–215.
[7] Milde, K., Sand, W., and Bock, E., "Thiobacilli of the Corroded Concrete Walls of the Hamburg Sewer System," *Journal of General Microbiology,* Vol. 129, 1983, pp. 1327–1333.
[8] Sand, W., "Importance of Hydrogen Sulfide, Thiosulfate, and Methylmercaptan for Growth of Thiobacilli During Simulation of Concrete Corrosion," *Applied Environmental Microbiology,* Vol. 53, 1987, pp. 1645–1648.
[9] Sand, W. and Bock, E., "Biodeterioration of Mineral Materials by Microorganisms—Biogenic Sulfuric and Nitric Acid Corrosion of Concrete and Natural Stone," *Geomicrobiology Journal,* Vol. 9, 1992, pp. 129–138.
[10] Sand, W., Milde, K., and Bock, E., "Simulation of Concrete Corrosion in a Strictly Controlled H_2S-Breeding Chamber," *Recent Progress in Biohydrometallurgy,* G. Rossi and A. E. Torma, Eds., Associazione Mineraria Sarda, Italy, 1983, pp. 667–677.
[11] Schremmer, H., "Über Betonangriffe durch Schwefelwasserstoff," *Zement-Kalk-Gips,* Vol. 17, 1964, pp. 417–424.
[12] Thistlethwayte, D. K. B., *Control of Sulfides in Sewage Systems,* Butterworth, Melbourne, Australia, 1972.
[13] König, W. A., Ludwig, K., Sievers, S., Rinken, M., Stölting, K.H., and Gunther, W., "Identification of Volatile Organic Sulphur Compounds in Municipal Sewage Systems by GC/MS," *Journal of High Resolution Chromatography and Chromatography Communications,* Vol. 3, 1980, pp. 415–416.
[14] Rinken, M., Aydin, M., Sievers, S., and König, W. A., "Quantifizierung Flüchtiger Schwefelverbindungen in Bezug Auf Die Korrosion von Betonabwasserkanälen," *Fresenius Z. Anal. Chemie,* Vol. 318, 1984, pp. 27–29.
[15] Wierig, H. J., "Final Report from the Hamburg Research Project: Building Materials," *Biogene Schwefelsäurekorrosion in Teilgefüllten Abwasserkanälen,* R. Bielecki and H. Schremmer, Eds., Leichtweißinstitut der TU Braunschweig, Braunschweig, Germany, 1987, pp. 33–49.
[16] "Sulfide in Waste Water Collection and Treatment Systems," *ASCE Manuals and Reports on Engineering Practice,* American Society of Civil Engineers, 1989, p. 69.
[17] Dumas, T., "Calcium Aluminate Mortars and Concrete: An Application to Sewer Pipes in Harsh Environments," in *Proceedings of the International Conference on the Implication of Ground Chemistry and Microbiology for Construction,* University of Bristol, Great Britain, 1992.

Bibliography

Bielecki, R. and Schremmer, H., *Biogene Schwefelsäurekorrosion in Teilgefüllten Abwasserkanälen,* Leichtweiß—Institut der TU Braunschweig, Braunschweig, Germany, 1987.
Bock, E. and Sand, W., "Microbially Influenced Corrosion of Concrete and Natural Sandstone," *Microbially Influenced Corrosion and Biodeterioration,* N. J. Dowling, M. W. Mittelman, and J. C. Danko, Eds., University of Tennessee, Knoxville, 1990, pp. 3.29–3.34.

Service Water Systems

Dirk H. J. Wagner,[1] *Wulf R. Fischer,*[2] *and Hasko H. Paradies*[3]

Correlation of Field and Laboratory Microbiologically Influenced Corrosion (MIC) Data for a Copper Potable Water Installation

REFERENCE: Wagner, D. H. J., Fischer, W. R., and Paradies, H. H., **"Correlation of Field and Laboratory Microbiologically Influenced Corrosion (MIC) Data for a Copper Potable Water Installation,"** *Microbiologically Influenced Corrosion Testing, ASTM STP 1232,* Jeffery R. Kearns and Brenda J. Little, Eds., American Society for Testing and Materials, Philadelphia, 1994, pp. 253–265.

ABSTRACT: A copper-corrosion process of unknown origin was observed in the cold and warm water supplies shortly after commissioning a county hospital in Germany. The cause of the damage could be attributed to microbial-influenced corrosion (MIC). An evaluation of the damage showed that corrosion is most likely to occur in intensively branched, horizontal pipework during prolonged periods of stagnation. The influences of operating conditions and design installation on the corrosion process could not be separated.

The operating conditions and design installation can be separated in test rigs using the occurrence manifestation characteristics for this corrosion process as a measure for the likelihood of corrosion. After an induction period of 200 days the corrosion is most often found under intermittent and stagnant conditions in the test rigs. Furthermore, a seasonal influence can be observed. It was shown in experiments performed in the laboratory that it should be possible to considerably minimize this induction period found in the test rigs.

KEYWORDS: microbiologically influenced corrosion (MIC), copper, potable water

Introduction

A copper-corrosion process of unknown origin in a county hospital in Germany was observed in the cold and warm water supplies shortly after commissioning the hospital. The cause of the damage has been attributed to microbiologically influenced corrosion (MIC) [*1*].

A field study in the county showed that the corrosion failure in the hospital was not unique, but was by far the worst case. Similar damage has occurred in large public buildings; private houses have not been affected [*2,3*].

Damage that occurred in three large public buildings over a period of ten years was evaluated, showing that after an induction period of three and a half years breakthroughs of copper tubes occurred stochastically. An evaluation of a high number of samples taken from these buildings after five, eight, and ten years showed that 20 to 100% of the copper tube walls remained. No trend with which to predict the lifetime of a copper installation

[1] Junior scientist, Märkische Fachhochschule, Laboratory of Corrosion Protection, Frauenstuhlweg 31, D-5860 Iserlohn, FRG.

[2] Senior scientist, Märkische Fachhochschule, Laboratory of Corrosion Protection, Frauenstuhlweg 31, D-5860 Iserlohn, FRG.

[3] Senior scientist, Märkische Fachhochschule, Laboratory of Biotechnology, Frauenstuhlweg 31, D-5860 Iserlohn, FRG.

could be observed. Although only one corrosion system was affected (hard-drawn copper tubes and soft, unbuffered reservoir water), a stochastic distribution of the resistance to corrosion was found.

According to the German Standard DIN 50 930, Part 5 "Corrosion Behavior of Metallic Materials in Water; Copper and Copper Alloys," perforations in cold water installations consisting of copper piping should only be observed if more than one of the following parameters has an unfavorable value: (1) design of installation and operating conditions, (2) kind of commissioning for the installation, (3) material and material surface conditions, and (4) chemical and biological composition of the water. If the formation of a protective layer on the material surface is disturbed by potable water of unfavorable composition, or other unfavorable parameters, perforations of tubes can be expected. No perforations would be expected in the relevant water distribution area according to the assessments mentioned in DIN 50 930.

To determine the influence of other parameters leading to the perforations, more than 500 failed copper pipe samples taken from the county hospital were examined. The damage occurred mainly in two sections of the hospital that included intensively branched, horizontal pipework subjected to prolonged periods of stagnation. In the area with vertical, straight runs of pipework and short periods of stagnation, no perforations and no deep pits (none >0.1 mm) were observed. Furthermore, a gas pressure test was performed with this water supply one year before commissioning the hospital. During the winter period before commissioning, the supply was filled with water and the hospital installation was used as a substitute heating system [*4*]. This has to be regarded as another factor with an unfavorable influence.

The failure analysis showed that it is not possible to separate the influence of the parameters design installation from the operating conditions on the corrosion process. This separation is a prerequisite for the evaluation of countermeasures and a more profound understanding of the corrosion mechanism.

A separation of design and operation parameters is possible with test rigs set up in the hospital. A test rig necessarily simulates a short, unbranched floor supply. The results of the failure analysis in the county hospital showed that a low corrosion rate can be expected with this installation design. The influence of operating conditions can be worked out in a test rig. A time period between the setup of a test rig and commissioning the rig is avoided.

This paper will deal with the influence of operating conditions on the likelihood of MIC. Two test rigs were installed in this hospital, one at a place where the water was fed into the hospital installation, and the other one at a place where the water has passed many hospital installations. Furthermore, a possible influence of the hospital installation itself on the likelihood of corrosion was investigated.

To rate the results obtained from these test rigs, the typical features for MIC, as described in Ref [*1*], are used: (1) uptake of copper into the potable water, (2) formation of black layers of copper(II)-oxide; (3) formation of exopolymeric substances, and, (4) general attack and pitting at the same time.

After two-and-a-half years of operating time, the simulation of the corrosion process was successful in both test rigs, but with a lower corrosion rate than in the damaged water distribution system of the hospital [*5*]. The corrosion rate in the rigs corresponds to that in the area with a low damage probability in the hospital. These results are within the spectrum of the results occurring in the hospital. It takes a certain period of time until the typical characteristic features are observed in the test rigs for the first time.

Based on this knowledge, this paper will deal with the following questions:

(1) Can typical induction periods be determined for the single characteristic features of this type of corrosion?

(2) Are the results obtained from the test rigs comparable with results of exposure tests and laboratory loops?
(3) Is it possible to understand the spectrum of the observed corrosion behavior in terms of the influence of operating conditions?

The results obtained from these investigations are also important in determining the relevant time period for investigating corrosion performance, because it is desirable to predict corrosion behavior from such investigations.

Experimental Procedure

The commissioning of the test rigs consisting of copper (German Standard: SF-Cu, F37; ISO-Standard: Cu-deoxidized high phosphorous (DHP) was performed in January 1990. Different operating conditions were simulated in parallel water lines by the use of: solenoid valves with time control, stop-cocks and flow-controls. These conditions were: (1) constant flow, (2) intermittent conditions, (12-h stagnation, with a water change every hour), and, (3) stagnation (water change every 24 h). The measurements in the test rigs during the last 30 months relevant for this investigation are as follows: Copper tubes were collected after two- to four-month exposure. For regular controls, water samples were collected every one or two weeks from the test rigs to determine the copper concentration by atomic absorption spectroscopy (AAS).

The occurrence of spots of black layers was determined using a stereo microscope, and exopolymeric substances (EPS) were detected performing the Periodic acid-Schiff reagent (PAS) test according to Chamberlain et al. [*6*]. Copper tubes were stained in 10% (w/w) citric acid to reveal pitting attack. Pit depth was measured using a stereo microscope by focusing on the non-attacked surface and then on the bottom of the obviously deepest pit.

Starting in May 1991, exposure tests were performed in the laboratory, simulating stagnant conditions with water taken from the county hospital, and a laboratory loop was set up that worked under intermittent operating conditions with the same water. Further experimental details are described in Ref [*7*].

Results

Uptake of Copper into the Potable Water

The copper concentrations obtained from the different water samples are rated in Fig. 1*a* through *f*. The distribution of the obtained values is dividied into two domains, (1) copper concentrations of 0.3 mg/L $< c <$ 3 mg/L and, (2) concentrations of more than 3 mg/L.

Figure 1*a* shows the rating of all water samples obtained from the test rigs. From the initial installation, copper concentrations between 0.3 and 3 mg/L were measured. After 160 days of operation, the majority of all samples investigated were in this range. Critical values of more than 3 mg/L were obtained after an induction period of 200 days. A further increase could be observed during the following three months, then samples exceeded the critical value up to 560 days. No critical values could be observed in the time period of 600 to 760 days. Values of more than 3 mg/L were found from 120 to 800 days and then vanished. Only one further excursion was observed after 960 days.

Figures 1*b* and 1*c* compare the influence of the hospital installation on the uptake of copper ions. Samples taken at the place of the water inlet to the hospital show few concentrations >3 mg/L after 240, 520, 840, and 960 days. Water samples taken at the place where the water had passed many installations showed values beyond 3 mg/L continuously from 200 to 560 days. Two further excursions were noticed after 760 and 800 days (Fig. 1*c*).

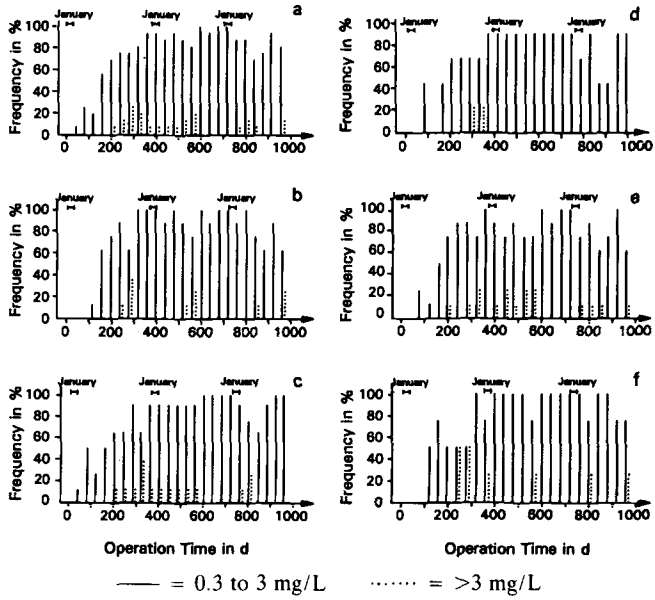

FIG. 1—*Rating of water samples concerning the uptake of copper into the potable water as a function of operation time: (a) rating of all samples; (b) samples taken from a place where the water is fed into the hospital installation; (c) samples taken from a place where the water has passed many of the installations of the hospital. Samples exposed to (d) Constant flow; (e) intermittent conditions and (f) stagnant conditions.*

The influence of the operating conditions on the uptake of copper can be seen in Fig. 1*d* through 1*f*. Under constant flow conditions, the concentration exceeded 3 mg/L after 280 and 320 days. Operating at intermittent conditions caused an uptake of copper of more than 3 mg/L in about 50% of the samplings after 240 and 280 days. Under stagnant conditions, an irregular uptake could be observed after 240, 280, 360, 560, 800, and 960 days. Using the concentration range of 0.3 mg/L $< c <$ 3 mg/L as a parameter for the uptake of copper, no influence of the hospital installation or the operating conditions on the corrosion process could be derived.

Occurrence of Black Oxide Layers

Figure 2 shows the occurrence of black deposits evaluated from all samples taken from the test rigs. Figs. $2a_1$ and $2a_2$ show the results obtained from the top and bottom halves of the copper tubes cut between the 3 and 9 o'clock position. The data in both diagrams have the same shape, indicating that no difference can be detected between the two halves of the copper tubes. So, no preferred orientation for the formation of the black spots can be seen. Therefore, in discussing the formation of EPS and pitting attack, the tubes are no longer separated into top and bottom halves in Figs. 3 and 4.

Small black spots on a bare copper surface occur from the first sampling. After 240 days, about 80% of the samples show this behavior (Fig. $2a_1$ and $2a_2$). With further operation time, the bare surfaces were covered by black spots or stripes, or both, mixed with bluegreen alkaline corrosion products. The black spots were no longer detectable, but they did not vanish as indicated by the dotted line in Fig. 2.

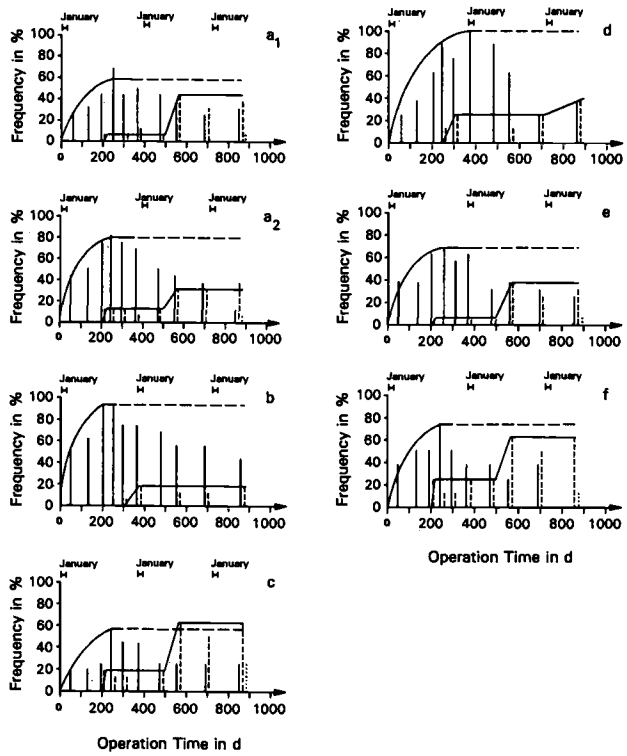

FIG. 2—*Rating of copper samples concerning the formation of black oxide layers as a function of operating time; (a) through (f) as described in Fig. 1.*

a_1 = *Top halves of the copper tubes.*

a_2 = *Bottom halves of the copper tubes.*

The first occurrence of black spots mixed with alkaline corrosion products was detected after 200 days of operating time. The frequency of about 20% remained constant for a whole year. After 560 days, an increase up to 40 ± 5% was noticed and continued to remain constant. After 870 days, black spots underneath blue-green tubercules were observed indicating continuation of the corrosion process.

Black spots on a bare copper surface developed rapidly (Frequency 90%) on copper samples taken from the rig at a place where the water was fed into the hospital installation (Fig. 2*b*). Black spots mixed with bluegreen corrosion products were detected for the first time after 300 days for about 20% of the samples. This frequency remained constant. After the water had passed many installations of the hospital, it became more corrosive (Fig. 2*c*). The frequency of black spots on a bare copper surface was lower (50%) than in Fig. 2*b* because many more black spots mixed with bluegreen corrosion products could be detected. This is the case for the first time after 200 days with a frequency of 15%, then remained constant for nearly one year. In the time period of 490 to 570 days, an increase up to 60%

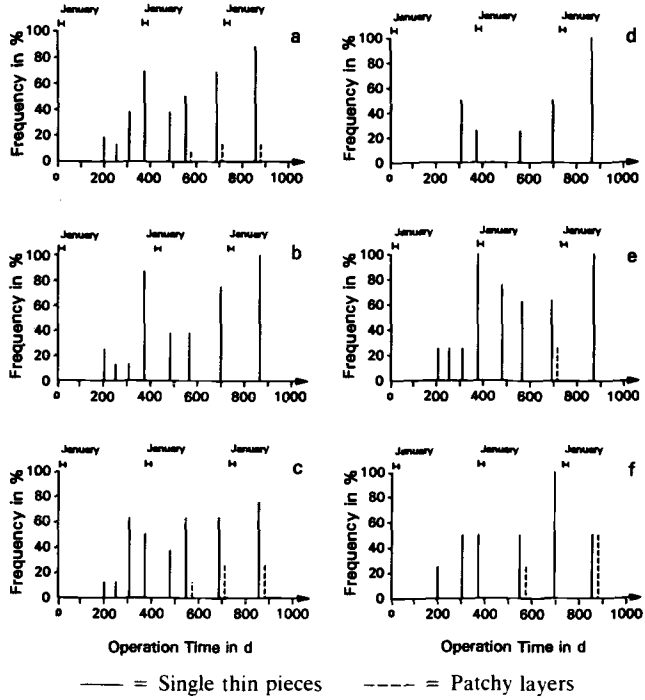

FIG. 3—*Rating concerning the formation of EPS on copper samples as a function of operating time; (a) through (f) as described in Fig. 1.*

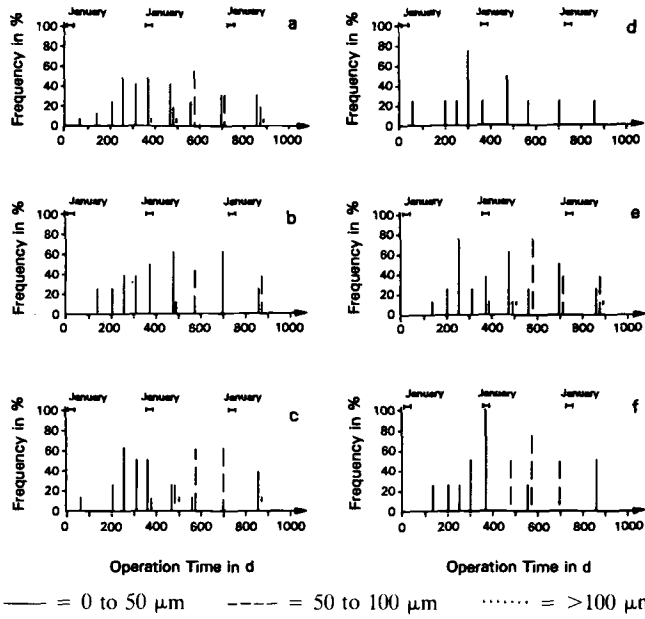

FIG. 4—*Rating of copper tubes concerning pitting attack as a function of operating time; (a) through (f) as described in Fig. 1.*

was observed. During further samplings until 870 days, 60% of the samples showed black spots mixed with bluegreen corrosion products. After this time, black spots underneath bluegreen tubercules were observed indicating the continuation of the corrosion process (Fig. 2*c*). This observation has not been made to date in samples taken from the rig at the place where the water is fed into the installation.

The influence of the operating conditions on the formation of black spots mixed with bluegreen corrosion products that increase with stagnation time can be seen in Fig. 2*d* through 2*f*. The number of black spots on a bare copper surface decreased with increasing operation time. No clear influence can be derived for the constant flow conditions (Fig. 2*d*). The black spots mixed with bluegreen corrosion products occurred first after 240 days. A slight increase could be seen after 570 days. A more significant effect was obtained under intermittent conditions. After about 200 days, approximately 5% of the investigated samples showed this effect for nearly one year. After 500 to 570 days the number of samples increased to 40%. The evaluation of the samples under stagnant conditions showed the same effect, but to a greater extent. Here, an increase from 20 up to 60% could be observed. Black spots underneath green tubercules were observed for the first time after 870 days during intermittent and stagnant conditions.

Detection of Exopolymeric Substances (EPS)

The detection of EPS is described by the occurrence of (1) single thin pieces and (2) patchy layers. Figure 3*a* shows the results obtained with all investigated samples. After 200 days, single thin pieces of EPS were detected for the first time and then increased up to 90% in these samples. Patchy layers were found after 570 days. To date (after three years operating time), about 25% of the samples showed this effect.

The influence of the installation of the county hospital is shown in Fig. 3*b* and 3*c*. After 200 days, in samples taken from the test rig at a place where the water was fed into the installation, only single thin pieces of EPS were found. The number of samples with a positive result increased with operating time up to 100% after 870 days (Fig. 3*b*). These single thin pieces of EPS were also found after 200 days in samples from the rig at a place where the water passed many hospital installations (Fig. 3*c*). No significant differences were detected among the single thin pieces. After 570 days, patchy layers of EPS were detected and were also found during further samplings with a frequency up to 25% (Fig. 3*c*).

An influence of the operating conditions on the EPS formation can also be noticed (Fig. 3*d* through 3*f*). Only single thin pieces were found under constant flow conditions after 310 days with an increasing frequency up to 100%. Single pieces occurred under intermittent and stagnant conditions after 200 days. With increasing time a higher number of samples also showed this effect. During one sampling patchy layers were detected after 700 days, under intermittent flow conditions, and after 560 and 870 days under stagnant conditions.

Pitting Attack

Because of the high number of pit depths in the range of 10 μm $< l_{max} <$ 50 μm, no trends were determined (Fig. 4). Pits were observed from the first sampling. In Fig. 4, the maximum pit depths are separated into two domains, (1) 50 μm $< l_{max} <$ 100 μm and (2) $l_{max} >$ 100 μm. No conclusions about pit propagation can be drawn from these results. Pits with $l_{max} >$ 50 μm occurred after 400 days operation time in a stochastic distribution. The influence of the hospital installation site on the formation of pits cannot be detected, although the pits

with $l_{max} > 100$ μm occurred at the test rig at a place where the water had passed many installations of the hospital (Fig. 4*b*, *c*).

A qualitative trend can be derived from the results with the different operating conditions (Fig. 4*d* through *f*). No pits deeper than 50 μm were found under constant flow conditions. Approximately the same number of pits at 50 μm $< l_{max} <$ 100 μm occurred under intermittent and stagnant conditions. Pits with $l_{max} > 100$ μm were found only during one sampling under intermittent conditions. No dependence of the pit formation on the operation time of the rigs was observed.

Discussion

Four characteristics of MIC were used to determine the influence of operating conditions and design of the hospital installation on the corrosion process leading to the damage. The uptake of copper is rated in three different concentration ranges, (1) $c < 0.3$ mg/L, (2) 0.3 mg/L $< c <$ 3 mg/L, and (3) $c > 3$ mg/L. The limiting value of 3 mg/L was chosen because it is recommended by the European Community as the maximum concentration acceptable in potable water; 0.3 mg/L is discussed in Scandinavia as a maximum value. Values above 3 mg/L are regarded as unacceptable in potable water while values between 0.3 and 3 mg/L are acceptable concentrations. The formation of black deposit layers is divided into (1) black spots on a bare copper surface, (2) black spots mixed with alkaline corrosion products consisting of posniakite and malachite, and (3) black spots underneath bluegreen tubercules. The occurrence of EPS is distinguished as (1) single thin pieces and (2) patchy layers. Pit depths are divided into the following classes: (1) 10 μm $< l_{max} <$ 50 μm, (2) 50 μm $< l_{max} <$ 100 μm and (3) $l_{max} > 100$ μm. Pit initiation with $l_{max} < 10$ μm cannot be detected because general attack occurs at the same time. So, these two measures cannot be used to assess the likelihood of corrosion. It is known from practical experience that pits with $l_{max} < 100$ μm tend to repassivate while pits with $l_{max} > 100$ μm tend to remain active leading to the perforation of the tube.

The different extents of these four characteristics obtained as results of the test rigs will be used to discuss the dependence of operating conditions and the hospital installation on the likelihood of corrosion. The rating of the likelihood of corrosion is given in Table 1. The non-appearance of black spots and pieces of EPS, as well as copper concentrations <0.3 mg/L show that no MIC is occurring. Black spots on a bare surface, pits of 10 μm $< l_{max} <$ 50 μm and copper concentrations 0.3 mg/L $< c <$ 3 mg/L are not regarded as significant parameters because they do not indicate corrosion in the test rigs. Black spots on a bare surface can only be detected as long as no other corrosion products are formed covering the black spots.

TABLE 1—*Rating the likelihood of corrosion based on the extent of the manifestation characteristics.*

	Corrosion Likelihood			
Parameter of Manifestation of Corrosion	+ +	+	0	−
Uptake of copper	>3 mg/L[a]	>3 mg/L	0.3 to 3 mg/L	<0.3 mg/L
Spots of black layers	underneath tubercules	mixed with posniakite or malachite	on a bare copper surface	not detectable
Formation of EPS	patchy layers	single thin pieces		not detectable
Pit depth (l_{max})	>100 μm	50 to 100 μm	10 to 50 μm	

[a] The concentration must be below 3 mg/L again for at least 200 days of operating time.

The occurrence of the characteristics of MIC (1) uptake of copper $c > 3$ mg/L, (2) formation of single pieces of EPS, (3) black spots mixed with posniakite or malachite, and, (4) pit depths 50 μm $< l_{max} <$ 100 μm are regarded as a start of the MIC process. At least two or more of the above parameters must be met. A greater degree of these manifestations, (1) the formation of black spots underneath tubercules, (2) patchy layers of EPS, (3) hole depths $l_{max} > 100$ μm, and, (4) uptake of copper $c > 3$ mg/L, when the concentration was below this value again for at least 200 days operating time, represents an increase of the likelihood of corrosion. For this assessment, at least one of these parameters and the conditions that are regarded as a start of the corrosion process, as described above, must be met.

An evaluation of pitting attack shows that it can only be used as a qualitative measure not showing any trends in the MIC process. The maximum pit depth is used as a parameter. Only a very small area of a sample surface is investigated in this way, so no average values for rating the likelihood of corrosion are obtained from these results. The other three characteristics are much more representative of the likelihood of MIC.

Table 2 shows an evaluation of the data based on the first occurrence of the parameters listed in Table 1. The time difference between the commissioning of the test rig and the first occurrence is called the induction period. A further subdivision is performed concerning the black spots mixed with posniakite and malachite, that is, this manifestation occurring with more or less than 20% frequency for the evaluation of these induction times.

The uptake of copper, spots of black layers and formation of EPS, show a first induction period of about 200 to 250 days corresponding to July through August 1990. Based on these three parameters, no influence of operating conditions and hospital installation on the induction period can be observed. As defined above, this induction period corresponds to the start of MIC. An increase in the likelihood of corrosion after 570 days (July 1991), which is indicated as a second induction period where at least one further parameter must be fulfilled, can be noticed for the lines working under intermittent and stagnant conditions, but not in the lines with constant flow. The same holds true for a third induction period

TABLE 2—*Induction periods of the different extents of the single manifestation in days based on the rating shown in Table 1.*

	All Samples	Water Feeding into the Installation	Water has Passed Many Hospital Installations	Constant Flow	Intermittent	Stagnation
Uptake of copper	200[a]	250[b]	200[a]	300[c]	200[a]	250[b]
		530[d]				570[d]
Spots of black layers	200[a]	300[c]	200[a]	250[b]	200[a]	200[a]
	570[e]		570[e]		570[e]	570[e]
	880[f]		880[f]		880[f]	880[f]
Formation of EPS	210[a]	210[a]	210[a]	300[c]	210[a]	210[a]
	570[e]		570[e]			570[e]
Pit depth l_{max}	370[g]		370[g]		370[g]	
	480[h]	480[h]	480[h]		480[h]	480[h]

[a] July 1990.
[b] August 1990.
[c] October 1990.
[d] June 1991.
[e] July 1991.
[f] June 1992.
[g] January 1991.
[h] May 1991.

after 880 days (June 1992) using the spots of black layers underneath tubercules as an indicator.

The first induction period of 200 days can be observed in both test rigs at a place where (1) the water was fed into the hospital installation and (2) the water had passed many installations. The latter one also shows the induction period in July 1991 and June 1992. In the rig at the place where the water entered the hospital, only the uptake of copper lets one assume an induction period in July 1991. This shows that the likelihood of corrosion is higher in the test rig installed at the place where the water had passed many hospital installations.

It can be seen in Table 2 that the pit depths do not follow the trend described above. The values for this parameter vary. So, this parameter cannot be used as an indicator of MIC. To date, in the lines with constant flow, pit depths did not exceed 50 μm which confirms the results described above concerning the influence of operating conditions.

These results show a seasonal influence on this corrosion process. The highest likelihood of corrosion can be expected in the summer period from June to August. The likelihood of corrosion is smaller during the other seasons of the year.

To get a quantitative measure of the extent of the individual manifestations of MIC, the frequency of occurrence is evaluated for the operation time of 870 days (Table 3*a*). It can be seen that the occurrence of MIC covers a broad spectrum of 0 to 78% and is dependent on operating conditions and location of the test rig. Pit depths >100 μm, patchy layers of EPS, and black spots underneath bluegreen tubercules cannot be evaluated because of the low frequency of occurrence. The frequency of the other parameters is rated in Table 3*b* (the highest frequency of each individual characteristic is equal to 100%) to show the influence of the operating conditions and the installation on the likelihood of corrosion. No significant influence can be assigned to the uptake of copper (0.3 to 3 mg/L), the formation of single pieces of EPS and pit depths (10 to 50 μm, 50 to 100 μm). The black spots mixed with bluegreen corrosion products and uptake of copper ($c > 3$ mg/L) show a higher likelihood of corrosion at the place where the water has passed many installations of the hospital. Concerning the different operating conditions, pit depths of 10 to 50 μm and uptake of copper (0.3 mg/L $< c <$ 3 mg/L) could not be differentiated. The other parameters show clearly that the line operating with intermittent and stagnant flow conditions has the higher likelihood of corrosion. Stagnant and intermittent operating conditions cannot be distinguished based on these results.

The results obtained from the laboratory loop and exposure tests in the laboratory after one year of operating time are rated in Fig. 5 according to the terms given in Table 1. It can be seen that EPS and pitting attack were detected in the exposure tests after only five days. Because these two parameters are fulfilled, the MIC process had already started after this period of time. In samples taken from the laboratory loop, two parameters were positive after fifty days of operating time: (1) the formation of spots of black layers mixed with posniakite and malachite, and, (2) the formation of single pieces of EPS. So, the MIC process started after this period of time. This indicates a reduction of the induction period and considerable acceleration of the corrosion process in the laboratory.

Conclusions

An induction period of about 200 days can be observed for three characteristics of MIC in the test rigs, (1) the uptake of copper, (2) the formation of spots of black layers and (3) the formation of EPS. These three characteristics, typical for MIC, occur at the same time and cannot be differentiated. The influence of these parameters on each other cannot be

TABLE 3*a*—*Frequency of the different extents of the single manifestation in %.*

	Manifestation					
	EPS Single Thin Pieces	Black Spots Mixed with Posniakite/Malachite	Pit Depth 10 to 50 μm	Pit Depth 50 to 100 μm	Uptake of Copper 0.3 to 3 mg/L	Uptake of Copper >3 mg/L
All samples	39.1	14.5	31.4	11.5	75.1	7.3
Place where the water feeds into the installation	37.6	7.3	35.6	10	74.5	5.2
Test rig where the water has passed many installations	38.2	22.9	27.7	16.6	77.7	7.6
Constant flow	24.5	10.6	30	0	77.9	2.0
Intermittent	48	10.9	33.9	18.3	73.8	9.5
Stagnation	32.6	26	30.4	17.9	77.1	8.2

TABLE 3*b*—*Rating of these frequencies; the highest frequency is equated to 100%.*

All samples	81.5	55.8	88.2	62.8	96.4	76.8
Test rig where the water feeds into the installation	78.3	28.1	100	54.6	95.6	54.7
Test rig where the water has passed many installations	79.5	88.1	77.8	30.7	99.7	80.0
Constant flow	51.0	40.8	84.3	0	100	21.0
Intermittent	100	41.9	95.2	100	94.7	100
Stagnation	68.0	100	85.4	97.8	99	86.3

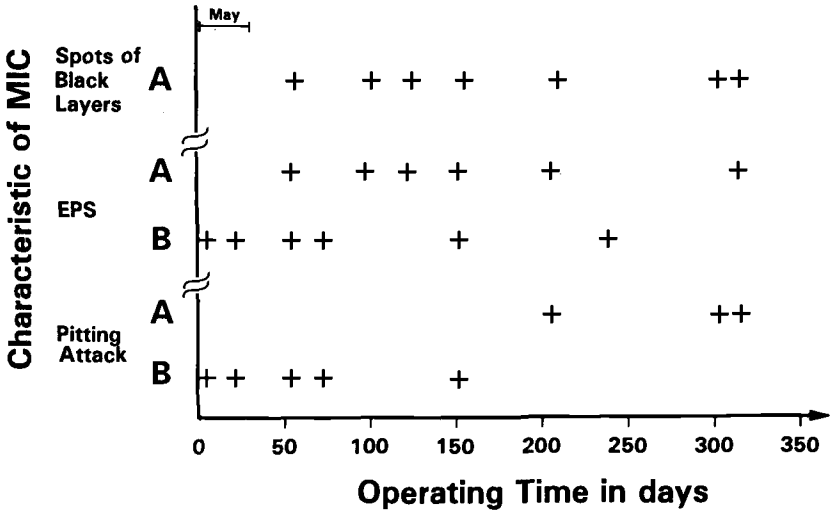

FIG. 5—*Results obtained from the laboratory loop (a) and exposure tests in the laboratory (b) concerning the different manifestations of corrosion as a function of operating time.*

separated. Formation of EPS shows that microbiology is an important parameter regarding MIC.

The highest likelihood of corrosion was observed in the summer period of every year (June through August) and was correlated to the formation of EPS. During this period the water temperature was high in the reservoir from which the water was taken. A high level of microbiological activity in the water can be assumed for this period of time. During other periods of the year, the likelihood of corrosion is much lower. This can also be regarded as a possibility that microbiology is a parameter in the corrosion process. A seasonal influence on MIC can clearly be seen.

The same process resulting in MIC occurred in the test rig at a place where the water feeds into the hospital installation and in the test rig at a place where the water has passed many installations of the hospital. The likelihood of corrosion was found to be higher in the latter which indicates the influence of horizontally installed copper pipework in the hospital. The same result occurred from the evaluation of damaged copper samples from the hospital. Therefore, the installation within the hospital seems to have an influence on the likelihood of corrosion.

An influence of the operating conditions can also be observed. The likelihood of corrosion is higher during intermittent and stagnant conditions than during constant flow conditions. A separation of the influence of intermittent and stagnant conditions is not possible based on these results. These results also confirm the observations of the evaluation of damage in the county hospital.

The results obtained from the evaluation of damage from the county hospital (the highest likelihood of corrosion for horizontally installed copper pipework with prolonged periods of stagnation was most susceptible to corrosion) were confirmed by the results of the test rigs. With two test rigs in the building, it was possible to separate the influence of the design installation and the operating conditions. The different results obtained by various operating conditions cover the spectrum of the observed corrosion behavior for copper pipes in the hospital.

Pit depths cannot be used as a specific parameter for predicting MIC or the lifetime of the installation, because no trends could be derived from pit depth data.

The induction period can be reduced considerably in a laboratory loop and exposure tests, showing that it is possible to accelerate the corrosion process in the laboratory. This is a prerequisite for the evaluation of countermeasures and a more profound understanding of the mechanism. Within a very short period of time, MIC is established in the loop. If further loops are taken into operation, they will be inoculated with water from this loop which has now been operating for one year. With this procedure, it should be possible to overcome seasonal influences.

It is shown that the likelihood of the occurrence of characteristics of MIC is very small during the start-up of a copper piping installation, but increases drastically after an induction period. All experiments that do not take into account this induction period are not necessarily relevant, because incorrect conclusions about the likelihood of corrosion may be predicted from the results of short-time experiments.

References

[1] Fischer, W. R., Paradies, H. H., Wagner, D., and Hänßel, I., "Copper Deterioration in a Water Distribution System of a County Hospital in Germany Caused by Microbiologically Influenced Corrosion—I. Description of the Problem," *Werkstoffe und Korrosion*, Vol. 43, 1992, pp. 56–62.

[2] Kuplin, M. and Fischer, W. R., "A Field Inquiry Concerning the Cause of Pitting of Copper in Water Distribution Systems," in preparation.

[3] Fischer, W. R., Paradies, H. H., Hänßel, I., and Wagner, D., "Copper Deterioration in a Water Distribution System of a County Hospital in Germany Caused by Microbiologically Influenced Corrosion" in *Microbially Influenced Corrosion and Biodeterioration*, N. J. Dowling, M. W. Mittleman, and J. C. Danks, Eds., 1991, pp. 8–47.

[4] Wagner, D., Fischer, W. R., and Paradies, H. H., "Test Methods on Microbial Induced Corrosion in Different Loops," in *12th Scandinavian Corrosion Congress and Eurocorr '92, Proceedings*, Vol. I, T. J. Tunturi, Dipoli, 1992, pp. 651–665.

[5] Wagner, D., Fischer, W. R., and Paradies, H. H., "Copper Deterioration in a Water Distribution System of a County Hospital in Germany Caused by Microbiologically Influenced Corrosion—II. Simulation of the Corrosion Process in Two Test Rigs Installed in This Hospital," *Werkstoffe und Korrosion*, Vol. 43, 1992, pp. 496–502.

[6] Chamberlain, A. H. L., Angell, P., and Campbell, H. S., "Staining Procedures for Characterising Biofilms in Corrosion Investigations," *British Corrosion Journal*, Vol. 23, 1988, pp. 197–198.

[7] Wagner, D., Fischer, W. R., and Tuschewitzki, G. J., "Microbiologically Induced Pitting Corrosion of Copper Pipes," International Copper Association 453, Sept. 1992.

[8] Grauer, R., "Solid Corrosion Products—I. Magnesium, Zinc, Cadmium, Lead and Copper," *Werkstoffe und Korrosion*, Vol. 31, 1980, pp. 837–850.

Fumio Kajiyama,[1] *Kiyoshi Okamura,*[1] *Yukio Koyama,*[1] *and Komei Kasahara*[1]

Microbiologically Influenced Corrosion (MIC) of Ductile Iron Pipes in Soils

REFERENCE: Kajiyama, F., Okamura, K., Koyama, Y., and Kasahara, K., **"Microbiologically Influenced Corrosion (MIC) of Ductile Iron Pipes in Soils,"** *Microbiologically Influenced Corrosion Testing, ASTM STP 1232,* Jeffery R. Kearns and Brenda J. Little, Eds., American Society for Testing and Materials, Philadelphia, 1994, pp. 266–274.

ABSTRACT: Corrosion of ductile cast iron in soils containing iron-oxidizing bacteria (IOB), sulfur-oxidizing bacteria (SOB), iron bacteria (IB), and sulfate-reducing bacteria (SRB), or both, was studied in the laboratory by applying electrochemical techniques such as EIS and corrosion potential measurement. Weight loss measurements were directly correlated to the EIS measurements, thereby establishing a good correlation to estimate the general corrosion rates from the EIS measurements. EIS technique provided information on the nature of corrosion processes involved in MIC phenomena.

KEYWORDS: microbiologically influenced corrosion (MIC), ductile iron, soil, iron-oxidizing bacteria (IOB), sulfur-oxidizing bacteria (SOB), iron bacteria (IB), sulfate-reducing bacteria (SRB), electrochemical impedance spectroscopy (EIS) technique

Since the first report by Kuhr and Vlugt [*1*] in 1934, sulfate-reducing bacteria (SRB) have been the focus of many investigations involving microbiologically influenced corrosion (MIC). In recent years, however, the roles of other species of bacteria (acid producing bacteria and metal depositing bacteria, among others), have increasingly been emphasized. The authors analyzed localized corrosion failures on buried ductile cast iron pipes and identified iron-oxidizing bacteria (IOB), sulfur-oxidizing bacteria (SOB), and iron bacteria (IB) as causing soil corrosion. The contribution of SRB was found to be small [*2*].

In the present study, ductile cast iron coupons were subjected to a series of laboratory tests involving soils containing IOB, SOB, IB, and SRB, or both. The extent of corrosion determined from weight loss measurements was correlated with the results of periodical electrochemical measurements. It was revealed that the electrical impedance spectroscopy (EIS) technique could provide direct information as to the rates of corrosion as well as the nature of corrosion processes.

Experimental Procedures

Burial Testing

Each soil corrosion cell was prepared by burying a three-electrode probe in a 1 dm^3 Pyrex® glass cell that was filled with a particular soil.

[1] Research engineer, research engineer, research engineer, and general manager, respectively, Tokyo Gas Co. Ltd., Fundamental Technology Research Laboratory, 16–25 Shibaura, 1-Chome, Minato-ku, Tokyo, 105, Japan.

A total of ten kinds of soil were collected from the Tokyo metropolitan district where the presence and high activities of bacteria (IOB, SOB, IB, and SRB, or both) had been recognized. Two additional burial tests were conducted in the soils sterilized with respect to IOB and SRB, or both, by treating for 36 ks in the autoclave at 383 K, at 100 kPa.

The three-electrode probe was a triangularly-spaced type in which 30-mm long × 20-mm wide ductile iron and platinum plates were positioned in parallel, with a 15-mm spacing, as the working and auxiliary electrodes, respectively, and a commercial double-junction type of saturated Ag/AgCl electrode was used as the reference electrode. To simplify the corrosion system, an exposed surface area of 6 cm^2 was obtained for both working and auxiliary electrodes by applying waterproof paint leaving two surfaces opposite to each other.

Each soil corrosion cell was held at 303 K in an incubator for a period of 7.78 Ms. During the testing period, the EIS and the corrosion potential measurements were taken at regular intervals.

Electrochemical Measurements

Electrochemical impedance data were determined with a three-electrode system comprised of a three-electrode probe, a potentiostat, and a frequency response analyzer by applying 10 mV rms of sinusoidal waves over the frequency range from 10 kHz to 1 mHz. Electrochemical impedance data were plotted on a Cole-Cole diagram, and from a charge transfer resistance, R_{ct} was to be read.

Corrosion Potential Measurements

Corrosion potential was obtained by measuring the potential of working electrode by means of an electrometer relative to a Ag/AgCl reference electrode. All the Ag/AgCl potential measurements were corrected for the temperature and referred to $Cu/CuSO_4$ electrode at 298 K [*3*].

Environment Analysis

Soils were investigated with respect to Eh(oxidation reduction potential), pH, the amount of FeS, and the number of bacteria both before and after the testing. Samples were collected from the immediate vicinity of each working electrode. Bacterial counts were made in accordance with the most probable number method. Details have been described in Ref *4*.

Corrosion Rate Calculations

Upon conclusion of burial testing, every probe was removed from each soil corrosion cell, followed by cleaning and weight loss determination. The weight loss measurements were then converted into corrosion rates by applying Faraday's law.

Corrosion rates estimation from R_{ct} measurements was made according to the relationship in Eq 1 as follows [*5*]

$$d = 4.12 \times 10^{-13}/(R_{ct})_{av} \quad (1)$$

where d (m/s) is the general corrosion rate and $(R_{ct})_{av}$ (ohm m^2) is the charge transfer resistance averaged over extended periods. Several keys for increased accuracy of estimation will be discussed later.

Results and Discussion

Corrosion Rates Estimation

Figures 1 to 3 show the typical electrochemical impedance data obtained in the presence and predominant activities of IOB, IB, and SRB, respectively. Tables 1 to 3 represent the results of environmental analyses to identify the predominant bacteria in the respective soil corrosion cells. Table 1 shows that obligately anaerobic SRB were isolated from the oxygenated and acidic environments. The SRB were supposedly in association with the activities of IOB that could effectively consume oxygen in the immediate vicinity of SRB. In the case represented by Fig. 2 and Table 2, the activities of IB resulted in the tuberculation, followed by the evidence for this interpretation with SOB and SRB beneath the tubercles leading to enhanced corrosion. On the other hand, in the case of Fig. 3 and Table 3, SRB were the only species present.

It can be seen from these figures that the majority of the electrochemical impedance data were characterized by the appearance of only one, though frequently depressed, capacitive semicircle, with the infrequent appearance of the two overlapping, depressed, capacitive semicircles. The capacitive semicircles were frequently accompanied by an inductive loop, as represented in Figs. 1 and 3.

Since the impedance data were basically capacitive in nature, the corrosion rate could be estimated from the charge transfer resistance R_{ct}, determined from the diameter of each semicircle. If the impedance spectrum curve had no intersections with the $-\mathrm{Im}[Z] = 0$ axis, extrapolations were made according to the procedures schematically represented in Fig. 4. Such procedures were devised on a trial-and-error basis so that the fit of the calculated corrosion rates to those from the actual weight loss measurements would become excellent.

Figures 5 to 7 show the time dependence of R_{ct}^{-1} and corrosion potential E_{corr} for respective soil corrosion cells, as represented in Figs. 1 to 3. The charge transfer resistance averaged

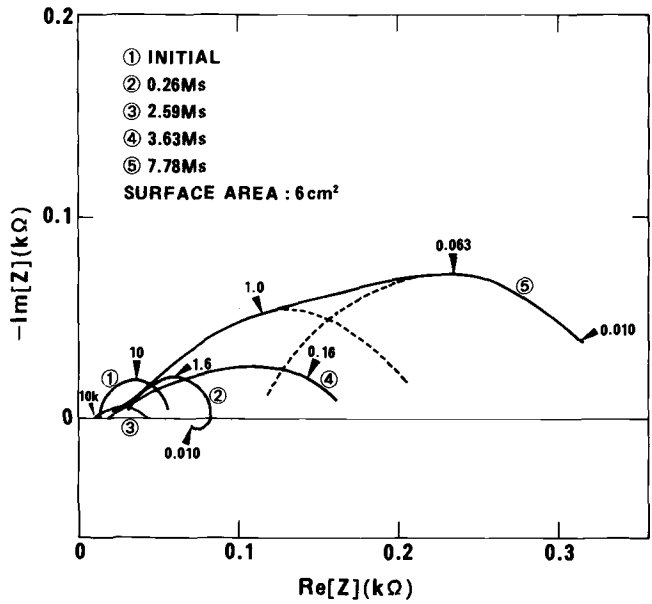

FIG. 1—*Sequential complex plane impedance plots under active IOB conditions. Numbers on the diagram stand for frequency in Hz.*

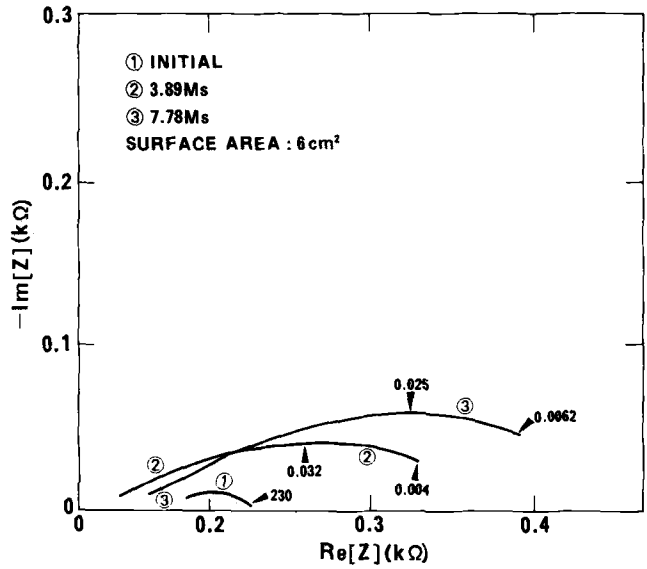

FIG. 2—*Sequential complex plane impedance plots under active IB conditions. Numbers on the diagram stand for frequency in Hz.*

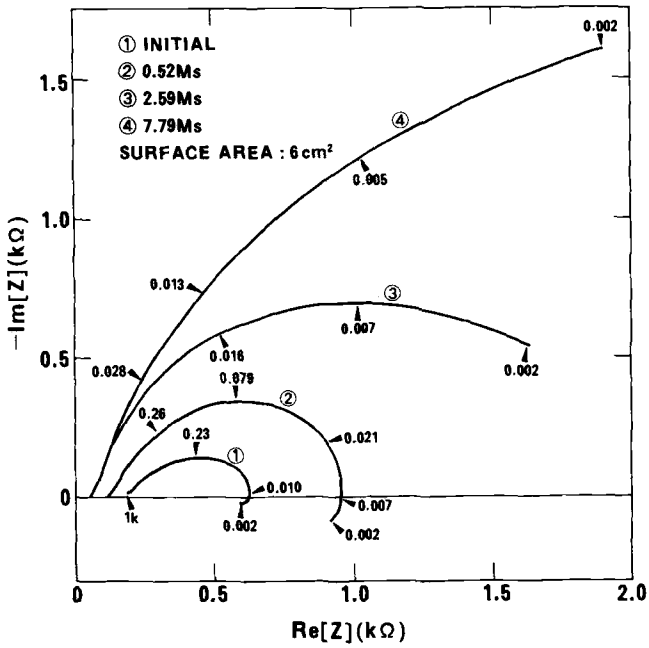

FIG. 3—*Sequential complex plane impedance plots under active SRB conditions. Numbers on the diagram stand for frequency in Hz.*

TABLE 1—*Results of environmental analyses under active IOB conditions in test soil.*

Time, Ms	Location in Soil Box	Eh, V versus NHE	pH	FeS, wt. ppm	Number of Bacteria, per kg of Soil			
					SRB	IOB	SOB	IB
0	bulk	0.655	2.82	1110	7×10^4	8×10^9	2×10^5	0
7.78	electrode/soil interface	0.409	3.36	549	4×10^4	3×10^8	0	0

over extended periods was then determined by graphical integration, followed by the substitution of Eq 1 for $(R_{ct})_{av}$ to obtain the general corrosion rate.

Corrosion Rates

Figure 8 shows the results of laboratory MIC testing wherein the corrosion rate estimated from electrochemical impedance data was plotted against that determined from the actual weight loss measurement.

Although whole data for 10 kinds of soils with varying soil properties and microbial activities were plotted together, all data fell closely around the 1:1 line. This 1:1 relationship was achieved by manipulating the EIS data to fit the desired result.

In connection with Fig. 8, the following is also noteworthy:

(1) Corrosion in the presence of IB was localized and accompanied by the tuberculation leading to the enhanced corrosion rates as high as 1×10^{-11} m/s. Four data points fell concentrically around the same spot.
(2) Corrosion rates in the presence of IOB ranged from 1.87×10^{-11} m/s (the highest corrosion rate observed in the present testing) to 1×10^{-12} m/s.
(3) Measured corrosion rates in the presence of SRB remained at levels more than one to two orders of magnitude lower than those of IOB, SOB, or IB.
(4) Sterilization resulted in a decrease in corrosion rates from 1.87×10^{-11} m/s to 1×10^{-12} m/s with respect to IOB; likewise, from 3.23×10^{-12} to 3.17×10^{-13} m/s, with respect to SRB.

Impedance Spectra and Bacterial Species

Bacterial species dependence of the impedance spectra is schematically represented in Fig. 4.

TABLE 2—*Results of environmental analyses under active IB conditions in test soil.*

Time, Ms	Location in Soil Box	Eh, V versus NHE	pH	FeS, wt. ppm	Number of Bacteria, per kg of Soil			
					SRB	IOB	SOB	IB
0	bulk	0.519	8.22	5	2×10^8	0	4×10^8	$++^a$
7.78	electrode/soil interface	0.559	4.06	8	7×10^7	0	5×10^9	$+++^a$

[a] As one-by-one counting of IB is not easy because these bacteria usually form agglomerated strings, a 3-level semiquantitative indicator system, +, ++, and +++ is employed here to classify the IB population.

TABLE 3—*Results of environmental analyses under active SRB conditions in test soil.*

Time, Ms	Location in Soil Box	Eh, V versus NHE	pH	FeS, wt. ppm	Number of Bacteria, per kg of Soil			
					SRB	IOB	SOB	IB
0	bulk	0.591	5.91	116	2×10^6	0	0	0
7.78	electrode/soil interface	0.254	7.14	253	1×10^{10}	0	0	0

In the presence and high activities of IOB and SOB, or both, in the acidic soils of pH 2 to pH 3, frequently encountered in Neogene strata or reclaimed lands containing higher concentration of sulfate ion as 1400 wt. ppm, severe microbiologically accelerated corrosion was observed without producing any protective corrosion products. A small diameter, hence a small R_{ct} of capacitive semicircle was frequently accompanied by an inductive loop, which is characteristic of environments containing high levels of sulfate [*6*]. Marked decrease in the corrosion rate was evident at around 3 Ms (Fig. 5), together with the decrease of the amount of FeS and the number of SOB (Table 1). This indicated the possibility that high activities of IOB brought about the death of SOB. The IOB also died, due to the lack in the nutrients required to maintain the bacterial proliferation in the soil corrosion cell. A

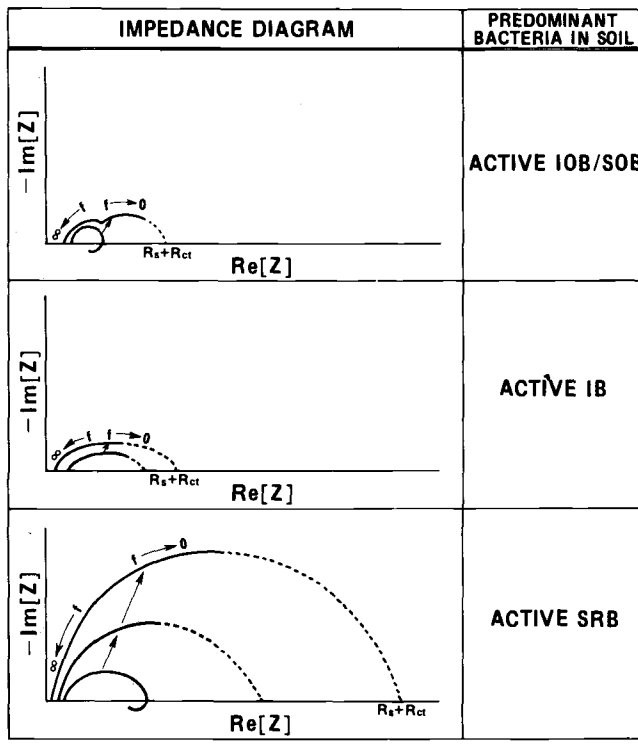

FIG. 4—*Schematic EIS spectra characteristic of corrosion of ductile cast iron resulting from the activity of the cited classes of bacteria in soils.*

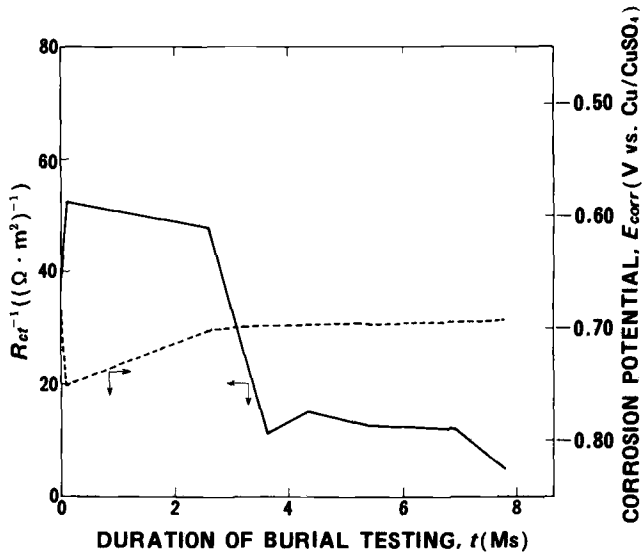

FIG. 5—*Time dependence of* R_{ct}^{-1} *and* E_{corr} *for corrosion of ductile cast iron in soils under active IOB conditions.*

sharp reduction in E_{corr}, observed immediately after the beginning of exposure in Fig. 5, was a feature common to the corrosion cells. Both soils and solution media were affected by the presence and high activities of IOB. Reflecting the loose and less protective nature of the corrosion products, E_{corr} remained at relatively low levels around −0.7 V versus Cu/$CuSO_4$.

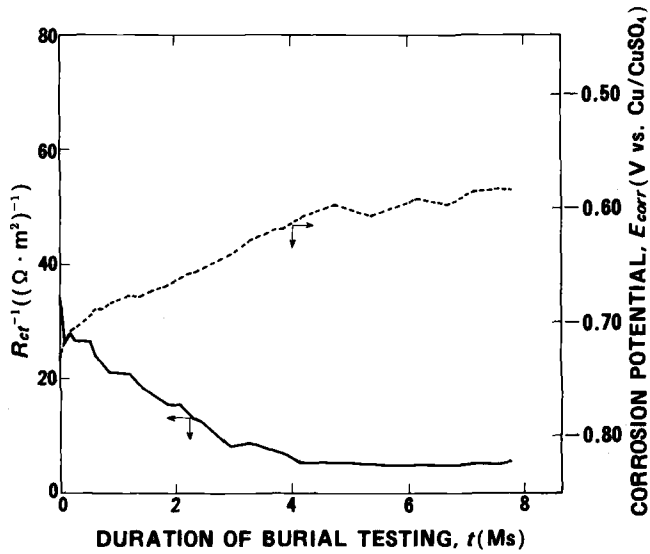

FIG. 6—*Time dependence of* R_{ct}^{-1} *and* E_{corr} *for corrosion of ductile cast iron in soils under active IB conditions.*

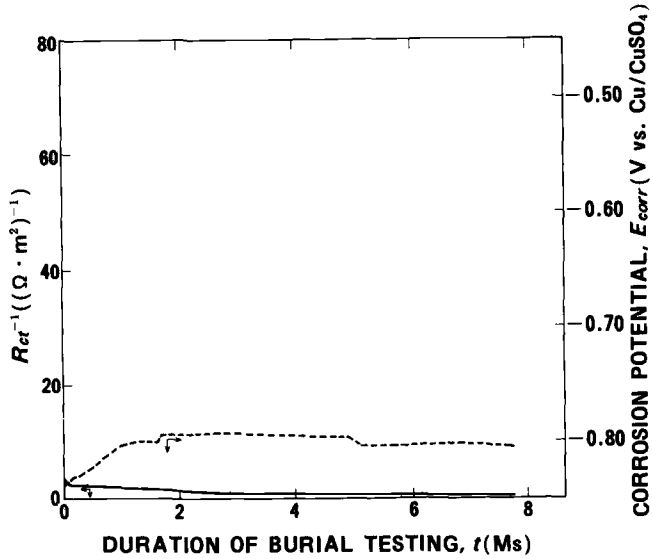

FIG. 7—*Time dependence of* R_{ct}^{-1} *and* E_{corr} *for corrosion of ductile cast iron in soils under active SRB conditions.*

In the presence and high activities of IB in a neutral environment, only capacitive semicircles appeared throughout the testing period, as evident in Fig. 2. Increased IB counts with relatively high levels of SOB and SRB counts and decreased soil pH (Table 2) indicate that the dense tuberculation created differential aeration cells that effectively excluded

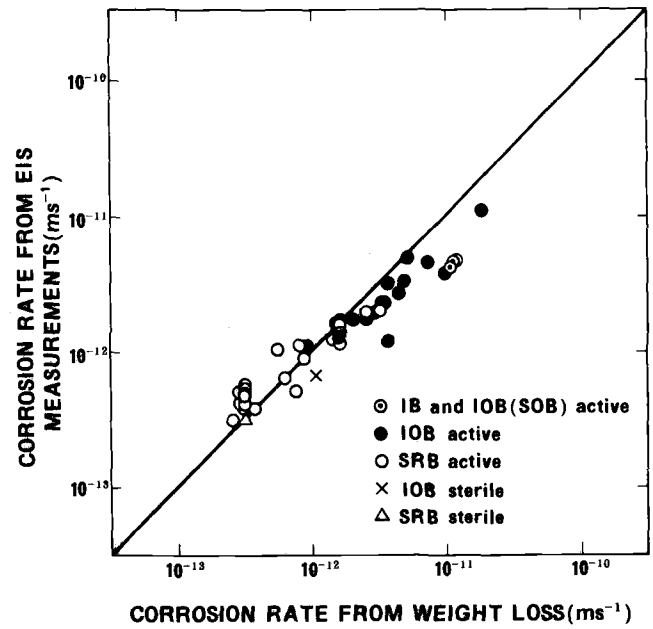

FIG. 8—*Relationship between corrosion rate predicted from EIS measurements and that determined from weight loss measurements.*

oxygen from the area immediately beneath the tubercles. The removal of oxygen thereby accelerated the synergistic proliferation of SOB and SRB beneath the tubercles that lead to enhanced corrosion rates. In response to such an observation, the form of corrosion on the working electrode was characterized as referred to graphitic corrosion. It is to be noted that ennoblement of corrosion potential with time, ultimately rested at around -0.6 V versus $Cu/CuSO_4$, as shown in Fig. 6. This was probably due to the production of dense tubercles comprised of FeOOH and $FeCO_3$.

In the presence of active SRB, an inductive loop characteristic of the sulfate containing environments appeared at the early stage of exposure. The indicative loop was replaced in due time by a strongly increased R_{ct} of semicircles supposedly due to the blocking of active sites by thin and continuous FeS films [7]. Although the production of such FeS films led to low corrosion rates, corrosion potentials were maintained at extremely low levels at around -0.8 V versus $Cu/CuSO_4$ as evident in Fig. 7. This suggests that -0.8 V sites can act as macroanodes in the dissimilar soil corrosion cell.

The relationship between the corrosion rates associated with certain bacteria and the levels of corrosion potential suggest that there can be, for each type of bacteria, a threshold potential for the initiation of MIC and an optimum potential range for MIC in the soil. This demonstrates that the bacteria can tolerate a wide range of environmental conditions.

Conclusions

Laboratory MIC testing of ductile cast iron was conducted by applying the EIS technique. The conclusions based on the test are as follows:

(1) Microbiological activities enhanced the rates of corrosion of ductile cast iron in the soils in approximately the following ascending order: SRB, IOB, and IB in symbiosis with SOB.

(2) Rates of MIC of ductile cast iron in the soils could be estimated based on the EIS measurements according to the equation $d = 4, 12 \times 10^{-13}/(R_{ct})_{av}$, where d is the general corrosion rate (m/s), and $(R_{ct})_{av}$ is the charge transfer resistance (ohm m^2) averaged over extended periods.

References

[1] von Wolzogen, Kuhr, C. A. H., and van der Vlugt, L. S., "De Grafiteering van Gietijzer als Electro-Biochemish Process in Anaerobic Gronden," *Water*, Vol. 18, No. 16, 1934, pp. 147–165.

[2] Kajiyama, F. and Kasahara, K., "Microbiologically Influenced Corrosion of Buried Ductile Iron Pipes and Their Electrochemical Behavior," *Proceedings of the 38th Japan Society of Corrosion Engineering*, Tokyo, 1991, pp. 243–246.

[3] Uhlig, H. H. and Revie, R. W., *Corrosion and Corrosion Control*, Third Ed., Wiley-Interscience, New York, 1985, p. 34.

[4] Kasahara, K., Kajiyama, F., and Okamura, K., "The Role of Bacteria in the Graphitic Corrosion of Buried Ductile Cast Iron Pipes," *Zairyo-to-Kankyo*, (in Japanese), Vol. 40, No. 12, 1991, pp. 806–813.

[5] Kasahara, K. and Kajiyama, F., "Determination of Underground Corrosion Rates from Polarization Resistance Measurements," *Corrosion*, Vol. 39, No. 12, 1983, pp. 475–480.

[6] Kasahara, K. and Kajiyama, F., "Application of AC Impedance Measurements to Underground Corrosion Monitoring," *Proceedings of 9th International Congress on Metallic Corrosion*, Toronto, 1984, pp. 296–302.

[7] Kasahara, K. and Kajiyama, F., "Role of Sulfate Reducing Bacteria in the Localized Corrosion of Buried Pipes," *Proceedings of the International Conference on Biologically Induced Corrosion*, National Association of Corrosion Engineers (NACE), Houston, 1985, pp. 171–183.

Wulf R. Fischer,[1] *Dirk H. J. Wagner,*[2] *and Hasko H. Paradies*[3]

An Evaluation of Countermeasures to Microbiologically Influenced Corrosion (MIC) in Copper Potable Water Supplies

REFERENCE: Fischer, W. R., Wagner, D. H. J., and Paradies, H. H., **"An Evaluation of Countermeasures to Microbiologically Influenced Corrosion (MIC) in Copper Potable Water Supplies,"** *Microbiologically Influenced Corrosion Testing, ASTM STP 1232,* J. R. Kearns and B. Little, Eds., American Society for Testing and Materials, Philadelphia, 1994, pp. 275–282.

ABSTRACT: Unexpected pitting of copper pipes in drinking water installations has appeared mainly in public buildings (often in hospitals) at a small number of places around the world (for example, Germany, Scotland, Saudi-Arabia). Experience and scientific based knowledge about pitting corrosion of copper does not indicate a remarkable susceptibility in the respective drinking water installations. Because substances of biological origin were mixed with the solid corrosion products, the following hypothesis was generally accepted: microbiologically influenced corrosion (MIC).

Though the mechanism of MIC is by no means clear in detail, promising countermeasures have to be developed, substantiated and introduced into practice to protect existing installations. In this paper, the arguments for qualified actions are described and, when available, the success of these measures are mentioned. It can be stated that the likelihood of MIC in copper can be reduced to technically acceptable or even to negligible values by a combination of some well-known methods of corrosion protection.

KEYWORDS: microbiologically influenced corrosion (MIC), pitting corrosion, copper, drinking water, corrosion protection

Background

In 1986 and 1987, we were confronted with pitting of copper plumbing networks (German Standard: SF-Cu; ISO Standard: Cu-DHP). Four different cases were investigated. A brief summary of the relevant facts is listed in Table 1.

All four cases have one fact in common: the solid corrosion products are mixed up with a gelatinous acid-insoluble film. Chemical analysis of the gelatinous films elucidates that they consist of polysaccharides [*1,2*] or polysilicates or both [*3*]. The polysaccharides must be of biological origin. We investigated the chemical composition of the solid corrosion products for the German case in more detail and found other chemicals, for example, lactate and pyruvate, indicating biological activity [*2*].

[1] Professor, Märkische Fachhochschule, Laboratory of Corrosion Protection, Frauenstuhlweg 31, D-5860 Iserlohn, Germany

[2] Junior scientist, Märkische Fachhochschule, Laboratory of Corrosion Protection, Frauenstuhlweg 31, D-5860 Iserlohn, Germany

[3] Professor, Märkische Fachhochschule, Laboratory of Biotechnology, Frauenstuhlweg 31, D-5860 Iserlohn, Germany.

TABLE 1—*Observations of corrosion damage.*

Country, Type of Building	Composition of the Gelatinous Film	Shape of the Pits
Germany, hospital	polysaccharide	semihemispherically shaped
Saudi Arabia, hospital	polysaccharide	semihemispherically shaped
Scotland, hospital	polysaccharide, partially with polysilicate	semihemispherically shaped/pin-hole-sized
Sweden, private houses	polysilicate	semihemispherically shaped

The second fact that all four cases have in common is the composition of the water: it is soft, weakly buffered, with a low salt content prepared from surface water. Water treatment is briefly described in Table 2. These corrosion damages could not be explained by referring to the scientific based knowledge and experience from practice as described in [*4–9*], or as laid down in DIN 50930, Part 5, Corrosion Behaviour of Metallic Materials in Water; Copper and Copper Alloys.

In addition to the polysaccharides, an exceptional level of biological activity within the pitted pipes was established, in the German case, by the metabolic or degradation products mentioned previously, and, in the Scottish cases, by tremendous oxygen consumption during periods of stagnation.[4] However, in the Swedish case, the influence of microbiology to the corrosion damage was not significant.

Therefore, a first hypothesis for the mechanism may be substantiated by these facts:

> The physical and chemical properties of the gelatinous films in combination with metabolic and degradation products of biological origin influence the nature and chemistry of the electrolyte at the phase boundary with the metal. The increase of pitting is determined by this change in the water composition at the phase boundary.

Especially in the Swedish and German cases, some surface areas, although completely covered by the gelatinous film, had a shiny appearance without detectable signs of electrolytic attack. This situation arose when either the chemical or physical or both (for example, status of adherence) properties of the gelatinous films were not uniform or when the chemical composition of the electrolyte in and underneath these films caused and stabilized pitting. The different manifestations of the electrolytic attack for the different cases are summarized in Table 3. Though the surface is completely covered by the gelatinous film, the manifestation of the electrolytic attack may differ.

A model for the explanation of pitting is described in Ref *10*. Geesey demonstrated the chemical interaction of polysaccharides with copper ions and the transport of these ions through the gelatinous film. Since no validated, generally accepted model for the description of the relevant pitting corrosion is available, no specific types of microorganisms can be suspected, although it has been suggested that some bacteria will attack the copper and some others will not when they become sessile on the copper surface [*10–13*]. A physical model for the explanation of pitting corrosion taking into account the transport properties of the gelatinous films is described in Ref *14*.

[4] W. Keevil, personal communication, CAMR Consultancy, Salisburg, UK.

TABLE 2—*Description of water sources and treatments.*

Case	Water Source	Water Treatment
Germany	storage lake	pH-adjustment: CO_2 + lime, disinfection: Cl_2 + ClO_2
Saudi Arabia	seawater	distillation, mixture with well water, partially demineralized by reverse osmosis, disinfection: Cl_2
Scotland	boggy lake	flocculation, pH-adjustment: lime, disinfection: Cl_2
Sweden	mixture lake and well water	pH-adjustment: CO_2 + lime, disinfection: no information

Aspects for the Evaluation of Countermeasures

Several parameters influence the MIC susceptibility of copper to microbiologically influenced corrosion (MIC). As shown in Fig 1: the quality of the copper surface; operating conditions, design, and commissioning; the chemical composition of the water; and the corrosion-relevant biological activity have to be taken into account.

The potential for corrosion can be classified based on the corrosion rate or the expected extent of the manifestation of corrosion, especially by the end of the expected time of use. Copper pipes are delivered in the following conditions: hard, halfhard, and soft. Though the different qualities are installed in different quantities, no influence of the hardness of the tube on the likelihood corrosion is detectable. For this reason, the influencing quality of the copper surface cannot be used for the evaluation of countermeasures.

In setting up a new copper installation, generally accepted recommendations concerning commissioning and design of the installation and the operating conditions should be followed to avoid MIC. Pressure testing and operating conditions determine the likelihood of corrosion as well as pipe size, actual flow rates, storage vessel size, conditions of maintenance and cleanliness, and temperature control. The likelihood of corrosion remains small even in bigger municipal buildings, where the system is designed to include more vertical than horizontal runs. There is significant evidence that large plumbing systems are most prone to corrosion [*15*]. The highest rate can occur when a high degree of branching and a lot of horizontal runs are present. The likelihood of corrosion in domestic water distributions is small. Nevertheless, the signs of MIC may be detectable, although the number of corresponding failures remains very small.

A long period of time following installation and pressure testing can increase the likelihood of corrosion, especially when the water used for pressure testing stays in the copper tubing.

TABLE 3—*Manifestations of electrolytic attack.*

Case	Pits		General Attack (Roughening of the Surface)	Appearance as Electropolished
	Semi-hemispherical	Pin Hole		
Germany	X[a]		X	X
Saudi-Arabia	X		X	
Scotland	X or	X	X	
Sweden	X		X	X

[a] X: influence detectable.

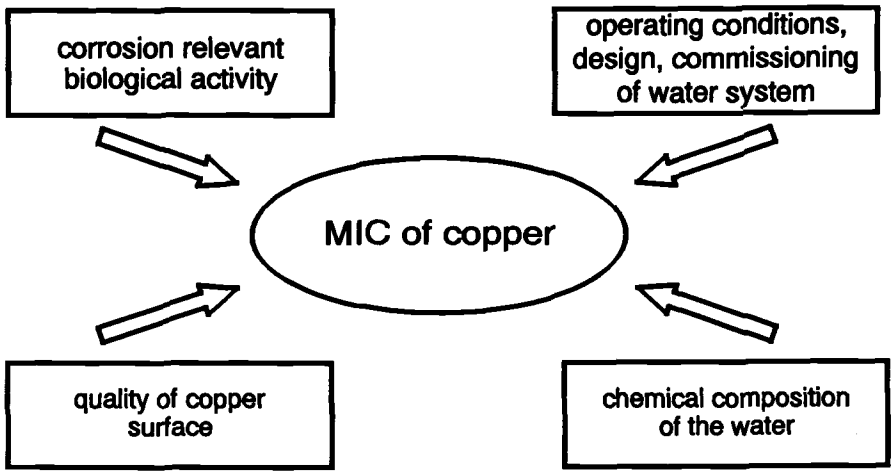

FIG. 1—*Parameters influencing the likelihood of MIC.*

The introduction of water into the system for pressure testing and other purposes can be harmful unless the system can be flushed on a regular basis. The possibility of stagnant pockets of water and partly filled pipes must be avoided.

The likelihood of corrosion is very small when a constant flow of water is established. Corrosion is at a maximum under intermittent flow conditions when periods of stagnation are prolonged [*15*].

All of these arguments can be considered when setting up a new copper installation. Only a few can be applied as a basis for countermeasures in potable water supplies that have already been operating for a certain time and where damage has occurred. To save a damaged installation, one has to focus on two parameters: (1) corrosion-relevant biological activity and (2) chemical composition of the water.

Corrosion-Relevant Biological Activity

The corrosion relevant biological activity is influenced by several parameters as shown in Fig. 2: the type of microorganisms; their metabolic state, that is, alive or dead; their motility, that is, planctonic or sessile; and their growth rate and input from the water source into the potable water supply. As mentioned previously, different types of microorganisms have different influences on the likelihood of MIC, but there is no general information available about the properties of specific microorganisms within a consortium. So the development of specific and sensitive countermeasures, for example, influencing nutrients, is not yet possible. The most important goal is to decrease the quantity of microorganisms in potable water supplies.

Several possible countermeasures and their influence on the parameters previously mentioned are listed in Table 4. All of these countermeasures may be applied in affected potable water installations.

Ultraviolet (UV) irradiation was applied in some of the four cases. The observation of the corrosion behavior shows that this measure applied alone is not sufficient. Filtration can be used in two ways: to influence the nutrients and the microorganisms. Filters that are not maintained regularly may become a source of infection, therefore, the specialists responsible for the hygienic aspects of the water do not recommend the use of filters. Flocculation

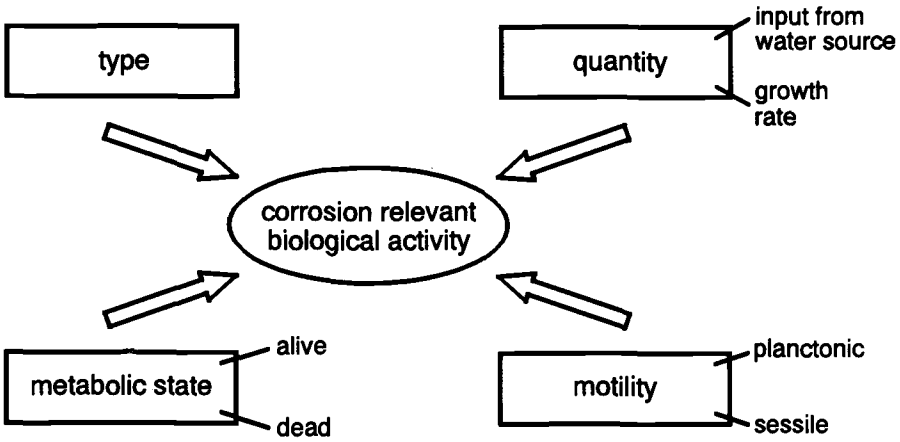

FIG. 2—*Main parameters determining corrosion-relevant biological activity.*

should affect biological activity like filtration, but the authors have no experience with this countermeasure.

It has been observed in the field that an installation is much more susceptible to pitting when exposed to a water supply that is increasingly contaminated by sources of infection. All sources for pollution that can increase the number of microorganisms should be avoided, such as, open water tanks, open reservoirs and dirty or irregularly maintained filters. Tubes leading into taps that are seldom used should be cut off from the installation.

Within the temperature range of 25 to 45°C, the generation rate of microorganisms reaches a maximum. Most of the microorganisms occurring in potable water can be killed by keeping the temperature above 55°C. Below 12°C the growth rate is reduced considerably. It has been shown in laboratory experiments that no relevant corrosion could be observed on copper samples exposed to water above 55°C [*16*].

Besides disinfection by filtration, no relevant experience from practical applications is available concerning this countermeasure. Laboratory investigations show that the number of colony-forming units can be decreased remarkably by chlorination. This countermeasure is not applicable in hospitals.

Since sessile microorganisms are especially likely to be involved in the corrosion mechanism, all countermeasures to decrease the number of sessile colonies are promising. Sessile microorganisms and the gelatinous film can be removed by a special hot citric acid treatment

TABLE 4—*Possible measures and their effect on the corrosion-relevant biological activity.*

Countermeasure	Type	Quantity	Metabolism	Motility
UV irradiation	X[a]		X	
Filtration		X		
Flocculation		X		
Removal of sources of infection	X	X		
Water temperature	X	X	X	
Disinfection	X	X	X	
Rinsing or pressure cleaning of the tube surface	X	X		X

[a] X: influence detectable.

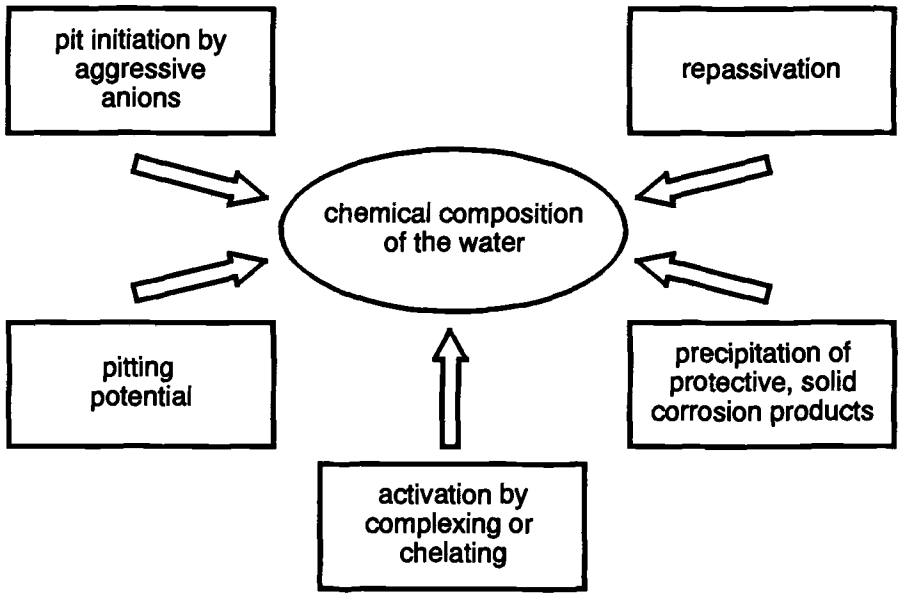

FIG. 3—*Main factors determining the corrosion behavior of copper in water distribution related to the chemical composition of the water.*

with high flow rates, as performed in the German case. The cleaning procedure as described in the German standard DIN 1988 Technical Rules for Potable Water Installations can be applied regularly and removes weakly adherent or sedimented corrosion products and microorganisms.

Corrosion behavior is improved by the countermeasures discussed in this section, but these countermeasures are not sufficient to solve relevant corrosion problems. Therefore, these measures obviously have to be supported by others that change the chemical composition of the water.

Chemical Composition of the Water

Pit initiation may be caused by localized changes in physical or chemical properties or both of an existing protective layer or by establishing localized conditions that inhibit the formation of a protective film. Besides the corrosion potential, pit initiation depends on the chemical composition of the potable water. Figure 3 shows several parameters determining corrosion behavior that can be related to the chemical water composition, mainly to the anions in the potable water. These anions influence the pitting potential, the precipitation of protective solid corrosion products, repassivation, and pit initiation and cause an activation of the corrosion process by complexing or chelating effects.

The influence of different anions on the induction of pit initiation, repassivation and precipitation of protective layers is summarized in Table 5. Chloride was detected to cause pit initiation [*17*]. Repassivation is supported by chloride and bicarbonate and inhibited by sulfate.[5] Therefore, the likelihood of pitting is mainly determined by the ratios of chloride/bicarbonate and chloride/sulfate. The pH is another important factor for repassivation;

[5] W. R. Fischer, unpublished results.

TABLE 5—*Influence of anions on pitting of copper and uptake likelihood of copper ions in the water.*

	Induction of Pit Initiation	Repassivation	Precipitation of Protective Layer	Activation by Complexing Agents	
				Cu^+	Cu^{2+}
pH		X[a]	X		
HCO_3^-	X		X		X
Cl^-	X	X+[b]	X+	X	
Cl^-/SO_4^{2-}		X−[c]			
HCO_3^-/SO_4^{2-}	X+	X−			

[a] X: influence detectable.
[b] X+: beneficial influence.
[c] X−: detrimental influence.

when pH stays below 3.8 within the pit, repassivation is inhibited [*18*].[5] The pit growth rate depends on potential, pit depth, and the chemical composition within the occluded corrosion cell. The pH change from the bulk water to the electrolyte within the occluded corrosion cell depends mainly on the buffering capacity of the water, for example, the bicarbonate concentration. The formation of a protective layer of the copper in the water distribution system is affected by pH, bicarbonate, and chloride.

This is a first attempt to discuss the influence of the chemical composition of the electrolyte on the likelihood of pitting by common parameters of water composition as described in Ref *19*. Two other important factors must be recognized, complexing and chelating agents. Bicarbonate forms complexes with copper(II)-ions and chloride forms complexes with copper(I)-ions [*20*].

The increase of bicarbonate concentration was successfully used in the Swedish case and improved corrosion behavior in a German MIC case.[6] The ion exchange of sulfate for chloride was used successfully in Germany to stop pitting corrosion by facilitating repassivation [*21*]. There is no reason that this countermeasure should not show the same beneficial effect under conditions that promote MIC.

Combinations of Different Countermeasures

UV irradiation, addition of bicarbonate, and their combination were used successfully to improve corrosion behavior. The permanent increase of water temperature above 55°C solved the corrosion problem in warm water supply systems. Further possible combinations, such as flocculation and ion exchange, are expected to show comparable beneficial effects, but, to date, no practical experience can be used to validate these suggestions.

Many well-known and economical countermeasures have been discussed in this contribution. It can be shown by field experience and theoretical considerations that a combination of different methods should be applicable in each case to protect existing copper installations.

References

[*1*] Fischer, W. R., Hänßel, I., and Paradies, H. H., "First Results of Microbial Induced Corrosion of Copper Pipes" in *Microbial Corrosion*, Vol. 1, C. A. C. Sequeira and A. K. Tiller, Eds., Elsevier Applied Science, London and New York, 1988, p. 300.

[6] A. Baukloh, personal communication, Kabelmetal, Oshabrück, Germany.

[2] Fischer, W. R., Paradies, H. H., Wagner, D., and Hänßel, I., "Copper Deterioration in a Water Distribution System of a County Hospital in Germany Caused by Microbiologically Influenced Corrosion—I. Description of the Problem," *Werkstoffe und Korrosion*, Vol. 43, 1992, p. 56.

[3] Linder, M. and Lindmann, E. K., Internal Report, Swedish Corrosion Institute, Stockholm, Sweden, Oct. 1987.

[4] Lucey, V.-F., "Pitting Corrosion of Copper in Potable Water," *Werkstoffe und Korrosion.*, Vol. 26, 1975, p. 185.

[5] Lucey, V.-F., "Pitting Corrosion of Copper—A Review," in *Symposium: Corrosion of Copper and Copper Alloys in Buildings*, Japan Copper Development Association, Tokyo, 1982, p. 1.

[6] Campbell, H. S., "Pitting Corrosion of Copper Water Pipes," in *Proceedings of 2nd International Congress on Metallic Corrosion*, National Association of Corrosion Engineers, Houston, TX, 1966.

[7] Linder, M. and Lindmann, E. K., in *Proceedings of the 9th Scandinavian Corrosion Congress*, Copenhagen, 1983, pp. 569–581.

[8] Holm, R., "Corrosion of Copper Pipes in Fresh Water—Swedish Experiences," in *Symposium: Corrosion of Copper and Copper Alloys in Buildings*, Japan Copper Development Association, Tokyo, 1982, p. 76.

[9] v. Franqué, O., "Pitting Corrosion of Copper Tubes in Cold Water-Situation and Experiences in the Federal Republic of Germany," in *Symposium: Corrosion of Copper and Copper Alloys in Buidings*, Japan Copper Development Association, Tokyo, 1982, p. 135.

[10] Geesey, G. G., Mittelman, M. W., Iwaoka, T., and Griffiths, P. R., "Role of Bacterial Exopolymers in the Deterioration of Metallic Copper Surfaces," *Materials Performance*, Vol. 2, 1986, pp. 37–40.

[11] Geesey, G. G., Jang, L., Jolley, J. G., Hankins, M. R., Iwaoka, T., et al., "Binding of Metal Ions by Extracellular Polymers of Biofilm Bacteria," *Water Science Technology*, Vol. 20, 1988, pp. 161–165.

[12] Jolley, J. G., Geesey, G. G., Hankins, M. R., Wright, R. B. and Wichlacz, P. C., in *Applied Spectroscopy*, Vol. 43, 1989, pp. 1062–1067.

[13] Angell, P., Campbell, H. S., and Chamberlain, A. H. L., "Microbial Involvement in Corrosion of Copper in Fresh Water," ICA Report 405, International Copper Association, New York, 1992.

[14] Fischer, W. R., Wagner, D., and Paradies, H. H., "New Types of Corrosion Caused by Organic Membranes," in *Microbial Corrosion-2*, C. A. C. Sequeira and A. K. Tiller, Eds., Institute of Materials, London 1992, pp. 155–165.

[15] Wagner, D. H. J., Fischer, W. R., and Paradies, H. H., "Correlation of Field and Laboratory Microbiologically Influenced Corrosion (MIC) Data for a Copper Potable Water Installation," in this volume, pp. 253–265.

[16] Walker, J. T., Keevil, C. W., Dennis, J., McEvoy, J., and Colbourne, J. S., "The Influence of Water Chemistry and Environmental Conditions on the Microbial Colonisation of Copper Tubing Leading to Pitting Corrosion Especially in Institutional Buildings," ICA Project 407, Final Report 1988–1990, International Copper Association.

[17] Fischer, W. R. and Füßinger, B., "Influence of Anions on the Pitting Corrosion of Copper in Potable Water," in *12th Scandinavian Corrosion Congress and Eurocorr 92 Proceedings*, Dipoli, Vol. 1, 1992. p. 769.

[18] Pourbaix, M., "Some Reference of Potential-pH Diagrams to the Study of Localized Corrosion," *Journal of the Electrochemical Society*, Vol. 123, 1976, p. 27.

[19] "Bekanntmachung der Neufassung der Trinkwasserverordnung," Teil 1, No. 66, *Bundesgesetzblatt* 1990.

[20] Hollemann, A. F. and Wiberg, E., *Lehrbuch der Anorganischen Chemie*, Walter de Gruyter, Berlin, New York, 1976.

[21] Kruse, C.-L. and Ensenauer, P.-K.-J., in *Sanitär und Heizungstechnik*, Vol. 52, 1987, pp. 758–763.

Jiunn S. Luo,[1] *Xavier Campaignolle,*[1] *and David C. White*[1]

Microbiologically Influenced Corrosion (MIC) Accelerated Testing Using a Flow-Through System

REFERENCE: Luo, J. S., Campaignolle, X., and White, D. C., **"Microbiologically Influenced Corrosion (MIC) Accelerated Testing Using a Flow-Through System,"** *Microbiologically Influenced Corrosion Testing, ASTM STP 1232*, Jeffery R. Kearns and Brenda J. Little, Eds., American Society for Testing and Materials, Philadelphia, 1994, pp. 283–292.

ABSTRACT: Microbes recovered from sediments, slime, tubercles, or corrosion coupons were characterized into functional groups, identified by fatty acid patterns and used in a flow-through test system. Test solutions were prepared as field conditions and supplemented with nutrients for the growth of microbes. Four-sided working electrodes were fabricated to simplify experimental design by combining four steel disks from the same stock into one probe. Concentric electrodes were made to simulate localized corrosion and study the effect of bacteria upon stability of localized corrosion. Electrochemical techniques such as: open circuit potential, electrochemical impedance spectroscopy, and galvanic current measurements were performed to evaluate the corrosion of mild steel in solutions containing different combinations of bacteria. Actual microbial community on the electrode surface was recovered by culture methods for viable counts upon termination of experiments. Preliminary results indicated that this test system provided an accelerated testing to simulate field exposures.

KEYWORDS: microbiologically influenced corrosion (MIC), accelerated testing, multi-electrode, concentric electrode

Biofouling of industrial cooling water systems, marine fouling on offshore structures, and sulfide contamination of oil and gas reservoirs have emphasized the need for a better understanding of microbiologically influenced corrosion (MIC). Recently, there has developed a greater recognition of the complexity of the MIC process. It was proposed [*1–3*] that the mechanisms of MIC can be categorized into three groups: (1) production of differential aeration and concentration cells by biofilm formation resulting from the availability of dissolved oxygen at the metal/solution interface, (2) production of acidic metabolities, that is, organic and inorganic acids, or both, or the end products of fermentation growth by bacteria, and (3) interference in the cathodic process under oxygen-free conditions by obligate anaerobic bacteria and their metabolic sulfide products. However, the use of pure strains of bacteria in experiments has been criticized as being nonrepresentative of actual field situations. Therefore, it is necessary to develop an accelerated test system that can simulate field conditions with known ecological, physiological, and nutritional requirements for bacteria involved in corrosion processes. This paper describes the use of a flow-through system, electrochemical monitoring methods, and bacterial cell counts to evaluate MIC of mild steel in seawater and cooling water systems.

[1] Post-Doctoral research associate, research associate, and executive director, respectively, University of Tennessee, Center for Environmental Biotechnology, Knoxville, TN 37932-2567.

Experimental Procedure

Preparation of Microbial Cultures

Bacteria used in experiments were isolated from field solutions and corrosion coupons. Corrosion products were aseptically transferred to a test tube containing 10 mL of medium consisting of (in g/L): glucose 2, sodium lactate 2, NH_4Cl 0.5, KH_2PO_4 0.1, and $MgSO_4 \cdot 7H_2O$ [*4*]. This medium was then inoculated into three different types of solutions designed to be enriched for aerobic, fermentative, or sulfate-reducing microbial consortia. Total fatty acid composition of the consortia was measured after saponification in methanol to form the methyl esters. A Microbial Identification System including a Hewlett-Packard 5980A capillary gas chromatograph, autosampler, and computer with microbial identification database (Microbial ID, Inc., Newark, DE) was used to identify the consortia. Prior to starting an experiment, each culture was transferred to, and incubated in, a fresh culture medium for desired periods, centrifuged at 5000 rpm for 20 min and resuspended in a test solution. Test systems were inoculated with bacteria several times during the duration of an experiment to achieve adequate microbial populations and accelerate MIC testing.

Electrochemical Cell

A sterilizable, flow-through electrochemical cell, as shown in Fig. 1, consisting of a 600 mL glass beaker included: (1) a working electrode, (2) a Pt coated Nb mesh counter electrode, (3) a saturated calomel reference electrode, (4) a 0.2 μm sterile filter ventilation port, (5) a magnetically driven, Teflon®-coated stir bar, and (6) a test solution inlet and outlet. A

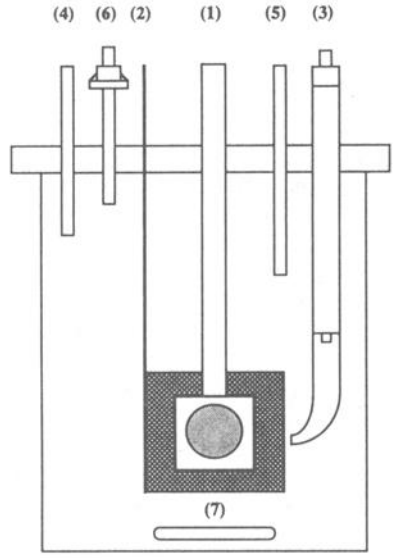

1. Working electrode
2. Counter electrode
3. Reference electrode
4. Solution intlet
5. Solution outlet
6. 0.2 um air filter
7. Stir bar

FIG. 1—*Electrochemical cell arrangement.*

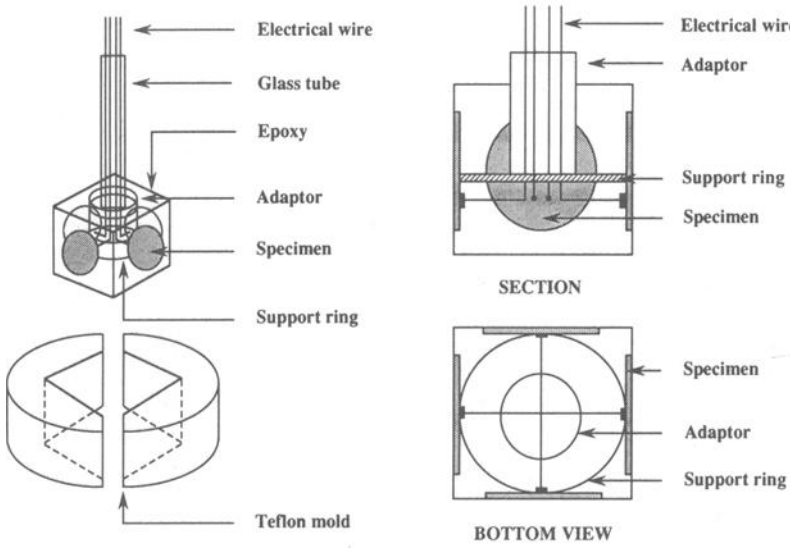

FIG. 2—*Schematic illustration of a four-sided electrode probe.*

four-sided working electrode [5] was fabricated to simplify experimental design by combining four 16-mm diameter AISI 1020 carbon steel disks into one probe, as illustrated in Fig. 2. It was reported that no interferences or crosstalk were observed between electrodes, and the interfacial chemistry at the metal/solution interface was reproducible [5]. In addition, a concentric specimen, as shown in Fig. 3, of AISI 1020 carbon steel was constructed to investigate localized corrosion (pitting) influenced by micro-organisms, where two circumferential steel electrodes were separated by a Teflon insulator ring and embedded in epoxy. The surface area ratio between the large circumferential electrode (25.4-mm diameter) and the small central electrode (2-mm diameter) was about 160:1. Under ambient atmospheric conditions, localized corrosion was simulated by cathodically polarizing the large electrode to −1200 mV Standard Calomel Reference Electrode (SCE) for 3 h, while the small electrode was left at its open circuit potential of −530 mV (SCE) [6]. After this preconditioning phase, the galvanic current between the cathode and the anode was monitored to determine the influence of bacteria upon pitting corrosion.

Test Solutions

Test solutions consisted of both synthetic seawater and cooling water. The preparation of synthetic seawater was based on ASTM Standard Specification for Substitute Ocean Water (ASTM D1141) with several modifications. The solution included (in g/L): NaCl 33.2, $MgCl_2$ 1.11, $CaCl_2 \cdot 2H_2O$ 1.32, Na_2SO_4 4.09, $NaHCO_3$ 0.21, KCl 0.695, KBr 0.101, NaF 0.003, and $SrCl_2 \cdot 6H_2O$ 0.025. Additional nutrients for marine bacteria growth (in g/L): NH_4Cl 0.1, yeast extracts 0.01, sodium lactate 0.05, glucose 0.01, vitamins 1 mL and KH_2PO_4 0.05 were added to accelerate the growth of inoculated bacteria. A simulated cooling water contained (in g/L): NaCl 0.073, NH_4NO_3 0.05, Na_2SO_4 0.12, $MgCl_2 \cdot 6H_2O$ 0.154, KH_2PO_4

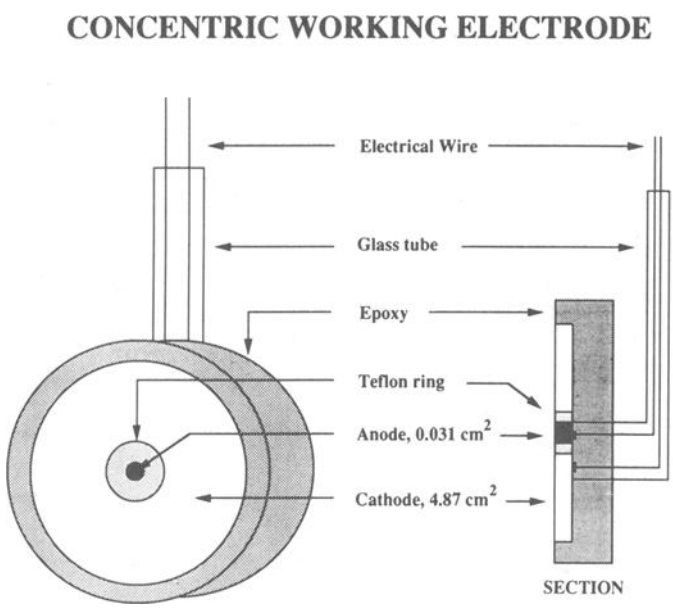

FIG. 3—*Schematic illustration of a concentric electrode.*

0.038, K_2HPO_4 0.124, $FeCl_3 \cdot 6H_2O$ 0.33 mL of a 10 mM solution and Hutner's salt solution 1.0 mL was also prepared. Total organic carbon content of the cooling water was adjusted to about 0.35 g/L by adding sodium lactate 0.8 g/L and sodium succinate 0.5 g/L.

Test Procedures

Prior to the start of each experiment, all specimens were wet polished in sequence with 240, 400, and 600 grit SiC paper, ultrasonically cleaned with distilled water, degreased with acetone, and sterilized with 70% alcohol for 20 min. The electrochemical cell was sterilized with ethylene oxide using the precautions defined previously [*4*]. All inlets and outlets for the cell were autoclaved to achieve sterilization. Test solutions were autoclaved at 121°C for 2 h and solution pH values were adjusted to 7.8 and 7.2 for the synthetic seawater and simulated cooling water, respectively, using either 0.2 M NaOH or HCl. During the test period, the solutions were maintained at ambient temperature, and the flow rate was controlled at 60 ± 5 mL/min by a dual-channel peristaltic pump.

Open-circuit potential (OCP) of test specimens was monitored at intervals of 1 h by a Hewlett-Packard model 3458A multimeter via a Keithley model 706 scanner controlled by a computer. Electrochemical impedance spectroscopy (EIS) analysis was performed by using the Zplot® software (Scribner Associates, Inc.), a Solartron model 1255 frequency response analyzer, and a potentiostat/galvanostat model 273 from EG & G Princeton Applied Research. Sinusoidal potentials of 5 mV were applied between 5 mHz and 10 KHz at 5 steps/decade. For cathodic polarization and galvanic current measurements, a Sycopel model DD10M potentiostat was used.

Total bacterial cell counts from bulk solutions and specimen surfaces were enumerated by acridine orange direct counts (AODC) after fixation in 2.5% glutaraldehyde [*7*]. Additionally, viable plate counts and the most probable number technique (MPN) [*8*] were employed to estimate specific aerobes and sulfate-reducing bacteria, respectively.

Results and Discussion

Microbial Activity Monitored by Open-Circuit Potential Measurement

MIC of mild steel in cooling water systems was studied by placing a four-sided electrode probe in the solution containing *Pseudomonas fluorescens* (*Lux*), hereafter referred to as 5RL, and *Desulfovibrio gigas* (*D. gigas*) for a time up to 200 h. 5RL was selected on the basis of its ability to reduce oxygen concentrations in the lower layers of the biofilm as the biofilm develops [9]. *D. gigas* is an anaerobic, dissimilatory sulfate-reducer. It was detected that 1.0E + 08 cells/mL 5RL and 1.0E + 06 cells/mL *D. gigas* existed in the culture media after 3 days of incubation. It is believed that the established 5RL biofilm on the metal surface may provide prerequisite anaerobic environments for *D. gigas* growth. Hence, inocula of 5 mL of 3-day old 5RL and *D. gigas* cultures into the electrochemical cells were performed at specimen exposure times of 0 and 96 h, respectively.

Typical open-circuit potential (OCP) versus time plots for specimens in the sterile and 5RL + *D. gigas* solutions are given in Fig. 4. For the sterile control, the OCP of specimens remained steady at −230 mV (SCE) for approximately 80 h and then decreased gradually to −350 mV (SCE). While in the solution containing 5RL, a rapid potential drop occurred after about 30 h of exposure and then maintained a −750 mV (SCE) for 10 h, followed by an abrupt increase in potential toward −300 mV (SCE) and kept increasing steadily until

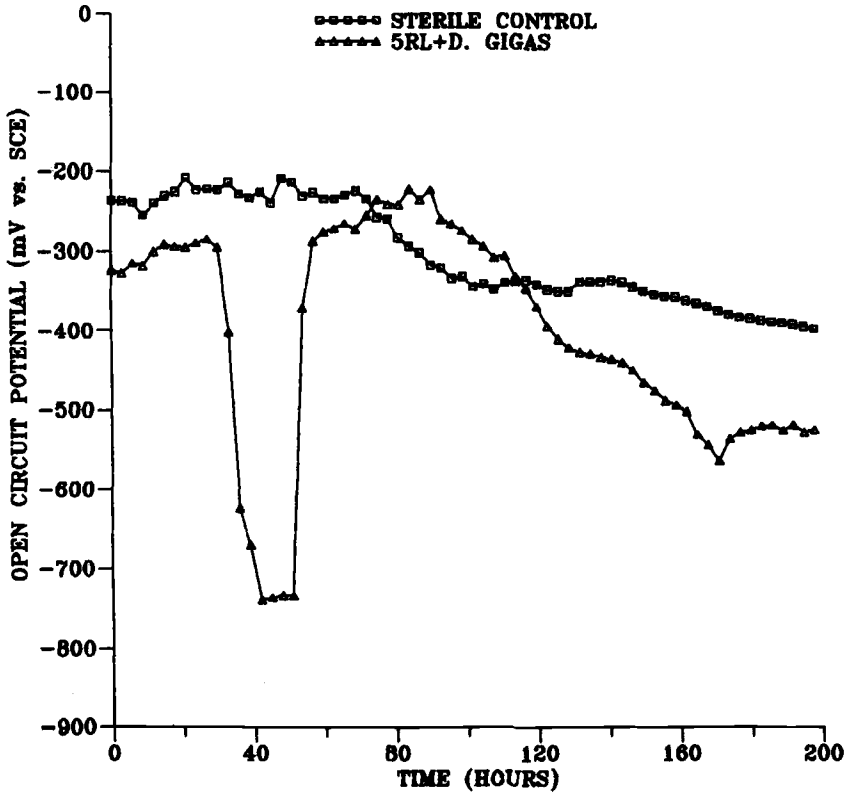

FIG. 4—*OCP versus time plots for specimens in the sterile simulated cooling water with and without inoculation of bacteria.*

D. gigas was added (at specimen exposure time of 96 h). The addition of *D. gigas* caused a gradual decline in potential from approximately −300 to −500 mV (SCE) throughout the rest of the experiment.

It is generally recognized that localized corrosion occurs when environmental effects induce heterogeneities on the metal surface. The physical presence of microbial cells on the surface, in addition to their metabolic activity, modifies electrochemical behaviors of the metal at the metal/solution interface. Adsorbed cells grow, reproduce, and form colonies that are physical anomalies on the metal surface, resulting in local anodes and cathodes. Under aerobic conditions, areas under respiring colonies become anodic and surrounding areas become cathodic [2]. Therefore, it is possible to infer that the colonization of 5RL on the steel surface, followed by nucleation of localized attack, caused a sudden drop in OCP. Subsequent sustained potentials at about −750 mV (SCE) indicated the propagation of the local attack. However, a mature biofilm could prevent the diffusion of corrosive species, such as oxygen, to the metal surface, thereby reducing the metal corrosion [*10*]. Hence, a relatively sharp increase in OCP (Fig. 4) could imply a uniform 5RL biofilm covered on the metal surface. In the presence of *D. gigas,* changes of OCP correlated to both activities of 5RL and *D. gigas* on the metal surface, that is, *D. gigas* modified the biofilm produced by 5RL so as to affect *D. gigas* colonization rates. Since 5RL has been frequently cited as a typical genus of slime forming bacteria, the established 5RL biofilm provided the prerequisite anaerobic habitat for *D. gigas* metabolic activity and growth. This was confirmed by viable counts, which showed 5.0E + 06 cells/cm^2 5RL and 1.0E + 03 cells/cm^2 *D. gigas* on the coupon surface at specimen exposure time of 120 h, while 1.0E + 08 cells/cm^2 5RL and 1.0E + 05 cells/cm^2 *D. gigas* were detected after 200 h of exposure.

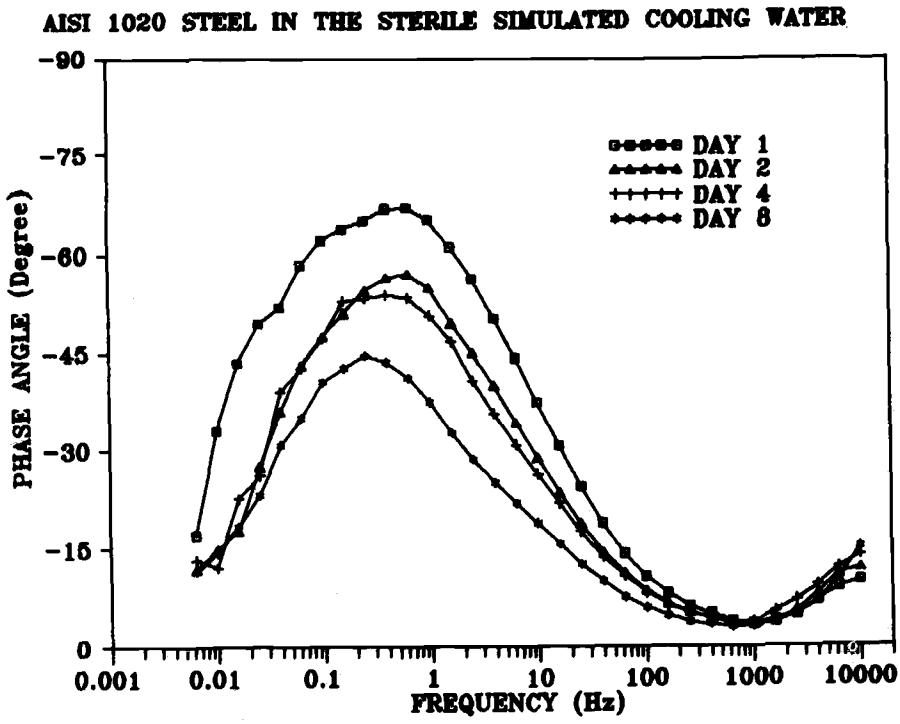

FIG. 5—*Bode plots for a specimen in the sterile simulated cooling water at various immersion times.*

Prediction of Biofilm Formation by EIS Technique

The activity of the biofilm estimated as volatile fatty acid production correlates with the average corrosion rate in terms of charge transfer resistance measured by EIS [*11*]. It was reported [*12*] that EIS can be used to study mechanisms of MIC with little or no damage to the numbers of viable bacteria in a biofilm, or to the activity of the bacteria. However, when corrosion reactions are complicated by diffusion constraints, that is, bacteria strongly adhered to metal surface and introduced diffusion gradients [*13*], Nyquist plots do not permit a reasonably accurate extrapolation of charge transfer resistances. Moreover, it was recognized [*14*] that the combination of microbial films and corrosion products often encountered in MIC causes the impedance to become very high at low frequencies, thus shifting the maximum phase angle to lower frequencies. As a result, an increase of the phase angle at the lowest frequency may reflect the formation of biofilms. Figures 5 and 6 present the phase angle versus frequency plots for four-sided specimens in the sterile cooling water with and without inoculation of 5RL + *D. gigas* at various immersion times. It is apparent that in the sterile control (Fig. 5), no significant changes of phase angle at the lowest frequency (5 mHz) occurred, while in the 5RL + *D. gigas* solution (Fig. 6), a steady increase in the angle (at 5 mHz) was observed. AODC from the coupon surfaces confirmed that the formation and aging of 5RL and *D. gigas* biofilms resulted in an increase of the phase angle at the lowest frequency.

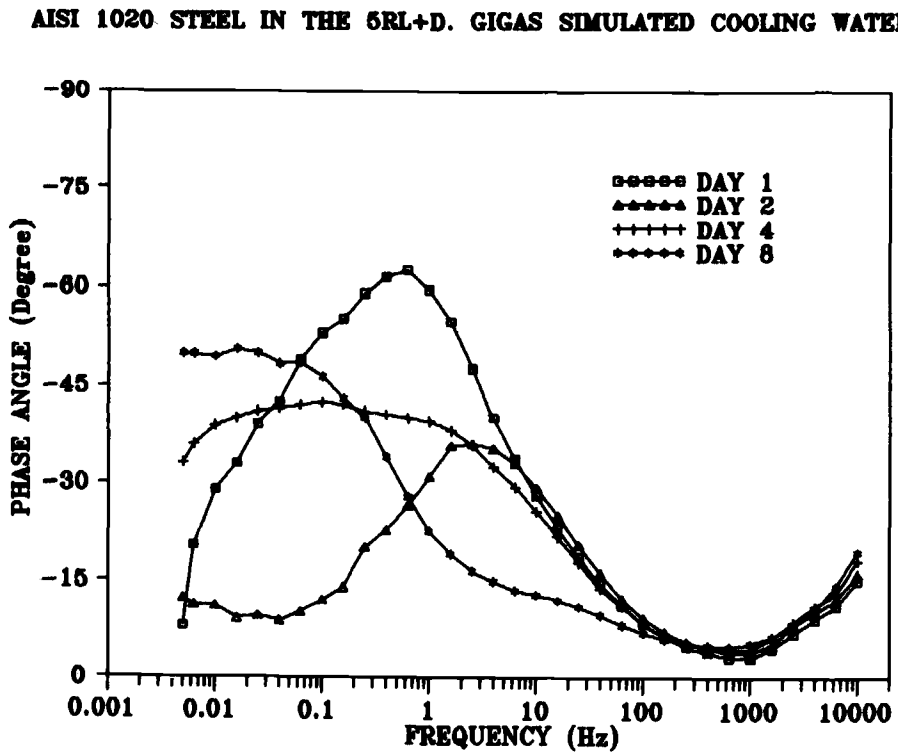

FIG. 6—*Bode plots for a specimen in the simulated cooling water containing 5RL* + D. gigas *at various immersion times.*

Effect of Sulfate-Reducing Bacteria Upon Pitting Corrosion

It is generally recognized that major field failures due to sulfate-reducing bacteria (SRB) are often in the form of localized corrosion, such as pitting. Pitting corrosion can be described as galvanic cells electrically short-circuited through the body of a metal. In the presence of active pits, galvanic currents between corroded areas and noncorroded sites should be persisted. In order to address these features, the galvanic currents of the preconditioned concentric specimens in the aerobic synthetic seawater containing *Vibrio natriegens, Desulfovibrio vulgaris,* and both were monitored. *V. natriegens* is a slime-forming, acid-producing heterotrophic aerobe, and *D. vulgaris* is a dissimilatory, sulfate-reducing anaerobe, which is ubiquitous in natural seawater. Since hydrogen evolution from cathodic polarization is beneficial to the growth of *D. vulgaris* [*15*], inoculation of bacteria into the flow-through electrochemical cells was performed before cathodically polarizing the large electrode to −1200 mV (SCE).

Figure 7 shows the galvanic current density between the anode and the cathode at open circuit as a function of time for concentric specimens exposed to aerobic synthetic seawater with different bacteria inocula. In all cases, a relatively sharp decrease in current density was followed by a steady final current density. In the presence of *D. vulgaris* alone, a higher

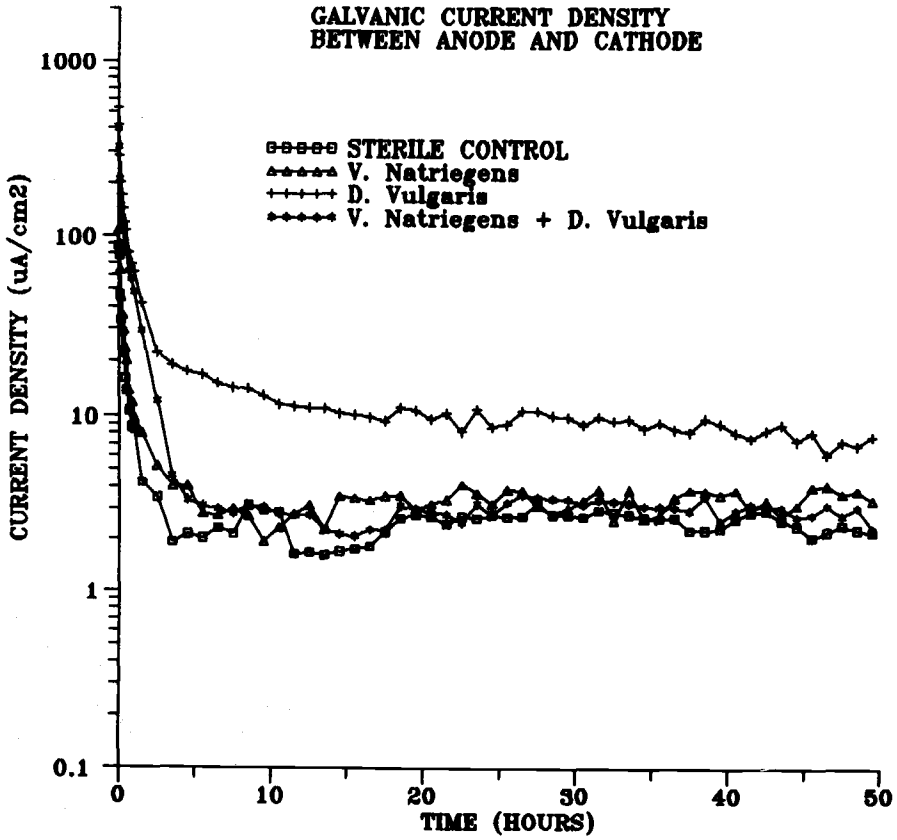

FIG. 7—*Galvanic current density between the anode and the cathode for concentric electrodes exposed to the synthetic seawater containing different types of bacteria.*

final current density (10 $\mu A/cm^2$) was obtained in comparison with that of sterile control or solutions with *V. natriegens*. It is possible to infer that the formation of a *V. natriegens* biofilm could make the anode and the cathode identical and that the galvanic currents between them became infinite. However, biofilms composed only of *D. vulgaris* are able to sustain the localized corrosion created by preconditioning the specimens. It was noticed that AODC of anodic and cathodic surfaces showed equivalent amounts (1.0E + 06 cells/cm^2) for the *V. natriegens* monoculture and the coculture but elevated numbers (2.0E + 07 cells/cm^2) of *D. vulgaris* on the anodic surface in the condition where the coupling current persisted. Consequently, the value of the galvanic current established between the anode and the cathode after the preconditioning phase can be a criterion to evaluate localized corrosion influenced by microorganisms [*16*].

Conclusions

(1) The utilization of the flow-through electrochemical cell associated with inoculation of bacteria accelerated MIC testing.
(2) In the presence of bacteria, changes in specimen open-circuit potential correlated with changes in the Bode plots from EIS measurements, which revealed the development of biofilms.
(3) Galvanic current measurements between the separated anode and cathode of the concentric electrode can be a useful technique to determine localized corrosion influenced by microorganisms.

References

[*1*] Ford, T. and Mitchell, R., "The Ecology of Microbial Corrosion," *Advances in Microbial Ecology*, Vol. 11, K. C. Marshall, Ed., Plenum Press, New York, 1990, pp. 231–262.
[*2*] Little, B. J., Wanger, P. A., Characklis, W. G., and Lee, W., "Microbial Corrosion," *Biofilms*, W. Characklis and K. C. Marshall, Eds., John Wiley & Sons, New York, 1990, pp. 635–670.
[*3*] Hamilton, W. A., "Sulphate-Reducing Bacteria and Anaerobic Corrosion," *Annual Review of Microbiology*, Vol. 39, 1985, pp. 195–217.
[*4*] White, D. C., Jack, R. F., Dowling, N. J. E., Franklin, M. J., Nivens, D. E., Brooks, S., Mittelman, M. W., Vass, A. A., and Isaacs, H. S., "Microbially Influenced Corrosion of Carbon Steel," Proceedings of the National Association of Corrosion Engineers (NACE), CORROSION/90 Conference, Paper 103, NACE, Houston, 1990.
[*5*] Nivens, D. E., Jack, R. F., Vass, A. A., Guckert, J. B., Chambers, J. Q., and White, D. C., "Multi-Electrode Probe for Statistical Evaluation of Microbiologically Influenced Corrosion," *Journal of Microbial Methods*, Vol. 16, No. 1, 1992, pp. 1–12.
[*6*] Guezennec, J., Mittelman, M. W., Bullen, J., White, D. C., and Crolet, J-L, "Stabilization of Localized Corrosion on Carbon Steel by Sulfate-Reducing Bacteria," United Kingdom Corrosion/92 Conference, The Institute of Corrosion, London, UK, 13–15 Oct. 1992.
[*7*] Hobbie, J. E., Daley, R. J., and Jasper, S., "Use of Nuclepore Filters for Counting Bacteria by Fluorescence Microscopy," *Applied and Environmental Microbiology*, Vol. 33, No. 5, 1977, pp. 1225–1228.
[*8*] Collins, C. H. and Lyne, P. M., *Microbiological Methods*, 4th Edition, Butterworth Inc., Boston, 1976, p. 204.
[*9*] Patel, T. D. and Bott, T. R., "Oxygen Diffusion Through a Developing Biofilm of *Pseudomonas fluorescens*," *Journal of Chemical Technology and Biotechnology*, Vol. 52, 1991, pp. 187–199.
[*10*] Pederson, A. and Hermansson, M., "The Effect of Metal Corrosion by *Serratia Marcescens* and a *Pseudomonas SP.*," *Biofouling*, Vol. 1, 1989, pp. 313–322.
[*11*] White, D. C., Nivens, D. E., Mittelman, M. W., Chambers, J. Q., King, J. M. H., and Sayler, G. S., "Non-Destructive On-Line Monitoring of MIC," Proceedings of the National Association of Corrosion Engineers (NACE), CORROSION/91 Conference, Paper 114, NACE, Houston, 1991.
[*12*] Franklin, M. J., Nivens, D. E., Guckert, J. B., and White, D. C., "Effect of Electrochemical Impedance Spectroscopy on Microbial Biofilm Cell Numbers, Viability, and Activity," *Corrosion*, Vol. 47, No. 7, 1991, pp. 519–522.

[*13*] Costerton, J. W. and Boivin, J., "Microbially Influenced Corrosion," *Biological Fouling of Industrial Water Systems: A Problem Solving Approach*, M. W. Mittelman and G. G. Geesey, Eds., Water Micro Associates, San Diego, CA, 1987, pp. 56–76.

[*14*] Dowling, N. J. E., Stansbury, E. E., White, D. C., Borenstein, S. W., and Danko, J. C., "On-Line Electrochemical Monitoring of Microbially Influenced Corrosion," *Microbial Corrosion: 1988 Workshop Proceedings*, G. J. Licina, Ed., Electric Power Research Institute, Palo Alto, CA, Chapt. 5, pp. 1–17.

[*15*] Guezennec, J., "Influence of Cathodic Protection of Mild Steel on the Growth of Sulphate-Reducing Bacteria at 35°C in Marine Sediments," *Biofouling*, Vol. 3, 1991, pp. 339–348.

[*16*] Campaignolle, X., Luo, J. S., Bullen, J., White, D. C., Guezennec, J., and Crolet, J-L, "Stabilization of Localized Corrosion of Carbon Steel by Sulfate-Reducing Bacteria," Proceedings of the National Association of Corrosion Engineers (NACE), CORROSION/93 Conference, Paper 302, NACE, Houston, 1993.

Author Index

Subject Index

ISBN 0-8031-1892-9